turboexpanders

and process applications

Heinz Bloch
Claire Soares

G|P
P|

TURBOEXPANDERS AND PROCESS APPLICATIONS

This Page Intentionally Left Blank

TURBOEXPANDERS AND PROCESS APPLICATIONS

Heinz P. Bloch
Claire Soares

Gulf Professional Publishing
an imprint of Butterworth-Heinemann

Boston • Oxford • Auckland • Johannesburg • Melbourne • New Delhi

Information contained in this work has been obtained by Butterworth-Heinemann and the authors from sources believed to be reliable. However, neither Butterworth-Heinemann nor its authors shall be responsible for any errors, omissions, or damages arising out of the use of this information. This work is published with the understanding that Butterworth-Heinemann and its authors are supplying information, but are not attempting to render engineering or other professional services. If such services are required, seek the assistance of the experienced companies listed in Appendix C, "Turboexpander Contacts and Addresses," or other appropriate professionals.

Gulf Professional Publishing is an imprint of Butterworth–Heinemann.

Library of Congress Cataloging-in-Publication Data
Bloch, Heinz P., 1933–
Turboexpanders and process application / Heinz Bloch and Claire Soares.
p. cm.
ISBN 0-88415-509-9
1. Turboexpanders. 2. Heat recovery. I. Soares, Claire. II. Title

TJ266 .B58 2001
621.406--dc21 00-054358

British Library Cataloguing-in-Publication Data
A catalogue record for this book is available from the British Library.

The publisher offers special discounts on bulk orders of this book.
For information, please contact:

Manager of Special Sales
Butterworth–Heinemann
225 Wildwood Avenue
Woburn, MA 01801-2041
Tel: 781-904-2500
Fax: 781-904-2620

For information on all Butterworth-Heinemann publications available, contact our World Wide Web home page at: http://www.bh.com

10 9 8 7 6 5 4 3 2 1

Printed in the United States of America

Contents

Dedication

To the Memory of Dr. Judson S. Swearingen,
January 11, 1907–September 5, 1999

Those who knew him well called Dr. Swearingen a man of many talents, a superb theoretician, and hands-on manager. He was one of the rarest breed of individuals: An inventor and entrepreneur with a genius-level feel for machine behavior.

His pioneering works, over one hundred mechanical and natural gas and/or hydrocarbon processing patents and numerous articles, led the way to a cryogenic expander technology that has become an inseparable part of the gas processing industry.

Preface

We planned this book to be an up-to-date overview of turboexpanders and the processes where these machines are applied in a modern, cost-conscious plant environment. Therefore, the text addresses construction features, application criteria, functional parameters, and selection guidelines. It is clearly intended for the widest possible spectrum of engineering, technical support, maintenance, operating, and managerial personnel in process plants, refineries, air liquefaction, natural gas separation, mining, design contracting, and many other industries.

The book covers both cryogenic turboexpanders that are used to recover power from extremely cold gases, and hot gas expanders that recover power from gases reaching temperatures well in excess of 1,000°F. Because energy recovery applications ranging from 75–25,000 kW exist in virtually any process that uses high-temperature and/or high-pressure gases, properly designed turboexpanders will play an increasingly important role in modern industry. It is our hope that we have managed to thoroughly explain why, when, and how to use these machines—in both theory and practice. We, therefore, delve into issues and guidelines, overview comments and details, procedures, and techniques that most turboexpander owner/operators and specifying engineers need to know.

To the best of our knowledge, this is the first comprehensive text that elaborates on the rather skimpy treatment given to turboexpanders elsewhere. It is clearly the first book explaining magnetic bearing applications for this machinery category.

In terms of audience, this book should be of unique interest to a very wide spectrum of engineers, technicians, supervisors, operators and managers in virtually every user plant environment. Recent technical graduates, experienced and advanced individuals from air separation facilities, chemical plants, refineries, natural gas processing plants, mining, design contracting, and other industries will benefit from this highly practical, well-illustrated text.

Written and compiled with the active assistance of industry experts and experienced turboexpander users, the book covers theory to the extent necessary to understand operating principles and overall application criteria. The interaction of components and controls, auxiliaries, and subsystems is given extensive coverage and provides continuity and readability.

The reader will find both chapter sequences and the index organized for rapid retrieval of pertinent information. Referring to this text will equip every turboexpander job level and job function with an understanding of technical matters relating to a wide variety of processes and equipment types. It combines process and mechanical technology as it applies to these machines and presents both "overview information" and more detailed explanations for the various categories of readers and interested parties.

The following are some examples of the book's problem-solving potential.

A.	JOB FUNCTION:	Equipment Selection Engineer
	RESPONSIBILITY:	Bid Evaluation
	PROBLEM:	Receives offers from bidders whose component selections differ; needs to understand the advantages and disadvantages of certain design features
	HOW SOLVED:	This text will provide guidance.
B.	JOB FUNCTION:	Plant Manager
	RESPONSIBILITY:	P&L, Plant Profitability, Safety
	PROBLEM:	Receives contractor's proposal for an energy conservation project, which includes a turboexpander driving a generator.
	HOW SOLVED:	Understands operating principles and relative complexity after reviewing this text.
C.	JOB FUNCTION:	New engineer
	RESPONSIBILITY:	Contact person between project group and operations department.
	PROBLEM:	Confronted with a machine he knows nothing about; has no knowledge of a particular process that uses turboexpanders.
	HOW SOLVED:	Finds a thorough explanation in this text.

Rotating machinery users seem to fall into one of two categories: those who *need* to conserve operational costs and those who merely *want* to conserve operational costs. Either category makes sense in today's business environment, where companies concern themselves with downsizing and restructuring on an unprecedented scale. The (occasionally dubious) logic cited for this includes competitive positioning, global profile extension, and overhead streamlining. Superimposed on these learnings are issues such as increased environmental legislation and profitability targets.

Against this backdrop, the quest for more efficient processes, more reliable equipment, downtime avoidance, and maintenance cost reductions is understandable. How are these pursuits structured? Better yet, how *should* they be structured? The answer is the real best-of-class, high profitability performers who are hard at work changing old ways of thinking. They are willing to reassess work processes and work procedures. Best-of-class companies also revisit the basics while, understandably, engaging in the search for new and advanced technologies.

Interestingly, modern turboexpanders cater to all of these approaches. That's why it is incumbent upon technical personnel engaged in process engineering or power generation to become thoroughly familiar with this sometimes under-rated equipment category. In the truly forward-looking companies, turboexpanders are being considered for an ever-increasing field of industrial fluid moving and energy conservation tasks.

With these facts in mind, we have compiled and updated material provided by turboexpander technology experts. Editing their work proved to be a real challenge. Although we occasionally found small differences in items concerning technical detail, we discovered that some of the oldest papers and presentations on both art and science of turboexpander technology are not only still readable, but continue to be totally relevant and applicable today.

We sometimes kept certain information contained in a particular author's work even though the same topic is given partial coverage elsewhere in this book. We tried to remember that we wanted to achieve technical relevance, readability, and balance. Occasionally, we decided that the inclusion of a parallel text offered a different or additional perspective, perhaps with new or different illustrations, or an interesting but straightforward mathematical treatment.

As the reader progresses through this book, he or she will uncover in successive chapters additional layers of information that give insight into how the original, generally small and somewhat "prototypish" turboexpanders became the giant monsters of our day. They have not yet reached their full and undoubtedly massive applications potential.

Indeed, turboexpanders deserve to move into the limelight. Many of these machines are contributing to the profitability of modern process plants, while at the same time protecting the environment. They are highly reliable machines that represent mature technology. And that is why we compiled this text—to acquaint the serious manager and technical specialist with modern turboexpanders and the processes that benefit from them.

Much credit goes to the manufacturing companies and writers that have designed and produced the machines and applications. Others are to be commended for writing and explaining, and for not allowing doubters and detractors to derail their enthusiasm and drive. First and foremost among these pioneers stands Dr. Judson Swearingen, who founded the Rotoflow Company and whose name is listed numerous times in the various references that other solid contributors have cited in their own work product. These pertinent references are given at the end of each chapter.

Acknowledgments

We are grateful to the following manufacturers and publishing companies for providing us with reference material:

- Atlas Copco / Rotoflow (a division of Atlas Copco)
- Babcock Borsig
- Bearings Plus
- Compressor Controls Corporation
- Dresser Rand
- Demag Delaval
- Elliott Company
- GHH-Borsig
- Hydrocarbon Processing (Gulf Publishing Company)
- Mafi-Trench
- MAN-Gutehoffnungshuette
- Nova Magnetics
- Revolve Technologies
- Sulzer-Roteq
- S2M (Société de Mécanique Magnétique)
- Turbomachinery International

Heinz P. Bloch
Claire Soares

Note 1. Conversion factors are given in Appendix A.
2. Please also review Appendix B and C for additional names.

This Page Intentionally Left Blank

CHAPTER ONE

Why and How Turboexpanders Are Applied

Turboexpanders are expansion turbines, rotating machines similar to steam turbines. Commonly, the terms "expansion turbines" and "turboexpanders" specifically exclude steam turbines and combustion gas turbines. Turboexpanders (Figure 1-1) can also be characterized as modern rotating devices that convert the pressure energy of a gas or vapor stream into mechanical work as the gas or vapor expands through the turbine. If chilling the gas or vapor stream is the main

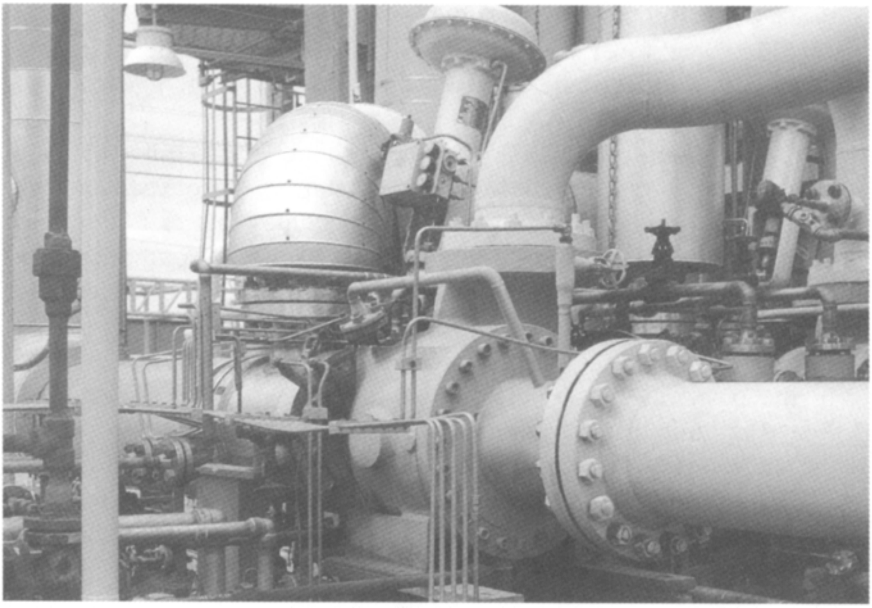

Figure 1-1. Modern turboexpander installation. *(Source: Atlas Copco.)*

objective, the mechanical work so produced is often considered a byproduct. If pressure reduction is the main objective, then heat recovery from the expanded gas is considered a beneficial byproduct.

In each case, the primary objective of turboexpanders is to conserve energy. Contemporary turboexpanders do this either by recovering energy from cold gas (cryogenic type) or from hot gases at temperatures of over 1,000 degrees. Current commercial models exist in the power range of 75 kW to 25+ MW, so many applications are possible.

Changing market conditions, accentuated by growing environmental awareness on a global scale, are improving market receptivity for the turboexpander. Machinery manufacturers, quick to sense this market potential, have developed design features within their turboexpander ranges that offer user-friendly features, promoting ease of maintenance and operation, and aid design optimization.

TURBOEXPANDERS FOR ENERGY CONVERSION*

Substantial energy can be recovered using low-grade waste heat, process gas, or waste gas pressure letdown.

Centrifugal (radial inflow) turboexpanders are well adapted to such energy conservation schemes and, with recent developments that have increased their reliability, are suitable for unattended service on a 24-hour, 7-day week operational basis. Some of the recent developments include better shaft seals, thrust bearing monitoring, and superior control devices.

Turboexpanders are well qualified to meet the requirements of energy conservation. Decades of development in turboexpander technology have resulted in highly efficient machines that can be applied in the profitable recovery of energy from waste heat sources and gas pressure letdown. Increasing demand and the progressive depletion of energy sources point to the need for conservation and for the recovery of energy from sources once thought unprofitable.

In the past, the use of the turboexpander as an energy recovery device was limited for a number of reasons:

- The return on capital investment did not justify a power recovery system unless more than several thousand horsepower was recovered.

**Sources: Atlas Copco (Rotoflow) Corporation and Babcock-Borsig.*

- Finding a market for recovered power was difficult when there appeared no immediate use for it within the plant.
- Continuity and reliability of this energy source was required if it were used as "base load," which required standby equipment, spares, and appropriate operator attention.
- Lack of confidence in new power recovery schemes that were not yet proven made both government and private industry reluctant to invest in these systems.

Recently, there has been a substantial shift in conditions and user attitudes. With increasing cost of power, the return on capital investment has vastly improved. A more favorable regulatory climate and changes in attitude of utility companies toward returning electricity to their grid have made novel power producing schemes practical and attractive.

High-efficiency expanders and their relatively short payback period made even smaller units economically attractive. These machines have demonstrated a high degree of reliability. Hundreds of units have been in continuous uninterrupted service for many years; this has removed the need for backup equipment and has demonstrated that unattended operation is entirely feasible.

What follows is a summary of turboexpander applications, an overview of what constitutes the present state-of-the-art, and the features incorporated in turboexpander design, which enable it to meet a host of power recovery requirements.

TURBOEXPANDER APPLICATIONS

For many years, turboexpanders have been used in cryogenic processing plants to provide low-temperature refrigeration. Power recovery has been of secondary importance. Expander efficiency determines the amount of refrigeration produced and, in gas process plants, the amount of product usually depends on the available refrigeration. Accordingly, there is a large premium on efficiency and, of course, on reliability.

The main market for turboexpanders has been in low-pressure air separation plants, expanding down from 5 bar, and in hydrocarbon processing plants, expanding natural gas from as high as 200 bar. The air separation expanders are roughly divided into two types. The first type ranges from a few horsepower up to 100 hp. Here, the expander power is too small to be economically recovered and is, therefore, absorbed by an oil brake or similar device. The second type ranges from 100 hp to over 2,000 hp, where the power is used to drive electric generators or process booster compressors.

Hydrocarbon gas expanders range in the order of 100 hp to 8,000 and more hp. The majority of these machines are usually designed for power recovery duty, with a process compressor directly driven by the expander. The gas is usually expanded from an inlet pressure in the 100 bar to 50 bar range, down to outlet pressures in the 50 to 15 bar range. This results in an expansion ratio of 2:1 to 4:1, a very suitable expansion for a single-stage expander. Typical efficiencies range from 84% to 86%.

There are numerous, large turboexpanders operating in the pressure range of 130–200 bar, most of them in well-head natural gas service.

Expanders are also used for the purification of gases, such as H_2 or He, by condensing contaminants. These are usually small units, 5–50 hp, operating at speeds from 45,000–70,000 rpm, and not usually considered economical for power recovery.

POWER RECOVERY TURBOEXPANDERS

As mentioned earlier, the number of power recovery applications is steadily increasing. Large and small demonstration plants are operating, or are about to begin operation. Some of these were built to study or minimize potential problem areas for new, large power plants in the planning stage. Indeed, the potential is for large-scale utilization of such sources as ocean-thermal energy, solar heat, geothermal, waste heat, natural gas, waste gas pressure letdown, and undoubtedly others.

The cycles in these power recovery applications are relatively simple. Figures 1-2 and 1-3 are typical examples. The cycle configurations involve the removal of solids or liquids ahead of the expander, and often the incoming stream is heated so its temperature will not reach its frost point at the discharge. This addition of heat also increases the amount of available power. Some examples of this application are expansion of waste gas, waste products of combustion in oxidation processes, waste carbon dioxide, and expansion of high-pressure synthesis gas streams.

If gases were to be expanded in conventional impulse or axial reaction turbines, care would have to be taken to discharge just above the dew point of the expanded gas. If gas were to enter the turbine at

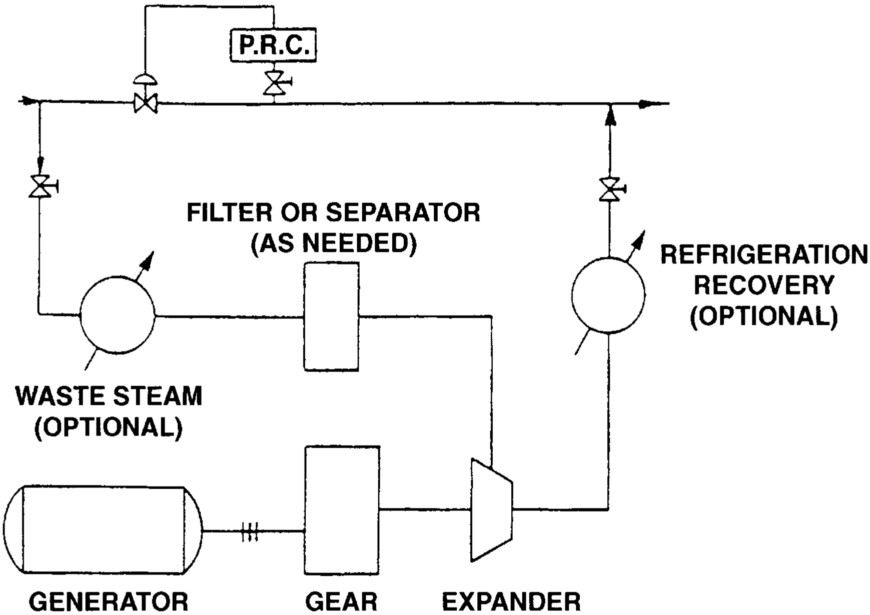

Figure 1-2. Turboexpander in gas pressure letdown service (power recovery cycle).

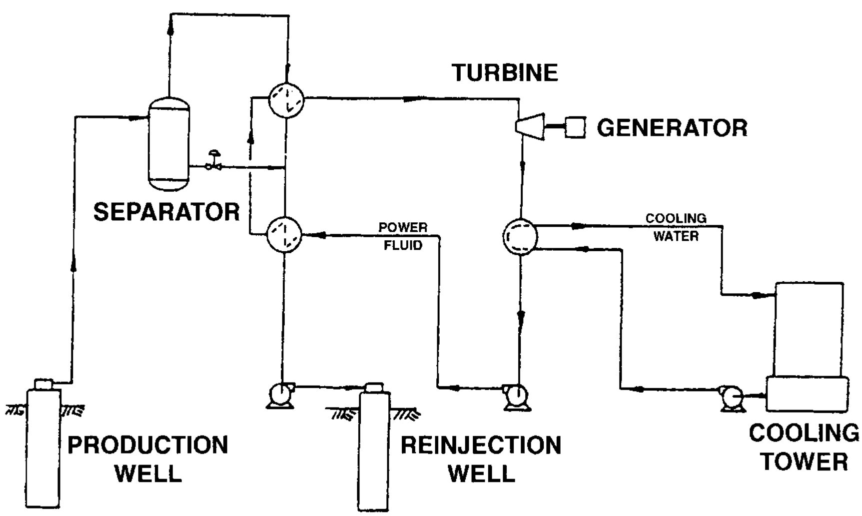

Figure 1-3. Simplified binary geothermal cycle using power expansion turbine.

or near its dew point, the turbine would operate in the condensing range, resulting in two-phase flow in the turbine outlet. This condensate has caused severe erosion problems in ordinary turbines; however, the design of the radial inflow turbine solved these problems, as will be discussed later.

Consider a 1,200 kW power recovery expander-gear-generator designed to be installed in parallel with a natural gas pressure letdown station. The expander shown in Figure 1-2 receives the process gas at 11 bar and 42°C and expands it to 5 bar. In this case, the temperature at the discharge is calculated to be 1°C, and since the gas contained water vapor, it will condense in the expander. This will bring the gas to a suitable dew point, and droplets are removed in a separator downstream of the expander.

Another application for turboexpanders is in power recovery from various heat sources utilizing the Rankine cycle. The heat sources presently being considered for large scale power plants include geothermal and ocean-thermal energy, while small systems are directed at solar heat, waste heat from reactor processes, gas turbine exhaust and many other industrial waste heat sources. Some of these systems are discussed below in greater detail.

There are two general geothermal resources, dry (steam) fields and wet (brine) fields. More than 800 MWe is being produced from such dry geothermal steam fields in Northern California. The wet fields usually cannot be used in this manner and Rankine cycle-type systems, called binary plants, are being considered at such locations. At the wet fields found in the Imperial Valley of Southern California, the geothermal fluid is a 250°C brine, which does not lend itself for use in conventional steam turbines.

In a typical binary cycle (Figure 1-3), power recovery is accomplished by pumping the hot water or brine from underground wells through heat exchanger equipment to boil a working fluid maintained in a closed cycle. The resulting vapor is expanded to drive the turbine-generator and then recondensed and pumped back into the heat exchanger to repeat the cycle. This expansion of the vapor produces saleable power, so efficiency is at a premium. Several working fluids are suitable for binary cycles, and include iso-butane, iso-pentane, propane, and certain hydrocarbon mixtures. For years now, suitable turboexpanders with high efficiency, reliability, and seal systems have been available to meet the various geothermal requirements.

A study of this type of application was aimed at developing the conceptual design for a radial reaction turbine. Conducted by Rotoflow for EPRI (Electric Power Research Institute in Palo Alto, California), the study led to a 65 MWe gross output turboexpander operating at 3,600 rpm and directly coupled to a synchronous generator. The turbine design has a double (back-to-back) rotor, 122 cm in diameter, placed between the bearings with a single inlet port and double discharge ports.

A hydrocarbon mixture was selected as the working fluid and the vapor at the inlet to the turbine was 33.3 bar at 143°C. The vapor was being expanded to 5 bar, at a condenser temperature of 63°C. Since this plant was to be located in the Southern California desert, the condensing was to be done with air; this explains why a high expander discharge temperature had to be selected. Rotoflow made a comprehensive study to determine how the machine would be affected by the large change in ambient temperatures found at this location, which can vary from a high of 50°C in summer to well below freezing in winter. Less drastic, but nevertheless serious, excursions can be experienced from day to night. Although such wide swings may cause extensive condensation in typical turbines, these varying conditions can be efficiently and safely handled in modern turboexpanders.

One of the problems that complicates plant design in wet geothermal fields is the extreme corrosiveness of the brine. The previously described system involved pumping the brine to the plant, and then from the plant into the ground, thus keeping the brine from flashing and causing severe scaling in casings, pipes, and heat exchangers.

To circumvent this problem a pilot plant was constructed by Daedalean Associates in Maryland under the sponsorship of the U.S. Department of Energy (DOE), using direct-contact heat exchangers. The working fluid in this design, in this case iso-pentane, is sprayed in direct contact with the geothermal brine and vaporized. The fluid and water vapor at 66°C are expanded from 3 bar to 1 bar in a 100 kw expander/integral-gear/generator unit. Testing showed that only 1 ppm of the iso-pentane was absorbed in the "boiler" brine.

Much attention is also being given to solar energy. It does not appear that direct solar heat is economically feasible as a large power plant energy source; however, this resource has great potential for a number of process and heating applications.

One form of solar heat does offer interesting possibilities and is referred to as OTEC (Ocean-Thermal Energy Conversion). The OTEC power plant principle uses the solar heat of ocean surface water to vaporize ammonia as a working fluid in a Rankine cycle. After the fluid is expanded in the turbine, it is condensed by the 22°C colder water pumped from the ocean depths. A successful demonstration platform was designed and constructed with funding from several private companies; it has a 50 kW ammonia turbine/gear/generator unit, which expands the ammonia from 7 bar and 21°C, to 6.5 bar at 10°C.

Both the boiler and the condenser were designed for a 5.5°C temperature approach, using the 27°C surface water for heating and 4°C water pumped from 663 m below the surface at a location 2.5 km off the west coast of the big island of Hawaii.

POWER ABSORPTION METHODS

The turboexpanders frequently used in refrigeration processes develop power, but recovery of this power has often been of secondary importance. A number of power absorption methods are directly applicable to energy recovery expanders.

Direct-Connected Compressor

The most popular method of absorbing turboexpander power is by means of a single-stage or two-stage centrifugal compressor, mounted directly on the expander shaft. In a cryogenic process, there is nearly always a place where this compression energy can be used. Adding a compressor load to the system is inexpensive with turboexpander designs where the bearings also support the compressor impeller. On these machines, an impeller, casing, and seal are all that needs to be added.

Gear and Generator

If a plant has no use for a compressor and power is of value, a gear speed reducer and electric generator represent a widely used and reliable method for the recovery of energy. This generator arrangement usually consists of a high-speed gear, couplings, and a generator. Other rotating machinery, such as a pump, may also be used to absorb the energy.

An expander with integral speed reducing gear represents a simplified version of this concept. Here, the pinion gear is on the turboexpander shaft. As shown in Figure 1-4, the pinion gear directly engages the low-speed master gear and reduces the speed of the available power

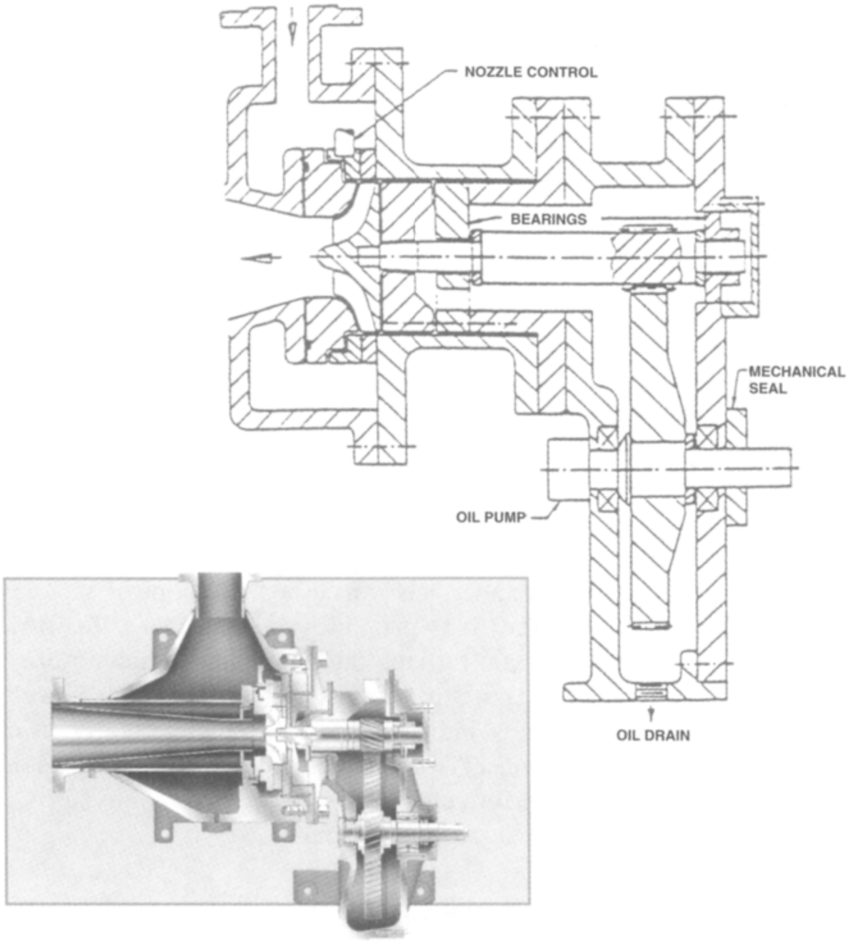

Figure 1-4. Cross-section of an expander with integral gear for power recovery.

to 3,600 or 3,000 rpm, as required. This arrangement has several advantages. It permits easy application of a mechanical seal on the low-speed shaft that hermetically seals the expander gearbox. These integral gear units are designed for pressurization up to 10 bar.

Integrally geared units eliminate the power losses incurred by high-speed pinion gear bearings of an external reduction gear and the windage-related losses of a high-speed coupling. Moreover, alignment issues and noise problems are thus addressed.

TURBOEXPANDER QUALITIES

From the preceding applications and from many hydrocarbon applications, it is apparent that a turboexpander is a special turbine that should be designed with quality features to meet the following requirements:

- Maintain high efficiency with varying flow
- Toleration of dust or condensation of gas stream
- Bearing strength to avoid damage if the rotor should be unbalanced by ice deposits, or damaged by erosion
- High efficiency (usually requiring high speed)
- Proven reliability
- Positive shaft seals or other special seals
- Wide range of sizes

Variable Flow Control

A high-quality turboexpander has variable flow control nozzles capable of withstanding the total pressure and acting as the flow control for the main gas stream through the plant. The variable nozzle should be matched with a rotor to give high efficiency over a wide range of flows. Figure 1-5 is indicative of this range, usually from 50% to 120% of design or wider. They should be designed for negligible blow-by and for durable performance, even if constantly moved by a pressure-controller or other controlling signal.

Expansion of Condensing Streams

To use turboexpanders for condensing streams, the rotor blades must be shaped so that their walls are parallel at every point to the vector resultant of the forces acting on suspended fog droplets (or dust particles). The suspended fog particles are thus unable to drift toward the walls. Walls would otherwise present a point of collection, interfering with performance and eroding the blades. Hundreds of turboexpanders are in successful operation involving condensing liquids.

Dust-laden streams can also cause operational problems. A turboexpander that can efficiently process condensing streams (gas with fog droplets suspended) can usually handle a stream with suspended solid particles, as long as the particle size does not exceed 2–3 μ. The newer designs reduce erosion of expander back rotor seals by disposing of

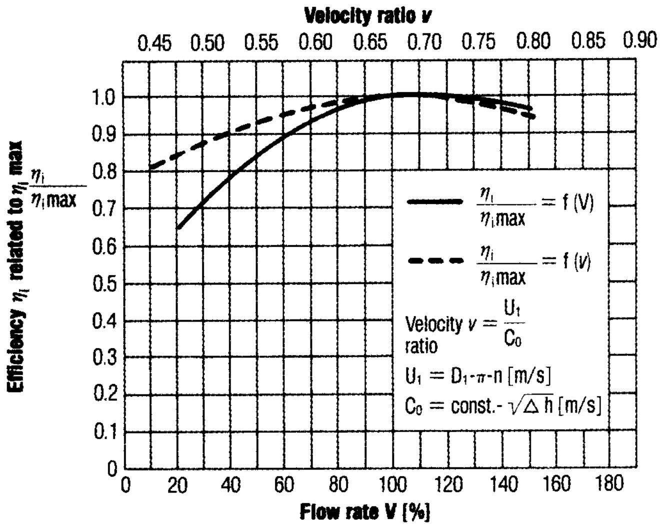

Figure 1-5. The typically flat turboexpander efficiency characteristic with various flowrates is shown here. Efficiency versus the velocity ratio *v* (ratio tip speed to spouting velocity) is also shown. *(Source: Atlas Copco.)*

the dust that accumulates at the seal and discharging it through the balance holes in the expander rotor. Large expanders can be designed to handle dust or particles up to 10 μ.

Thrust Bearing Force Meters

Machines with an expander inlet pressure on the order of 10 bar carry thrust loads usually within the capabilities of the thrust bearings. At higher pressures it is essential to carefully balance the thrust loads against each other. Thrust loads, even though originally correctly balanced, may change greatly and exceed the thrust bearing load-carrying capacity. This imbalance of thrust loads may be caused by either erosion of a seal, icing, or off-design operating conditions. This problem has been solved by a force measuring meter on each thrust bearing, and in some cases, a thrust control valve that controls the thrust by control of pressure behind the thrust-balancing drum (Figure 1-6).

Because of features such as these, the reliability of turboexpanders is exceptionally good. Operation for several years without repair is not uncommon.

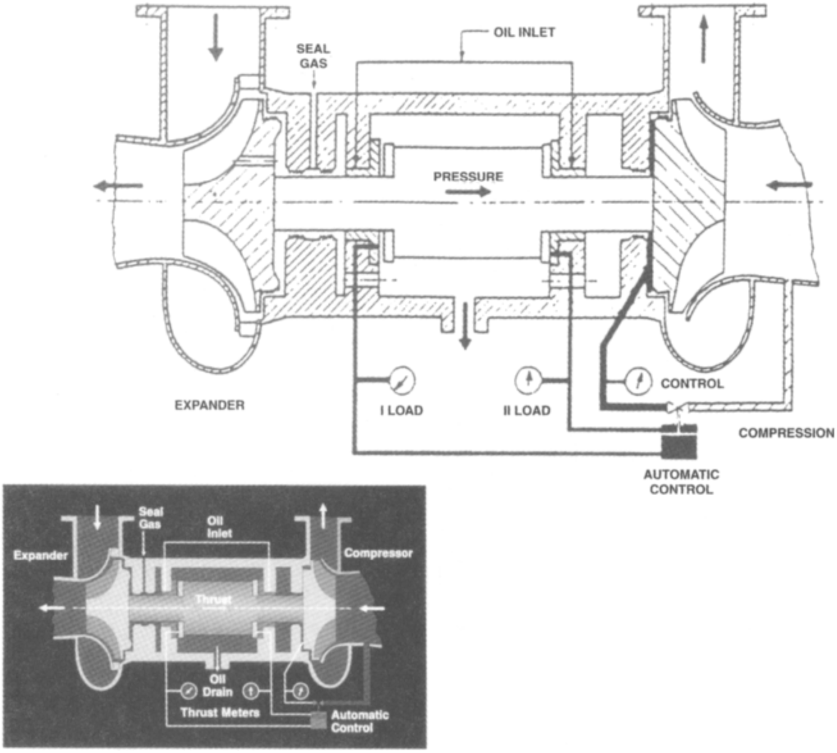

Figure 1-6. Rotor thrust and metering schematic.

Shaft Seals and Bearings

Virtually all cryogenic turboexpander seals are either of the close-fitting labyrinth or noncontacting (dry) gas seal type (Figure 1-7). Conventional mechanical seals are not generally used; high velocities prohibit the use of contacting-face seals in these machines. However, the generally lower speed, hot gas turboexpanders often employ modified mechanical contact seals (Figure 1-8).

With close-clearance seals it is important that the shaft be closely maintained in its rotating position; flexible shaft design (operation above the first lateral critical) is usually not acceptable. Bearings that maintain the closest alignment of the shaft are obviously the best for such applications and, for this purpose, close-clearance journal-type bearings are used.

Adjustable seals employ a tapered shaft-conical labyrinth seal design. Seal clearance can be maintained by adjusting the axial position of the seal, a procedure not possible with other types of seals.

Buffered labyrinth seals permit injection of buffer gas between the labyrinths for maximum process gas containment without oil contamination.

Carbon ring seals can be used in moderate pressure applications. They permit less leakage than a labyrinth seal design and they can be operated dry, buffered with gas, or buffered with liquid.

Oil bushing seals are used to seal in hazardous and/or toxic gases when a buffer-gas source is not available. Oil is injected into the seal to isolate process gas from the lubrication system and atmosphere. Excess oil-gas mixture drains into a trap which returns the gases to the process gas stream and the oil to an atmospheric reservoir.

Dynamic dry gas seals minimize leakage. They eliminate the need for an oil-film seal and expensive seal support systems. The dry gas seal can be applied in single, double or triple configurations. It is recommended when leakage can be hazardous and/or costly.

Drainer seals mix seal gas and a small amount of bearing oil in a cavity behind the labyrinth seals. The oil/gas mixture is separated in a drainer to minimize dilution and eliminate the need for external oil degassing tanks. Seal gas is vented from the top of the drainer and can be recovered in a recovery system. Oil is returned to the lubrication system.

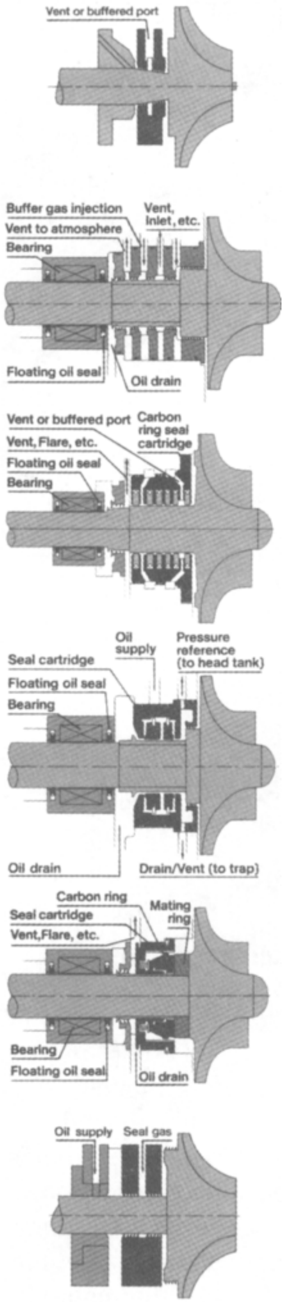

Figure 1-7. Seal configurations exployed in modern turboexpanders. *(Source: Atlas Copco.)*

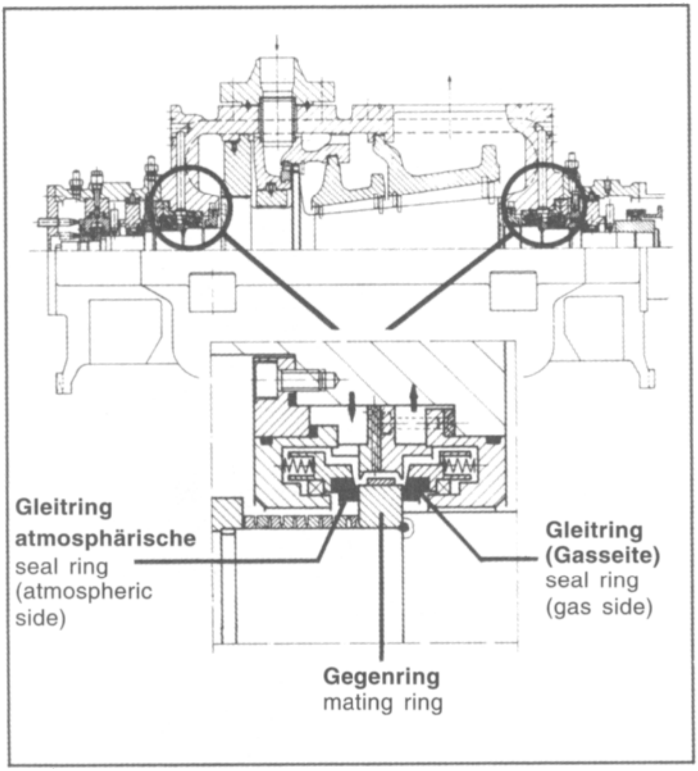

Figure 1-8. Special mechanical seals (contact seals) used in hot gas turboexpanders. *(Source: GHH-Borsig.)*

Size-Related Problems

Turboexpanders currently in operation range in size from about 1 hp to above 10,000 hp. In the small sizes, the problems are miniaturization, Reynolds Number effects, heat transfer, seal, and mechanical problems, and often include bearing and critical speed concerns. In intermediate sizes, these problems become less significant, but bearing rubbing speeds and vibration become increasingly important.

Vibration becomes critical in the intermediate ranges because structural members are relatively less massive and the speeds are high enough to match the resulting natural frequencies in some cases. Thorough testing of rotors is essential, and extensive work has been done in this area.

In intermediate and larger sizes the thrust bearing problem requires more attention, but it has been effectively solved recently by the introduction of the thrust force meter and thrust force adjustment valve, described earlier.

SUMMARY

Presently, designs for radial inflow turboexpanders in sizes up to 70 MW are available for use in geothermal power plants. Following are some of the most important features that make turboexpanders ideal for the recovery of power from the vast available resources of pressurized gas streams.

- Mechanical designs of low-temperature, high-speed machinery are routine.
- Stiff shaft designs have eliminated shaft and bearing criticals in the entire operating range.
- Rotor resonance problems are well known to the designers and are, in most cases, totally eliminated.
- Thrust bearings, often the most problematic component in high-speed machinery, can be accurately monitored and controlled.
- Condensing streams and some dust in gas can be handled without erosion.

Turboexpanders can be used for energy recovery and, in some instances, their application avoids losses in the form of cooling. In other instances, these machines recover energy from waste heat or from pressurized gas streams that would otherwise have to undergo pressure reduction in mechanical letdown valves.

In practical terms, the application of expansion turbines depends on the relationship between the possible gain of mechanical energy and the required investment cost. Typical commercial applications for turboexpanders include:

- Chemical and petrochemical industries
  —FCC
  —Nitric acid
  —Acetic acid
  —Terephthalic acid, or PTA (see Figure 1-9)
- Natural gas and oil industry

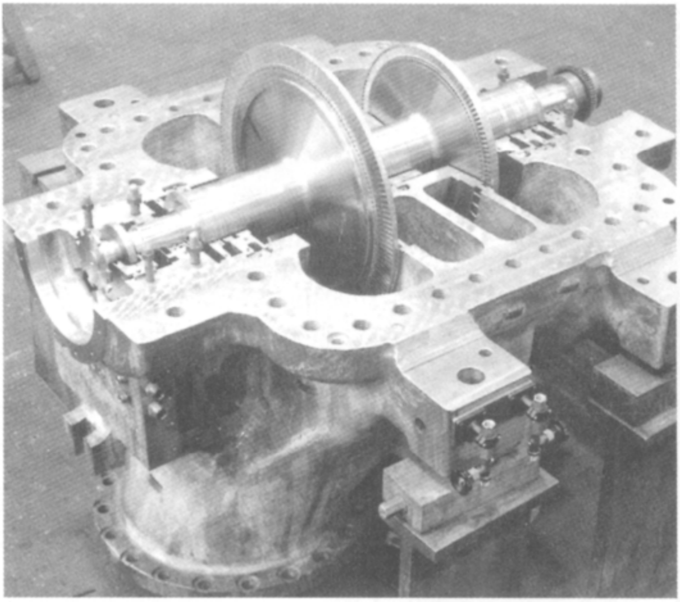

Medium:
reactor Off-Gas
Inlet pressure:
21 bar/7.7 bar
(304,5/11,7 psia)
Temperature:
170°C/150°C
(338/302°F)
Outlet pressure:
1,3 bar
(18,9 psia)
Output:
4,560 kw
(6,115 hp)
Speed:
7,330 rpm

Figure 1-9. Two-stage process gas expansion turbine for a terephtalic acid plant. *(Source: GHH-Borsig.)*

—Pipeline pressure reduction
—LNG, LPG (see Figure 1-10)
—Liquefaction of methane
- Coal gasification and hydration
- General industrial power recovery
- Mine cooling

On the one hand, expansion turbines operate directly in the gas flow with the purpose of efficiently using pressure gradients. On the other hand, these machines operate in the more indirect way in a thermodynamic cycle. A good example is, of course, the Rankine cycle, which generally consists of an evaporator, an expansion turbine, condenser, and pump. Turboexpanders simply take advantage of the temperature gradients existing in this cycle.

Gas expansion turbines may embody different designs depending on the process media and associated systems. Special requirements may pertain to duties such as sealing off toxic, flammable, caustic, corrosive, erosive, and high-temperature media. These requirements may lead to sealing geometries that are common to turbines and turbocompressors.

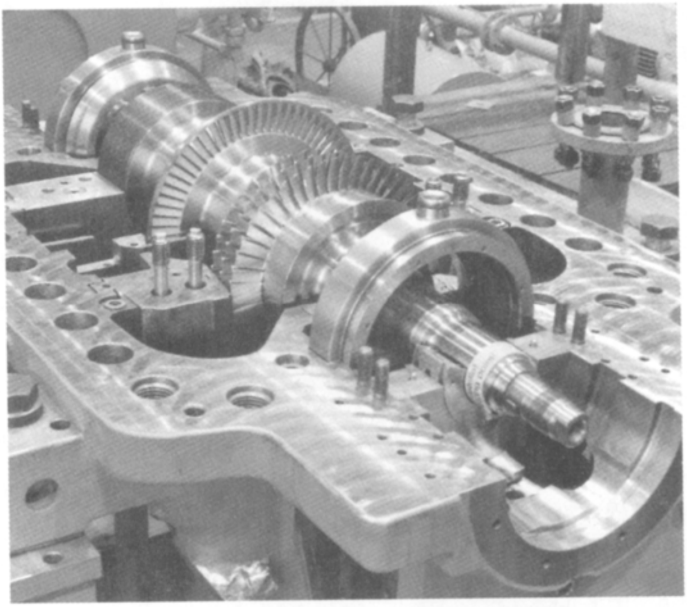

Inlet pressure:
40 bar a
(575 psia)
Temperature:
95°C (203°F)
Back pressure:
9 bar a
(129 psia)
Output:
4,180 kw
(5,605 hp)
Speed:
12,890 rpm

Figure 1-10. Multistage turboexpander in natural gas letdown service. *(Source: GHH-Borsig.)*

Expander design requires precise knowledge of thermodynamics gas properties. Pertinent calculation methods involving real gas equations of state are common practice to compressor as well as expander technology. However, the control systems governing or tracking gas expansion on turboexpanders need to be individually adapted to project requirements to ensure safe and reliable operation under design and off-design conditions.

BIBLIOGRAPHY AND ADDITIONAL READING

1. Holm, J., 1969. "The application of turboexpanders for energy conservation," ASME Paper 69 VIBR-58.
2. Swearingen, J. S., 1971. AIChE Annual Institute Lecture.
3. 8,000 hp Natural Gas Expander-Compressor, installed at Petro-Canada Exploration, Inc., Empress Plant at Empress, Alberta. Canada.
4. *Chemical Engineering* 75, No. 11, p. 146, May 21, 1968.
5. *Stodola: Steam and Gas Turbines,* Peter Smith Publishers, p. 312 (Steam Quality).

6. Diagram from paper by The Ben Holt Co. "Advanced Binary Cycles for Geothermal Power Generation."
7. EPRI Contract No. RP928-3.
8. Daedaleon Associates, Springland Research Center, Woodbine, Maryland.
9. Lockheed Missiles and Space Co., Sunnyvale, California, Subcontract YF80C1230A.
10. Swearingen, J. S., 1966. U.S. Patent 3,232,581 (February).
11. Swearingen, J. S., 1970. U.S. Patent 3,495,921 (February).
12. Swearingen, J. S., 1971. U.S. Patent 3,610,775 (October).
13. Swearingen, J. S., 1971. Japanese Patent 617,904 (September).
14. Swearingen, J. S., 1974. U.S. Patent 3,828,610 (February).
15. Swearingen, J. S. and Mafi, S., 1969. "Experimental Investigation of Vibrations in High Speed Rotating Machinery," ASME Paper No. 69 VIBR-58.

CHAPTER TWO

Turboexpander Fundamentals

The following provides a more detailed review of turboexpander theory, including basic gas flow as is applicable to industry applications. As was mentioned in Chapter 1, industrial low temperature (cryogenic) operations have dramatically increased in capacity and variety over the past several decades. Their important applications include separation of air, recovery of ethane and propane from natural gas, liquefaction of natural gas and other gases, gas purification, and power recovery. This rapidly growing trend has attracted a good deal of interest, and the modern turboexpander is an important contributor to the development of industrial low-temperature operations.

BASIC APPLICATIONS

A turboexpander generates the deep, low-temperature refrigeration industrially used for gas separation and liquefaction, and a number of related purposes. It does so by the mechanism of constant entropy expansion, together with the production of power (a byproduct). The power is generated from the decrease in enthalpy of the stream itself. A turboexpander is a high efficiency turbine with numerous special features. These features make it conveniently usable and reliable for small volumetric flows at the low temperatures (and often rather high pressures) usually found in these applications.

Turboexpanders have been used in air separation processes since the mid-1950s. The early designs were small and the mechanical problems encountered were mainly related to miniaturization and the unavailability of good bearings for the high speeds. The rotors were only a few inches in diameter and speeds were in the range of 20,000–50,000 rpm. Higher efficiency, lower maintenance, and reduced size were the expected benefits beyond those attainable from precursor equipment, such as reciprocating expanders.

Reciprocating expansion engines have been used since the early twentieth century and are still used to some extent, especially for volumetric flows below 10 ft^3/min. Reciprocating machines often suffer from high maintenance, excessive size, valve problems, and the fact that liquid will damage the valves. For these reasons they have largely been replaced by turboexpanders, even down to sizes around 1 hp.

The success of expanders was predicted in the 1940s. More recently, processes similar to those used in air separation have been applied in other fields. These new applications have progressed as a result of the parallel development of new processes and improved heavy-duty turboexpanders.

Moreover, there have been improvements in the economics of the processes themselves. The following review of turbine technology recaps the evolution of the turboexpander.

There are three general types of turbines. One is the common impulse turbine shown in Figure 2-1. In it, all of the pressure energy is converted to velocity in the nozzle. The resulting high-velocity stream impinges on U-shaped blades in the rotor. The rotor blades move at half the velocity of the gas jet, and the gas exiting the rotor blades is directed backward with respect to the rotor. In this design the gas leaves without significant residual absolute rotational velocity. Approximately 8% of the available energy is lost in making the U-turn between the rotor blades.

The reaction turbine, shown schematically in Figure 2-2, is generally more efficient. In its primary (stationary) nozzles only half the pressure energy of the gas stream is converted to velocity. The rotor with a blade speed matching the full-jetted stream velocity receives this jetted gas stream. In the rotor blades the other half of the pressure energy is used to jet the gas backward out of the rotor and, hence, to exhaust. Because half the pressure drop is taken across the rotor, a seat must be created around the periphery of the rotor to contain this pressure. Also, the pressure difference across the rotor acts on the full rotor area and creates a large thrust load on the shaft.

A further improvement in turbine design led to the radial reaction type seen in Figure 2-3. Compared to the pure reaction type, the radial reaction machine has a reduced discharge diameter. In this design the gas, again half expanded in the primary nozzles and jetted tangentially into the rotor, matches the peripheral speed of the rotor and flows radially inward within the rotor, leaving it at a lesser diameter. This arrangement reduces the velocity required from the secondary (rotor)

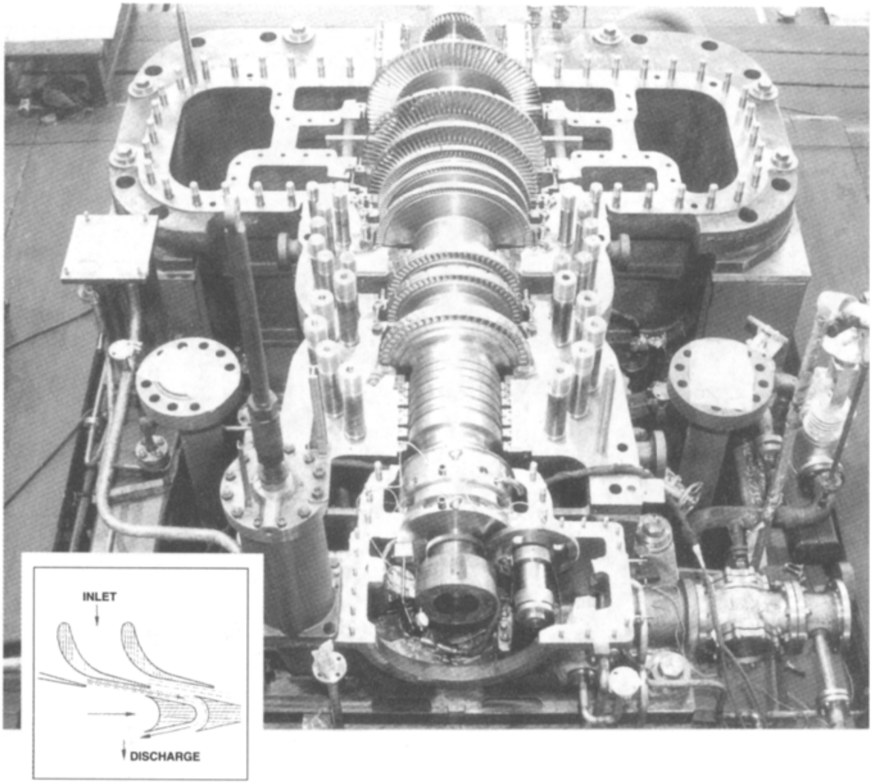

Figure 2-1. Steam turbine using impulse blading. *(Source: Mitsubishi Heavy Industries.)*

nozzles with correspondingly lower nozzle friction loss. It also reduces the diameter of the rotor seal, which reduces both the seal leakage and the shaft thrust load.

The radial reaction turbine is the most efficient of the three available types. Although used in large water turbines, it is not used in large steam turbines because of their large volumetric flow, and because adapting it to multistaged configurations is rather cumbersome. However, the radial reaction design is well suited to turboexpanders for the above reasons, as well as other reasons that merit brief explanation.

GAS PATH EQUATIONS AND ANALYSIS

Successful commercial expander processes depend on the design and production of suitable high-speed turbine rotors and nozzles capable

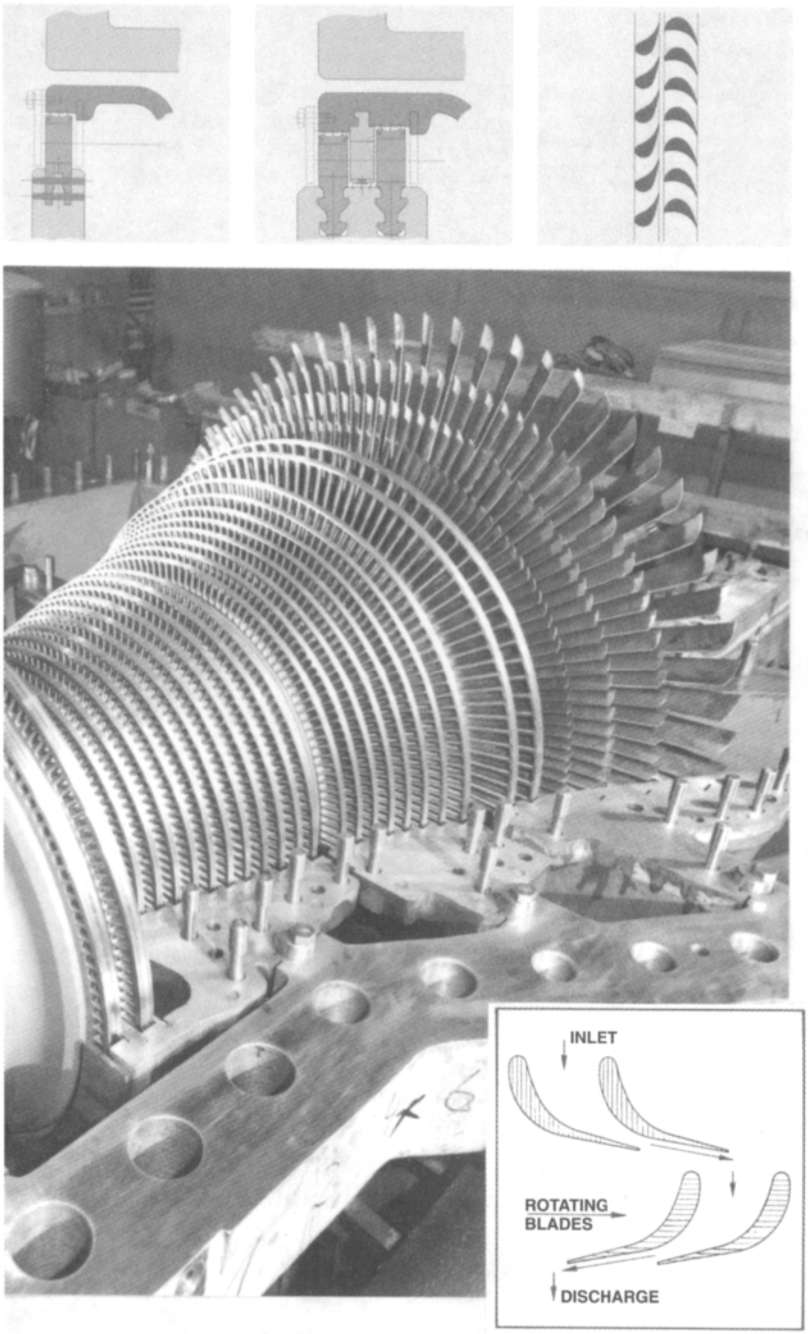

Figure 2-2. Steam turbine using reaction blading. *(Source: GHH-Borsig.)*

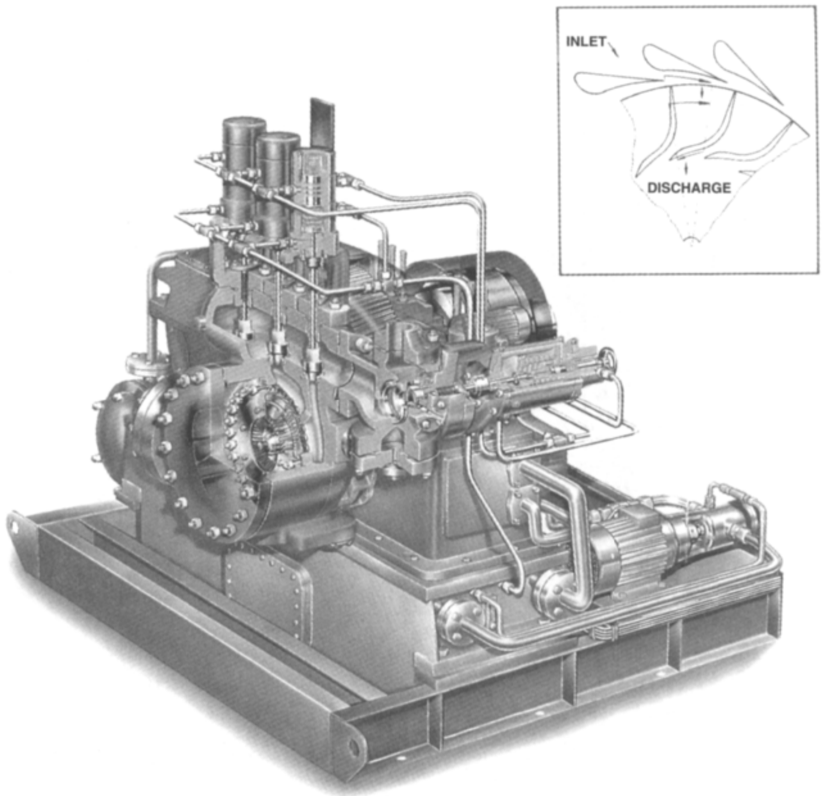

Figure 2-3. Radial reaction turbine. *(Source: Kuehnle, Kipp, and Kausch.)*

of reliable operation under extreme conditions of low temperature and a wide range of pressures. A unique combination of thermodynamics, mechanics of fluid flow, and physics of rotational equipment were addressed in the development of both the equipment and its application to processes. Two widely used processes are of interest here.

Figure 2-4 shows a low temperature (–300°F) application of a turboexpander in the separation of air in a simplified cycle. The air is cooled in a heat exchanger down to near its liquefaction point, and then some further heat is removed by the turboexpander while a portion of the stream is condensed. By visualizing a heat envelope around the process it can be seen that virtually all the energy decrease

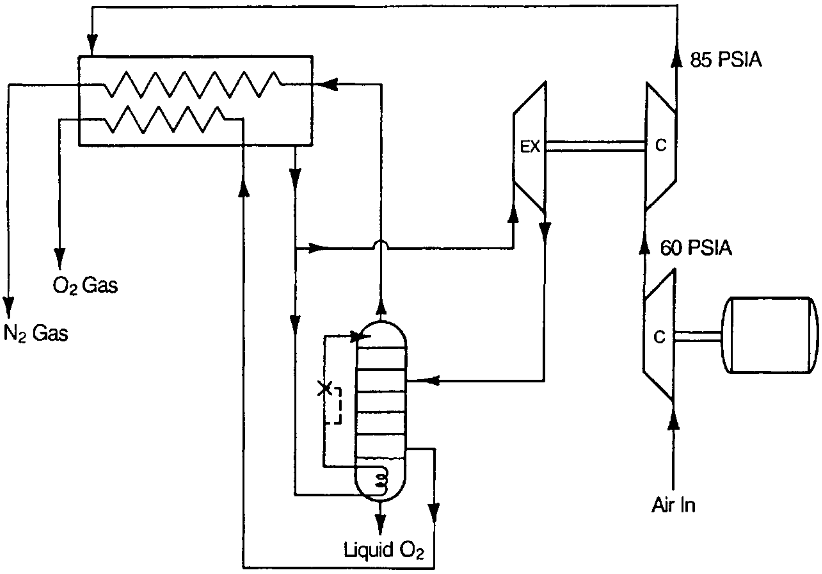

Figure 2-4. A low temperature application of a turboexpander in the separation of air.

in the turboexpander is make-up for the temperature difference at the warm end of the heat exchanger plus the heat leak (if no cold or liquid product is removed). Air separation can be performed by charging the process with air at 70–85 psia.

Older processes used Joule-Thomson cooling entirely. The Joule-Thomson effect is defined as the cooling that occurs when a highly compressed gas is allowed to expand in such a way that no external work is done. This cooling is inversely proportional to the square of the absolute temperature. The system worked satisfactorily, but it required much higher pressures to remove the same amount of energy.

Figure 2-5 shows another application for turboexpanders, one that requires –100 or –150°F for the separation of propane and heavier hydrocarbons from a natural gas stream. The product is almost always recovered as a liquid, which introduces a large additional refrigeration load. The residue gas discharge pressure usually must be maintained as high as possible, so efficiency is important.

This cycle illustrates several desirable features of a low-temperature process. First, the expander should be applied at the lowest temperature level in the cycle because this is where it is the most thermodynamically effective, that is, it has the best Carnot or Second Law

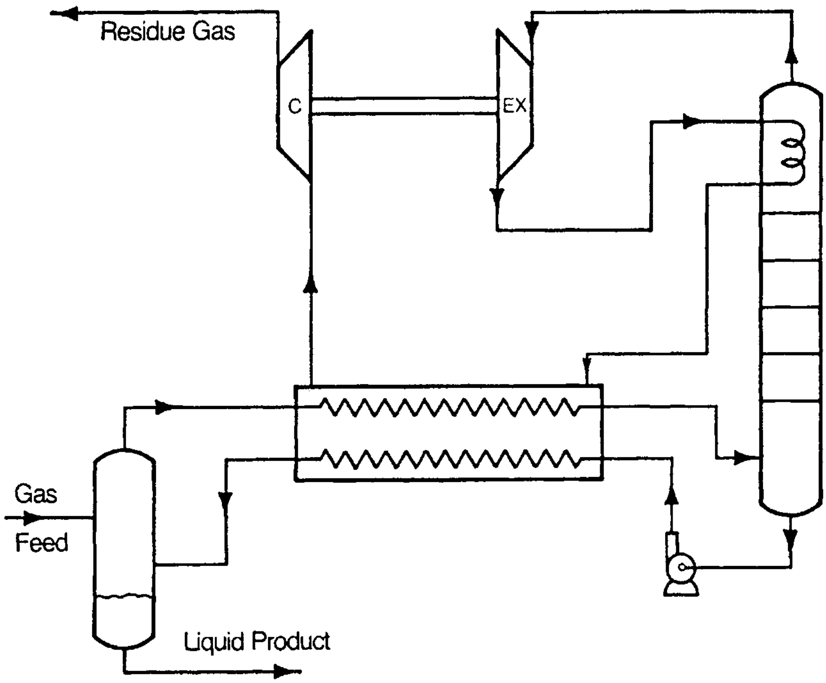

Figure 2-5. Turboexpander applied to the separation of propane and heavier hydrocarbons from a natural gas stream.

efficiency. Second, the temperature difference in the heat exchanger should be reasonably low. A third favorable feature is its conservation of refrigeration.

Refrigeration conservation is illustrated by the handling of the raw liquid accumulating at the bottom of the tower. These conditions yield substantial quantities of dissolved, undesirable light constituents, and are at least partially vaporized in the heat exchanger as the crude liquid stream is counter-currently warmed by the raw gas. The latent heat absorbed by this boiling stream offsets the heat liberated when part of the light constituents unavoidably dissolves in the raw liquid as it condenses out of the feed stream in the high-pressure side of the heat exchanger. This practice of refrigeration economy is of greater importance than is sometimes appreciated.

The success of these two processes, one requiring refrigeration at –300°F, and the other at –125°F, poses the questions: What are the preferred applications for turboexpanders? Why not use them in air conditioners or other commonly used refrigeration systems?

Looking at this low temperature refrigeration as to power requirement, one expander horsepower removes its heat equivalent to 2,545 Btu/hr, as compared with 12,000 Btu/hr, about 4.7 times as much. This is referred to as a "ton" of refrigeration. Thus, the turboexpander must develop 4.7 hp to generate a ton of refrigeration; however, it delivers 4.7 hp back as power.

Refrigeration represents work according to the Second Law. The arrangement of a turboexpander system functioning as a refrigeration machine is shown in Figure 2-6. It usually consists of a conventional compressor with inter- and aftercoolers rejecting heat to ambient temperature, a heat exchanger, and turboexpander, the power from which helps drive the compressor.

In Figure 2-6 consider the compressor and aftercooler as an isothermal compressor operating at T_2 with an efficiency E_e. Assume negligible pressure drop and temperature difference in the heat exchanger (normally only a few degrees), and assume the working fluid to be a perfect gas. Further, consider the removal of a quantity of heat Q_e at an average low temperature T_1 by the turboexpander. This requires that it deliver shaft work equal to Q_e.

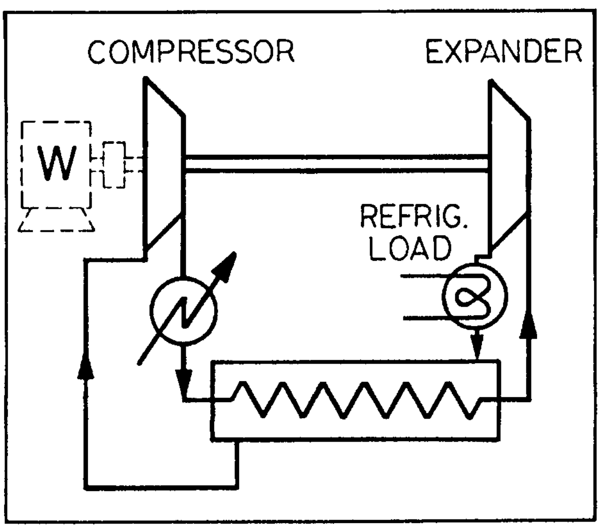

Figure 2-6. Turboexpander system functioning as a refrigeration machine.

If the expander efficiency is η_e across the expander, the ideal work would be

$$\Delta H_e = \frac{Q_e}{\eta_e} \tag{2-1}$$

The theoretical (isothermal) compression work in the compressor is

$$\frac{Q_e}{\eta_e} \bullet \frac{T_2}{T_1} \tag{2-2}$$

The actual compressor work W_e, is this latter quantity divided by compressor isothermal efficiency η_c; thus,

$$W_e = \frac{Q_e}{\eta_e \eta_c} \bullet \frac{T_2}{T_1} \tag{2-3}$$

Mechanical work equal to Q_e is returned to the compressor, so the net work to the compressor is,

$$W = W_e - Q_e = Q_e\left(\frac{T_2}{\eta_e \eta_c T_1} - 1\right) = Q_e \frac{T_2 - \eta_e \eta_c T_1}{\eta_e \eta_c T_1} \tag{2-4}$$

The Second Law theoretical work is,

$$W_{theor.} = Q_e \frac{T_2 - T_1}{T_1} \tag{2-5}$$

Hence, the Second Law efficiency is,

$$\begin{aligned} \frac{W_{theor.}}{W} &= \frac{(T_2 - T_1)\eta_e \eta_c}{T_2 - \eta_e \eta_c T_1} = \frac{\eta_e \eta_c T_2 - \eta_e \eta_c T_1}{T_2 - \eta_e \eta_c T_1} \\ &= \frac{T_2 - \eta_e \eta_c T_1 + (\eta_e \eta_c - 1)T_2}{T_2 - \eta_e \eta_c T_1} \\ &= 1 - \frac{T_2(1 - \eta_e \eta_c)}{T_2 - \eta_e \eta_c T_1} \end{aligned} \tag{2-6}$$

A plot of this efficiency, assuming commonly available equipment, is shown by the expander curve in Figure 2-7. (For a more detailed treatment of efficiency and equipment sizing, refer to the Appendix). The family of curves shows the power efficiency of conventional refrigeration systems. The curves for the latter are from published handbook data and refer to the evaporator temperature as the point at which refrigeration is removed. If the refrigeration is used to cool a stream over a temperature interval, then the efficiency is obviously somewhat less. These curves illustrate several refrigeration temperature intervals. Comparing these curves to the expander curve shows that the refrigeration power requirement by expansion compares favorably with mechanical refrigeration below –50 or –100°F. The expander efficiency is favored by lower temperature at which heat is to be removed.

It can also be concluded from Figure 2-7 that if the process can justify the complexity, it is better to use conventional means rather than expanders to absorb heat at moderate temperatures in the range of ambient to –50°F, although frequently, for expediency, expanders

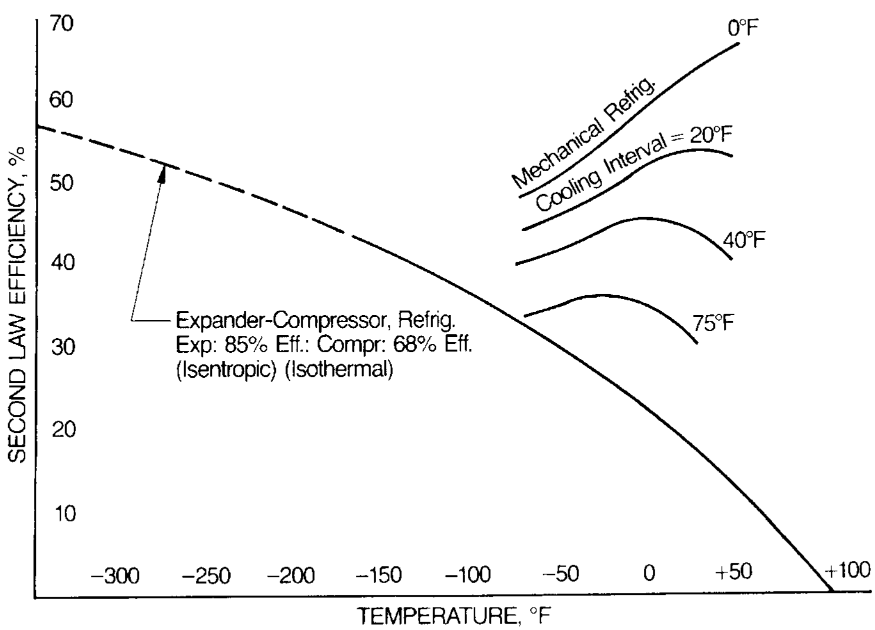

Figure 2-7. Mechanical versus turboexpander refrigeration.

are used anyway. This use of refrigerant for lower grade refrigeration is illustrated in a recently developed cycle for the recovery of propane and heavier fractions from natural gas. The LPG recovery process in Figure 2-8 is similar to that shown in Figure 2-5. For ease of comparison the two flow diagrams have been made as similar as possible.

This new process differs from the older process in one important respect: the flash gas off the raw cold liquid in the new cycle is recompressed and cooled in an aftercooler to cause partial condensation. This liquid is returned to the heat exchanger to accomplish the moderate temperature refrigeration. With this done, the expander needs to be concerned only with the lower temperature refrigeration duty, which has another important advantage. The recirculation of this refrigerant, which is largely propane, produces a low-pressure vapor phase over the product liquid. In turn, this serves to shield the liquid so that only negligible amounts of methane and ethane dissolve in it.

This new process provides a refrigeration system within the cycle itself for accomplishing the moderate temperature refrigeration, which otherwise would have to come from the expander at greater power

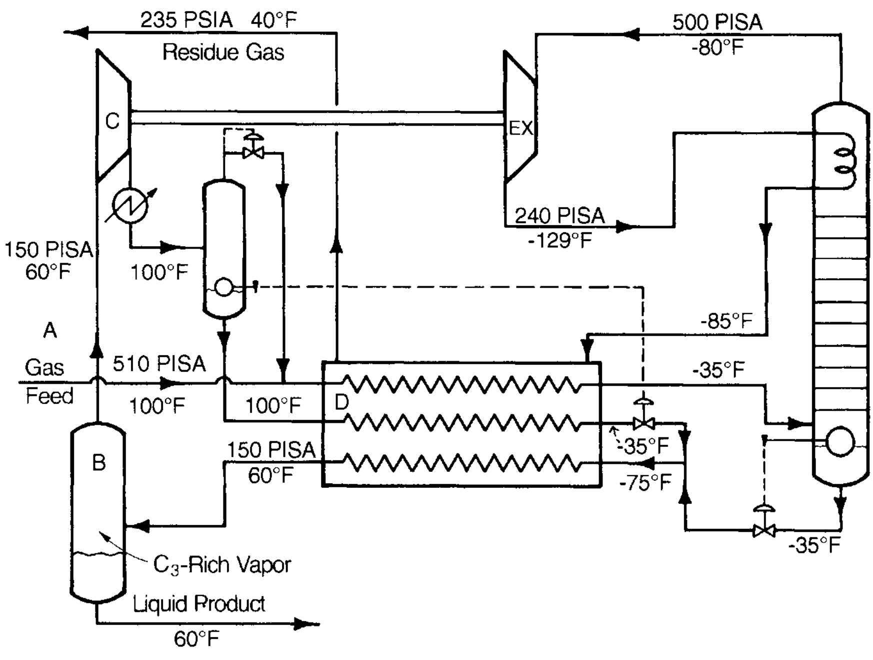

Figure 2-8. LPG recovery process.

expenditure. Also, it produces a product liquid which is not "wild," meaning that it has a low content of the more volatile gases.

SPECIFIC CRYOGENIC APPLICATIONS

The largest number of turboexpanders are applied in low-pressure air separation plants, expanding from 75 or 150 psi (517 or 1,034 kN/m^2) However, the greatest part of the total applied horsepower goes into hydrocarbon processes.

When a larger amount of refrigeration per pound of air (or other expanding gas) is required, the gas is expanded through a wider expansion ratio. Turboexpander efficiency deteriorates when the expansion ratio per stage becomes high, such as 10:1 or higher. However, two-stage turboexpanders have been made for as high as 35:1 (700 to 20 psia, or 4,830 to 140 kN/m^2), attaining above 80% efficiency.

A few separation plants have reciprocating expanders for 2,000 to 3,000 psi (13,800–20,700 kN/m^2) inlet pressure. The incoming pressurized gas is about –40°F (–40°C) and is not clean enough to operate satisfactorily in small turboexpanders. However, several turboexpanders have been put into air service during the last decades at 1,500 psia (10,300 kN/m^2) for liquid production.

There are numerous large turboexpanders operating in the pressure range of 2,000–3,000 psi. Most are for wellhead natural gas, but a few applications are for power recovery.

Hydrogen and helium liquefaction takes place at a much lower temperature than air liquefaction. To attain this low temperature and in part to circumvent heat exchanger constraints, it is more practical to cascade the expanders. In cascading setups, one turboexpander produces refrigeration at a higher level than the other. This arrangement not only improves the temperature approach in the heat exchangers, but can be integrated with the purification process where methane, nitrogen, or other contaminants are removed.

Expanders can also be used for the purification of gases by freezing out contaminants. This can be accomplished by switching exchangers as in Frankl heat accumulators used in air separation plants. In this case, the cold waste nitrogen dries out the switched exchanger. It can be done more efficiently and with less pressure reduction in switching heat exchangers . Figure 2-9 shows an expansion-type drying or vapor recovery cycle where the desired product or impurity is frozen out of the stream. The advantages of this cycle are low pressure loss and

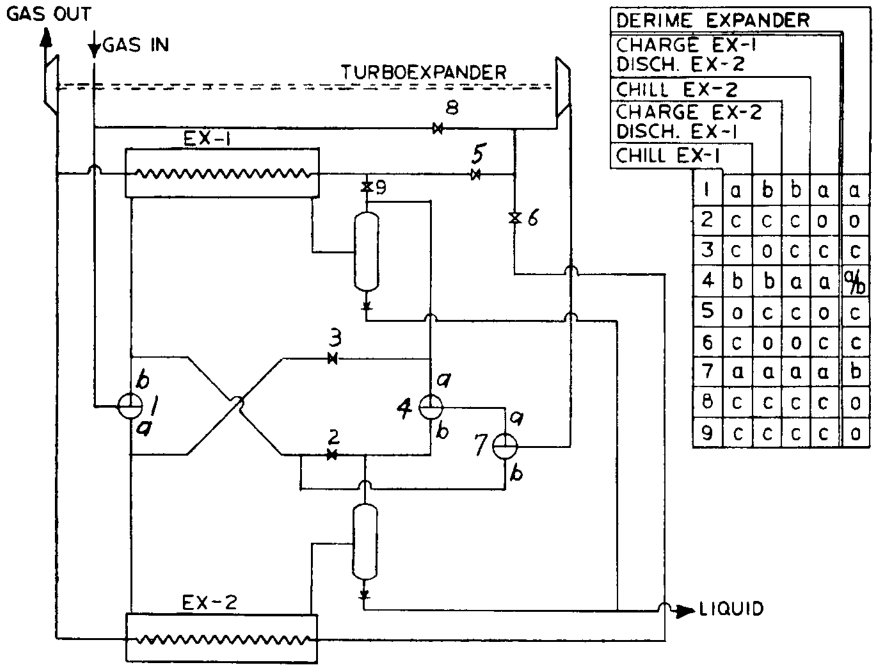

Figure 2-9. Expansion-type vapor recovery system.

complete drying; there is no bypassing when the heat exchangers shift. In this cycle one of the heat exchangers is warmed sufficiently to melt the frozen contaminant and collect it while the second exchanger is fully purifying the gas. Little refrigeration is lost warming and cooling the heat exchanger because it is done by the switched streams. The latent heat and the small temperature difference necessary to make the process operate are removed by the turboexpander.

Numerous applications where the recovery of power is important are being explored and exploited to an increasing degree. These are classified as turboexpander applications because of the importance of reliability and high efficiency. Turboexpanders meet these requirements and are available in the needed capacity ranges. A 5,000 hp (3,727 kW) compressor-loaded turboexpander is shown in Figure 2-10.

The cycles in these power recovery applications are relatively simple. They involve the removal of solids or liquids ahead of the expander, and often the incoming stream is heated so its temperature will not reach its frost point at the expander discharge. This heating also increases the amount of available power. Some examples of this

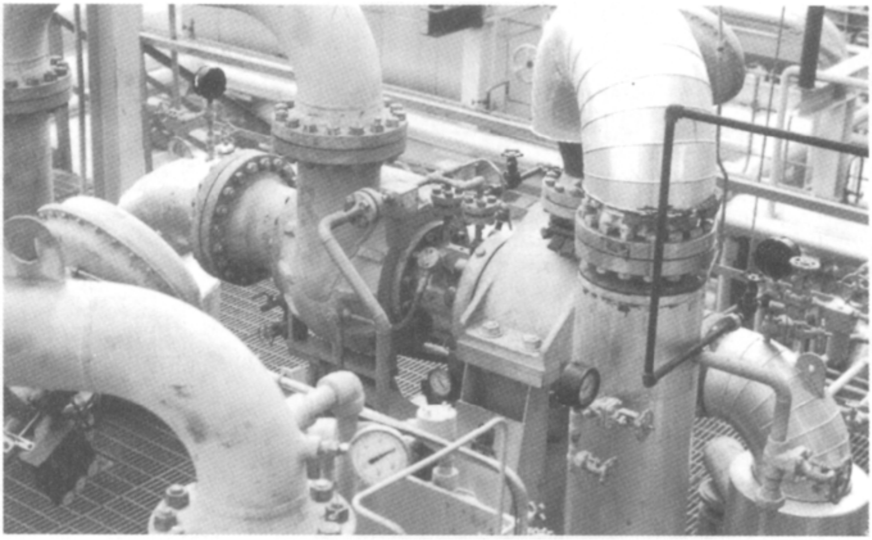

Figure 2-10. Atlas Copco expander, rated at 3,731 kW (5,000 hp), used for pressure letdown at a plant in Salionze, Italy.

application are expansion of waste gas, waste products of combustion in oxidation processes, waste carbon dioxide, and expansion of high-pressure synthetic gas streams.

There is a Second Law thermodynamic advantage in operating an expander at as low a temperature as possible. In most applications it has been arranged to discharge just above the dew point of the expanded gas. If the cold compressed gas could enter the expander at or near its dew point, the expander would then operate condensing and at the lowest possible temperature. Such condensate has traditionally been troublesome in turbines, but this has been solved in modern turboexpanders.

When large amounts of low-temperature refrigeration are required, efficiency becomes more important than expediency. It is desirable to take advantage of the lowest possible expansion temperature. This leads to expansion from an inlet pressure above the critical pressure and near the critical temperature, and often results in a high percentage of liquid in the expander. By optimizing the isentropic expansion range, the cycle efficiency is good, especially if the expander power can be usefully and economically recovered. This places rigorous requirements on the turboexpander including operating in the condensing mode, as discussed further below. Such plants are already in successful operation and many more will surely follow.

FUTURE APPLICATIONS

Due to the greater variety of expanders and their advanced quality and capabilities, many future uses are possible.

One application is the expansion of liquids or flashing liquids. Although this does not seem to be a very large power application, but all of the power removed from a cryogenic process reduces the amount of heat introduced into the process by turbulence.

A stream of 100 gpm (379 l/min) liquid expanding from 1,000 psi (6,900 kN/m^2) to 100 psi (690 kN/m^2) if it does not flash will develop approximately 40 hp (29.9 kW). Flashing usually more than doubles the power. Although this is only a small fraction of the total required refrigeration, it is near the coldest point in the system and is valuable. A hundred hp is the equivalent to a quarter of a million Btu per hour (73.3 kW) of heat. This would vaporize 2,900 lb (1,315 kg) per hour of liquid nitrogen at an absolute pressure of 20 psi (138 kN/m^2).

When these liquid or flashing liquid turboexpanders are installed, the operators are often surprised at the improved process efficiency.

Another application for turboexpanders is in power recovery from geothermal heat. This is accomplished by using the hot water from underground hot water wells (250°C) to boil a working fluid maintained in a closed cycle. The resulting fluid vapor is expanded to recover the power and then recondensed and pumped back into the heat exchanger to repeat the cycle. This expansion of the vapor produces saleable power, so efficiency is at a premium. Suitable turboexpanders are available and operating at high efficiency. Moreover, they exhibit high reliability of all mechanical components.

Finally, there are an increasing number of streams of pressurized industrial gases containing contaminants, such as corrosive or polymerizing liquid mist, tar, and the like, on which the pressure is being released, and the quantities of available power are significant.

STATISTICAL ASPECTS OF TURBOEXPANDER REQUIREMENTS

Figure 2-11 illustrates the potential severity of three problems that tend to correlate turboexpander inlet pressure: thrust bearings, erosion of rotor and nozzles, and radial bearings.

In a radial turbine there are enormous centrifugal forces acting radially outward on the stream within the rotor. If this stream contains

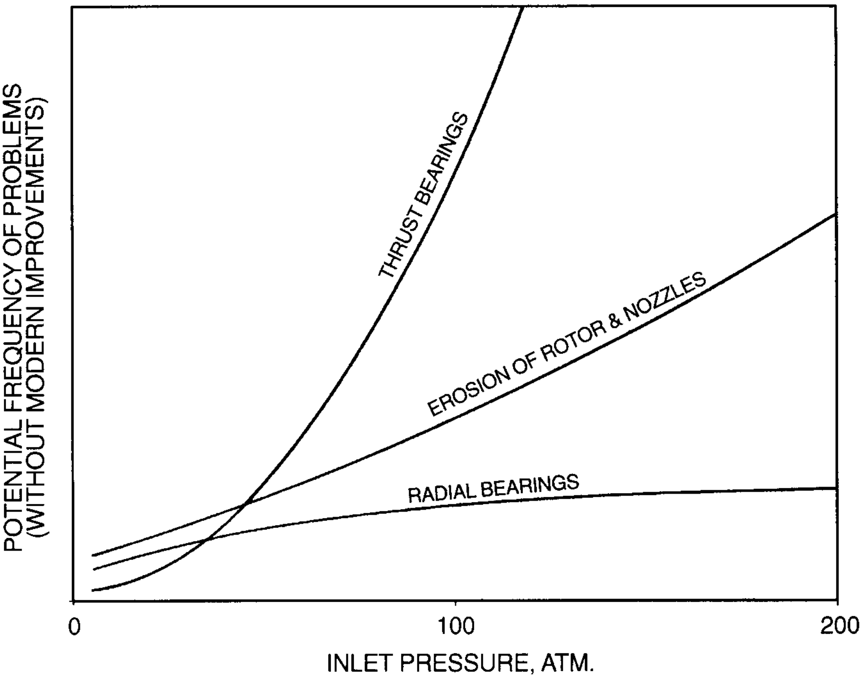

Figure 2-11. Potential frequency of problems without benefit of modern improvements, statistically related to inlet pressure (1 atm ≈ 101.3 kNm^{-2}).

solids such as welding beads or dust, these solids tend to accumulate in the rotor and cause rapid erosion. Erosive action tends to increase with pressure; at higher pressures the screen is more likely to fail. A more dense gas sweeps more scale and welding beads along with it. High-pressure streams often originate from more contaminated zones. Also, the inlet stream is warmer and may not have been well processed and cleaned.

Turboexpanders usually operate at low temperatures where there is the possibility of ice or other frozen solids condensing and partially plugging and unbalancing the rotor. This risk may be somewhat greater at high pressures because the expander inlet temperature is likely to be correspondingly higher and the residual water vapor content high enough to cause trouble—assuming the dryers have failed. Furthermore, at higher pressure the required speed is often higher. Elevated pressure and speed tend to increase the radial bearing requirements, although heavy bearing loads may be encountered at low pressure as well.

In a well-designed turboexpander the journal peripheral velocity is roughly proportional to the rotor tip velocity, and in heavy-duty applications the journal peripheral velocity is high. For thrust bearings, the thrust loads are designed to be equal and opposite. Typical deviations in the magnitudes of these separate thrust forces are 5%–10%. This load deviation error is well within the capacity of available thrust bearings for expanders with inlet pressures of a few hundred psi (recall that 1 psi = 6.9 kN/m^2). As pressures approach 1,000 and more psi, automatic thrust force metering and control become necessary.

RADIAL REACTION VERSUS IMPULSE DESIGN

As mentioned earlier, turboexpander are generally of radial reaction turbine design because this geometry is often most efficient. In an ordinary impulse turbine the high velocity stream from the nozzles makes a U-turn in the rotor blades, and this U-turn consumes 8%–10% of the energy.

The reaction turbine avoids this U-turn and its efficiency penalty. In the reaction turbine half of the pressure energy is spent across the rotor, so there must be a seal around the rotor. With the rotor inlet at its periphery, the discharge from the rotor may now be chosen at a reduced diameter radial, or quasi axial, shaft-concentric position. Since the discharge is obviously smaller in diameter, the rotor seal will also be smaller in diameter because it only needs to surround the discharge portion of the rotor. As a consequence, seal loss is reduced and shaft thrust decreases as well. Likewise, the discharge or secondary nozzle losses are reduced because the gas exits at lower velocity.

However, there are limits to the diameter reduction because too small an exit opening would increase the axial discharge velocity and the resulting losses would overtake the other savings. An intermediate design, the radial reaction design, is often the most efficient compromise. Both shop and field testing have confirmed this to be the case.

Large, single-stage hydraulic turbines that must be highly efficient are virtually always of this configuration. On the other hand, large multistage steam turbines avoid this geometry simply because the fluid entry and discharge porting of radial reaction turbines would result in design complexities.

EFFICIENCY AND SIZING CALCULATIONS

The efficiency of expansion turbines (partial admission axial, full admission axial, and radial inflow turbines) is a function of the following four basic parameters.

Specific speed $$N_s = \frac{N\sqrt{Q_3}}{(778\Delta h)^{3/4}}$$

Specific diameter $$D_s = \frac{D_2(778\Delta h)^{1/4}}{\sqrt{Q_3}}$$

Pressure ratio $$P_r = P_1/P_3$$

Reynolds number $$R_e = \frac{U_2 D_2}{\nu_2}$$

where N = shaft speed (rpm)
Q_3 = exhaust volume flow (ft^3/sec)
Δh = Ideal enthalpy differential available by process (Btu/lb)
U_2 = turbine tip speed (ft/sec)
D_2 = tip diameter (ft)
ν_2 = Kinematic viscosity of process gas at turbine inlet (ft^2/sec)

For the preliminary estimate of the expected efficiency of expansion turbines, in most cases it is sufficient to neglect Reynolds number effects ($R_e \geq 10^5$) and use the efficiency and specific speed correlations shown in Figure 2-12 for partial admission axial impulse, reaction radial inflow and full admission impulse and reaction axial turbines. Due to the economic advantage of the radial turbine, the radial inflow turbine is the best selection when operating in the specific speed range $20 < N_s < 140$, whereby the optimum efficiency will be achieved at $N_s = 80$.

The machine selection is also a strong function of the specific expansion pressure ratio, whereby the following rule-of-thumb applies:

Partial admission axial turbines	$P_r \leq 40{:}1$
Radial inflow turbines	$P_r \leq 30{:}1$
Full admission axial impulse turbines	$P_r \leq 30{:}1$
Full admission axial reaction turbines	$P_r \leq 5{:}1$

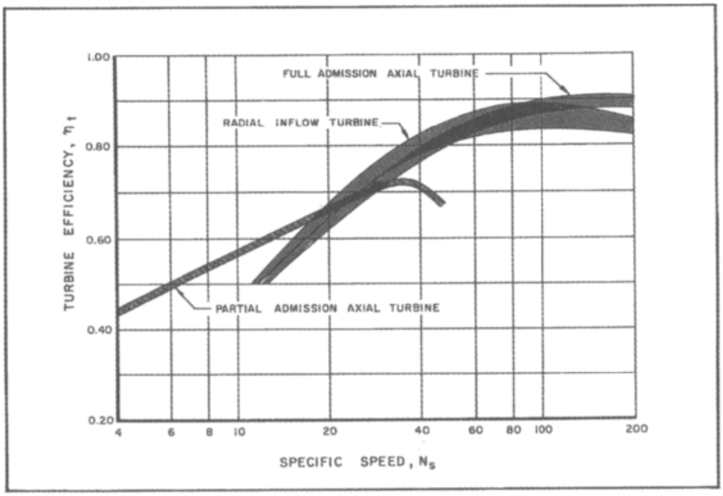

Figure 2-12. Efficiency of various expansion turbine types as a function of specific speed, N_s

$$N_s = \frac{N\sqrt{Q_3}}{(778\Delta h)^{3/4}}$$

N = shaft speed (rpm)
Q_3 = exhaust volume flow (ft^3/sec)
Δh = ideal enthalpy differential (btu/lb)

Because high-pressure ratio requirements coincide in most cases with low specific speed designs, only partial admission axial or radial inflow turbines are seriously considered.

To calculate the specific speed, N_s, it is necessary to select a reasonable shaft speed. First, calculate the approximate shaft power by assuming

$\eta_t = 0.80$
$SHP = 1.41\ w\Delta h\eta_t$
w = weight flow (lb/sec)
Δh = ideal enthalpy differential (Btu/lb)

For the calculated shaft horsepower, Figure 2-13 presents the speed trend of present advanced bearing technology. Any speed below the limiting line can be used for calculating the specific speed. With N

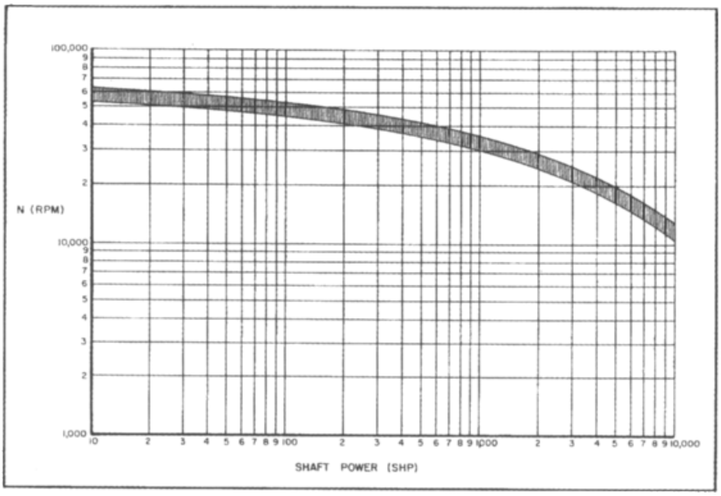

Figure 2-13. Shaft speed N (rpm) as a function of horsepower according to present oil bearing technology.

established, Figure 2-12 indicates the maximum expected turbine efficiency. If the maximum speed has already been selected and $N_s < 20$, a partial admission axial machine should be selected. If $N_s > 140$, the speed should be decreased, or the design of a full admission axial reaction turbine should be seriously considered. Since most present air separation and petrochemical process specifications lend themselves to the selection of radial inflow expansion turbines, the following preliminary sizing calculations are limited to the radial inflow turbine.

Observing the relationship

$$U/C_o = \frac{N_s D_s}{154}$$

where U = tip speed (ft/sec)

C_o = spouting velocity (ft/sec)

$C_o = 223\sqrt{\Delta h}$

It is sufficient to know $U/C_o = f(N_s)$ for preliminary sizing of the machine. For this purpose, Figure 2-14 presents proven experience of $U/C_o = f(N_s)$. With U/C_o given, the tip speed is determined by $U = (U/C_o)\ 223\sqrt{\Delta h_{ad}}$ (ft/sec). Figure 2-14 also shows a tentative value of the degree of reaction of radial in-flow turbines.

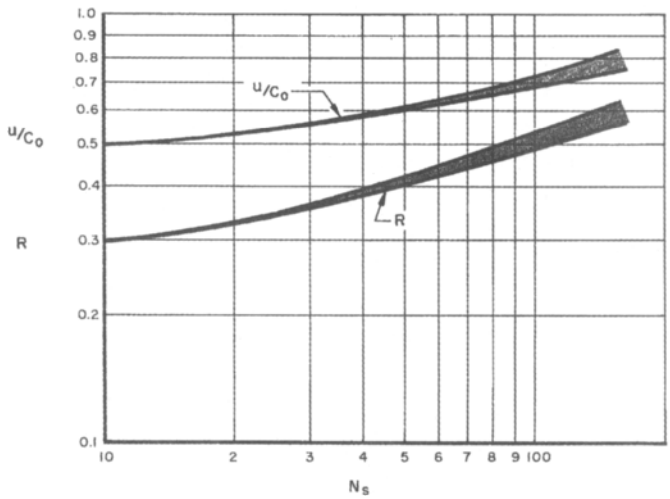

Figure 2-14. $U/C_o = f(N_s)$ and degree of reaction, R, for radial inflow expansion turbines.

Although the tip speed of brazed or fabricated aluminum turbine wheels must be limited to U = 900 ft/sec, the selection of aluminum forged and three-dimensionally machined turbine wheels provides superior mechanical integrity and exceptional mechanical reliability up to tip speeds of U = 1,600 ft/sec. Using forged titanium wheels, a tip speed of 2,000 ft/sec can be achieved as demonstrated by advanced jet engine practice. With N known, the tip diameter D (inches) is determined by the equation

$$D = 229\ U/N \text{ (inches)}$$

Having established a preliminary value of expected efficiency, shaft horsepower, and machine size, the detailed aerodynamic and mechanical design of the machine can be accomplished by a team of process and turboexpander specialists. For this purpose, accurate data must be supplied for the following process parameters:

Δh = ideal enthalpy differential (Btu/lb)
x = equilibrium moisture content at turbine discharge (% of total weight flow)
v_3 = specific volume at turbine discharge (ft^3/lb)
w = total turbine inlet weight flow (lb/sec)

T_1 = inlet temperature (°R)
P_1 = inlet pressure (psia)
P_3 = turbine exit pressure (psia)

Additionally, gas composition, average molecular weight, and average specific heat value must be supplied.

SUMMARY

To summarize, turboexpanders can efficiently expand:

air	hydrogen sulfide
ammonia	isobutane
carbon dioxide	methane
carbon monoxide	natural gas
ethylene	nitrogen
freon	oxygen-rich gases
helium	steam
hydrocarbon mixtures	uranium hexafluoride
hydrogen	other gases and vapors
hydrogen-rich gases	liquids (even with H_2S)

Pressures: Turboexpanders can be designed to operate at up to 3,000 psi and higher inlet pressures as required by conditions. Expansion pressure ratios can also be adjusted for each process over a wide range. A majority of efficient expansion ratios are below 5:1, although pressure ratios up to 10:1 can be accommodated with reasonable efficiency. Smaller, lower pressure units are popular for air separation and helium liquefaction. Intermediate pressure (100–1,000 psi) and high pressure expanders (1,000–3,000 psi) are widely used in natural gas processing and industrial gas liquefaction.

Temperatures: Turboexpanders are routinely used to process gas streams ranging from 600°F down to a few degrees above absolute zero. Competent manufacturers would be delighted to respond to inquiries about higher temperature applications.

Wheel sizes: Wheel diameters range from 1.75 in. for cold helium expanders up to 55 in. for compressor impellers.

Horsepower: Turboexpanders are rated from a few horsepower to thousands of horsepower. Units operating above 1,000 hp are largely used for natural gas treatment and energy recovery. Smaller units are used for inert and hydrocarbon liquefaction and air separation.

Adaptability: Expander internals (rotors, impellers, inlet nozzles, etc.) can be redesigned at moderate cost to accommodate changes in process conditions, such as lower pressure, changing gas composition, and flowrate.

BIBLIOGRAPHY AND ADDITIONAL READING

1. Claude, G., *Compte rend,* Vol. 134 (1902), pp. 1568–1570.
2. Swearingen, J. S., "Method and apparatus for removing vapors from gaseous mixtures by freezing," U.S. Patent No. 3,418,820 (1968).
3. Swearingen, J. S., "Turboexpanders and processes that use them," *Chem. Eng. Progress,* Vol. 68 (1972), No. 7, pp. 95–102.
4. Abadie, V. H., "Predicting expander performance," ASME Paper No. WA/PID-19 (1969).
5. Houghton, J. and Mclay, J. D., "Turboexpanders aid condensate recovery," *Oil and Gas Journal,* (5 Mar. 1973), pp. 76–79.
6. Swearingen, J. S., "Turbine wheel," U.S. Patent No. 3,610,775 (1971).
7. Swearingen, J. S., "Turbine wheel," Japan Patent No. 617,904 (1971).
8. Swearingen, J. S., "Thrust measurement and control," French Patent No. 70.44263 (1971).
9. Swearingen, J. S., "Thrust meters," Italy Patent No. 903 075 (1972).
10. Drost, G., "Maintenance of turbomachinery in cryogenic applications," *Cryog. Ind. Gases* (Nov/Dec 1969), pp. 29–30.
11. Swearingen, J. S., "Apparatus for extracting energy from gas," U.S. Patent No. 2,804,021 (1954).
12. Swearingen, J. S., "Anticavitational power absorber," U.S. Patent No. 3,375,903 (1968).
13. Swearingen, J. S., "Heat generation and hydraulic power," U.S. Patent No. 3,507,577 (1970).

CHAPTER THREE

Application of Cryogenic Turboexpanders

The practical applications for cryogenic turboexpanders are best illustrated by industry case history reports that follow.

METHANE (NATURAL GAS) LIQUEFACTION

OPTIMIZING EFFICIENCY IN METHANE LIQUEFACTION

Although the gas discussed in this chapter is methane, processes and equipment for other gases can be evaluated with this study of work, temperature differences, and efficiencies in methane liquefaction. This approach can be used to appraise almost any cryogenic process for best efficiency. Gas liquefaction is carried out either by stage (cascade), mechanical refrigeration, by the use of turboexpanders, or a combination of the two. The technology of mechanical refrigeration has progressed to an advanced point. This cannot be universally claimed for the application of expansion turbines where compromises in good performance have sometimes been tolerated. When efficiently planned, however, turboexpansion cycles can be excellent.

Gas can be condensed by (a) mechanically refrigerating it, (b) compressing and expanding it, using turboexpanders, or, (c) pressure effects such as by Joule-Thomson cooling and overcoming the vapor pressure. The liquefaction of methane can involve all three of these effects. These effects can be separately evaluated to show the effectiveness of each in producing liquid.

The simple cycle in Figure 3-1, presented as the basis for this study, serves to illustrate these effects and to provide a basis for their evaluation.

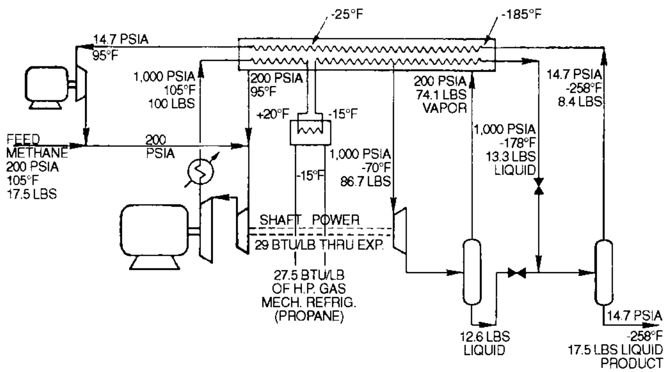

Figure 3-1. This example flow scheme for methane liquefaction uses compression, turboexpansion, and mechanical refrigeration.

Thermodynamics

The removal of heat at a low temperature and its rejection at a higher temperature requires work. This is stated simply by the Second Law of thermodynamics, one form of which is

$$W = Q_1 \frac{T_2 - T_1}{T_1}$$

The validity of this equation is illustrated by using an expansion engine and compressor to lift 1 Btu from, as an example, 50°R and rejecting it at 500°R. This can be illustrated by isothermal compression of an idealized gas at 500°R with a perfect compressor, cooling the compressed gas in a perfect heat exchanger to 50°R without pressure loss, then expanding the gas in sufficient quantity at 5°R (isothermally) to absorb 1 Btu. This expanded gas is then returned through the idealized heat exchanger and recompressed for recycling. The volume to be recompressed is 100 times as great as that which is expanded because the absolute temperature is 100 times as great. The compressor requires 100 Btu of work energy, while the expansion engine develops 1 Btu of work energy.

A net quantity of 99 Btu of work is required to transfer 1 Btu of heat from 50°R to 500°R. Substituting in the Second Law equation gives this same result:

$$W = 1\ \text{Btu}^{*}\ \frac{500-5}{5} = 99\ \text{Btu}^{**}$$

*heat **Work

This concept is now applied to the liquefaction of methane initially at atmospheric pressure and 105°F, 105°F being selected because it is a common industrial heat rejection temperature. The theoretical quantity of work (expressed in Btu of work equal to 778 ft-lb, of work) required to cool 1 lb of methane down to its liquefaction point and then to absorb the 219.7 Btu of latent heat of liquefaction at –258°F, is shown in Figure 3-2. It amounts to 510.8 Btu of work per pound of methane and is not to be confused with Btu of heat, although the quantities in this case are not very different. This amount of work per pound of methane is equivalent to 352 hp/MMcfd. An actual process with its expected inefficiencies would require twice this much work.

EXAMPLE PROCESS

An illustrative process for producing the liquefaction of methane is shown in Figure 3-1. It has not been optimized and rounded-off

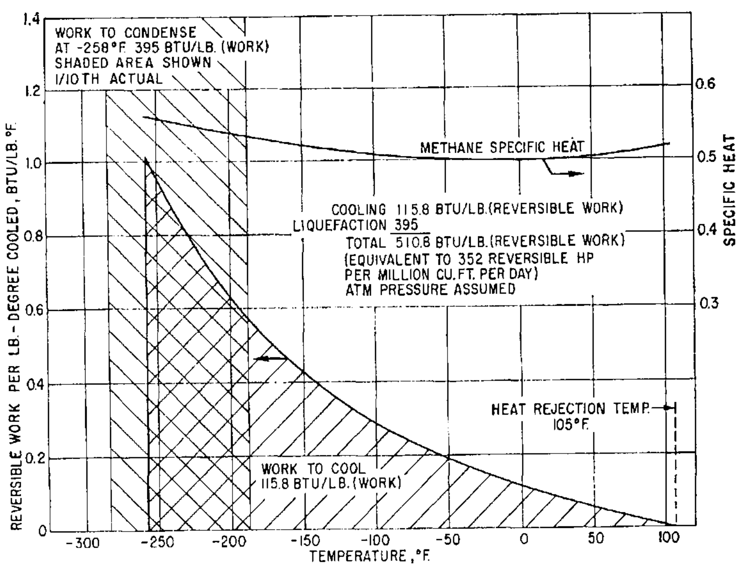

Figure 3-2. Theoretical work to liquify 1 lb of methane.

numbers are used. This particular flow schematic is specially selected for a number of reasons, which will become apparent. Describing the process briefly, gas is shown fed to the system at 200 psia where it joins a recycle stream at that pressure, and the combined stream is recompressed to 1,000 psia. This stream is cooled and divided, and the larger portion of it is then passed through a turboexpander where it is expanded to 200 psia and partially condensed. The remaining unexpanded portion is further cooled at 1,000 psia and liquified, and its pressure is then reduced to 200 psia. This liquid is now combined with the liquid separated from the 200 psia turboexpander discharge stream and flashed to atmospheric pressure for production of a storable liquid. The flash gas is warmed, recovering its refrigeration effect, and recompressed to 200 psia for recycling. (This may in some cases be salable or usable as fuel gas without recompression.) The uncondensed portion of the 200 psia expander discharge stream is warmed, recovering its refrigeration effect, and then recycled. The power from the turboexpander is recovered in a compressor operated in series with the main high pressure compressor.

This process is shown on a Pressure-Enthalpy diagram in Figure 3-3. The dashed lines trace the streams through the diagram.

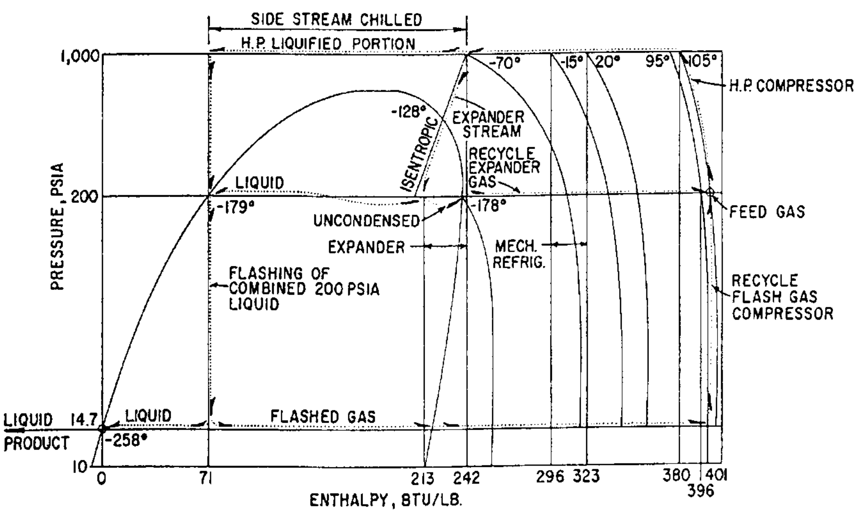

Figure 3-3. The example process in Figure 3-1 is charted on this pressure-temperature-enthalpy diagram; dashed lines trace the streams through the diagram.

The heat quantities in the countercurrent heat exchanger streams are balanced by a small amount of propane refrigeration at –15°F.

Temperature Differences

Figure 3-4 shows the temperature differences in the heat exchanger where the lower curve is the 1,000 psia stream to be cooled, and the upper curve (for simplicity) is the composite of both the 200 psia stream and the 14.7 psia stream being warmed. The two curves diverge and the mechanical refrigeration brings them to within a 10° approach, again at –15°F. The lower, oppositely curved section of the high-pressure curve is for further cooling and liquifying of the small, high-pressure, side stream gas.

It is important to keep the temperature differences in a low-temperature heat exchanger from becoming too wide, especially at its low temperature end because here the temperature difference represents work loss. The temperature difference is shown in Figure 3-4 by areas marked X, Y, and Z. The associated work losses are these areas divided by the square of their respective absolute temperatures and multiplied by 565, the heat rejection temperature. Their respective magnitudes

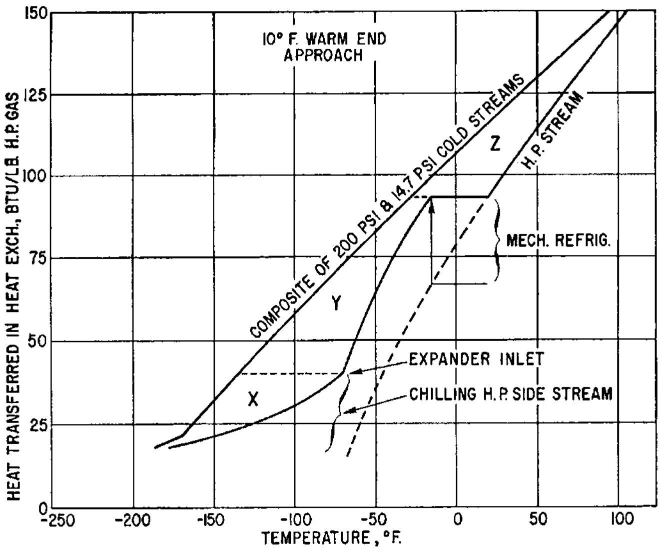

Figure 3-4. Temperature distribution in the main heat exchanger from the example process.

are X = 5.6 Btu, Y = 7.0 Btu, and Z = 3.8 Btu of work per pound of high-pressure gas being cooled (or 32, 40, and 21.7 Btu for a total of 93.7 Btu of work per pound being liquified).

Work Inputs

Table 3-1 gives the work inputs to the system and the overall thermodynamic efficiency of the process. An accounting of the work quantities supplied to the various functions in the process is given in Table 3-2.

There are three actions or functions occurring. One of these actions is performed by the expander/compressor combination, which is accomplishing refrigeration. Another is performed by mechanical refrigeration using propane as the refrigerant. These two actions are more apparent than the third, which is performed by compression causing condensation and Joule-Thomson cooling.

Referring again to Table 3-2, the main high-pressure compressor work is 159 Btu per pound of high pressure methane flow. Of this stream, 86.7% goes through the turboexpander. In the turboexpander

Table 3-1
Distribution of work used by the liquefaction process
(Basis: 1 lb of 1,000 psia stream)

		Charge at atm press.	Charge at 600 psig***
*Low press. compr. (recycle)		22.4 Btu	14.0 Btu
*Work in 200 psia, feed		46.5	−20.0
*H.P. compr.	159 Btu		
**Less expander 29 × .867 (exp. flow)	−25.2	133.8	133.8
Mech. refrig.		14.0	14.0
Total		216.7	141.8
Dividing by .175 liquified, get		216.7/.175 = 1,239 Btu/lb of liquid	141.8/.175 = 810 Btu/lb of liquid
Theor. work to liquify (From Figure 3-2)		510.8 Btu/lb	
Efficiency of process (with charge at atm press.)		510.8/1,239 = 41.25%	510.8/810 = 63.1% (equiv. 558 hp per MMscfd)

**68% Isothermal efficiency; heat rejected at 105°F*
***85% Isentropic efficiency.*
****And 18% consumed as fuel taken from L.P. recycle.*

Table 3-2
Accounting of the work in the liquefaction process—effectiveness of various functions (Process shown in Figure 3-1. Basis: 1 lb of 1,000 psia gas)

Expander/Compressor	Actual work, Btu	Function eff., %	Theor. work to process, Btu
H.P. compressor work = 159 × .867 × .60/.963	85.9	—	—
(total) (expndr. flow) (z)			
Exp. work recovered .29 × .867	-25.2	—	—
Net work	60.7	35.8	21.75
Compression liquefaction and Joule-Thomson			
Remainder of H.P. compr. work (159–85.9)	73.1	—	42.50
Low press. compr. (recycle)	22.4	58.2*	13.03
(charge)	46.5	—	27.05
	142.0	—	—
Mechanical refrigeration	14.0	43.0	6.01
Total	—	—	110.34
Deduct: Wasted work (heat exch.)	—	—	−16.40
(flash gas)	—	—	−4.49
Net work (For .175 lb liquid)	—	—	89.45
Net work/lb 89.45/.175	—	—	510.8
Compare theor. (From Figure 3-2)	—	—	510.8

**Average efficiency for the three.*

the average compressibility of this stream is 0.6. The remaining 0.4 portion of the energy must be accounted for and is included in the compression or Joule-Thomson effect. (Actually, this number is .363 instead of .4 because the average compressibility under compressor conditions is .963 instead of 1.0.)

The 0.6 portion of the 159 Btu of high-pressure compressor input work acting on the expander amounts to 85.9 Btu (work). The expander recovers 29 Btu of work per pound passing through it. A 0.867 fraction of the high-pressure stream passes through it, which gives 25.2 Btu of work, and this results—after being credited to the work input—in a net use of 60.7 Btu for this function. This net work at 35.8% efficiency (see "Efficiencies") gives theoretical work or worth of 21.75 Btu toward actually cooling and condensing the liquid product.

Mechanical refrigeration requires 14 Btu of work, which at 43% functional efficiency, contributes 6.01 Btu of theoretical work.

Using the compression/Joule-Thomson action, of the 159 Btu of work put into the high-pressure compressor, 85.9 Btu is used by the turboexpander as explained above, and the difference of 73.1 Btu is the input power applied to this effect. It acts at 58.2% efficiency and introduces 42.5 Btu of theoretical work. The small recompressor uses 22.4 Btu of work compressing the flash gas. Although not mentioned, if the work in the 200 psi feed stream had to be compressed from atmospheric to 200 psia, it would require 46.5 Btu of actual work. These streams, again at 52.5%, give 11.78 and 24.42 Btu of theoretical work, respectively. The theoretical contributions of these three functions (expander/compressor, mechanical refrigeration, and compression/Joule-Thomson) combined give 110.34 Btu of work.

The heat exchanger temperature difference wastes 16.4 Btu of work. Also, there is an estimated 4.49 Btu of flash energy wasted when the 200 psi liquid is flashed to atmospheric pressure. These two drains on the theoretical work, amounting to 20.89 Btu, are deducted leaving 89.45 Btu of theoretical work applied to the process. This liquifies 0.175 lb of product for 1 lb of circulated high-pressure gas. Dividing 89.45 Btu by .175 gives 510.8 Btu of theoretical work per pound of liquid product. This compares with the calculated 510.8 Btu theoretical work shown in Figure 3-2.

Efficiencies

Figure 3-5 shows the efficiencies of the various functions plotted against temperature. The curve marked "expander-compressor" is based

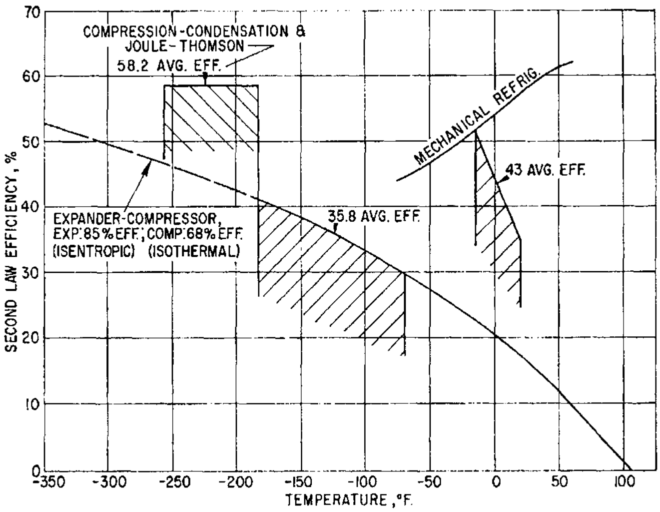

Figure 3-5. Thermodynamic efficiencies of the three liquifying mechanisms.

on this machine's thermodynamic efficiency. In turn, this is based on the Second Law for removing heat from an environment at any particular temperature and rejecting it at 105°F when operated with an infinitesimal heat exchanger temperature difference, but with an 85% efficient turboexpander and a 68% isothermally efficient compressor. (The loss due to the finite heat exchanger temperature difference was separately considered earlier).

The mechanical refrigeration curve is calculated from data in the NGPSA (Natural Gas Processors Suppliers Association) Data Book. This curve represents refrigeration at a fixed temperature. In the process shown in Figure 3-1, the lowest temperature (–15°F) must be maintained to cool the gas to that point, and the average efficiency over the range through which the gas is cooled falls as shown, the average being 43%.

The third curve, that of the compression/Joule-Thomson cooling, shows 58.2% efficiency. This is calculated based on the difference in the accounting shown in Table 3-2 and is the "practical" efficiency of this effect. It would be 68%—that of the compressor—except for several losses, such as the warm end temperature difference and a small, not easily recoverable, portion of the flash loss.

The efficiency of the compression effect is high and its quantity large, favored by high pressure. However, it would not have the opportunity to act to this degree in the absence of the turboexpander, therefore the latter is the key to a large fraction of this high-efficiency effect. It is important to minimize losses such as those connected with large heat exchanger temperature differences.

The benefits of using the turboexpander are further enhanced by applying it to a cycle at the lowest convenient temperature and by the capability of this machine to operate with a condensing stream.

Process Refinement

A possible refinement to the process can be made, particularly to the 4.49 Btu lost on flashing the 200 psia saturated liquid to atmospheric pressure. If this were flashed first to 80 psia and then flashed to atmospheric pressure, over half of the flash gas would be released at 80 psia. The expansion of this gas in a turboexpander would recover almost half of the total flash loss, and the liquid yield would increase 4.74% plus contribute 1% of the plant power.

As an indication of turboexpander sizes, for each million cubic feet per day of liquid product, this flash gas turboexpander would be "sized" at 6 hp; the main turboexpander at 99 hp; the main 1,000 psia compressor at 626 hp (including the stage driven by the turboexpander), and the flash gas compressor at 88 hp. The feed gas is at 200 psi and contains a substantial amount of energy above the 14.7 psi level. Otherwise, it would require 183 hp to compress the feed gas.

The mechanical refrigeration system for producing LNG, generally known as the cascade cycle, is shown in Figure 3-6.

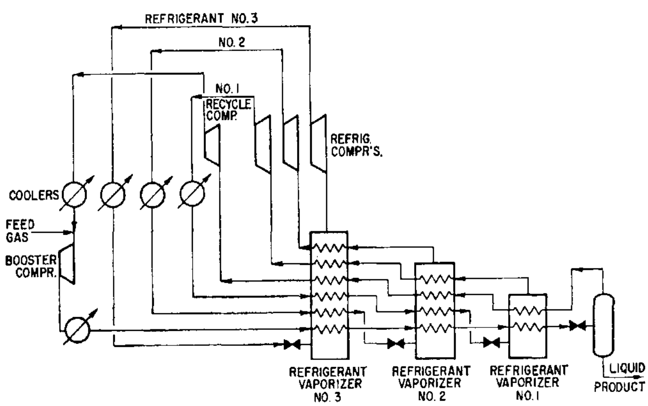

Figure 3-6. Scheme for liquifying methane using the cascade refrigeration system.

In summary, starting with 105°F gas at atmospheric pressure, the theoretical work necessary to liquify one pound of methane is 510.8 Btu or 352 hp/MMcfd. The simplified liquefaction process, as illustrated, uses a turboexpander/compressor and a small propane refrigeration unit. The 41.25% efficiency breaks down as follows: one-fourth contributed by the turboexpander/compressor at 35.8% efficiency; one-sixteenth contributed by the mechanical propane refrigeration unit at 43% efficiency, at a moderate temperature where its efficiency is high; and a large fraction—eleven-sixteenths—contributed at 58.2% efficiency by compression and Joule-Thomson condensation energy.

The process illustrates the use of mechanical refrigeration in its high-efficiency temperature range; the maximum use of compression energy because of its high efficiency; and the use of turboexpansion at a low temperature—its Carnot efficiency is best at low temperatures, especially because it permits large use of the efficient pressure effect.

COMPARISON OF EXPANDER AND CASCADE CYCLES FOR LNG

Although not proven, the general consensus is that large base-load plants for liquifying natural gas should use a cascade cycle. Reported thermodynamic efficiencies for expander cycles liquifying natural gas (assumed to be pure methane) vary from about 36% to 48%, whereas the efficiencies of cascade cycles (including the modified one using a mixed refrigerant) vary from about 32% to 42%. It is, therefore, not possible to draw a clear-cut conclusion about the relative power requirements. It appears that the best expander cycle is competitive with the best cascade for base-load plants, as far as power usage is concerned, and may be lower in first cost.

Generally, the cascade cycle, including the mixed-refrigerant (MRC) type, is more complex than the expander cycle. It also requires a larger investment and is more difficult to control, which is apparent when comparing flow diagrams of the two processes. Figure 3-7 is a diagram of a typical cascade using three fluids: propane, ethylene, and methane. Contrast this with the expander cycle published by Swearingen, or the expander cycle of Becker in Figure 3-8. The purification system for the feed gas is omitted in both cases for the sake of simplicity.

The main advantage of a cascade over an expander cycle is presumed to be the lower power requirement. Since power is a large percentage of the total cost in large capacity plants, the possible

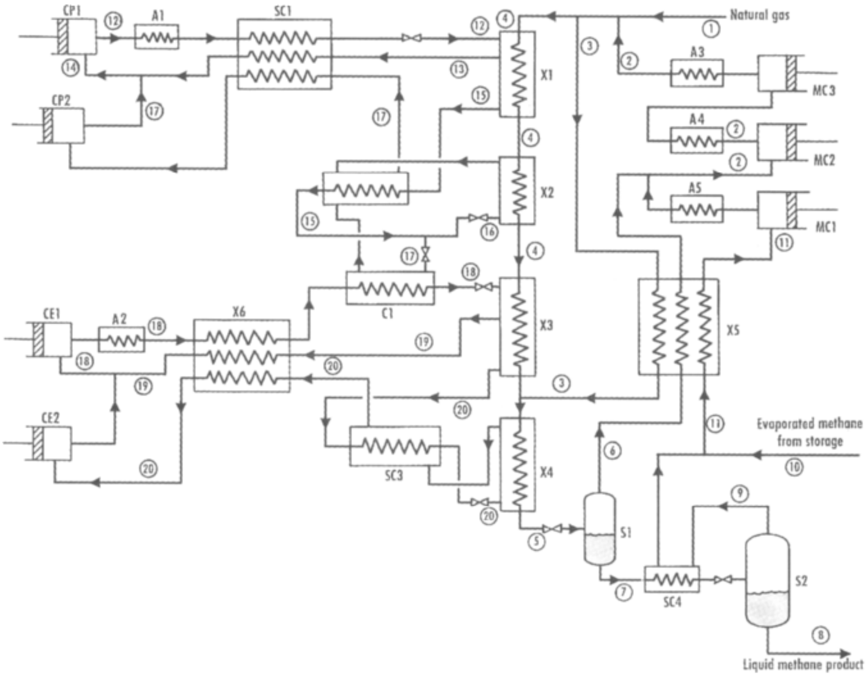

A1 . . . A5	Compressor aftercoolers
C1	Ethylene condenser
CP1	First stage of propane compressor
CP2	Second stage of propane compressor
CE1	First stage of ethylene compressor
CE2	Second stage of ethylene compressor
MC1, MC2, MC3	Three stages of recycle methane compression
SC1	Propane liquid subcooler. Cooled by returning propane vapor.
SC2	Propane liquid subcooler. Cooled by returning propane vapor.
SC3	Ethylene liquid subcooler. Cooled by returning C_2H_4 vapor.
SC4	Methane liquid subcooler. Cooled by CH_4 vapor from S1.
S1, S2	Phase separators
X1	Exchanger cooling NG by evaporating propane at intermediate pressure
X2	Exchanger cooling NG by evaporating propane at low pressure
X3	Exchanger cooling NG by evaporating ethylene
X4	Exchanger condensing NG by evaporating ethylene
X5	Exchanger cooling NG by recycle CH_4 streams
X6	Exchanger cooling C_2H_4 vapor by returning C_2H_4 vapors

1 . . . 11 incl.	Natural gas and CH_4 streams
12 . . . 17 incl.	Propane streams
18 . . . 20 incl.	Ethylene streams

Figure 3-7. Typical cascade cycle.

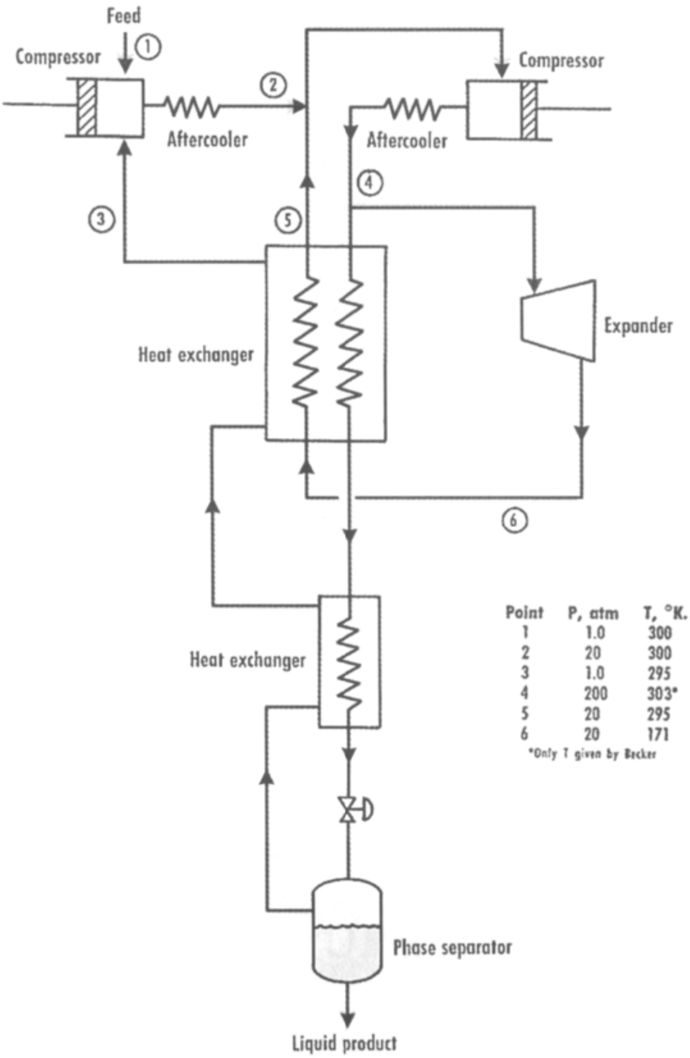

Point	P, atm	T, °K.
1	1.0	300
2	20	300
3	1.0	295
4	200	303*
5	20	295
6	20	171

*Only T given by Becker

Figure 3-8. Single-acting expander cycle.

savings in power cost might more than balance an increase in fixed charges. A reliable comparison of the power requirements for the two processes is difficult to make for several reasons. First, there are no large base-load plants using an expander cycle and, hence, figures on power usage are calculated ones. Second, the analysis of a cycle under practical conditions requires making assumptions about compressor and expander efficiencies, heat-exchanger temperature differences, pressure drops in flow lines, heat leaks, and the percentage of expander-generated power that can be applied to compression of the gas.

Furthermore, appreciable differences can arise from simply using different sources of data on gas properties. There are very few calculated power requirements for a cascade process under practical operating conditions that have been published and, therefore, available for a direct comparison between the two processes. Additionally, published figures on the actual power requirements for many cascades are actually for natural gas, whereas the calculated figures are based on the liquefaction of pure methane.

Although natural gas contains several other hydrocarbons in addition to methane and small concentrations of other gases, it is believed that the assumption of pure methane is acceptable for the purpose of comparing different cycles. In spite of these difficulties, a comparison based on the available data is worthwhile.

Dr. Judson Swearingen calculated the power requirement of his cycle to be 900 hp/MMscfd of gas liquified. In other units this figure becomes 1,239 Btu/lb or 5.80 kw-hr/lb-mole. This corresponds to a thermodynamic efficiency of 41.25% based on the minimum possible work for a completely reversible cycle. As before, this is calculated by means of the following equation readily derived from the two laws of thermodynamics:

$$W_{min} = \Delta H - T_o \Delta S \tag{3-1}$$

where ΔH = difference in enthalpy between the initial state of the gas and the liquid at 1 atm

ΔS = entropy difference for the same initial and final states

T_o = the average temperature at which heat can be rejected to the environment

Some values of W_{min} are given in Table 3-1. In all cases, the liquid product is saturated liquid at 1 atm. It is clear from these figures that the initial state of the gas has considerable influence on the power requirement, and comparisons between processes must take this into account.

Calculations of the power requirement for Swearingen's cycle using his values of the pressures, initial gas temperature, sink temperature, and expander efficiency resulted in an efficiency of 43.0%. Increasing the expander intake temperature from this value of –70°F to –10°F increased the efficiency to 45.6%. For the cycle shown in Figure 3-8, Becker gave as the work requirement 0.47 kw-hr/m^3 of liquified methane for the optimum intermediate pressure of 20 atm and an expander efficiency of 80%. His minimum work was 0.226 in the same units, and therefore the efficiency was 44.3%.

Becker also analyzed a similar cycle in which the expansion valve was replaced by a turbine and obtained an efficiency of 48.1%. Analysis of Becker's single-expander cycle gave an efficiency of about 40%.

Cascade Cycles

Published analyses of cascade cycles by means of energy balances under conditions comparable to those used in analyzing expander cycles are very scarce. Longwell and Kruse tabulated computer-calculated compressor and expander powers for a C_3H_6-C_2H_4-CH_4 cascade. For a feed of 1,566 lb-moles/hr at 515 psia and 60°F, 490 lb-moles of LNG and two gaseous products were produced.

Since only 31% of the feed was converted to LNG, this cascade is not comparable with the expander cycles considered in which all the feed was converted to liquid. When the efficiency was calculated by Equation 3-1 it turned out to be only 2.15%.

Ward reported power consumption for a plant using the mixed-refrigerant cycle. Compressor power was 9,460 kw for an LNG production rate of 28,550 m^3/hr. This converts to 3.37 kw-hr/lb-mole of liquid. The minimum work for a feed-gas pressure of 37 atm, an assumed feed-gas temperature of 80°F, and an assumed heat-sink temperature of 80°F = 1.09 kw-hr/lb-mole of liquid. This gives an efficiency of 32.4%.

Emery et al. reported these data on the Marathon-Phillips plant in Alaska, which uses a C_3H_6-C_2H_4-CH_4 cascade:

Feed (99.5% CH_4) at 620 psia and 75°F
LNG produced = 172.6 × 10E6 scfd
Total compressor power = 85,600 hp

Using these data, it is possible to calculate a work requirement of 3.20 kw-hr/lb-mole of LNG. The minimum work for the given feed state and a heat-sink temperature of 80°F = 1.05 kw-hr/lb-mole and the efficiency = 32.8%. See Table 3-3 for typical values.

Table 3-3
Minimum work for methane liquefaction

Initial state of CH_4			Minimum work of liquefaction		
P, atm	T, K.	t, °F.	Heat-sink temp., °F.	BTU/lb	kw-hr/lb mole
1.00	300	80	80	470	2.21
1.00	324	105	105	512	2.40
15	300	80	80	292	1.37
30	300	80	80	247	1.16
50	300	80	80	213	1.00
35	289	60	60	214	1.004

The interpretation of this figure is not entirely clear because an unknown amount of fuel gas is produced by flashing the liquid, and some of the compressor power is used to compress this gas. It is reasonable, however, to assume that the error resulting from this would be relatively small.

Salama and Eyre reported a power consumption of 125,000 hp for a standard cascade producing 300 × 10E6 scfd of LNG with a feed gas of 750 psia. This is equivalent to a usage of 417 hp/MMscfd. Assuming the gas enters the plant at 80°F and that heat can be rejected at this temperature, the minimum reversible power = 154 hp/MMscfd, or the thermodynamic efficiency = 37.0%.

Ritter cited a figure of 46,900 bhp for a three-fluid cascade liquifying 102 MMcfd. Natural gas was available at 465 psia and 100°F. No pressure or temperature was given, but assuming 1 atm and 32°F, the work of the compressors equals 3.01 kw-hr/lb-mole. The minimum work for this case is 1.243 kw-hr/lb-mole, corresponding to an efficiency of 41.3%.

Ritter also gave the flow diagram for an expander cycle and reported data from which an efficiency of 35.9% for the cycle and an expander efficiency of 80% were calculated. When the same cycle was analyzed using an expander efficiency of 85%, an efficiency of 36.9% was obtained for the cycle.

Barber and Haselden analyzed two cascade cycles, one of which was designated "normal" and the other "cascade with cold compression." They reported thermodynamic efficiencies of 40.0% and 42.1%, respectively. An expander cycle designated "Heylandt" was also analyzed and an efficiency of 37.5% reported.

ETHYLENE PLANT EXPANDERS

Cryogenic processes using turboexpanders facilitate high levels of ethylene recovery from refinery gas while producing byproducts of hydrogen- and methane-rich gas. In a cryogenic process, most of the ethylene and almost all of the heavier components are liquified and ethylene is separated from this liquid.

Radial inflow turboexpanders are the best equipment for this application because they handle condensing streams, provide a high expansion ratio in a single stage, and are custom-built to accommodate the plant's process conditions.

Most ethylene plants operate continuously with the expanders operating at or near design conditions. If necessary, due to their unique design characteristics, radial inflow turboexpanders can accommodate a wide range of process conditions without significant losses in thermal or mechanical efficiency. Expanders may be loaded with booster compressors, gear-coupled generators, dynamometers, or other in-plant mechanical equipment such as pumps. In ethylene plants, turboexpanders are typically used in either post-boost or pre-boost applications.

In post-boost applications, the turboexpander operates under generally equalized pressure conditions (i.e., the turboexpander discharge pressure is approximately the same as the compressor inlet pressure).

In pre-boost applications, the turboexpander discharge pressure is considerably lower than the compressor inlet pressure. This situation requires special consideration when designing the turboexpander and auxiliary systems. In pre-boost designs, compressing the gas to a higher pressure produces more refrigeration in the turboexpander. Figure 3-9 shows a cross-section of an expander-compressor unit.

Generator-loaded expanders are used when compression is not required and additional sources of electric power are desirable. Depending on operating conditions such as rpm and power level, integral or external gearboxes transmit power to an induction or synchronous generator. Figure 3-10 depicts the integral gearbox.

When power levels are low or cannot otherwise be utilized, a dynamometer or an air brake (blower) may be used. Figure 3-11 shows a typical dynamometer-loaded turboexpander cross-section.

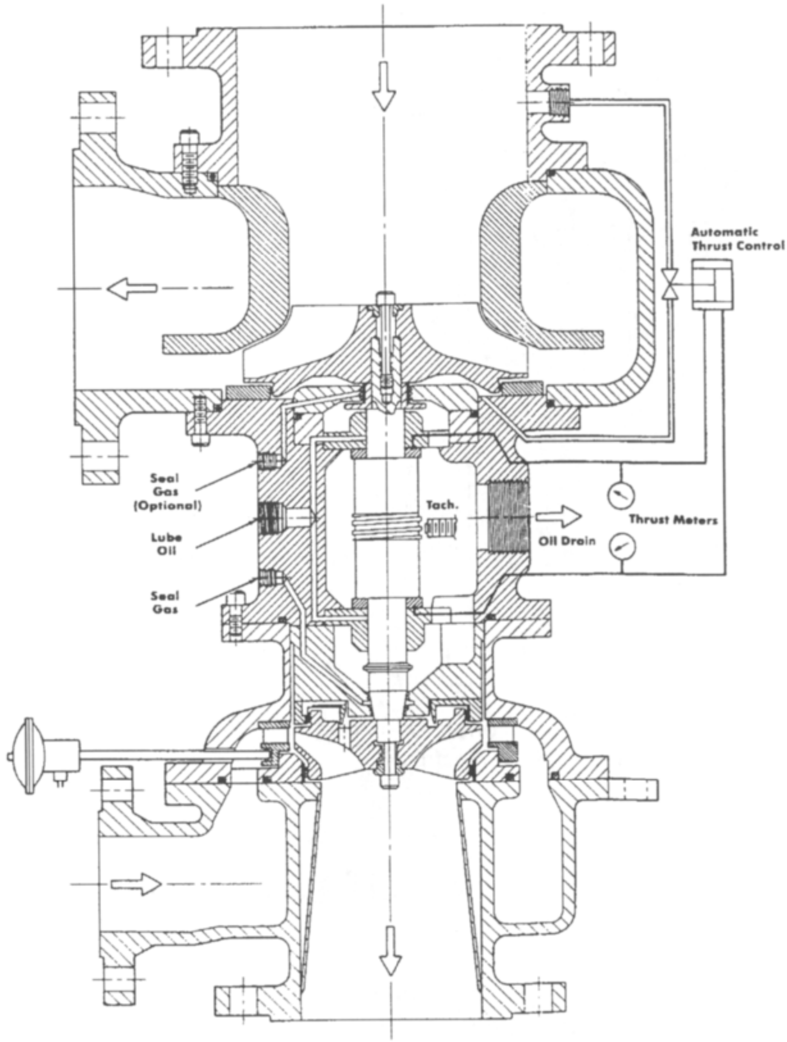

Figure 3-9. Expander-compressor cross-section. *(Source: Atlas Copco.)*

The choice of a turboexpander load may be influenced by the desire to optimize refrigeration. In other words, a dynamometer load may be chosen over a generator load due to speed considerations. Additionally, there are other constraints imposed on optimal design. Factors such as impeller peripheral velocity (tip speed), bearing design, axial load balance, material selection, and manufacturing methods (which have greatly improved in the recent decades) all have an influence.

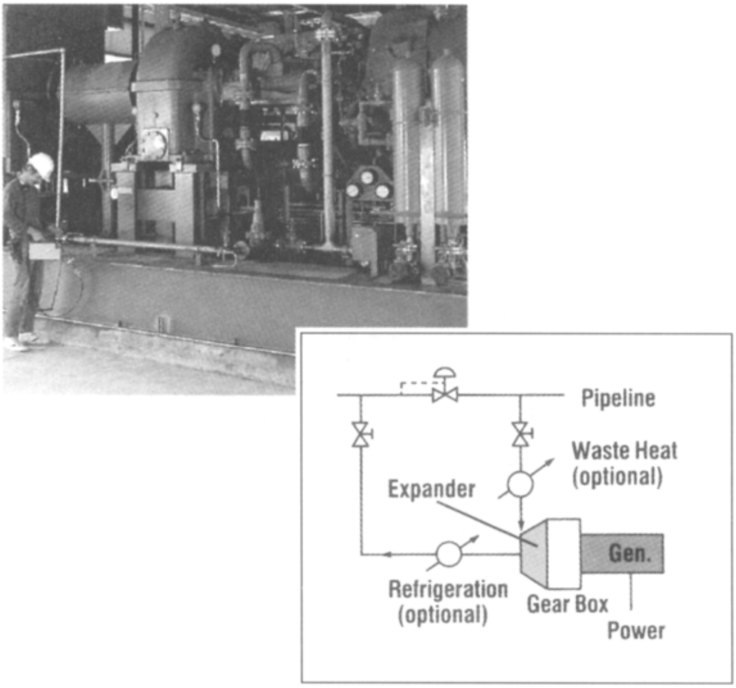

Figure 3-10. One of eight generator-loaded Rotoflow expanders used to convert geothermal energy to electricity.

EXPANSION OF CONDENSING STREAMS

All turboexpanders in ethylene plants work in two-phase operation and two critical issues must be addressed. One is to make certain that internal parts exposed to flow are not damaged, and the other is to maintain thermal efficiencies as high as for single-phase operation. These issues are both solved by the resulting force directions for the vectors of centrifugal force (10–15° from the radial direction) while blade loading is kept optimized using the desired blade geometries.

Expander Efficiency

Expander efficiency is related to gas flow, enthalpy drop, and shaft rotating speed. The combination of these parameters defines impeller blade geometries required to maximize thermal efficiency. Expander

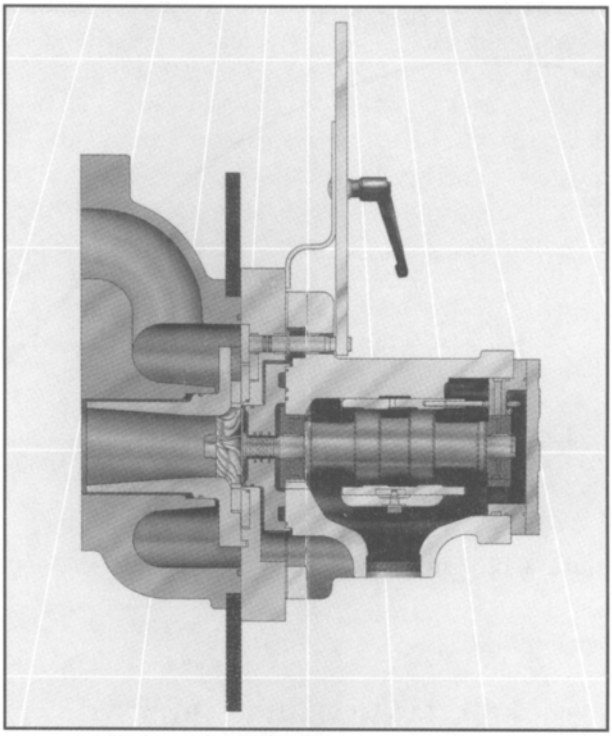

Figure 3-11. Expander-dynamometer cross-section.

efficiency versus enthalpy drop is shown in Figure 3-12. As depicted, efficiency is relatively flat over a range from 10 Btu/lb (23 J/g) to 60 Btu/lb (140 J/g). In other words, within this range, turboexpander design efficiency is not sensitive to enthalpy drop across the expander. When enthalpy drop is below the lower limit, turboexpander thermal efficiency drops sharply. The main reasons for this are velocity losses, in the former case, and mechanical constraints, in the latter case.

Expander performance will shift as plant conditions—such as gas flowrate, gas inlet, and discharge pressure—gas composition, and inlet temperature change. Calculation of expander thermal efficiency from field data is not accurate because expander discharge flow normally consists of two phases, gas and liquid. Efficiency calculations should always be cross-checked with the shaft power produced before any decision on expander performance is made.

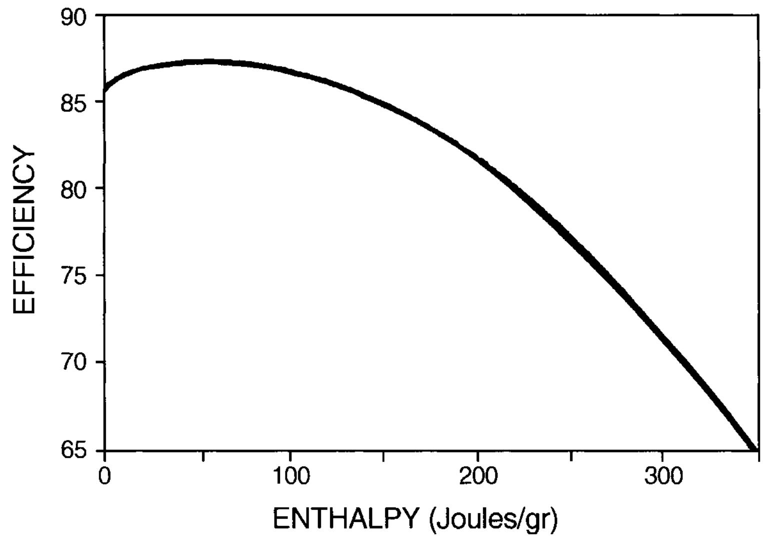

Figure 3-12. Expander enthalpy drop versus efficiency.

MECHANICAL RELIABILITY

As previously discussed, the reliability of turboexpanders has increased considerably since their first application in ethylene plants in the early seventies. This is mainly due to a better understanding of rotordynamics, material selection, and improvements in mechanical design. Most ethylene plant turboexpanders have stiff shaft and bearing construction. Recent high tip speed turboexpanders have also used this design. The primary advantage of the stiff shaft design is that it provides excellent shaft control with minimal damage should the rotor develop an out-of-balance condition. Damage to the blades, ice formation in the wheel, or a liquid slug entering the machine can all cause rotor unbalance.

Flexible shaft design requires that a machine run above its critical speed. Any unbalance will cause the center of gravity to shift, often causing high vibration and heavy wear of the seals. In some cases, due to dilution of the lubricating oil, flexible shaft machines may run at critical speed causing severe damage to rotating parts.

The stiff shaft design has lower clearance requirements, which allows non-contacting seals to be used. Contacting seals, if used, would eventually wear resulting in a drop in performance and possible failure from high thrust loads.

Journal bearings used in stiff shaft machines are designed to handle high dynamic loads during emergencies. Bearings are rigid to shift the oil film resonance frequency well above the maximum running speed. Magnetic bearings have recently been used successfully in ethylene plant machinery and are worthy contenders for traditional oil bearings in turboexpanders.

Most turboexpanders use close-fitting, labyrinth-type seals to minimize gas leakage. In ethylene plants, seal gas usually has a low molecular weight. Low molecular weight seal gas increases the velocity through the labyrinth seal, possibly causing erosion. To protect the labyrinth from high velocity gas, drainers may be installed. Dry gas seals represent another important and generally attractive alternative resulting in reduced gas leakage.

Automatic Clamping System

Ethylene plants are usually designed for a wide range of flow variations. Turboexpanders handle flow variations by means of adjustable inlet guide vanes. Inlet guide vanes maintain reasonably constant thermal efficiency over a wide range of flows. Process gas pressure variation may cause separation of the nozzle adjusting ring and nozzle segments resulting in blow-by or excess clamping, which inhibits or prevents proper operation. Automatic Clamping Systems (ACS) address this problem. Since ACS were implemented in turboexpander design, inlet guide vane operation and, hence, performance has significantly improved.

High Efficiency Boosters

Initially, ethylene plants did not pay much attention to booster performance. In the mid-1950s, booster efficiencies in the mid-sixty percentile range were acceptable to industry. Since booster efficiency, especially in the pre-boost configuration, has a significant effect on refrigeration and therefore on capital investment, higher efficiencies are very desirable. Booster efficiency has since improved and values in the low eighty percentile range are commonly achieved. There is a cumulative effect in the pre-boost system. Higher outlet pressure results in more power for the expander that drives the compressor. When this cycle reaches equilibrium, optimum refrigeration is produced.

Dust-Free Design

Process gas flowing through turboexpanders should be relatively clean. Normally it is recommended that solid particle size not exceed 5–10 μ; with a maximum concentration of 40 mg/m^3. Clean gas is required not only to prevent erosion, but also because higher concentrations have a measurable effect on expander performance. Large particles cause disturbances in flow, which may result in a 2%–3% drop in thermal efficiency. High gas velocities carry solid particles through the inlet guide vane channel causing erosion and damage to seals and impeller blade tips. If particulate matter is introduced in spite of precautions, Figure 3-13 shows a design to harmlessly discharge dust particles to the expander discharge and prevent accumulation of dust particles behind the impeller. Erosion of labyrinth seals may also result in thrust unbalance, which, in turn, may cause serious damage to the turboexpander if undetected and uncorrected.

Automatic Thrust Balance System

Changes in speed or process gas pressure can change the axial position of the turboexpander shaft. Labyrinth seal wear in the turboexpander may also cause thrust force unbalance. To decrease the load

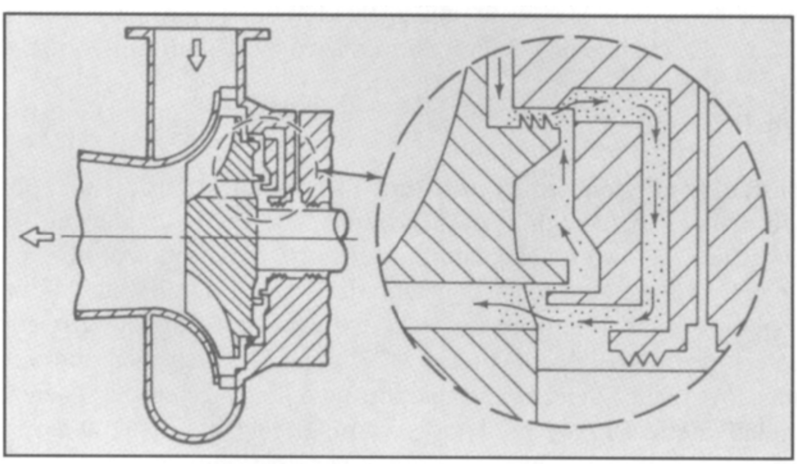

Figure 3-13. "Dust-free" turboexpander geometry. *(Source: Atlas Copco.)*

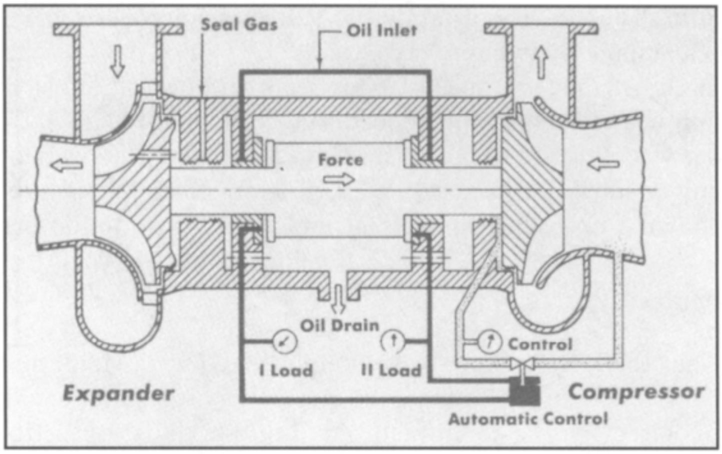

Figure 3-14. Atlas Copco thrust control system.

on the thrust bearing and control the shaft position within acceptable limits, the thrust control system illustrated in Figure 3-14 is used.

The Automatic Thrust Balance System is a dynamic adjusting system. Hydrodynamic pressure at the thrust bearing face, an indication of thrust loads, is continuously monitored and fed to either side of a piston, which, in turn, adjusts the pressure acting behind the compressor wheel.

OPERATING HISTORY

Turboexpanders, after initial troubleshooting during start-up and commissioning, and as long as they are properly maintained and operated, will function reliably and efficiently for many years. As is so often the case in an operating environment, machines are sometimes unfairly blamed for problems in ethylene plants as well. The turboexpander is no exception here, however, it is important to remember that it is only one piece of equipment in these complex plants and all equipment is interrelated. Troubleshooting and cause and effect analysis should be performed with sufficient operating data and from an overall system perspective. For example, high expander vibration may be due to bearing damage, liquid carryover from the inlet separator, compressor surge, or lack of a proper lubricating oil supply. Other examples include operation at reduced speed due to nozzle leakage,

leakage in the Joule-Thomson bypass valve, or improper setting of the booster compressor bypass valve.

High thrust may be due to improper operation of thrust control, operation beyond the recommended range, or liquid slugs hitting the expander wheel due to improper inlet piping design. The overall system productivity should be checked and verified by obtaining data regularly and following procedures in the manufacturer's instruction manuals.

Maintenance Practice

Turboexpanders are relatively simple machines. Major problems may be avoided by following the normal maintenance procedures recommended by the manufacturer. Regular daily operating data collection or log sheets make troubleshooting much easier for both plant personnel and the turboexpander manufacturer. Operating conditions far from design conditions may result in damage to internal parts. For example, both turboexpander impeller and seal may be damaged from improper oil filtration or from vibration, the latter occasionally produced by an outside source such as gas pulsation. Thrust bearings may be damaged due to inadequate oil pressure, liquid slugs introduced to the impeller, sudden changes in operating pressure, or booster compressor surge. Shaft seals may be damaged by improper seal gas filtration.

Generally, the following items should be frequently checked:

- Thrust loads on the bearings
- Seal gas pressure and flow
- Lube oil pressure
- Differential pressure across the lube oil filter
- Differential pressure across the inlet screen
- Pressure behind the expander and compressor impellers
- Oil reservoir level
- Oil inlet temperature to the bearings

Turboexpanders Equipped with Magnetic Bearings

Existing lubricated bearing standards were the starting point for designing turboexpanders with magnetic bearings. Machines of this type are primarily installed in air liquefaction and air separation plants. They range in size from about 100–2,000 kw and are configured as shown in several earlier illustrations.

Since the early 1980s, major producers of turboexpanders have been able to supply these machines with bearings upgraded to fully magnetic, oil-free design. Initially, typical mid-size machines were described by the following parameters:

- Turboexpander power of 600 kw
- Maximum continuous speed of 33,000 rpm
- Turboexpander isentropic efficiency of 86%
- Compressor polytropic efficiency of 79%

Shaft and Bearing Design

Based on the chosen standard, the shaft was originally designed for a maximum continuous speed of 52,000 rpm. This maximum continuous speed was limited by:

- The journal bearing diameter (based on the bearing manufacturer's experience)
- The maximum outer diameter of thrust bearing (based on thrust collar design and allowable stresses)
- The first or free-free rotor bending mode frequency (based on the required margin for operation below the critical speed)

Additionally, the following dimensions controlled the minimum shaft length of earlier machines:

- Journal bearing length (based on an assumed load capacity)
- Axial length of thrust bearing (given by manufacturer)
- Auxiliary bearing and shaft vibration probe length (given by manufacturer)
- Shaft sealing length (based on seal configuration and pressure drop)

Using the above pre-existing parameters, the rotors were retrofitted with suitable magnetic bearings. Magnetic bearings are a far-reaching technological development, as will be discussed later in Chapter 6.

Power losses of the magnetic bearings due to eddy currents were calculated by the bearing manufacturer. For thrust bearings, the losses were small enough to be labeled zero, whereas journal bearing losses were given as 0.4–0.7 kw. Additionally, windage losses were calculated to reach values from 3–5 kw at maximum continuous speed in a pressurized bearing housing. Because it was expected that heat transfer from the hot compressor side could never be precisely calculated, it was assumed from the beginning that a certain amount of cooling gas would be needed to absorb and transfer about 1–2 kw of the total power loss. To achieve the required cooling, approximately 100–300 scm/h of nitrogen were needed.

Bearing Load and Cross-Coupling Stiffness Measurements

One advantage of using active magnetic bearings is the feasibility of continuously measuring bearing forces during operation. Thrust bearing currents can now be used to control the pressure on the balance piston. In other words, hydraulic means of maintaining rotor thrust balance (discussed earlier) must now compete against electromagnetic means of achieving the same goal.

In addition to tracking static bearing loads, it is also possible to measure dynamic bearing loads and destabilizing forces. This allows the manufacturer to calculate cross-coupling stiffness related to bearing planes.

Economic Comparisons

Economic comparison is often separated into installation and operating costs. Assigning a cost of 100% to a turboexpander with conventional bearings, a machine with magnetic bearings will cost 140%. Additional criteria to consider include space requirements, foundation costs, product leakage to atmosphere, energy required for cooling water, and oil supply pumps.

Generally, the initial cost advantage of purchasing a turboexpander equipped with conventional bearings is usually negated by operating cost savings over a period of three to five years. Reliability-focused owner-operator companies are likely to specify magnetic bearings.

ECONOMICS OF TURBOEXPANDERS IN CLEAN APPLICATIONS

Natural gas must meet certain specifications before it qualifies for fuel. It should also meet certain dew point characteristics before entering a transmission pipeline. Water dew point is controlled and maintained by stationary equipment such as molecular sieves or dehydration by glycol. Hydrocarbon dew point, on the other hand, can be controlled by either stationary equipment, such as a Joule-Thomson valve, or by a turboexpander. The former method is relatively simple but limited in capability and, more importantly, wastes energy. The latter option includes more costly rotating equipment, but provides a wide range of capabilities including recovery of cold energy. Turboexpander applications have proven to be the most cost effective and energy-saving method versus other process options.

Improving the economics of gas plant design, construction, and operations is essential to ensure the approval of future de-bottlenecking, capacity expansion, and new projects. The economics include not only capital investment, life cycle operations, and maintenance costs, but also the monetary equivalents of safety, reliability, and availability.

The trend in gas plant design has been to maximize train capacity in an effort to take advantage of the economy of size. At the same time, gas plant designers are constrained by the maximum size of processing equipment of proven design. Table 3-4 shows the trend in gas plant train sizes in the last three decades.

Onshore or offshore gas plants are designed for either LNG rejection and gas injection, or LNG rejection and transmission for sale. In the case of offshore plants, onshore facilities further process the natural gas before transmission for sale. In either case, natural gas must be treated and then refrigerated to make rejection of heavy hydrocarbons possible. In plants where natural gas is treated for sale purposes, water and hydrocarbon dew points of the gas must also be controlled.

GAS TREATING METHODS

There are several process options to treat gas and reject liquid. A typical pipeline gas specification with respect to thermal value is shown in Table 3-5.

Table 3-4
Gas plant train sizes (thousand tons / year)

Year of design	Nominal train capacity range
1960–1970	0.5–1.1
1971–1978	1.2–1.6
1979–1991	2.0–2.6
1992–1996	3.5–4.5

Table 3-5
Example pipeline quality natural gas

Major and minor components, mole %	Minimum	Maximum
Methane	75	—
Ethane	—	10
Propane	—	5
Butanes	—	2
Pentanes and heavier	—	0.5
Nitrogen and other inert	—	3–4
Carbon dioxide	—	3-4
Trace Component		
Hydrogen sulfide		.25–1.0 gr/Nm^3
Mercaptan sulfur		.25–1.0 gr/Nm^3
Total sulfur		5–20 gr/Nm^3
Water vapor		7.0 lb/28 M Nm^3
Oxygen		.2–1.0 ppmv
Other Characteristics		
Heating value, MJ/m^3 gross saturated	35	43

Liquids: Free of liquid water and hydrocarbons at delivery temperature and pressure.
Solids: Free of particulate in amounts deleterious to transmission and utilization equipment.

One option for water dew point control is to alter the freezing point by glycol contact before cooling. The second option is to dry the gas by molecular sieve prior to refrigeration and subsequent separation of heavy components for hydrocarbon dew point conditioning.

A third alternative design is to chill the gas and separate the water content. In this option, water and hydrocarbon specifications may be satisfied simultaneously if the gas temperature is kept above hydrate formation. This option is the simplest process and most engineering studies have shown it to be the least expensive gas treatment method.

Hydrocarbon dew point control is achieved by cooling the gas. There are three cooling alternatives: free expansion or Joule-Thomson expansion, external refrigeration, and using a turboexpander. Joule-Thomson expansion does not always produce the needed refrigeration over the life of the plant and, hence, is not considered as a viable option in most studies. A Joule-Thomson valve, however, is always used as a bypass for the other options.

A comparison of the alternative process designs must take into consideration capital and life-cycle operating and maintenance costs, technical issues and equipment integrity, number of vessels and rotating equipment, availability and reliability, personnel safety, and environmental issues. A schematic of dew point control by using a turboexpander in an ethylene plant is shown in Figure 3-15, and a schematic of dew point control using a turboexpander in a gas plant is shown in Figure 3-16.

An early study involving a gas processing plant design for an offshore platform in the North Sea was performed in the early 1970s. This study indicated that the turboexpander option contained fewer vessels and equipment. The study results are listed in Table 3-6; note that the turboexpander also represented the option with the lowest operating cost. This plant processed natural gas from a condensate reservoir in a dense phase state.

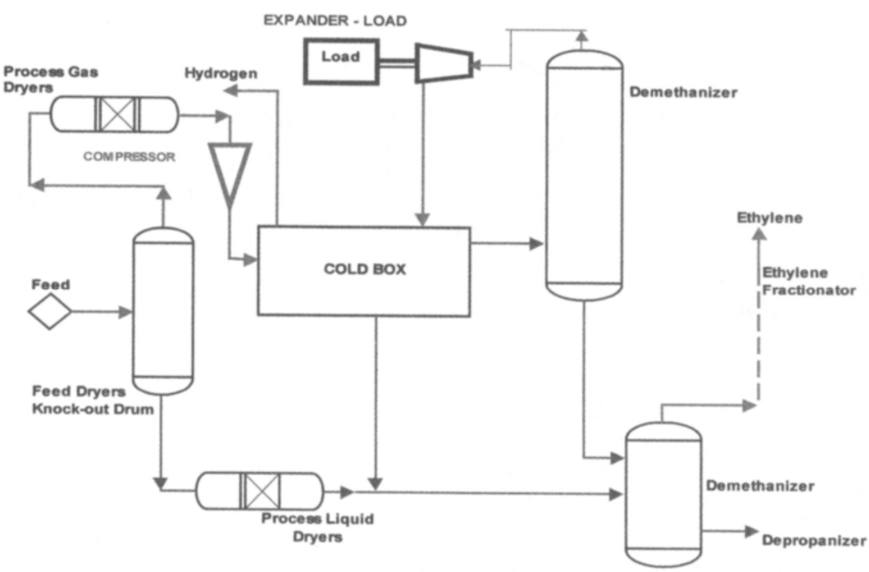

Figure 3-15. Dew point control in an ethylene/MTBE plant.

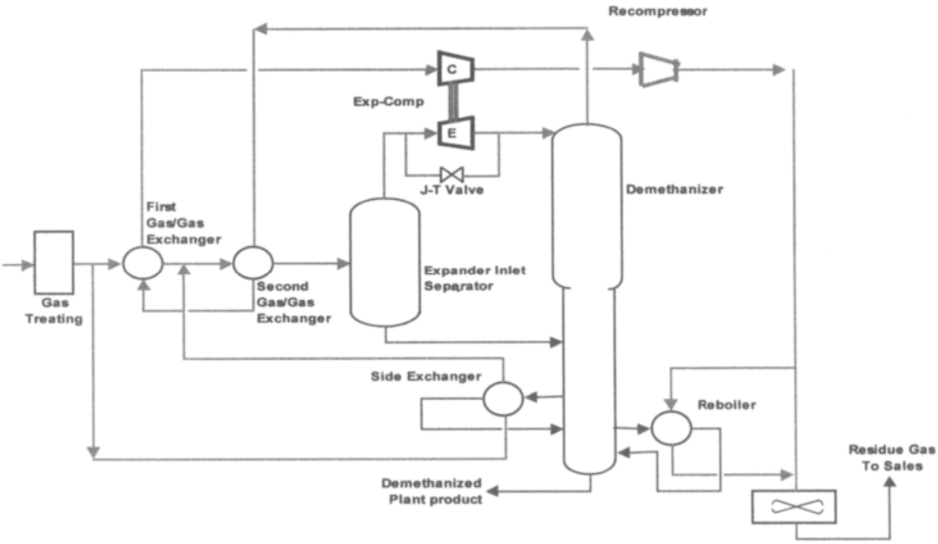

Figure 3-16. Dew point control in a gas plant.

Table 3-6
Comparison of equipment requirements (an offshore 2.5 MMscmd plant)

	Refrigeration plant	Turboexpander plant
Pressure vessel	12	4
Heat exchangers	25	7
Storage tanks	5	2
Towers	4	0
Heaters	2	1
Compressors	3	3
Dehydrators	3	3
Filters	0	2
Turboexpanders	0	1
Total	72	23
Fuel gas (MMSCFD)	2.02	1.8 (10.9%)
Electric power (Kw)	500	212 (57%)

In a similar study, Exxon describes an onshore plant where once again gas processing with a turboexpander was chosen over the other alternatives. The results of that report are detailed in Table 3-7.

One of the most comprehensive economic studies was done in two phases. The first phase addressed whether the location of the treating facilities should be offshore or onshore. The second phase evaluated the process design options. The outcome of the first phase recommended onshore natural gas treating facilities; the second phase recommended implementation of the turboexpander process design. The process options evaluated for this project are listed below:

Option 1:	Initial Installation—Joule-Thomson Expansion
	Future Installation—Propane Refrigeration
Option 2:	Turboexpander Throughout the Project Life
Option 3:	Initial Installation—Turboexpander
	Future installation—Propane Refrigeration

A further detail of this study included sensitivity analysis for the area of heat exchangers, discount rate, and fuel cost. The results are listed in Table 3-8. Option 2, the turboexpander scheme, was selected in terms of energy and maintenance savings, as well as enhanced reliability, availability, and safety.

THERMODYNAMIC BEHAVIOR OF HYDROGEN/NATURAL GAS MIXTURES

The process gas of ethylene plants and methyl tertiary butyl ether plants is normally a hydrogen/ methane mixture. The molecular weight of the gas in such processes ranges from 3.5 to 14. The thermodynamic behavior of hydrogen/methane mixtures has been and continues to be extensively researched. The gas dynamic design of turboexpanders, which are extensively used in such plants, depends on the equations of state of the process gas. Optimum performance of the turboexpander and associated equipment demands accurate thermodynamic properties for a wide range of process gas conditions.

The existing equations of state (i.e., Benedict-Webb-Rubin (BWR), Soave-Redlich-Kwang, and Peng-Robinson) have some practical limitations. The equations of state developed by the University of Illinois

(text continued on page 76)

Table 3-7
Comparison between expander plant and conventional plants

	Process power (Kw) consumed	Process cooling duty (Kw)	No. of items of equip.	Total power consumption	
				Optimum (Kw)	Deviation (conventional) (Kw)
External refrigeration with no recycles	9,000	19,400	38	28,400	+250
External refrigeration with gas recycle	8,800	20,200	36	29,000	+850
External refrigeration with NGL recycle to LP separator	9,150	19,000	33	28,150	0 (Base)
Turboexpander with NGL recycle to LP separator	8,650	18,750	30	27,400	–750

Table 3-8
Sensitivity analysis
(Net present value: $1,000,000)

	Option 1	Option 2	Option 3
Power imported from the national grid			
Fuel cost at .033 $/standard m^3			
Discount rate at 10%			
Minimum area heat exchanger	184.33	181.00	186.83
Maximum area heat exchanger	180.50	183.67	188.67
Power imported from the national grid			
Fuel cost at 0.133 $/standard m^3			
Discount rate at 10%			
Minimum area heat exchanger	224.67	220.00	224.17
Maximum area heat exchanger	219.50	220.50	226.33
Power imported from the national grid			
Fuel Cost at .0706 $/standard m^3			
Discount rate at 7%			
Minimum area heat exchanger	267.17	262.67	269.50
Power imported from the national grid			
Fuel Cost at 0.282 $/standard m^3			
Discount rate at 7%			
Minimum area heat exchanger	330.33	324.83	329.00
All power generated on the site			
Fuel cost at .0706 $/standard m^3			
Discount rate at 10%			
Minimum area heat exchanger	117.17	110.33	119.00
All power generated on the site			
Fuel cost at 0.282 $/standard m^3			
Discount rate at 10%			
Minimum area heat exchanger	247.17	240.00	243.50

(text continued from page 73)

also have only a limited range of applications. By using the various equations of state, especially in the vapor-liquid equilibrium region, research by Zudkevich and Joffe showed that various model predictions are not the same and that they also differ from actual field results. The field data collected for hydrogen/methane mixtures are in the range of 100–200°F; these mixtures contained some polar components (i.e., H_2S and CO_2).

Thermodynamic properties of hydrogen in hydrocarbon mixtures have been studied in the past by using correlation techniques. Most of these mathematical models are for single-phase gas mixtures with high pressures and warmer than cryogenic temperatures. Process plants such as ethylene plants, Methyl Tertiary Butyl Ether (MTBE) plants, and hydrogen purification plants, operate at medium pressures with cryogenic temperature and in the two phase region. An accurate vapor-liquid equilibrium condition for the hydrogen rich mixture is an essential prerequisite in the design of process plants handling such mixtures.

Zudkevich and Joffe evaluated the available mathematical models for the equations of state of hydrogen mixtures. Evaluations were made using field performance data from several plants. These researchers noted that there are several applications that require accurate thermodynamic data for hydrogen rich hydrocarbons. Some of these applications are listed below.

Methyl Tertiary Butyl Ether (MTBE)

The need for high-octane, unleaded gasoline and clean air has led to an increasing demand for oxygen containing additives to gasoline, such as MTBE. This product reduces the carbon monoxide in the exhaust gas while enhancing the octane number of the gasoline. The process requires refrigeration in which peak cold is generated by expansion of a hydrogen rich hydrocarbon gas. In the process design where refrigeration is achieved by expander trains, the turboexpander feed contains hydrogen mixed with light hydrocarbons up to and including butane.

Ethylene and Propylene Plants

High ethylene recovery from the tail gas that is normally used as a fuel is possible by using a turboexpander. All ethylene process plants using the turboexpander move the gas in two-phase operation. As was mentioned earlier, through a cryogenic process most of the ethylene and almost all of the heavier hydrocarbon components are liquified in one process. In another process, ethylene, is separated from the liquid. Turboexpander feed gas contains hydrogen and light hydrocarbons such as methane, ethane, ethylene and trace acetylene. Many refineries are also using a similar process to fractionate propylene from the liquid feed.

Hydrogen Purification

Traces of impurities such as nitrogen, carbon monoxide and methane may be separated after liquefaction at deep cryogenic temperatures. The preferred process design uses turboexpanders to produce these deep cryogenic temperatures.

All the above applications require accurate thermodynamic data of the hydrogen rich hydrocarbons.

SUMMARY

To recap, a turboexpander is a radial inflow turbine. The expansion process is accomplished in two steps: primary and secondary expansion. Primary expansion occurs in the inlet guide vanes and secondary expansion occurs in the radial wheel. The process is isentropic and thermally efficient with recoverable cold energy. Turboexpanders used in dew point control require the following:

- The turboexpander should tolerate the process gas stream at a saturated state and condensation through the expander wheel.
- Robust rotor design is needed to handle unbalance caused by ice deposits.
- High axial loads must be accommodated and thrust control systems are required.
- Positive shaft sealing must be achieved.
- Systems and component design must be robust when the process gas contains dust particles.
- Design criteria must include high reliability and availability.

In addition to the above, turboexpanders used in LNG rejection and dew point control require that consideration be given to the following:

- The turboexpander must handle a variable process gas flow while maintaining high efficiency.
- The machine must accommodate a wide inlet pressure range.
- The recompressor must cover a performance map of relatively wide-ranging characteristics.

Tables 3-9 and 3-10 show typical examples of turboexpander installations with unique design characteristics. Examples of LNG rejection and dew point control are shown in Table 3-9, while examples for LNG rejection and gas injection are shown in Table 3-10.

ROTOR SYSTEMS FOR TURBOEXPANDERS IN LNG PLANTS

As is the case with turboexpanders for other applications, the preferred choice for LNG machines with oil lubricated bearings is the stiff shaft design. The primary advantage of this design is that it provides excellent shaft control with minimal damage should the rotor become unbalanced. Damage to the blades, ice formation in the wheel, or a liquid slug entering the turboexpander can all cause rotor unbalance. Flexible shaft design requires that a machine run above its critical speed. Any unbalance will cause the center of gravity to shift, often causing excessive vibration and heavy wear of the seals and, in some cases, due to dilution of the lubricating oil, causing severe damage to rotating parts. The stiff shaft design has lower clearance requirements that allow noncontacting seals to be used. Contacting seals eventually wear resulting in a drop in performance and possible

Table 3-9
Typical examples for LNG rejection and dew point control

Application	Onshore	Onshore
Site	St. Fergus	Norway
No. of trains	2	3
Capacity per train (MMscmh)	15	30
Turboexpander power (Kw)	6,000	5,000
Bearing type	Oil lubricated	Magnetic
Bearing environment	Pressurized	Atmospheric
Shaft deal	Labyrinth	Dry face

Table 3-10
Typical examples for LNG rejection and gas injection

Application	Offshore	Offshore
Site	Congo	Nigeria
No. of trains	2	1
Capacity per train (MMscfh)	6	15
Turboexpander power (Kw)	4,000	13,000
Bearing type	Magnetic	Oil lubricated
Bearing environment	Pressurized	Pressurized
Shaft seal	Labyrinth	Labyrinth

failure due to high thrust loads. Journal bearings used in stiff shaft systems are designed to handle high dynamic loads during emergencies. Bearings are rigid to shift the oil film resonance frequency well above the maximum running speed.

The majority of turboexpanders in LNG applications use close-fitting, labyrinth-type seals to minimize seal gas leakage. A lean and warm seal gas is injected into the seal cavity to protect the bearing system from the cold expander process gas. Conical shaft seals still predominate because they have the advantage of preventing liquid accumulation in the seal. For this reason, the seal region tends to eliminate cross-coupling effects and also protects the seal against erosion.

Dry gas seals, when economic considerations allow, are another alternative for reducing gas leakage. Dry face-seal systems have been used successfully and field experience has proven their effectiveness.

MAGNETIC BEARING ROTOR SYSTEMS

The design and manufacture of active magnetic bearings has advanced in the last decade. The list of successfully installed turbomachines with active magnetic bearings is growing rapidly and ever-larger turboexpanders are being fitted with these bearings. A cross-section of a rotor supported by magnetic bearings is shown in a later chapter. Two rolling ball bearings are used as auxiliary bearings to support the rotor when the magnetic bearing system is not powered and levitating and in the event of a crash-landing. The bearing environment is isolated from the process gas by a dry-face or dry-gas seal. This isolation is achieved by the dry-gas seal having both inboard and outboard labyrinths.

The vented cavity is located between the runner and the outboard labyrinth where nitrogen is injected into the outboard labyrinth. Outward leakage of nitrogen dilutes natural gas that leaks through the dry-face seal and diluted natural gas is vented to an atmospheric flare system. Inboard nitrogen leakage, on the other hand, enters the bearing housing. This leakage accomplishes both cooling of the rotor and purging of the bearing housing. The fact that the active magnetic bearing environment is always purged with nitrogen qualifies this bearing housing for certification by certain air quality regulatory agencies.

SIDE LOAD ISSUES

Gas dynamic radial loads are not considered in oil bearing rotor systems because the load capacity of oil bearings is quite high. On the other hand, the design of radial magnetic bearings is based on both rotor dynamic and gas dynamic criteria. Rotor dynamic analysis is performed based on conventional design parameters such as rotor weight, bearing span, and bearing stiffness. Evaluating gas dynamic radial loads, however, is a challenging task. Computational fluid dynamics is employed to estimate gas dynamic radial loads that, for the most part, are due to non-uniform pressure fields around the expander and compressor wheels. Non-uniform pressure fields create non-uniform density and, therefore, the wheels' reaction to resistance produces non-uniform radial load. The radial loads on expander and compressor wheels are transferred to the bearings.

The Congo turboexpander mentioned in Table 3-10 is equipped with active magnetic bearings with a pressurized bearing housing vented to the compressor inlet. Even though the turboexpander discharge contains 25% condensates, the gas loading on the magnetic bearing is negligible. This is due to the design of the fluid passage to avoid any non-uniform pressure distribution around the expander wheel.

TURBOEXPANDER AVAILABILITY

As discussed earlier, the drive for more economical design of gas plants has contributed to trends toward constructing single train plants, units of greater power, and units of higher gas volume capacity. Because of the elimination of spare units, single train plants require units of high reliability. Turboexpanders have proven to be of high availability and reliability. The availability of several turboexpander

Table 3-11
Turboexpanders with oil bearings

Plant	Availability
Turboexpander compressor Dew point control duty AMOCO Empress Plant, Canada	99.80
Turboexpander compressor Dew point control duty TOTAL St. Fergus Plant, UK	99.86
Turboexpander generator Power recovery Mammoth Pacific Plant, USA	99.50
Turboexpander generator Power recovery Steamboat Geo Plant, USA	99.80

Table 3-12
Turboexpanders with active magnetic bearings

Plant	Availability
Turboexpander compressor Liquid rejection/oas injection application ELF Congo, N'Kossa, Congo	99.95
Turboexpander compressor Ethylene Plant QGPC, Qatar	99.95

units with oil bearings is shown in Table 3-11. Table 3-12 illustrates availability data of turboexpanders with active magnetic bearings.

The above data shows that field operation of turboexpanders for treating natural gas from condensate reservoirs, as well as from associated and nonassociated gas reservoirs, is more economical in comparison with other treating methods. These machines have proven to be highly reliable. Moreover, recent design features and technology have enhanced their performance to the point where the achievable energy and operating cost savings cannot be ignored.

BIBLIOGRAPHY AND RECOMMENDED READING

1. Salama C. and Eyre D. V., *Chem. Eng. Prog.* 63, No. 6, pp. 62–67, 1967.
2. Swearingen, J. S., *Oil and Gas Journal,* Oct. 6, 1969.
3. Becket, R., *Linde Reports on Science and Technology,* No. 8, pp. 3–5, 1966.
4. Din, F., *Thermodynamic Functions of Gases,* Vol. 3, Butterworths, 1961.
5. Longwell, P. A. and Kruse, J. W., *Adv. Cryo. Eng.* 15, pp. 18–27, 1970.
6. Ward, D. E., Chapter 19 in *Advanced Cryogenics.* C. A. Bailey, Ed. Plenum Press, 1971.
7. Emery, W. B., Sterrett, E. L., and Moore, C. F., *Oil and Gas Journal,* Jan. 1, 1968, pp. 55–59.
8. Ritter, C. L., *Chem. Eng. Prog.* 58, No. 11, pp. 61–69, 1962.
9. Barber, N. R. and Haselden, G. G., *Trans. Instr. Chem. Engrs.* 35, pp. 77–86, 1957.
10. Linnett, D. T. and Smith, K. C., *Adv. Cryo. Eng.* 15, pp. 8–17, 1970.
11. Stokes, B. K., Expander Plants, Exxon Production Research Company, July 1981.
12. Swearingen, J. S., "Turboexpanders and Processes That Use Them," *Chemical Engineering Progress,* Vol. 68, No. 7, July 1972.
13. "Application of Active Magnetic Bearings to Industrial Rotating Machinery," printed matter of Bearing Manufacturer S2M, Vernon, France.
14. Ruckert, A., "Program SR3 zur Berechnung der Selbst-und Unwuchterregten Querschwingungen Gleitgelagerter Rotoren mit Zusatzeinfluessen," Forschungsbericht Heft 273 der Forschungsvereinigung Antriebstechnik, Frankfurt/M., Germany, 1990.
15. Wachel, J. C., "Rotordynamic Instability Field Problems," 2nd Workshop on Rotordynamic Instability of High Performance Turbomachinery, Texas A&M University, 1982.
16. Kenneth, E. A. and Robert, X. P, "Influence of Gas Seals on Rotor Stability of a High Speed Hydrogen Recycle Compressor," 17th Turbomachinery Symposium, Texas A&M University, 1982.
17. Agahi, R. R., Ershaghi, B., Leonhard, M., and Ispas, I., "Side Load Effect on Turbomachines with Active Magnetic Bearings," ICMB, Zurich, Switzerland, August 1994.

18. Agahi, R. R., Ershaghi, B., and Baudelocque, L., "Turboexpanders with Pressurized Magnetic Bearings for Off-Shore Applications," MAG '95, Alexandria, VA, August 1995.
19. Agahi, R. R. and Ershaghi, B., "Integrated Monitoring and Controlling of Turboexpander Compressor with Active Magnetic Bearing," Turbomachinery Asia '94, Singapore, July 1994.
20. Agahi, R., Ershaghi, B., Leonhard, M., Bosen, W., and Brunet, M., "The First High Power Natural Gas Turboexpander Compressor with Magnetic Bearings and Dry-Face Seals," Revolve 1992, Calgary, Canada, June 1992.
21. Barnwell, J. and Wong, W., "Expanders Do Payouts Offshore North Sea," 5th Offshore Southeast Asia, Singapore, February 1984.
22. Bird, D., "Efficiency and Reliability of Large Turboexpanders: 25 Years of Operating Experience at Amoco Canada's Empress Facility," AIChE National Meeting, Houston, Texas, March 1997.
23. Brooks, C. R. M. and Noble, C., "The Magnus Challenge-North Sea's Deepest and Most Northern Platform," 64th Annual GPA Convention, Houston, Texas, March 1985.
24. Coyle, D. A., Durr, C. A., De La Vega, F. F., Hill, D. K., and Collins, C., "LNG Plant Design in the 1990's," 74th Annual GPA Convention, San Antonio, Texas, March 1995.
25. Diaz, P. J., "Options to Increase the Condensate Production in a Refrigeration Extraction Plant," 73rd Annual GPA Convention, New Orleans, Louisiana, March 1994.
26. Lillard, J. K. and Nicol, G., "An Operating History of Turboexpanders in the Supercritical Fluid Regime," 73rd Annual GPA Convention, New Orleans, Louisiana, March 1994.
27. McGlashan, R. S. and Hviding, G., "Troll Onshore Development: Balancing Costs, Energy Efficiency, and Emissions," 71st Annual GPA Convention, Anaheim, California, March 1992.
28. Musamma, A., "Improvement of Arun Treating Unit," 73rd Annual GPA Convention, New Orleans, Louisiana, March 1994.
29. Ross, I. and Robinson, T., "Offshore Gas Conservation Utilizing a Turboexpander Based Refrigeration Extraction Cycle," Offshore Europe Conference, September 1981.
30. Engineering Data Book, Natural Gas Processors Suppliers Association, Section 2, Volume 1, 1994.
31. Agahi, R. and Eshaghi, B., "Ethylene Plant Turboexpander Improvements" AIChE, 4th Ethylene Producers Conference, March 31, 1992.

32. Peng, D. Y. and Robinson, D. B., "A Two Constant Equation of State," *I.E.C. Fundamentals,* 15, pp. 59–64, 1976.
33. Soave, G., *Chem. Engr. Sci.,* 27, No. 6, p. 1197, 1972.
34. Benedict, W. and Rubin, *Chem. Engr. Prog.* pp. 47, 419, 1951.
35. Newton, R. H., ibid, 27, 302, 1935.
36. Chao, K. D. and Seader, J. D., *AIChE Journal,* pp. 598–605, December 1961.
37. Grayson, H. G. and Streed, G. W., "Vapor-Liquid Equilibria for High Temperature, High Pressure Systems," 6th World Petroleum Congress, Germany, June 1963.
38. Zudkevitch, D. and Joffe, J., "Correlation and Prediction of Vapor-Liquid Equilibria with the Redlich-Kwong Equation of State," *AIChE Journal,* Vol. 16, No. 1, pp. 112–119, January 1970.
39. Mohsen-Nia, M., Moddaress, H., and Mansoori, G. A., "A Simple Cubic Equation of State for Hydrocarbons and Other Compounds," SPE Paper No. 26667, Proceedings of the 1993 Annual Technical Conference and Exhibition of the Society of Petroleum Engineers, Houston, Texas, 1993.
40. Dresser-Rand (Olean, New York) sales publication, "Power Recovery Expanders," 1999.

CHAPTER FOUR

Application of Hot Gas Turboexpanders

The list of practical applications for hot gas turboexpanders is continuously growing. The following discusses the most common applications.

NITRIC ACID PLANT APPLICATIONS

NITRIC ACID PRODUCTION[1]

Since the first application of turbocompressors (Figure 4-1) in large-scale production of nitric acid as a raw material for fertilizers, explosives, plastics, and a variety of other chemical products, the requirements on processes as well as on rotating equipment have become increasingly demanding. Environmental as well as economic considerations have heavily influenced the development of such plants.

Nitric acid, or "aqua fortis" as it was called in medieval times, has been known and used by mankind for centuries. At first, it was produced by heating a mixture of sodium nitrate (Chile saltpeter) and sulfuric acid. The product obtained was sodium hydrogen sulfate, and the nitric acid vapors escaping during this process were condensed:

$$NaNO_3 + H_2SO_4 \rightarrow NaHSO_4 + HNO_3$$

Nitric acid was generated in this manner prior to the year 1900, and its production depended on the availability of Chile saltpeter. The increasing importance of nitrogen compounds as a fertilizer rendered this method inadequate to satisfy the escalating demand. In 1903, the

[1]*Sources: Sulzer Turbomachinery (Sulzer Roteq) Winterthur, Switzerland, and MAN-GHH, Oberhausen, Germany.*

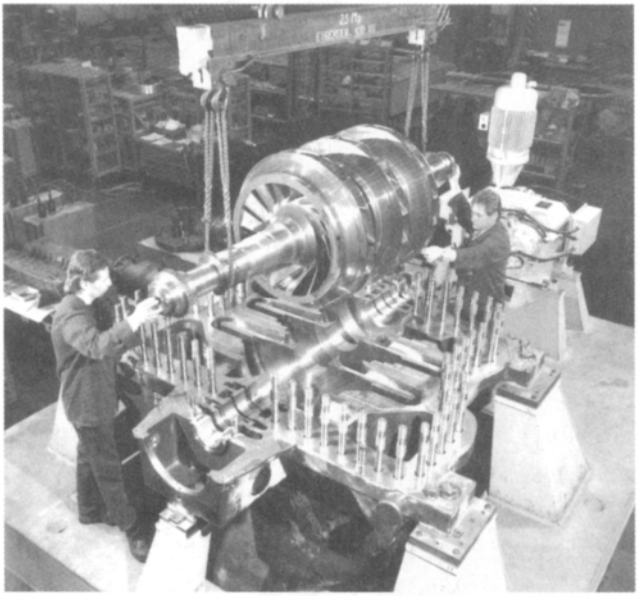

Figure 4-1. Assembling a nitrous gas compressor at a GHH manufacturing plant.

electric arc process was discovered, which enabled the manufacture of nitric acid with air or a mixture of nitrogen, oxygen, and electric energy as basic raw materials.

Figure 4-2 represents a schematic of an early industrial plant employing a compressor to circulate the gas. The pressure level was, of course, rather low, only about 1.3 bar. Air was subjected to a high-voltage electric arc, resulting in the formation of nitrogen oxide (NO). Passing through a system of heat exchangers and a conversion chamber forming nitrogen dioxide (NO_2), the gas finally condensed at low temperature precipitating di-nitrogen tetroxide (N_2O_4) as a snow-like solid. This was further treated to obtain nitric acid ($2N_2O_4 + 2H_2O + O_2 \rightarrow 4HNO_3$). However, the low yield and the amount of electric energy required, prompted the search for more economic production methods.

In 1838, Frederic Kuhlmann discovered the formation of nitrogen oxide (NO) during the catalytic oxidation of ammonia. Wilhelm Ostwald developed the production methods in 1902 and established the base for today's major commercial processes. However, industrial production began only after Haber and Bosch developed the synthesis of ammonia around 1916.

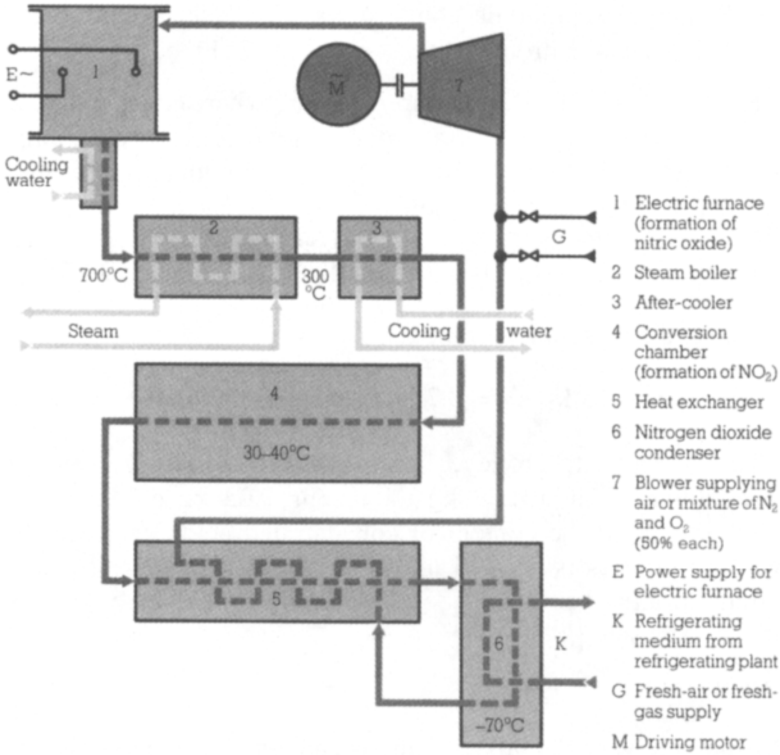

Figure 4-2. Example of a production plant for nitric acid from the nitrogen and oxygen of atmospheric air (electric-arc method).

Suitable stoneware was used to build the earlier plants, limiting the pressure levels. The development of stainless steel gave momentum to the continuing search for process improvements.

Manufacturing Processes

Weak nitric acid at concentrations between 50%–70% is manufactured according to one of the following main processes using air and ammonia as raw materials.

- *Process 1:* Ammonia combustion at atmospheric pressure and absorption of the nitrous gas at 3–12 bar
- *Process 2:* Ammonia combustion at 3–12 bar and subsequent nitrous gas absorption at the same pressure level

- *Process 3:* Ammonia combustion at an intermediate pressure of 2–5 bar and nitrous gas absorption at 7–15 bar

Process 2 is a single-pressure process, whereas processes 2 and 3 are dual-pressure. The overall process equation can be expressed as $NH_3 + 2O_2 \rightarrow HNO_2 + H_2O + 412$ kJ. Introducing the molecular weights into this equation yields

$$17 \text{ kg } NH_3 + 64 \text{ kg } O_2 = 63 \text{ kg } HNO_2 + 18 \text{ kg } H_2O$$

or, using air to supply the necessary oxygen:

$$1 \text{ kg } NH_3 + 16 \text{ kg air} = 3.7 \text{ kg } HNO_2 + 1.06 \text{ kg } H_2O + 12.24 \text{ kg } N_2$$

Theoretically, to produce 1 kg of nitric acid requires at least 0.27 kg of ammonia and 4.33 kg of air (or 1.02 kg of oxygen). These weights refer to the content of concentrated acid. Realistically, however, the process is divided into three successive stages: combustion, oxidation, and absorption.

Combustion

Ammonia vapor is mixed with air and converted into nitrogen oxide at an elevated temperature in the presence of a catalyst, which generally contains noble metals such as platinum and rhodium. The optimal gauge temperature is maintained by controlled ammonia and combustion air preheating. The reaction is highly exothermic:

$$4NH_3 + 5O_2 \rightarrow 4NO + 6H_2O + 907 \text{ kJ}$$

Using air to supply the necessary oxygen, the following quantities of gas are present according to the above equation and given 1 kg of ammonia:

$$1 \text{ kg } NH_3 + 10 \text{ kg air} \rightarrow 1.76 \text{ kg NO} + 1.59 \text{ kg } H_2O + 7.65 \text{ kg } N_2 + 13{,}340 \text{ kJ}$$

Oxidation

Nitrogen oxide is oxidized with the excess oxygen from the previous process phase to form nitrogen dioxide. The reaction is exothermic:

$$2NO + O_2 \rightarrow 2NO_2 + 113 \text{ kJ}$$

The oxidation requires 0.94 kg of oxygen. Using air, the quantities involved are

$$1.76 \text{ kg NO} + 4 \text{ kg air} \rightarrow 2.7 \text{ kg } NO_2 + 3.06 \text{ kg } N_2 + 3{,}330 \text{ kJ}$$

After complete conversion of NH_3 to NO_2, the following total quantities are present:

$$2.7 \text{ kg } NO_2 + 1.59 \text{ kg } H_2O + 10.71 \text{ kg } N_2 = 15 \text{ kg of mixture}$$

Absorption

Finally, the nitrogen dioxide is converted into nitric acid with water and oxygen, theoretically, according to the following formula:

$$4NO_2 + O_2 + 2H_2O \rightarrow 4HNO_2 + 340^* \text{ kJ}$$
(*with 60% acid concentration)

The quantities involved are

$$2.7 \text{ kg } NO_2 + 2 \text{ kg air} + 0.53 \text{ kg } H_2O \rightarrow 3.7 \text{ kg } HNO_2$$
$$+ 1.53 \text{ kg } N_2 + 4{,}990 \text{ kJ}$$

At the end of the process, the total quantities present will be

$$3.7 \text{ kg } HNO_2 + 1.06 \text{ kg } H_2O + 12.24 \text{ kg } N_2 = 17 \text{ kg of mixture}$$

This corresponds to the total weight of primary substances necessary as expressed by the overall process equation, namely, 1 kg of ammonia and 16 kg of air. The total theoretical heat liberated amounts to 21,660 kJ or 5,855 kJ/kg nitric acid.

The changes in the various reactions are never complete; therefore, the amount of air required and, hence, the quantities of gas circulated, are greater than those corresponding to the theoretical reactions.

While nitric acid is being formed, partial reactions occur that lead to a separation of nitric oxide:

$$3NO_2 + H_2O \rightarrow 2HNO_3 + NO + 135 \text{ kJ}$$

The quantities of nitric acid and nitric oxide produced depend on the excess of oxygen and water.

Undesirable Reactions

An oxygen deficiency leads to the burning of ammonia to nitrogen according to

$$4NH_3 + 3O_2 \rightarrow 2N_2 + 6H_2O + 1{,}270 \text{ kJ}$$

Other possible undesirable reactions include:

- Cracking of NH_3 to N_2 and H_2
- Decomposition of NO to N_2 and O_2
- Reaction of NO with NH_3 producing N_2

These reactions can be limited or prevented by proper plant design, correct mixing of the burner gas, and keeping the catalyst activity high. Modern plants convert about 97% of NH_3 to NO.

It is obviously an advantage to recover the large amount of heat liberated, for example in steam boilers and heat exchangers. This is realized after the combustion of ammonia, which occurs at around 900°C. The oxidation of nitrogen oxide to nitrogen dioxide is favored by high pressure and low temperature. Hence, there must be efficient and continuous heat removal by means of water cooling, or by the absorption condensate. The low-temperature heat thus removed must serve purposes other than power generation.

Acid Concentrations

Concentration by simple distillation of weak acid is only possible up to about 68%. Higher concentrations of 80%–90% can be obtained by dehydrating weak acid with sulfuric acid.

Modern processes for strong acid are based on direct oxidation of ammonia with air or oxygen, with the first two steps being similar to the weak acid process. Various processes exist allowing co-production of weak and strong acid.

Weak nitric acid reacts with NO according to the formula

$$NO + 2HNO_3 \rightarrow 3NO_2 + H_2O$$

Further processing of the enriched NO_2 with different and competing methods—some requiring low temperature and others requiring high pressure—results in the production of di-nitrogen tetroxide, N_2O_4. It reacts with air and water to form a high-strength acid of about 85%:

$$2N_2O_4 + O2 + 2H_2O \rightarrow 4HNO_3$$

The resulting nitric acid can be concentrated further by simple distillation.

Plant Pressure Level Considerations

The higher the plant pressure, the lower the capital cost due to lower equipment volume. In other words, the increased wall thickness is more than compensated for in terms of costs by the smaller dimensions of the equipment. Lower pressure, however, gives a higher yield and lower catalyst consumption during ammonia combustion, as well as longer operating time of the catalyst.

A high pressure level results in a higher energy requirement with possibly higher utility costs. On the other hand, today's strict environmental pollution laws with regard to NOx discharged into the atmosphere are easier to meet at higher pressures, and oxidation of NO to NO_2 is favored by increased pressure and low temperature.

Although the turbomachinery is the heart of the plant, it represents only about 15% of the total installation. Therefore, from a cost viewpoint its influence on the chosen process and pressure level is rather small.

Today's tendency to concentrate high production capacities, in excess of about 500 t/d, in single-stream plants has resulted in mostly dual-pressure installations. A medium pressure level is mostly used for catalytic oxidation, and a higher pressure for absorption. For very large single capacity plants, the pressure level moves towards the upper values. A high degree of heat recovery is also gaining more importance.

Figure 4-3 shows ammonia combustion at atmospheric pressure and absorption at gas compressor discharge pressure. This schematic illustrates Process 1 in a low-pressure combustion plant. It also introduces the turboexpander in tail gas service. Figure 4-4 illustrates the size of the machinery involved in composite turbomachinery trains used in nitric acid plants. The gear units in the foreground are located at either end of the four-stage compressor. A typical control and instrument diagram for Process 1 is depicted in Figure 4-5, including additional nomenclature and symbols.

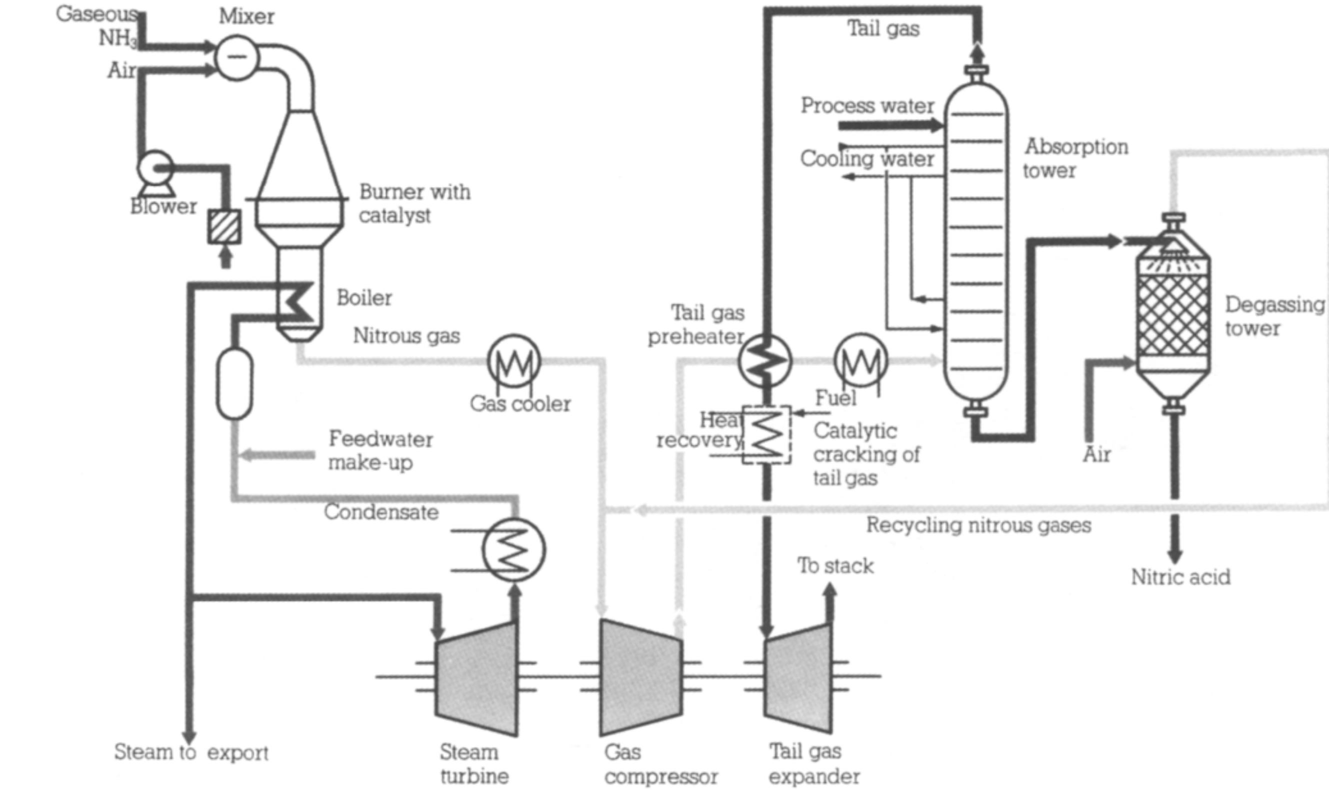

Figure 4-3. Ammonia combustion at atmospheric pressure, absorption at gas compressor discharge pressure of 3–12 bar (Process 1, low-pressure combustion).

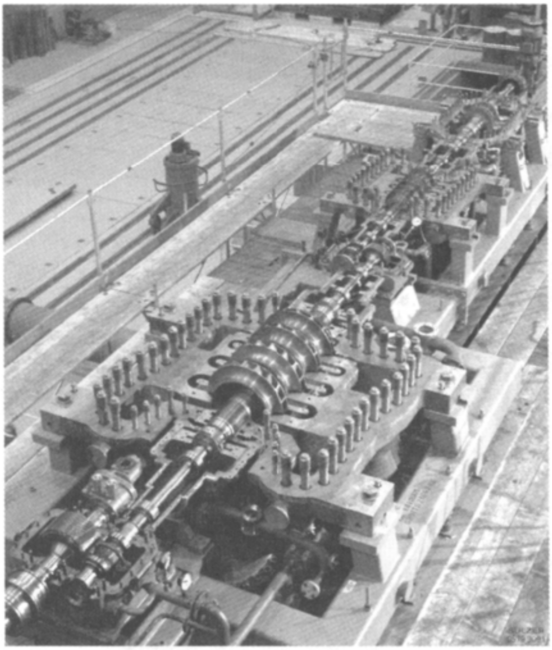

Figure 4-4. Compressor train in Argentina compressing nitrous gases. Mass flow = 26,400 Nm^3/h; Pressures = 0.82/12.8 bar; Power input = 3,390 kW; Power recovered by expander = 1,750 kW.

The elevated pressure in Process 2, shown schematically in Figure 4-6, again includes a tail gas expander as part of the combustion air compressor train (Figure 4-7). A typical control and instrument diagram for Process 2 is given in Figure 4-8. The nomenclature described in Process 1 also pertains here.

Finally, the dual-pressure cycle of Process 3 can be seen schematically in Figure 4-9, and in its physical configuration in Figure 4-10. Note that the lineup starts with the axial flow air compressor to the left, the radial flow nitrous gas compressor is in the middle, and the expander in the right foreground. Figure 4-11 shows the typical control and instrument diagram for Process 3.

Tail gas expanders are thus an integral part of modern nitric acid plants. However, these turbomachinery trains are also part of a combined turbomachinery train comprised of a prime mover and two or more compressor casings.

(text continued on page 99)

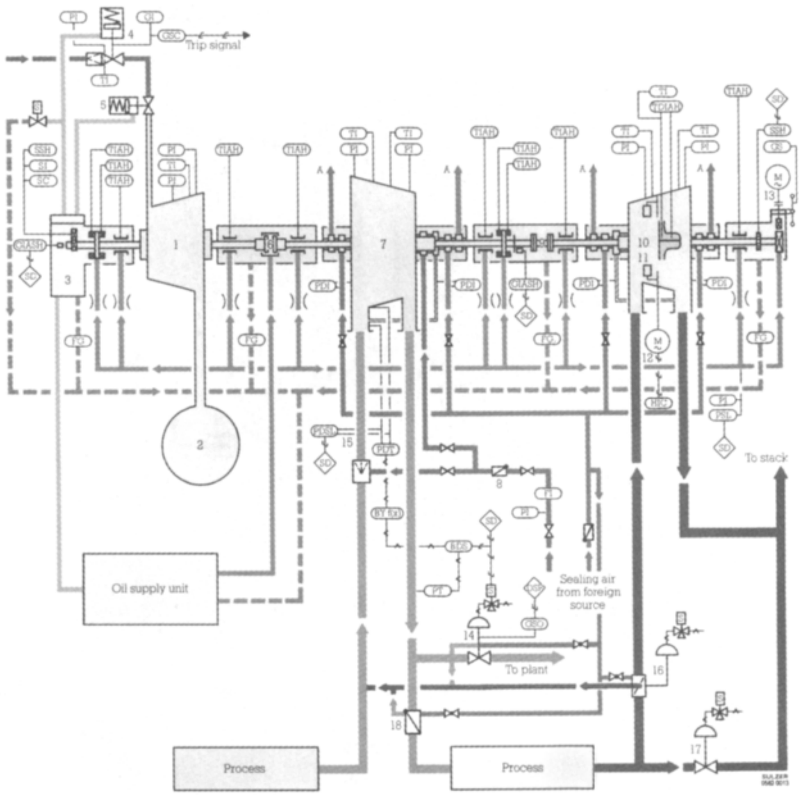

List of reference numbers and functional description

1 Steam turbine
2 Condenser
3 Governor gear block
4 Emergency stop valve
5 Nozzle control valves for speed governing
6 Flexible coupling
7 Nitrous gas compressor (axial or centrifugal type) with air-sealed labyrinth shaft seals
8 Gas compressor steam cleaning facility with steam injection in the compressor suction main and in the discharge-side labyrinth gland
9 Solid coupling with flexible intermediate shaft
10 Tail gas expander without or with adjustable inlet guide vanes (11) and guide vane setting motor (12), labyrinth shaft seals with air sealing
13 Turning gear
14 Gas compressor anti-surge (ON–OFF) control circuit, comprising transmitters, computers and pneumatic control valve
15 Reverse flow protection (on axial compressors only) as supplementary protection device against surging, working independently of the control circuit
16 Expander emergency stop valve with pneumatic actuator and solenoid valve
17 Expander bypass (stack) valve with pneumatic actuator and solenoid valve
18 Non-return valve

Figure 4-5. Typical control and instrument diagram for Process 1.

Line symbols

Nitrous gas
Tail gas
Air
Lube oil supply
Oil return
Control oil supply
Steam
Electric signal line
Pneumatic signal line

Valve and apparatus symbols

Two-way valve
Three-way valve
Butterfly valve
Non-return valve
Valve with control trim
Diaphragm valve actuator (pneumatic)
Piston valve actuator (pneumatic or hydraulic)
Spring
Solenoid valve actuator
Electric motor, ~ AC
A Atmospheric outlet
FC Control element closes on failure of auxiliary energy supply
FO Control element opens on failure of auxiliary energy supply
Silencer

Mechanical symbols

Flexible coupling
Solid coupling
Journal bearing
Thrust bearing of tilting-pad type
Gear
Labyrinth-gland chambers

Instrument and controller symbols

The first letter indicates the measured or initiating variable:
P Pressure
T Temperature
PD Pressure difference
F Flow
G Position
H Hand
B Anti-surge control

The succeeding letter indicates the display or output function:
I Indication
A Alarm
S Switch function
C Control
G Sight glass without measurement
Y Relay, computer

The last letter indicates the extreme value at which the alarm/switch function is trigged:
H High
L Low
C Closed
O Open

Switch function processing:
Driver shut-down
Driver start permission

Figure 4-5. ***(Continued)***

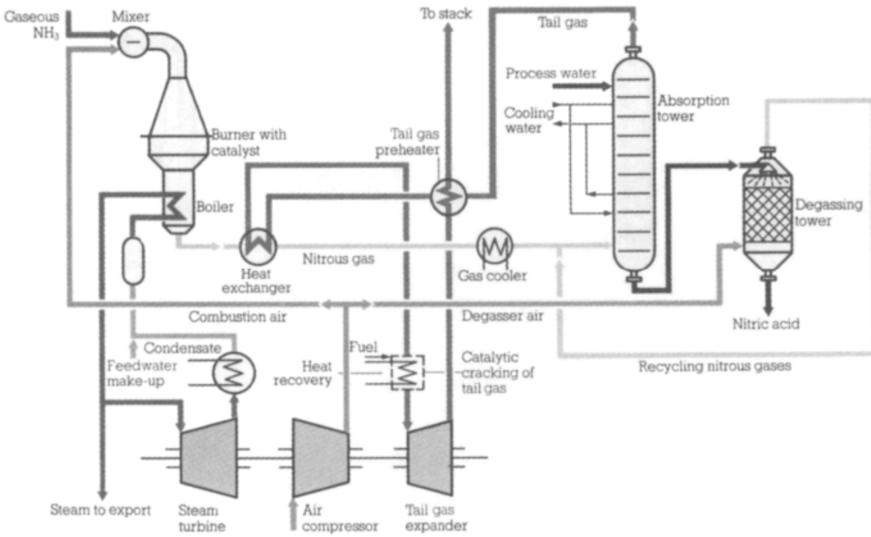

Figure 4-6. Ammonia combustion and absorption at air compressor discharge pressure of 3–12 bar (Process 2, elevated pressure). a = medium pressure, 3–6 bar; b = high pressure, 6–12 bar, with intercooling or booster compressor.

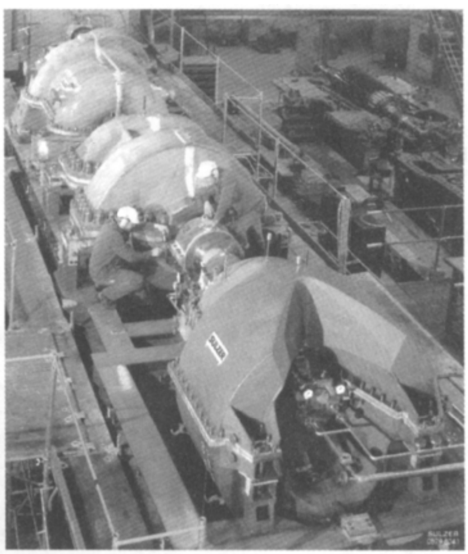

Figure 4-7. Combustion air compressor train. Mass flow = 98,000 Nm^3/h; Pressures = 1.0/7.4 bar; Power input = 10,000 kW; Power recovered by expander = 8,900 kW.

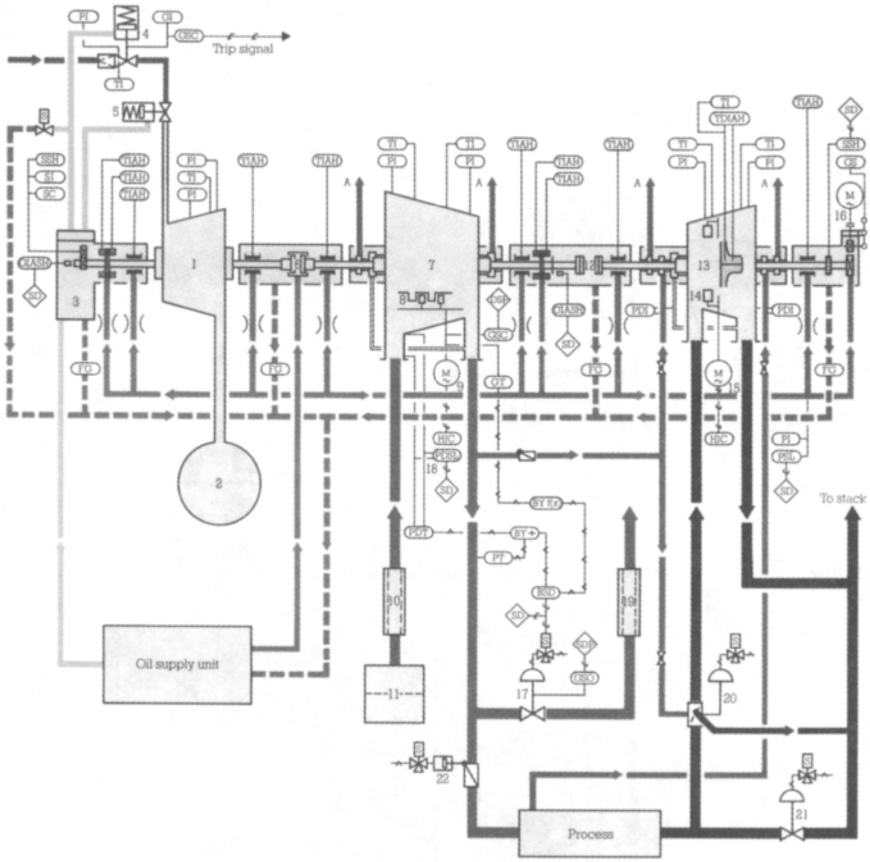

List of reference numbers and functional description

1 Steam turbine
2 Condenser
3 Governor gear block
4 Emergency stop valve
5 Nozzle control valves for speed governing
6 Flexible coupling
7 Air compressor (axial or centrifugal type) without or with adjustable guide vanes (8) and guide vane setting motor (9)
10 Suction line silencer
11 Air intake filter
12 Solid coupling with flexible intermediate shaft
13 Tail gas expander without or with adjustable inlet guide vanes (14) and guide vane setting motor (15), labyrinth shaft seals with air sealing
16 Turning gear
17 Air compressor anti-surge (ON–OFF) control circuit, comprising transmitters, computers and pneumatic blow-off control valve
18 Reverse flow protection (on axial compressors only) as supplementary protection device against surging, working independently of the control circuit
19 Blow-off silencer
20 Expander emergency stop valve with pneumatic actuator and solenoid valve
21 Expander bypass (stack) valve with pneumatic actuator and solenoid valve
22 Non-return valve with pneumatic actuator and solenoid valve

Figure 4-8. Typical control and instrument diagram for Process 2.

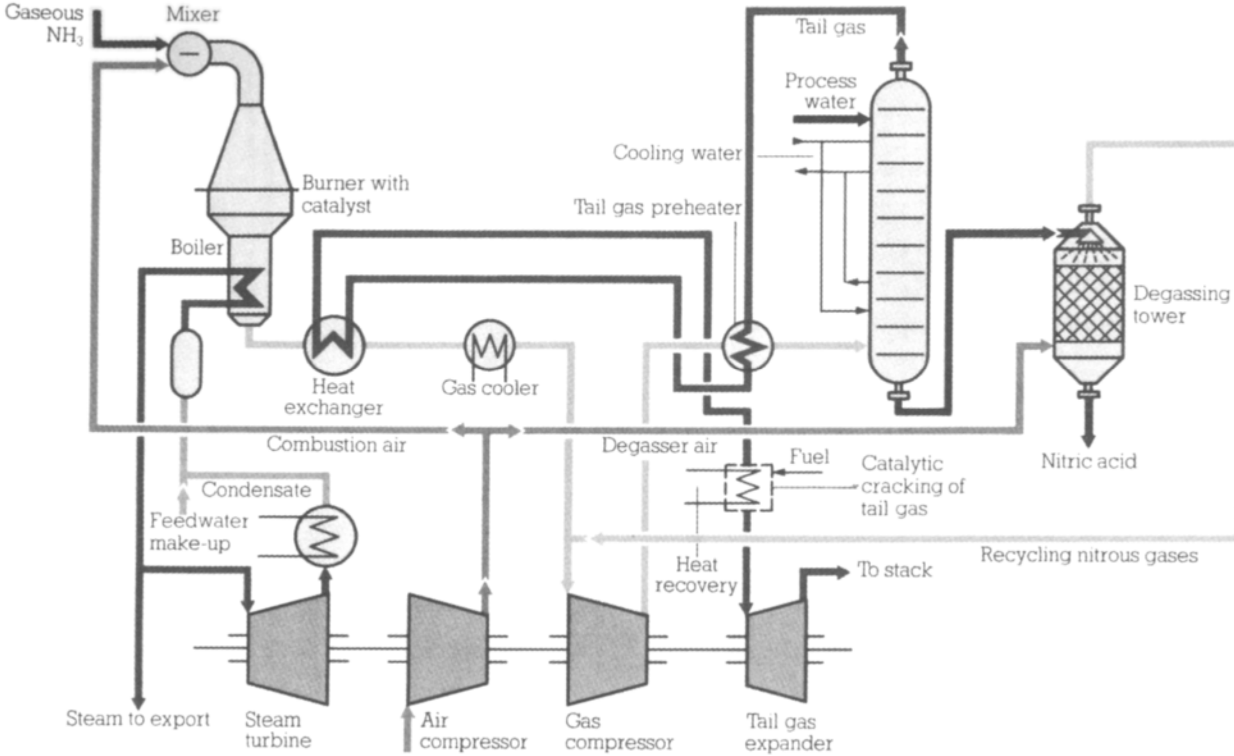

Figure 4-9. Ammonia combustion at air compressor discharge pressure of 2–5 bar, absorption at nitrous gas compressor discharge pressure of 7–15 bar (Process 3, dual-pressure cycle).

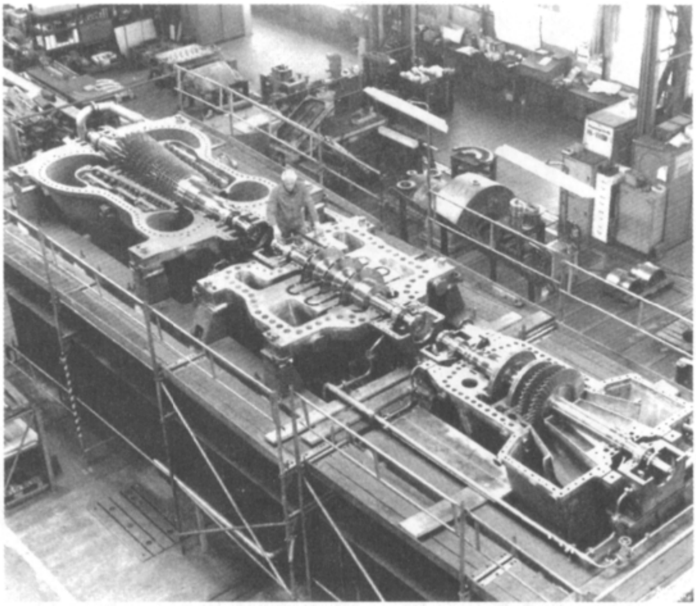

Figure 4-10. Compressor train for dual-pressure installation consisting of an axial flow air compressor with adjustable stator blades and a radial flow nitrous gas compressor and expander. Mass flow: air = 139,000 Nm^3/h, nitrous gases = 122,500 Nm^3/h; Pressure: air = 0.82/4.75 bar, nitrous gases = 4.38/10.8 bar; Power input total = 16,840 kW; Power recovery by expander = 10,950 kW.

(text continued from page 93)

SELECTION AND DESIGN OF TURBOCOMPRESSORS FOR NITRIC ACID PLANTS

Although this book deals almost exclusively with modern turboexpanders, the tail gas expander in nitric acid plants enjoys a somewhat special relationship with the compressors that are almost always associated with this turbotrain.

Centrifugal Compressors

Figure 4-12 presents an overall picture of the compressor duty ranges and machine combinations applied in a typical nitric acid plant, including capacities and pressure ratios. The diagram represents typical

(text continued on page 102)

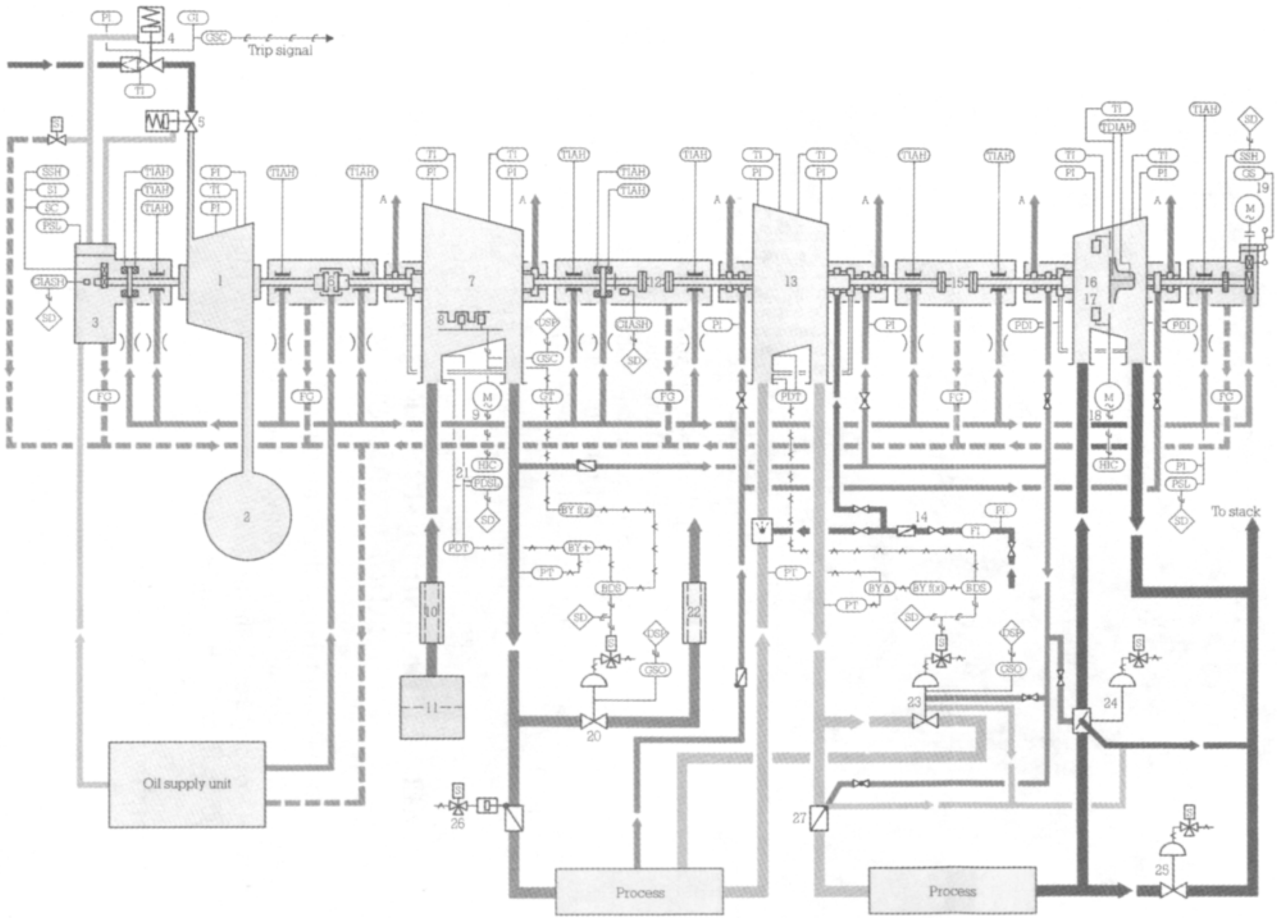
Trip signal
Oil supply unit
Process
Process
To stack

List of reference numbers and functional description

1 Steam turbine
2 Condenser
3 Governor gear block
4 Emergency stop valve
5 Nozzle control valves for speed governing
6 Flexible coupling
7 Air compressor (axial type) without or with adjustable guide vanes (8) and guide vane setting motor (9)
10 Suction line silencer
11 Air intake filter
12 Solid coupling with flexible intermediate shaft
13 Nitrous gas compressor with air-sealed labyrinth shaft seals
14 Gas compressor steam cleaning facility with steam injection in the compressor suction main and in the discharge-side labyrinth shaft seal
15 Solid coupling with flexible intermediate shaft
16 Tail gas expander with or without adjustable inlet guide vanes (17) and guide vane setting motor (18), labyrinth shaft seals with air sealing
19 Turning gear
20 Air compressor anti-surge (ON–OFF) control circuit, comprising transmitters, computers and pneumatic blow-off control valve
21 Reverse flow protection as supplementary protection device against surging, working independently of the anti-surge control circuit
22 Blow-off silencer
23 Gas compressor anti-surge (ON–OFF) control circuit, comprising transmitters, computers and pneumatic recirculating control valve
24 Expander emergency stop valve with pneumatic actuator and solenoid valve
25 Expander bypass (stack) valve with pneumatic actuator and solenoid valve
26 Non-return valve with pneumatic actuator and solenoid valve
27 Non-return valve

Figure 4-11. Typical control and instrument diagram for Process 3.

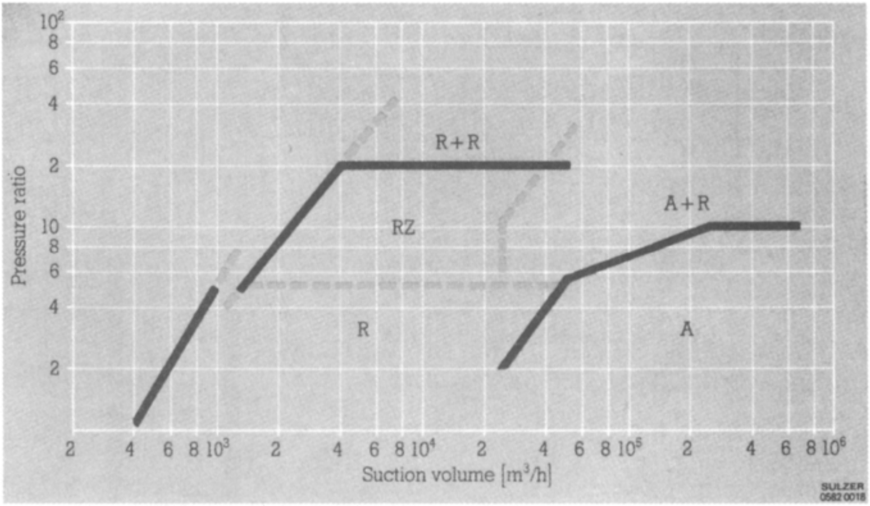

Figure 4-12. Duty range for turbocompressors in nitric acid plants. The diagram refers to atmospheric air and gases with similar properties, such as nitrous gas (A = axial, R = radial flow compressor).

(text continued from page 99)

performance envelopes for the various compressor types. Although it is valid for air, it can also be used for nitrous gas compression since the thermodynamic properties and volume flows for nitric acid facilities are sufficiently similar.

For small flowrates, the single-casing radial compressor without intercooling is employed for delivery pressures of up to 4–6 bar. Higher pressures of up to 15 bar are attained with intercooled machines of single- and double-casing design.

The various application fields in Figure 4-12 are served by the machines illustrated in Figure 4-13 ("RZ") and Figure 4-14 ("R"). R + R indicates two type-R compressors in series, A + R refers to an axial machine followed by a radial compressor, and so forth.

Axial Compressors

Above a minimum intake flowrate of about 50,000 m^3/hr and depending on the required discharge pressure, axial compressors (Figure 4-15) offer certain advantages. Their polytropic efficiencies,

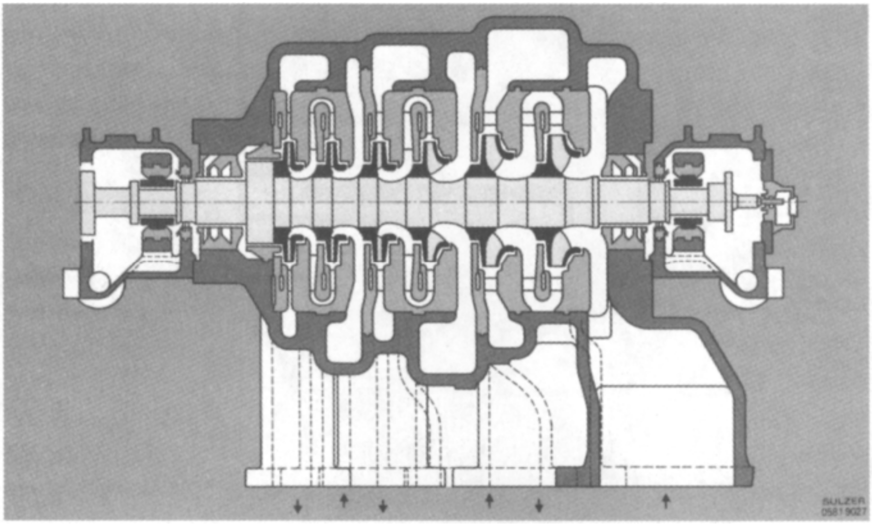

Figure 4-13. Sidestream radial machines of four to eight stages with horizontally split casing and one or two pairs of intermediate nozzles, generally for connecting external intercoolers.

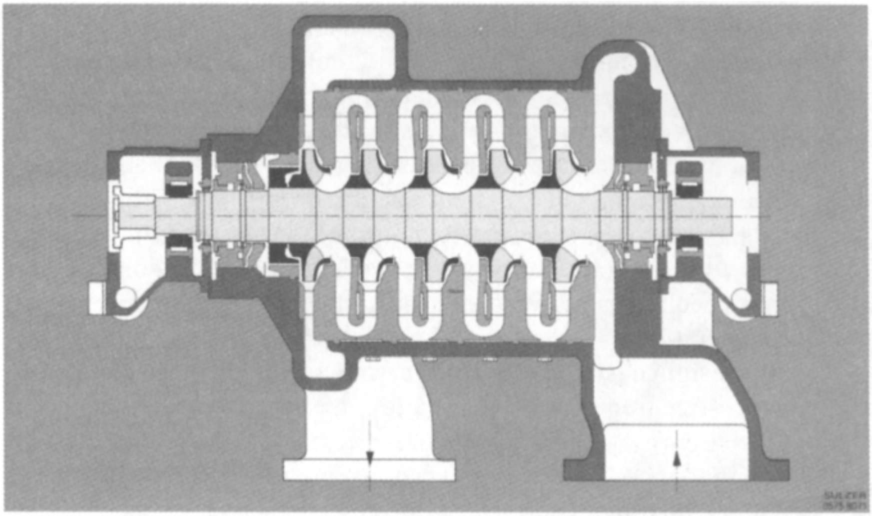

Figure 4-14. Radial machines of one to eight stages with horizontally split casing, partcularly suitable for compressing nitrous gases. There are no dead spaces provoking buildup of an ammonium nitrate salt.

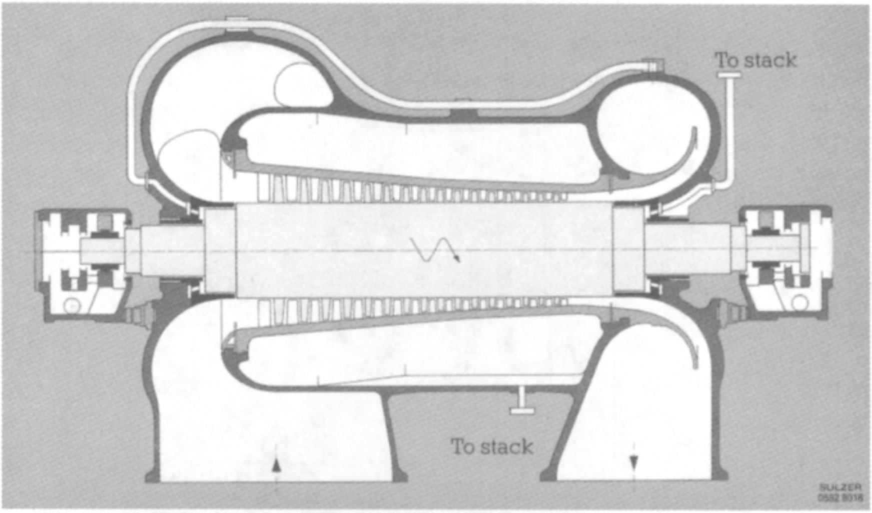

Figure 4-15. Axial compressor with fixed stator blades, double-casing design, and forged monoblock rotor. Particularly suitable for compressing nitrous gases. There are no dead spaces provoking buildup of ammonium nitrate salt.

for a given pressure ratio, are between 3%–7% higher than those of corresponding centrifugal machines.

When used to compress air, the axial compressor may be equipped with adjustable stator blades, either partially (Figure 4-16) or on all stages. In the case of a motor serving as the associated driver or with a generator coupled to the train, the adjustable stator blade feature allows more efficient control than suction throttling. With a steam turbine as the associated driver, stator blade adjustment may be combined with the obvious shaft speed control. This combination allows for special operating conditions, such as startup, or extreme part-load operation.

A well-designed stator blade adjusting mechanism is absolutely maintenance-free, requires no lubrication, and is completely protected against the ingress of dirt or moisture.

The design of an axial compressor is greatly influenced by the degree of its blading reaction. Accordingly, an experienced manufacturer may select two types of blading for its modern turbocompressors, namely one with 50% reaction, the other with 80% reaction, each having its specific merits. The 50% reaction offers such advantages as

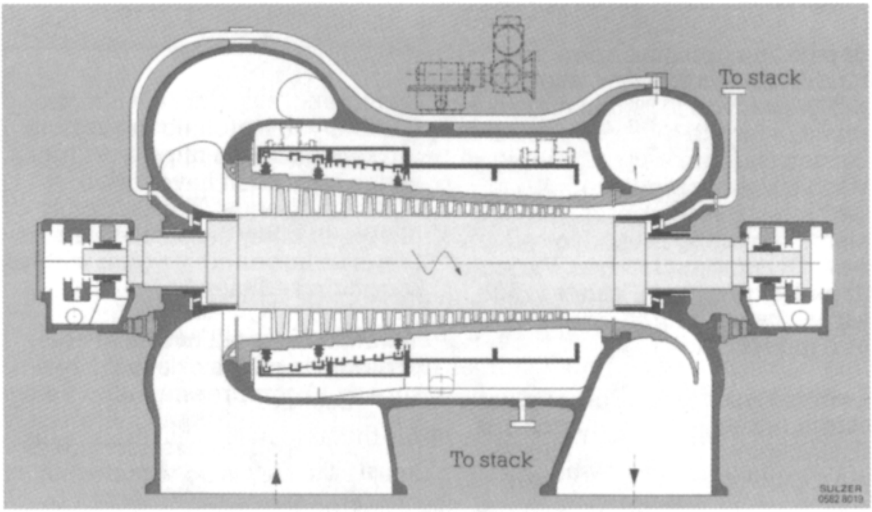

Figure 4-16. Axial compressor with adjustable stator blades, either partially or on all stages. Double-casing design and forged monoblock rotor. This design offers a wide operating range especially in combination with speed control.

- Higher circumferential speed capability due to inherently lower blade tip Mach number
- Higher mass flow at a given speed
- Wide useful flow range by varying stator blade angles
- Steep head flow characteristics for stable operation

With 80% reaction blading, the advantages are

- Higher head per stage at equal tip speed and, therefore, fewer stages to reach a given process pressure ratio
- Wide useful flow range by virtue of variable speed control

Having two degrees of reaction available facilitates the matching of turbocompressors in nitric acid plants, especially in dual-pressure installations, because these two different degrees of reaction may be mixed within the same compressor.

Depending on the operating conditions, the first few stages are of 50% reaction to obtain maximum capacity for the selected speed. In the downstream stages, where Mach numbers are lower due to the higher gas temperatures, 80% reaction blading is used to reduce the total number of stages. Variable stator blade control, either full or partial, can also be used with mixed blading.

A compressor fully equipped with 80% blading reaction turns at a slower speed than one with 50% reaction having the same rotor diameter. This offers flexibility in matching the various turbomachines in nitric acid trains, which often have different optimum speeds. This flexibility often allows eliminating an intermediate gear without sacrificing efficiency.

Whether to install two axial compressors in series or a low-pressure axial compressor followed by a high-pressure radial compressor (for larger capacities and higher final pressure) should be decided by the compressor application engineers. They must select the most suitable layout that will match the speeds of all the associated machine casings for optimum efficiency and life-cycle cost. This speed and performance matching is generally made on the basis of the manufacturer's train performance curves, as illustrated in Figure 4-17.

Shaft Seals

Due to the extremely toxic nature of nitrous gases, losses to the atmosphere must be avoided. Nitrous gas compressors and expanders are fitted with suitable shaft seals, often equipped with connections for seal air and vents to the stack. The simplicity of the seal and its associated system make it a reliable element and easy to maintain.

When labyrinth seals (Figure 4-18) are employed in modern turbomachines, they typically consist of thin, stainless J-shaped steel strips on the rotating part. These J-strips are secured by a caulked-in stainless steel wire and are easily replaceable. Locating the labyrinth strips in the rotating part reduces the risk of heat-induced rotor distortion. If rubbing occurs, the thin metal is likely to become abraded without the casing and the rotor becoming excessively hot.

SELECTION AND DESIGN OF TAIL GAS EXPANDERS

Selection of a tail gas expander depends on the temperature and pressure on the inlet conditions of the nitrous gas. The pressure equals that of the compressor outlet minus the pressure losses in the cycle. Depending on process and plant size, these losses amount to 0.3–2.0 bar. The inlet temperature may vary widely from plant to plant. Figure 4-19 shows an expander in the 10,000 kW power output category.

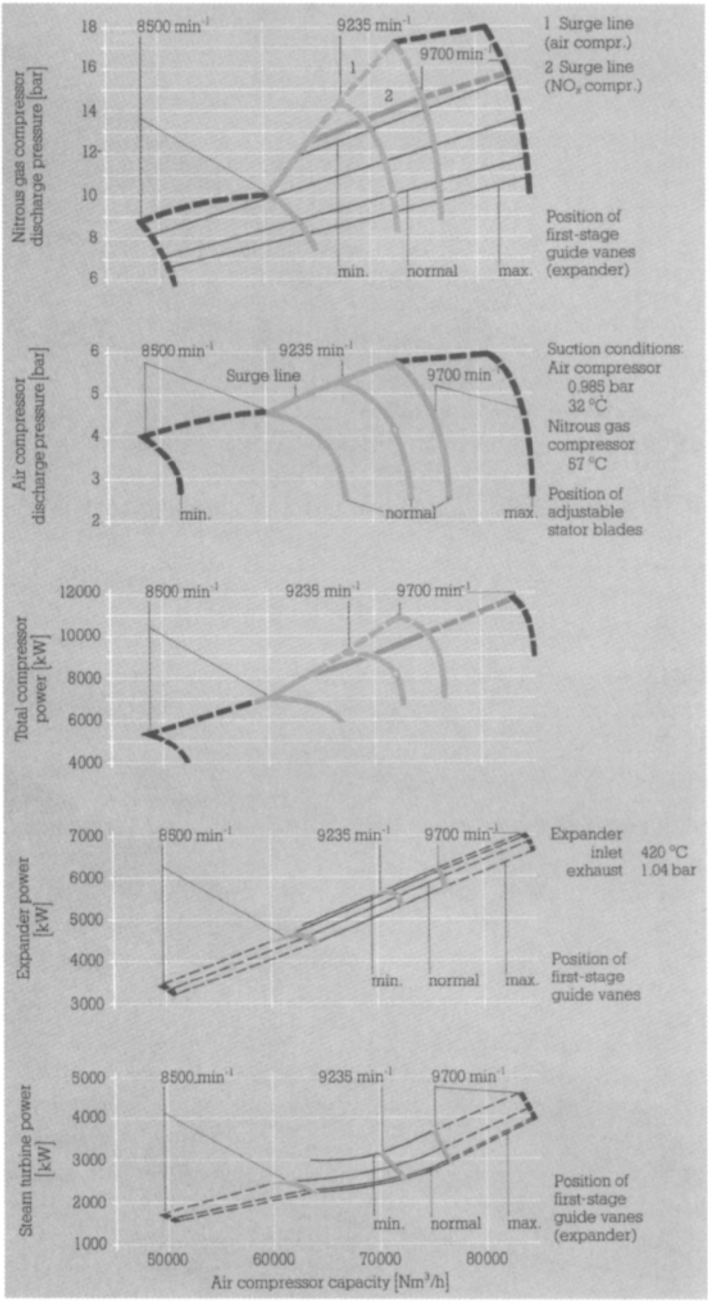

Figure 4-17. Typical performance curves for a turbine-driven compressor train in a nitric acid plant.

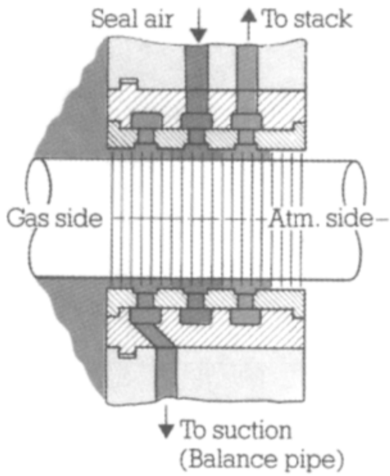

Figure 4-18. Labyrinth seal for nitrous gas equipped with seal air connection.

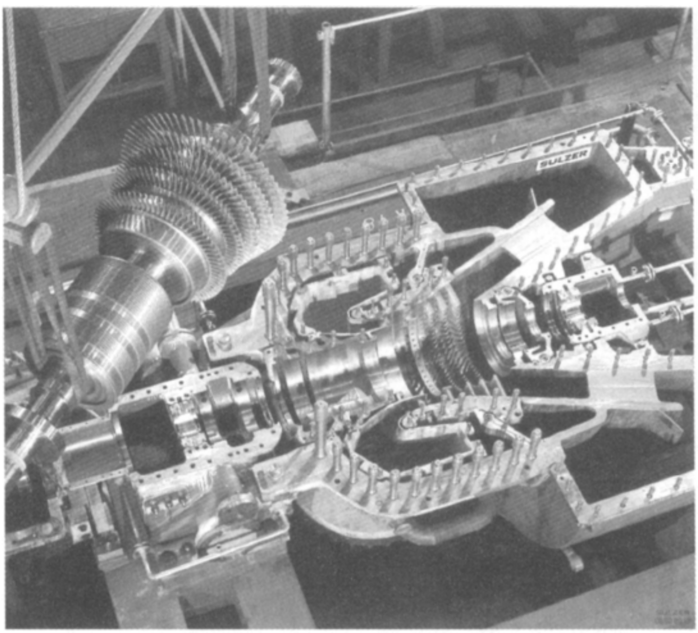

Figure 4-19. Tail gas expander for 7.4 bar, 700°C maximum inlet; and power output at 10,000 kW.

Figure 4-20 shows typical duty ranges of hot gas expanders offered by one major manufacturer.

If the tail gases are heated in counterflow with the hot gases from the compressor outlet, this temperature generally does not exceed 250°C, but it may reach 500°C if heated by the hot combustion gases coming from the burner outlet. One method to reduce the amount of NOx discharged to the atmosphere is catalytic cracking of the tail gas after the absorption column using a fuel rich in hydrogen. Tail gases up to 730°C are thus possible, which permits the compression input power to be covered almost completely by the expander. The reaction yields carbon dioxide and water vapor, neither of which is considered a pollution hazard.

Most of the large tail gas expanders are axial type. Multistage uncooled expanders, illustrated in Figures 4-21 through 4-23, are

(text continued on page 112)

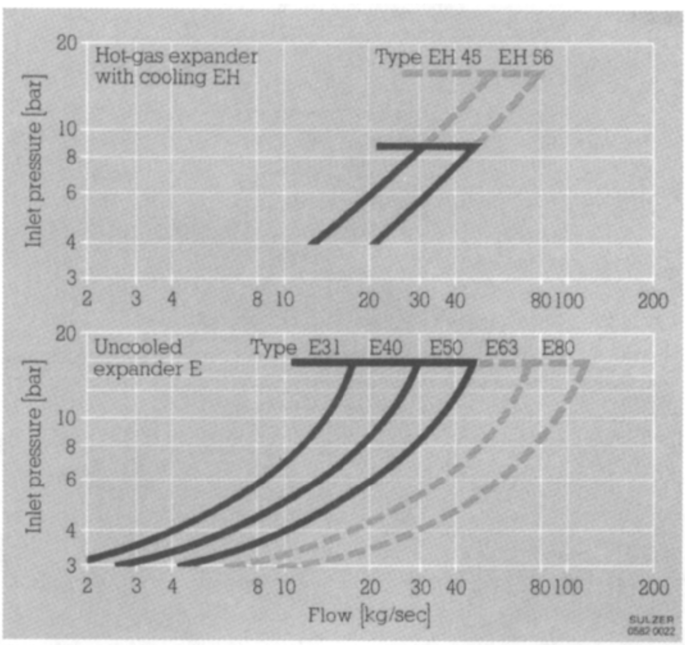

Figure 4-20. Duty range of expanders for nitrous gases in nitric acid plants. The bottom diagram refers to uncooled expanders (inlet temperature 500°C) and the top diagram refers to cooled expanders (inlet temperature 730°C).

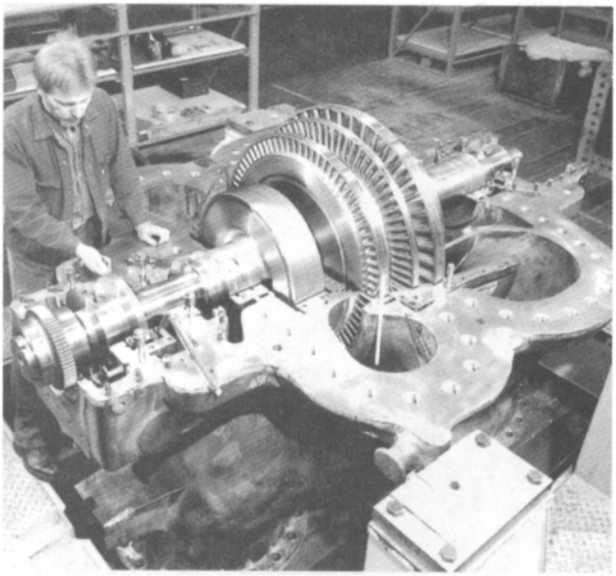

Figure 4-21. Tail-gas expander for a 945-t/day two-pressure nitric acid plant; P = 11,200 kW, n = 5,850 rpm. *(Source: GHH-Borsig.)*

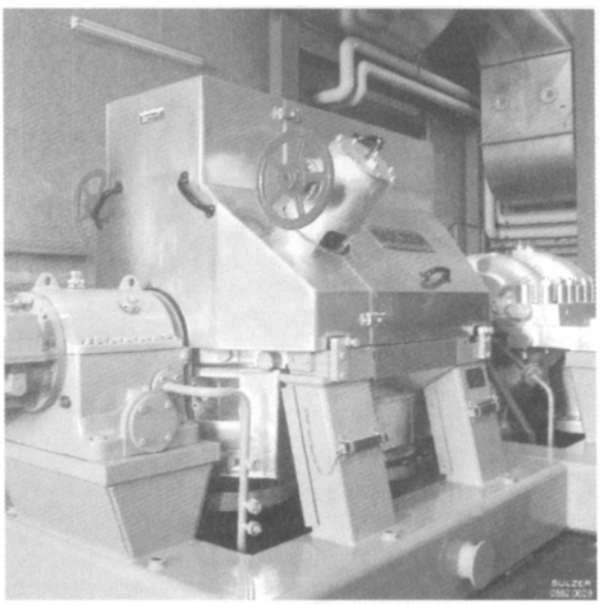

Figure 4-22. Expander with inlet valves. *(Source: Sulzer-Roteq.)*

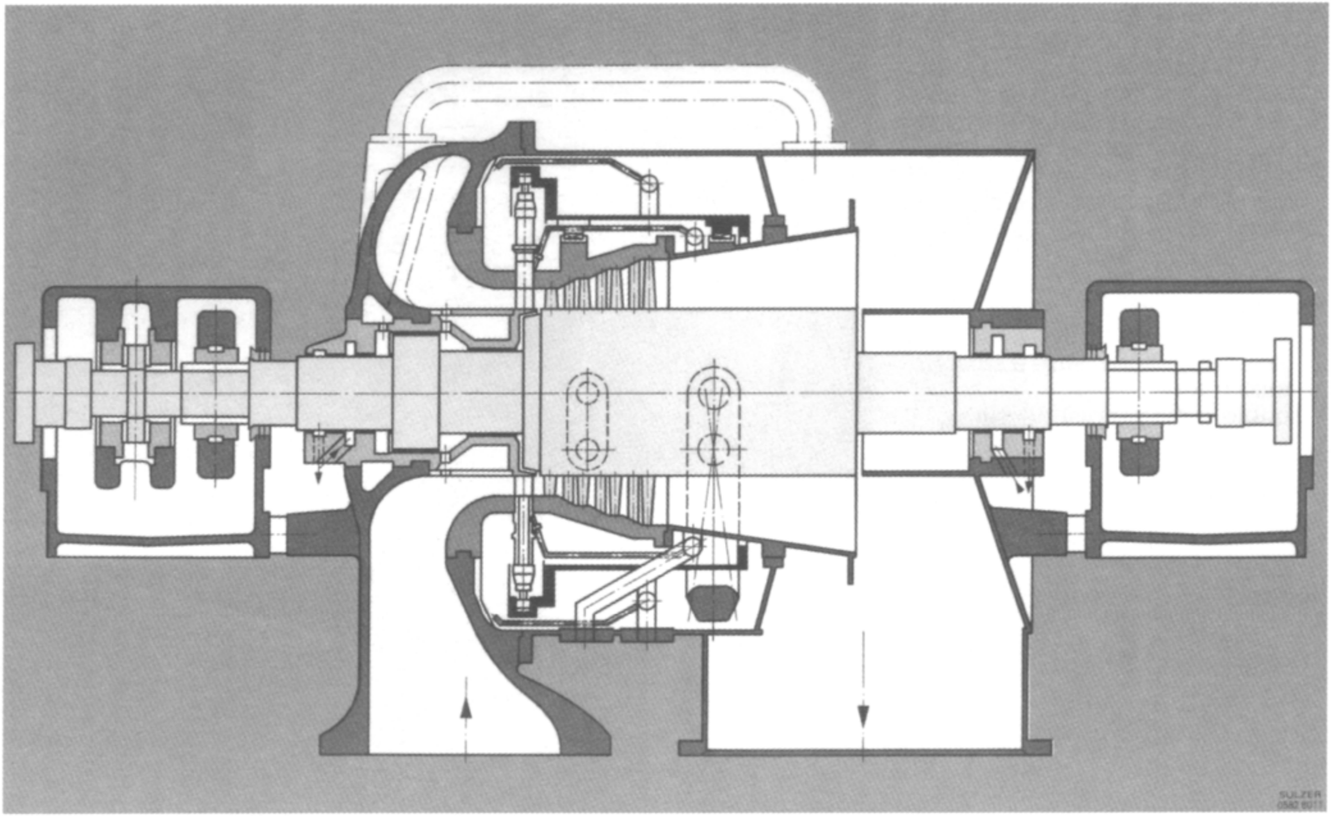

Figure 4-23. Multistage expander cross-section.

(text continued from page 109)

adopted for "low" temperatures (up to 510°C). For higher temperatures, multistage cooled expanders are employed. These expanders are designed directly from the industrial gas turbine. Typical configurations are shown in Figure 4-24.

Uncooled Expanders

Sulzer Turbomachinery (Sulzer Roteq) employs the casing design illustrated in Figures 4-21 through 4-23 for gas inlet temperatures up to 510°C at 13 bar. The maximum design pressure is 17 bar at 485°C; these machines are built with four stages for power ratings up to 20 MW. The ferritic inlet section is made of 12% Cr steel casting, minimizing deformation at high temperature. The exhaust section is of welded design. The rotor blades are mounted in circumferential grooves of the forged monoblock rotor and the rotor is given a full speed balance.

Circumferential grooves in the stator blade carrier take up the blades of the second to fourth stages. The first row of stator blades is adjustable. Circumferential grooves in a separate blade carrier accommodate the stator blades.

Two or four lobe bearings are used in these expanders, determined by the function of the rotor-dynamic requirements. A double-acting thrust bearing may be mounted, if required. Labyrinth seals with connections for seal gas are standard equipment, however, dry gas seals are available.

Using the design and operating experience of adjustable stator blades in axial compressors, major manufacturers use first-stage guide vane adjustment for many expander models. Depending on process requirements and customer preference, the adjustment can be made during operation by an electric motor or manually with the expander at standstill. Expanders equipped with first-stage stator blade adjustment allow for optimal matching to the process conditions and improved efficiency at part-load operation, particularly in combination with guide vane control of the axial air compressor.

Adjusting the stator blades leads to full arc admission at all operating conditions, and blade excitations due to partial admission are thereby avoided. On well-designed hot gas expanders the adjusting mechanism is generally located between the blade carrier and outer

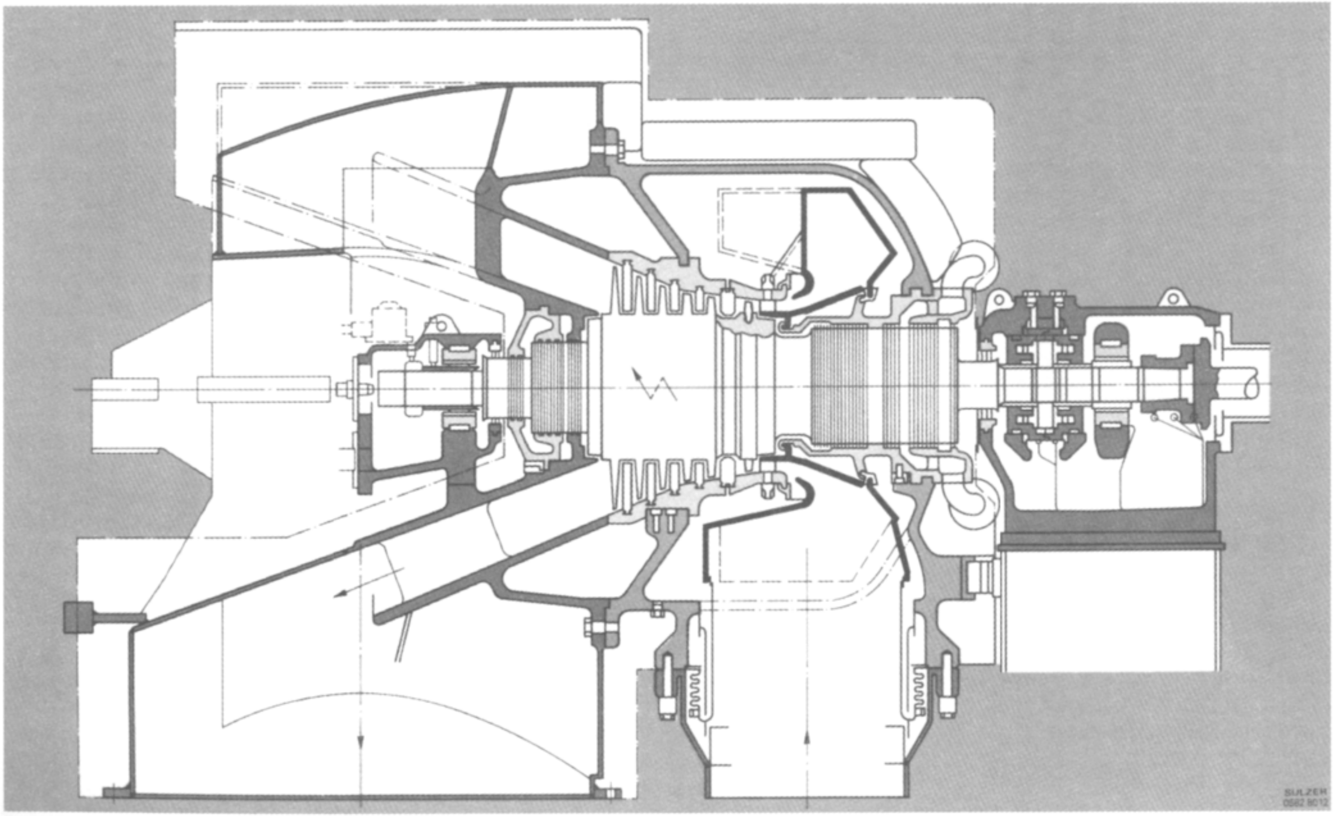

Figure 4-24. Cooled, multistage, hot gas expander.

casing. This ensures it is well protected and essentially maintenance-free. For higher gas temperatures, this space is ventilated by a small amount of air to keep the space temperature below 300°C.

For gas temperatures in excess of 380°C, experienced manufacturers often mount the adjustable guide vanes in special ceramic bearings. The shaft end of each blade is fixed to a lever, which is connected to a hinge-mounted adjusting cylinder. Axial movements of the cylinder open or close the blading.

The smaller framed hot gas expanders are often equipped with two control valves, each controlling a segment of 30% and 20%, respectively, of the total inlet. It is possible to vary the inlet cross-sectional area of these segments, within limits, by later replacing individual nozzles with blind fillers or vice-versa. Other machines may feature full arc admission without control valves.

Cooled Expanders

In many hot gas expanders, cooling air at 200–240°C is admitted to the space between the inner and outer inlet casing. From there, approximately half of the cooling air flow moves to the inlet section of the blade carrier, cooling it from the outside. Additionally, an aerodynamically shaped annular gap produces a film of cooling air on the inside of the blade carrier. Through bores in the blade carrier and the second-stage stator blade, a portion of the air flows to the rotor surface, cooling the downstream section of the rotor.

The second half of the cooling air flow is directed to the front end of the rotor and from there through an aerodynamically shaped annular gap to the rotor surface, forming a film of cooling air down to the second stage. A small portion of this latter air flow is diverted to the labyrinths for sealing and cooling purposes.

SELECTING A PRIME MOVER FOR TURBOTRAINS IN NITRIC ACID PLANTS

Just as compressors are an indispensable element of the turbotrain of which the hot gas expander is a part, so is the principal driver. Therefore, the following briefly highlights the more important aspects of these drivers.

The considerable amount of heat generated in nitric acid plants suggests that steam be produced and used to drive the compressors.

Energy recovery has been standard practice from the early days of ammonia oxidation plants; with escalating energy costs energy recovery is becoming increasingly important.

Modern nitric acid plants are designed for energy self-sufficiency during normal operation. Except for the startup phase, process heat generated will equal energy consumed by the compressors. Moreover, in many cases surplus energy can be exported in the form of steam, for example.

The difference between the power consumed by the compressor train—the biggest consumer of energy—and the energy recovered by the expander is compensated for by an additional driving unit. Depending on the process, this machine is required to supply from 5%–85% of the compression power in normal operation.

The tail gas leaving the absorption tower is available at elevated but low temperature. To exploit it for energy recovery in an expander, it must be suitably heated. The higher the tail gas temperature entering the expander at equal mass flow and pressure, the higher the expander output is and, consequently, the required normal operating power of the associated prime mover or "complementary driver" is smaller. However, the heat used to increase the temperature of the tail gas is no longer available to produce useful steam. The plant designer must, therefore, optimally split the total available heat. This decision may influence which type of complementary driver is best.

Electric motors may be considered in cases where it is considered advantageous to export surplus steam outside the nitric acid plant. Condensing steam turbines are normally used to bridge the power deficit. Extraction-condensing turbines make it possible to use some of the available steam for heating purposes.

A back-pressure (noncondensing) turbine may also be used if there is a profitable use for intermediate-pressure steam. In the unlikely event that large quantities of steam are required, additional high-pressure steam from an external source might be necessary. However, while it is theoretically possible that the amount of heat generated in the nitric acid plant will be insufficient to cover the entire demand, this is not usually a valid concern.

In cases where low-cost fuel is available, a gas turbine may be chosen. This would obviously make it possible to export the surplus steam. Some compressor trains in nitric acid plants are, indeed, using a gas turbine as the associated or complementary driver.

An energy distribution schematic demonstrating export for power generation, heating, or a combination of both, is shown in Figure 4-25. In this modern plant, efficient heat recovery supplies steam to a district heating system. Electric power generation is demand-based. Suppose during winter less power is necessary to compress the same mass air flow, then more surplus steam would be available. Constant inlet steam pressure, constant speed, and adjustable extraction pressure—each independent from the other—form the control concept. For startup, the system is switched to speed control. The complete control approach constitutes a stand-alone system and the available energy is automatically distributed.

The driving unit must be designed to meet the starting conditions as well as normal operation. At startup it generally must provide approximately 20%–40% of the normal compression power. In a plant using a hot gas expander, the power input at startup may be considerably higher than the drive rating during normal operation. The complementary driving unit must then be dimensioned for overload when starting, which means slightly poorer efficiency during normal operation.

When the power deficit is covered by an electric motor, the initial motor load may be a multiple of its normal power output because the expander is unable to contribute any power at startup. Depending on plant design and startup requirements, a motor power of 50%–75% of the rated compressor power is sufficient for startup purposes. Careful engineering studies are always appropriate in this case.

With a steam turbine, the turbocompressors can be readily matched to the different plant operating conditions. Under continuous load, this type of installation is powered by the steam resulting from ammonia combustion. Consequently, an outside steam supply is needed for startup. This may be a separate boiler or another external source with live-steam properties not necessarily corresponding to those obtained from the nitric acid plant. The steam turbine must be of robust design because of the different pressure and temperature levels.

A range of industrial steam turbines with a choice of reaction and impulse blading are available to satisfy these needs. They virtually guarantee an optimal solution to the various problems encountered when combining compressors, expanders, and turbines to form an efficient, reliable nitric acid train. A typical train is depicted in Figure 4-26.

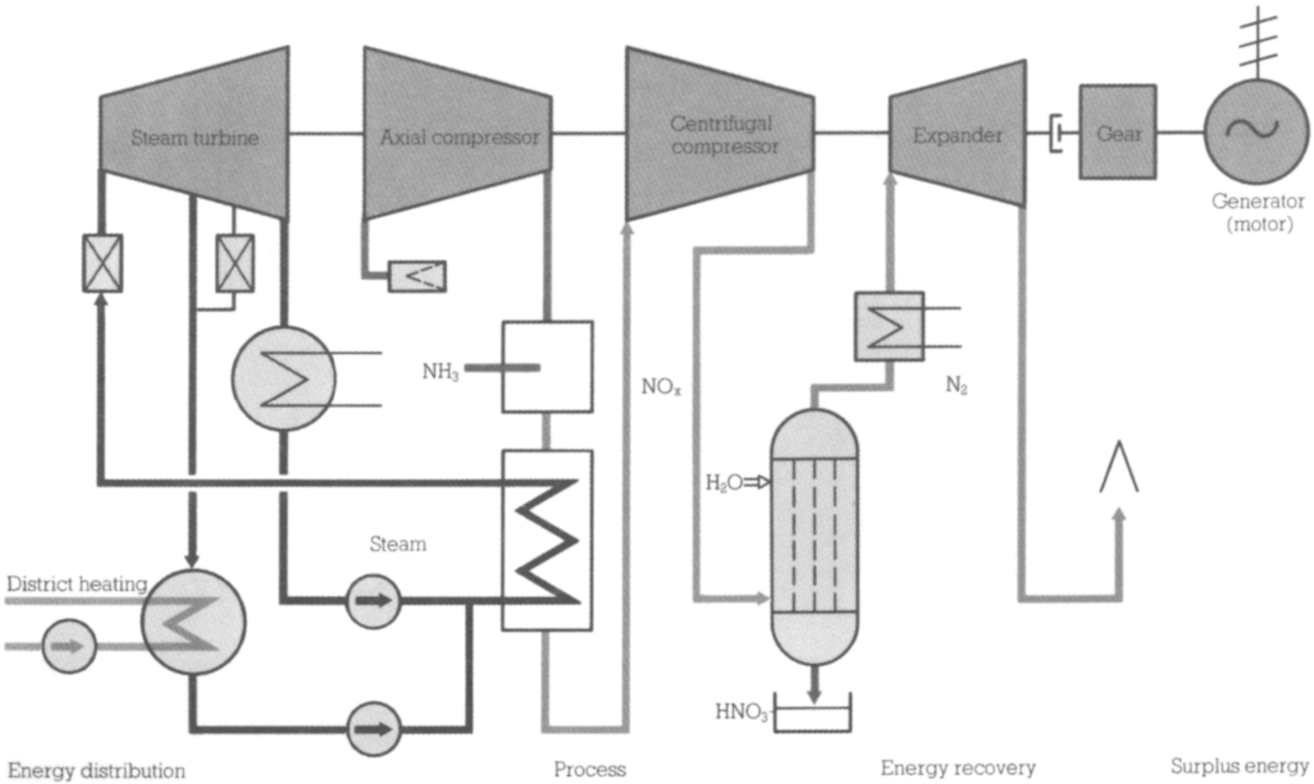

Figure 4-25. Nitric acid plant at Fredericia (Denmark) with a four-machine turbogroup and generator. Power output to district heating system = 0–27 MW; Power output to electric grid = 0–5.8 MW; Steam turbine = 10.8 MW; Axial compressor = 8.2 MW; Centrifugal compressor = 4.1 MW; Expander = 7.4 MW; Nitric acid production = 650 t/d.

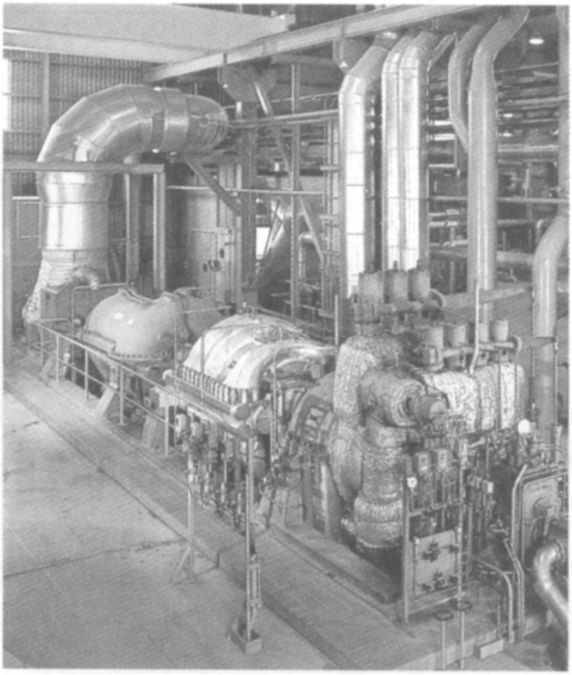

Figure 4-26. Nitric acid plant at Fredericia (Denmark) with turbogroup and generator.

When combining compressors, expanders, and turbines, the speeds, thermal expansions, and thrust loads on shaft systems exist at different magnitudes and directions. These must be managed and accommodated with skill and experience.

Design Considerations

Nitrous gases originating from the combustion units in nitric acid plants carry small amounts of unreacted ammonia, NH_3. The ammonia may react with the nitrous gas to form microscopic particles of ammonium nitrate that adhere to solid surfaces. Within a short time, there is a growing layer of ammonium nitrate salt covering the internal surface of the nitrous gas compressor (Figure 4-27). This layer can obstruct the flow passages because it tends to increase the power consumption, provoke excessive vibrations, and even present a safety hazard since ammonium nitrate explosions can occur.

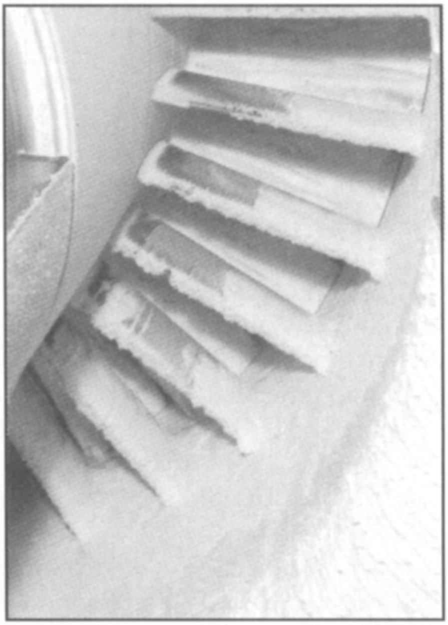

Figure 4-27. Ammonium nitrate salt deposits in the inlet of a nitrous gas axial compressor.

To remove these undesirable but unavoidable salt deposits, a significant amount (about 1% of mass flow) of boiler feedwater at 80–90°C is periodically injected. Injection nozzles are typically located in the inlet section, in the return channels, and in the labyrinth seals on the discharge side of nitrous gas compressors. This periodic flushing of the compressor with water does have certain disadvantages:

- Water droplets may cause erosion, especially in axial compressors
- Water and nitrous gases combine to form nitric acid and cause corrosion
- Ammonium nitrate deposits are not completely removed
- Temperature shocks may cause horizontal flange joints to open, allowing nitric acid to enter

Periodic steam injection at just one suitable location will circumvent these disadvantages and can result in complete and exceedingly rapid (often less than one minute) removal of ammonium nitrate irrespective of the location within the compressor. The two available flushing methods are compared in Figure 4-28.

The entire turbotrain can be "packaged" as shown in Figure 4-29. Providing a special lifting arrangement (Figure 4-30) can greatly facilitate its installation.

Obviously, large turbotrains require modern coupling arrangements. At least one manufacturer, Sulzer-Roteq, makes extensive use of solid couplings between compressors and expanders. The thrust bearing is usually located in the low-pressure compressor.

Solid coupling methods use an intermediate shaft, flexible enough to allow for misalignment of the same order of magnitude as other types of couplings. This intermediate shaft connects the shaft ends of the two machines (Figure 4-31). For direct turbine drive the turbine is generally equipped with its own thrust bearing and coupled to the compressor train with a gear coupling or, preferably, a contoured diaphragm coupling.

If an intermediate gear is necessary, some manufacturers use single helical gears provided with thrust collars on the pinion shaft, as shown in Figures 4-32 and 4-33. The thrust collars not only neutralize the

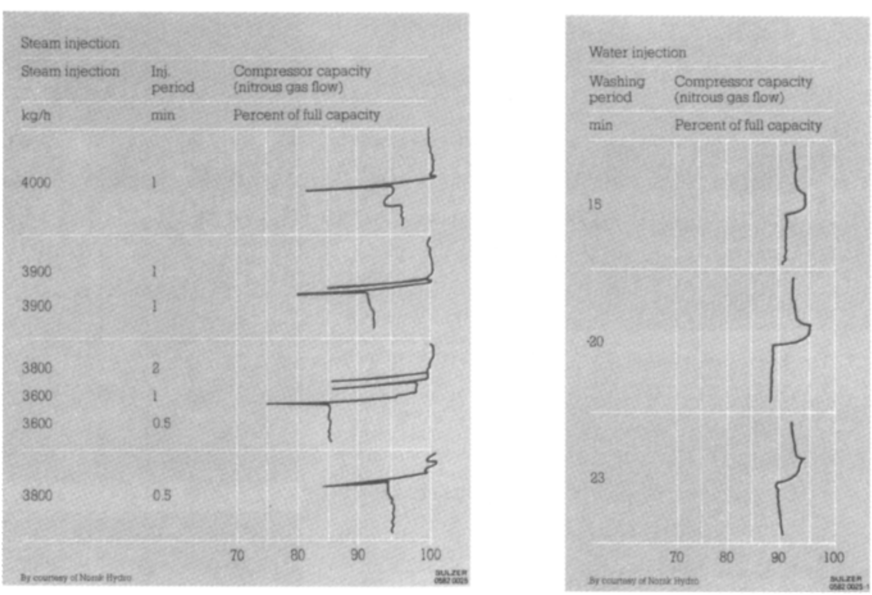

Figure 4-28. Comparison of effect on compressor flow capacity using steam injection and water injection.

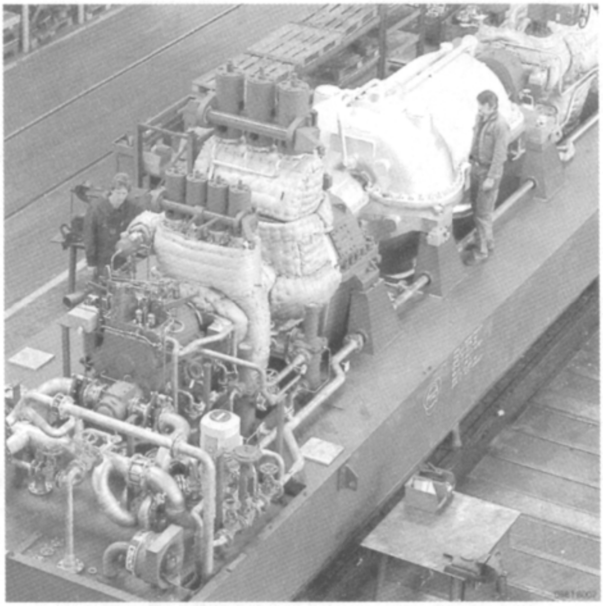

Figure 4-29. 360-t/d packaged unit—top foundation plate 13 m long, 3.6 m wide, 0.93 m high. The oil system is situated at the front end, followed by the steam turbine, compressor, and expander. The oil coolers are located separately.

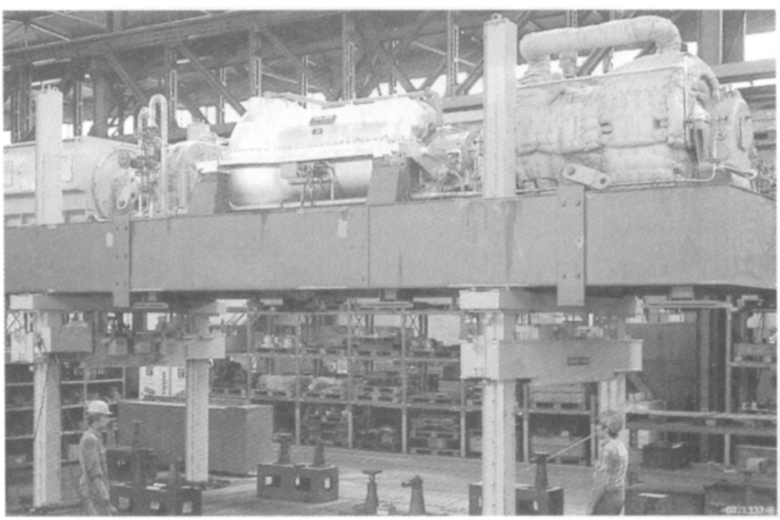

Figure 4-30. "Packaged" trubomachinery train furnished with sophisticated "lifting legs."

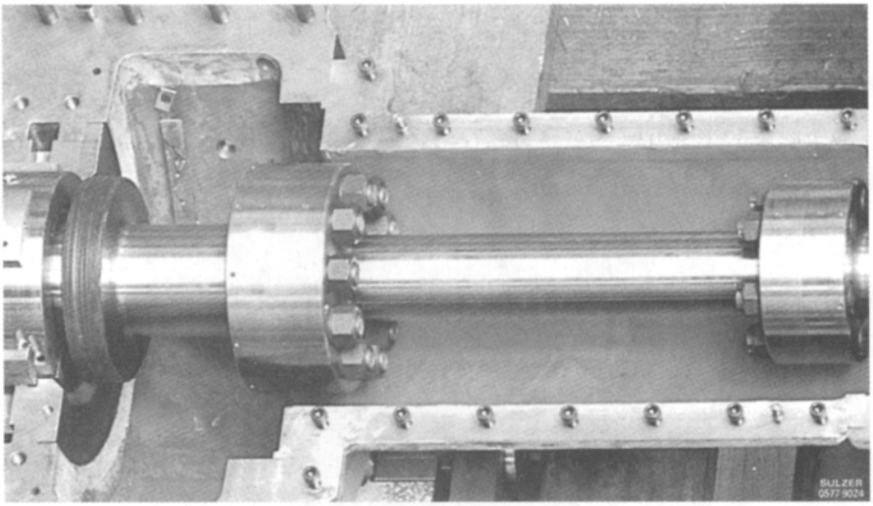

Figure 4-31. Intermediate shaft with connected shaft ends.

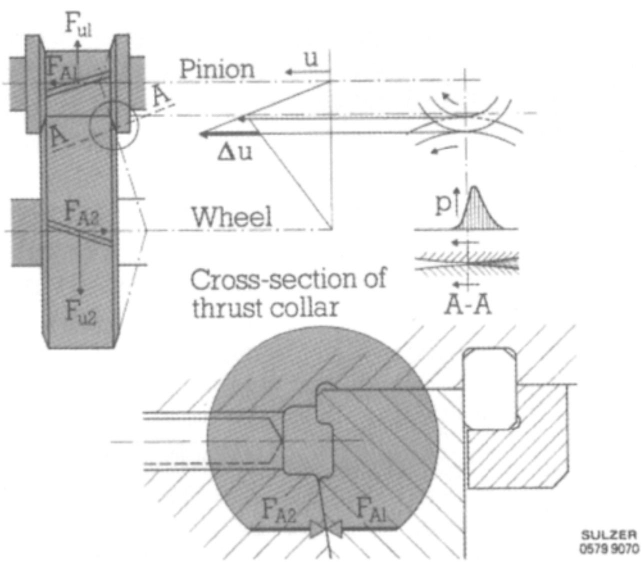

Figure 4-32. Method of axial thrust transfer in a single helical gear with thrust collar.

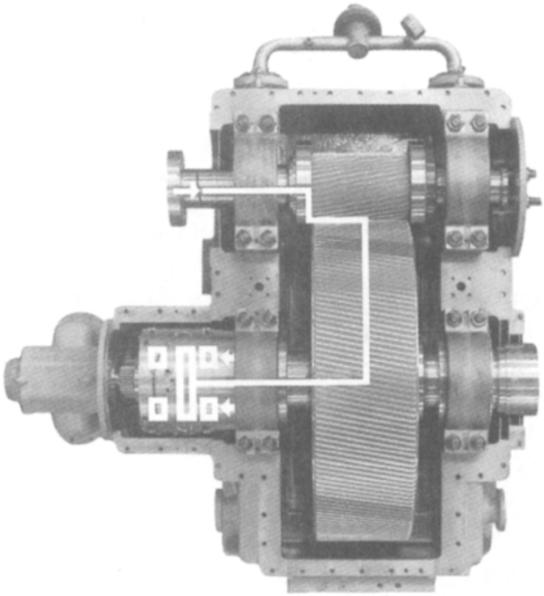

Figure 4-33. Working principle of thrust transmission shown on a single helical precision gear.

axial thrust created by the meshing of the teeth cut at an angle to the axis of the shaft, but also transmit the unbalanced axial thrust of the high-speed rotor train to the thrust bearing on the low-speed section. Due to the oil film, the pressure zone is spread over an enlarged surface with a pressure distribution similar to that of a standard oil-lubricated journal bearing. Thrust transmission is, therefore, effected with lower mechanical loss than would be expected with commercially available thrust bearings. Other manufacturers use double helical gearing whose inherent thrust balance allows the use of relatively small, low-loss thrust bearings.

A number of coupling options exist with motor drivers. The main gear is often equipped with a simple shoulder bearing, does not have thrust collars, and is connected to the compressor train with a solid coupling. Other manufacturers opt to use flexible couplings and conventional thrust bearings.

Whenever a hot-gas expander is employed, the thrust bearing of the compressor train is located in the expander. This coupling arrangement minimizes the coupling overhung mass, thus reducing the risk of undue rotor sensitivity, dynamic instabilities, and perhaps the occasional phenomenon of torque lock leading to additional loading of the axial thrust bearing.

Turbotrain Safety Systems

The compressors in the train arrangement are equipped with anti-surge controls operating a blow-off (air compressor) or bypass valve (nitrous gas compressor). If dual-casing turbocompressors are used, the ideal technical solution is to equip each machine with its own blow-off or bypass valve. This allows the installation to operate within a stable range and deliver any useful quantities between maximum and virtually zero. Where a two-casing set for air and nitrous gas is operated at more or less constant load, sometimes only the low-pressure air compressor is equipped with anti-surge control and a blow-off valve. The high-pressure compressor is then protected by a simple "open-closed" outlet valve controlled by a thermostat and differential pressure switch.

Safety systems are typically divided into emergency trip/shutdown functions, controlled (slow) shutdown, alarm activation, or startup annunciation of auxiliary equipment such as oil pumps.

Detecting transducers at the measuring points are electrical, pneumatic, or hydraulic. The resultant circuits and sequences can be seen from the typical functional diagram in Figure 4-34. An emergency shutdown immediately triggers the following operations:

- Driving units shut down by closing the main stop valve and the steam turbine regulating valves and at the same time closing the butterfly valve upstream of the expander (closing time 2–3 sec)
- Production stops by closing the ammonia inlet valve at the burners
- Compressor surging is prevented by opening the bypass of the expander and the blow-off valves of the low- and high-pressure compressors

In the latter case, the plant is not purged and some nitrous gas will remain in the equipment. The entire installation is shut down within 6–8 min after the first signal is initiated.

Emergency shutdowns represent an exception, controlled or "slow" shutdowns are the normal mode. Slow shutdowns are triggered either

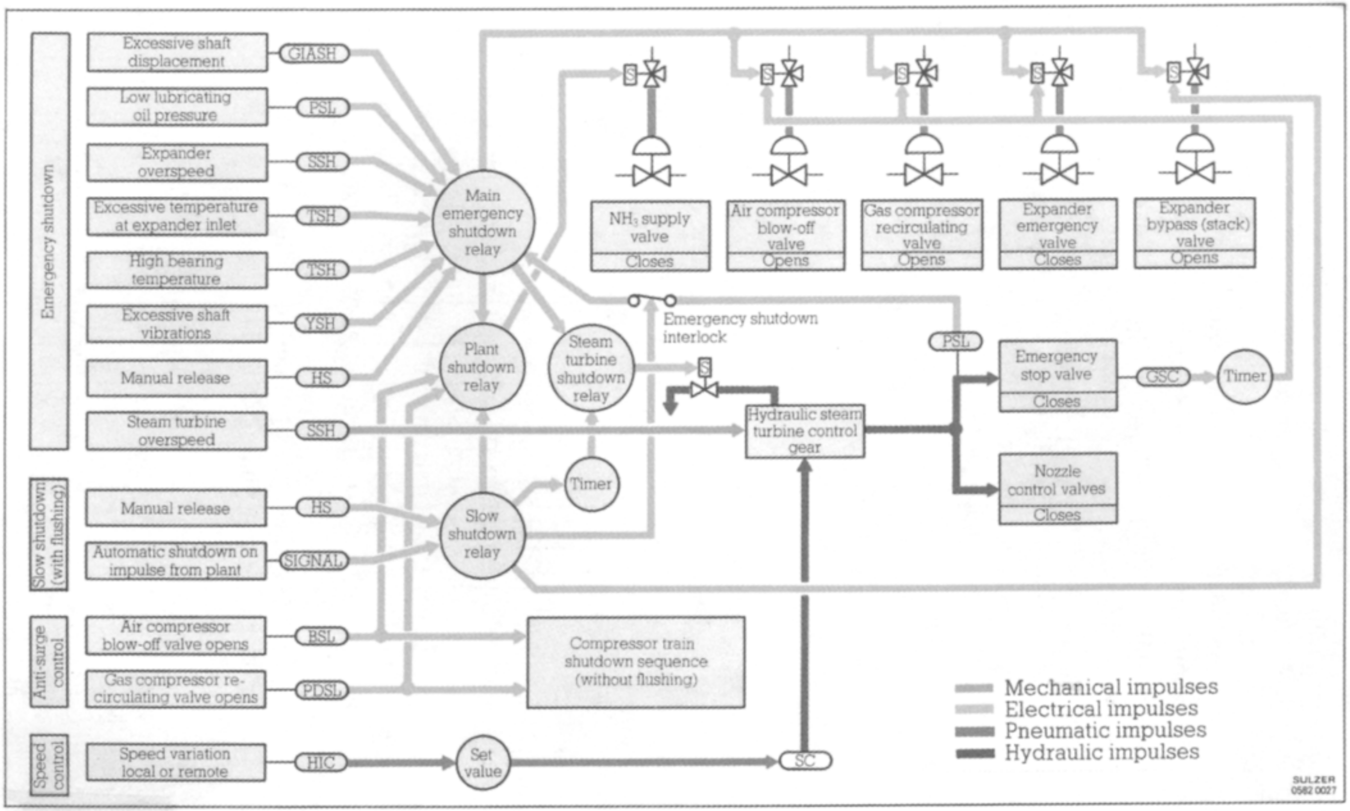

Figure 4-34. Function diagram of the safety systems for emergency and slow shutdowns, and of the speed regulating devices.

from the control panel or by automatic means after receiving an appropriate signal from the production plant. The control relays have delayed action to ensure adequate gas-freeing of the plant during the shutdown. Auxiliary fans are occasionally used for gas-freeing or purging duty.

Apart from the systems triggering emergency and slow shutdowns, nitric acid plants normally include supervisory instrumentation to indicate abnormal operating conditions. (These instrument functions are not shown in Figure 4-24.) Additionally, there are self-contained safety devices, such as check valves in the discharge piping of both gas and air compressors. These check valves prevent backflow of pressurized gases during reduced speed or shutdown events. Check valves are also fitted in the condensate, lubricating oil, and control oil circuits. The various safety provisions incorporate first-out indications; in other words, they allow operating personnel to trace the initiating impulse that led to the shutdown.

Startup Procedures

Starting up the turbocompressor installation of a nitric acid plant does not present a problem. As mentioned earlier, during the startup phase the expander is not able to contribute any power. Accordingly, electric motor drivers must initially provide power in excess of the nominal operational rating.

Smooth starts are possible with steam turbine installations that include an auxiliary boiler because the startup phases of the turbocompressor can be matched to different plant operating conditions. Aside from process-related timing issues, the time elapse or machinery startup duration is generally determined by the temperature gradients admissible on both steam turbine and expander. These factors are influenced by the relative expansion rates of the fixed and rotating components in these machines.

Figure 4-35 shows typical starting times for different train configurations. The different startup phases include:

- Idling or warming up of the steam turbine
- Increasing speed to an rpm at the lower limit of the critical speed range
- Waiting for steady state (temperature stabilization)
- Traversing rapidly through the critical speed range
- Waiting for new steady state at about 90% of nominal speed

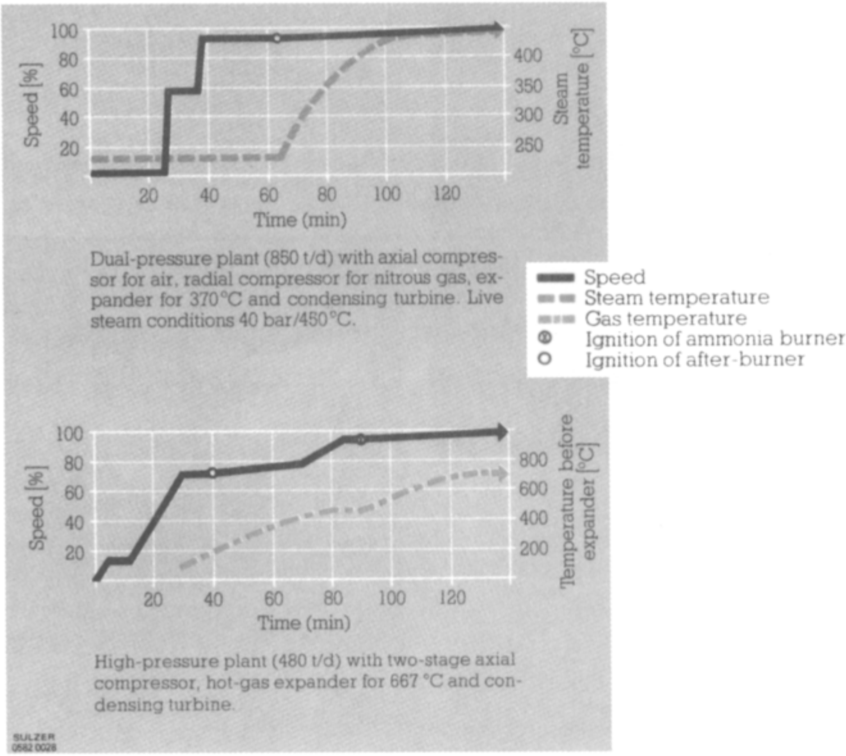

Figure 4-35. Typical starting diagrams.

- Igniting ammonia burner
- Ramping-up to full load with the power contribution from the expander

After achieving full load, the operating pressure is adjusted with the regulating devices of the expander.

When restarting an installation that is still moderately hot, difficulty is often experienced during the initial phase due to the use of saturated steam (from the auxiliary boiler), which is cooler than the superheated steam raised by ammonia combustion. Consequently, a sturdy steam turbine must be chosen, capable of withstanding the thermal stresses imposed.

Table 4-1 lists the principal components that make up typical turbotrains in nitric acid plants. Note the somewhat sophisticated metallurgy for these machines.

Table 4-1
Material selection for nitric acid turbotrains

Components	Air compressor		NO_2 compressor		Expander	
	Radial	Axial	Radial	Axial	510°C	710°C
Casing	GG-20	GG-25	GX5CrNi174	GX5CrNi174	GX22CrMoV121	GS-17CrMo55
Inner casing						X10 CrNiTi 18 9
Diffuser casing						GS-17CrMo 55
Exhaust casing					X2CrNiMo 18 12	HI
Adjusting cylinder		HI				
Diaphragm	GG-20		GX5CrNi174			
Return channel	GG-20		GX5CrNi174			
Blade carrier	GGG-40			GXSCrNi174	GX22CrMoV121	GX22CrMoV121
Stator blades		X20Cr13		X22CrNi17/V80	X20CrMoV121	NiCr20TiAL
Stage 2						GX45
Stages 3–6						X20CrMoV121
Rotor blades		X20Cr 13		X22CrNi17/V80	X20CrMoV121	NiCr20TiAL
Stages 3–6						X20CrMoV121
Impeller	23CrNiMo747		X6CrNJMoCu145			
Shaft seals	GG-20	GG-25	GX5CrNi174	GX5CrNi174	GX22CrMoV121	GS17CrMoV55
Labyrinth strip	X6CrMo17/17440	Ni99.2	X6CrMo 17	NI 99.2	X10CrNiTi189	X10CrNiTi189
Caulking wire	X8Cr 17	X8Cr17	X8Cr17	X8Cr17	X8Cr17	X8Cr17
Dummy piston	34CrNiMo6	28CrNiMoV85	X22CrNi17	X22CrNi17	X20CrMoV121	X20CrMoV121
Bearing pedestal	GGG-40	GGG-40	GGG-40	GGG-40	GGG-40	GGG-40
Rotor shaft	34CrNiMo6	28CrNiMoV85	X22CrNi17	X22CrNi17	X20CrMoV121	X20CrMoV121
Tie bolts	34GrNiMo6	34CrNiMo6	34CrNiMo6	34CrNiMo6	X20CrMoV121	X20CrMoV121

Lube Oil Units

Lube oil units are typically available in two versions: the manufacturer's standard or in accordance with APl Standard 614. The major components of a unit are the oil tank, auxiliary oil pump, double filter and, selectively, one or two oil coolers. All components of the smaller units are mounted on a common bedplate, separated from the other components. The oil can be heated by an electrical or steam-powered heating unit. The necessary instrumentation is a standard supply item and, if requested, the switches and motors can be prewired. The main and auxiliary oil pumps are driven by different types of drivers (e.g., one by an electric motor and the other by either a small steam turbine or by direct connection to the shaft end of a major machine casing in the turbotrain).

INTEGRALLY GEARED PROCESS GAS RADIAL TURBINES[2]

As mentioned earlier, a variety of turbomachines are required to produce nitric acid. In the case of small plants, these machines represent a substantial investment. A combination of proven air compressor modules with newly developed expansion turbines and nitrous gas compressors on a single gearbox provides a new, low-cost alternative and gives the plant owner/contractor useful potential for faculty optimization (Figures 4-36 through 4-38).

Nitric acid as a raw material has many applications in the chemical industry, ranging from mineral fertilizers through plastics and explosives. In the past, large or very large plants have been designed to produce up to 1,500 mt of acid per day with a maximum of five turbomachines. These machines typically included a steam turbine, an axial air compressor, a radial NOx compressor, a tail gas (hot gas) expander (also called power or expansion turbine), and a motor-generator combined in a single train via couplings and intermediate gears.

The more recent combination of standardized compressor modules and customized components with integrally geared radial turbines has opened new possibilities. Integrally geared radial turboexpanders represent considerable design flexibility and this, in turn, allows

[2] *Source: Based in part on information published in* Compressor Tech, *January/February 1999. Data provided by GHH-Borsig and additional material made available by Demag Delaval.*

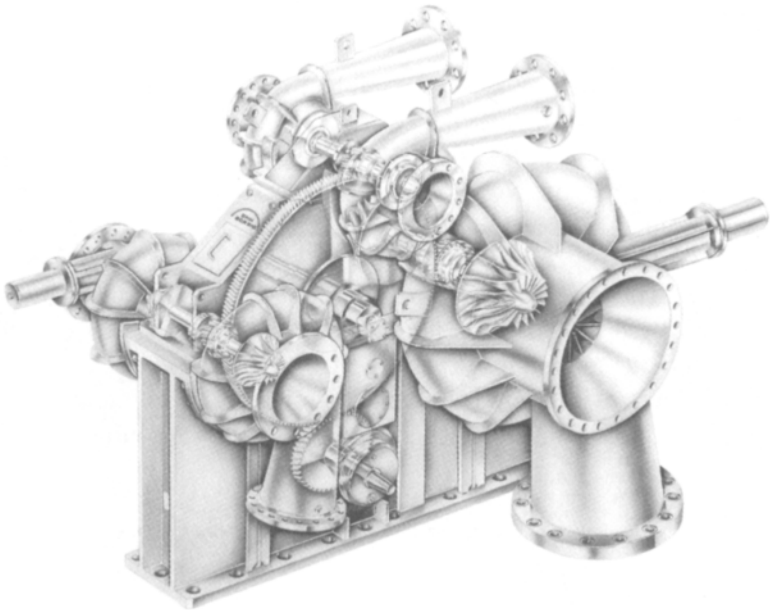

Figure 4-36. A single integral gear box connects one or more expanders to several compressor stages. *(Source: GHH-Borsig.)*

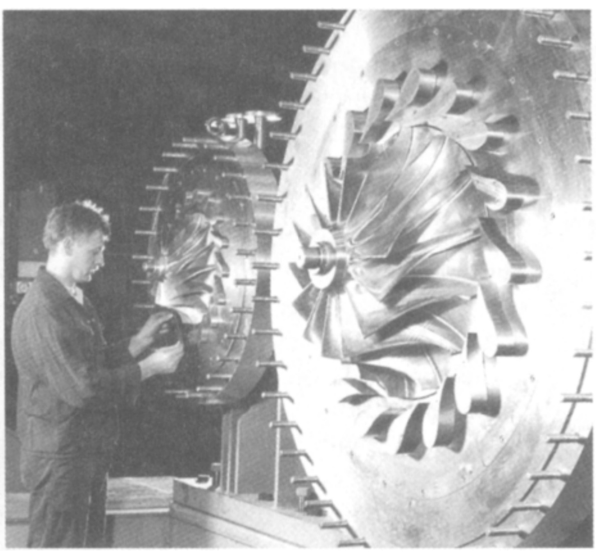

Figure 4-37. Two radial inflow expanders mounted on a single gear box. *(Source: GHH-Borsig.)*

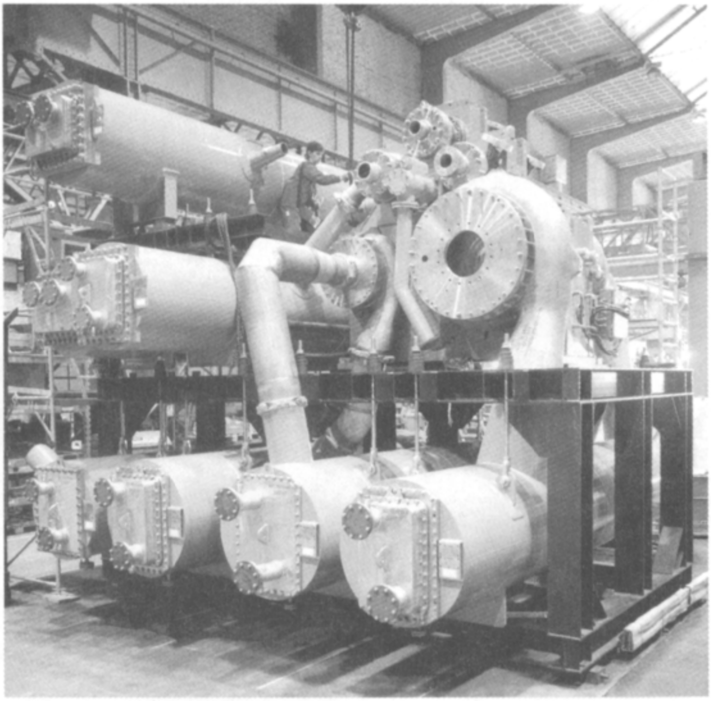

Figure 4-38. Ten-stage, integrally-geared compressor. *(Source: GHH-Borsig.)*

economical facilities to be built for small and medium-sized plants. Moreover, this relatively new concept of an integrally geared turbomachine is certainly not confined to nitrous acid plants. A number of PTA and DMT plants have profited from this development and other applications are sure to follow.

In the case of nitrous acid plants, application of integrally geared process gas radial turbines and compressors are used in plants with capacities ranging from 120–600 t/day and higher. For air compression, up to three compressor stages are connected in series. To increase efficiency, the inlet temperature of the individual stages is reduced by using two external intermediate coolers.

Standard assemblies from the range of geared compressors made by competent manufacturers have proven successful for many years as the compressor stages. The compressor cases are mounted at the overhung ends of the one or more pinion shafts engaged by a large-diameter bull gear (Figure 4-39). Three or more pinion shafts surround

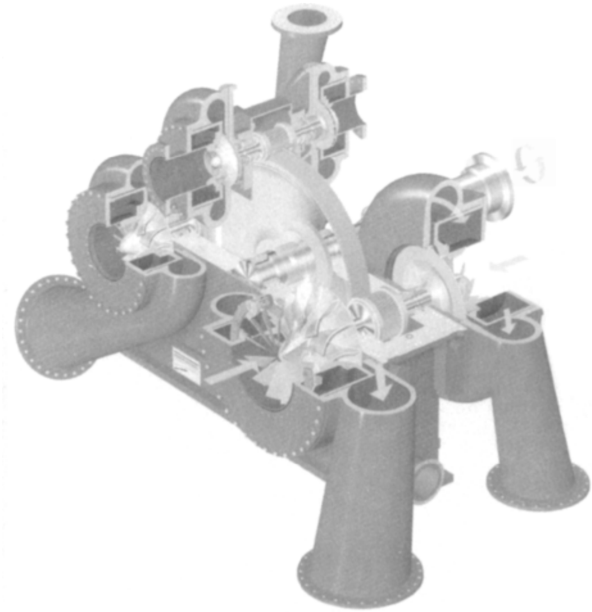

Figure 4-39. Integrally geared multistage compressor. *(Source: Demag Delaval.)*

the bull gear and one or two of the pinion shaft ends carries the radial inflow tail gas expander. To control the turboset, inlet guide vanes are used upstream of the first air compressor stage. This enables the air volume and pressure in the plant to be adjusted within certain limits.

Depending on plant size, the hot gas expander is supplied either with (Figure 4-40) or without variable inlet guide vanes. Adjustment features are not required in small plants where throughput at constant or full-load capacity is anticipated.

As previously mentioned, the expander turbine is only one component of the train or turboset. A motor-generator or a mechanical drive steam turbine might also be included. Although the motor is directly coupled to the bull or main gear of the integral gear set, the speed ratio must be selected to allow the steam turbine to operate at its optimum efficiency. An intermediate gear may be used to reduce the relatively high turbine speed to the required value.

Because there is considerable design flexibility in accommodating optimum turbine speed, standard mechanical drive steam turbines are often chosen. The offset arrangement (Figure 4-41) provides additional freedom for the turboset component layout.

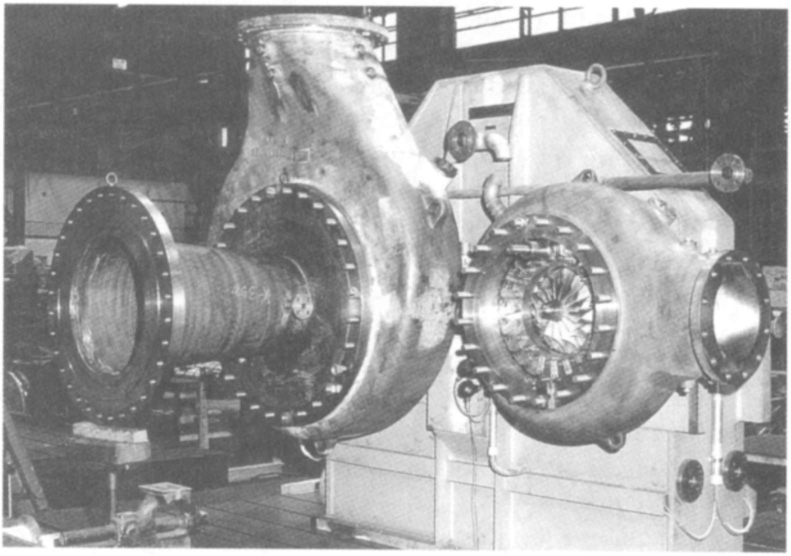

Figure 4-40. Two-stage radial inflow expander with variable inlet guide vanes (right). *(Source: Demag Delaval.)*

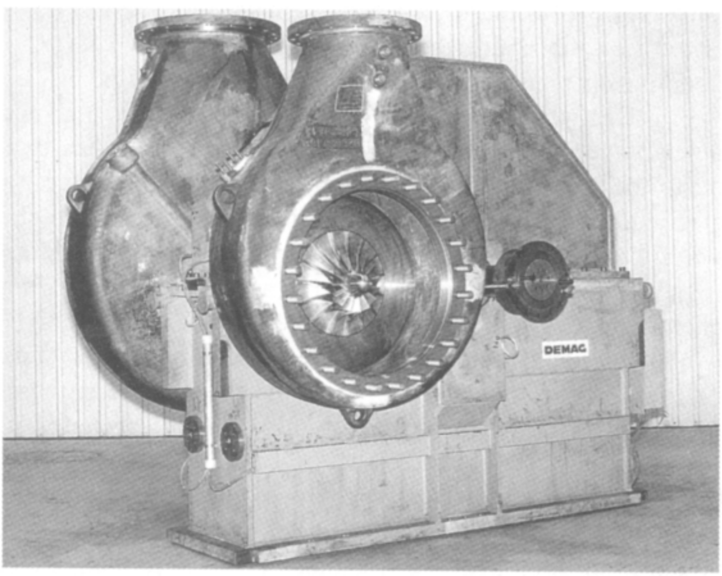

Figure 4-41. Offset arrangement facilitates component layout. *(Source: Demag Delaval.)*

Monitoring should include the usual parameters worthy of surveillance in high-speed turbomachinery: the temperature of journal bearings, vibration and axial position of the pinions, inlet and discharge temperatures combined with discharge pressure from the individual compressor stages, and various lube oil system devices. Competent manufacturers make sure all measurement locations are completely prewired on the machine and made available at predefined interfaces or in terminal boxes for connection at the plant site.

Lubrication is typically provided by two separate oil pumps—a direct shaft-driven pump on the gear case and an auxiliary electric motor-driven oil pump that is usually mounted on a lube skid or similar sub-base. Oil filters, oil coolers, and oil heaters complete the lubrication system, which has many (if not all) features in common with traditional auxiliary systems. A typical schematic is shown in Figure 4-42.

A small expander recovers the tail gas energy. To maintain its compact design, the impulse principle known from steam turbine design has generally been adopted. This enables the inherent thermal and pressure energy to convert back into mechanical energy with a minimum number of stages and good efficiency. It is generally sufficient to arrange two such stages in series to handle the pressures and temperatures that are encountered in the expander. An admission pressure and temperature of around 145 psi (10 bar) and 752°F (400°C) can be reduced to atmospheric pressure and about 212°F (100°C).

Depending on plant size and expander manufacturer, power levels of between 2,720–5,440 hp (2–4 MW) are typically being recovered, but higher power levels are not unusual. New approaches have been adopted in the manufacture of both rotors and stationary components for small radial turboexpanders. Unlike conventional technology employing single blades, both inlet guide vanes and impellers wheels are designed and manufactured as integral, and not built-up (composite), components. Impellers or wheels are milled out of high-strength forged disks while the stator components, depending on size, are fabricated by spark erosion from a ring or made as precision castings. These manufacturing methods ensure maximum flexibility in the implementation of specific design requirements.

Rigorous design reviews must include the often highly complex resonance behavior of impellers and blading to ensure vibration-free or vibration-tolerant design of these critical turboexpander components. In other words, the manufacturer must perform comprehensive theoretical and experimental studies of the blade oscillations in the rotating system.

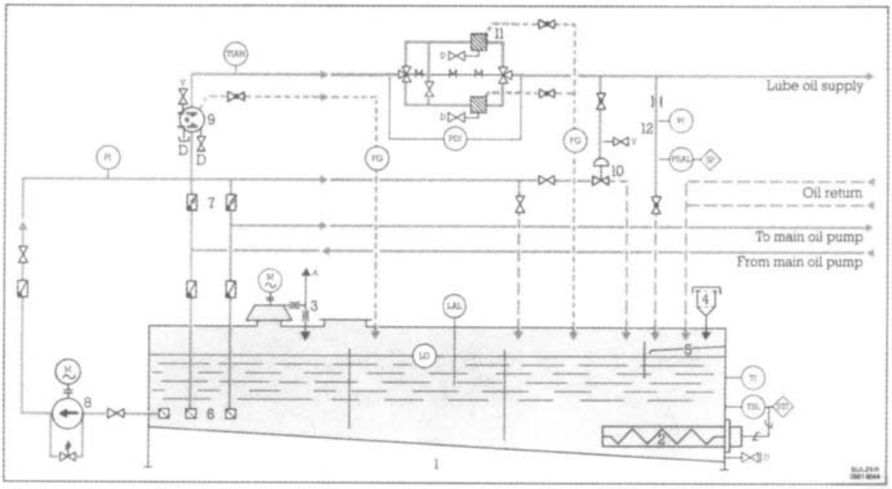

Scope of supply and functional description

1 Lube oil tank with auxiliary equipment
2 Electric oil heaters
3 Oil mist fan
4 Filling sieve and breather
5 Degasifier plates
6 Suction strainers
7 Safety arrangement (4 non-return valves) in the main oil pump suction and discharge lines to prevent back-flow of oil if the compressor and hence the main oil pump should accidentally turn in reverse direction
8 Auxiliary oil pump, electric-motor-driven; automatic start-up of the pump in the event of oil pressure drop
9 Oil cooler
10 Oil pressure control valve, maintaining the bearing oil pressure at 1.5 bar
11 Twin oil filter, each of the filter screens being sized for full flow, with transfer valve for filter changeover during operation and PDI pressure loss indicator
12 Testing device for checking the automatic start-up of the auxiliary oil pump

Line symbols

Oil supply
Oil return
Vent
Cooling water
Electrical connection
Oil mist
Mechanical connection

Valve and apparatus symbols

Globe valve
Three-way valve
Needle valve
Non-return valve
Suction strainer
Non-return valve with bore
Diaphragm valve actuator
Spring-loaded safety valve
Orifice
Drain plug
A Atmospheric outlet
D Drain
V Vent

Instrument symbols

Measured variables (first letter)
P Pressure
T Temperature
PD Pressure difference
F Flow
L Level
Passive function (following letter)
I Indication
A Alarm
S Switch function
G Sight glass without measurement
Extreme values (last letter)
H High
L Low
Signal processing
Compressor driver start-up interlock
Start-up of auxiliary oil pump

Figure 4-42. Lube oil schematic, Sulzer standard.

TURBOEXPANDERS IN GEOTHERMAL APPLICATIONS*

Since 1970, a great deal of work has been devoted to efficiently extracting heat from such underground sources as steam pockets or hot and usually pressurized brine streams. These geothermal sites are widely distributed throughout the world. Turboexpanders have demonstrated excellent capabilities in converting this heat energy into electricity through a binary cycle process.

More specifically, there are two general geothermal resources: dry steam fields and wet brine fields. In the dry geothermal fields, energy is recovered from the expansion of steam flashed from the hot well streams. Thousands of megawatts are being produced from such dry geothermal steam fields in Northern California and Washington State in the U.S. A typical application is Unocal's geothermal power plant in the Salton Sea, located in Imperial Valley, California. In this project, the high pressure steam (23 bar) from the separator is directed through a Rotoflow turboexpander operating at a back-pressure of about 9 bar. The turboexpander is a 15,000 rpm radial inflow, variable inlet vane, reaction-type turbine, with a power output rating of 4.4 MW. This unit has been in commercial operation since 1990.

The flashed steam method is less efficient and its requirements for steam properties—cleanliness, high temperature, and high pressure—are usually unavailable in most geothermal fields. The situation is different with the binary cycle system, which is quite efficient and widely used. This "wet" system involves the transfer of heat from the hot well stream into a more manageable boiling fluid to generate power through a turboexpander.

One problem that complicates plant design in wet geothermal fields is the scaling in casings, pipes, and heat exchangers. To overcome this problem, a pilot plant was constructed by Daedalen Associates in Maryland, under the sponsorship of the U.S. Department of Energy (DOE), using direct-contact heat exchangers. In this design the working fluid, isopentane, was sprayed in direct contact with the geothermal brine and vaporized. The fluid and water vapor at 66°C was expanded from 3 bar to 1 bar in a 100 kW expander/integral-gear/generator unit built in 1978. This was the world's first binary cycle in a geothermal application.

* *Based on information supplied by the Rotoflow Div. of Atlas Copco.*

However, the open-loop pilot plant approach was not widely adopted due to the significant loss of working fluid to the brine in the direct-contact heat exchanger. A study of a closed-loop binary cycle system was completed by Rotoflow for EPRI in the late 1970s. In a typical closed-loop binary cycle, power recovery is accomplished by pumping hot water or brine from underground wells through heat exchanger equipment to boil a working fluid maintained in a closed cycle. The resulting vapor is expanded to drive the turbine-generator set, producing salable power; the vapor is then recondensed and pumped back into the heat exchanger to repeat the cycle. Several working fluids are suitable for binary cycles including isobutane, isopentane, propane and hydrocarbon mixtures.

THE BEN HOLT PROCESS DESIGN

A very successful project began in the early 1980s when the Ben Holt Company (Pasadena, California) designed and constructed a 10 MW air-cooled, closed-loop binary cycle at their Mammoth Geothermal Plant, located on the eastern slope of the Sierra Nevada mountain range in California.

The Mammoth-Pacific plants are the world's first commercial application incorporating two closed-loop systems (hence, "binary process") designed to protect the environment and conserve water. This is illustrated in Figure 4-43.

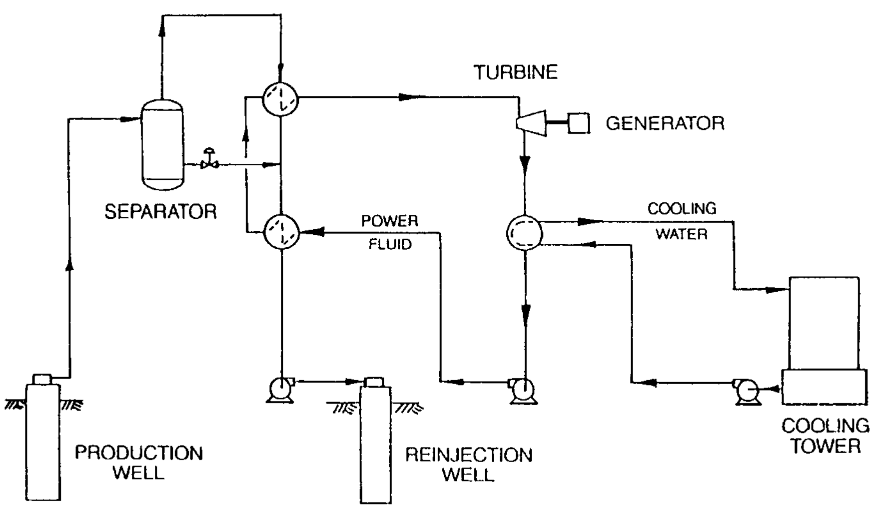

Figure 4-43. Typical binary cycle used in geothermal plants.

In the "primary binary loop," production wells recover 170°C hot water from the geothermal reservoir and deliver 3,036 m^3/hr at 14 bar to heat exchangers in the power plant. Water leaves the heat exchangers at 70–90°C and is recycled to the ground through a re-injection well at a depth of 400–600 m. In the "secondary binary loop," the heat from the hot water evaporates the isobutane working fluid at 36 bar and 150°C (Table 4-2).

Power is generated by the pressurized gas expanding through an 11,000 rpm single-stage, radial-inflow turbine expander, which drives a synchronous generator. Exhaust gas from the expander is liquified by air-cooled condensers and is pumped back to the heat exchangers to repeat the cycle.

The original Pacific Lighting Energy Systems (PLES) plant uses two generator-loaded expanders. The power plant has operated successfully for years, providing the incentive for expanding the project. Indeed, two more power plants of nearly identical design were built in the Mammoth expansion after final approval of the permits for construction were obtained in 1989. The newer plants each use three generator-loaded expanders, with a combined power output of 30 MW. They have been in commercial operation for many years and many other plants soon followed.

Unique Design Features for Geothermal Energy Recovery Applications

Radial inflow turboexpanders offer several performance features that are especially well suited to geothermal applications. First and foremost, these machines can handle a wide range of operating conditions. This is important because most geothermal fields are located in the deserts and mountains and the condensing must be accomplished with air coolers. A comprehensive study was conducted to determine the effect of the unusually wide range of ambient temperatures on the machine design. These can vary from a high of 50°C in the summer to well below freezing in winter or even from day to night. Such a wide swing requires a change of expander discharge pressure, resulting in a change of discharge volume flow and possibly extensive condensation in the turbine.

Turboexpanders require variable flow control nozzles capable of withstanding the total pressure and acting as the flow control for the main gas stream through the plant. The variable nozzles are matched

Table 4-2
Application performance data for Mammoth Lakes, CA geothermal power generating plants

Parameters	Plant No. 1	Plants No. 2 and No. 3
Site area including wells	360,000 m^2 (90 acres)	200,000 m^2 (50 acres)
Plant site area	8,000 m^2 (2 acres)	16,000 m^2 (4 acres)
Number of production wells	4 @ 180 m deep (600 ft deep)	4 @ 180 m deep (600 ft deep, each plant)
Number of reinjection wells	3 @ 400–600 m deep (1,400–2,000 ft deep)	2 @ 400–600 m deep (1,400–2,000 ft deep, each plant)
Hot water	170°C, 14 bar a, 836 m^3/h (340°F, 190 psi, 3,800 gpm)	170°C, 14 bar a, 1,100 m^3/h, each plant (340°F, 190 psi, 5,000 gpm, each plant)
Isobutane data	150°C, 36 bar a, 1,150 m^3/h (300°F, 500 psi, 5,200 gpm)	150°C, 36 bar a, 1,900 m^3/h, each plant (300°F, 500 psi, 8,500 gpm, each plant)
Number of expander-generators	2	3 each plant
Type of expander	Single-stage, radial-inflow	Single-stage, radial-inflow
Type of generator	4,100 volt synchronous	4,100 volt synchronous
On-site kW use	2,000 kW	4,000 kW each plant
Net kW to Gnd. 2 Generators	12 MW maximum	16 MW each plant maximum
Equivalent homes served	12,000 maximum	9,000 to 16,000 each plant
Oil saved	67 tpd (156,000 bpy)	60–90 tpd (117,000–208,000 bpy) each plant
CO_2 greenhouse gas avoided	200 tpd (80,000 tpy)	150–270 tpd (60,000–107,000 tpy) each plant
Estimated project life	30 years	30 years

Project Owner/Operator: Pacific Geothermal Co. and Mammoth Binary Power Co.
Project Engineering: Ben Holt Co., Pasadena, CA.
Expander-Generator Manufacturer: Rotoflow Corporation Inc., Los Angeles, CA.

to the turbine wheel to give high efficiency over a wide range of flows (see Figure 1-5). The large volume ratio capability permits use of simple, single-stage expanders.

With a lower temperature, the turbine is best used by allowing the back-pressure to fall and thus obtain more power. In radial inflow turbines, the relative velocity at the turbine inlet is small. Any changes are, therefore, far less significant than with high relative velocity impulse wheels. Commonly, a turboexpander tolerates as much as a 30% change from its designed enthalpy. The effect on efficiency was shown earlier in Figure 3-12.

Modern radial inflow expanders can handle any amount of condensation at discharge without a significant loss of efficiency. Droplets resulting from incomplete vaporization in closed-loop isobutane systems "float" through the turbine with negligible impingement because the flow passage is essentially parallel to the blading.

Occasionally, a wider range of operating conditions must be accommodated due to changes occurring in geothermal fields (e.g., change of brine temperature or flowrate). In these instances, the expander can be redesigned simply and easily to suit the new conditions. It should be noted that in a geothermal plant efficiency is at a premium. One percent improvement in efficiency in a 40 MW plant can increase plant profitability by a quarter of a million dollars per year.

Another feature of radial inflow turboexpanders is their high efficiency and maximum power output and their mechanical operation reliability. Relatively high operating pressures and running speeds are usually required by expanders in geothermal binary process services to deliver the best performance (up to 90% with certain larger wheels) and maximum power output. At higher pressures and speeds it is essential that the design take into account the reliability of the turpoexpander:

- Thrust forces must be balanced over the full range of operating conditions. Even though correctly balanced, occasional erosion of a seal or off-design operations can cause the thrust load to vary widely and exceed the thrust bearing load-carrying capacity. In quality machines, a patented thrust balance system automatically senses and compensates for sudden pressure changes.
- The design of shaft seals must strive to reduce wear of these critical components. An overhung turbine design should use a stiff shaft that operates below its first shaft critical speed. This will greatly limit the extent of damage in the event of accidental or

unforeseen equipment distress. Using a stiff shaft has another advantage, which allows the use of a labyrinth-type noncontacting seal. Buffered labyrinth seals serve to recover and recycle the isobutane and can virtually eliminate waste and pollution. Similarly, novel dry gas seals can also be used to provide positive sealing and eliminate seal gas recovery systems.

- Bearing oil film critical speeds (bearing resonance) and oil swirl problems must be addressed. The rigidity and strength of soundly engineered shaft and bearing systems can ensure operation without risking vibration problems. Both conventional and active magnetic bearings can provide reduced sensitivity to unbalance due to dust accumulation or wear. Properly engineered, either bearing type can provide substantial resistance to deposit-initiated operating abnormalities.

Turboexpander designs heeding these design concerns have proven to be exceptionally suited for geothermal applications. Continuous operation for several years without repairs is not unusual.

Economics

The cost of producing power varies with the capacity and temperature of geothermal brine and the cooling method selected. For illustration purposes, the estimate of the installed cost of a binary cycle geothermal plant is \$1,500/kW + \$250,000. Using an average revenue of \$0.07 per kW/hr, a 1 MW geothermal plant will have a three-year payback period.

TURBOEXPANDER APPLICATION IN CATALYTIC CRACKING UNITS[3]

PROCESS OVERVIEW

Fluid catalytic cracking (FCC) is considered the primary conversion process in an integrated refinery. For many refiners, the cat cracker is the key to profitability because successful operation of the unit can determine whether or not a refiner stays in business and remains competitive.

[3] *FCC process description adapted by permission from* Fluid Catalytic Cracking Handbook, *R. Sadeghbeigi, Gulf Publishing Company, Houston, Texas, 2000, pp. 3–17.*

There are over 400 cat crackers operating worldwide, with a total processing capacity in excess of 12 MMbpd. Several companies such as Exxon-Mobil, Shell, and Total have their own designs, however most current operating units have been designed or revamped by major engineering contractors such as UOP, Brown & Root, M. W. Kellogg, and Stone & Webster. Although the mechanical arrangements in individual FCC units may differ, their common objective is to upgrade low-value feedstocks to more valuable products. It is important to note that, worldwide, about 45% of all gasoline produced comes from the FCC and ancillary units, such as the alkylation unit.

The FCC unit uses a microspheroidal catalyst, which fluidizes when properly aerated. The main purpose of the unit is to convert high-boiling fractions called gas oil to high-value, high-octane gasoline and heating oil. Gas oil is the portion of crude oil that boils in the 650–1,050+°F (330–550°C) range and contains a diversified mixture of paraffins, naphthenes, aromatics, and olefins.

Figure 4-44 shows how a typical cat cracker fits into the refinery process. The crude unit is the first processing unit in the refining sequence. Here, the raw crude is distilled into several intermediate products. The heavy portion of the crude oil that cannot be distilled in the atmospheric tower is heated and sent to the vacuum tower. The tar from the vacuum tower is sent to be processed further in a delayed coker or resid processing units.

The gas oil to a conventional cracker is primarily from the atmospheric column, the vacuum tower, and the delayed coker unit. Additionally, many refiners blend some atmospheric or vacuum residue with the cracker feedstocks to be processed in the FCC unit.

REACTOR DESCRIPTION

The reactor-generator (Figure 4-45) is the heart of the FCC process. In a modern cat cracker, virtually all of the reactions occur in the riser over a short period 2–4 sec before the catalyst and the products are separated in the reactor. However, some thermal and nonselective catalytic cracking reactions continue to occur in the reactor housing. A number of refineries are modifying the riser termination devices to eliminate this problem.

From the preheater, the feed enters the riser near the base where it contacts the incoming regenerated catalyst. The ratio of catalyst to oil is normally in the range of 4:1 to 9:1 by weight.

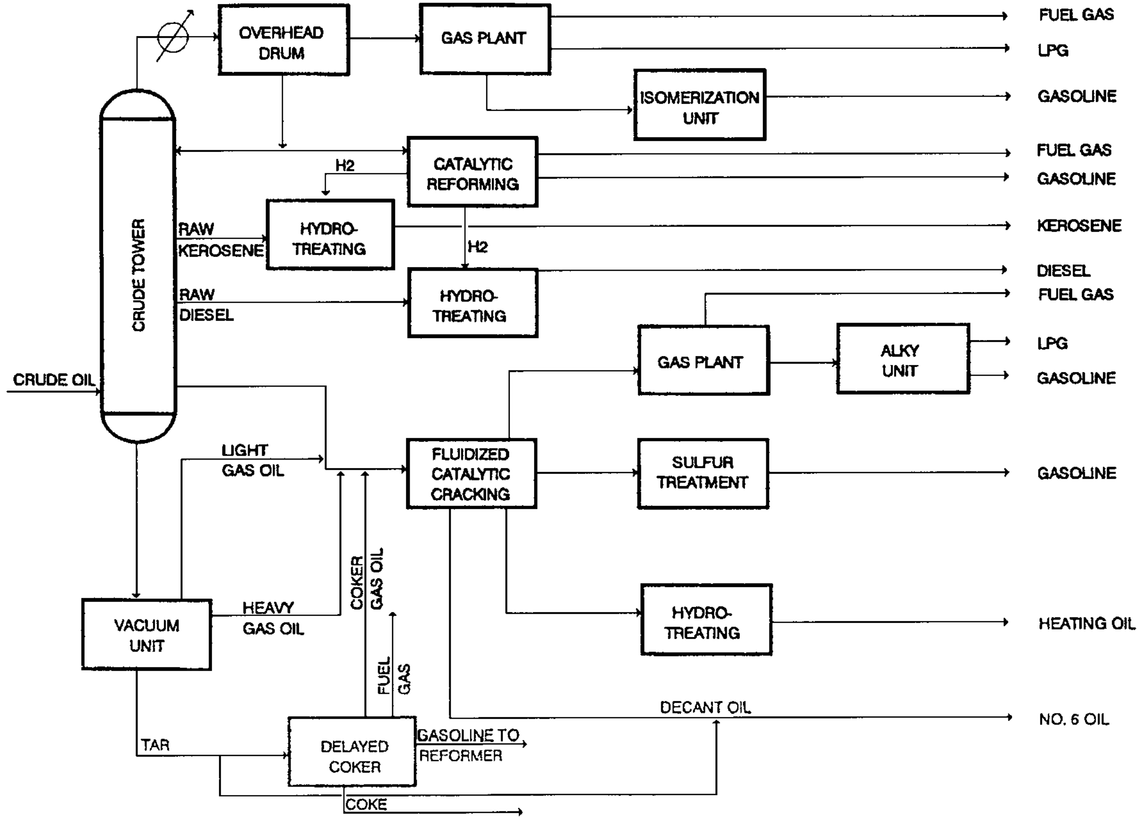

Figure 4-44. A typical high-conversion refinery.

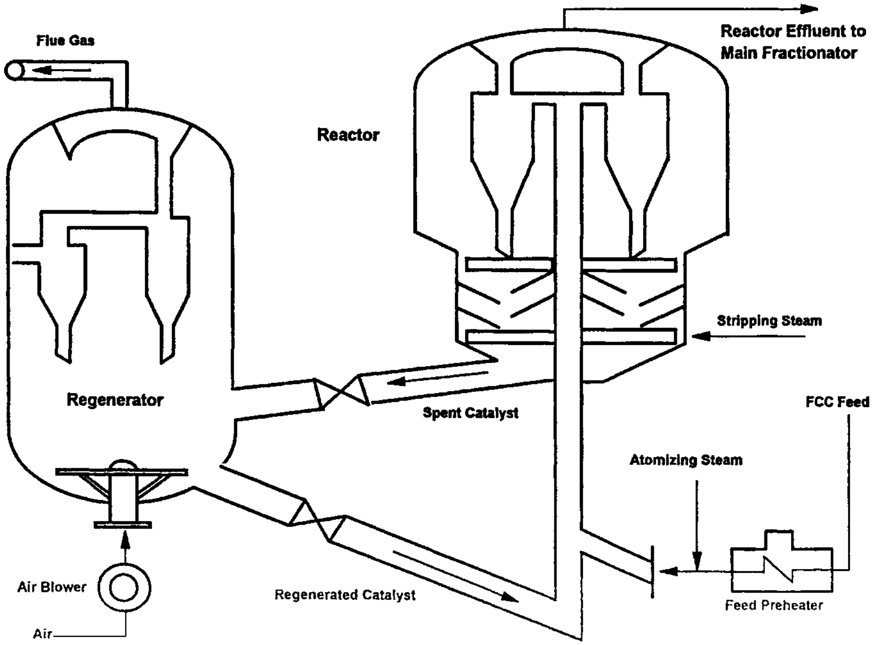

Figure 4-45. A typical FCC reactor-regenerator.

The heat absorbed by the catalyst in the regenerator provides the energy to heat the feed to the desired reactor temperature. The net heat of the reaction occurring in the riser is endothermic (i.e., it requires energy input). This energy is provided by the circulating catalyst. The catalytic reactions occur in the vapor phase and, as soon as the feed is vaporized, cracking reactions begin simultaneously. The expanding volume of the generated vapors lift the catalyst and carry it up the riser.

The riser (Figures 4-46 and 4-47) is essentially a vertical pipe usually having a 4–5-in. thick refractory lining for insulation and abrasion resistance. Typical riser dimensions are 2–6 ft in diameter and 75–120 ft in length. The ideal riser simulates a plug flow reactor, where the catalyst and vapor travel along the length of the riser at the same velocity with minimum back-mixing.

Efficient contacting of the feed and the catalyst is critical for achieving the desired cracking reactions. Steam is commonly used to atomize the feed because feed atomization increases the availability of feed at the reactive acid sites on the catalyst. Employing a high-activity zeolite catalyst ensures virtually all of the cracking reactions

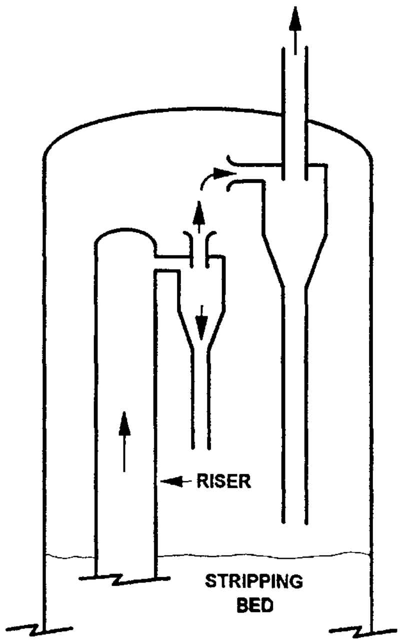

Figure 4-46. Riser cyclone.

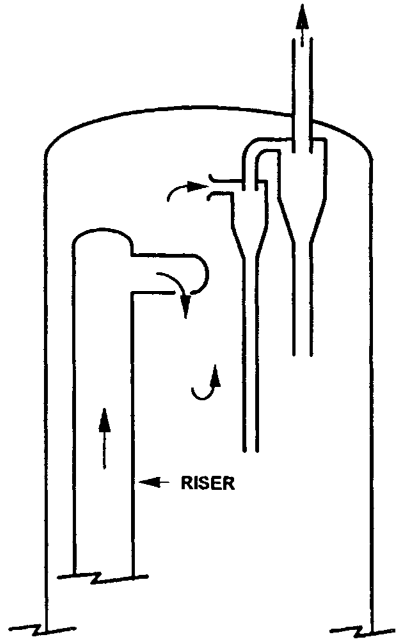

Figure 4-47. "Rough cut" cyclone.

occur in the riser in a less than 2 sec. Risers are normally designed for an outlet vapor velocity of 50–75 ft/sec, with an average hydrocarbon residence time of about 2 sec, based on outlet conditions. As a consequence of the cracking reactions, a hydrogen-deficient material called coke is deposited on the catalyst, reducing catalyst activity.

Catalyst Separation

After exiting the riser, the catalyst enters the reactor. In modern FCC operations, the reactor serves two basic functions: as a disengaging space for the separation of catalyst and vapor, and as the housing for the reactor-internal cyclone.

Nearly every FCC unit employs some type of inertial separation device connected on the end of the riser to separate the bulk of the catalyst from the vapors. Most units use a deflector device to turn the catalyst direction downward. On some units, the riser is directly attached to a set of cyclones. The term "rough cut" cyclones (Figure 4-47) generally refers to this type of arrangement. These schemes separate approximately 75%–99% of the catalyst from the product vapors.

Most FCC units use either single or two-stage cyclones (Figure 4-48) to separate the remaining catalyst particles from the cracked vapors. The cyclones collect the catalyst and return it to the stripper through the use of diplegs and flapper valves. The product vapors exit the cyclones and flow to the main fractionator column for recovery. The efficiency of a typical two-stage cyclone system is 99.995+%.

It is important to incorporate process and mechanical provisions to separate catalyst and vapors as soon as they enter the reactor. Otherwise, the extended contact of the vapors with the catalyst in the reactor will allow recracking of some of the desirable products. Furthermore, the extended residence time also promotes thermal cracking of the desirable products.

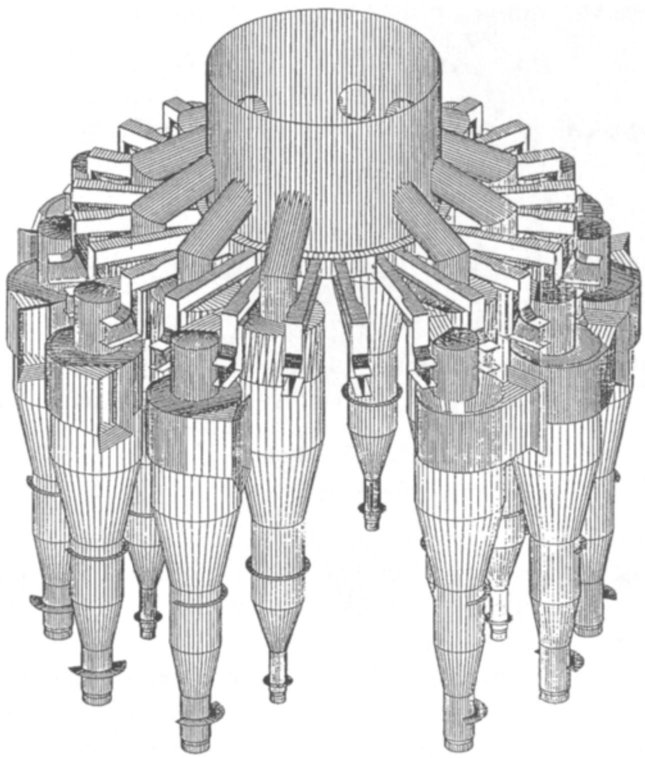

Figure 4-48. A two-stage cyclone system. *(Source: Bill Dougherty, BP Oil Refinery, Marcus Hook, PA.)*

Stripping Section

As the spent catalyst falls into the stripper, valuable hydrocarbons are adsorbed within the catalyst bed. Stripping steam, at a rate of 2–5 lb/M-lb of circulating catalyst, is used to strip these hydrocarbons from the catalyst. Both baffled and unbaffled stripper designs (Figure 4-49) are in commercial use. An efficient stripper design incorporates optimum countercurrent contacting between the catalyst and steam. Reactor strippers are commonly designed for a steam superficial velocity of 0.75 ft/sec and a catalyst flux rate of 500–700 lb/min-ft^2 of circulating catalyst. At too high a flux, the falling catalyst tends to entrain steam, thus reducing the effectiveness of stripping steam.

Not all hydrocarbon vapors can be displaced from the catalyst pores in the stripper. A fraction of them are carried with the spent catalyst into the regenerator. These vapors have a higher hydrogen-to-carbon ratio than the coke on the catalyst. The drawbacks of allowing these hydrogen-rich hydrocarbons to enter the regenerator are:

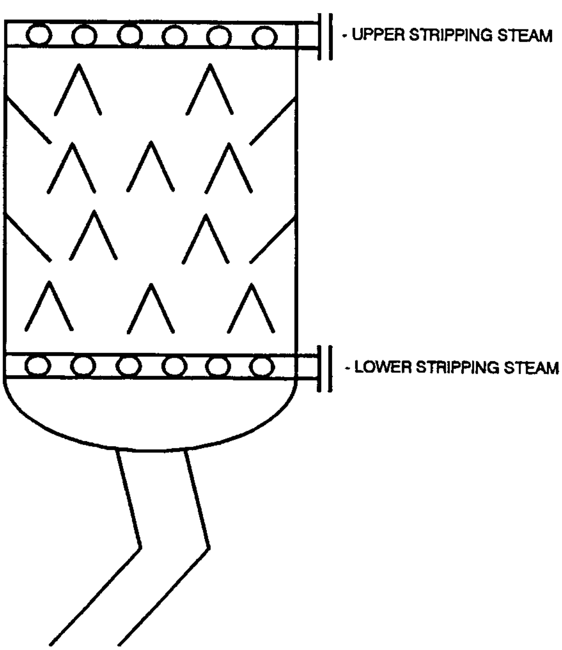

Figure 4-49. An example of a two-stage stripper.

- Loss of liquid product. Instead of the hydrocarbon burning in the regenerator, they could be recovered as liquid products.
- Loss of throughput. The combustion of hydrogen to water produces 3.7 times more heat than the combustion of carbon to carbon dioxide. The increase in the regenerator temperature caused by excess hydrocarbons could exceed the temperature limit of the regenerator internals and force the unit into a reduced feed rate mode of operation.
- Loss of catalyst activity. The higher regenerator temperature combined with the formation of steam in the regenerator reduces catalyst activity by destroying the catalyst's crystalline structure.

The flow of the spent catalyst to the regenerator is typically controlled by the use of a valve that slides back and forth. This slide valve (Figure 4-50) is used to control the catalyst level in the stripper. The catalyst level in the stripper provides the pressure head that allows the catalyst to flow into the regenerator. The exposed surface of the slide valve is usually lined with a suitable refractory to withstand erosion.

REGENERATOR DESCRIPTION

The regenerator has two main functions: It restores catalyst activity and supplies heat to crack the feed. The spent catalyst entering the regenerator contains between 0.8–2.5 wt% coke, depending on the quality of the feedstocks. Components of coke are carbon, hydrogen, and trace amounts of sulfur and nitrogen, which burn according to the reactions shown in Table 4-3.

Air is the source of oxygen for the combustion of coke and is supplied by a large air blower. The air blower provides sufficient air velocity and pressure to maintain the catalyst bed in a fluid state. The air enters the regenerator through an air distributor (Figures 4-51 and 4-52) located near the bottom of the vessel. The design of an air distributor is important in achieving efficient and reliable catalyst regeneration, and a number of designs are available from major FCC unit licensors. Generally, air distributors are designed for a 1–2 psi pressure drop to ensure positive air flow through all nozzles.

There are two regions in the regenerator: the dense phase and the dilute phase. At the velocities common in the regenerator, 2-4 ft/sec, the bulk of catalyst particles are located in the dense bed immediately above the air distributor. The dilute phase is the region above

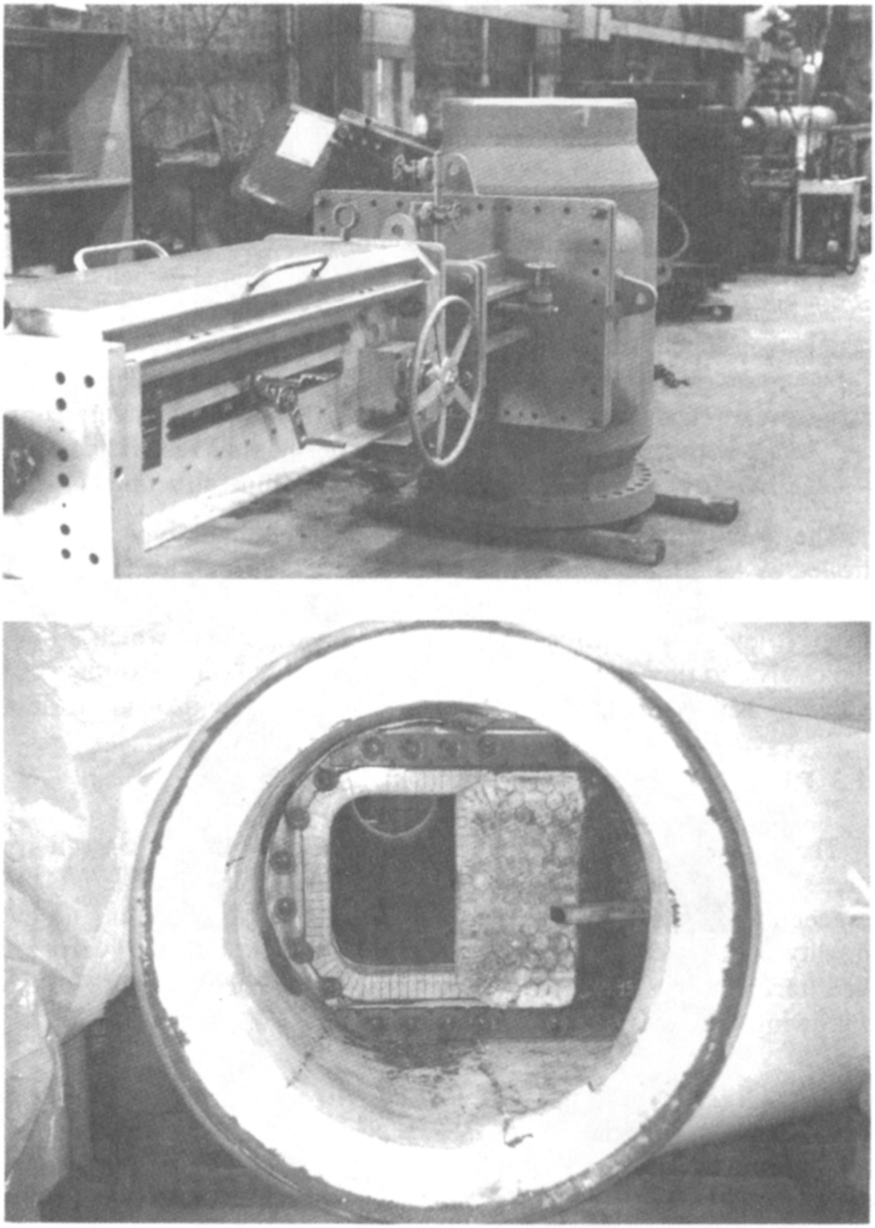

Figure 4-50. Catalyst slide valve. *(Source: Enpro Systems, Channelview, Texas.)*

Table 4-3
Typical reactions occurring in FCC units

			K Cal/Kg of C, H_2, or S	BTU/lb of C, H_2, or S
$C + 1/2\ O_2$	$\rightarrow$	CO	2,200	3,968
$2CO + O_2$	$\rightarrow$	$2CO_2$	5,600	10,100
$C + O_2$	$\rightarrow$	CO_2	7,820	14,100
$H_2 + 1/2\ O_2$	$\rightarrow$	H_2O	28,900	52,125
$S + xO$	$\rightarrow$	SO_x	2,209	3,983
$N + xO$	$\rightarrow$	NO_x		

Figure 4-51. Air distributor—"pipe grid" design version. *(Source: Enpro Systems, Channelview, Texas.)*

the dense phase up to the cyclone inlet and has a substantially lower catalyst concentration.

Standpipe and Slide Valve

From the regenerator, the regenerated catalyst flows down a transfer line commonly referred to as a standpipe. A standpipe provides the necessary pressure head needed to circulate the catalyst around the

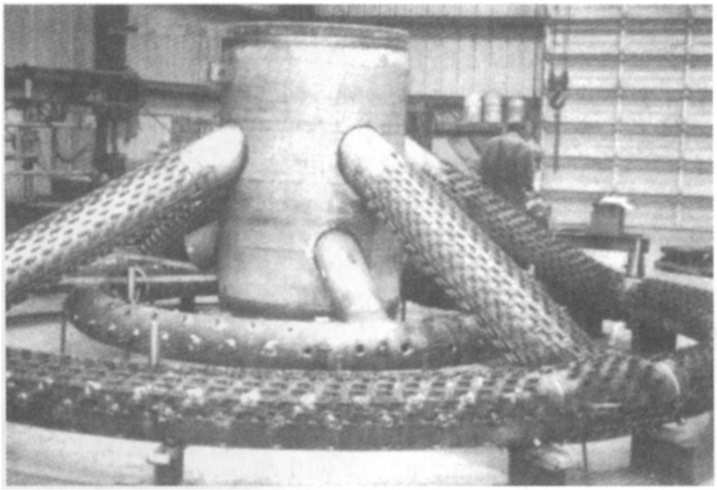

Figure 4-52. Air distributor—"air ring" design. *(Source: Val-Vamp, Inc., Houston, Texas.)*

unit. In some units, standpipes are extended into the regenerator, and the top section is often called a catalyst hopper. The hopper, which is internal to the regenerator, is usually an inverted cone design. Its function is to provide sufficient time for the regenerated catalyst to be aerated before entering the standpipe. Standpipes are typically sized for a flux rate in the range of 100–300 lbs/sec-ft^2 of circulating catalyst. In most cases, sufficient flue gas is carried down with the regenerated catalyst to keep it fluidized, however, longer standpipes may require external aeration. Aeration is ensured by injecting a supplemental gas medium, such as air, steam, nitrogen, or fuel gas, along the length of the standpipe. The catalyst density in a well-designed standpipe is in the range of 35–45 lbs/ft^3.

The flowrate of the regenerated catalyst to the riser is commonly regulated through the use of either a slide or plug valve. The operation of a slide valve is similar to that of a variable orifice. Slide valve operation is automatic. Its main function is to supply enough catalyst to heat the feed and achieve the desired reactor temperature.

Catalyst Separation

As the flue gas leaves the dense phase of the regenerator, it entrains catalyst particles. The amount of entrainment largely depends on the flue gas superficial velocity. The larger catalyst particles, 50–90 μ, fall back into the dense bed. However, for the smaller particles, 0–50 μ, the flue gas velocity is sufficient to suspend them in the dilute phase and carry them out of the regenerator and into the cyclones.

Most FCC unit regenerators employ 6–16 sets of primary and secondary cyclones in series, depending on unit size. These cyclones are designed to recover catalyst particles that are larger than 20 μ. The recovered catalyst particles are returned to the regenerator via the diplegs. The flue gas exits the cyclones through a plenum chamber.

The distance above the catalyst bed in which the flue gas velocity has stabilized is referred to as the transport disengaging height (TDH). At this distance, there is no further gravitation of catalyst. The centerline of the first-stage cyclone inlets should be at TDH or higher; otherwise, excessive catalyst entrainment will cause extreme catalyst losses.

Flue Gas Heat Recovery Schemes

The hot flue gas leaving the regenerator plenum holds an appreciable amount of energy. A number of heat recovery schemes are used to recover this energy. In some units, the flue gas is sent to a CO boiler where both the sensible and the combustible heat are used to generate high-pressure steam. In other units, the flue gas is exchanged with boiler feed water to produce steam through the use of shell/tube or box heat exchangers.

In most units, the flue gas pressure is reduced to atmospheric pressure across an orifice chamber. The orifice chamber is a vessel containing a series of perforated plates designed to maintain a given back-pressure upstream of the regenerator pressure control valve.

In some larger units, a turboexpander is used to recover this pressure energy. To protect the expander blades from erosion by the catalyst, the flue gas is first sent to a third-stage separator to remove the fines. The third-stage separator, which is external to the regenerator, consists of a large number of swirl tubes designed to separate 70%–95% of the incoming particles from the flue gas.

A power recovery train—occasionally called a string—(Figure 4-53) employing a turboexpander usually consists of four main elements or casings: the expander, a motor-generator, an air blower, and a steam turbine. The steam turbine is used primarily for startup and often to supplement the expander for generation of energy. This topic will be discussed in more detail later in this chapter.

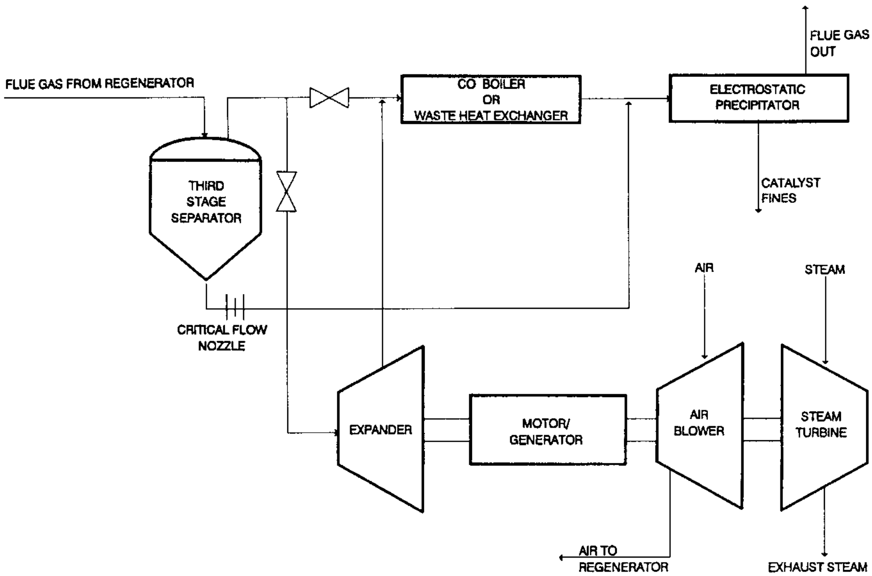

Figure 4-53. A typical flue gas power recovery scheme.

The motor-generator can either produce or absorb power. In some FCC units, the expander horsepower exceeds the power needed to drive the air blower. In this case, the excess power is transmitted to the refinery power grid. If the expander generates less power than required by the blower, the motor-generator provides the power to hold the entire train at the desired speed.

From the expander, the flue gas travels through a (waste heat) steam generator to recover additional energy. Depending on local environmental regulations, an electrostatic precipitator (ESP) or a wet gas scrubber may be placed downstream of the waste heat generator prior to releasing the flue gas to the atmosphere. In some units, an ESP is used to further remove catalyst fines in the range of 5–20 μ from the flue gas. In other units, a wet gas scrubber is used to remove both catalyst fines and sulfur compounds from the flue gas stream.

Catalyst Types

Many substances exhibit catalytic properties to a greater or lesser degree, but only a few compounds are satisfactory for commercial cracking. A good catalyst is a compound that has a high activity so that only small quantities are necesary. High activity alone, however, is not enough. The catalyst must have the ability to produce desirable products. For example, a catalyst must not produce too much coke. High coke yields are extremely undesirable because whatever feed weight goes to coke is lost so far as useful products are concerned, and the coke deposited on the surface of the catalyst lowers its activity. This coke deposit must be burned off to regain activity and regeneration is an expensive process.

The catalyst must also be selective to valuable products. Gasoline is desirable, therefore high yields must be produced, but it must be high-octane gasoline. C_3's and C_4's are sometimes required for polymerization, alkylation, and chemical production. Certain catalysts give high yields of these compounds, especially the unsaturated components. Gases, such as methane and hydrogen, are undesirable so the yield of these products must be suppressed.

A good catalyst is also stable. It must not deactivate at the high temperature levels (1,300–1,400°F) experienced in modern regenerators. It must also be resistant to contamination. While all catalysts are subject to contamination by certain metals, such as nickel, vanadium, and iron in extremely minute amounts, some are affected much more than others. While metal contaminants deactivate the catalyst slightly, this is not serious. The important effect of the metals is that they destroy a catalyst's selectivity. Hydrogen and coke yields rise rapidly, and the gasoline yield decreases. The effect is so serious that feeds containing less than 0.5 ppm nickel have caused debits amounting to $7,800/day in a 35,000 B/D fresh feed unit using "3A," a catalyst described below. While zeolite catalysts are not as sensitive to metals as 3A catalysts, they are more sensitive to the carbon level on the catalyst. Since all commercial catalysts are contaminated to some extent, it has been necessary to develop a measurement that reflects the degree of contamination.

Over the years, thousands of compounds have been tried as cracking catalysts. These compounds fall into two general categories: natural and synthetic. Natural catalyst, as the name denotes, is a naturally occurring clay that is given relatively mild treating and screening before use. The synthetic catalysts are more important because of their widespread use. Two main types of synthetic catalysts are currently in use: amorphous and zeolitie.

For many years the most common catalyst was an amorphous or noncrystalline type called 3A. Initially, all 3A catalyst contained 13%

alumina and 87% silica. To improve activity maintenance, the alumina content was increased to 25%. Both 13% and 25% alumina grades continue to be used; the choice at a given refinery is based on the specific situation. Another amorphous-type catalyst, containing silica-magnesia and called 3E, has also been used in several commercial versions. A major step in catalyst development was the introduction of crystalline zeolitic, or molecular sieve catalysts. First used commercially in 1962, they are now employed by over 90% of U.S. industry. Their activity is very high, some of the active sites being estimated at 10,000 times the effectiveness of amorphous silica-alumina sites. Because the zeolite crystals are too small to be used directly, and because of their extremely high activity, small amounts such as 3%–25% of zeolite are impregnated on amorphous clay or silica-alumina base to make commercial catalysts.

With the many types of cracking catalysts available today, catalyst selection has become an important part of refinery planning. For a given refinery situation, both the level and type of conversion are important. For example, a 75% conversion level can be achieved at moderate reactor temperatures with highly active catalyst, producing maximum yields of good octane gasoline. Or, a 75% conversion level can be achieved at high reactor temperatures with moderately active catalyst, producing maximum yields of olefinic gases and a gasoline product with very high octane. By changing catalyst types, a refiner has wide flexibility in choosing the conversion level and product slate that best meets their particular requirements. Generally, catalyst types are selected to suit feedstock quality, desired conversion level, and regional and seasonal product distribution requirements.

DESIGN ISSUES RELATING TO FCC TURBOEXPANDERS

In the mid-to-late 1960s, some were reluctant to use turboexpanders in FCC units. The reasons for the non-implemention often included:

- The low catalyst recovery system efficiency
- The difficulties of designing the turboexpanders for this service
- The investment cost required with minimal emphasis on pollution control

The problem of efficient catalyst recovery from the flue gas has since been overcome by Shell, which has an external separator design available for licensing. The Shell separator proved successful in reducing catalyst carryover in the flue gas to a level of concentration and particle size range that is acceptable for expander service. Other refiners have had success with designs that do not use the Shell separator, but which are nevertheless able to achieve a level of performance equally acceptable for such service.

The second problem in the foregoing list exists because the design of expanders for FCC service is a rather specialized field, especially in larger sizes of axial design. Only a handful of manufacturers are fully able to supply such expanders. The designs are generally similar (Figure 4-54) and all appear to offer machines that can reasonably be expected to remain on-stream for periods equal to the extended runs now common on major refiner's FCC units.

In order to overcome apprehension regarding erosion of turbine blades during service and the hazards attending such failure, provision is made for visual inspection by a strobe light and camera while in operation. Scheduled inspection by a camera (borescope) permits

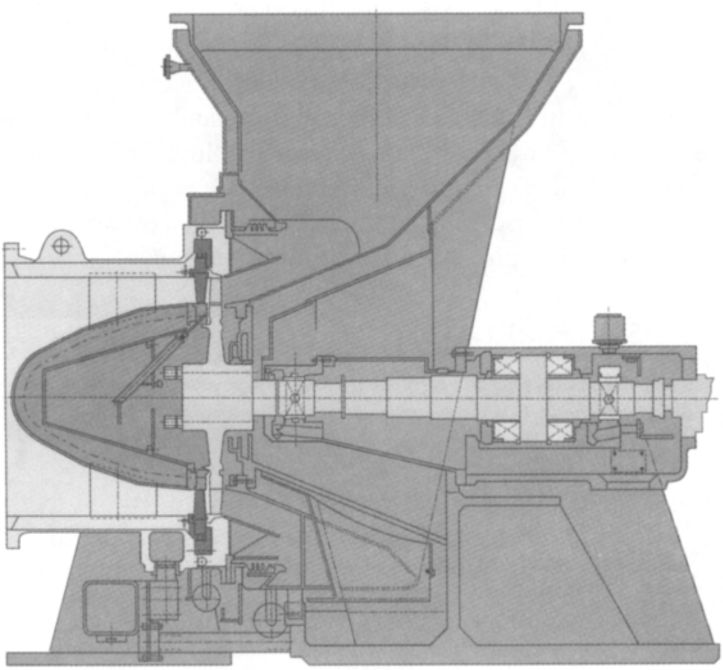

Figure 4-54. Cross-section of an Elliott single-stage hot gas expander.

reasonable predictions of the remaining bladelife. Bladelife has now been extended up to three years and is a direct function of the efficiency of the catalyst separator.

The problem of economic justification for the required investment is a matter that depends on the individual refinery situation. However, it is almost certain that more refiners will be installing such equipment in the future. The ability of the equipment to operate satisfactorily has been amply demonstrated and this will increase the refiner's desire to consider and use flue gas expanders for FCC installations (Figure 4-55). For typical sizes, refer to Figure 4-56.

Many locations worldwide now have very strict requirements in regard to atmospheric pollution due to gaseous and particulate exhausts. Regulations will become even more stringent in the future. Emphasis on pollution control will make the improved separator a desirable (and in some cases, necessary) expenditure even without the expander. Thus, a portion of the investment cost of creating a suitable environment for the expander can be assigned or allocated to pollution control.

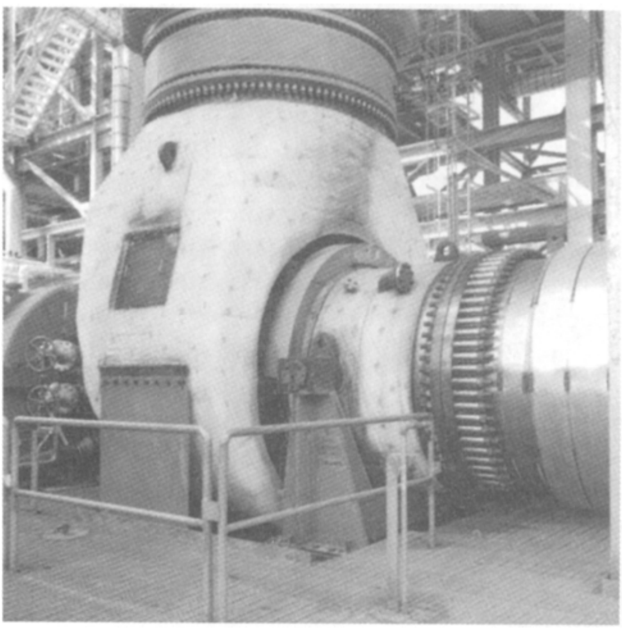

Figure 4-55. Elliott hot gas expander installed in an FCC power recovery string rated at 42,000 hp (31,330 kW).

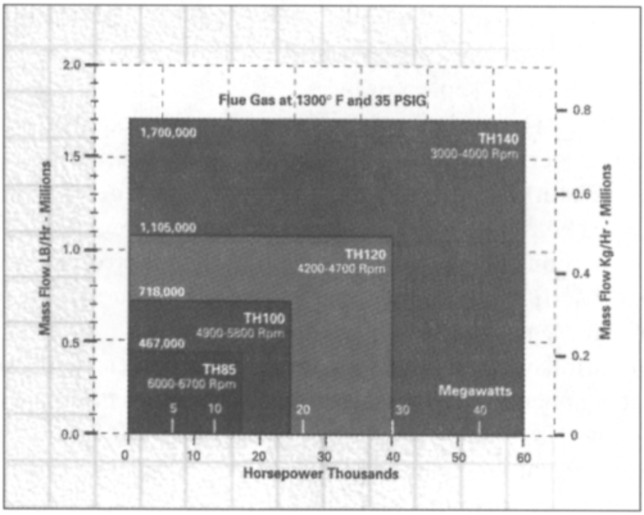

Figure 4-56. Typical size chart for hot gas expanders in FCC units. *(Source: Elliott Company.)*

If the refiner does not have a CO boiler and the combination of an expander and CO boiler can be used in the economic study, there is little doubt as to the attractiveness of the return. Although the CO boiler is probably the easiest to justify economically, this is not the case with the expander. The difficulty in justifying the expander stems, in part, from the average refiner's tendency to view it as an experimental installation and, therefore, overdesign it. It is important for the refiner to remember that "Best-of-Class" owner/user companies reap substantial profits from their hot gas expander installations. Interested refiners should perhaps consider engaging a competent engineering designer to make the study. This approach eliminates some of the danger of having the design influenced by the refiner's preconceived ideas. An objective study may result in economy of design without prejudicing the safety and operating capability of the completed installation. Whether refiner-designed or contractor-designed, low and high pressure are two types of installation that should be considered.

Low and High Pressures

The low pressure regenerator is usually found in units that have not been designed for the expander. In such cases, the expander may not be able to recover as much horsepower as required to supply the air blower.

A second type of design allows the regenerator to operate at a pressure high enough so that the expander has a horsepower recovery potential exceeding the requirements of the air blower. Most new FCC units are likely designed for higher pressure.

Both the high- and low-pressure units face the same issues regarding catalyst recovery and expander design. However, controls may differ in those designs that produce more horsepower than can be used by the primary driven machine.

It is most likely that in designing a new FCC unit the expander will drive the air blower and produce enough horsepower in the "end-of-bladelife" condition to supply the horsepower required by the air blower at the expander's end-of-run efficiency. There would also be an allowance for deviations from expected expander performance and air blower performance. Thus, the expander can be expected to have available, at start of run, a considerable amount of excess horsepower. This excess horsepower must be used in some economic manner without jeopardizing the continued safe operation of the FCC unit over its normal on-stream run time.

Consider the supposition that the excess horsepower sink is to be an electric power generator, which is tied into the refinery power system. If the refinery power system fails or if there is a fault in the generator system, the total generated horsepower normally going into the electrical power network becomes available for acceleration of the expander/blower train. This sequence of events may not appear to be a serious situation. It certainly would not be serious in the case of a steam turbine or other motive fluid turbine where a high pressure source is used and throttle valves are relatively small. However, in the case of an FCC expander the flue gas flow is quite large and has relatively low pressure. The inlet valve to the FCC expander is large and actuation time for full stroke may vary from 10–70 sec. This compares unfavorably with the normal steam turbine trip which functions in less than 1 sec. Since an expander/blower train may have as much as 33% total expander output as excess horsepower suddenly available for acceleration, it is possible to reach trip speed in 3–10 sec. Valve dependency, which take in excess of 3 sec to operate, becomes a real concern and a potential hazard.

It can be extremely dangerous to making simple assumptions or endeavor to conduct separate analyses of the expander and blower. The only satisfactory method to arrive at a safe, efficient, and practical design is to consider the air blower, regenerator, expander, and CO boiler as a single system. It follows that the requisite system calculations must completely cover the probable range of normal and emergency conditions. All piping hydraulics, control valves, and machine controls in the system must be included. For each possible condition a complete calculation is necessary, which includes:

- Stoichiometry of combustion
- Material balance on the regenerator
- Air blower performance
- Air line hydraulics
- Flue gas line hydraulics to the expander, including the regenerator pressure control valve
- The expander performance
- The expander exhaust line hydraulics through the CO boiler and stack

Obviously, if over-simplifying assumptions are to be avoided, a tremendous amount of trial-and-error calculation is involved in such a study.

Design Guides

With the aid of the computer and suitable programs, design calculations are feasible at a reasonable cost. Moreover, these calculations can be made without having to make questionable assumptions. A program has been developed by the Brown & Root Company that gives good results, enabling companies to perform quality studies.

A series of curves (Figures 4-57 through 4-60) indicate some of the design considerations that apply to expander installations. Some curves are purposely presented with parameter dimensions omitted; these curves then are qualitative rather than quantitative. Figure 4-57 is typical of a centrifugal air blower or air compressor, while Figure 4-58 represents an axial air blower (compressor). Expander performance is depicted in Figure 4-59, and expanders and blowers are compared in Figure 4-60.

The normal procedure to set design ratings for the blower is to calculate the blower design discharge pressure required for the design flow. Applying whatever safety factor is considered necessary, a design

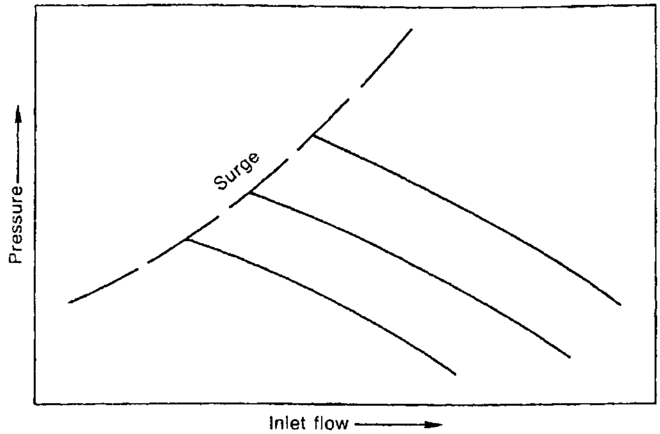

Figure 4-57. Centrifugal compression relationships.

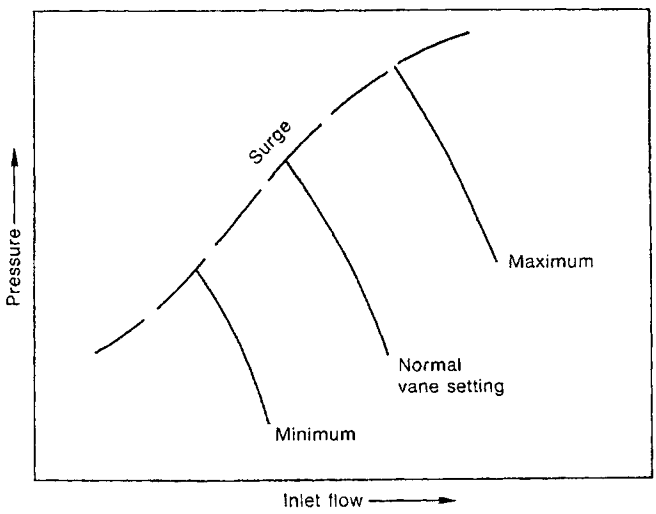

Figure 4-58. Axial compression relationships.

specification is then written for the resulting flow and pressure. The proposals are checked against these requirements. Also, a check is made to ensure that the machine is not in surge at design turndown rates. A similar procedure is followed for the expander. The train is checked for starting characteristics to ensure that there is starting capability.

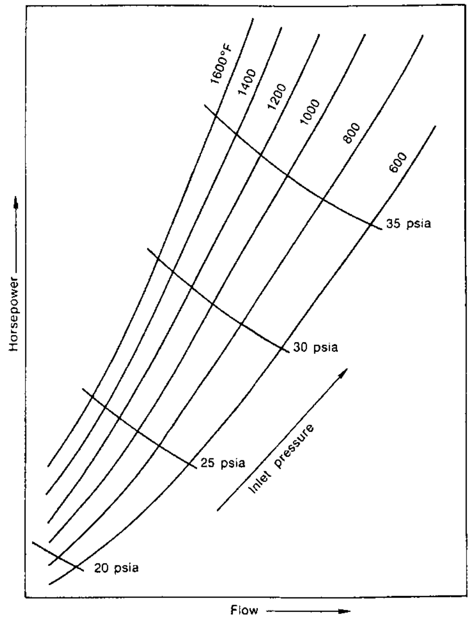

Figure 4-59. Typical expander parameters.

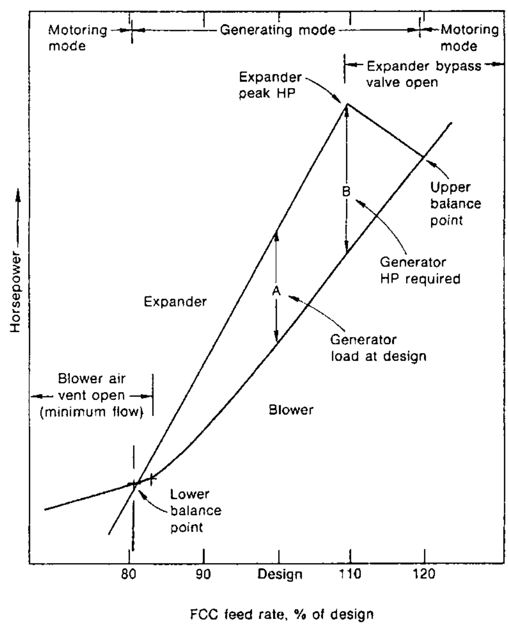

Figure 4-60. Expander deliver capacity versus blower capacity requirements.

Although the foregoing approach is acceptable design practice, it may not be sufficient for most installations. If the design point is used in size determinations, the generator will probably be sized incorrectly. Note how available excess horsepower varies in Figure 4-60. At low flow conditions the expander does not produce enough horsepower to satisfy air blower demand. Therefore, a motor/generator combined in one machine is a possible solution. As the fresh feed flow (and air flow) is increased, the horsepower output of the expander increases until it finally equals that required by the air blower. Beyond this flow the expander output increases until the pressure drop through both the flue gas system and expander increases to the upper limit where the regenerator excess pressure valve begins to open and gas will bypass the expander. This incipient bypass point coincides with the peak of the expander curve and gives the excess horsepower *B* available for the generator—as compared to the smaller excess horsepower *A* available at design conditions. As flow through the regenerator continues to increase past the bypass point, the expander excess horsepower decreases as a result of the flow-related increase in pressure drop through the regenerator overhead system. Finally, regenerator overhead flow increases to a point where expander output power once again equals air blower power requirements. At flue gas flows beyond this balance point, the expander horsepower is insufficient to supply the required power to the primary driven machine (i.e., the air blower).

The foregoing discussion of the system horsepower curves assumed only a single parameter of FCCU operating conditions. There are limitless combinations for which horsepower curves can be drawn for the expander and blower. Some of these are shown in Figures 4-61 through 4-66 and are discussed below.

Regenerator Pressure

Regenerator pressure is fixed by the design and control of the dilute phase regenerator operation. The effect of the regenerator pressure controller set point is shown in Figure 4-61. This pressure determines when the expander bypass valve begins to open. Thus, an increase in regenerator pressure will cause the expander to deliver more power than is required by the slightly increased power requirements of the air blower. The excess horsepower *B* increases to *C*. The Brown & Root computer program assumes that this pressure is known and fixed by controlling the regenerator.

(text continued on page 167)

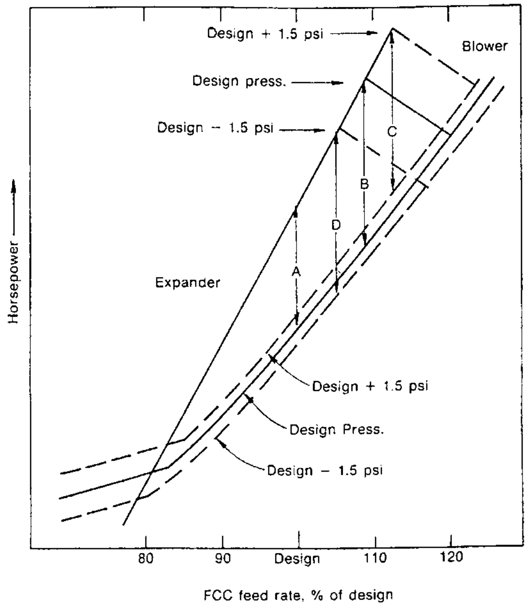

Figure 4-61. Effect of regenerator pressure.

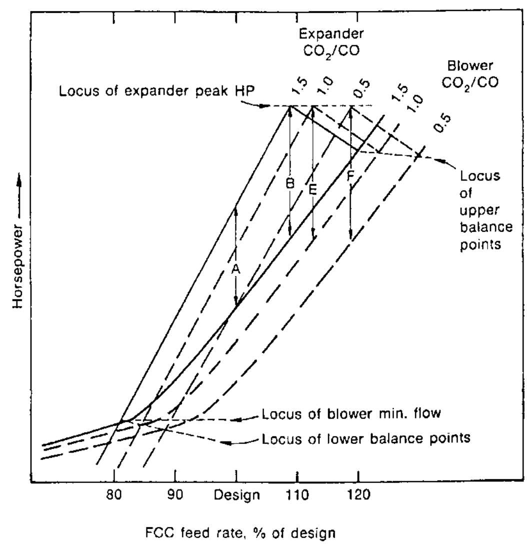

Figure 4-62. Effect of CO_2/CO ratio in the exhaust gases.

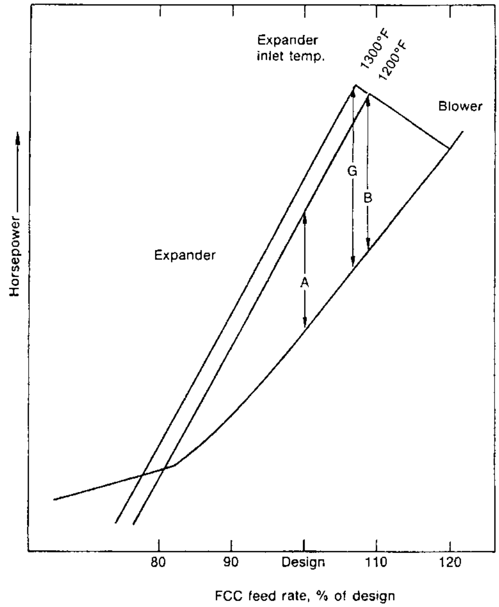

Figure 4-63. Effect of expander inlet gas temperature.

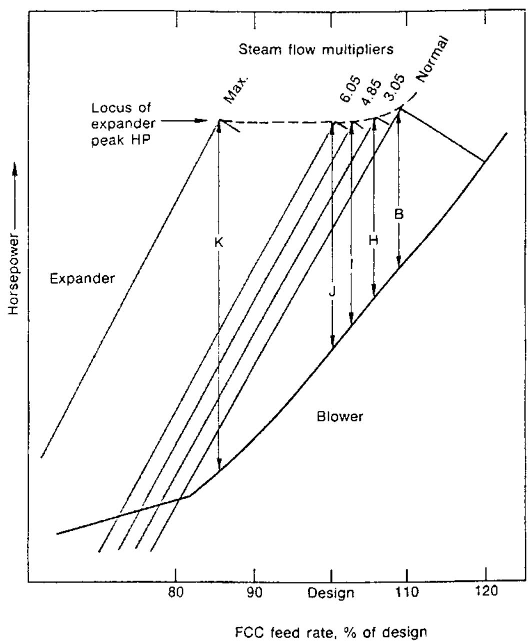

Figure 4-64. Effect of steam in the exhaust gases.

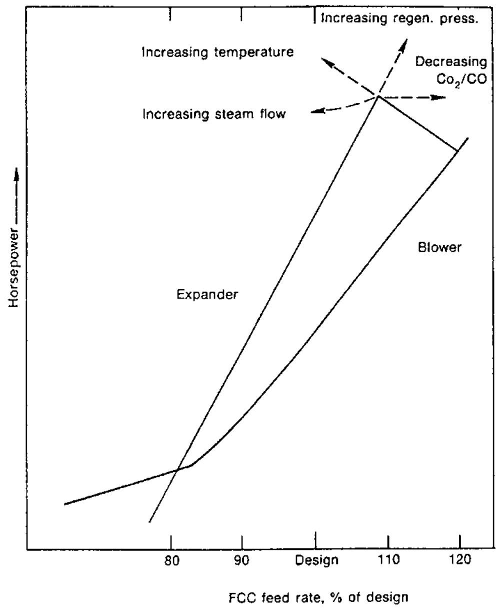

Figure 4-65. Comparative effects of various parameters.

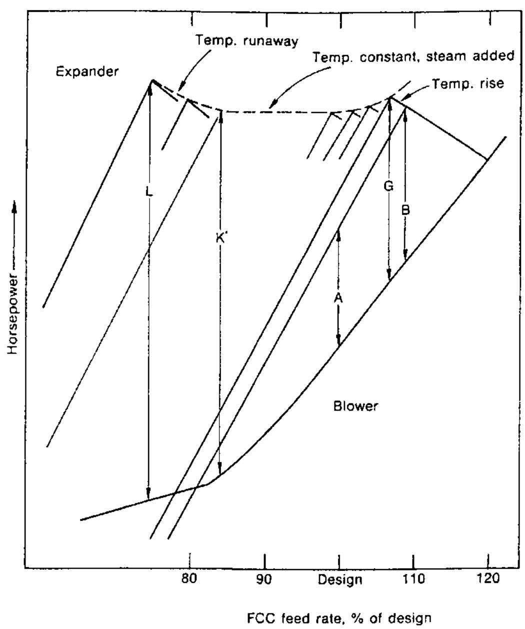

Figure 4-66. A progression toward temperature runaway.

(text continued from page 161)

Carbon Dioxide and Monoxide Ratios

CO_2/CO ratios are related to both the expander and blower horsepower curves. This effect is depicted in Figure 4-62 in which the design CO_2/CO ratio of 1.5 for a given feed rate is shown as solid lines. As the CO_2/CO ratio decreases, less combustion air is required and less flue gas is generated. In other words, less horsepower is required by the blower at the same time that less flue gas is available to the expander. Both expander and blower horsepower curves move to the right and the peak generating loads change only slightly as shown by comparing excess horsepower *B* with amounts *E* and *F* for lower CO_2/CO ratios. Low ratios are preferred in cracking operations because more feed can be run with a given installed air blower.

Temperature changes for the flue gas to the expander produce the effects shown in Figure 4-63. The expander inlet temperature at design is 1,200°F. As the expander inlet temperature rises, the expander horsepower curve moves to the left and upward while the change in the blower curve is insignificant. The results are that the lower horsepower balance point moves to the left and down, the peak of the expander curve moves to the left and up, the peak generator load increases to *G*, and the expander bypass valve opens at a lower feed rate.

Note that the increase in peak generator load is not simply the amount of increase in the peak expander horsepower. Since the peak has moved to the left as well as up, the coincident horsepower required by the blower has been reduced and the equivalent of this reduction is also added to the peak generator load.

An increase in ambient air temperature will decrease the available energy for the generator. This assumes that the fresh feed and coke burn remains constant. The expander horsepower does not change, but the air blower horsepower increases with increased air temperature, causing the excess energy to decrease. Steam and water may need to be added to the flue gas flow at various points in the system to control afterburning. In Figure 4-64, the solid curves are for a normal flow of steam. The dotted curves are for increases in the steam rate by 3.05 times, 4.85 times, and 6.05 times the normal flowrate.

Again, the blower horsepower curve is not appreciably changed. The expander horsepower curves, however, are moved to the left. Note that the locus of peaks moves to the left and down initially, then moves horizontally to the left with the addition of steam. The effects are due to a reduction in the molecular weight of the flue gas and an increase in the volume of the flue gas. This combination moves the peak expander horsepower to the left and down. Increases beyond about five times normal steam quantity cause only horizontal change in the peak because of the lessening effect on weight flow through the expander, but continued increase in actual volume of flow. Thus, the excess horsepower increases as shown by *H, I,* and *J.*

Factors Influencing Peak Power Output

A composite of the factors influencing peak expander horsepower is shown in Figure 4-65. Decreasing feed rate or regenerator pressure moves expander peak power down and to the left along the expander curve. Decreasing CO_2/CO ratio in the flue gas moves expander peak power horizontally to the right. Increasing the temperature of the flue gas going to the expander moves the peak power in essentially a straight line upward and to the left. Increasing steam moves the expander peak power in a curving path downward and to the left until it becomes horizontal to the left after the steam rate is more than about five times the normal steam rate.

Power Failure

An important part of designing a power recovery train is to consider the case of a generator failure. In the previously reported study, the selected generator has a rating that is approximately one-third of the rated capacity of the expander. If the system were operating at rated capacity *B* when a failure occurred either in the electrical network or in the generator itself, approximately one-third of the expander output horsepower would be available for acceleration of the train. The resulting acceleration is quite rapid and results in reaching trip speed in approximately 3 sec. If, on the other hand, the generator was at normal generating load represented by *A* at the time of power failure, the time to trip would be 8 sec or more. If the expander train did not have any blower and all of the load was generating capacity, the time to trip on loss of generating capability would be less than 1 sec.

These short times are significant when considering that a standard FCCU slide valve will probably move at 1 in./sec—if it doesn't stick.

Remember that ordinary pneumatic control instrumentation can have an appreciable lag time, therefore, valve action probably will not start for 3 sec.

The solution is to provide valves and actuators that will operate in time to prevent "excessive" overspeeding of the train. The control pickup and transmission system must be electronic to provide essentially instantaneous response. Actuators must be foolproof and powerful, as well as quick acting.

Operator Response

A forecast of operator response is another important factor to consider in developing design specifications. For example, consider the unit in this study is operating at design conditions where the CO_2/CO ratio is 1.5, flue gas temperature is 1,200°F, and the steam rate is normal. Figure 4-66 illustrates this condition and how expander horsepower minus blower horsepower at design would give the excess power available for the generator, as represented by line *A*.

What happens if the expander were operating at peak power so that the excess power supplied to the generator is represented by line *B*? Assume afterburning occurs to cause a temperature rise. In the events that follow, there will be variations detectable in the blower horsepower requirements, but they will be small compared to the others that occur. If the unit was in lined-out operation before the afterburning occurred, the operators will be reluctant to disturb the regenerator-reactor balance.

It is reasonable to assume there would be no operator intervention in time to prevent a 100°F rise in expander inlet temperature. Line *G* represents the power delivered to the generator at the higher temperature of 1,300°F. Either the operators or a controller will likely add a water spray to prevent a further rise in temperature.

If the regenerator temperature continues to rise, additional quantities of steam will be added in the form of water spray by either manual or automatic means—first, through one set of injection nozzles in the overhead line, then through another set elsewhere. It may become necessary to add steam to the cyclones in order to maintain 1,300°F to the expander. Spray nozzles in the dilute phase might also be used if the temperature continues to rise.

Steam Rate Increase

With each additional increase in steam rate, the expander curve in Figure 4-66 moves to the left and the excess power delivered to the generator becomes increasingly larger. At maximum steam addition rates, the excess power is represented by line K'. Note line K' in Figure 4-66 is similar to line K in Figure 4-64, except that the expander in Figure 4-66 is operating at a higher temperature.

Any further increase in regenerator temperature will not be corrected by steam because the maximum steam rate has already been reached. Therefore, line L represents one condition in a progression of uncorrected temperature rises.

It is important point to note that most operating situations that move the expander curve to the left will result in large increases of excess power being absorbed by the generator. The power capacity of the generator under these conditions would be much greater than that required at normal design. Thus, other forms of control are needed to avoid the need for an oversized generator.

Power System Stability

Power system stability studies can provide some insight into the effects of power failure. The calculations can become tedious if performed manually because of the iterative steps required to obtain satisfactory answers. Therefore, a computer program is used to supply the iterative answers in a short time and with comparable accuracy.

Consideration of the effects of power failure and the resulting loss of speed control must include peak shaft torque, which can be supplied to the shaft as the train speeds up. Of even more concern is the sudden braking (also called "breaking") effect, which may result if acceleration has occurred and the power circuits are re-energized after acceleration has taken place. Power outages or dips longer than a few cycles should lock out the breakers so that reclosure cannot be effected until the speed has been brought below generating speed so that the motor/generator is in motoring mode when re-energized.

Results of studies to determine the effect of stator vane control on acceleration are shown in Figures 4-67 and 4-68. The first control step shown in Figure 4-67 is to have the stator vanes normally on flow control with a 2 sec lag in the flow control. On reaching trip, the stator vanes drive to the wide open position after a 1 sec lag. The vanes move at design speed.

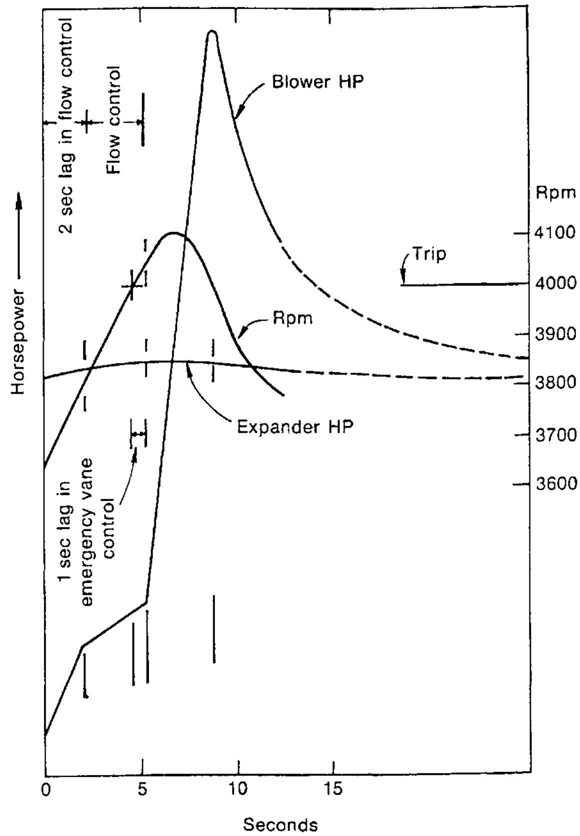

Figure 4-67. Acceleration caused by power failure.

Note that during the first control step the lag in the flow control allows the air flow to increase as rpm increases and a relatively steep rise in blower horsepower results. At 2 sec the flow control acts and reduces the rate of increase in blower horsepower.

The trip operates at approximately 4.25 sec, but no effect is seen until the 1 sec lag in the trip actuation of the vanes has passed. Thus, it is after the 1 sec lag that the vanes start driving to the wide open position at the design actuation rate. The result is a sharp increase in air flow and blower horsepower. Note that this flow is going into the regenerator since no "SNORK" valve has been included in the calculations. The acceleration reaches a peak at about 6.5 sec and blower horsepower peaks at about 8.25 sec, with the vanes fully open at 8.5 sec. Sometime over 30 sec the horsepower of the blower and expander will equalize. If no other action results they will stabilize.

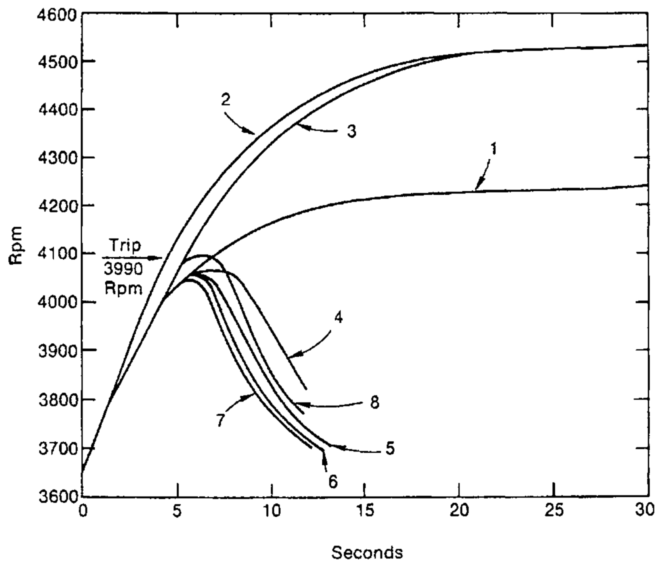

Figure 4-68. Acceleration effects under various conditions: (1) Vanes fixed; (2) Vanes on flow control, no time lag; (3) Vanes on flow control, 2 sec lag; (4) Vanes fixed until trip, trip moves 5°/sec; (5) Same as 4 except moves vanes 10°/sec; (6) Same as 4 except moves vanes 15°/sec; (7) Same as 4 except moves vanes 20°/sec; (8) Vanes on flow control, 2 sec lag, 10°/sec.

It is interesting to note that very little change in expander horsepower has resulted. The "surge" capacity of the regenerator system has maintained essentially the same flow to the expander, and most of the expander horsepower change is due to a variation in efficiency.

A number of variations of the stator vane control are shown in Figure 4-68. Only rpm versus time in seconds is shown. All curves are based on starting from a maximum generator load at the time of generator failure.

Curve 1 shows a fixed vane case, which is the equivalent of having no stator vanes or having stator vanes that are inoperative. Curve 2 represents stator vanes that exercise instantaneous flow control (no lag) with no trip action. Curve 3 is for stator vane control with a 2 sec lag and no trip action. Curves 4, 5, 6, and 7 are for fixed stator vanes until trip, with trip driving them to the wide open position (after 1 sec lag) at rates corresponding to half design rate, design rate, one, and one-half design rate, respectively. The faster the action of the vanes, the lower the rpm peak. However, although not shown on the curves, the faster action also increases the blower horsepower peak and, consequently, increases the peak torque on the shaft and couplings. Curve 8 corresponds to the curve of Figure 4-67. The rpm peak is higher because the flow control action takes place between 2 sec from power failure and 1 sec after trip. However, this closely represents the actual case that could be expected in an installation where vanes were on flow control and no other trip devices were provided.

Control Cautions

Caution should be taken to prevent excessive acceleration. One solution is to provide for opening of the compressor discharge vent valve to increase the compressor flow and increase blower horsepower. This is effective with a centrifugal compressor, however, not with an axial compressor unless the compressor is provided with adjustable stator vanes that are reliable. This can be seen from the performance curve. The head versus flow curve for a given vane setting is extremely steep and opening the vent valve is ineffective. However, if the vanes operate fully open and the vent valve opens, the combined effect is satisfactory. The vent valve must not be oversized.

Another solution is to eliminate the air exiting the unit on the assumption that if no air goes in, no flue gas comes out to drive the expander. Again, this is not very effective because the unit acts as a large surge bottle and the large flue gas valves are relatively slow. Before the flue gas back-pressure valves have acted, excessive acceleration may result.

Noise control is worth mentioning. The turboexpander and axial compressors are noise producers and consideration must be given to the need for providing noise abatement. Silencers on vents and noise insulation housings on machines should be considered and have been proven effective.

Application Concerns

A satisfactory study of the application of the flue gas expander to a particular fluid catalytic cracking unit must include the following steps:

Step 1. Selection of normal operating conditions for the regenerator system. This sets normal air blower flow and head, and expander flow and head. If the proposed installation is being designed for an existing FCC unit, only a limited choice of conditions is available. In the design of a new FCC unit, however, it is possible to balance the cost of high-pressure regenerator design against the value of the energy recovered by means of the flue gas expander to arrive at a set of normal operating conditions that derives maximum return from the invested capital.

Step 2. System calculations over the entire range of possible operating conditions are required. The range must cover from the air blower minimum flow point to the expander bypass point for all reasonable variations in the applicable parameters of CO_2/CO ratio, fresh feed rate, flue gas temperature, ambient air temperature, and so forth.

Step 3. The final selection of a specific air blower and turbo-expander must be made after fully considerating the results of Steps 1 and 2. The normal operating point must be located on the system operating map (similar to Figure 4-66) so that reasonable latitude is available in operating variables between normal operating point and air blower minimum flow, and between operating point and expander bypass point.

Step 4. A study of starting characteristics of the train is necessary to select the correct startup driver rating (motor and/or steam turbine).

Step 5. The selection of an electric generator size must be made on the basis of the results of Step 2 with full consideration of the various parameters as shown in Figure 4-66.

Step 6. Acceleration calculations should be made to determine the effects of electrical power failure. Overspeeding of the train can be destructive if controls are inadequate to limit the peak speed within reasonable bounds.

Interest in the application of turboexpanders turbine to FCC unit is very high, and deservedly so. The power recovery turboexpander offers practical improvement in FCC unit operating economics. Modern designs that encompass the entire system have fully overcome problems and concerns that may have existed decades ago. Expander metallurgy is available to vastly reduce erosion rates experienced when turboexpanders were first applied in FCC units. Should issues arise, they can be addressed and fully resolved through complete analysis and proper follow-up. A summary of design considerations is given in Table 4-4.

POWER GENERATION FOR THE FCC PROCESS

As energy costs increase the importance of efficiency in each process grows. This is certainly true for the Fluid Catalytic Cracking (FCC) process where energy recovery from the hot pressurized regenerator flue gas has become commonplace since the 1970s. Initially, power from the FCC unit was recovered in an expander that was connected to the main air blower. Toward the end of the twentieth century, there was increased interest in using the hot pressurized flue gas in the FCC process for generating electricity. Today, users have the choice of either application; both achieve power recovery effectively.

The system that generates only electricity from the hot flue gas is called a Total Power Generation (TPG) system. The following reviews the design considerations related to common string arrangements, the use of synchronous versus induction generators, the TPG operational differences compared to the traditional FCC string, and a typical control system for the TPG train.

Table 4-4
Summary of design considerations

- Catalyst entrainment to expander
- Maximum design temperature at expander inlet
- Design CO_2/CO ratio
- Regenerator pressure
- Expander metallurgy
- Design ambient air temperature
- Effect of cooling sprays on expander horsepower
- Effect of erosion on expander output
- Actuation time for emergency controls
- FCCU turndown requirements
- Selection of adequate motor/generator size
- Adequate sizing of shafts, couplings, and bearings for maximum torque conditions

String Arrangements

Figure 4-69 shows a typical five-body FCC main air blower string consisting of an expander, axial compressor, steam turbine, speed-reducing gear, and generator. Although other arrangements are possible, this setup contains all the elements that are required in the main air blower train, or string. The axial compressor supplies air to the regenerator. The steam turbine provides startup power, additional power generation capability, and power for the main air blower if the motor/generator or expander is out of service. The expander supplies the power for the main air blower and excess power is used to generate electricity. The motor/generator, usually the induction type, generates electricity from the excess power, supplements the steam turbine power if the expander is out of service, and supplements the steam turbine during startup or provides all the startup power if there is no steam turbine in the string. Since the generator must operate at a constant (synchronous) speed, the gear ratio is selected so that the main bodies in the string will operate at a speed that optimizes their efficiency.

Figure 4-70 shows a four-body TPG train (string). As before, the expander supplies power to the generator. The steam turbine supplies power to the generator, provides startup power, and provides control for synchronization. The generator provides electricity, and the gear is used to allow the expander and steam turbine to operate at near optimum efficiency with the generator at its desired speed.

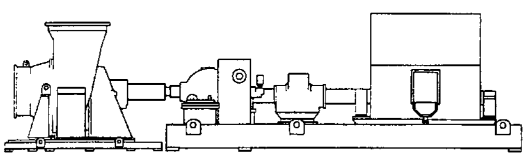

Figure 4-69. Five-body FCC string.

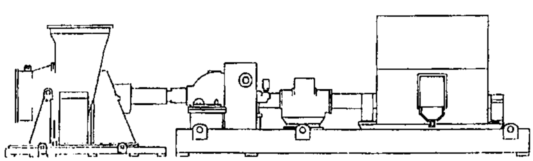

Figure 4-70. Four-body total power generation (TPG) string.

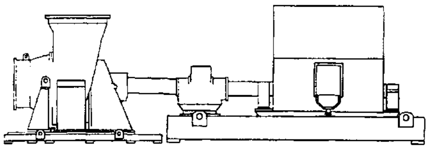

Figure 4-71. Three-body TPG string.

The typical three-body TPG string is shown in Figure 4-71. With this arrangement the generated electricity is limited by the expander output. Additionally, both startup and synchronization must be accomplished by the expander instead of the steam turbine.

Single versus Two Trains

If there is an existing main air blower train (or string; the terms are used interchangeably), it is relatively easy to add a separate TPG string. It is also possible during the planning stage of the main air blower to make provisions for the addition of an expander and generator to the main air blower train.

Some of the design considerations of one full power recovery string versus separate air blower and TPG strings are listed Table 4-5. One full FCC power recovery string will take up less area and, therefore, may initially be less expensive. However, when there is a separate TPG string, a synchronous generator will reduce plant utility costs. With the full string layout the expander and generator are a part of the process; with separate strings the TPG and process operations are independent of each other.

Generator Type

Deciding whether to use an induction or the synchronous generator must also be made. Design considerations of induction and synchronous generators are shown in Table 4-6. An advantage that favors the induction type is that it is easier to synchronize. An advantage that favors the synchronous type is the improved plant load power factor correction. Generally, induction generators are used on full power recovery FCC strings and synchronous generators are used on TPG strings. However, generator types must be selected on a case-by-case basis.

(text continued on page 180)

Table 4-5
Design considerations, full versus separate TPG strings

Full FCC string		Separate air blower and TPG string	
Design considerations		**Design considerations**	
• Minimum amount of real estate • Large string inertia • Synchronization of generator less accurate	• Larger steam turbine or bootstrap required • Expander and generator part of process • Addition of expander requires prior planning • Induction M/G decreases power factor • Loss of production on loss of generator or expander	• Independent start-up, steam turbine sized for blower • Process line-out independent of expander • Reduced exposure of expander to high catalyst loadings • Retrofit with minimum disturbance • Synchronous generator helps power factor • Outage of generator or expander does not affect production	• Requires more area • Lower string inertia on load loss • Synchronization requires increases sophistication

Table 4-6
Design considerations in generator selection

Generator Comparisons			
Synchronous		**Induction**	
• Plant load power factor correction • Not limited in size; solid-pole rotors available in larger sizes • When you lose the tie line, you can still supply the rest of the plant	• Requires sophisticated control of excitation voltage (Requires d.c. excitation source.) Speed regulation must be precise (only when disconnected from tie line) • Can't handle overloads as well as induction system (except when synchronous system is oversized). Limited pull out torque. (Normally 200%.) Requires short circuit current protection	• No synchronization problems (Gets excitation from utility line or in-plant synchronous condenser) • Better able to handle overloads. Large pull out torque as a generator. No short circuit protection required.	• Makes plant power factor worst • Limited to about 16,000 hp (at 3600 rpm) because of laminated rotor • If utility tie line is lost, you lose power unless synchronous condensers are installed in the plant

(text continued from page 177)

Operational Differences

There are several operational differences between the TPG arrangement and the full FCC string including the normal operating speed, synchronization, and startup.

The normal operating speed of the full string can vary as much as 5%. The normal operating speed of the TPG string is usually constant at synchronous speed or, at most, a +1% speed for an induction generator drive.

The full FCC string is synchronized using the governor controls on the steam turbine. Synchronization of the three-body TPG string is accomplished through the control system and large expander valves.

Startup of the full string is normally a bootstrap operation with the expander being heated as the process vessels and piping experience the process-dependent temperature increase. The expander is exposed to many hours of off-design conditions and abnormal catalyst loadings during the startup period. For the TPG system, the entire process is brought to steady-state before startup begins. If there is no steam turbine, the TPG string is put on turning gear. Next, steam is added to remove the string from the turning gear and raise it to nominal speed. Flue gas is then gradually added to increase the train speed to synchronous conditions and control the heating rate of the expander. After synchronizing, flue gas is increased to full flowrate, and the steam is backed out until the generator is producing full steady-state power.

TYPICAL CONTROL SYSTEMS

Modern control systems use microprocessors, programmable logic controllers (PLCs), and/or minicomputers to provide the various functions required by the TPG string. The control systems must encompass the valve arrangements, startup, synchronizing, and trip conditions. Figure 4-72 illustrates this concept. This control system is used in many FCC hot gas expanders designed and manufactured by Jeannette, a Pennsylvania-based Elliott Company. It can easily accommodate each of these conditions.

Valve Systems

During normal operation, the valve system for the TPG expander is basically the same as the expander in the full FCC power recovery

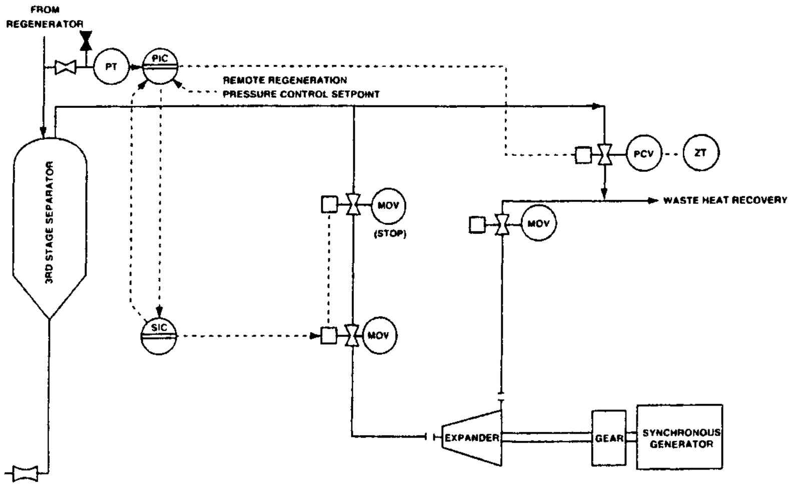

Figure 4-72. Simplified turboexpander control schematic.

string (Figure 4-72). The expander inlet butterfly valve maintains regenerator pressure control with the upstream motorized stop valve fully open.

Instead of using the expander main bypass valve for regenerator pressure control, it is also possible to install a small bypass valve, say 30%, downstream of the expander inlet butterfly valve, bypassing to the expander exhaust line as shown in Figure 4-73. Although this valve may not appear necessary, it can provide additional flexibility and protection.

Startup

After performing the usual pre-start activities, such as activating the lubricating oil, the TPG string is placed on turning gear. After making the necessary checks, steam is admitted between the expander inlet stop valve and butterfly valve as shown in Figure 4-74. The stop valve is closed at this time. After the expander is soaked to steam temperature, flue gas is gradually added at a rate not to exceed the expander allowable heating rate. As the flue gas rate is increased, the TPG string increases in speed. Care should be exercised to ensure the expander exhaust casing temperature rating is not exceeded and that string torsional critical speeds are avoided. The amount of flue gas is increased until the speed is slightly below synchronous speed. At this point, the TPG string is ready for synchronization.

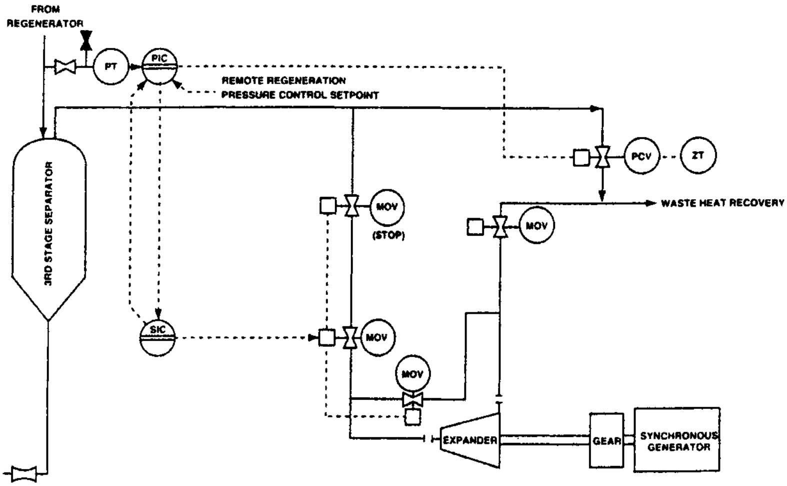

Figure 4-73. Expander bypass control schematic.

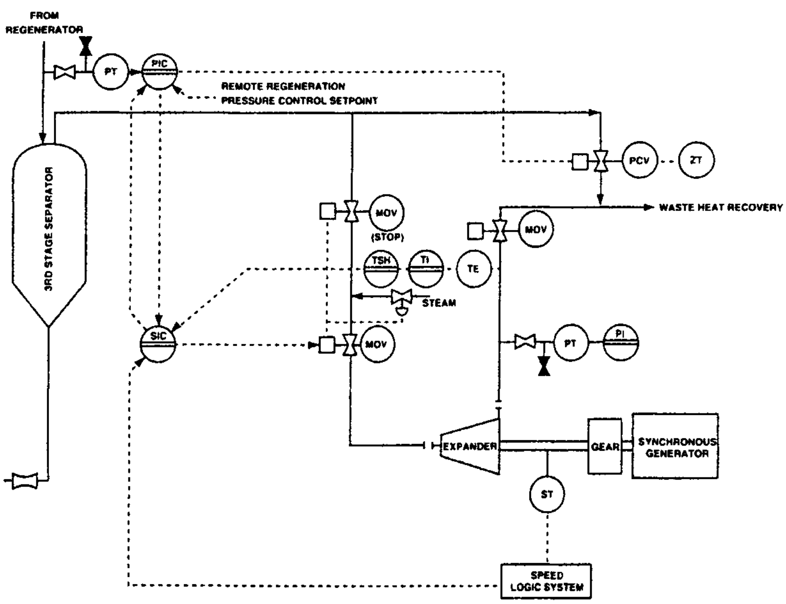

Figure 4-74. Typical startup schematic for turboexpanders in FCC units.

Synchronization

Once the switchgear and other electrical facilities are ready, the steam ahead of the expander inlet butterfly valve is increased so that the speed is slightly above the synchronous speed. This ensures that the expander exhaust casing temperature rating is not exceeded during synchronization. As shown in Figure 4-75, the small bypass valve located downstream of the expander inlet butterfly valve is gradually opened until the speed of the string exactly coincides with the synchronous speed. The generator is then synchronized with the power grid. Full load should then be placed on the generator by increasing the flue gas and backing out the control steam consistent with the expander heating rate. With the expander at full load, regenerator pressure control is maintained by the expander inlet butterfly valve.

Overspeed Protection

One of the most sensitive situations for the TPG string is during emergency conditions. Because of the lower inertia of the three-body

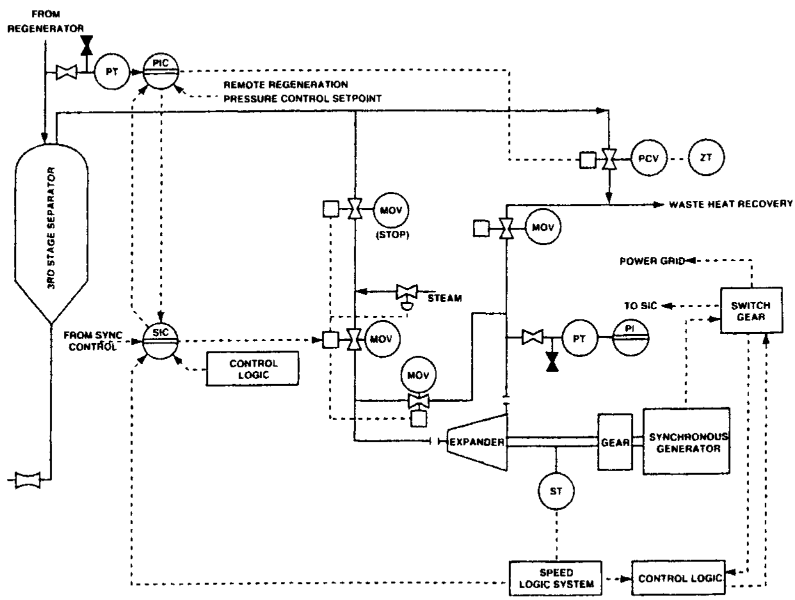

Figure 4-75. Control settings during speed synchronization of turboexpander in FCC service.

TPG string as compared to the five-body, "full" FCC string, overspeed of the TPG string is critical and the potential for higher overspeeds is significantly increased. For this reason, special consideration in the control system must be given to loss of generator load and coupling breakage. These are worst-case scenarios, but it should be noted that overspeed is also critical for the TPG system because of the large valves involved and because a large amount of energy is stored between the valves and the nozzle ring of the expander. A typical overspeed control system for the TPG is shown in Figure 4-76.

If the breakers that connect the generator to the grid are suddenly opened, there is an instantaneous loss of total load on the expander. Immediately, the TPG string will increase in speed. When the breakers open, a signal is sent to the controller, and the controller directs the expander inlet butterfly valve to close and the small expander bypass valve to snap open. Simultaneously, regenerator pressure control transfers to the main expander bypass valve. With the expander inlet butterfly valve closed, flue gas energy no long enters the expander. When the fast-acting, small expander bypass valve opens it is equally important that the stored energy between the inlet butterfly valve and

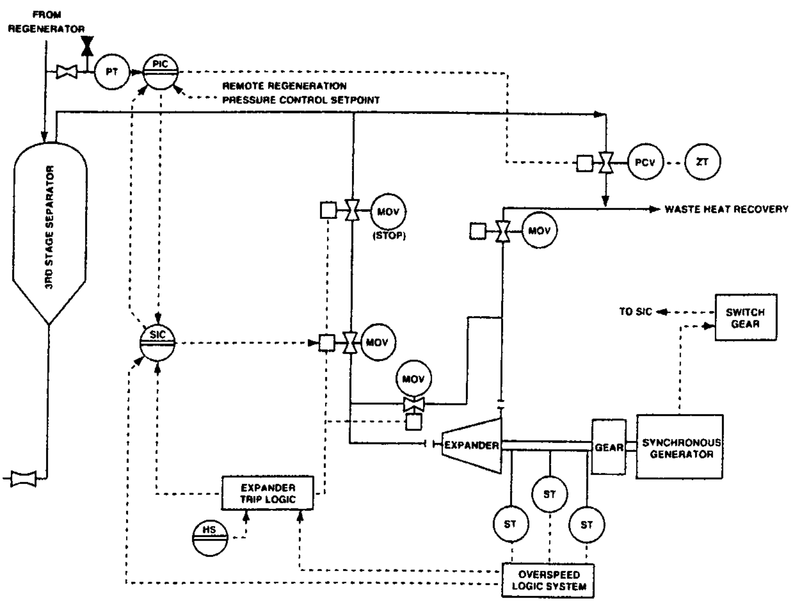

Figure 4-76. Overspeed control schematic.

the expander be quickly dissipated. This control sequence assures that the overspeed of the TPG string is kept to a minimum during loss of generator load.

The overspeed of the expander can be even greater if there is an instantaneous failure of the coupling between the expander and gear. In this instance, the expander is developing full power, but there is no load to slow the rate of increase in speed because the inertia effects of the gear and generator cannot come into play. A coupling failure represents the most severe test on the expander rotating elements and control system.

The first action required during this situation is to sense the overspeed condition. Well-engineered controls continuously monitor the expander speed rate-of-change and consider it the signal that indicates an emergency condition. As a backup, modern controls also incorporate an electronic two-out-of-three voting trip system. Upon sensing that an overspeed condition exists, the trip logic directs the expander inlet butterfly valve to close and the main expander bypass valve assumes the regenerator pressure control function. During an overspeed condition, it is even more important that the small expander bypass valve be available so that the stored energy ahead of the expander is dissipated as quickly as possible. The small bypass valve diverts flue gas from the expander so that it will not enter the expander and be used to develop power. It also causes the expander inlet pressure to rapidly decrease, thus reducing the energy available in the flue gas that does enter the expander. Therefore, the small bypass valve located between the expander and the inlet butterfly valve reduces the expander power in not one, but two ways.

FCC DYNAMIC COMPUTER SIMULATIONS

The complex FCC system involves not only turbomachinery, but also related process components. All of these must be properly designed and sized to operate within system parameters from startup to steady state design point, and through shutdown. System response to emergency conditions is also mandatory. Computer simulation is, therefore, an integral part of the design process. A computer program capable of this simulation is described below.

Elliott's digital simulation program (EDSCAN) was developed to assist customers in designing reliable and economic FCC systems. The program is used for analyzing any type of Elliott equipment, associated process components, and control systems. Verification of program results was performed using two methods. The first used a comparison of actual string overspeeds with predicted or calculated results, which showed very good correlation (Figure 4-77). The second method used a test facility with an arrangement as shown in Figure 4-78. The facility included an Elliott air compressor, adjustable piping configurations, and an antisurge system. Various transients were run with system responses dynamically recorded and compared to EDSCAN predictions. Comparison of these results permitted the manufacturer to perfect the various computer component elements that are used throughout EDSCAN. Elliott now offers EDSCAN as a valuable and proven tool to assist in the complex design of FCC systems.

For FCC applications, a rigorous analysis typically involves transient evaluations of expander coupling failures, generator load drops, compressor and surge system operation, and control valve malfunctions. The results of these evaluations permit optimum selection of control valves and control strategies.

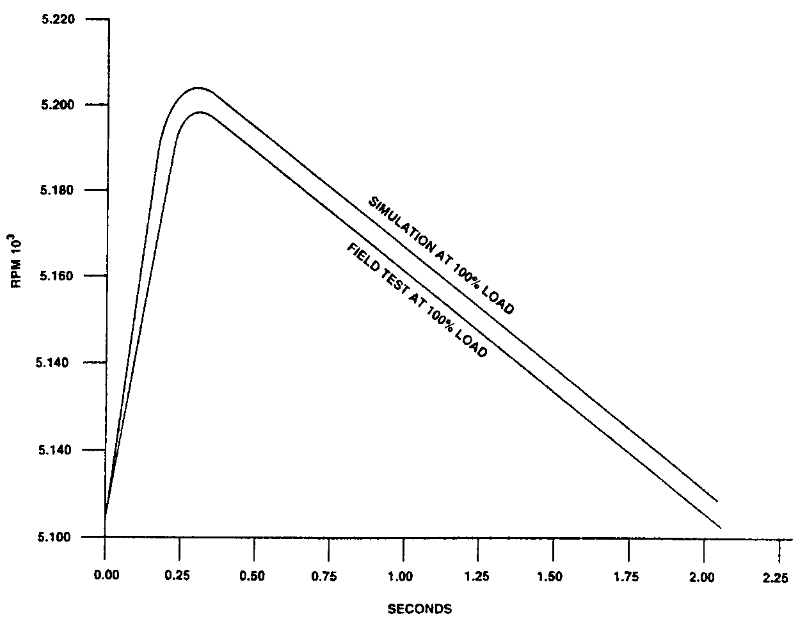

Figure 4-77. Speed changes during instantaneous load drop event; calculated and experimental values.

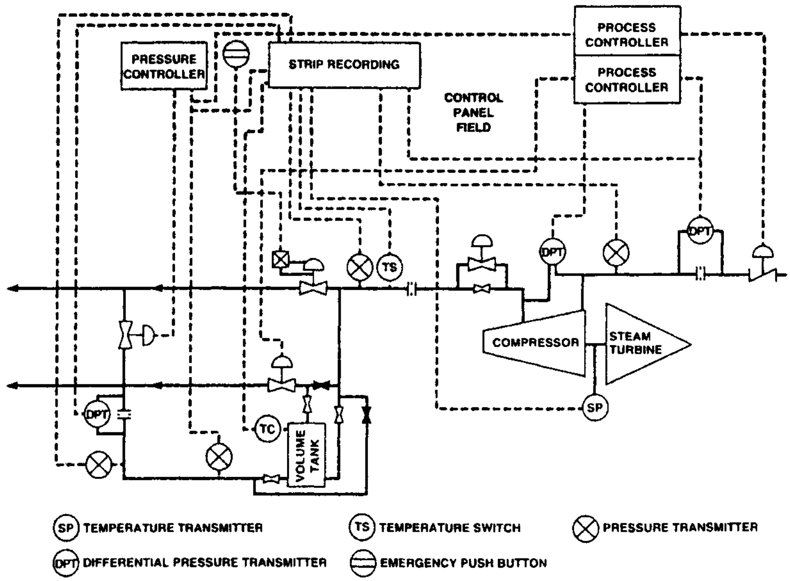

Figure 4-78. Dynamic process simulation test arrangement used by the Elliott Company.

Power Recovery Strings (PRS)

The power and benefits achievable through the use of EDSCAN are best demonstrated by reviewing recent case histories. A typical power recovery string block diagram is shown in Figure 4-79. The characteristics of each major component, associated piping volumes, and control systems are modeled.

The regenerator (Figure 4-80) is represented by a simplified model that includes the total volume and mass balance calculation. The regenerator exit temperature is assumed constant for the duration of the transient. The third-stage separator is handled as a fixed volume and associated pressure drop. Blow-down (bypass) flow is subtracted from the input flow.

The expander inlet valves are modeled using the exact Cg versus position characteristics supplied by the valve vendor. The specified valve stroking times can be varied as part of the analysis. A controller positions the valves to hold constant regenerator pressure.

The expander performance is modeled using normalized flow function versus pressure ratio and normalized efficiency versus velocity

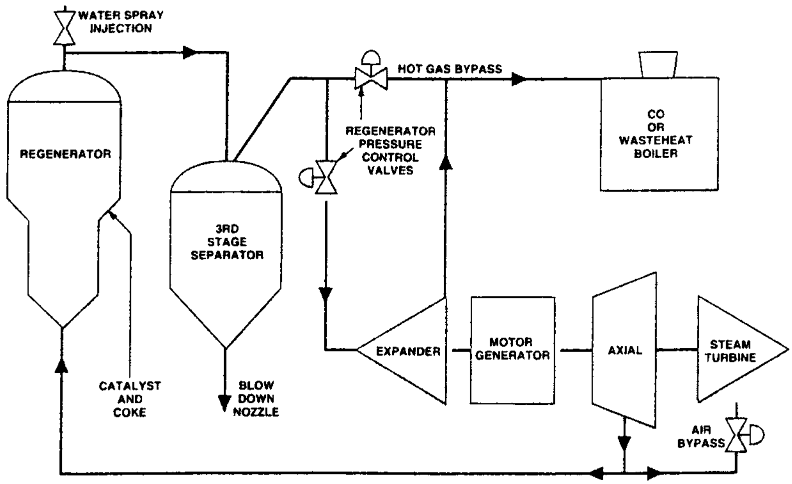

Figure 4-79. FCC power recovery string block diagram.

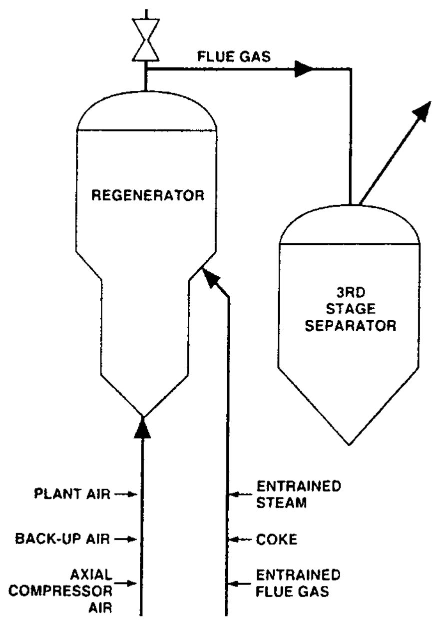

Figure 4-80. Regenerator and third-stage separator.

ratio. The velocity ratio is a function of the available energy of the gas, pitch line diameter, and operating speed. From these relationships, the horsepower developed may be calculated for any combination of inlet conditions and speed.

The motor/generator is modeled as an energy source/sink limited by its specific design capabilities. As a generator, it will absorb all excess power available while holding speed constant (synchronous) as long as it is electrically connected to the utility grid.

Axial compressor performance is modeled using a normalized operating map of pressure rise versus inlet volume flow. Lines of constant guide vane position and normalized efficiency are included. For given inlet air conditions, guide vane position, and calculated system resistance, the operating point on the compressor map is established. The guide vanes are typically positioned by a controller (Figure 4-81) to hold constant mass flow and the antisurge system controller prevents the compressor from operating to the left of the surge control line by modulating the blow-off (bypass) valve.

Steam turbine performance is modeled using a standard steam flow versus horsepower map and valve position versus steam flow. The turbine inlet valve(s) is positioned by the governor system to maintain constant speed (or another parameter when synchronized).

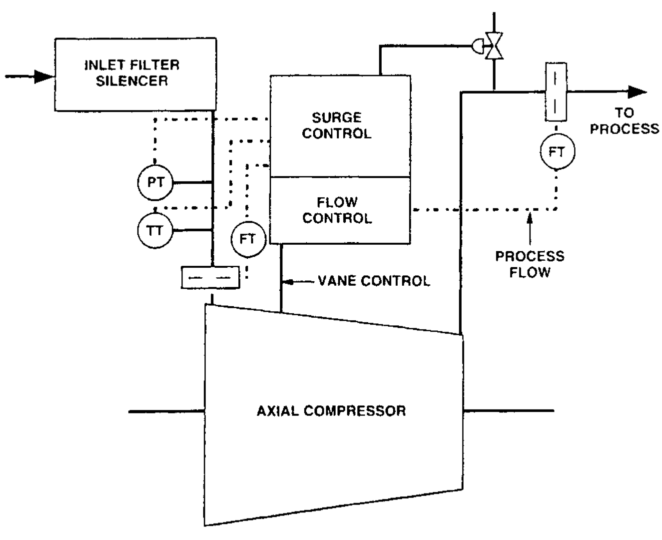

Figure 4-81. Axial compressor antisurge and guide vane control.

Using these relationships, horsepower is calculated to satisfy the governor requirements.

All turbomachinery models consider rotor inertia, bearing losses, and windage. The interconnected piping is modeled as a pressure drop and a volume.

Expander Coupling Break

The most difficult transient to handle safely is a break of the expander coupling (worst-case scenario). In order to contain speed within acceptable limits, a fast-acting inlet valve and a differential speed sensing switch are often required. The speed switch detects a change in speed between rotors across the expander coupling as shown in Figure 4-82. Using the fast-acting valve and speed switch limits expander overspeed to less than 33%. The steam turbine and compressor part of the string decelerated following the overspeed trip.

Generator Load Drop

Although not as difficult to handle as a coupling break, an opening of the generator breaker while producing maximum power is possible

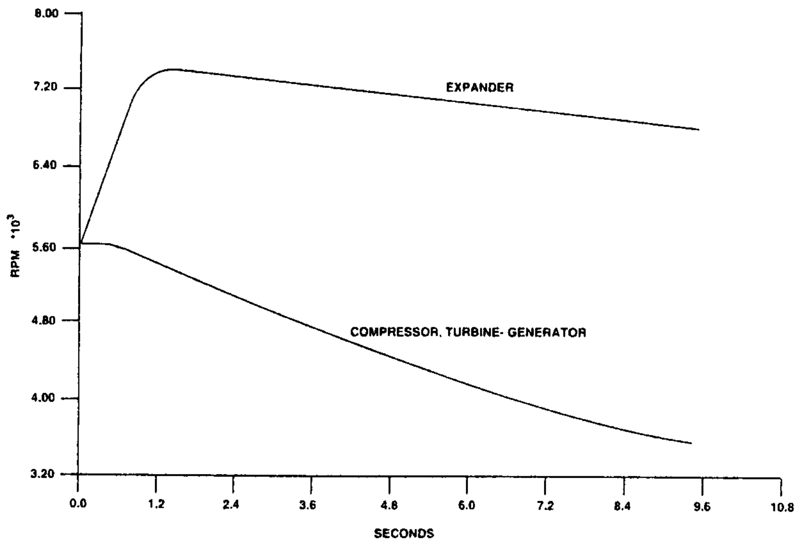

Figure 4-82. Speed versus time plot during coupling failure.

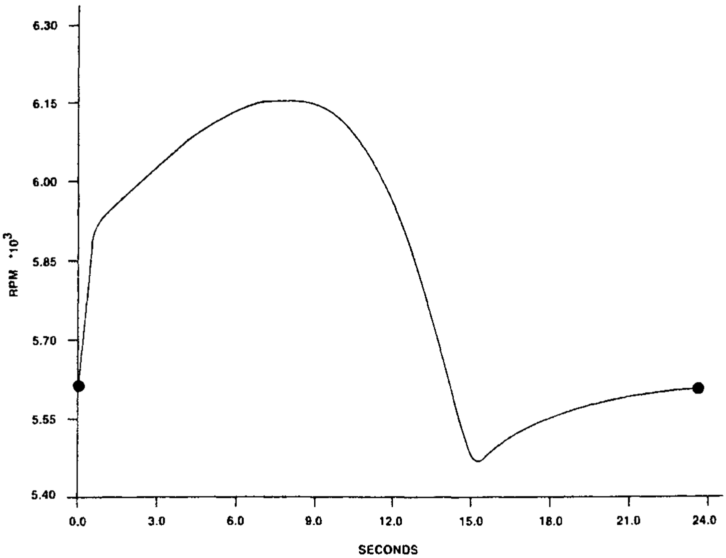

Figure 4-83. Speed versus time plot during generator full load drop (PRS string).

during operation. Figure 4-83 shows a sudden rise in string speed until the overspeed trip causes the inlet valve to close and the bypass valve to open. This action, in turn, causes the speed to peak at less than 10% over design, and then decelerate back to design speed where the steam turbine governor re-establishes control.

Control Valve Malfunction

A major operating concern is maintaining constant outlet pressure at the regenerator. Control systems and valving are designed to minimize regenerator pressure fluctuations to the greatest extent possible, even during malfunctions of the control systems themselves.

An example is shown in Figure 4-84, which represents the regenerator pressure following a malfunction of the expander bypass valve. The bypass valve trips open in 1 sec while the expander inlet valve maintains control. The regenerator pressure drops approximately 2.0 psi before starting to recover. The inlet valve stroking time was 10 sec and the controller settings were 5% proportional band and 30 sec reset.

A second plot of the same transient is shown in Figure 4-85. This shows the power balance between the string components during the

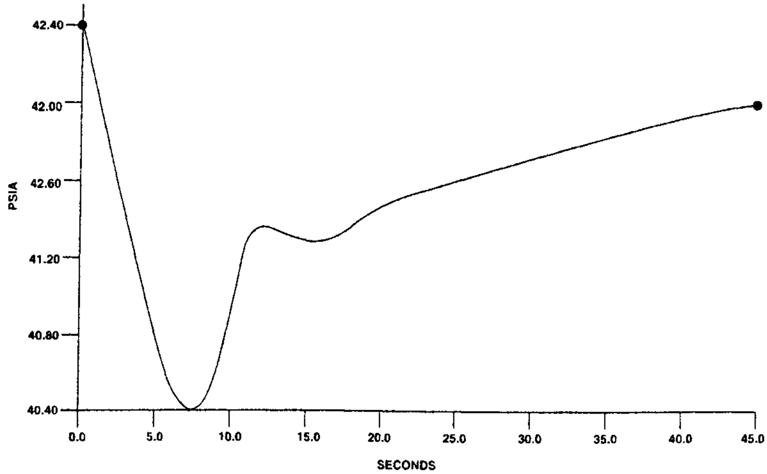

Figure 4-84. Regenerator pressure deviation during expander bypass valve malfunction.

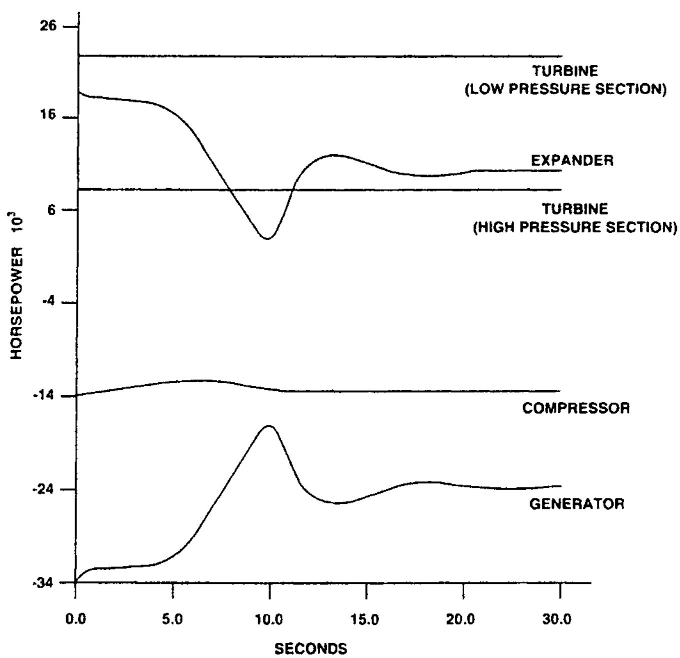

Figure 4-85. Power balance between string components during malfunction of bypass valve.

bypass valve malfunction. The major effect is a drop in the expander output with a corresponding drop in the generator output.

Total Power Generation (TPG)

A TPG block diagram is shown in Figure 4-86. It is similar to the FCC diagram except a second inlet valve is added to assure trip action and a bypass valve is added to reduce overspeed and aid in startup. The only rotating elements are the expander and generator and, possibly, gear (Figure 4-87).

Coupling Break

An expander coupling break on the TPG string (Figure 4-88) is similar to that on the PRS string. The only difference is the use of a bypass valve between the expander inlet valve and the expander. This bypass valve significantly effects the dissipating energy around the expander. The predicted overspeed in this example was 12% compared to a 33% overspeed for a similar transient shown earlier in Figure 4-82, which did not have the downstream bypass valve.

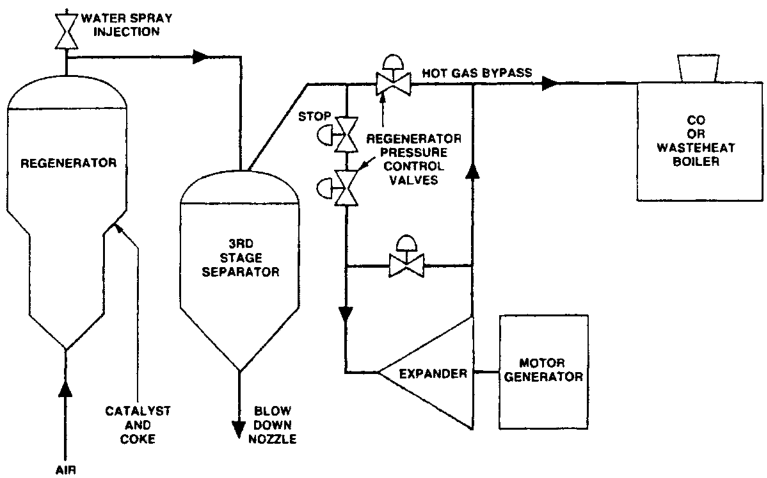

Figure 4-86. Total power generation with FCC turboexpander.

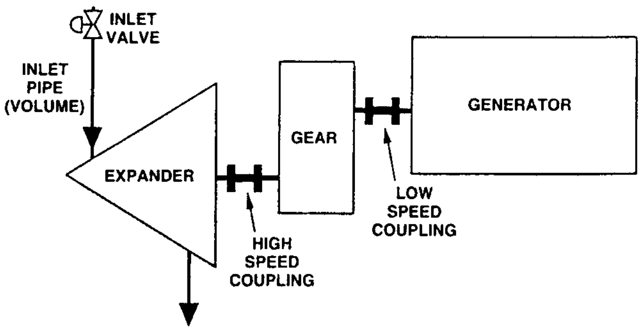

Figure 4-87. Main rotating elements comprising a TPG string.

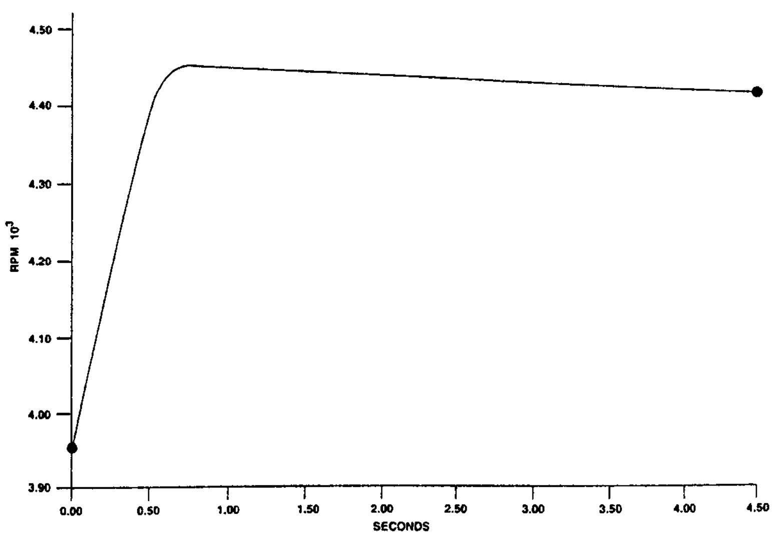

Figure 4-88. Speed versus time relation during expander high-speed coupling failure.

Generator Load Drop

A generator load drop of 100% is shown in Figure 4-89. For a valve closure time of 1 sec, a 5% overspeed is predicted. Note the comparison to the power recovery string in Figure 4-83, where a 10% overspeed was predicted with a 10 sec valve closure. The much larger rotor inertia of the full power recovery string allows the use of a slower and less expensive valve.

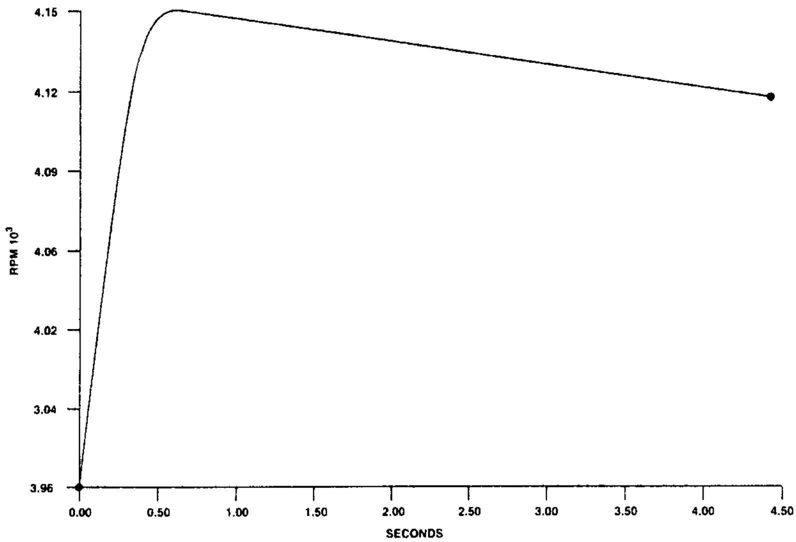

Figure 4-89. Speed versus time relation during generator full load drop (TPG string).

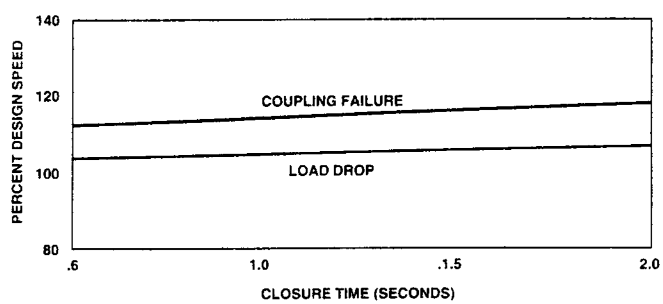

Figure 4-90. Predicted overspeed versus valve closure time.

Valve Closure Study

Figure 4-90 demonstrates the predicted overspeed versus inlet valve closure rates ranging from .6 sec to 2.0 sec for both coupling failure and generator load drop. The study showed that a valve with a 2.0 sec closure time could meet all overspeed criteria at a significant savings over the faster closure valves. The relatively small difference in overspeed between the coupling failures and generator load drops is mainly due to the opening of the downstream bypass.

MICROPROCESSOR-BASED TURBOMACHINERY MANAGEMENT SYSTEMS

Digital control methodologies similar to the Elliott Digital System program evolved from successful and proven reliable high-speed air compressor management and control approaches.

Today's digital systems accomplish these requirements through a base system of hardware and software. Elliott's system is the MACS PACK, which stands for data Monitoring, data Acquisition, Control System PACKage. The base system is more than a traditional control panel that contains gauges, monitors, individual controllers, annunciators, and lights. It takes all these traditional functions and adds turbomachinery management characteristics such as:

- Condition status with the information displayed in an easy to interpret format (Figure 4-91)
- Condition trending with the operator able to choose any four parameters simultaneously
- Predictive maintenance through the use of trend information
- Turbomachinery equipment diagnostic capabilities
- Communication to the host computer, modem, printer, and other controllers

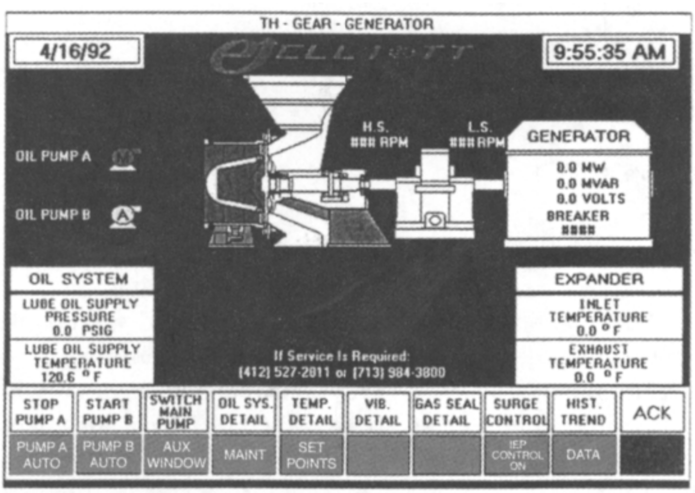

Figure 4-91. User-friendly information display panel.

DIGITAL SYSTEM OVERVIEW

Before discussing the turbomachinery management attributes of digital systems, it is helpful to review the hardware, software, and MACS PACK components.

EDS Hardware

The selection of digital systems hardware focuses on the turbomachinery string (Figure 4-92). In general, the philosophy is to transmit all available turbomachinery information back to the main Central Processing Unit (CPU) for status, use, and archiving. On every string there is a variety of sensors used for controlling and monitoring. Any monitored point using RTDs, thermocouples, or 4–20 ma signals is attached to Signal Conversion Modules (SCM) located in unit junction boxes. These SCMs contain high-speed input processors to convert analog signals to digital signals and send the information to the main CPU. All SCMs (up to 128 with 16 inputs each) carry digital information to the digital system via a single wire. Not only does this arrangement provide significant installation savings, but also the signals are isolated and immune to surrounding noise. Devices, such as digital governors, digital antisurge controllers or vibration monitors, are integrated into the modern digital systems via serial communication.

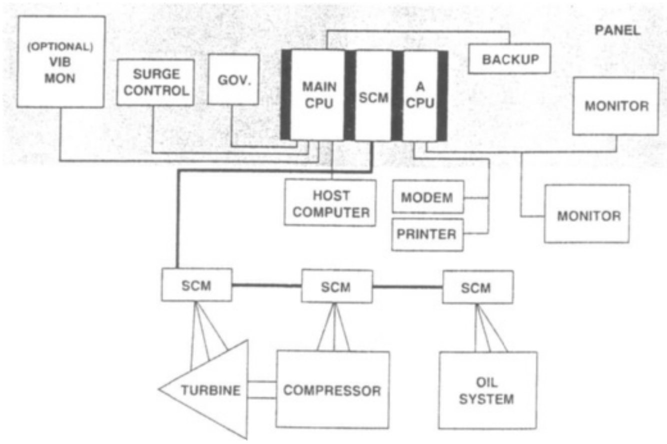

Figure 4-92. Block diagram of a proven digital supervisory and monitoring system for turbomachinery trains. *(Source: Elliott Company.)*

Elliott has also developed the Laser Sentry System, which is a monitoring device used in FCC applications. The system detects solid particles entrained in gas streams on a continuous and real-time basis. It is a good example of a device that can be easily integrated into the EDS to provide enhanced data management.

Systems such as the EDS use a dual microprocessor system. As can be seen in Figure 4-93, critical parameters of memory, input/output, alarm/trips, and host computer communication are handled in the main processor. To maintain fast response time, this processor is kept free of less critical tasks such as operator interfacing, trending, and archiving. A second processor, an administrative CPU, is used for these less critical yet important tasks.

Once the information is entered into EDS it is available for display, communication, status, manipulation, and archiving. A color graphic operator interface (VGA high resolution monitor with integral keyboard) is provided. The standard operator interface with combined screen and keyboard was selected based on location flexibility, ease of use, and compatibility with future EDS packages. A backup two-line display/keyboard is provided should the main operator interface(s) or the Administrative CPU fail.

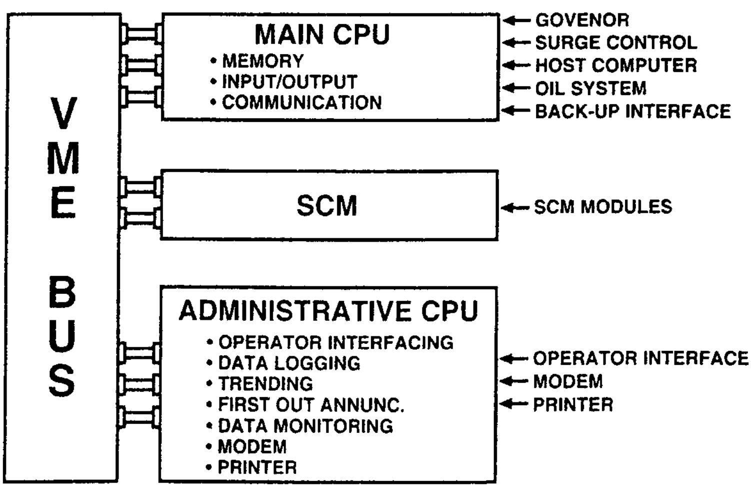

Figure 4-93. Dual microprocessor system used to supervise and control turbomachinery. *(Source: Elliott Company.)*

Software

The software employed for the critical elements (memory, alarming, tripping, and communicating with the host computer) uses a real-time operating system and resides in the main CPU. The administrative CPU employs multitasking software that performs important tasks such as modem communication, trending, and archiving.

MACS PACK

This is the base package in each Elliott Digital System. Hardware and software of the EDS described above are integrated into a program that provides the following:

- Graphic screens to display system parameters in an easy to understand format (Figures 4-94 through 4-98).
- Control of the oil system.
- Single point interfacing allowing the operator to control, manage, and monitor the turbomachinery from one screen and keyboard.
- Alarm and trip functions.
- Annunciation including time tagged information for problem location, time of occurrence, time of acknowledgement, and time of return to normal.

(text continued on page 202)

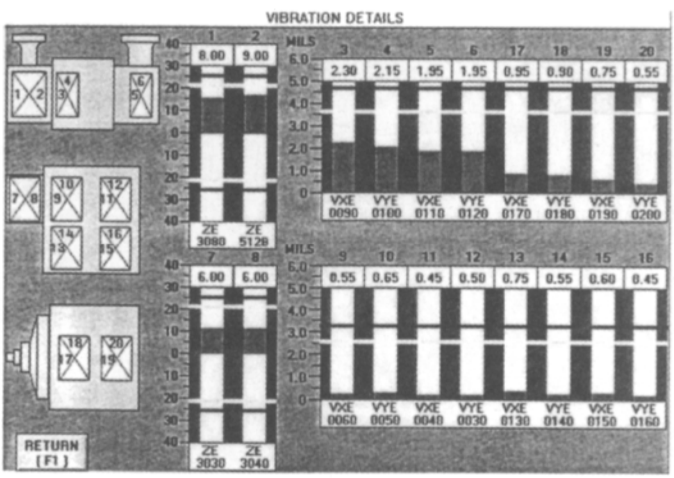

Figure 4-94. Graphic display screen indicating vibration behavior.

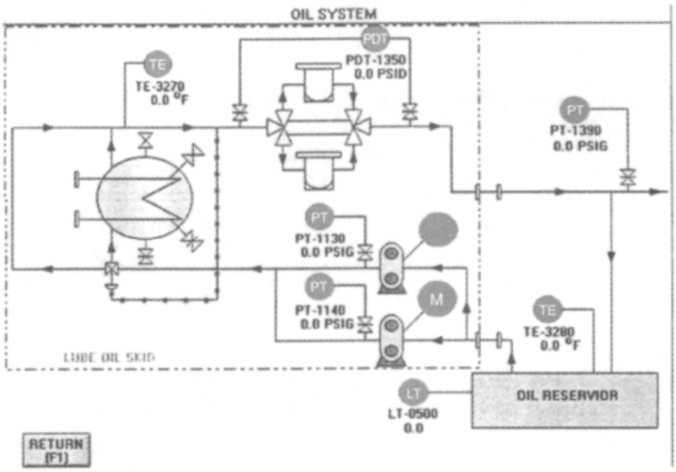

Figure 4-95. Graphic display of oil system status.

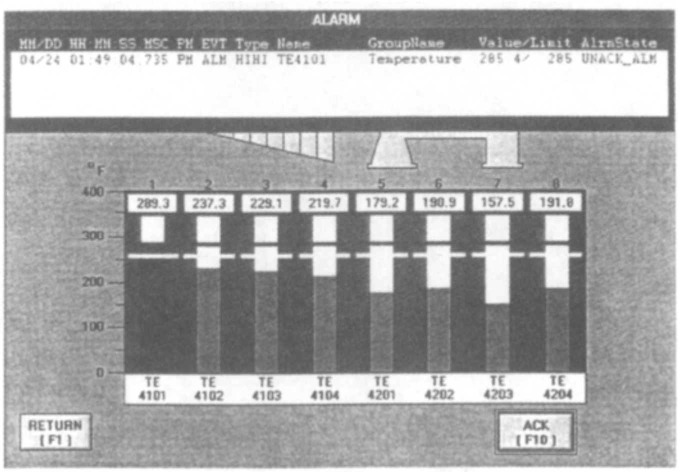

Figure 4-96. Alarm status displays.

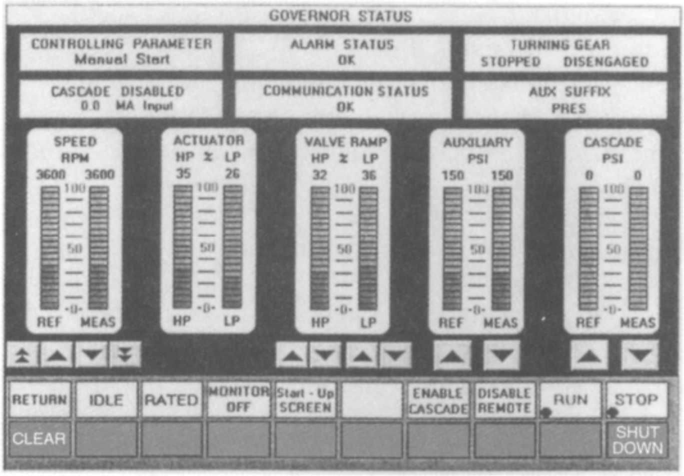

Figure 4-97. Graphic display of governor status.

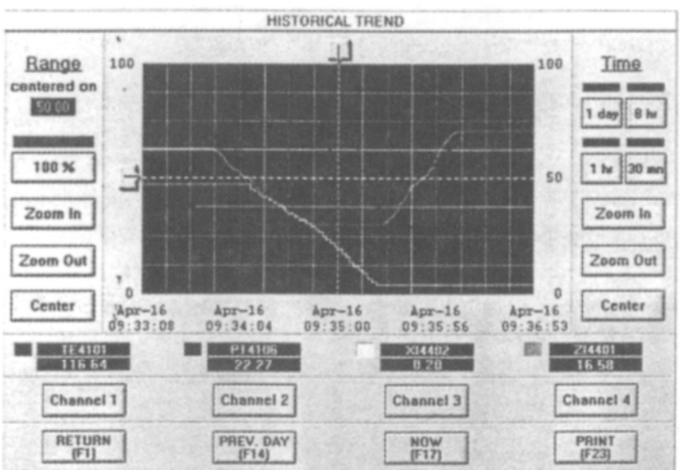

Figure 4-98. Historical trend display.

(text continued from page 199)

- Data archiving and downloading.
- Modem communication for data evaluation by specialists at remote locations.
- Trending of all archived data.
- Information transfer to printer including trend graphs.
- Communication to a host computer via Modbus protocol.
- Comprehensive display of controller data (e.g,., Woodward 505 governor).

Data Management and Communication

The capabilities of the EDS range from tighter operational control to avoidance of unscheduled maintenance shutdowns. Some of the important management parameters inherent in EDS are listed below.

Management by Operator, Owner, Machinery Builder, and Service Support Expert

Along with the capability for the operator to evaluate and trend, information can be communicated to a host computer. Additionally, archived data may be sent by modem to a remote location for use in planning, reporting, or expert evaluation by support personnel.

Single-Point Interfacing

Whether the operator interface is next to the unit or in the control room, the operator can manage the turbomachinery from a single point. From this single point, faster evaluation and implementation of changes can be initiated.

Expansion Packages

Good management requires the ability to stay current with technology. For this reason the EDS has been designed on a hardware platform (Figure 4-99) that provides expansion capabilities for new hardware and software packages. The many available packages include:

- Antisurge control for custom compressors.
- Turbine and compressor online performance for use in equipment predictive maintenance.
- Expert system for turbine vibration.

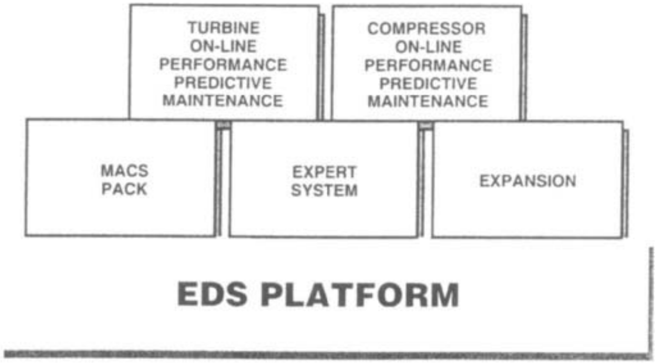

Figure 4-99. Elliott digital system platform.

Economic Impact

The objective of any management package is to provide a positive economic impact on the project. These objectives are met by

- Setting control and monitoring parameters at the factory to streamline installation and startup.
- Providing single wire connections between the unit-mounted junction boxes and the digital system, which reduces field wiring costs.
- Trending capability that allows better scheduling of major maintenance programs.
- Communicating of data to other computers, which facilitates comprehensive operating reports.

The foregoing demonstrates that modern digital devices offer highly reliable, state-of-the-art microprocessor technology that controls turbomachinery strings, monitors operating data, stores data for subsequent evaluation, communicates to other systems, and can expand with future technologies.

LASER SENTRY

A major concern in the application of power recovery expanders in the FCC process is catalyst carryover from the third-stage separator that enters the expander.

In cooperation with United Technologies' Research Center, Elliott has developed a monitoring device that detects solid particles entrained in gas streams. This device, which Elliott has named "Laser Sentry," provides a means to monitor average particle density of entrained particulate in gas streams continuously and in real time.

The capabilities of the Laser Sentry are particularly useful in FCC installations for the purpose of monitoring the performance of catalyst removal equipment. It can detect abnormal amounts of catalyst in the gas stream and also provide an early warning to the plant operator.

General Description

A simplified cross-section of the Laser Sentry is shown in Figure 4-100. A helium-neon laser projects a beam of light across the center of the inlet piping upstream of the expander. The beam strikes a fiber-optic phototransducer located opposite the laser. As the particulate-laden gas passes through the laser beam, portions of the beam are dispersed in all directions. The amount of light striking the photosensor is inversely proportional to the amount of particulate present. The resultant signal from the phototransducer is fed to a microprocessor, which contains a photoamplifier and the necessary logic to indicate the quantity of particulate present. The laser source and the phototransducer never come in contact with the gas. The gas is contained in the process line via two air-purged, fused silica lenses in front of the laser and phototransducer hardware.

Additional software is available that estimates changes in average particulate size. This permits trend monitoring of the performance of third-stage separators. (This ability to continuously monitor average particle density and changes in particle size is unique to the Laser Sentry.) There are nine signals available from the Laser Sentry signal

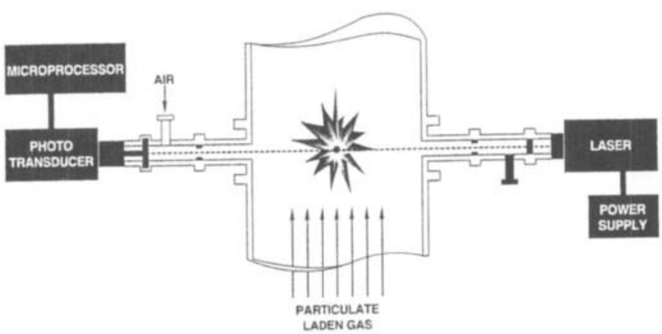

Figure 4-100. Monitoring of catalyst entrainment (Elliott "Laser Sentry").

processor that can be monitored by a host computer. With the addition of the particle size software, the estimated particle density and size can be continuously calculated and displayed. The available signals also serve a diagnostic function. The signals can be used to evaluate laser performance and process window condition. Alarm signals are also available that will alert operators of abnormal particle density conditions.

The Laser Sentry is also a useful device for monitoring the presence of catalyst in gas streams. It can be installed in any new or existing FCC installation and can interact with the EDS or existing instrumentation and can activate new or existing alarm/shutdown devices. In summary, this device serves as an extremely capable "early warning" system to avoid problems caused by catalyst carryover during process upsets.

POWER RECOVERY EXPANDER REPAIR

How long does it take to repair a hot gas expander, and what are the essential activities that are involved in effecting such repairs? These valid questions are best answered by highlighting a specific example.

In April 1990, an Elliott two-stage FCC power recovery expander (Figure 4-101) experienced severe damage due to a process upset that occurred during the startup cycle. The power developed by the expander is used to drive an axial compressor and a motor/generator. The high efficiencies of axial compressors provide a positive power balance because the power generated by the expander exceeds the compressor requirements. The excess power is used to generate electrical power, which the refinery can use in-house or sell back to the local utility.

Any downtime of an expander results in significant lost revenue. When this particular damage occurred, the user no longer obtained power from the process to drive the equipment. Instead, the user was forced to buy electricity to drive the axial compressor. Depending on the power capability of the expander, losses of $300,000 per month or greater may be experienced.

At the time of the damage, it was recommended that the expander be shipped back to the repair facility for inspection to determine the repair requirements. If the inspection showed the repair was feasible, the repair facility could be quickly supported by the plant's main service and engineering personnel. The close proximity of the main manufacturing facility was also an additional bonus. Parts too large for the repair facility to handle could be machined at the main plant.

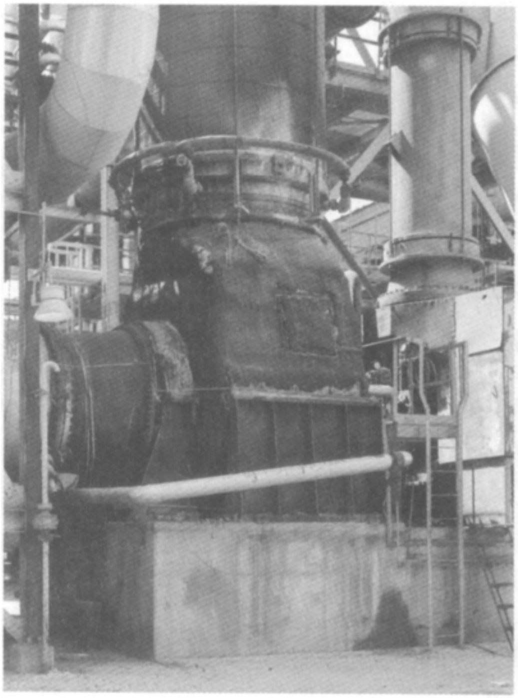

Figure 4-101. Elliott two-stage power recovery expander.

The inspection process involved considerable work, due to the amount of damage experienced. The following steps were involved in the inspection process; they can be considered typical of recommended procedures:

- Initial inventory and documentation of parts received.
- Visual inspection and assessment of all major components to determine whether further inspections were warranted or the piece was beyond repair.
- Dye penetrant inspection of the hardware to determine the extent of distress in order to develop material requirements and repair techniques.
- Dimensional and runout inspections to determine the extent of deformation to bores, turns, flange faces, and fit areas.

Upon completion of the inspection process the results were reviewed, and the following requirements were defined for each major component of the hot gas expander and its respective subassemblies:

- Was the piece repairable based on inspections or should it be scrapped?
- Could the piece be restored to original drawing specifications or were design and dimensional changes required?
- What was the specific mechanical and/or weld repair process each piece was to undergo?
- What material was required in the forms of plate, forgings, or castings to conduct the repair?
- What new miscellaneous parts, such as nuts, bolts, studs, and so forth, were required?

Prior to the authorization from the user to begin repair, two complications arose that could adversely affect the initially established delivery date. The first item was the delivery time for the nickel alloy rotor and stator blades. To circumvent this problem, the user agreed to provide an order to Elliott to begin purchasing the material for the blades. The second item was a requirement for the redesigned stator blade assemblies to eliminate a warpage condition experienced during abnormal operating conditions (Figure 4-102). No drawings existed for the redesign on this unit. However, to show commitment to the project, the manufacturer agreed to generate the necessary layout and detail drawings to incorporate this redesign in the repair. This was done prior to approval of the repair and shows the cooperation between mature sellers and buyers.

It was known that once presented with the repair quote and procedure, the user would also consider the possibility of purchasing a new expander. However, the lead time for the repair was approximately one-half that for a new expander. By not having to purchase electricity, the cost savings more than justified the repair. Additionally, the owner company was satisfied by assurances given by the expander manufacturer to provide a unit in essentially new condition.

Repair approval was given at the end of November 1990 and a scheduled shipping date of September 1991 was set. The first repair step was to place the material on final order. For the parts to be manufactured at the main plant, the raw material was ordered by the repair facility and shipped to the main plant for machining. Where possible, forgings were substituted for weldments or castings. Lead times for forgings were significantly less than the other forms of material, and the forgings were received in a rough-machined state, which reduced the time to complete machining operations.

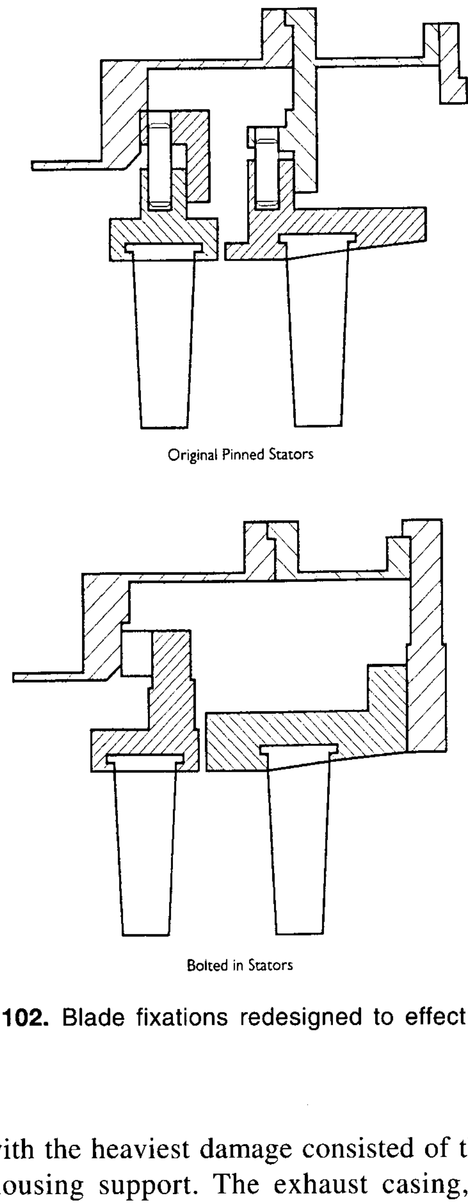

Figure 4-102. Blade fixations redesigned to effect rapid repair.

The areas with the heaviest damage consisted of the exhaust casing and bearing housing support. The exhaust casing, which is bolted to the bearing housing support, was torn from its attachment and deformed beyond repair. Numerous cracks around its supporting struts were found and the flexible expansion joint welded to the exhaust casing was twisted and torn. To facilitate repair, the attachment end of the exhaust cone was completely removed and a new ring forging welded in its place. After welding, this area was locally stress relieved.

As deformation of the casing existed, all new vertical and horizontal centerlines of the casing were reestablished. This was a critical concern as the exhaust casing was used to establish the datum for the repair and assembly of the expander. Drawing requirements were obtained by providing additional stock on the ring forging welded to the casing. Thus, it was ensured that once new centerlines were established, the bolting surfaces could be machined at drawing dimensions without having to worry about rework. Upon completion of the machining operations and welding on the new bellows assembly, the exhaust casing underwent a final dye penetrant inspection and air test to qualify it.

The bearing housings and supports required extensive repair. All of the housing bores were pounded out, particularly the bearing bores, which were pounded out up to one-quarter inch. Ninety percent of the threaded fasteners had been ripped out of their respective threaded holes and the dowel holes were all oval. The sealing steam chamber of the bearing support was ripped away from the main support structure.

All bores and fit areas of the housings and supports were built up with welding. The plate forming the sealing steam chamber was completely cut away and a new piece welded in its place. With the assistance of the main plants repair technology and materials engineering groups, requirements to weld up all damaged holes were developed and accomplished. Upon completion of the welding, the housings and support underwent localized stress relief operations where applicable. The bearing housing then underwent complete re-machining operations to return all bore and fit areas to drawing specifications. All threaded holes were drilled and tapped, and new dowel holes drilled and reamed.

The inlet casing experienced severe distortion in addition to damage to the first-stage stator blade assemblies. Based on inspection readings, a re-machining drawing was generated to show clean-up requirements and also assist in establishing the proper location of the redesigned first-stage stator housing. The inlet nose cone was twisted inside of the casing and required complete replacement.

A new nose cone was obtained and initial machining performed by the repair facility. The nose cone is supported by six radial pins. The nose cone and inlet casing were sent to the main plant to ensure the pin hole locations were properly positioned. Here, the inlet casing was assembled and oversized pin holes were drilled and reamed in the pieces. Pins made to fit the holes were also machined. Repair machining of the three trunnion bores was then performed to ensure the casing would be located in the correct axial position on its support.

The main plant's manufacturing facility was also responsible for producing the new diffuser and first- and second-stage stator assemblies, in addition to many other miscellaneous parts. The owner/user's spare rotor was used as part of the rebuild. Complete disassembly, dimensional, and penetrant inspections of the rotor were conducted. New blades were installed in the discs. Final qualifications of the rotor included rotor stud stretch tests, balancing, and mechanical and electrical runout checks.

As the final part of the repair process, the expander underwent a trial assembly at the repair facility. The actual job assembly and disassembly fixtures were used during the trial assembly. No significant problems were encountered and internal clearances were to specifications. As the assembly bed plate at the repair facility did not exactly duplicate the user's baseplate, there was some concern that readjustment would be required in the field to obtain clearances. To facilitate the field assembly process, appropriate pins and fixtures were manufactured to hold axial and concentric positions of the diffuser and stator as they were in the repair shop. The entire expander trial assembly was completed one month ahead of schedule.

The next step was to install instrumentation and conduit, disassemble the expander, preserve, and ship. These steps were completed and the major components shipped by mid-September 1991. To assist the user, the bearing housing was shipped air freight and was installed in early October, in preparation for alignment to the axial compressor. The earliery shipment of the expander permitted the user to improve the installation schedule. The expander was successfully placed in operation by mid-November 1991, and has since then operated flawlessly.

ECONOMIC EVALUATION OF FCC TURBOMACHINERY ALTERNATIVES

Power recovery systems are built around the one item of turbomachinery absolutely essential to the process: the air compressor. The first step in developing a viable string of process air equipment is, therefore, a decision regarding the type of air compressor.

Centrifugal compressors have served FCC processes well since about 1950. These machines are large, ruggedly designed units using labyrinth-type seals. Centrifugal units are capable of relatively large pressure ratios per stage, therefore, few stages are required for most applications. Centrifugal compressor performance is characterized by a more horizontal pressure rise at constant speed. Turndown at design pressure rise can reach as much as 55% of design flow. Constant pressure rise flow reduction is, however, accompanied by significant reductions in efficiency (Figure 4-103).

Striving for improved energy usage, refiners currently favor axial flow compressors for the FCC process. Axials are physically smaller and lighter weight than corresponding centrifugals. However, since only relatively small pressure ratios per stage are attainable, axials for FCC applications typically consist of 9–13 stages, depending on regenerator pressure requirements. With constant speed operation to deliver constant mass flow at constant discharge pressure with varying ambient temperatures, approximately half of the stationary blades are made adjustable. A more vertical pressure rise is typical of axial flow compressors. Constant pressure flow turndown to about 75% of design flow is possible with only modest efficiency decay (Figure 4-104). The operating characteristics of axial compressors can be tailored to meet process needs and can provide operating efficiencies up to 12% higher than obtainable with typical centrifugal compressors. Axial flow units are also readily matched to optimum speeds for turbines and power recovery expanders.

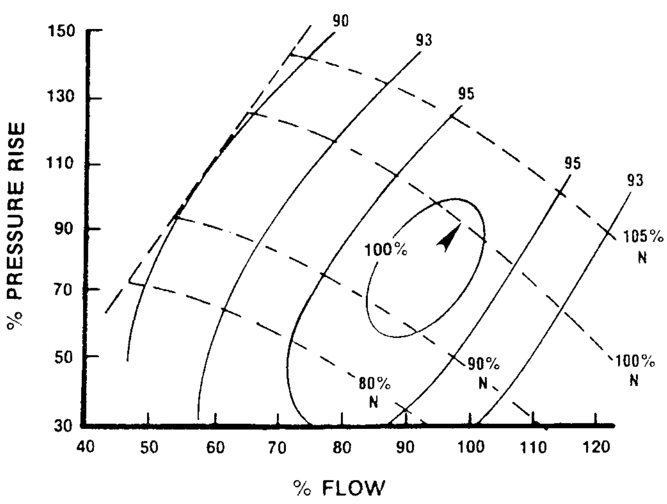

Figure 4-103. Typical centrifugal compressor performance map.

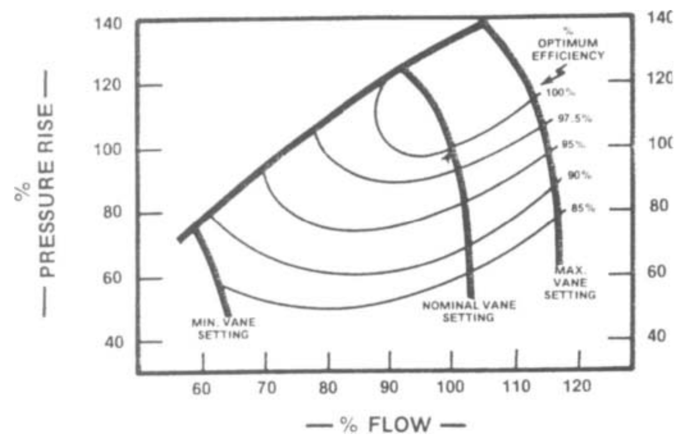

Figure 4-104. Typical axial compressor performance map.

The second step in developing the process air train is selecting the air blower main driver. This step includes many alternatives such as power recovery expanders, steam turbines, and electric motors. The following example illustrates these alternatives.

Basis and Assumptions for Example

1. Nominal 20,000 barrels per stream day FCC unit
2. Air Flow—350,000 lbs/hr at 45 psig
3. Regenerator operating at 35 psig
4. Expander operating conditions:
   Pressure: 30 psig/2.5 psig
   Temperature: 1,315°F
   Flow: 365,750 lbs/hr
   Allows 10% increase in mass flow in regenerator
   Allows 5% separator blowdown
5. Turbine startup feasible for power recovery strings

A 1992 vintage FCC unit with a capacity near 20,000 bbl/day is the basis of this example. An air flow of 350,000 lbs/hr at 45 psig is required to maintain a 35 psig regenerator pressure. The expander receives 365,750 lbs/hr of flue gas at 30 psig and 1,315°F.

Flue gas flow is estimated by allowing a 10% incease in mass flow in the regenerator vessel while taking a 5% decrease in flow for the third-stage separator blow-down. Power recovery strings are started by steam turbines.

As a first step in the driver analysis, the capital required to make each alternative operational is estimated. An orifice chamber is required to reduce the flue gas pressure for the steam turbine and motor alternatives. In this particular case, it is assumed that a third-stage separator is required for the power recovery alternatives only and that an electrostatic precipitator is used in all cases. Construction and engineering are estimated as percentages of total direct material and total material and construction, respectively. An allowance of 15% is made for contingency. Because the separator often includes a royalty fee, this item is added to the power recovery alternates. As shown in Table 4-7, the motor alternative will require the least capital. The power recovery alternatives require additional capital amounting to $4.63 and $4.75 per million respectively.

The incremental capital required for power recovery is offset by dramatic reductions in operating expenses. Electric rates are assumed to be 4.5¢/kW-hr used or 0.6¢/kW-hr of potential demand. Boiler feedwater and cooling water for condensation are valued at 75¢ and 35¢/M-lb, respectively. A value of $4.00/M-lb has been applied to steam used or generated. Quenching steam has been valued at 25¢/M-lb. The power recovery expanders have a minimal amount of quenching steam flowing through their systems to be certain that the steam is available when and if needed for temperature excursions above 1,350°F. The single-stage expander does not develop sufficient power for the full compressor demand. Motor supplemental power is assumed. The two-stage expander develops excess power via the induction motor. The waste heat system steam production is adjusted for lower flue gas temperatures with power recovery alternatives (Table 4-8).

Maintenance expenses are estimated at 3% for the required equipment. Spare wearing parts are allowed for the steam turbine. Every three years spare wearing parts and a rotor should be expensed for the power recovery cases. Expensing a rotor every three years is considered conservative especially for the two-stage alternative.

After an allowance for insurance and property tax, total operating expense is obtained for each alternative. Under the assumed conditions the steam turbine is very expensive to operate whereas the power recovery alternatives are nearly free.

(text continued on page 216)

Table 4-7
Capital required for FCC unit machinery alternatives

Direct Material Costs — Major Equipment	Steam Turbine Driven Air Blower	Motor Driven Air Blower	One Stage Expander Driven Air Blower	Two Stage Expander Driven Air Blower
Motor — Induction Type	—	310,000	231,000	231,000
Gear	—	122,000	80,000	80,000
Turbine — Main Driver or Start-up	468,000	—	200,000	200,000
Condenser	145,000	—	—	—
Expander	—	—	1,170,000	1,310,000
Orifice Chamber	200,000	200,000	—	—
Slide Valve/Expander Valves	300,000	300,000	200,000	200,000
Stack	210,000	210,000	210,000	210,000
Waste Heat System	518,400	518,400	383,900	360,000
Third Stage Separator	—	—	1,000,000	1,000,000
Precipitator	760,000	760,000	760,000	760,000
Bulk Material — Piping Structural, etc.	7,373,750	7,261,200	7,711,395	7,711,395
Total Direct Material Cost	9,975,150	9,681,600	11,946,295	12,062,395
Construction — 40% TDMC	3,990,000	3,872,600	4,778,500	4,778,500
Total Material and Construction	13,965,150	13,554,200	16,724,795	16,840,895
Engineering — 20% TM & C	2,793,000	2,710,800	3,344,900	3,344,900
Contingency — 15% TM & C	2,100,000	2,033,100	2,508,700	2,508,700
Royalty	—	—	350,000	350,000
Total Fixed Capital Required	18,858,150	18,298,100	22,928,395	23,044,495
Incremental Capital	560,050	—	4,630,295	4,746,395

Table 4-8
Operating expense projections for FCC unit machinery alternatives

Operating Expense — Utility	Steam Turbine Driven Air Blower	Motor Driven Air Blower	One Stage Expander Driven Air Blower	Two Stage Expander Driven Air Blower
Electricity — Potential demand — $.006/KWHR	—	—	268,430	268,430
Electricity — Usage — $.045/KWHR	76,355	3,546,400	186,745	(232,840)
Boiler Feedwater — $0.75/1000 LB	1,487,400	479,400	377,275	355,385
Steam — $4.00/1000 LB	2,812,240	(2,428,960)	(1,679,825)	(1,568,945)
Quenching Steam — $0.25/1000 LB	—	—	6,300	6,300
Cooling Water — $0.35/1000 LB	1,250,760	—	—	—
Total Operating Expense — Utility	5,626,755	1,596,840	(841,075)	(1,171,670)
Operating Expense — Maintenance				
General — 3% (F.C.R.)	565,745	548,945	687,850	691,335
Turbine	15,000	—	—	—
Expander — Expense Rotor in 3 Yrs.	—	—	136,500	152,835
Total Operating Expense — Maintenance	580,745	548,945	824,350	844,170
Insurance and Local Property Tax — 2% (F.C.R.)	377,165	365,965	458,565	460,890
Total Operating Expense	6,584,665	2,511,750	441,840	133,390

(text continued from page 213)

Having determined the capital requirements and operating expenses, an analysis of the overall economics of each driver is possible. Capital requirements are added to operating expense to yield the total annual expense. As expected, the turbine option need not be considered further. The power recovery alternatives do generate savings compared to the motor driven alternative. Allowing for federal income tax and adding back incremental depreciation yields a total incremental cash flow for each of the power recovery cases. Dividing the incremental capital required by the total incremental cash flow yields the payout period. Periods longer than three years are not generally considered economical (Table 4-9).

Calculation of the payout period does not, however, take into account the underlying economics of cash flow. The interest calculated in Table 4-9 is the interest for the first year. Declining interest over time directly translate to increased cash flow. To illustrate this situation, assume the useful life of this project is the same 15 years used for depreciation.

Assuming that the charge for electricity remains constant over the period, the relative operating costs are shown in Figure 4-105. The net incremental cash flow of the power recovery alternatives compared to the motor driven alternatives are illustrated in Figure 4-106. A two-year period is assumed between the first cash out-flow and the start-up of the unit. For the assumed operating conditions, the two-stage expander is preferred. Calculating the discounted cash flow rate-of-return involves establishing the yearly cash flow amounts and then applying the time value of funds to each amount. An iterative calculation is required to arrive at the percentage. For the single-stage expander the rate-of-return is 17.6%. The two-stage expander offers a 20.3% rate-of-return. A 20% rate-of-return is often considered economically sound. Note that payback periods, even under this analysis, are 5.1 and 4.5 years.

An additional modification to the economic analysis is easily made by using the annual cash flow analysis. Increasing costs over time can be analyzed for their impact on the economic evaluation. For example, Figure 4-107 shows the operating cost yield of applying a 15% annual rate-of-increase to electric rates. These results may be shocking at first, but by referring back to the operating cost calculations it is easy to see that electric power usage is greatly reduced by power recovery.

Table 4-9
Cost summary and payout for FCC unit machinery alternatives

	Steam Turbine Driven Air Blower	Motor Driven Air Blower	One Stage Expander Driven Air Blower	Two Stage Expander Driven Air Blower
Total Operating Expense	6,584,665	2,511,750	441,840	133,390
Annual Capital Requirements — Year #1				
Depreciation — 15 Yr. St. Line	1,257,210	1,219,875	1,528,560	1,536,300
Interest — 15 Yr. Fund 11%	2,557,635	2,481,675	3,109,665	3,125,410
Total Annual Capital Required — Yr. #1	3,814,845	3,701,550	4,638,225	4,661,710
Total Annual Expense	10,399,510	6,213,300	5,080,065	4,795,100
Gross Profit over Motor Alt.	N/A		1,133,235	1,418,200
Net Profit — 50% F.I.T.	N/A		566,618	709,100
Incremental Depreciation	N/A		308,685	316,425
Total Incremental Cash Flow — Yr. #1	N/A		875,303	1,025,525
Incremental Capital Required	560,050		4,630,295	4,746,395
Payout — Yrs.	N/A		5.3	4.6

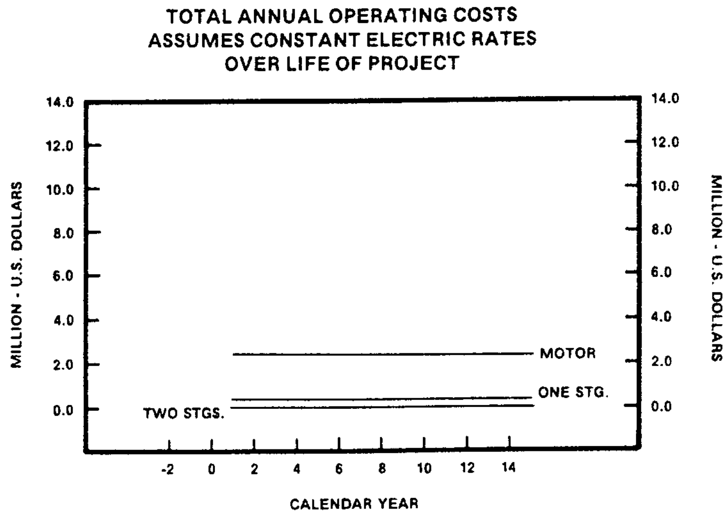

Figure 4-105. Relative operating costs for different FCC machinery alternatives.

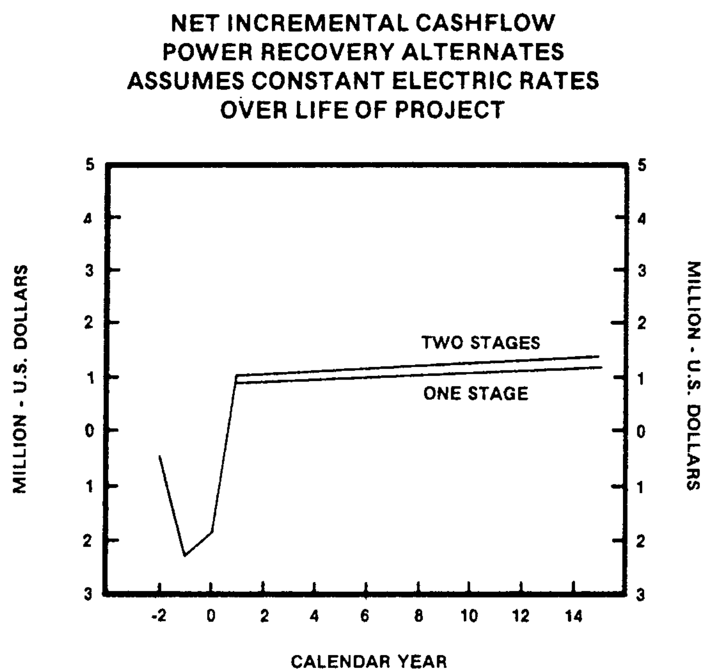

Figure 4-106. Net incremental cash flow for one- and two-stage power recovery expander schemes.

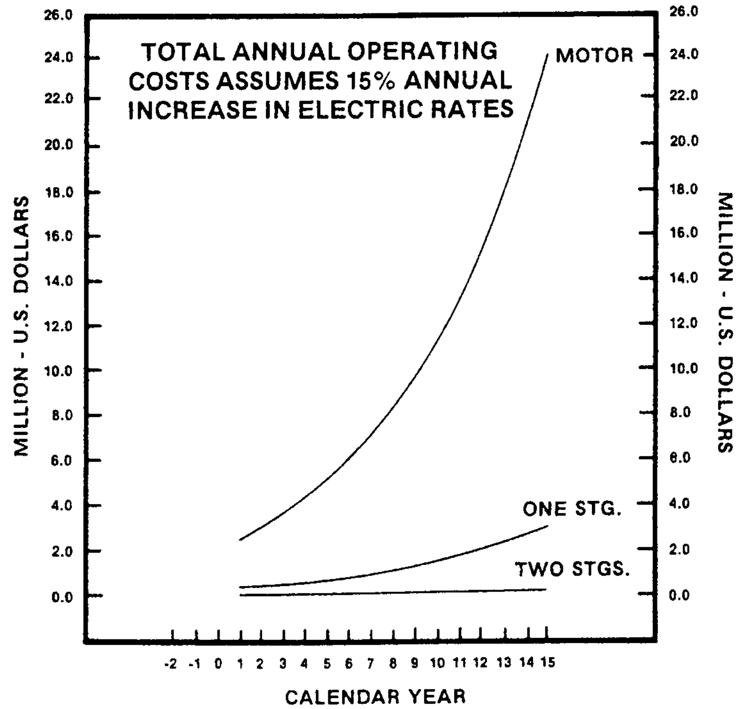

Figure 4-107. Total annual operating costs for three different FCC power recovery schemes.

The electric power usage is the primary expense incurred when using a motor driver. Table 4-10 documents these findings and the net incremental cash flow using one- and two-stage power recovery expanders is shown in Figure 4-108.

As Figure 4-108 shows, increasingly large cash flows develop in later years of operation. These large cash flows are essentially ignored by a simple payback period calculation.

Using the cash flows derived from the increasing utility rates, calculating the rate-of-return would show 33.8% for a one-stage unit and 35.5% for a two-stage unit. The corresponding payback periods are 3.7 years and 3.4 years.

Applying two important tax credits would improve the early years' cash flow and shorten the payback period. A 10% investment tax credit and a 10% energy tax credit applied to the incremental capital costs for the expanders yields nearly $1.0 million additional first-year cash

Table 4-10

Incremental capital	$4,630,295	$4,746,395
Payback based on first year's cash flow	5.3 years	4.6 years
Discounted cash flow method		
Rate-of-return	17.6%	20.3%
Payback period	5.1 years	4.5 years
Discounted cash flow method		
(15% annual rise in electric power rates)		
Rate-of-return	33.8%	35.5%
Payback period	3.7 years	3.4 years
Tax credits taken		
Constant electric rates		
Payback period	4.1 years	3.6 years

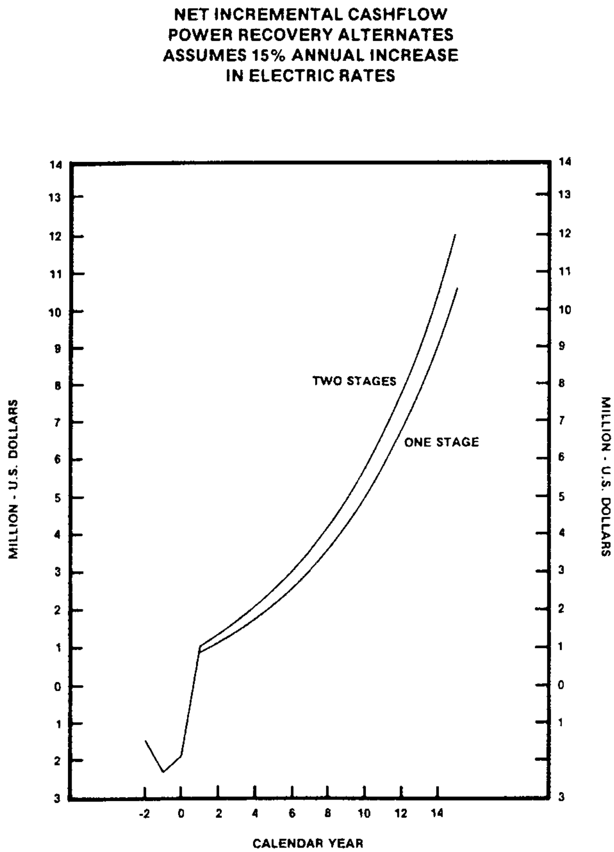

Figure 4-108. Net incremental cash flow using one- and two-stage power recovery expanders.

flow. Applying these credits to the constant electric power rate example reduces the payback periods to 4.1 and 3.6 years.

The next step is to address the startup drivers in the power recovery cases and determine the general equipment arrangements. Some general criteria used to begin determining the equipment arrangement include:

1. *Experience.* Has the customer or vendor used or supplied a particular arrangement?
2. *Process requirements.* Are there special startup and shutdown considerations such as catalyst loading and unloading and minimum air requirements?
3. *Customer preference.* Some hesitation exists to placing a motor/generator between the compressor and its main driver. In some cases, only direct-drive air strings are favored.

Plant layout and equipment considerations must also be factored into the decision. Some areas of special interest are:

1. *Piping layout.* The expander piping is large and expensive. The compressor nozzling is generally selected to minimize the impact on the expander piping. Steam turbine piping and possibly condensing equipment must also be considered.
2. *Induction motor mechanical considerations.* If the motor is placed between the compressor and the expander its shaft ends must be capable of full torque transmission. Unit torque requirements are generally well above those required by the motor rating. The result is specially designed motors.
3. *Induction motor electrical considerations.* When motor starting is desired, the startup torque requirements generally dictate the motor design. The electric current inrush at startup is significant. The plant electrical grid must be analyzed for compatibility.
4. *Steam turbine considerations.* The speed at which the turbine must operate and the steam conditions available influence the operating efficiency of the unit. Double-ended steam turbines require special consideration of thrust bearing sizing, overspeed protection, and governing systems.

Following these more technical evaluation issues, external constraints and operating economics must be analyzed. Startup of FCC air strings is accomplished using a secondary driver and includes the following considerations:

1. *Availability of steam.* If steam is readily available, a steam turbine completely satisfies the requirements under all conditions.
2. *Utility system restrictions.* Local utilities may restrict current application for motorizing and generation of power during normal operation.
3. *Economics of electricity versus steam startup.* Aside from utility restrictions, the cost of an electrical startup may be prohibitively high.

A thorough evaluation of the turbomachinery package process is required for each particular application. For most FCC units power recovery expanders are a sound investment. In cases where third-stage separation is required to meet emission standards, power recovery payback periods are reduced to even more attractive levels. New units and expansion of existing units provide energy conservation opportunities far too important to overlook.

DESIGN ASPECTS OF SECOND GENERATION HOT GAS EXPANDERS

With technological advances in the FCC process, the increased need for power recovery equipment has led companies to design a second generation of hot gas expanders. These expanders are a direct result of increased FCC regenerator operating pressures and temperatures (i.e., 40–45 psia, 1,300–1,400°F, respectively) and the demand for energy conservation in the form of recovered power of the regenerator exhaust flue gases that were often wasted. In the Elliott case, the task of designing a second generation of hot gas expanders was separated into two major areas, aerodynamic and mechanical design.

Aerodynamic Design

The aerodynamics associated with hot gas expanders is not new to competent manufacturers. Since the early 1940s, for example, Elliott has been a world leader in the manufacture of diesel and gas engine turbochargers. These turbochargers expand the engine exhaust gases to drive a compressor that supplies fresh air for the combustion process. Turbocharger inlet pressures and temperatures have steadily increased to current levels of 40 psia, 1,300°F, respectively. Elliott has also designed high temperature, 1,250°F, and high pressure, 110 psia, nitric acid expanders. Consider the four primary factors in controlling stage performance:

1. Velocity ratio
2. Stage reaction
3. Leakage and secondary losses
4. Gas conditions

Velocity Ratio

The velocity ratio is the single most important factor in determining the performance of an expander. The velocity ratio, μ, is a dimensionless parameter, relating the physical size of the expander to the gas conditions being considered. It is defined as:

$$\mu = u/C_o \tag{4-1}$$

where u = the expander blade speed
C_o = the equivalent velocity energy available

From dimensional analysis, the expander blade speed, u, is directly proportional to the wheel diameter, D, of the expander, multiplied by the rotational speed, N, of the expander, both of which are dependent on the volume flow of gas and mechanical stresses. The equivalent velocity energy, C_o, is dependent on the inlet gas conditions to the expander and can be directly translated into available energy by the following equation:

$$C_o = 223.7\sqrt{\Delta h_{SO}} \tag{4-2}$$

$$\Delta h_{SO} = c_p T_1\left[1-(r_p)\frac{k-1}{k}\right] \tag{4-3}$$

where Δh_{SO} = the available energy
T_1 = expander inlet temperature
r_p = expander expansion ratio
c_p, k = gas constants determined by the gas equations

The velocity ratio parameter is determined by relating the expander blade speed and the equivalent velocity energy available, which in turn enables determining the expander stage efficiency.

From Equation 4-1, it can be seen that the velocity ratio can be changed by:

1. Increasing the rotational speed, N
2. Using a larger rotor diameter, D
3. Decreasing the equivalent velocity energy, C_0 (i.e., adding more stages, therefore less energy per stage)

The physical size of the expander is dictated by the volume flow available to the expander. Therefore, to a large extent, the diameter is fixed and cannot be readily changed. Increasing the rotational speed also has its limits of mechanical stress that must be considered and, depending on the diameter, cannot easily be changed. Therefore, only by adding additional stages can the velocity ratio be increased. However adding more stages also has limitations, including:

1. Increased initial cost
2. Increased physical size
3. Increased rotor length
4. Decreased flow capacity (decreases the amount of flow that can be passed)
5. Increased stage velocity ratio

Obviously, adding several stages means additional material will be required. This will increase the overall physical size and cost of the machine. Significantly increasing the rotor length requires a between-bearing configuration. This, in turn, requires a radial inlet rather than the often more advantageous axial inlet. The effect on the flow capacity is shown in Figure 4-109. For a given pressure ratio, less flow will be passed by an expander having 4 stages than an expander having only a single stage or even two stages—an important factor to consider for future uprate. Having too many stages results in less energy taken across each stage, decreasing C_0 and, therefore, increasing the velocity ratio, which causes the efficiency to decrease.

Figure 4-110 depicts an efficiency curve versus velocity ratio for a reaction-type expander. The optimum efficiency will occur at a velocity ratio of .63. For a velocity ratio considerable greater or less than .63 a significant efficiency penalty can be expected. Considering the effects on the parameters mentioned above, it is easy to see the importance the velocity ratio has on the performance of the expander.

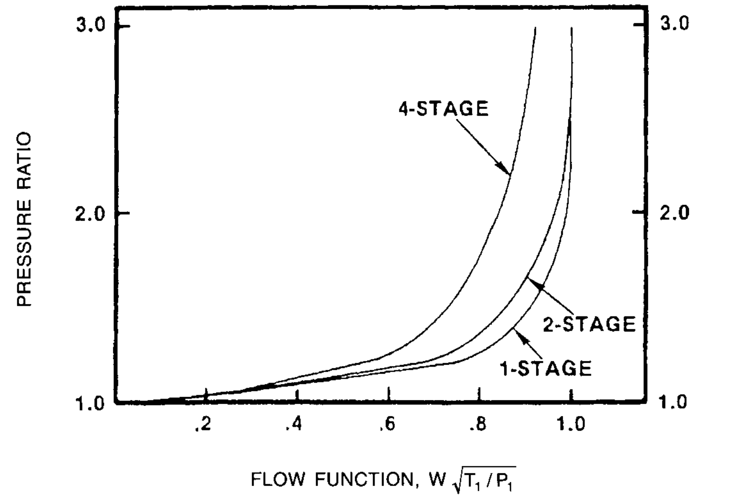

Figure 4-109. Effect of adding stages on expander flow capacity and pressure ratio.

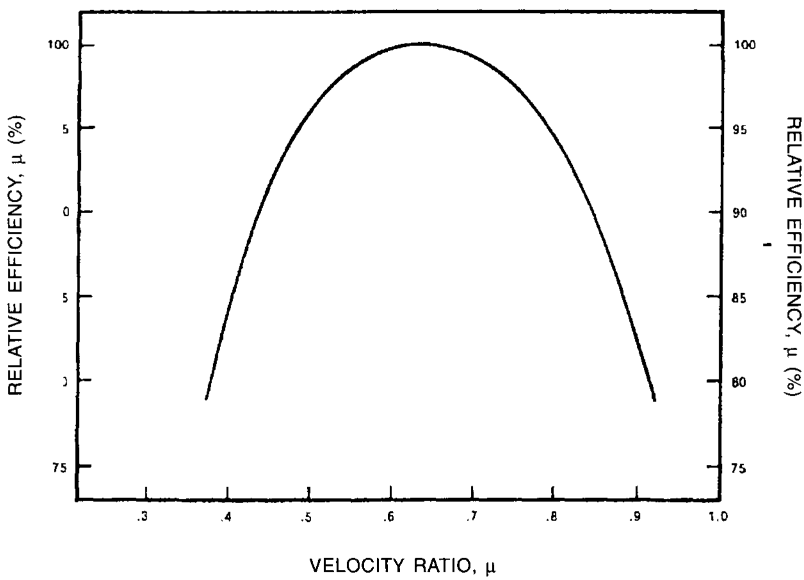

Figure 4-110. Velocity ratio versus efficiency.

Stage Reaction

As the gas expands through the stage, a partial expansion occurs in the fixed stator blades, followed by the remaining expansion through the rotating blades. The distribution of the gas through the stage can be controlled by the expander designer and is established as the stage reaction. The stage reaction then, is defined as the ratio of the energy expanded in the rotating blades to the energy available to the stage.

In Figure 4-111, this expansion process is shown on a Mollier diagram where Δh_{RS} = available energy across the rotor, Δh_{SS} = available energy across the stator, and Δh_{SO} = available energy across the stage.

In equation form, the stage reaction is defined as $R = \Delta h_{RS}/\Delta h_{SO}$. Although stage reaction is a complicated issue, certain areas should be discussed that the blade designer must consider together with their effects on expander performance. It is known that from a performance standpoint, the 50% reaction stage is the most efficient, assuming the

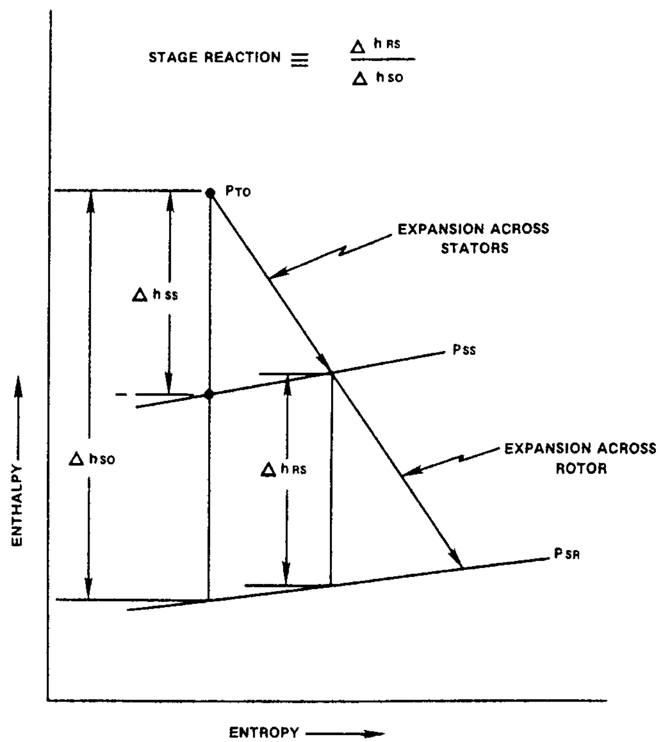

Figure 4-111. Mollier diagram for an expander stage.

velocity ratio is high and the leakage losses are low. This corresponds to conditions in normal reaction blading. However, if the available energy to the expander is large (i.e., greater than what can be efficiently handled in a single-stage application) the reaction will correspondingly increase. A higher reaction will have the following effects:

1. Increased energy across the rotating blades, which means a higher pressure drop across the rotating blades, thereby increasing the thrust loading.
2. Increased blade temperatures, resulting in higher blade stresses, further aggravating the material requirements for FCC expanders.
3. Increased blade relative velocities, resulting in higher blade relative Mach numbers and lower efficiencies.

Although expander designers are capable of controlling the stage reaction, they must also pay attention to constraints that are imposed by gas conditions.

Leakage and Secondary Losses

The control of leakage loss across the blades in a reaction expander is extremely important. Maintaining adequate clearance implies preventing mechanical rubs while at the same time minimizing the loss effect on expander efficiency.

Figure 4-112 shows the effect of the leakage flow across the tips of the rotating blades. The flow leaks from the pressure (concave) surface to the suction (convex) surface. Note that a higher pressure drop across the blades (i.e., higher reaction) increases the leakage rate. This effect can be seen in Figure 4-113 where it shows the effect of tip clearance as a fraction of passage height versus efficiency as a fraction of efficiency with no clearance, for various stage reactions. The efficiency not only decreases as the clearance is increased, but decreases as the stage reaction increases. Generally, to minimize leakage loss, stage reaction should be minimized and long blades should be used.

Additional leakage losses across the stator blades and shaft seal also play a key role in determining expander efficiency. This leakage can be controlled by keeping the clearances small, using a large number of restrictions, and installing shaft seals on the smallest practical diameter. Secondary losses, such as disc windage and frictional losses,

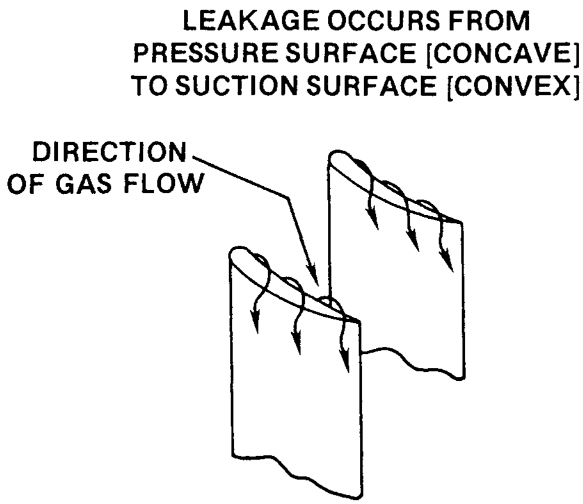

Figure 4-112. Effect of leakage flow across the tips of rotating blades.

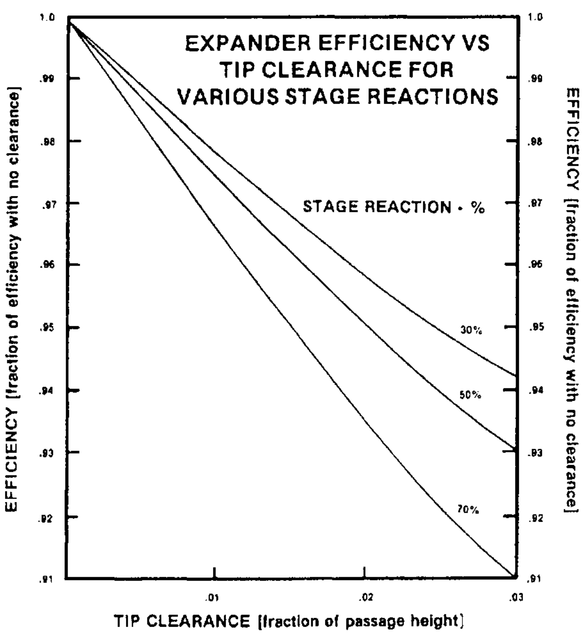

Figure 4-113. Effect of tip clearance (as a fraction of passage height) on expander efficiency.

although small, must also be considered in the final determination of expander efficiency. Disc windage losses are proportional to the cube of the speed and the diameter raised to the fifth power. Figure 4-114 shows the trend of wall frictional losses as a function of the blade height; losses are highest at the root and tip of the blade, as would be expected. The use of small base diameters and high rotational speeds will help in reducing windage and frictional losses.

Gas Conditions

The previous discussion of the velocity ratio parameter looked at the effect the available energy has on expander efficiency. The examples listed in Table 4-11 further illustrate this effect.

Example 1 shows the expander inlet conditions typical of past FCC applications with an expander inlet pressure of 30 psia and inlet temperature of 1,200°F. Example 2 shows the conditions prevalent in more recent FCC regenerator technology, where most of the CO is

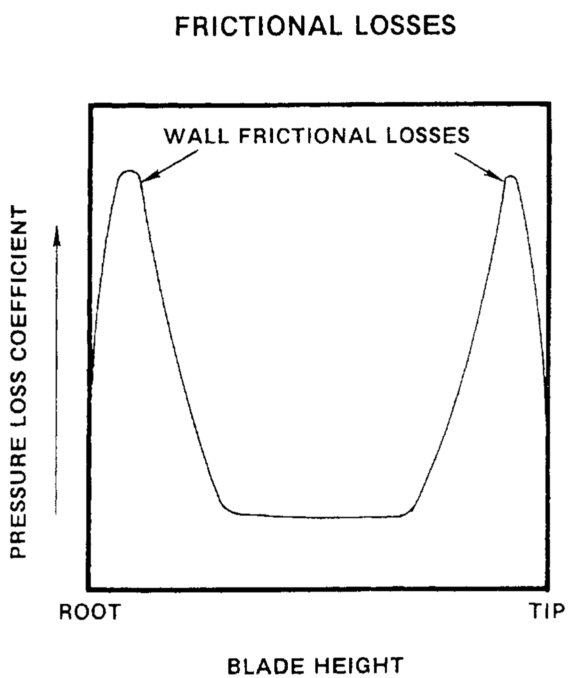

Figure 4-114. Trend of wall frictional losses as a function of blade height.

Table 4-11

	Inlet pressure (psia)	Inlet temp. (F)	Available energy (Δh_{SO})
Example 1	30	1,200	71.5
Example 2	42	1,300	110.4

**Gas Mole Wt. = 29.02; Exhaust Pressure = 15.2 psia*

converted into CO_2, with an expander inlet pressure of 42 psia and inlet temperature of 1,300°F.

Plotting these pressures and temperatures on a Mollier diagram (Figure 4-115), makes it possible to compare the amount of available energy for both examples. The available energy of Example 1 is 71.5 Btu/lb as compared to 110.4 Btu/lb for Example 2. In other words, increasing the inlet pressure from 30 to 42 psia and the temperature from 1,200 to 1,300°F results in over a 50% increase in available energy, which translates directly into recoverable power.

As mentioned earlier, because the number of stages has a significant effect in determining the velocity ratio, consider the effect the gas conditions have in determining the optimum number of stages. To make this determination, the following parameters should be considered:

1. The available energy to the expander, Δh_{SO}
2. The equivalent energy developed by a particular stage, $\Delta h_{STAGE} \propto u^2$
3. The optimum velocity ratio, $\mu = u/c_o$
4. The effects of the reheat factor, RF

This can be written as

$$M = (RF)\left(\frac{\Delta h_{SO}}{\Delta h_{STAGE}}\right)(\mu)^2 \tag{4-4}$$

where M = optimum number of stages.

Again, the importance of the velocity ratio can be seen because its effect is squared in this equation.

The reheat factor, RF, is a function of the pressure ratio across the machine, the stage efficiency, and the number of stages. The

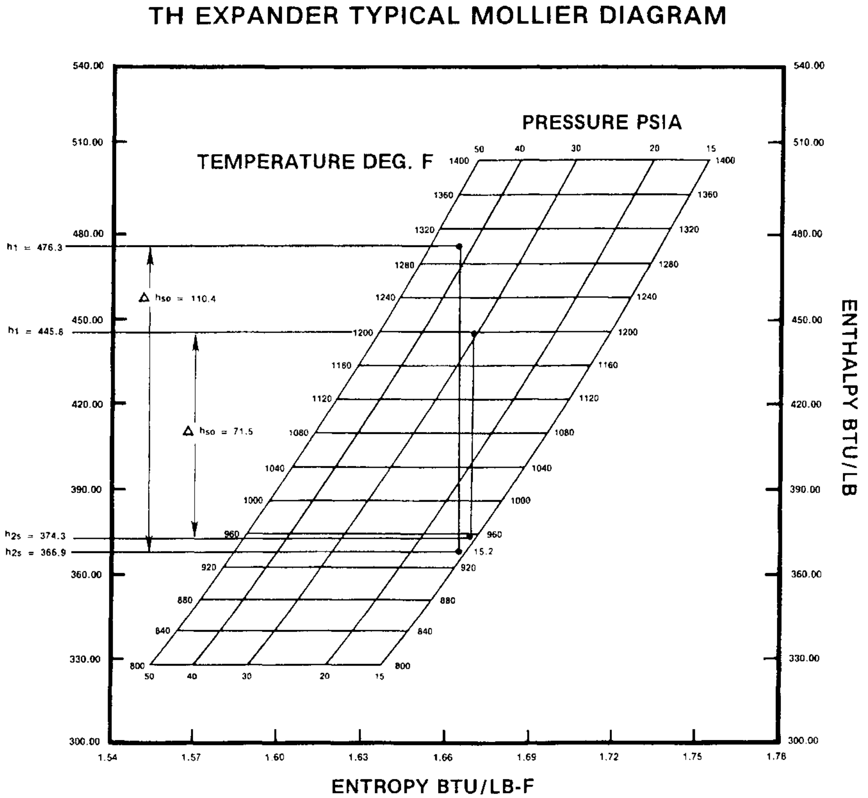

Figure 4-115. Pressures and temperatures from Table 4-11 transferred to Mollier diagram.

equivalent energy developed by a stage is proportional to the square of the blade speed.

For Example 2, recall the available energy is 110.4 Btu/lb. The energy developed by a stage is 22 Btu/lb. The reheat factor is 1.017 and the optimum velocity ratio (Figure 4-116) is .63. Substituting these values into Equation 4-4 yields:

$$M = (1.017)\left(\frac{110.4}{22}\right)(.63)^2 = 2.025$$

or the optimum number of stages is 2.

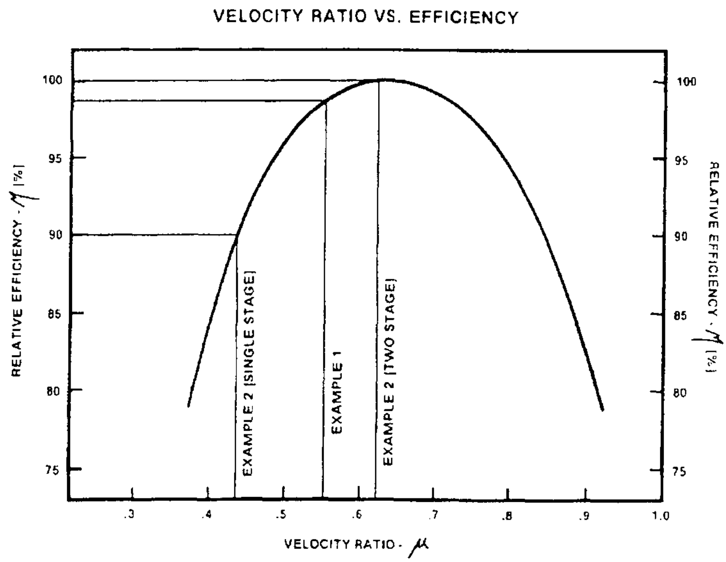

Figure 4-116. Optimum velocity ratio for expander stage.

The same calculation can be done for Example 1. With $\Delta h_{SO} = 71.5$ Btu/lb, $\Delta h_{STAGE} = 22$ Btu/lb, RF = 1.0 (for a single stage) and $\mu = .63$. Again, substituting the numbers

$$M = (1.0)\left(\frac{71.5}{22}\right)(.63)^2 = 1.290$$

or the optimum number of stages is one.

For a given flow of gas, and converting the available energy of Example 1 into an equivalent velocity energy from Equation 4-2, the actual velocity ratio for this example is .57. With this velocity ratio, the efficiency is 99% of its relative optimum value, as shown in Figure 4-116. For the same flow of gas as Example 1, the available energy of Example 2 can be converted into an equivalent velocity energy, then a comparison of efficiency can be shown for a single- and two-stage expander.

For a single-stage expander, these conditions convert to a velocity ratio of .44, reducing the efficiency to 90% of its relative optimum value. However, with a two-stage expander, the velocity ratio increases to a mean value of .62, moving the efficiency back along the curve to its peak value, resulting in the relative optimum efficiency selection.

Thus, with the two-stage expander, the efficiency is 11% greater than the equivalent single-stage expander, directly resulting in an 11% increase in recoverable power.

Summarizing, the best expander selection can be made from the following guidelines:

1. Use small rotor diameter and, therefore, longer blades. This helps reduce the physical size of the expander and maintain a high blade speed, thereby keeping the velocity ratio high. It also keeps tip leakage as well as disc windage and frictional losses to a minimum. The cost is also minimized—a major factor when considering the types of material required for these applications.
2. Use the highest rotational speed. This also helps reduce the physical size of the expander while keeping the velocity ratio high.
3. Provide the optimum number of stages. In modern FCC units, the gain in recoverable power using two-stage versus single-stage construction generally makes up for the incremental cost of two-stage expanders. The use of two stages also keeps the gas velocities at moderate levels, leading to longer blade life without sacrificing efficiency.

MATERIAL SELECTION FOR POWER RECOVERY TURBINES

Selecting materials for the hot end of power recovery turbines requires great care. Although inlet temperatures vary with the installation, they are usually in the range of 1,050–1,400°F. In selecting materials for service in this temperature range, the most important mechanical property is the stress rupture strength. Attention must also be given to coefficient of thermal expansion, oxidation resistance, weldability, as well as a number of other characteristics.

The first step is to establish the anticipated design life at rated speed and temperature. This is usually 100,000 hrs for the turbine disc. For the blading, generally called "buckets," the anticipated life may be 50,000–100,000 hrs, depending on anticipated erosion rates. In many applications buckets wear out due to erosion in less than 100,000 hrs, and in these cases it is unnecessary to select materials with extended stress rupture life. Evaluation of the stress rupture strength of high temperature materials requires preparing two types of curves. In the first curve (Figure 4-117) strength is plotted as a function of temperature with a series of curves for various projected lifetimes. These curves permit establishing the maximum allowable stress at any given temperature and are usually plotted for several materials.

In analyzing these data it is necessary to go beyond the curves and determine the expected behavior of the material with respect to notch sensitivity. Problems with notch sensitivity can often be corrected by modifying the processing steps and/or heat treatment.

It is important to note that material selection is based on the rated speed and temperature. If either the speed of the rotating parts (and, therefore, the stress) or the temperature is below the values on which the design is based, significantly longer life may be anticipated. When the operating temperature is below the design temperature by 50–100°F, a significant increase in life may be expected. Even 25°F can make an appreciable difference. The temperature of interest is the actual metal temperature, not the nominal inlet gas temperature. For example, allowance should be made for the temperature drop in the stationary blades or nozzles when determining the metal temperature

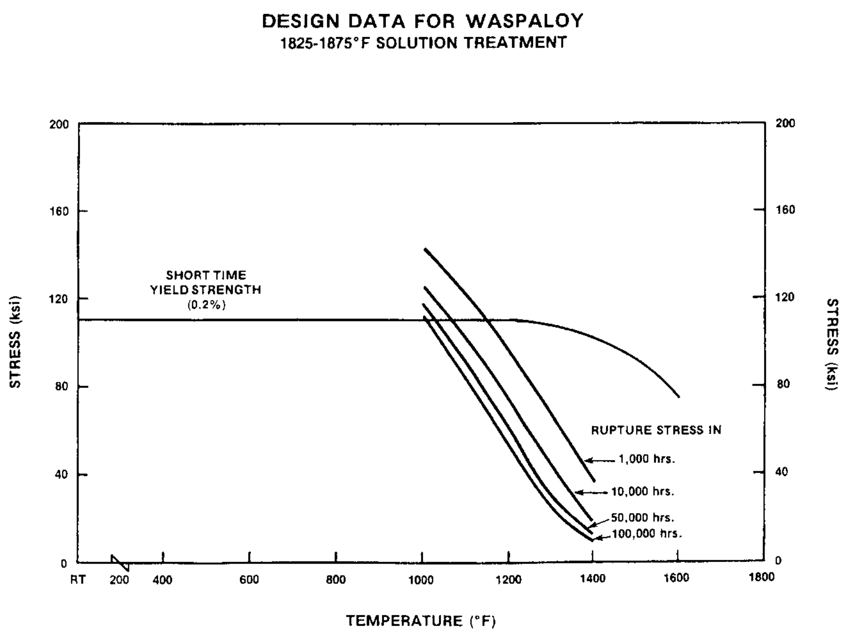

Figure 4-117. Temperature and stress limits related to design life of Waspaloy bucket material.

of the rotating buckets. In multistage turbines there are successively greater temperature reductions proceeding from the inlet to the discharge. In some cases, this permits later stages to be made of less highly alloyed, lower cost, more readily available materials than are required for the first row. The first row of blading is the hottest.

The second (Figure 4-118) curve, commonly called the Larson-Miller parameter curve, permits the evaluation of variations in operating conditions. Using this type of curve it is possible to estimate the life fraction of the material used under a given set of operating conditions including effects of upset conditions. As in Figure 4-117, upset conditions can have severe consequences. These temporary conditions, though brief, may require selecting a material of greater strength (and cost) than would be needed for nominal operating conditions.

While evaluating the mechanical properties of materials, attention must also be given to availability. Sometimes an alloy of attractive properties is not commercially available. It may be possible to obtain special heats for large parts such as appreciable quantities of plate, large forgings, and so forth, but it may be difficult to contain smaller quantities required for incidental pieces.

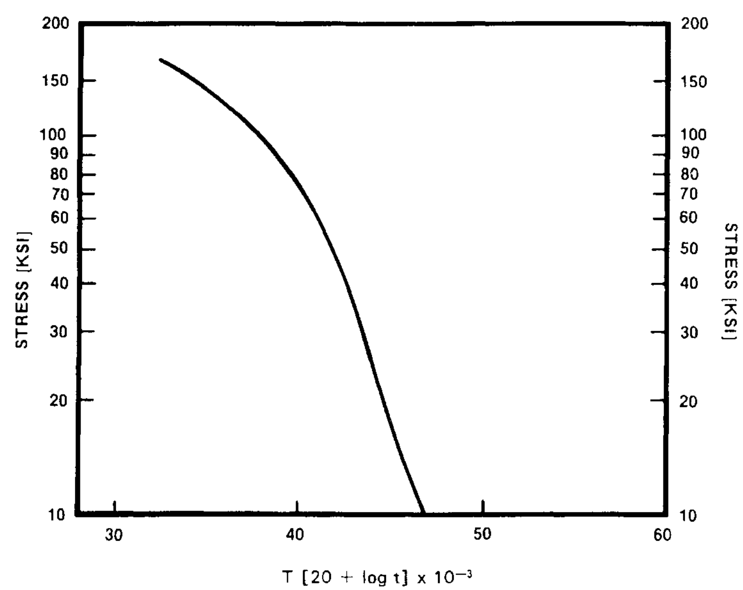

Figure 4-118. Larson-Miller parameter curves allow estimation of bucket life.

An appraisal must be made of the ease or difficulty that may be involved in the fabrication, welding, or machining of alloys being considered. Extensive fabrication and welding are involved with stationary parts. There are materials that have attractive mechanical properties, which are not used because of poor weldability. Frequently, such materials are difficult to obtain. Poor weldability leads to low demand, which is reflected in poor availability even for applications where welding is not required. Some materials are available only as castings, wrought products, or in a limited range of sizes. Step-wise progression in sizes is usually attainable provided the steps are not too large.

Based on the above criteria, good selections for turbine buckets and discs are A286, Incoloy 901, and Waspaloy. Inconel 718 is considered a possible replacement for Waspaloy in some temperature ranges simply because it does not contain cobalt, a metal that is occasionally in short supply. Stationary blades may be forged or cast from materials such as A286, Waspaloy, X40, or Inconel 713C, while casings may be fabricated from AISI Type 304 stainless steel, Inconel 600, or Hastelloy X.

Typical chemical analyses of these materials are listed in Table 4-12. Only two of these materials can be considered iron-based—Type 304 stainless steel and A286. X40 is cobalt-based and the others are all nickel-based (Incoloy 901 contains more nickel than iron). The desired longtime high temperature strength is obtained by adding various other elements including titanium, aluminum, molybdenum, columbium, tungsten, boron, and zirconium.

HOT CORROSION OF WASPALOY MATERIAL IN GAS EXPANDER ROTATING COMPONENTS

Selection of an alloy for high temperature operation depends on its ability to withstand the stresses imposed on it during service and on the corrosion resistance of the alloy to protect itself from various atmospheres in service. Waspaloy, used for rotating blades and discs in hot gas expanders, has generally been selected due to its ability to withstand the necessary stresses and to provide good oxidation resistance at elevated temperatures. The blade/disc components for hot gas expanders usually operate in the temperature range of 950–1,200°F. At these temperatures, the creep rupture properties of Waspaloy are excellent, which makes it a suitable candidate material. Since Waspaloy

Table 4-12
Typical chemical analysis of some alloys used in power recovery turbines

	C	Mn	Cr	Ni	Ti	Al	V	Mo	B	Co	Others
A286	0.06	0.40	15	25	2.0	0.2	0.25	1.2	0.005		
Incoloy 901	0.06	0.40	12	43	3.0	0.2		6.0	0.015		
Inconel 718	0.05	0.25	19	52	1.0	0.5		3.0			
Waspaloy	0.07	0.10	19	Bal.	3.0	1.4		4.2	0.005	13	Cb 5, Fe Bal.
X40	0.50	0.70	25	10						Bal.	Zr o.05
Inconel 713C	0.05	0.20	12	Bal.	0.7	6.0		4.5	0.010		W 7.5
Inconel 600	0.10		15	75							Cb 2.0, Zr 0.1
Hastelloy X	0.10	0.70	21	Bal.				9.0		1.5	Fe 8
Type 304	0.06		19	9							W 0.5, Fe 18

has approximately 18% chromium (Cr) in the alloy, the formation of protective oxide scales gives the material good oxidation/corrosion protection. However, certain gases, such as sulfur oxide (SO_x) and/or hydrogen sulfide (H_2S) atmosphere, can react with the protective oxide scale and cause it to deteriorate. Sulfur can then attack forming a nickel sulfide (Ni_3S_2) layer, which can lead to failure of the rotating components.

An Expander Blade Experience

Characterization and Identification of Corrosive Scale

Some manufacturers have experienced the above mentioned Ni_3S_2 scale formation phenomenon under certain gas conditions, which led to the failure of a rotating blade. One such experience involved a fracture that was distinctly intergranular with evidence of secondary intergranular cracks or grain separation across the fracture. Intergranular facets of the fracture were sharp and distinct with little evidence of any ductile mode. The fracture appeared to have occurred in a brittle intergranular mode.

The Ni_3S_2 constituent formed on the surface and scale formation was observed in all areas of the blade roots. The mechanism seemed to be more prevalent above the root pressure boundary than other areas of the blade root. Characterization of the scale was performed using a Scanning Electron Microscope equipped with an Energy Dispersion X-ray analyzer (EDX).

Characterizing and identifying the Ni_3S_2 scale is important in understanding the scale formation mechanism. Since the Ni_3S_2 occurred in a solid state, this phenomenon most likely occurred in the temperature range of 900–1,150°F. This temperature range is below the formation temperature of the liquid Ni_3S_2 phase of 1,193°F.

Fracture Mechanism

To explain the mechanism by which the formation of Ni_3S_2 scale can result in the fatigue failure of the blade disc, the effect of sulfur on the mechanical properties of nickel base alloys must be understood. Since the fracture modes are totally intergranular with evidence of

Ni_3S_2 and CrS (chromium sulfide) along the fractured face, a corrosive mechanism must have occurred. The sulfur-rich Ni_3S_2 phase acts as a source for sulfur to preferentially attack along the grain boundaries. The diffusion of sulfur along the grain boundaries occurs at a much faster rate than that through the Waspaloy matrix. The prestraining effect at the crack front also increases the diffusion of sulfur along the preferential grain boundaries.

Another possible theory for the fracture mechanism is based on the formation of the Ni_3S_2 scale altering the loading condition at the blade/disc root interface. The formation of the Ni_3S_2 scale in these locations changes the blade/disc root contact and can result in a high-point loading condition. This increase in loading condition of the blade/disc root interface can cause failure at operating conditions, whether by fatigue or possibly creep rupture. However, since both theories for the fracture mechanism depend on the formation of the Ni_3S_2 scale, the prevention of the corrosive condition is the remedy to the problem.

Determining Susceptibility of Ni_3S_2 Formation Using a Hot Gas Expander Analysis

Mechanism of SO_x Attack on Waspaloy

To fully understand the formation of the Ni_3S_2 scale under certain gas conditions, a brief description needs to be given on the chemical aspects of the protective (chromium oxide) Cr_2O_3/(nickel oxide) NiO scales that form at elevated temperatures. Under ideal oxidizing conditions, the alloy Waspaloy preferentially forms a protective oxide layer of NiO and Cr_2O_3 The partial pressure of oxygen is such that these scales are thermodynamically stable and a condition of equilibrium is observed between the oxidizing atmosphere and the scale. Even if the scale surface is damaged or removed, the oxidizing condition of the atmosphere would preferentially reform the oxide scales.

$$2\ Ni + O_2 = 2\ NiO$$

$$4\ Cr + 3\ O_2 = 2\ Cr_2O_3$$

If the atmospheres have sulfur present under an oxidizing condition, the oxide layer would still consist of Cr_2O_3 and NiO. The oxide layer formed limits the availability of sulfur to the underlying metal surface, but the rate of chromium diffusion from the body of the metal to this underlying metal surface is obviously unaffected and, thus, the chances of producing a protective scale are increased. This is supported by thermodynamics when considering free energy of formation at various temperatures for oxides and sulfides. In the 950–1,200°F temperature range, NiO/Cr_2O_3 layers are more likely to form than Ni_3S_2, even under oxidizing SO_2 atmospheres. When the gas atmosphere tends toward a more reducing condition, the sulfur attack becomes more prevalent. This leads to the formation of both CrS and $Ni3S_2$. At the eutectic temperatures above 1,193°F, the nickel sulfide forms a liquid phase that is capable of causing accelerated corrosion of the alloy, especially at the grain boundaries.

Determining Susceptibility of Ni_3S_2 Formation Using a Stability Diagram

Using thermodynamic calculations, a competent manufacturer can predict the susceptibility of the formation of Ni_3S_2 from any gas analysis. This is accomplished by determining the oxygen and sulfur partial pressures present in the gas analysis. Using a computer program, the gas analysis is programmed to calculate the equilibrium concentration of formation. This information is then used to calculate the partial pressure of oxygen and sulfur of the particular gas. By plotting this information on the nickel/NiO/Ni_3S_2 stability diagram, the susceptibility for the formation of Ni_3S_2 can be assessed. Figure 4-119 shows a stability diagram with gas analysis plots of A and B. Gas analysis A corresponds to a gas that has a more oxidizing condition under a certain pressure and temperature. In this condition, the Waspaloy material will favor the formation of the protective oxides NiO/Cr_2O_3 rather than the Ni_3S_2. However, with gas analysis B the gas is in a more reducing-type condition and will tend to form the corrosive Ni_3S_2 scale in preference to the protective oxides. This aspect is extremely important since preformed oxide scales in blade/disc pressure lands could be damaged or removed and would not preferentially reform under this gas condition. Consequently, the sulfur in the gas is more likely to react with Waspaloy to form Ni_3S_2, which could have detrimental effects on its material property. It is important to understand that this method does not precisely predict which way the reaction will

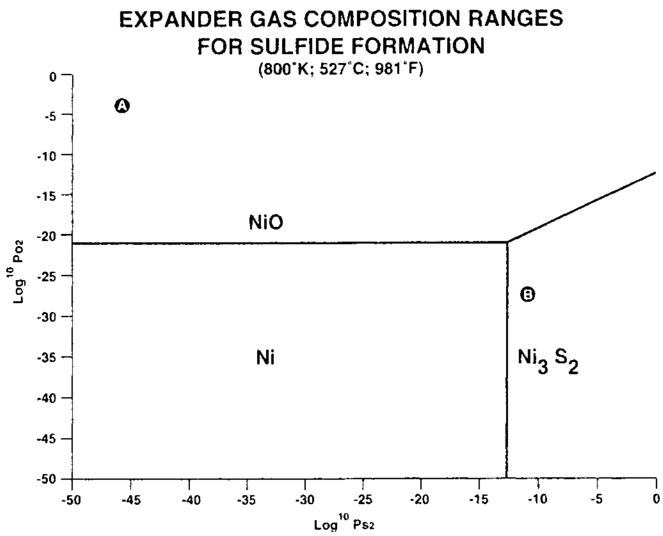

Figure 4-119. Stability diagram with region B indicating the more corrosive condition.

go; it mainly indicates a state or form that would most likely occur. If there is a change in temperature, the sulfide/oxide stability diagrams must be adjusted.

The importance of being able to predict the effect of a specific gas analysis on the formation of the corrosive scale is essential in the prevention of blade failures. Again, competent manufacturers have successfully developed a means of achieving this through the application of modern computer programs. However, the gas analysis provided must be as accurate as possible if the program and calculations performed are to have any real value.

Preventive Measures to Eliminate Ni_3S_2 Formation

Since competent manufacturers can accurately predict the susceptibility for the formation of the corrosive scale Ni_3S_2 for any gas analysis, it is possible to implement preventive measures. The preventive measure that is presently being used by Elliott and others is the use of a steam barrier. The principle of the steam barrier design is to inject steam into the inlet and exhaust chambers of the disc/blade area. The injection of steam into both these chambers creates a barrier of steam across the inlet and exhaust faces of the blade/disc roots. The steam barrier not only prevents any reducing-type effects from the expander gas, but will create an oxidizing effect due to the presence of the water (H_2O). This system has been designed and is operating in a number of applications where Ni_3S_2 susceptibility was identified.

Another prevention method is the application of a coating to the blade/disc root area to prevent the formation of Ni_3S_2. The coatings that are typically considered include aluminide coatings and chromide or chromium-rich diffusion coatings. An evaluation of the effect of these coatings on the creep rupture/fatigue life of Waspaloy material enables the expander manufacturer to determine the ability of the coating to withstand the loading conditions encountered.

Until the late 1990s, Waspaloy was still the best alloy available for the majority of hot gas turboexpanders used in industry and, until recently, it continued to offer the many special characteristic needed for hot gas expander applications. However, a new development followed in 2000 when the Ebara Corporation (Japan) released data on a nickel-base superalloy.

Sulfidation-Resistant Nickel-Base Superalloy for FCC Flue Gas Expanders

A nickel-base superalloy with excellent sulfidation resistance, high temperature tensile properties, and hot workability was developed by Ebara engineers as a material for the rotors of FCC gas expander turbines. Ebara investigated the effect of Mo, Ti, and Al additions on the sulfidation behavior of a Ni-20Cr-13.5Co alloy in H_2-H_2S mixtures at 600°C (1,112°F). It was found that increasing the Al content in the alloy improved the sulfidation resistance of AISI 685 (UNS N07001). Six mixtures of forged alloys in which the Al content was increased while the Ti content was decreased, were manufactured. Sulfidation tests and high-temperature tensile tests of these alloys indicated that the 1.5Ti-3.0Al alloy had twice the sulfidation resistance and almost equivalent tensile properties to those of AISI 685.

It was concluded that 1.5Ti-3.0Al should be considered the most suitable alloy for FCC flue gas expander rotors. A 1,400-mm diameter expander rotor disk was manufactured using this alloy. Test specimens removed from the disk rim showed that the disk had equivalent tensile properties at both room and elevated temperatures, and the same creep rupture strength as that of AISI 685.

TURBOEXPANDER TESTING

Although testing practices may vary between manufacturers, Elliott's approach is considered representative of experience-based testing of hot gas turboexpanders.

1. *Inlet Casing.* The inlet casing is hydrotested with temperature compensation. The maximum rating condition is 50 psi, 1,400°F inlet gas. For the hydrotest, the inlet flange and discharge section are blanked-off and the casing is then pressurized (Figure 4-120). A steady pressure is applied for approximately 30 min. During this time, the casing is thoroughly checked for any leakage at the weld joints.
2. *Exhaust Casing.* The exhaust casing, complete with expansion bellows, is given an air test. The air test pressure is dictated by the bellows construction and is a function of its size. For large units, about 9 psig is chosen, whereas the smaller units are typically tested at approximately 16 psig. The maximum design rating of a typical exhaust casing is 5 psig at 1,200°C.
3. *Rotor Heat Cycle.* As part of the rotor construction, Elliott conducts a heat cycling test of the rotor at the shaft-to-disk

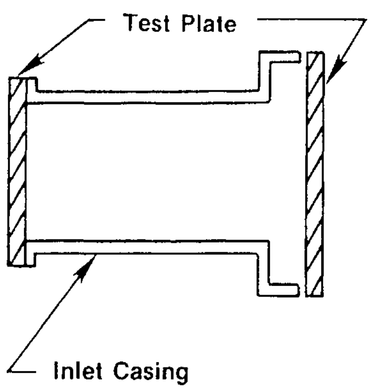

INLET CASING HYDROTEST

Figure 4-120. Casings are blanked-off for hydrotesting.

splined joint (Figure 4-121). The rotor is first check balanced, then the spline connection is heated to the operating temperatures—normally 500–600°F. After it cools, the rotor balance is rechecked. If the balance has shifted, the procedure is repeated until two consecutive balance readings are obtained. This assures that the disk-to-shaft joint will be thermally stable once the unit is installed in the field and reaches operational temperatures.

Once the final balance of the rotor is achieved, a check of the electrical runout is conducted. If this runout exceeds the standard specifications, corrective measures are taken.

4. *Mechanical Testing.* Once the unit is assembled, mechanical testing begins. All hot gas expanders are given a hot gas test. The test is conducted by recirculating hot gas from the discharge to the inlet. The heating is the result of windage friction of the disk in the casing.

As shown in Figure 4-122, the gas flows around the loop pumped by the windmilling turbine. Since this is a closed loop test, the loop is first purged of air using nitrogen. The unit is started with nitrogen in the loop and pressurized to 1–2 psig. As the temperature increases due to the windage heating, steam is added to the loop for temperature control. The steam will eventually displace the nitrogen during the test. The parameters measured during testing typically include:

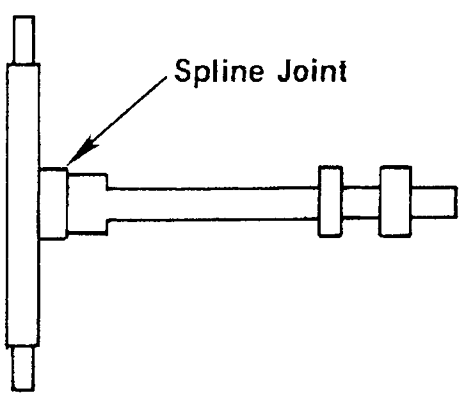

Figure 4-121. Hot gas expander wheel and shaft constitute the rotor. Note the splined engagement.

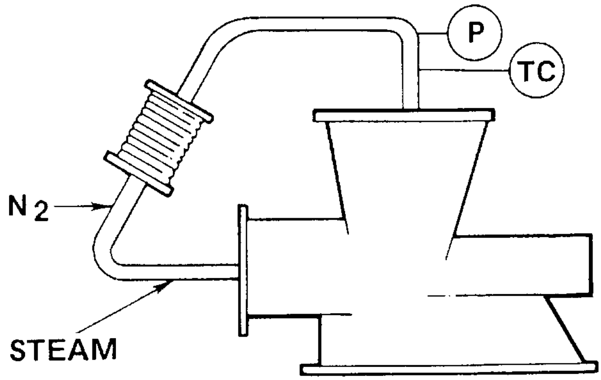

Figure 4-122. Closed-loop test setup.

- Vibration at each shaft probe
- Casing temperature
- Oil temperatures for the lube oil feed
- Throw-off temperatures from journal bearings and thrust bearing

The casing-internal instrument thermocouples are checked to ensure they are reading properly. RTDs and/or load cells are also checked during the test. The steam buffer seal controls are installed and functionally checked during the test.

Figure 4-123 outlines the basic test plan as an elapsed time versus unit speed plot. The initial operation increases the speed at approximately 10% increments as shown. The overall time to achieve test speed is approximately 3 hrs for the initial run-up, assuming a steam turbine drive. Once the unit has attained speed, the heating cycle begins. It may take from 4–8 hrs to attain the test temperature. Once the testing temperature is stabilized, the unit operates for 1 hr. After 1 hr, it is accelerated to its trip speed and the trip is checked for accuracy. The unit is then be brought back to normal operational speed and the test continues for an additional 3 hrs. Afterwards, the unit is tripped twice and the test is complete. After the trip test, the unit is cooled down. The overall testing time and cooling take approximately 16 hrs.

If there is a spare rotor sold with the order, the spare rotor is also heat cycled. If the customer requests, it too can be mechanically tested prior to shipment. If a motor drive is required, the initial run-up is

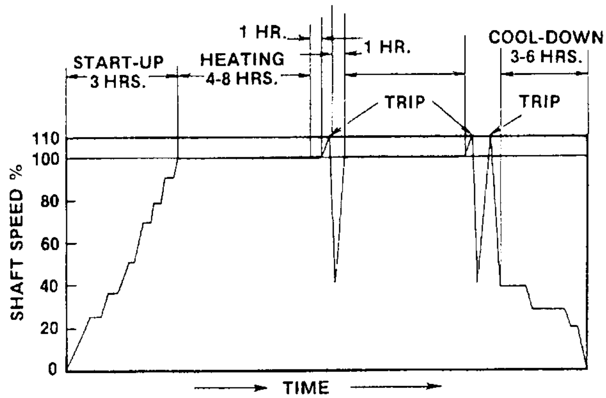

Figure 4-123. Basic testing and its speed versus time relationship.

completed using the shop steam turbine driver. However, once the rotor is checked and it is determined there are no clearance problems, it is accelerated to slow idle speed and then rapidly accelerated to design speed in order to simulate a motor start.

In addition to the mechanical testing, operation of the sight ports is checked to ensure they are properly oriented and that the blades can be seen when the unit is in operation. All assembly and disassembly tooling shipped with the job is used during the initial assembly. Tooling that is supplied with the job includes rails and lifting rigs for the rotor, bearing cap disassembly fixturing, and other casing fixtures required for rotor removal or disassembly and unique to the unit.

SOLID PARTICLE EROSION

In support of the power recovery expander market for fluid catalytic cracking units in refineries, some turboexpander manufacturers have an ongoing program to improve the solid particle erosion characteristics of the machine. Improved erosion characteristics will result in longer blade life, less downtime, and consequently greater profits for the users.

The following briefly reviews the parameters that affect erosion and the programs instituted by Elliott to obtain basic erosion data. The data from these studies have been integrated into Elliott's erosion prediction program. Table 4-13 lists some of the more important parameters affecting expander blade erosion from solid particles. Many of these parameters directly relate to the particle itself.

Table 4-13
Factors affecting expander blade erosion

1. Particulate concentration	g/acfm
2. Particulate velocity	ft/sec
3. Particulate angle of impact	degrees
4. Particulate size distribution	—
5. Particulate density	lb/ft^3
6. Particulate shape	—
7. Particulate attrition or friability	—
8. Blade base material	—
9. Blade coating material	—

The particle concentration, or the amount of foreign material entering the expander, is important to the life of the expander blading. The larger the quantities of catalyst dust ingested, the faster the expander blades will erode. Another important erosion parameter is the velocity of the particle. It is important to place a great deal of emphasis on controlling velocity because erosion increases exponentially with velocity, and, thus, decreases blade life. The angle at which the particle impacts the metal surface, the size distribution of the particles, and the particle density also have a significant effect on erosion. Other parameters that affect blade erosion are (1) particle shape, (2) particulate attrition rate, (3) blade base material, and (4) blade coating material.

How these factors affect erosion can be determined from the empirical equation shown in Table 4-14. The equation shows erosion rate proportional to a constant, the mass of the particle, its velocity, and angle of attack.

Table 4-14
Empirical equation of erosion parameters

$$\text{Erosion rate (loss of weight)} \approx K \frac{m_p V_p^2}{2} \alpha$$

K = Constant (depends on target material, particle abrasiveness and size distribution)

$\frac{m_p V_p^2}{2}$ = kinetic energy of particles (includes solids loading and particle velocities)

α = Angle of impingement on target blade surface

The constant, K, depends on the target material, particle abrasiveness, and size distribution of the particles. The kinetic energy of the particles is $M_p \times V_p^2 \div 2$. This parameter includes the solids loading, or concentration, and velocity of the particle. Alpha is the angle of impingement of the particle on the blade surface.

Programs are available to study each of these parameters. In the late 1980s, Elliott, with the assistance of the Research and Development Center of their then parent organization, Carrier Corporation, initiated three programs to study erosion. A materials and coatings program provided data on the relative erosion resistance of one base material to another and of one blade coating to another. A basic erosion parameter test program provided data on parameters such as the effect of impingement angle, velocity, particle size, and temperature. An erosion prediction program provided the tool that is required to study erosion resistance of different blade designs at specified operating conditions.

Table 4-15 lists base materials Elliott has tested. This list, which is continually being expanded, includes low alloy steels, high alloy iron base, nickel base, cobalt base materials, and others. Table 4-16 shows some of the coatings Elliott has tested. The list indicates the supplier, coating designation, and major components of the coating composition.

Test work for the materials and coating program and the basic erosion parameter test program was conducted in specially designed test rigs. Figure 4-124 schematically shows the general arrangement. A microblaster feeds the weighed sample of particulate nozzle, which directs the erosive particle to the erosion specimen. A vacuum line transports the dusty air from the test chamber to a filter system where all particulate matter is removed from the air. The basic method Elliott employed for determining the amount of damage to the specimens was weight loss. This required precise measurements of weight. A balance

Table 4-15
Materials tested for erosion resistance

AISI, ASTM, etc., Designations
403
1020
4340
4140
INCONEL 706
INCOLOY 901

Table 4-16
Coatings tested

Supplier	Designation	Material
Metco	P438	WC + Co, Ni
	P73F	WC + Co
	P81VF	Cr_2C_3 + NI, Cr
	P72F	WC + Co
Sermetel	J	AL, Si
	W + 5375	AL Ceramic
	W CLASS II	AL Ceramic
	W + 620	AL + Organic
Union Carbide	LW5N	WC + NI, Cr
	LC-1C	Cr_2C_3 + NI, Cr
	LW-1-40	WC + Co
	LA-2	AL_2O_3
	WT-1	WTiC
	LS-31	Co, Cr, NI, W
Lindberg	Tufftride	Nitride and Boron
	Boroloy	Diffusion Coatings

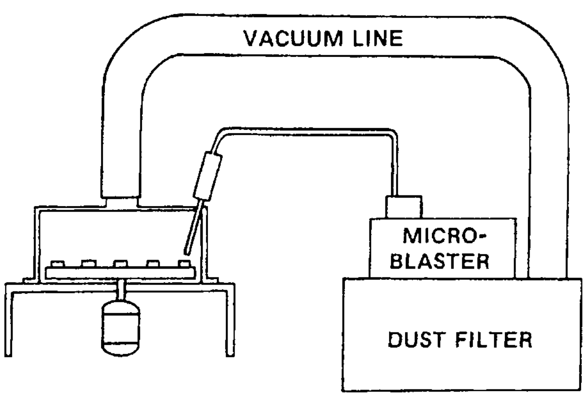

Figure 4-124. Particle velocity measurement.

scale that can be read to hundredths of a milligram was used. Generally, the amount of abrasive used was adjusted so that 2–10 mg of material were removed. The target specimens weighed approximately 24 g. Elliott also used a scanning electron microscope, which is of major value in studying surface features.

Figure 4-125 shows in more detail some of the components of the test cabinet. Abrasive particles are given an initial velocity by the primary air stream and then accelerated to a final speed by the secondary air stream. The final velocity of the abrasive particle is less than the velocity of the air and varies with particle size and density.

An important factor in the evaluation of test results is knowledge of particle velocity. It is more accurate to directly measure particle velocities than to depend on knowing the particle and fluid properties required to perform analytical calculations. Figure 4-126 schematically shows a rotating disk arrangement used to determine particle velocity. This measurement technique was an in-house development and is similar to a technique developed and later reported by the National Bureau of Standards. Conceptually, the method measures travel time of a particle over a known distance. In operation, the disks are rotated at a known slow speed to establish a reference mark on the outboard disc. Then the discs are rotated by the variable speed motor at a higher, known velocity. Particles passing from the nozzle through the slot in the first disc make a second mark on the outboard disc after crossing the space between. The distance between marks on the outboard disc is used to compute the particle velocity. Aerodynamic effects are a consideration, but have not been found to affect the velocity measurement.

A 1,200°F furnace was used for initial testing. Testing at atmospheric conditions, as well as at 1,000°F and 1,200°F, was followed by final testing at temperatures as high as 1,400°F.

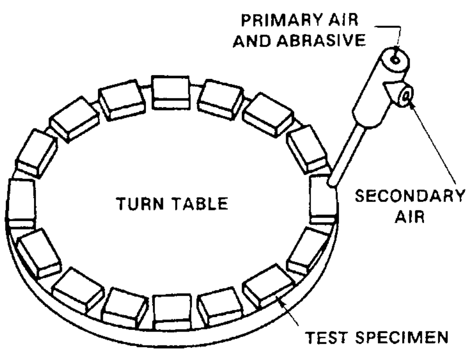

Figure 4-125. Test rig components used in erosion research.

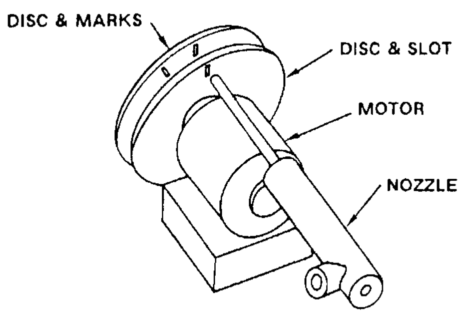

Figure 4-126. Overall arrangement of test rig used for erosion research.

An example of one of the data categories that can be obtained is illustrated in Figure 4-127. The specimen erosion proportional to volume removed is plotted versus particle velocity for four coating materials. The data for this plot were obtained at 1,200°F by impinging the specimen at a 20° angle to its surface with aluminum oxide particles. From this plot, it can be seen that coating "A" provides the least protection of the four coatings presented as evidenced by the large volume of coating removed.

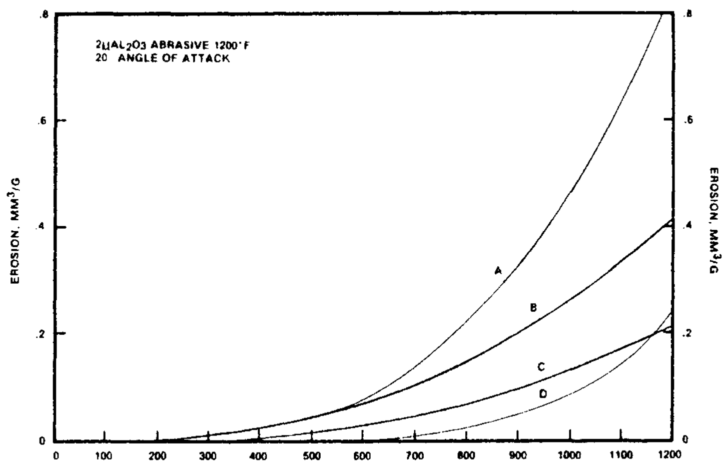

Figure 4-127. Data categories involved in erosion research are plotted as erosion versus velocity.

The value of the scanning electron microscope can also be recognized from this slide. Note that coating "D" has better erosion resistance than coating "C" up through a high velocity, but the opposite is true at higher velocities. Appropriate use of the SEM can determine whether or not the highest velocity data for coating "D" were influenced by particles wearing completely through the coating and eroding away some of the base metal, thereby, giving erroneous results. Other plots can be drawn from data obtained in these tests including the effect of (1) impingement angle, (2) particle size, (3) temperature, and (4) effect of abrasive size.

In analyzing erosion results, it is important to always consider gas and particle velocities. Figure 4-128 pictorially demonstrates typical velocity triangles for different particle sizes. The solid lines represent gas or wheel velocity, and the dashed lines represent typical particle velocities. Since the particle velocity lags the nozzle absolute leaving velocity C_1, the small particle has a velocity vector that is to the right of the gas velocity, W_1, relative to the rotor. Larger particles, in an absolute frame of reference, will have still lower velocities and, therefore, their relative velocity vectors are shifted further toward the right. Similarly, particles leaving the rotor blade have relative velocities less than the gas velocity W_2, and have absolute velocity vectors to the left of the absolute rotor leaving velocity C_2.

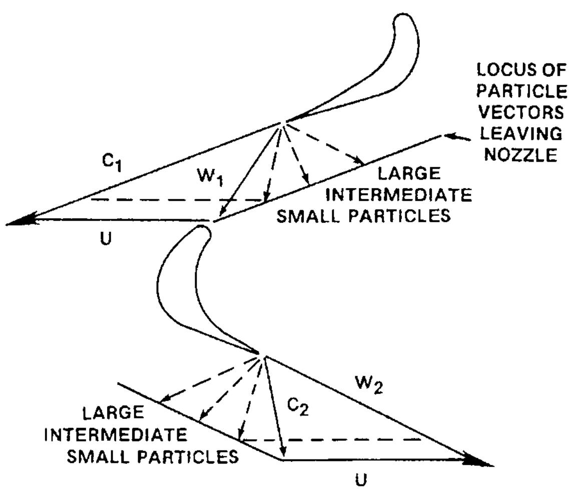

Figure 4-128. Typical velocity triangles for different size particles.

To study this behavior in an effort to design more erosion-resistant blades, the erosion prediction program was developed. Figure 4-129 shows how the blade-to-blade passage is modeled and Figure 4-130 highlights the nomenclature. The passage between adjacent blades is divided into cells in the transverse and axial directions. The computer keeps track of the particles as they are carried by the gas through the passage, and retains data on erosion caused by particles that hit the blade surfaces. Since this is a three-dimensional program, the erosion damage to the blade at sections from the hub-to-shroud is also calculated.

The three research programs just described provide interesting information, but the maximum benefit can only be obtained if the results can be integrated. Figure 4-131 demonstrates how the three programs are integrated. Analytical equations are used in the particle flow computer program to determine the trajectory, or path, of particles in a turbine. Empirical data and laboratory tests provide erosion data

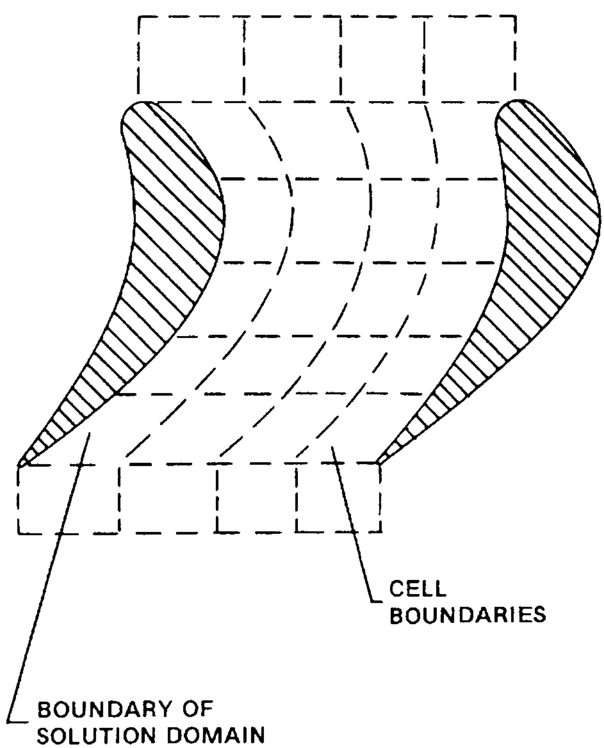

Figure 4-129. Blade-to-blade cell boundary conditions.

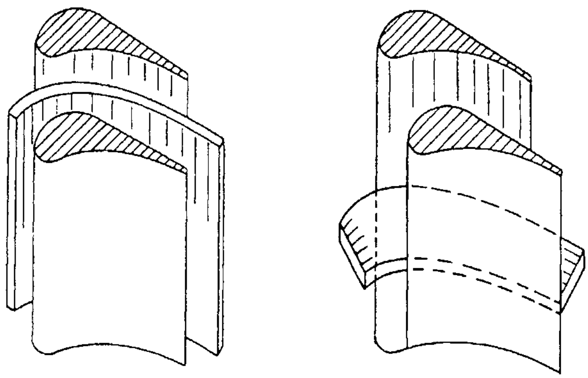

Figure 4-130. Prediction program nomenclature.

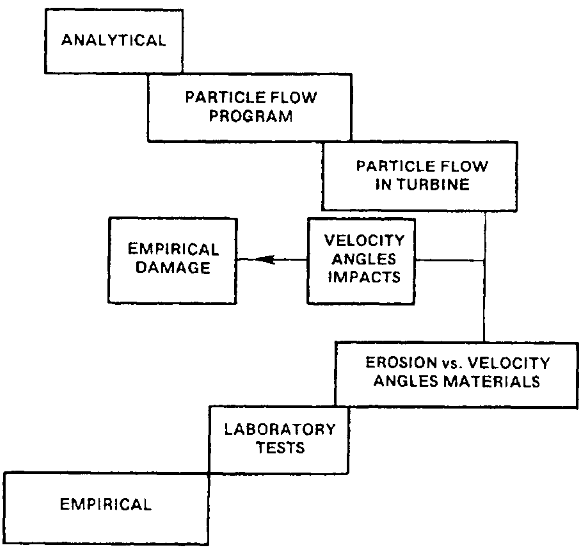

Figure 4-131. Integration of different erosion research programs.

versus velocity and angle of impingement for various particles and material combinations. The turbine particle flow program, which calculates the particle velocities, angles and impacts, uses the test information to calculate the predicted erosion damage. The qualitative results from this program have been verified by comparison with actual field results.

Figures 4-132 through 4-134 demonstrate the erosion damage results from the solid particle erosion program for the pressure surface of a rotating blade. Figure 4-132 is a plot of erosion at the base section of a rotor blade normalized to the trailing edge erosion versus the fraction of the path length. From this plot, the erosion is most severe at the leading edge, which is at the left side of the figure, and at the trailing edge, which is at the right side of the figure, with very minor damage between these extremes. Notice that the larger particles do very little damage. However, the smaller particles are responsible for about one-half the erosion, particularly at the trailing edge.

Figure 4-133 is a plot similar to the previous figure for the mean section, which is halfway up the blade height, however, there are some interesting differences. Although the greatest amount of erosion is still at the leading and trailing edges, there is much less erosion than at the base section. At least half of the trailing edge erosion is caused by the largest particles in the gas stream. The erosion at the tip section, Figure 4-134, is similar to the mean section erosion, except the levels are lower.

Figure 4-135 shows a composite of the erosion for five sections beginning with the base section and ending with the tip section. A rotor

(text continued on page 258)

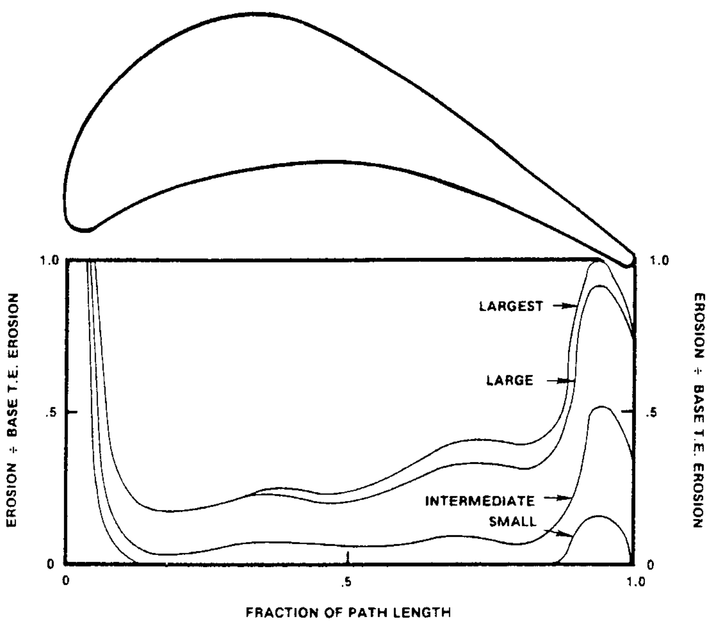

Figure 4-132. Erosion at rotor base section.

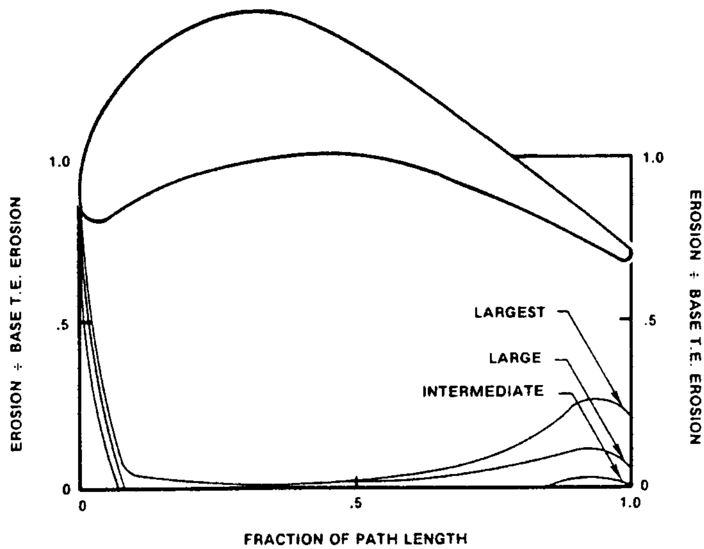

Figure 4-133. Erosion at rotor mean section.

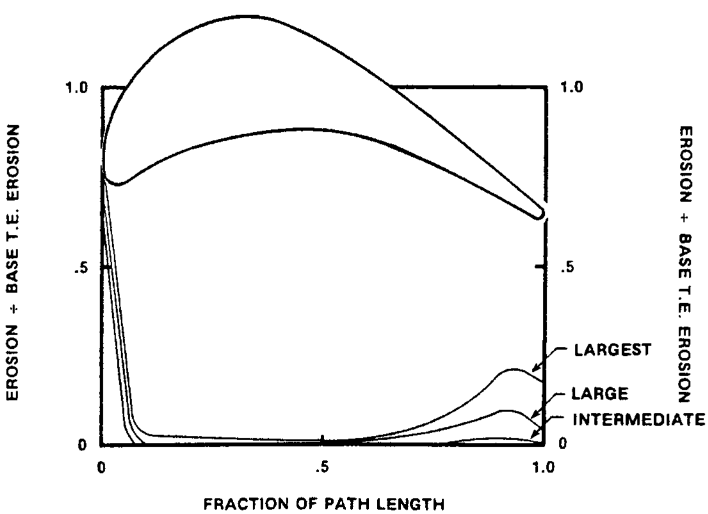

Figure 4-134. Erosion at rotor tip section.

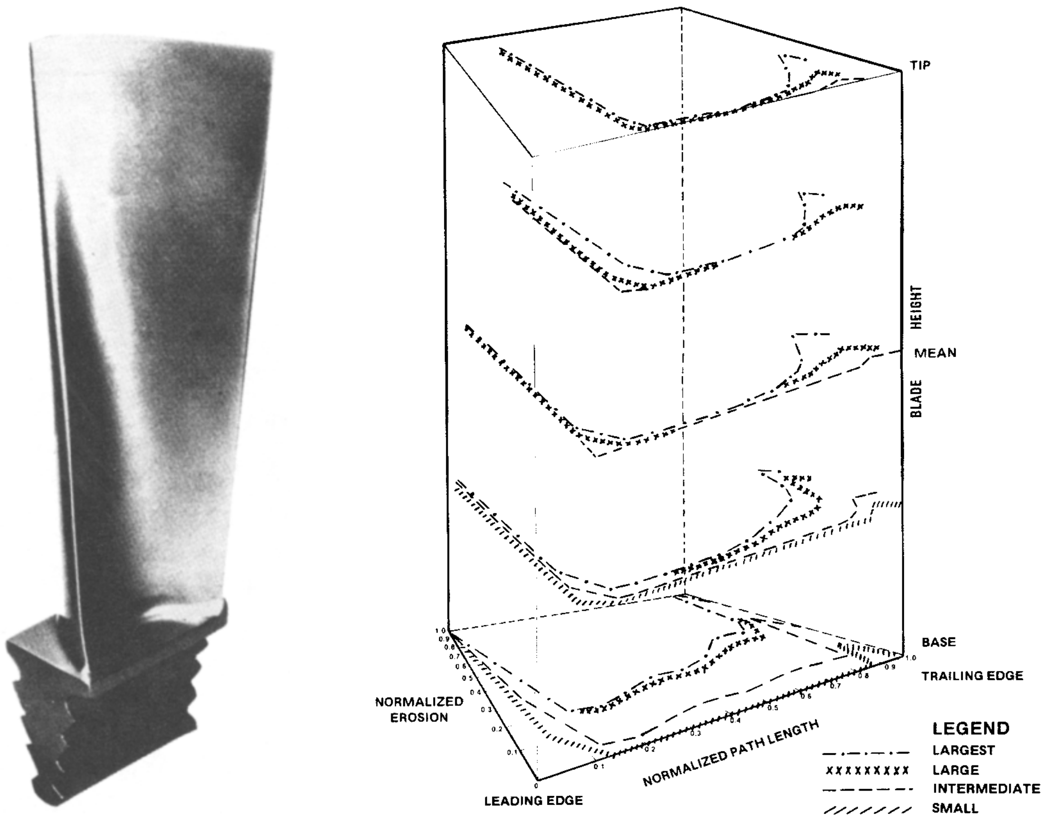

Figure 4-135. Composite of rotor blade erosion.

(text continued from page 255)

blade is shown on the left portion of the figure for comparison. The previous figures show that more erosion occurs near the base section than near the tip section of these tapered and twisted rotor blades for the distribution of particle sizes considered. It is interesting to note that constant section rotor blades would show a similar trend. The erosion picture, however, would change dramatically if the weight percent of particles larger than 10 μ were significantly increased.

Figure 4-136 shows the cumulative percent of erosion versus the fraction of path length at the mean section for several particle size ranges. At the leading edge, most of the erosion damage is caused by particles of intermediate size. Between 20% and 80% of the path length, the larger particles cause essentially all of the damage. Near the trailing edge, the largest particles in the gas stream cause more than 50% of the damage.

Figure 4-137 shows the leading and trailing edge of erosion versus fraction of the blade height. Once again, it can be seen that erosion decreases from the hub to the tip section. This plot also indicates that blade life is likely to be dictated by leading edge erosion. In actual practice, however, the leading edge of the blade is quite thick compared to the trailing edge. Therefore, when blade erosion is analyzed, more attention is directed to the trailing edge.

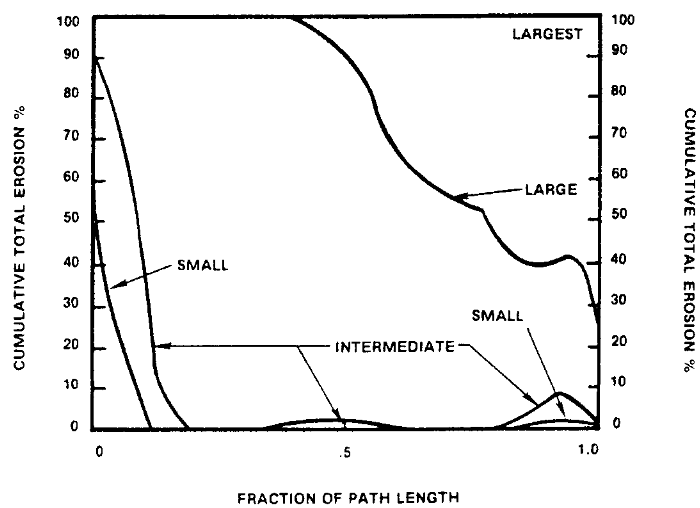

Figure 4-136. Cumulative percent erosion at mean section.

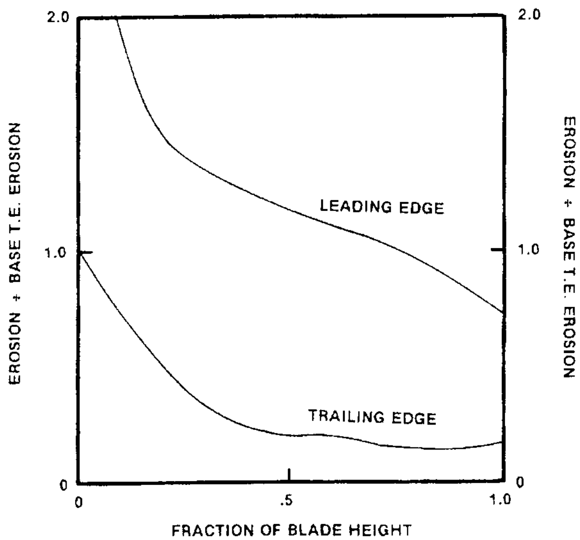

Figure 4-137. Leading and trailing edge erosion.

Additionally, the initial contact or suction surface of the blade is of concern. The Elliott program indicates that erosion of the suction surface is almost nonexistent; therefore, that erosion can be neglected in this instance. This conclusion is substantiated by actual field experience.

Figure 4-138 is a plot of the number of impacts per unit area and time versus the fraction of path length for the mean section of intermediate-size particles. It can be seen that some of the particles impact the blade surface at least once, and that first impacts occur over the entire surface. The density of second impacts is significant over only a third of the surface, and is prominent only near the trailing edge. The density of third impacts is relatively insignificant compared to the first impact density.

Elliott's erosion prediction program has also been used to analyze all the blade rows of a two-stage expander. This study confirmed that blade life of a two-stage expander is substantially greater than blade life of a single-stage expander.

As the above data demonstrates, an accurate erosion prediction program is vital to understanding blade erosion and how changes in blade design can affect the significance of erosion. Proprietary computer programs have certainly led to improved erosion resistance of many power recovery turbines. These recent blade design changes lead to

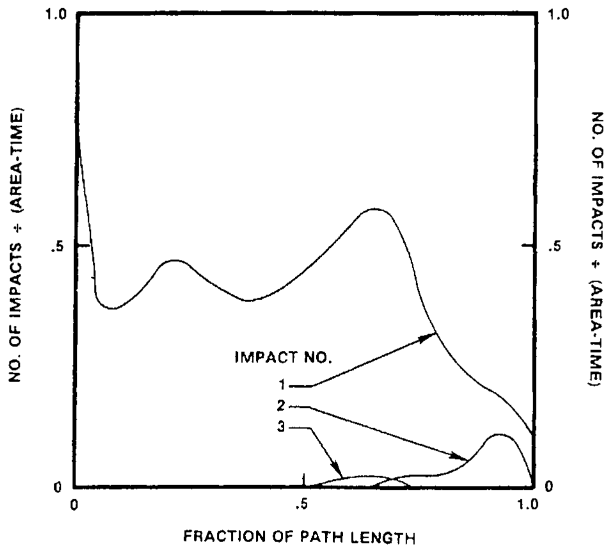

Figure 4-138. Impact density at mean section.

longer blade life, enhanced expander reliability, maintenance cost avoidance, and plant profitability.

POWER RECOVERY AND THE EDDY CURRENT BRAKE

As mentioned previously, increasing energy costs provide a powerful incentive to seriously consider the power recovery concept. Fluid catalytic cracker (FCC) power recovery is a means of recovering energy from the waste heat developed in the regeneration of the catalyst used for hydrocarbon cracking. The FCC power recovery process was shown earlier in Figure 4-53. This figure also showed the power recovery string, which consists of a hot gas expander, motor, compressor, and steam turbine in a tandem string arrangement. Figure 4-139 highlights the same concept in a somewhat different manner.

Some refineries that had not previously considered power recovery, have suddenly re-evaluated the economics with respect to their operations. Although they do not desire to replace their present motor or steam turbine driven compressors, they do want power recovery for electric power generation. This would permit commercial or co-gen power to be produced, or might simply reduce the load on the compressor drive motor.

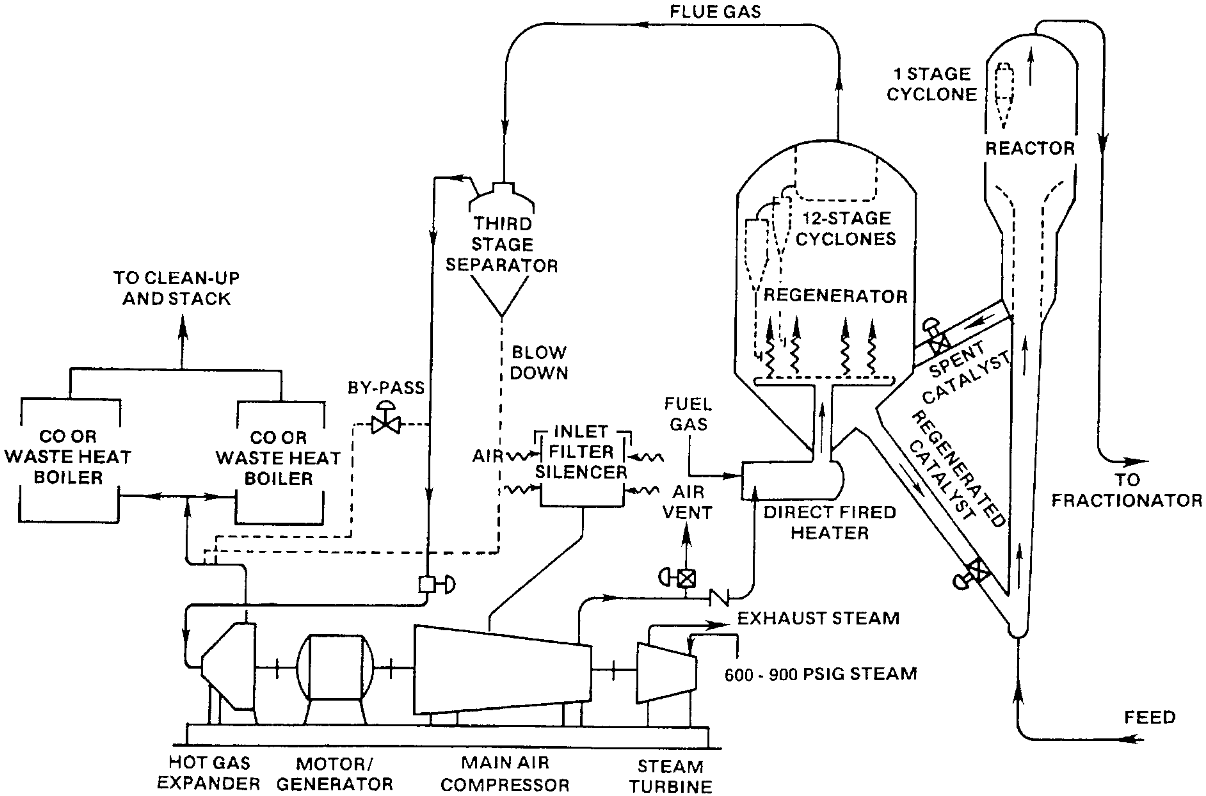

Figure 4-139. Typical FCC unit.

It is important to recognize that with an instantaneous shedding of the load in a power recovery string, acceleration is imminent. This condition is caused by the large volume of trapped gas in the piping upstream of the expander. The gas contains a significant amount of available energy, which must be dissipated by the expander or a bypass valve arrangement. Unfortunately, the specific volume of this gas demands large control valves and these tend to have slow reaction times. Therefore, much of the trapped gas will still pass through the expander and will, thus, provide undesirable driving torque. In the conventional FCC string shown in Figure 4-140, the compressor acts as a constant source of load. If the compressor were removed from the string, an alternative load source would be required. This load source would have to accommodate the following modes of operation:

1. Prevent runaway of the string in the case of a generator load loss. The large amount of available energy upstream of the expander must be dissipated.
2. Control acceleration of the string during an afterburn condition. The available energy of the string is increased as a result of higher inlet temperatures.
3. Have a means of bringing the unit up to the design speed. In the case of a synchronous generator, this speed control must be precise for synchronization.

Until recently, the only device capable of performing all three functions was the familiar eddy current brake shown in Figure 4-141. Eddy current brakes have been around for a long time and have been used for such diverse applications as controlling acceleration and deceleration of reversible rolling mills, speed governing of steam turbines, engine control in guided missiles, controlling tension on large

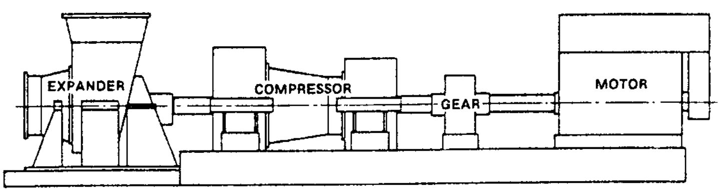

Figure 4-140. Conventional FCC machinery string.

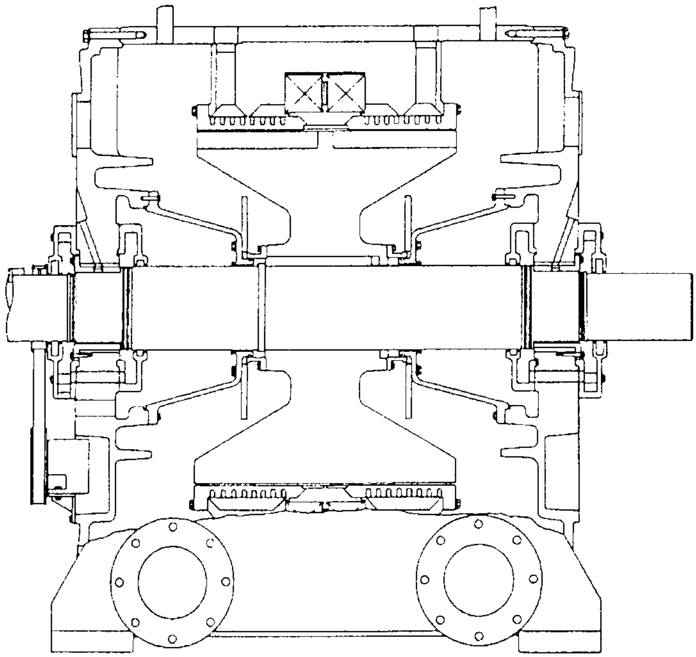

Figure 4-141. Eddy current brake.

paper mill rollers, and flywheel brakes. The original eddy current effect was discovered by French physicist Foucault in the mid-1800s. The Siemens-Schuckert Review of 1927 describes eddy current brakes for controlling rotating shafts. Wisconsin-based Eaton Industries manufactures eddy current brakes in sizes ranging up to 3,000 kW. Eddy current brakes are, therefore, "state-of-the-art."

The eddy current brake, in its simplest form, consists of a steel drum rotating an applied electromagnetic field. As the drum cuts the magnetic flux lines, eddy currents are generated in the disk and a resisting torque proportional to the magnetic field is generated. The coils are energized by a separate DC source such as a bank of batteries, which are under constant charge in a standby condition. Figure 4-142 shows an FCC string using the eddy current brake.

Having earlier described the three functions accommodated by eddy current brakes, the following examines how the brake performs in each circumstance.

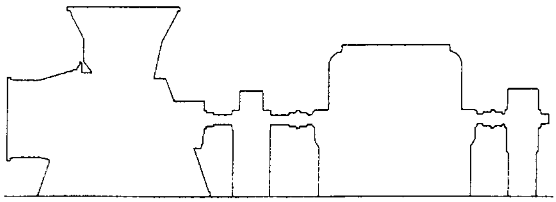

Figure 4-142. FCC string using an eddy current brake.

1. *Electrical Load Dump.* If an electrical load dump occurs during operation of the string, the switch gear signals the brake to energize to prevent string acceleration. Resisting torque from the brake is applied to the string within milliseconds. The brake controls are supplying approximately 900 V from the inverter/capacitor bank.

   Figure 4-143 represents a computer-generated plot that demonstrates the effectiveness of eddy current brakes in preventing overspeed of the string. The lower curve assumes the butterfly valve characteristic is linear from 60° open to the closed position. The rate of closure is 3.25 sec. (Butterfly valves are normally used to throttle the expander inlet gas.)

   The top curve of overspeed versus time demonstrates that the string will accelerate to 22% overspeed due to expansion of the gas trapped between the valve and expander nozzle ring. However, if an eddy current brake were part of the string, the acceleration of the string would be reduced to 11% overspeed. This would provide an important margin of safety.
2. *Afterburn Control.* Afterburn is the term for carbon monoxide burning downstream of the regenerator; this causes an increase in temperature upstream of the expander. Temperature sensors in the gas stream cause the brake to energize. This provides sufficient resisting torque to prevent acceleration until the afterburn is brought under control by water or steam injection.
3. *Synchronization Control.* During startup, partial load is applied to the eddy current brake. The expander is then throttled to a speed below synchronous speed, and the brake voltage controller varied to lower the voltage of the coil, causing a small speed

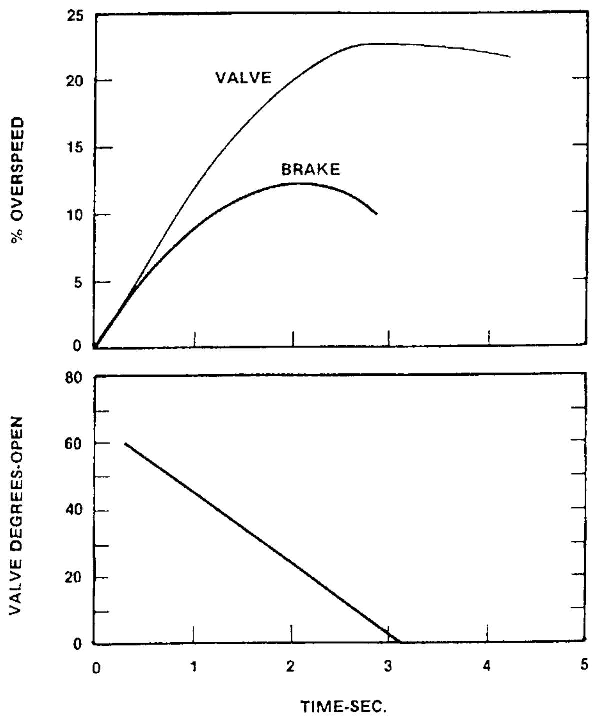

Figure 4-143. Computer-generated plot showing effectiveness of eddy current brake.

increase. This control has infinite variations. It permits the synchronous generator to be synchronized to the line frequency. In the case of an induction generator, it permits slow, smooth acceleration to design speed.

Figure 4-144 shows a family of characteristic torque versus speed curves for a typical eddy current brake. The dashed line indicates the partial load applied during startup. At about 75% of full speed, the voltage is slowly reduced from 50 V to approximately zero, thereby permitting the string to accelerate to synchronous speed. In some refineries, the FCC process is supplied with combustion air from a motor-driven compressor. These are generally older refineries that were designed and constructed before the advent of FCC power recovery. As demonstrated in Figure 4-145, the eddy current brake concept makes power recovery available to these refineries in the form of an

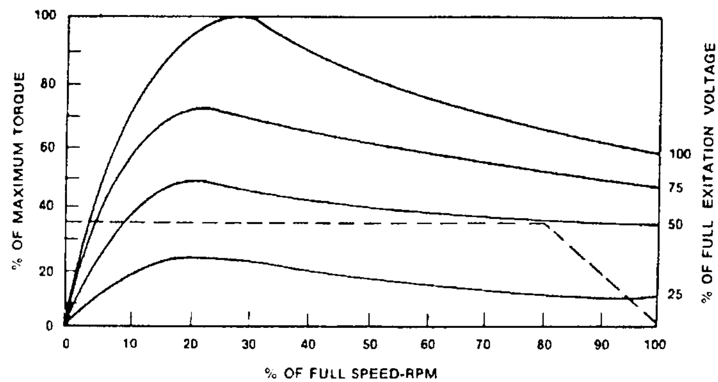

Figure 4-144. Typical torque versus speed curves for eddy current brakes.

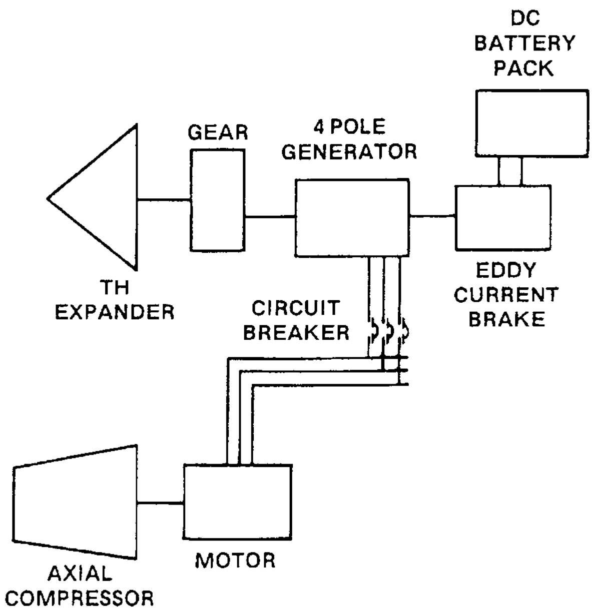

Figure 4-145. Power recovery string with eddy current brake.

expander-driven generator. This mode of on-site power generation allows removal of the compressor motor from the commercial power source. Locating the expander-generator train away from the compressor string may free up the compressor platform for equipment upgrades or capacity expansions that take up space.

> Where turbine-driven FCC compressor strings are used, the expander-driven generator can export co-gen power for sale to a commercial electrical network. This arrangement is shown in Figure 4-146.

Today's eddy current brake system is far superior to the mechanical switch-operated units of the past. Modern controls take advantage of all of the sophisticated logic found in microprocessor technology. This control system is functionally described in Figure 4-147. Each "black box" represents a separate control function with a master control called the "eddy current brake controller."

Leading turboexpander manufacturers have custom-designed the system for controlling eddy current brake strings to proven logic specifications. Elliott's brake control system has been designed for fail-safe operation, which results in seven different modes of operation: normal, ready mode, emergency stop condition, deceleration, generator load limit, maximum load limit, and generator synchronization.

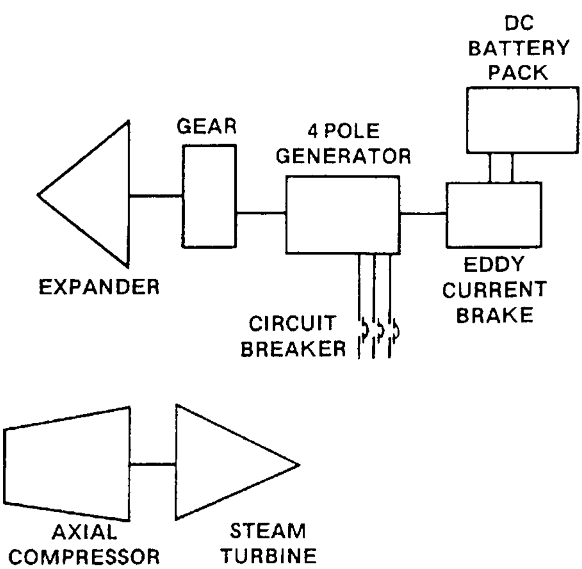

Figure 4-146. Expander-driven generator can export power. Note the eddy current brake.

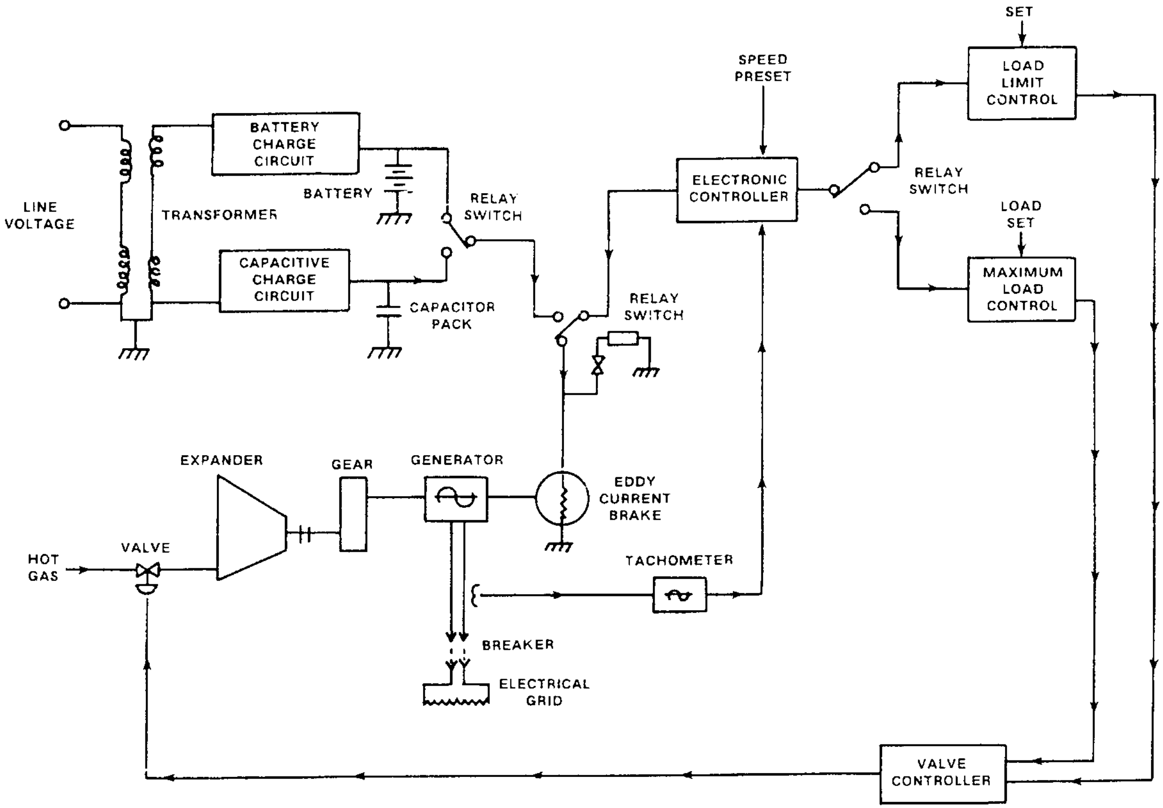

Figure 4-147. Elliott eddy current brake control schematic.

MODES OF OPERATION

While each mode is a separate function, the order of mode sequence depends on specific conditions.

During the *normal mode* (normal running operation), the brake is rotating at the speed of the generator. However, it is completely de-energized and, therefore, presents no load to the expander.

In the *e-stop/deceleration ready mode,* the high-voltage capacitor bank is under continuous charge from the rectified line voltage through a step-down transformer. A relay maintains the capacitor bank fully charged at all times. The controls are now in the *e-stop ready mode.* An alternate circuit, called the standby battery-charge circuit, is connected to line voltage through a step-down transformer. This charge circuit maintains the battery fully charged at all times. When the battery pack is fully charged, the charging current reduces to zero. This circuit is then in the ready position for applying sufficient voltage to decelerate the brake to a stop. A relay in the branch circuit, which supplies DC power to all the controls, is normally held closed. In the event of a power failure, this relay opens to apply excitation voltage from the battery pack to the brake.

E-stop mode operation is activated when an emergency stop or fault condition arises. Caused by an opening of the generator circuit breaker, the customer's contact will open causing the previously described capacitive discharge system to open. Immediately, full voltage from the capacitor bank is applied to the brake coil. Additionally, an e-stop water valve is de-energized permitting full water flow through the brake. After a short period, the e-stop relay switches to the normal deceleration mode, thereby, decelerating the string to a stop.

The purpose of the *deceleration mode* is to decelerate the unloaded system inertia to near zero rpm in a specified time period. As the e-stop relay switches to the deceleration mode, the brake coil is excited from the battery source at a lower, constant value voltage, which will produce sufficient torque to achieve the rated brake continuous thermal load. The system will then decelerate under a constant torque load.

The *generator load limit mode* is important in periods of normal operation when the expander exceeds the continuous rating of the generator. This occurs during a regenerator afterburn situation. During afterburn the available energy in the gas stream increases as a result of the higher inlet temperature, thereby increasing the power generation capability of the expander. When the generator output power (kilowatts) exceeds a preset limit, an electronic controller becomes energized. This controller regulates the brake to maintain the generator at its rated output by absorbing the excess expander torque, permitting the electrical grid connection to remain intact while the process is being brought under control. If the process cannot be brought under control within a preset time limit, a trip signal is initiated. This signal causes the expander valve to close. As the generator output decreases to zero, the main circuit breaker opens and the relay circuit initiates the deceleration mode. This circuit energizes the brake and decelerates the system to a stop by applying a constant torque. The generator load limit control can only be initiated when the electronics package is in the ready condition, earlier described as normal mode. If an energizing fault should occur during the generator load limit mode, the e-stop mode will override the load limit mode. The e-stop mode will, thus, initiate the emergency stop previously described.

The function of the *maximum load limit control mode* of operation is to limit the load of the string to an initially preset value. This value is indicative of the combined overload capability of the generator and brake. If the expander power is greater than this maximum capability, a contact closure immediately sends a signal to shut off gas to the expander. Once again, as the generator output reduces to zero, a protective relay will activate, thereby opening the main circuit breaker. Opening of this breaker initiates the deceleration mode. Any emergency fault during the maximum overload condition would switch the system to the e-stop mode followed by the deceleration mode.

Generator synchronization mode describes the method of speed control and generator synchronization. During startup of the string, the electronic controller is switched into the system to monitor the speed of the hot gas expander string. The monitored speed is then compared to a preset speed or synchronous speed. If a synchronous generator is used, suitable synchronizing equipment is used to slowly vary the signal to the electronic controller. This signals the controller to reduce brake torque until synchronous speed is attained. A synchronous generator could then be "brought into synchronization" with the line frequency of the grid. If an induction generator is used, synchronization equipment is not required. The generator is brought to synchronous speed by manually reducing the input voltage with a potentiometer.

Synchronization can only be accomplished with the emergency stop circuitry in the normal mode, previously described. If there is an emergency fault during the synchronization process, the e-stop contact will open and override the synchronization mode.

The eddy current brake controls for the power recovery string are designed for fail-safe operation of the eddy current brake. These controls provide all of the logic required to make the eddy current brake recovery string a viable contender for recovering power from previously wasted energy.

BIBLIOGRAPHY AND RECOMMENDED READING

1. Campbell, R. G., "Expanding the Mammoth Geothermal Project," Geothermal Resources Council Transactions, Vol. 15, October 1991.
2. Swearingen, J. S., "Power From Hot Geothermal Brines," *Chemical Engineering Progress,* July 1977.
3. Dakin, R., "Radial Inflow Turbines for Geothermal Application," Geothermal Resources Council, February 1986.
4. Kitz, K., "Salton Sea Unit 2 Innovations and Successes," Geothermal Resources Council Transactions, Vol. 15, October 1991.
5. Holm, J., "The Application of Turboexpanders for Enery Conservation, *IMechE,* 1981.
6. Agahi, R. and Ershaghi, B., "Expansion Turbine in Energy Recovery Applications, XVIIIth International Congress of Refrigeration, August 1991.
7. Krueding, A. P., "Power Recovery Techniques as Applied to Fluid Catalytic Cracking Unit Regenerator Flue Gas," U.O.P. Paper for presentation at AICHE Meeting, March 16–20, 1975.
8. Scheiman, A. D., "Analysis Shows FCC Power Recovery Payoff," *Oil and Gas Journal,* October 2, 1978.
9. Dziewulski, T. A. and Bews, J. H., "Recover Power from FCC Units," *Hydrocarbon Processing,* December 1978.
10. Lucenbach, E. C., "How to Update a Catalytic Cracking Unit," *Chemical Engineering Progress,* February 1979.
11. Scheiman, A. D., "Basics Key to Selection of FCC Make-up Driver," *Oil and Gas Journal,* October 16, 1978.
12. Pocock, A., "Economies of Power Recovery from Flue Gases of an Oil Refinery Catalytic Cracking Unit," Paper from Thermofluids Conference, Dec. 1–3, 1976, Hobart, Australia.

13. Ulke, A. and Rouleau, W. T., "The Effects of Secondary Flows on Turbine Blade Erosion," ASME Paper No. 76-GT.74.
14. "Proceedings of Hot Gas Expander Conference," Elliott Company, Jeannette, Pennsylvania, 1992.
15. Sales literature provided by Elliott Company, Jeannette, Pennsylvania, 2000.
16. Sales bulletins provided by Sulzer-Roteq, Winterthur, Switzerland, 1999.
17. Sales literature provided by Demag Delaval, Duisburg, Germany, 2000.
18. Sales literature provided by Dresser-Rand Company, Olean, New York, 2000.

CHAPTER FIVE

Specifying and Purchasing Turboexpanders

This chapter highlights and summarizes considerations dealing with expander subsystems, materials, manufacture, installation, component design, equipment maintenance and repair that might assist users in developing or evaluating turboexpander specifications.

CRYOGENIC EXPANDERS

A typical expander-compressor consists of three basic sections:

1. The expander section with inlet and outlet flanges.
2. The bearing housing or center section.
3. The compressor section with inlet and outlet flanges.

Standard turboexpander-compressor sets designed and manufactured by competent manufactureres embody many of the reliability improvement and maintenance cost reduction features inherent in API (American Petroleum Institute) standards for other turbomachines. To achieve close compliance, however, the owner/purchasers must know their specific needs or requirements. Nevertheless, it may not be practical, feasible, or economically justified to achieve full compliance with API specifications, which were generally devised without giving thought to the peculiarities of turboexpanders and their sometimes differing operating environments.

DESIGN CONSIDERATIONS

Off-Design Performance

Off-design performance of an expander-compressor set can be derived from the curves typically provided by the equipment manufacturer. Actual performance curves for a machine will generally be provided upon completion of performance testing at the manufacturer's facility.

Variable Inlet Guide Vanes

On quality machines, the expander variable inlet guide vanes (or nozzles) are designed to provide zero blow-by, positive actuation, and high efficiency over a broad operating range. This is often accomplished by using proprietary or patented mechanisms incorporating a pressure actuated sealing ring. This design eliminates side leakage and prevents nozzle galling. The mechanism should be designed to withstand full expander inlet pressure and can often be varied from approximately 0%–130% of the design flow through the machine.

Rotor Design Issues

Expander-compressor shafts are preferably designed to operate below the first lateral critical speed and torsional resonance. A flame-plated band of aluminum alloy or similarly suitable material is generally applied to the shaft in the area sensed by the vibration probes to preclude erroneous electrical runout readings. This technique has been used on hundreds of expanders, steam turbines, and other turbomachines with complete success. Unless integral with the shaft, expander wheels (disks) are often attached to the shaft on a special tapered profile, with dowel-type keys and keyways. The latter design attempts to avoid the stress concentrations occasionally associated with splines and conventional keyways. It also reduces the cost of manufacture. When used, wheels are sometimes secured to the tapered ends of the shaft by a common center stretch rod which is pre-stressed during assembly. This results in a constant preload on each wheel to ensure proper contact between wheels and shaft at the anticipated extremes of temperature and speed.

Sealing Systems

Manufacturers offering labyrinth-type shaft seals often opt to use a design incorporating a replaceable stainless-steel, rotating labyrinth running adjacent to a fiber-reinforced phenolic seal cartridge. In the event of seal contact, this design allows the phenolic to wear in a predetermined manner; it is thought to prevent damage to the rotating part. At least one manufacturer designs symmetrical shafts, allowing for interchangeability of seals between the expander and compressor side.

Bearing Configurations

Some manufacturers custom-design and manufacture their expander bearings. These include both pressure-dam and tilting pad-type journal bearings with fully integrated thrust bearings. The typical 360° journal bearings have an L/D ratio of approximately 0.6. Manufactured from brass and generally lined with a suitable babbitt composition, these bearings have an extensive and successful operating history for continuous use in diverse applications. Flexure pivot bearings and fully magnetic bearings are also in strong contention and may be an economically attractive option.

Turboexpander thrust bearings can be found at one or both ends of the shaft. On many machines, they are the fixed tapered-land type and are integral with the journal bearings. This proven design functions well under a wide range of radial and axial thrust loads. Again, flexure pad and magnetic thrust bearings are feasible and merit consideration.

Standard expander journal bearing configurations typically incorporate an imbedded resistance temperature detector (RTD) to measure bearing temperature and warn of possible bearing damage. An RTD can also be provided in the compressor bearing at the customer's request. The owner/purchaser should carefully examine the manufacturer's proposal data sheets for the bearing configuration and quantity of temperature probes supplied.

Expander Case Seals

It should be remembered that cryogenic expanders operate at extremely low temperatures and spring-loaded PTFE ("Teflon") cryogenic lip seals are, therefore, generally used for the expander casing. Properly designed, this highly reliable seal is also pressure actuated. Therefore, effective sealing does not depend on torqueing of case bolts. Elastomeric o-rings are used for sealing the compressor casing and parts not subjected to extremely low temperatures.

Compressor Diffuser

Modern compressors incorporate a parallel wall, vaneless diffuser that yields excellent off-design performance. On these machines, the estimated surge point is at approximately 65% of the design compressor flowrate.

Allowable Flange Forces and Moments

Expander process conditions induce thermal growth and/or shrinkage in the expander and compressor housing. Therefore, the expander case is normally centerline mounted and the compressor case is allowed to move along the centerline of the machine. Modern machines have allowable flange forces and moments that generally exceed three times NEMA (National Electric Manufacturers Association) requirements.

Rotor Balancing

All rotating parts must be dynamically balanced to an appropriate tolerance on precise electronic balancing equipment to ensure smooth operation over the entire operating speed range. Balance tolerances are set by API criteria for high-speed turbomachinery.

Seal Gas Systems

A simple, yet effective seal gas system consists primarily of a 5 μ filter and a differential pressure regulator. The regulator senses the pressure behind the expander wheel and automatically adjusts the seal gas pressure to the proper value. A single inlet connection is generally provided for hook-up to the customer's seal gas supply. The seal gas must be dry, oil free, and within the temperature range.

Trip and Main Inlet Valve

An expander emergency trip valve, capable of closing in less than one-half second, must be installed close to the expander inlet flange. A 60–80 mesh screen, differential pressure monitor, and shutdown must be installed between the trip valve and the expander inlet. Additionally, it is highly recommended that a 40–60 mesh screen be installed upstream of the compressor inlet for use during the initial startup period.

Vibration Monitoring Probes

Many of the prominent turboexpander manufacturers include, as standard supply, a radial eddy current probe near the compressor bearing. Multiple radial probes located near each of the two journal bearings are preferred and certainly highly recommended in larger frame size machines.

Conventional Lube Oil Systems

A lube oil system will be required unless, of course, the turboexpander is supplied with active magnetic bearings. The conventional lube oil system consists of a reservoir, electric cartridge or steam coil heater, lube oil pumps, one and preferably two (switchable) lube oil coolers, twin filters, accumulator, temperature monitor, pressure controls, and gauges. Whenever possible, this equipment should be mounted on a common support system skid together with the turboexpander-compressor train. It will rarely be advantageous to specify otherwise.

More often than not, a manufacturer's standard lubrication system incorporates many of the features inherent in the API standards. Nevertheless, when specifically required by customer specification, the lubrication system can be designed to comply almost fully with the applicable APl standards.

The reservoir may be either pressurized or atmospheric. It must have sufficient capacity to contain all oil during drain-back or shutdown. It must be equipped with an oil level indicator, a low-level alarm switch, safety relief valve, a pump for oil makeup during operation, drain valve, heater, mist eliminator, strainers, and required valves. Expander reservoirs must be designed and constructed in accordance with applicable ASME codes. Reservoir retention time is typically between 5–18 min depending on turboexpander size and manufacturer's sizing criteria. This is an area where the owner/purchaser should ask for the manufacturer's assistance.

Lube oil pumps are typically heavy-duty centrifugal or positive displacement type with a design capacity that covers the full range of anticipated operation. They can be either direct-driven by electric motors or coupled with disk or diaphragm-type couplings. Experienced turboexpander manufacturers will supply motors and couplings that are at least 25% oversized.

Lube Oil Coolers

Usually, either water-cooled or ambient air-cooled lube oil coolers are specified. They must be sized to provide continuous cooling at the most severe ambient conditions specified. Oil flow through the lube oil cooler is typically regulated by a temperature control system consisting of a controller inserted into the lube oil piping via a thermowell. The controller modulates a three-way transfer valve, which is actuated by a pneumatic diaphragm actuator and receives its signal directly from the controller. Temperature indicators allow local monitoring of lube oil temperatures.

Lube Oil Filters

Duplex, switchable filters are considered standard. A continuous-flow switching valve and 10 μ filtration elements should be provided.

Accumulators

A bladder or diaphragm-type accumulator should be supplied to provide proper lube oil supply to the bearings during expander-compressor coast-down in the event lube oil pressure is lost. The accumulator must be fitted with a preload filling system and necessary bleed and block valves.

Piping

All piping associated with turboexpander lubrication systems should be 300-series stainless steel. Using non-stainless piping upstream of the filters does not harmonize with the life-cycle cost goals of modern industrial plants. Whenever possible, lube oil piping connections should be welded.

Lube Oil Pressure Regulating Valve

Lube oil pressure is generally controlled by a self-contained pressure-regulating valve that automatically maintains a constant lube oil pressure across the bearings. The valve is normally adjustable, but is usually preset at the factory. The valve flow capacity must be sufficient to bypass excessive flow if both main and standby pumps are operating simultaneously.

Lube Oil Reservoir Heater

Many users prefer a thermostatically controlled, low power density electric heater (not exceeding 10 watts per square inch of area) that is submerged in the reservoir oil. Steam heaters are perfectly acceptable, but should be placed under the sloped reservoir floor. The space below this floor should be filled with a heat transfer fluid and be suitably vented.

Tubing and Piping Arrangement

All instrument tubing and subsystem piping should be arranged to allow free access to expander and major auxiliary equipment for operation and maintenance.

Instrumentation Highlights

Lube oil level in the reservoir should be monitored by a sensing device to indicate low lube oil level. Local and panel-mounted pressure gauges are necessary to monitor operation of the lube oil system and must be included in the manufacturer's scope of supply. The purchaser must distinguish between control room instrumentation and instruments mounted on a stand-alone (local) panel. There is also a tendency to place monitoring instruments on auxiliary equipment and piping. While this may cost less, it often complicates the operator's surveillance tasks.

First-out annunciators are highly desirable and should provide sufficient points to accommodate the specified alarm and shutdown functions. Standard features should include "acknowledge/silence," "lamp/test," and both audible and visible devices for general alarm indication. A dry auxiliary contact from the shutdown circuit must be provided for expander inlet trip valve actuation. Additional sets of contacts are useful for other alarm requirements.

All instruments and control devices on the control panel must have identifying nameplates of durable laminated plastic or similar engraveable material. Gauge nameplates, alarm light nameplates, and shutdown light nameplates should each have different color backgrounds.

Documentation and Testing

Set Points for Alarms and Shutdowns

All regulator, relief valve, and relay settings must be documented by the vendor. The expander-compressor lube system must be test-run at design differential pressure with the reservoir vented to atmosphere.

The reservoir relief valve should remain factory-set and sealed; it should not be adjusted to a "testing only" setting.

During testing, all alarm and shutdown functions must be simulated to verify proper operation of the annunciator display. The test technician must place his initials next to the tabulated set points as verification of completion.

Mechanical Testing

An expander-compressor unit must be mechanically tested and all mechanical tests should be witnessed by the owner-purchaser or his representative. If the manufacturer does not have the capability of testing with the fully bladed contract rotor, a "dummy" wheel may replace the compressor impeller. This dummy wheel is a disk with no blades, designed to duplicate the weight, center of gravity, and moment of inertia of the actual compressor wheel.

A slow roll check must be performed to detect any mechanical or electrical runout of the shaft.

Typically, speed is increased to maximum continuous speed in approximately 25% (of maximum continuous speed) increments. The expander-compressor should be held at each speed increment for a sufficient time to record pertinent data (i.e., vibration and bearing temperatures).

The rotor speed must then be increased to trip speed to check the overspeed trip setting, then reduced to maximum continuous speed and held for a minimum of 1 hr. Extended testing time should be allocated if necessary to reach satisfactory equilibrium conditions. The lube oil must be held near design inlet temperature during the mechanical test. Data logging should be done in 15 min intervals for all measuring points.

Compressor Performance Test

The compressor should be performance tested at or near the corrected aerodynamic speed. Suction throttling should be applied through the compressor speed range from near choke (stonewall) to surge. At least five data points must be established in this range. Two rounds of thermodynamic data (back-to-back) should be recorded at each data point. The thermodynamic data will need to be reduced and plotted as polytropic head and efficiency versus inlet flow, corrected to design speed.

Overspeed Test

This test is performed to verify the structural integrity of the expander wheels and the compressor wheels. The expander wheels should be instantaneously oversped during the mechanical test while assembled on the shaft. Compressor wheels should be oversped during the mechanical test or, alternatively, in a separate spin test facility.

Post-Test Disassembly

After successful completion of all testing, each rotating assembly must be disassembled for visual inspection of the rotor, bearings, and seals. Oversped wheels should be examined by the liquid penetrant method.

USING EXPANDER-COMPRESSOR CURVES TO PREDICT OFF-DESIGN PEFORMANCE

As was mentioned in Chapter 3, cryogenic natural gas processing plants commonly use turboexpanders to produce the required refrigeration. From a turbomachinery standpoint, the process is rather unique; the process gas itself is being expanded to produce refrigeration, while the power is absorbed by a direct-connected compressor. It is customary to allow the expander-compressor operating conditions and shaft speed to vary over a wide range in response to changing plant conditions.

While it is, of course, entirely possible to predict expander-compressor off-design performance using modern computer software, there are a large number of variables to be considered and it is not always easy to obtain a rapid overview. However, screening studies will benefit from graphical methods that allow the process designer to quickly determine the expander and compressor performance over the entire range of operation.

In developing these curves, which incidentally follow the trends illustrated in Figures 5-1 through 5-4, it was assumed that the plant is either a pre-boost or post-boost design with "conventional" gas composition and process conditions. For unusual plant designs, the expander manufacturer should be contacted.

EXPANDER UPGRADE AND REDESIGN EXPERIENCE

Cryogenic turboexpanders that were built and manufactured in the 1950s and 1960s are candidates for upgrading and revamping. While

(text continued on page 284)

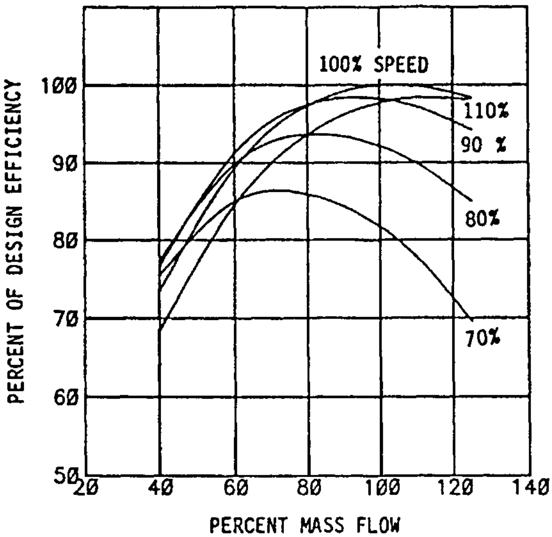

Figure 5-1. Typical expander efficiencies versus mass flow.

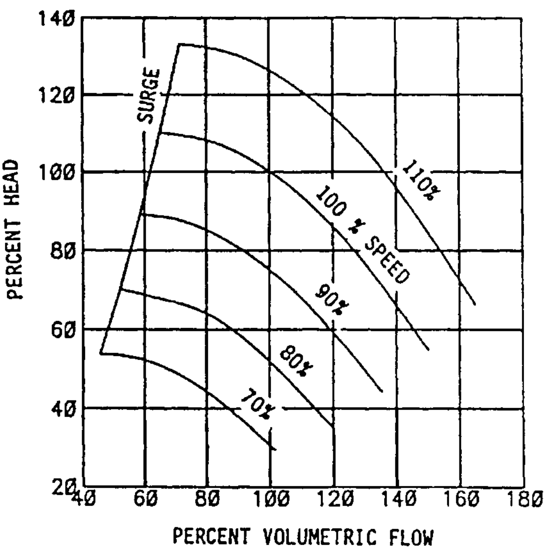

Figure 5-2. Compressor "boost" capacity is limited by the surge line.

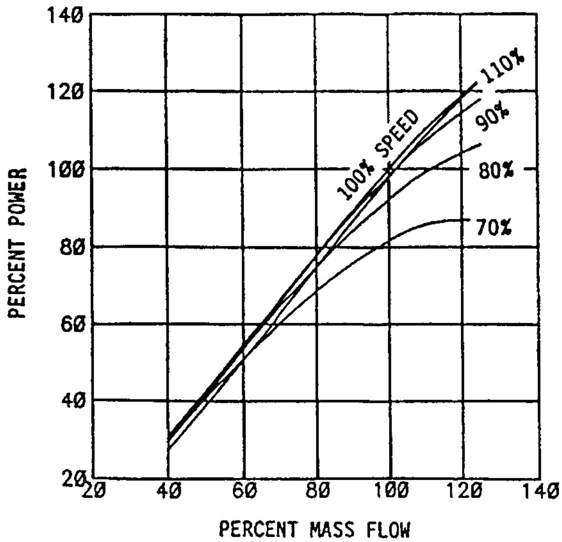

Figure 5-3. Expander power versus mass flow.

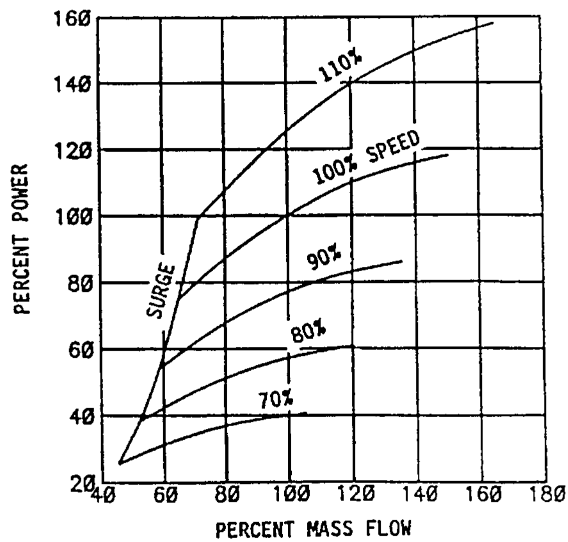

Figure 5-4. Compressor power versus mass flow.

(text continued from page 281)

many 1990s vintage machines have enjoyed flawless reliability and availability records, their older predecessors have occasionally suffered from such problems as:

- Leakage of lubricating oil into the process stream
- Loss of expander control due to abrasion of nozzle segment pins
- Loss of expander control due to nozzle segment/adjusting ring galling
- Chronic wheel failures of fabricated wheels
- Transient or chronic rotor imbalance due to cylindrical or splined wheel-to-shaft attachment

One experienced turboexpander manufacturer, Mafi-Trench Corporation (MTC), has extended its business into the repair, revamping, and upgrading of machines of various origins. A brief discussion of each problem and the MTC solution follows.

Leakage of Oil into the Process

Obviously, oil leakage may be caused by leaking mechanical seals. In turboexpander compressors, however, the most common cause is improperly designed labyrinth seals. Tapered labyrinth designs seem more prone to suffer from this defect.

In the tapered labyrinth (Figure 5-5), a fixed labyrinth seals against a tapered shaft. As the shaft moves axially, the clearance of the seal changes. This allows an excess seal gas flow. The resulting venturi effect actually drags the lubricating oil into the process stream. Also, since the tapered shaft seal makes it difficult to provide an effective oil slinger, the problem is compounded.

Seal gas systems are designed for dry, warm seal gas. However, condensation does occur occasionally. This condensation seems to accelerate erosion in the tapered area of the shaft. The most appropriate corrective action is often to replace the entire shaft.

Damage to the labyrinth requires replacement of the expander heat barrier or compressor shaft seal. A replacement design (Figure 5-6) uses a replaceable stainless-steel labyrinth mounted on the shaft. Because the seal is not tapered, axial movement of the shaft has little or no measurable effect on seal gas flowrates. Each labyrinth has an integral oil slinger incorporated into the design. Also, each rotating

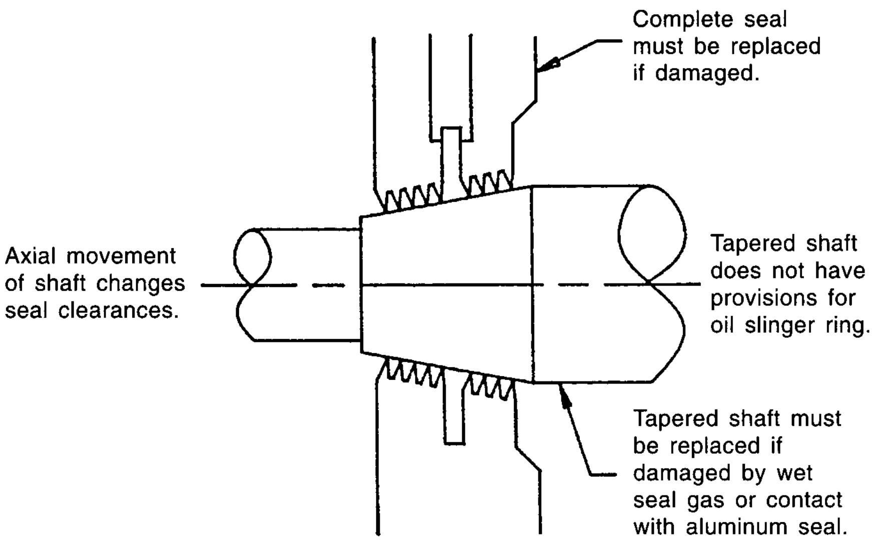

Figure 5-5. Typical tapered labyrinth assembly.

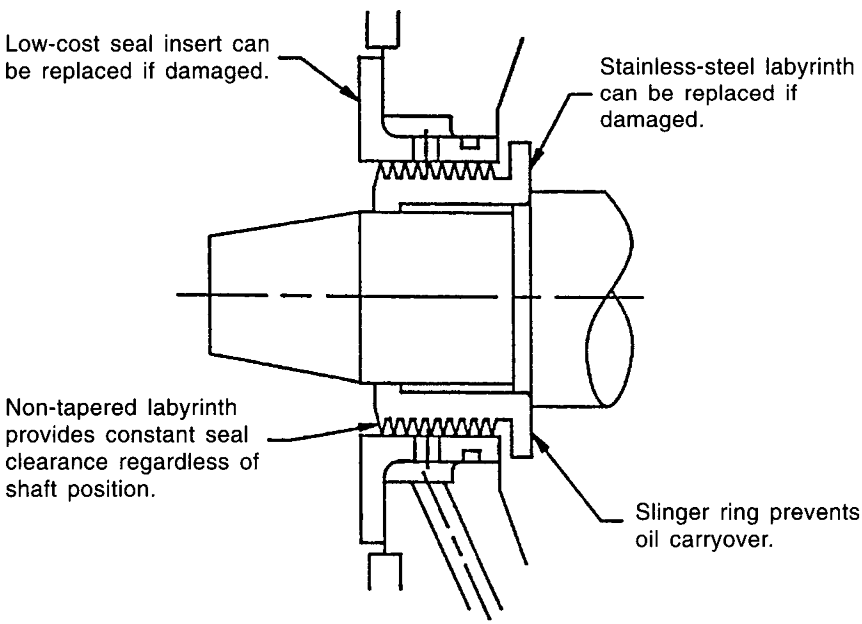

Figure 5-6. Advantageous replacement labyrinth seal. *(Source: Mafi-Trench.)*

seal mates with a replaceable micarta seal insert. This allows the entire seal assembly to be replaced without machining or replacement of the shaft, heat barrier, or compressor shaft seal.

Loss of Expander Control Due to Abrasion of Nozzle Against Pins

Expander nozzle designs often use a pin sliding in a groove to adjust the position of each nozzle segment (Figure 5-7). The groove is cut into a circular adjusting ring. As the ring is rotated, the pin is forced to slide up the side of the groove. This causes the pin, which has a very small contact area with the groove side, to rapidly wear. Due to many factors, each pin tends to wear at a different rate. The result is often a loss of efficiency due to unequal nozzle openings. Moreover, galling of the pin contributes to sticking of the nozzle assembly.

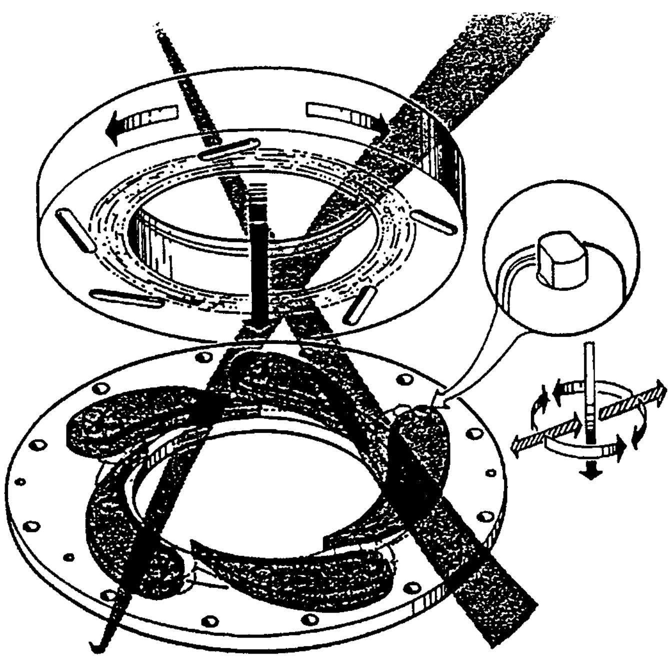

Figure 5-7. Expander nozzle adjustment via sliding pin engagement.

Loss of Expander Control Due To Nozzle Segment/Adjusting Ring Galling

The adjusting ring also serves as a pressure plate to hold the nozzle segments in place. This means there is constant fretting between the nozzle segments and adjusting ring. Eventually, the nozzle segments and adjusting ring become so galled that the actuator cannot overcome friction forces. The result is a loss of expander control. The pin and slot configuration also requires the pin to be pressed into the nozzle segment. This tends to upset metal around the pin hole and can prevent complete sealing of the nozzle.

MTC recommends a nozzle design similar to that shown in Figure 5-8, separating the pressure plate adjusting ring functions. This provides the following advantages:

- Movement around pins is rotational only
- Travel of individual nozzle segments is greatly reduced
- Pins float in the nozzle segments, allowing them to be lapped flat as a set, providing equal sealing of each segment.

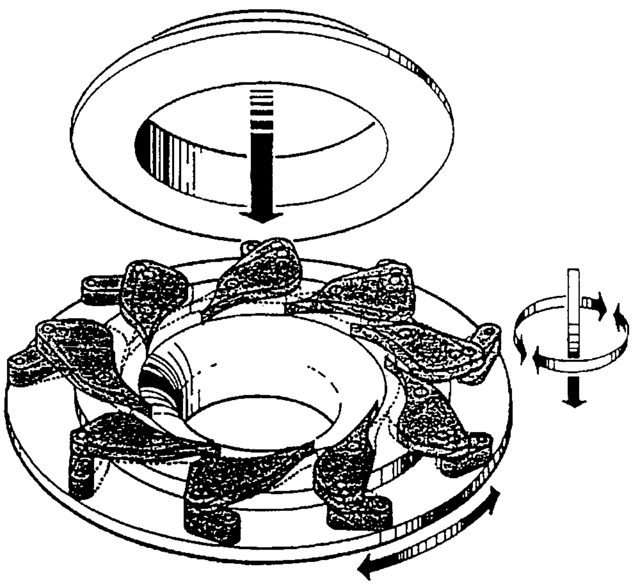

Figure 5-8. Expander nozzle adjustment geometry requiring component rotation around pins (no sliding in slots).

Malfunctions of pin and groove nozzle assemblies are probably the single major source of redesign requests.

Chronic Failures of Fabricated Wheels

Fabricating wheels from several pieces and then joining the pieces by welding or brazing is a common technique. On large open wheels, this technique is satisfactory. Unfortunately, few expander-compressors fall into this category. The small high-speed wheels in this type of machine are very difficult to assemble with acceptable quality. The passageways are often too small to allow proper welder access (Figure 5-9). Heat-affected zones tend to be in the most highly stressed areas and normal inspection methods are generally inadequate.

The result can be a wheel that fails prematurely. Often, a user will experience several wheel failures before deciding on a redesign (Figure 5-10). Yet, properly designed one-piece wheels have withstood decades of service without failures and, therefore, represent a desirable design in many cryogenic expanders.

Transient or Chronic Rotor Imbalance Due to Cylindrical or Splined Wheel-to-Shaft Attachments

During normal operation, a turboexpander-compressor rotor experiences wide swings in temperature and speed. These changes can cause the wheel bore to grow in relation to the shaft diameter. The result, on a cylindrical or splined attachment, is radial movement of the wheel on the shaft. This, in turn, could cause severe vibration, which can seriously damage the machine. Some manufacturers attempt to correct this problem by using an interference fit between the wheel and shaft. While this helps, it causes new problems. When an aluminum wheel is removed from the shaft, the soft bore tends to become galled. This is illustrated in the left portion of Figure 5-11. Upon reassembling the rotor, the interference fit is often lost. Further, because the galling is uneven, the wheel may no longer be concentric with the shaft.

Another wheel-to-shaft attachment uses a tapered fit (Figure 5-11, right portion). A center stretch rod constantly pulls each wheel onto the shaft. Should the wheel bore grow, the wheel remains centered and is drawn axially up the shaft taper. The tapered fit reduces galling risk during assembly and disassembly.

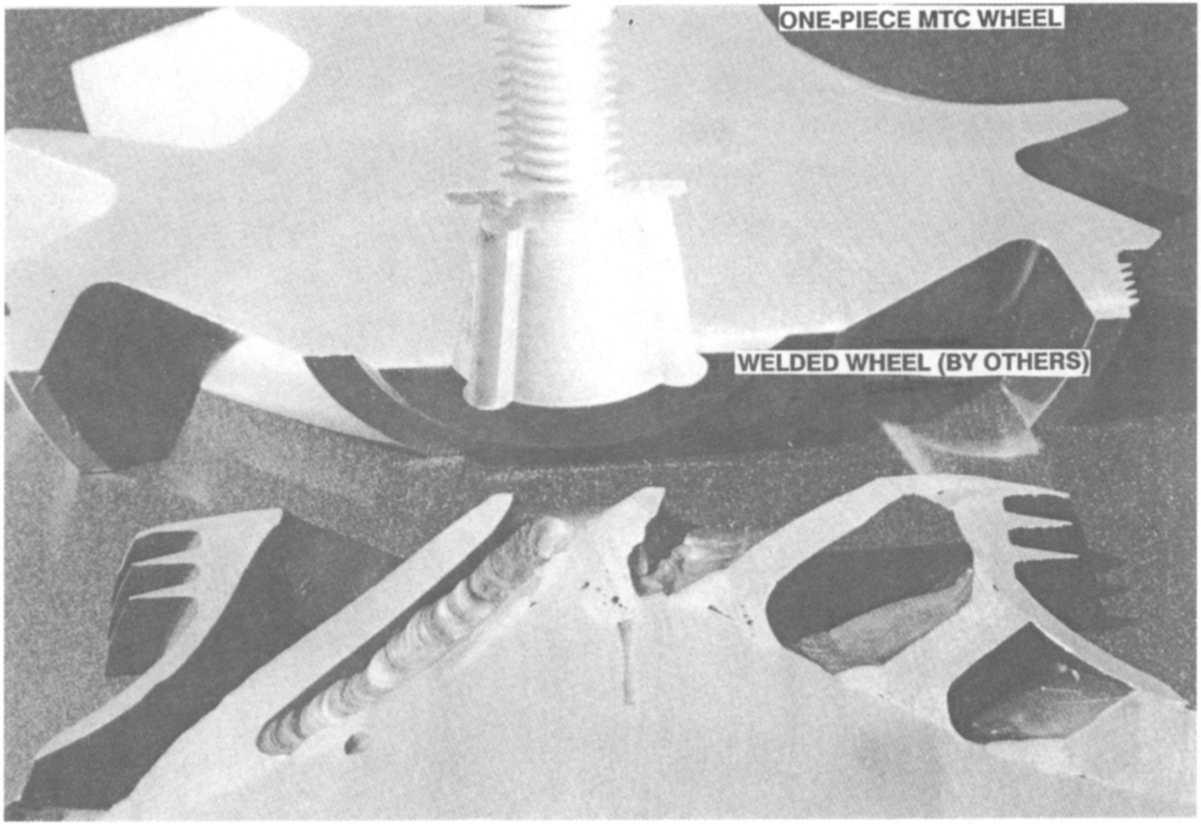

Figure 5-9. One-piece versus welded expander wheels (impellers).

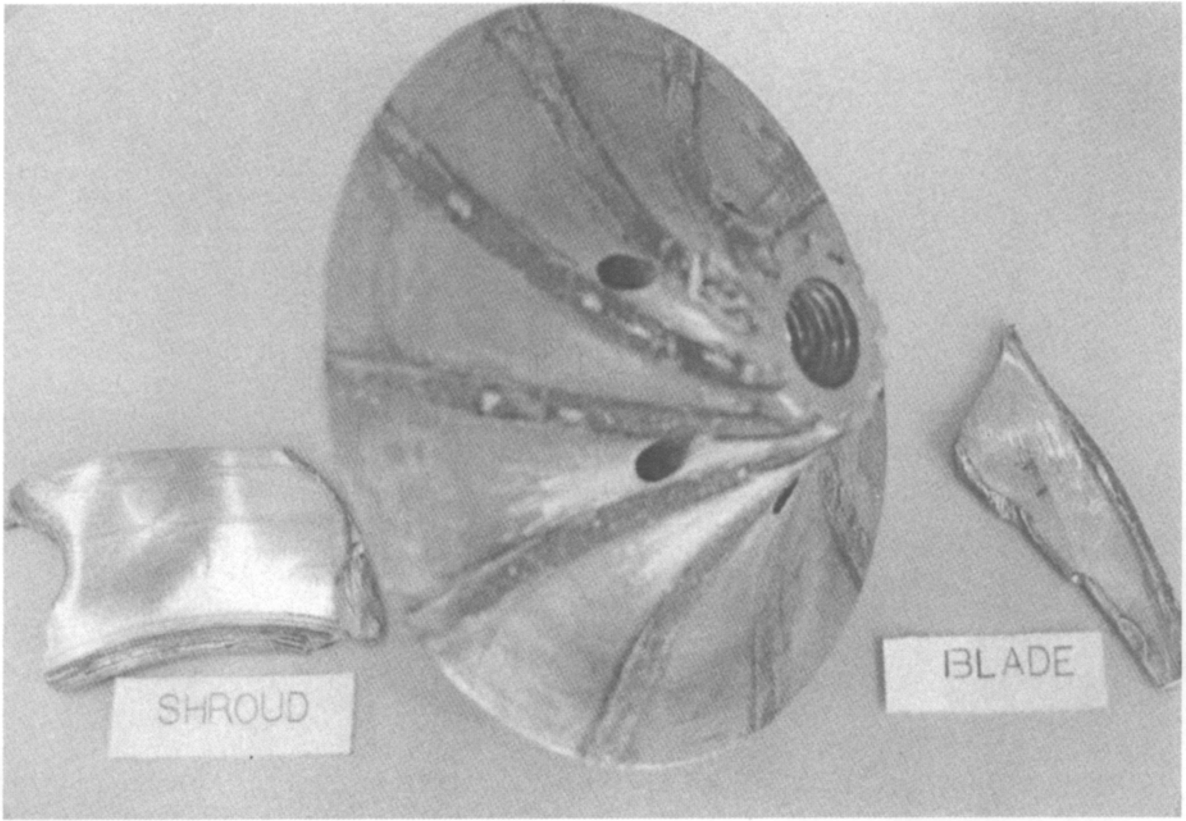

Figure 5-10. Expander wheel (impeller) failure.

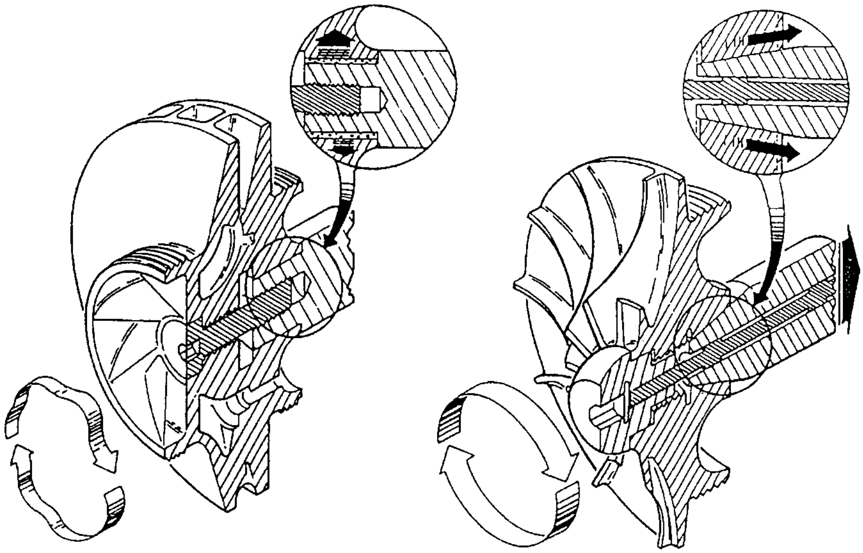

Figure 5-11. Wheel attachment designs.

TYPICAL EXPANDER-COMPRESSOR STARTUP

The following illustrates a typical startup sequence of a cryogenic expander. Don't forget to specify this document!

1. Turn on control power and check annunciator function. A number of alarms and shutdown lights should be illuminated:
   (a) Lube oil low differential pressure alarm (110 psi).
   (b) Lube oil low differential pressure shutdown (90 psi). Both lube oil differential pressure switches referenced to lube oil reservoir.
   (c) Seal gas low differential pressure alarm (30 psi).
   (d) Seal gas low differential pressure shutdown (20 psi). Both seal gas differential pressure switches referenced to expander wheel pressure.
   (e) Expander bearing low temperature shutdown on when bearing temperature below 70°F.
2. Check manual loading station at center of control panel. Select manual mode with 0–3 psi output.

3. Open seal gas block valve and verify seal gas 50 psi higher than expander wheel.
4. Open expander/compressor case drains and expander/compressor piping vents to vent any liquid and air from case and process piping. (Allow cases to purge 1–2 min, then close expander case drains.)
5. Close case drains.
6. Once case starts to pressure up (50 psi or better), switch No. 1 lube oil pump to manual.
7. Lube oil to bearings should be 150 psi higher than the reservoir pressure.
8. Once expander case pressure is above 150 psi or equal to tower pressure, activate XYZ. This will open both expander outlet (discharge) and compressor inlet valves.
9. Switch No. 2 lube oil pump to automatic.
10. Recheck control panel. All alarms and shutdowns should be clear. Allow time for seal gas temperature to reach +70°F and lube oil inlet temperature to reach 100°F. Depress shutdown reset. "Expander ready" light panel will illuminate.
11. Check expander bearing temperature in control room; a minimum temperature of 70°F is desired for startup.
12. Open manual block valve on compressor discharge.
13. Check the following:
    a. Expander outlet valve open.
    b. Compressor outlet valve open.
    c. Compressor inlet valve open.
    d. Lube oil pressure to bearings 150 psi above compressor inlet pressure.
    e. Seal gas pressure 50 psi above expander wheel pressure and temperature around 100°F.
    f. Lube oil temperature 100°F.
14. Open expander case drains and allow liquid to drain.
15. Place control ABC in "manual" with "0" on vane position gauge (expander inlet valve). Machine will speed up to about 5,000–10,000 rpm.
16. Open switch DEF. Observe GHJ opening.
17. Slowly increase ABC signal while monitoring synchronization signal and expander speed. When signals are the same, then switch to auto.

Startup Tips to Minimize Expander Problems

Approximately 97% of all turboexpander problems occur during the initial plant startup period. This critical period usually extends over several weeks, from the initial expander run until the plant pressures and temperatures are normalized and all related equipment is stabilized.

Some of the problems stem from outside factors unrelated to the turboexpander, including welding slag, dust, moisture, and so forth. Most others can be averted by systematically adhering to proper expander system checks and startup procedures.

Expander systems are normally shipped from the factory to the job site by truck. Road vibrations may loosen tube fittings and lube oil flange bolts. All screwed connections should be systematically re-tightened.

Before turning on the seal gas and lube oil pumps, initiate power to the control panel to confirm the indicator lights are functioning. At this time, there is no seal gas or lube oil pressure so the low lube oil alarm, low lube oil pressure shutdown, and seal gas alarm light should be on.

The electrical system should be checked to ensure that the Resistance Temperature Detectors (RTDs) are indicating the proper temperature. This temperature should have the same reading as the oil drain thermometer (usually a dial indicator).

The vibration indicator as well as the tachometer should read "zero." If these instruments are reading a higher number, a discontinuity or short circuit may exist in the electrical system. Sometimes, a ground loop on the electronic system can create a high level reading on the tachometer, RTD, or vibration monitor.

The stroke on the nozzle actuator must be checked for proper signal ranges. This is done by giving a 3–9 or 3–15 psi signal to the actuator rod motion.

If all systems are "go," turn on the seal gas. Open the expander and compressor case drains to purge systems. Close drains and check seal gas pressure. Seal gas temperature must be 70–80°F downstream of the regulator.

If the system is designed with a single seal gas pressure switch, the alarm and shutdown light on the seal gas will turn off. If the system is designed with a differential pressure switch, the differential will read almost "zero" until the expander case is pressurized. Therefore, an alarm and shutdown light will be on.

The lube oil pumps are now ready to be turned on. The pump and filter bypass valves should be open to avoid pressure pulses in the filter cartridges. Strong pressure pulses may cause filter cartridges to collapse. Typical filter elements will withstand 35–100 psi differential. If the pumps are turned on with each bypass closed, an instantaneous pressure of approximately 150 psi will hit the filters. This is due to the setting of the relief valves. For this reason, it is important to have on hand several extra seal gas and lube oil cartridges.

After the lube oil pumps have been running for approximaely 15 min, close the pump and filter bypass and slowly pressurize the system to establish normal lube oil pressure. The alarm and shutdown lights should turn off by pushing the reset button on the annunciator panel.

An important component in the lube oil system is the accumulator. It must be periodically checked for proper charge and bladder or diaphragm integrity. This can be done at any time. With bladder-type accumulators, close accumulator block valve, open drain valves, and observe the charge pressure. If there is no pressure, charge the bladder to the specified pressure. If pressure cannot be maintained, the bladder is defective and must be changed.

Note that diaphragm-type accumulators can be checked more easily and are more reliable than the less expensive bladder type. Here, a rubberized nylon diaphragm separates the nitrogen charge from the oil. An indicator rod protrudes into a transparent plastic dome and gives accurate, visual indication of the true volumes of nitrogen and lube oil.

If a system incorporates an air-fan type cooler, do not actuate the lube oil fan until the expander is in operation and the lube oil downstream of the cooler has reached 110°F.

The reservoir heater should be set at 80–100°F. Afterward, the heater cover should be closed and not touched again during the life of the machine (assuming that the thermostat stays operable).

The expander is now ready to be put into operation. Open the compressor inlet valve and expander discharge valve simultaneously. Then open the compressor discharge valve. Make sure the variable nozzles are in the closed position. Push the start button on the control panel to open the inlet shutdown valve.

The expander-compressor will attain a speed of 5,000–15,000 rpm, depending on the design horsepower of the machine. If the design pressure of the compressor suction is higher than the design pressure of the expander discharge (pre-boost type), increase the speed to approximately 80% of the design speed as rapidly as possible. This

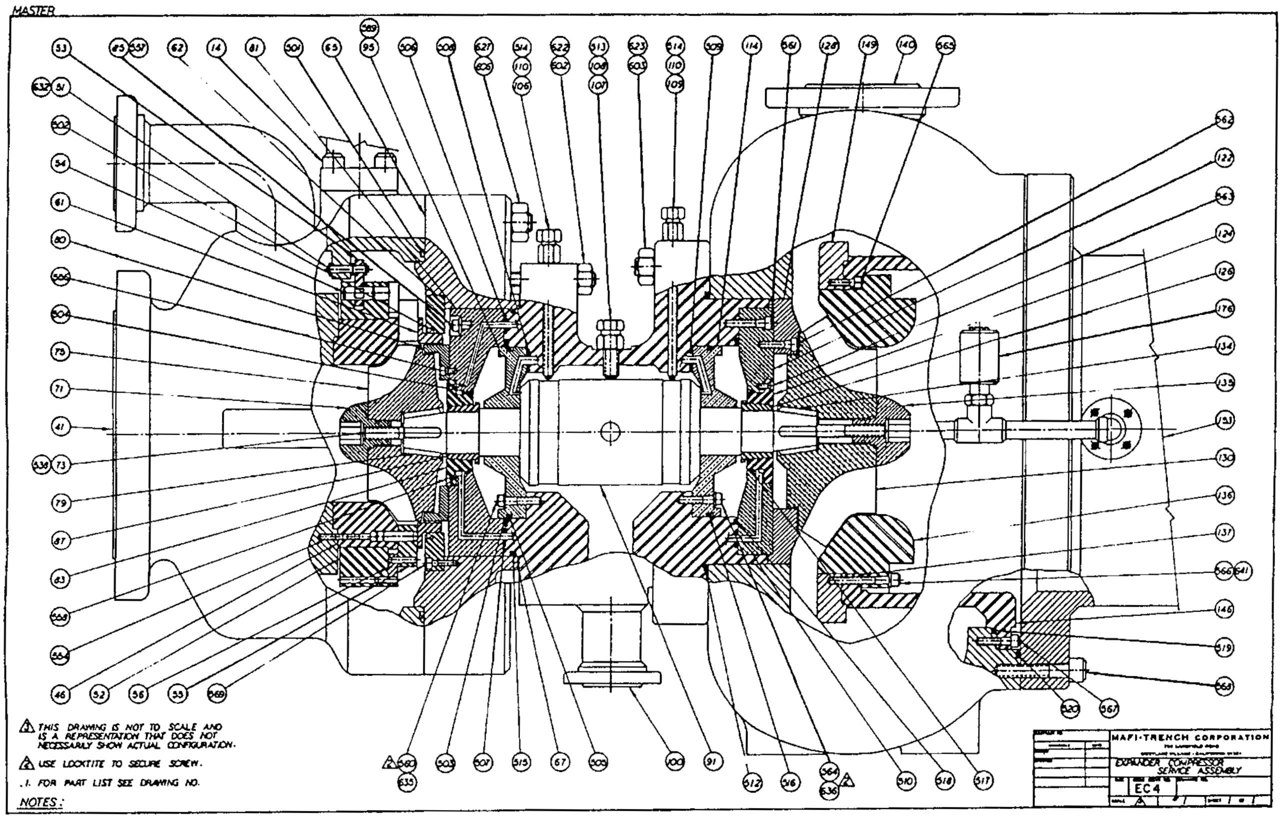

Figure 5-12. Typical cryogenic expander cross-section.

Table 5-1
Expander-compressor nomenclature

14	Actuator Mount Assembly	122	Compressor Shaft Seal
41	Expander Housing	124	Seal Insert(Compressor)
46	Expander Follower	126	Shaft Seal Ring (Compressor)
51	Actuating Pivot Pin		
52	Adjusting Ring	128	Compressor Wheel Seal
53	Actuating Lever	130	Compressor Wheel
54	Actuating Lever Pin	134	Shaft Key (Compressor)
55	Inlet Vane	135	Nose Cone (Compressor)
56	Adjusting Link	136	Compressor Follower
61	Pressure Ring	137	Gasket-Compressor
62	Pressure Ring Guide Follower		
65	Expander Housing Cover	140	Compressor Housing
67	Shim-Exp. Housing Cover	141	Compressor Housing
71	Nose Cone (Expander) Weldment		
73	Center Stretch Rod	146	Diffuser Bracket
75	Expander Wheel	149	Diffuser Plate
79	Shaft Key (Expander)	153	Compressor Inlet
80	Expander Wheel Seal	176	Auto Thrust Equalizer Assembly
81	Heat Barrier		
83	Seal Insert (Expander)	501/2	Teflon Seal
85	Washer-Heat Barrier	503–524	O-Ring
87	Shaft Seal Ring (Expander)	525	Teflon Ring
91	Shaft	526/7	O-Ring
95	Expander Bearing	552–558	Screw
100	Bearing Housing (Piping)	601–606	Stud
106*	Vibration Pickup (Expander)	615	Eyebolt
107	Tachometer Pickup or Tach Pickup Rework	621–627	Nut
		630	Lockwasher
108	Tachometer Pickup Locknut or Tach Pickup Spacer	635–638	Washer
109	Vibration Pickup or Vibration Pickup Assembly		
110	Vibration Pickup Locknut or Vibration Pickup Spacer		
114	Compressor Bearing		

* *Optional*

will minimize high start-up thrust loads. Conversely, if the compressor suction pressure is nearly equal to the expander discharge pressure (post-boost type), the expander speed may be increased at any desired rate.

Before the machine achieves design speed the tachometer setting should be checked. This can be done by lowering the set points until the overspeed alarm and shutdown are actuated. Once checked, the expander speed should be increased to design speed.

The typical nomenclature is shown in Figure 5-12 and described in Table 5-1.

POWER RECOVERY EXPANDERS FOR FCC UNITS IN MAIN AIR BLOWER OR GENERATOR DRIVE SERVICE

A general specification for modern power recovery (hot gas) expanders in FCC service is given below. This specification may be used as either a starting point for a plant-specific write-up, or as a generalized document that facilitates bid evaluation efforts. Remember that operational references are a shared vendor/contractor/plant operator (owner) responsibility.

A series of illustrations are included as examples of "real life" appearance of specified equipment and components being specified.

1.0 General Information

1.1 Scope

This specification covers the minimum requirements for the design, fabrication, materials, and testing of an overhung rotor axial flow, power recovery expander (Figure 5-13) used to drive a main air blower in Fluid Catalytic Cracking (FCC) service. In addition to the expander and main air blower, this string may also include a steam turbine, gear, and/or motor-generator.

The control of the process is based on the reactor-to-regenerator pressure differential. The pressure differential signal will be transmitted to the expander inlet butterfly control valve and expander bypass control valve, which will operate on split range control.

For Main Air Blower service with a steam turbine in the string, the unit shall be started by the steam turbine. The string shall be brought to minimum "N" rpm governor speed and stabilized. After proper checks and stabilization the unit shall be brought to rated speed, keeping in mind the critical speed and temperature requirements of the equipment in the train. After achieving rated speed, the expander inlet valve shall be opened while observing temperatures and applying cooling steam as necessary.

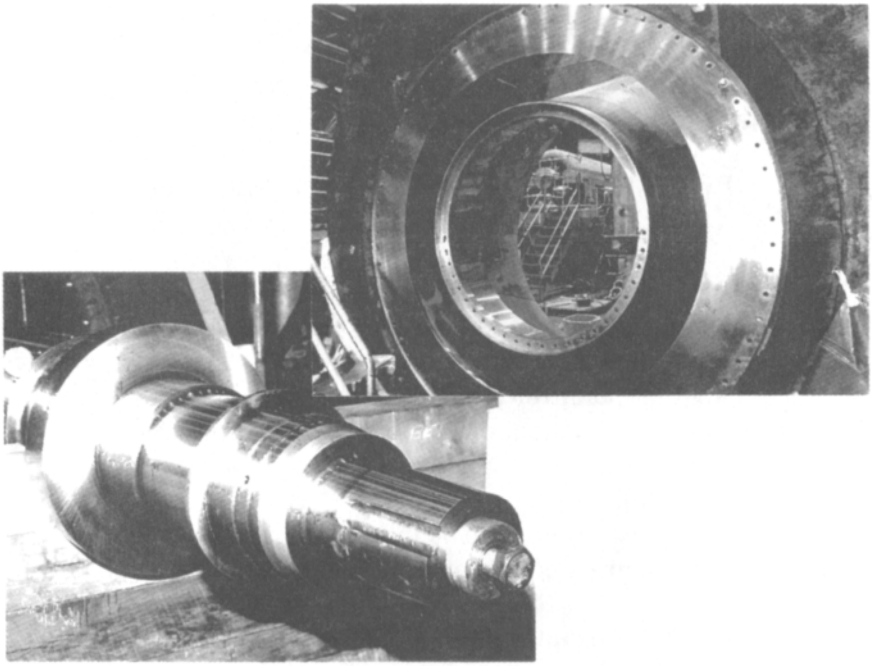

Figure 5-13. The Elliott TH expander is a single-stage hot gas expander with an axial inlet and vertical exhaust. The TH-line expanders range in horsepower from 4,000 to 50,000 and are of overhung rotor construction. The expander consists of four major components: the inlet casing and its supports, the exhaust casing, the bearing housing and support system, and the rotor.

For Generator Drive Service the expander-generator train will be started-up after the process is lined-out and at steady state. Steam will be admitted between the expander inlet butterfly valve and the block valve; the flue gas flowrate will then be gradually increased and mixed with the steam to control the heating/cooling rate of the expander and piping. The generator will be synchronized using the flue gas and the startup steam. The quantity of flue gas will gradually be increased and the steam backed out until the expander-generator is fully loaded.

For Main Air Blower service without a steam turbine in the string, the unit shall be started by first applying windage steam and then accelerating the train to rated speed using the electric motor. After achieving stable rated speed, the expander inlet valve will be opened while observing temperatures and applying cooling steam as necessary.

1.2 Applicable Specifications

ANSI B16.5	Pipe Flanges and Flanged Fittings, Steel, Nickel Alloy, and other Special Alloys
ANSI B31.3	Petroleum Refinery Piping
ANSI Y14.2M	Engineering Drawing and Related Practices—Line Conventions and Lettering
APl Std 612	Special-Purpose Steam Turbines for Refinery Services
APl Std 613	Special-Purpose Gear Units for Refinery Services
APl Std 614	Lubrication, Shaft-Sealing, and Control-Oil Systems for Special-Purpose Applications
APl Std 670	Vibration, Axial-Position, and Bearing-Temperature Monitoring Systems
ASME BPV Sect II	Materials
ASME BPV Sect VIII	Rules for Construction of Unfired Pressure Vessels
ASME BPV Sect IX	Welding and Brazing Qualifications
ASTM E94	Guide for Radiographic Testing
ASTM E125	Magnetic Particle Indications of Ferrous Castings
ASTM E142	Method for Controlling Quality of Radiographic Testing
ASTM E709	Practice for Magnetic Particle Examination
AWS D1.1	Structural Welding Code-Steel
ISO Std 3448	Industrial Liquid Lubricants—Iso Viscosity Classification
NEMA SM23	Steam Turbines for Mechanical Drive Service
NFPA 70	National Electrical Code, Articles 500 and 501 Hazardous Locations
OSHA	Occupational Safety and Health Standards of the U.S. Department of Labor

1.3 Definition of Terms

1.3.1 For Main Air Blower Service, rated speed (in revolutions per minute) is the speed at which the expander operates without consideration for any gear ratio. For Generator Drive Service, synchronous or rated speed (in revolutions per minute) is the speed at which the generator (electrical field) operates with consideration for any gear ratio.

1.3.2 Maximum continuous speed for generator drive duty is synchronous speed.

1.3.3 Trip speed is the speed at which an independent emergency device is activated and sends a signal to close the expander inlet butterfly valve system. This is approximately 105% of maximum continuous speed or synchronous speed (whichever is higher).

1.3.4 Overspeed is the speed at which the expander rotor is tested to prove its design capability for this service. Overspeed is 115% of maximum continuous speed.

1.3.5 Critical speed is when the frequency of a periodic exciting frequency applied to the rotor-bearing support system corresponds to the natural frequency of the system.

2.0 Expander

2.1 General

The expander design will be of axial entry (Figure 5-14), overhung rotor, stiff shaft construction with one or two rows of blading designed and constructed for 100,000 hrs of life and at least 3 yrs of uninterrupted continuous service. It is recognized that uninterrupted operation for this period of time involves factors beyond the Seller's control.

The design will have true centerline support of all components (Figure 5-15) with provisions to minimize stresses due to relative axial thermal expansion of the casings. The preferred method to reducing these axial stresses is through the use of an expansion joint in the exhaust casing (Figure 5-16). The design shall be such as to minimize the time required for rotor changeout.

2.1.1 The expander shall be capable of delivering the stated power at rated speed when operating at "normal" conditions as noted on the data sheets. The delivered horsepower shall be guaranteed with no negative tolerance.

2.1.2 The expander may be exposed to excessive inlet temperature conditions (afterburn) four times per year for 15 min each

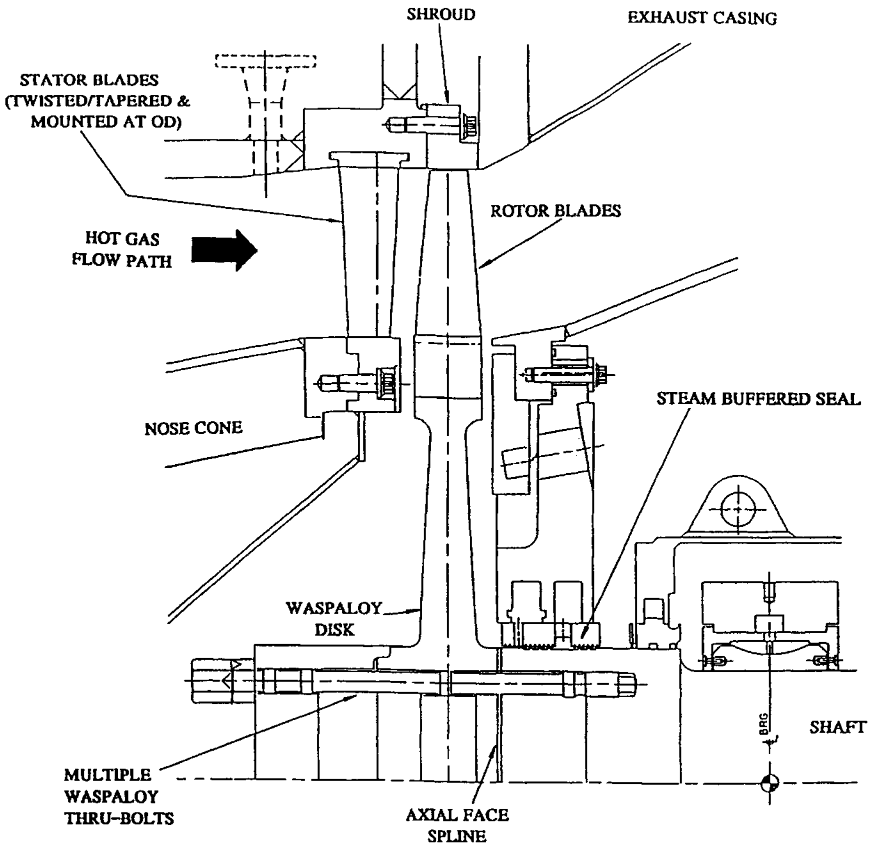

Figure 5-14. Axial entry hot gas expander, with principal parts identified.

with a maximum inlet temperature of 1,600°F. The expander shall be capable of continuous operation during this time.

2.1.3 The Seller shall provide curves for the rotating blades and the disk showing the percent of life consumed per unit time versus expander inlet temperature complete with sample calculations and total initial blade and disk life.

2.1.4 Velocity triangles at the mean section of the blading are to be submitted by the Seller. The blading shall be designed to minimize blade erosion caused by the particulate entrained in the flue gas with tapered and twisted rotor and stator airfoils. The blade design used shall have at least three years of successful operating time in FCC service for the frame proposed.

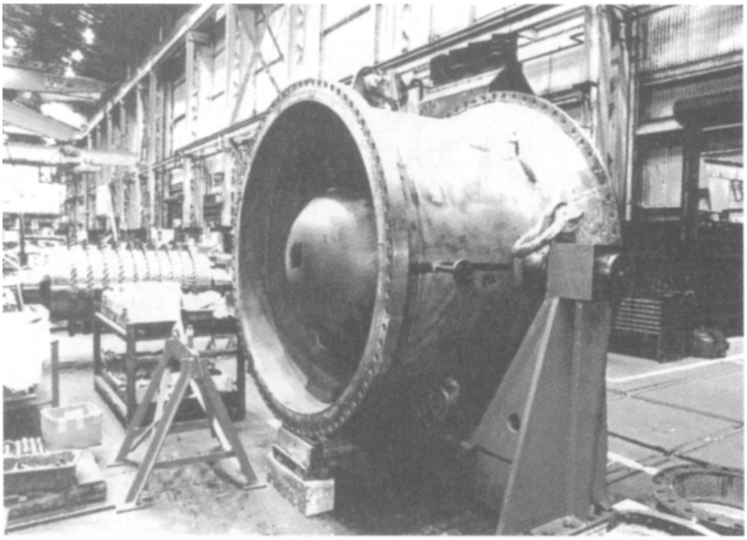

Figure 5-15. The inlet support, with the trunnion blocks, supports the inlet casing and is designed for thermal expansion of the casing while maintaining the centerline of the unit.

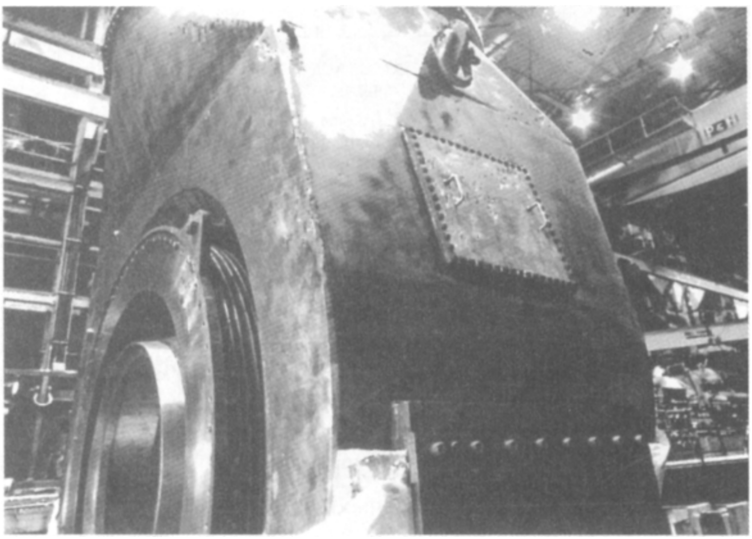

Figure 5-16. Casing and connections are designed to minimize distortions, prevent cracking, and allow relative movement during warmup and cool down. This view of the exhaust casing shows the stainless-steel expansion bellows.

2.2 Vibration and Balance

2.2.1 The rotor assembly (Figure 5-17) shall be multi-plane dynamically balanced at rated speed.

2.2.2 The shaft (Figure 5-18) shall be separately balanced prior to rotor assembly.

2.2.3 The maximum allowable mechanical-plus-electrical runout shall be 0.5 mils.

2.2.4 The maximum permissible vibration, in mils (0.001 in.), during shop test at rated speed shall be equal to the square root of 20,000 divided by the sum of rated speed plus mechanical and electrical runout for the overhung rotor design. Only the actual total measured runout may be subtracted from the unfiltered peak-to-peak amplitude measured during testing to attain the shaft vibration. The mechanical-plus-electrical runout subtracted from the unfiltered peak-to-peak amplitude shall not exceed 0.5 mils regardless of total runout.

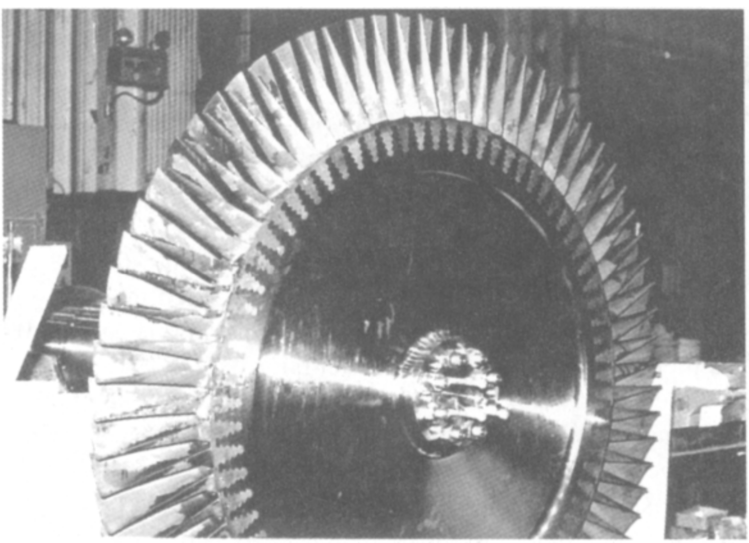

Figure 5-17. The rotor is an overhung design with the disk mounted to the inboard end of the shaft, positioned in the axial gas flow. Disk and blades are of Waspaloy material.

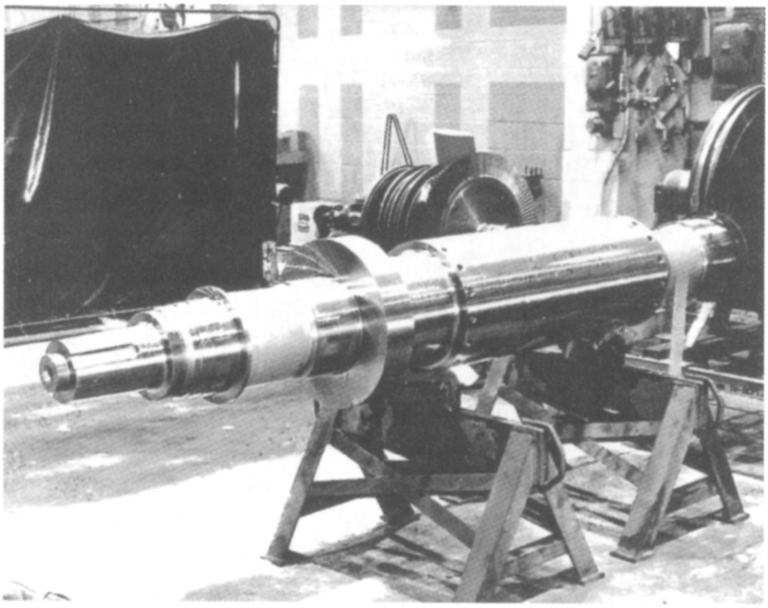

Figure 5-18. Finish-machined shaft showing integral thrust collar. The rotor is a stiff-shaft design.

2.3 Rotor Assembly

2.3.1 The shaft shall be capable of transmitting the maximum power at any operating point on the data sheet. The shaft end shall have a $\frac{3}{4}$ in./ft taper for a hydraulic-fitted coupling hub (Figure 5-19).

2.3.2 The disk shall be of forged material suitable for the temperature and service. The disk shall be designed to attain 100,000 hrs life, without any cooling, at the normal (guarantee) point including the temperature excursions.

2.3.3 The rotor studs (Figure 5-20) shall be ground of the same material as the disk and have rolled threads. The studs shall have provisions for positive locking to prevent unscrewing of the studs during operation.

2.3.4 The rotor blades shall be of the tapered/twisted, free vortex, reaction design (Figure 5-21). The blades shall be specifically designed for the dirty FCC flue gas application. Seller shall provide a Goodman Diagram for the highest stressed location

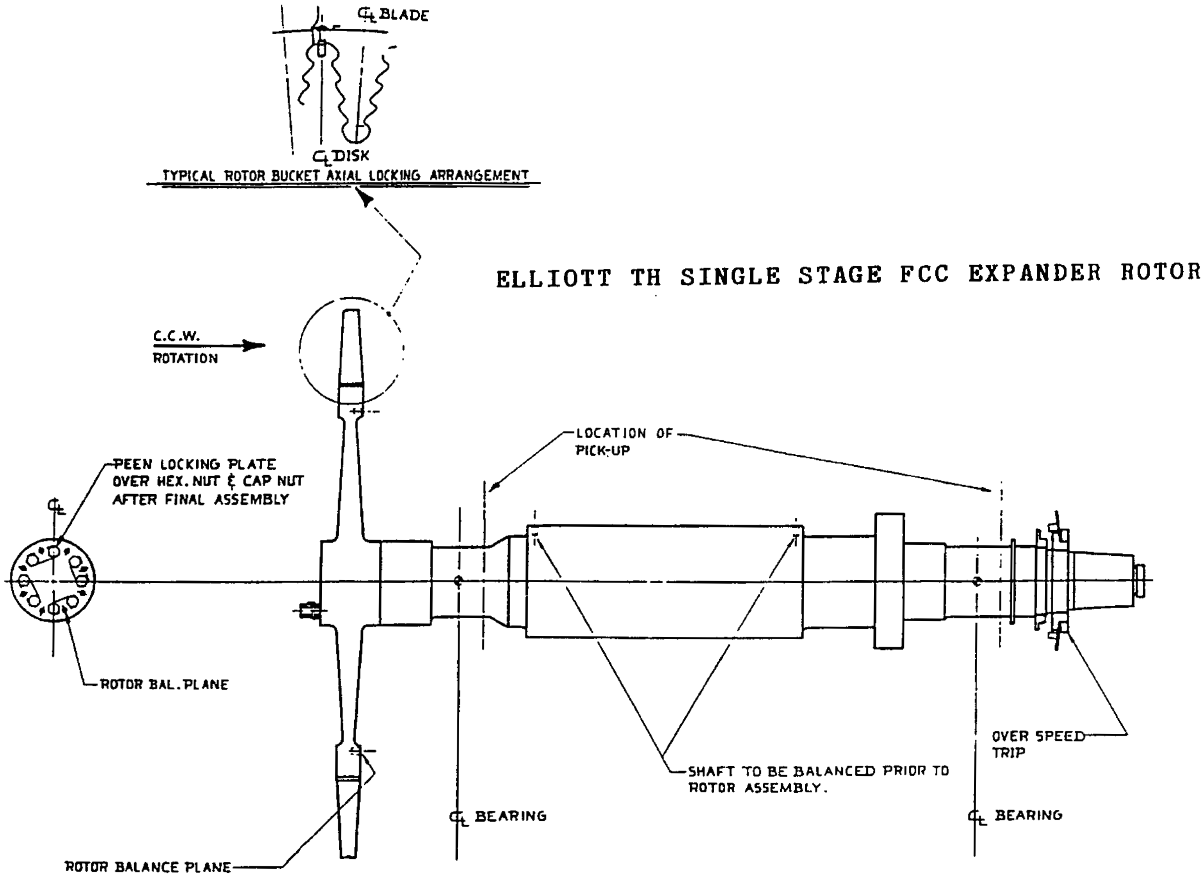

Figure 5-19. Rotor assembly showing tapered shaft end.

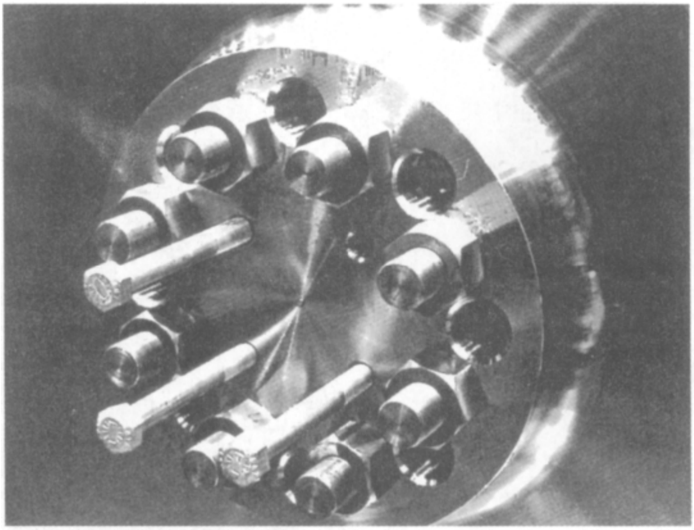

Figure 5-20. The disk containing the rotating blades is attached to the end of the shaft by means of eight studs with nuts. Disk-to-shaft juncture is an axial-face (curvic) spline, allowing transmission of torque and concentricity of the disk under high temperature conditions.

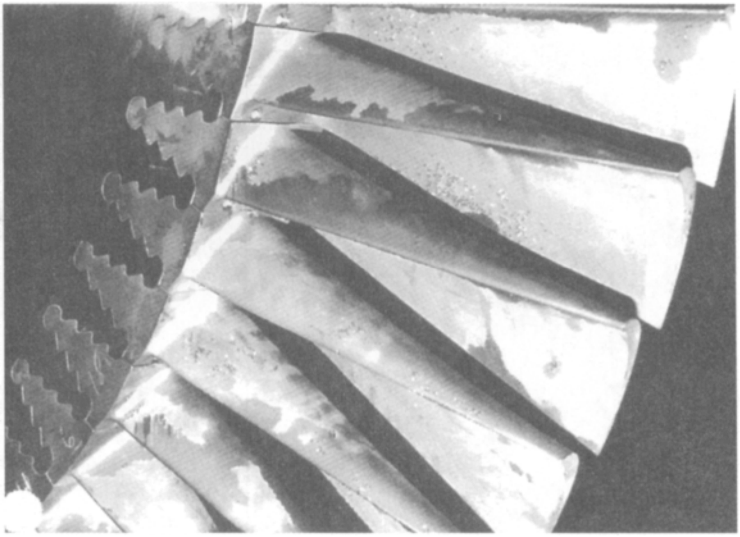

Figure 5-21. This picture shows the rotor blades from the inlet end. Root design is a four-land fir-tree type. A lock pin on each root platform locates the blade axially in the disc.

of the rotor blade at the normal (guarantee) point. The rotor blade shall be coated with chromium-carbide for erosion protection. The coating shall be applied to those areas that the Seller's blades typically experience erosion caused by the catalyst particles. The rotor blade material shall be compatible with the disk material. Seller shall provide a Campbell Diagram for the rotor blade. The blade natural frequency shall be at least 10% away from any exciting frequency, including nozzle passing frequency and the number of nose cone struts. The blade natural frequency shall be greater than four times rated speed.

2.3.5 The rotor assembly shall have a unique identification number permanently marked on the shaft. Blade and disk residual life curves shall be provided by the Seller. The disk/shaft attachment shall be redundant so that if the primary torque transmission path fails, a secondary path will prevent separation of the disk from the shaft.

2.4 Inlet Casing

2.4.1 The design of the main pressure containing inlet casing (Figure 5-22) shall be such that the hoop-stress levels at the metal temperature will not exceed the maximum allowable stress values specified in the ASME BPV Code for the material used. The construction rating for the inlet casing shall be adequate for the specified condition, but no less than 35 psig at 1,350°F; the rating shall be listed on the data sheets.

2.4.2 The nose cone (Figire 5-23) shall be the same material as the main barrel portion of the inlet casing and a parabolic shape to minimize stratification of the particulate in the flue gas. The struts that support the nose cone shall be aerodynamic in shape and located so that they do not cause uneven flow of the flue gas or particulate at the annulus just upstream of the stator blades. The struts (Figure 5-24) shall be designed to accommodate all forces transmitted through them without the presence of cracks at any time during the 100,000 hour design life of the expander.

2.4.3 The stator blades shall be made from a material suitable for the expected service conditions. A chromium-carbide coating shall be applied to the stator blades if the Seller has typically experienced erosion in this area due to the catalyst particulate.

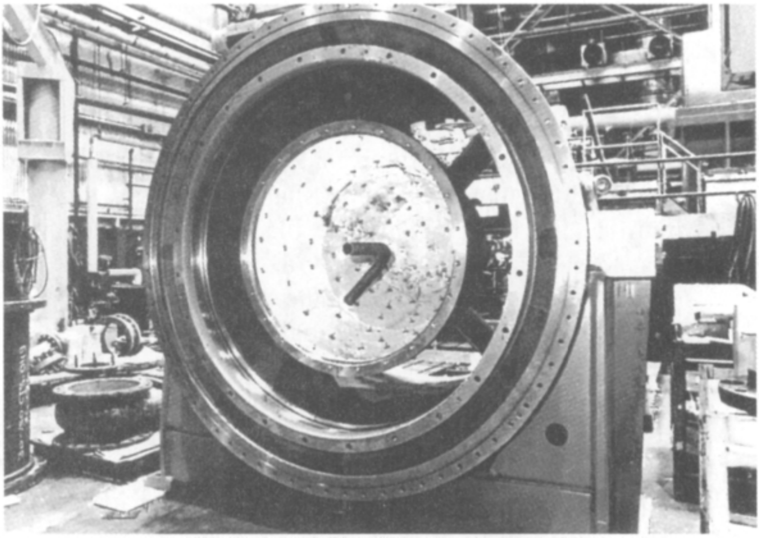

Figure 5-22. Upstream view of the inlet casing assembly. The nose cone is supported by struts that also allow entry of cooling steam and instrumentation into the cone.

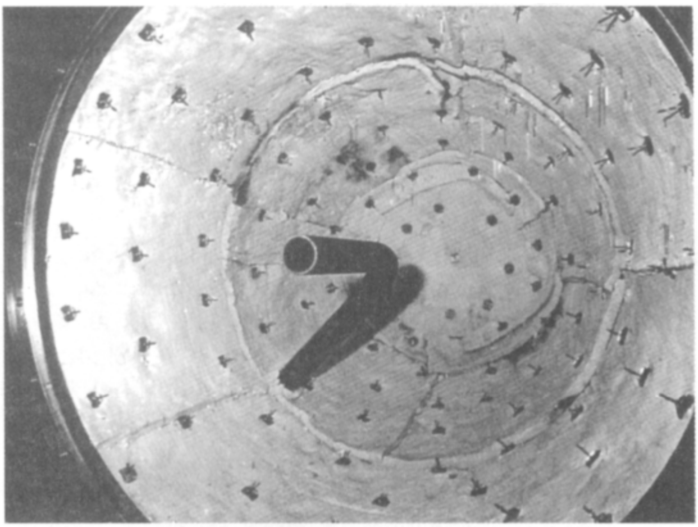

Figure 5-23. Interior of the nose cone showing terminus of the cooling steam line. The interior shielding consists of a 2-in. (50.8-mm) insulation thickness.

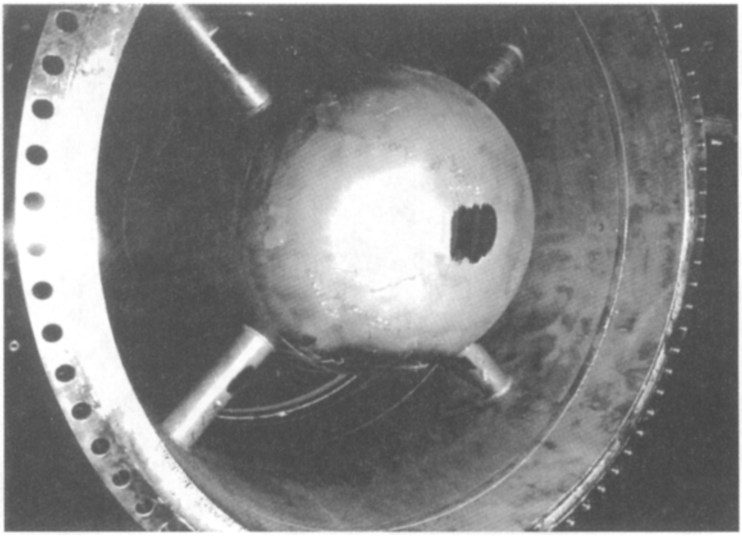

Figure 5-24. The struts transmit thrust loads imposed on the nose cone by flue gases to the inlet casing and its supports.

The stator blades shall be of the tapered/twisted, free vortex, reaction design to maintain even distribution of the catalyst particles as they pass through the blade path and to minimize erosion due to secondary flows. The stator blades shall be fixed in a fashion to minimize stresses to other components, and so that the forces take the most-direct route to the foundation.

2.4.4 Replaceable rotor and stator blade shrouds shall be provided. These shrouds shall be coated with an erosion resistant coating (Figure 5-25) compatible with the base material so as to minimize spalling of the coating during temperature transients.

2.4.5 The inlet casing support shall be designed with trunnions (see Figure 5-15) for true centerline support of the inlet casing. The support/casing system shall be designed for smooth movement of the inlet casing relative to the inlet support without sticking, binding, or uneven expansion during heating or cooling of the inlet casing.

2.4.6 Drains shall be provided at the low points of the inlet casing and be at least 1.5 in. in size, Class 300.

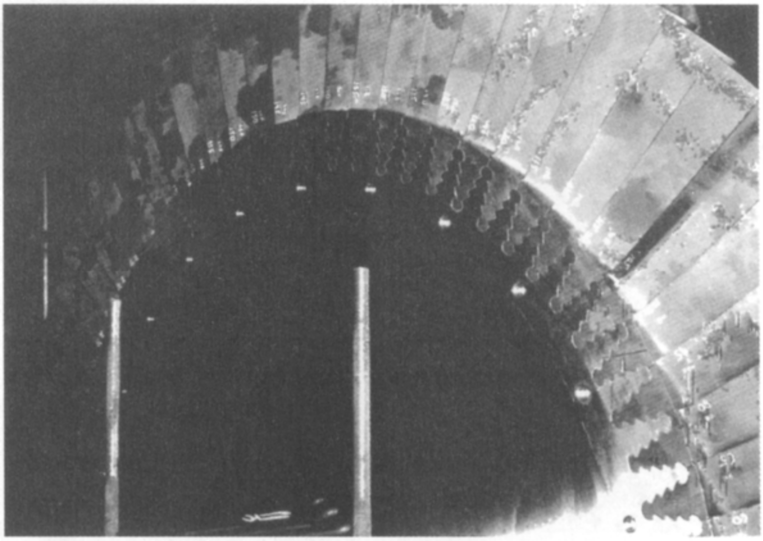

Figure 5-25. Rotor disk shown from the exhaust end. Blade trailing edges are coated with chromium carbide.

2.5.7 Auxiliary provisions

2.5.7.1 Two 1-in., Class 300 borescope connections shall be provided on the inlet casing to inspect the condition of the stator blades and the upstream side of the rotor blades during periods the expander is shut down without disassembly to the expander.

2.5.7.2 Cooling steam to the upstream side of the disk via the inlet casing shall be provided during times of temperature excursions to minimize the effect of the higher temperature on disk life. Also, provisions shall be made in the original design, without internal modification to the casing at a later date, to provide for steam that will prevent all ingress of flue gas to the upstream side of the disk.

2.5.8 The inlet flange shall be of the weldneck type with raised face designed in accordance with ASME BPV Code Section VIII. The flange shall be axial entry with a surface finish of 150–250 micro inches. The gasket shall be of the spiral-wound metal type with a seating stress of 10,000 psi.

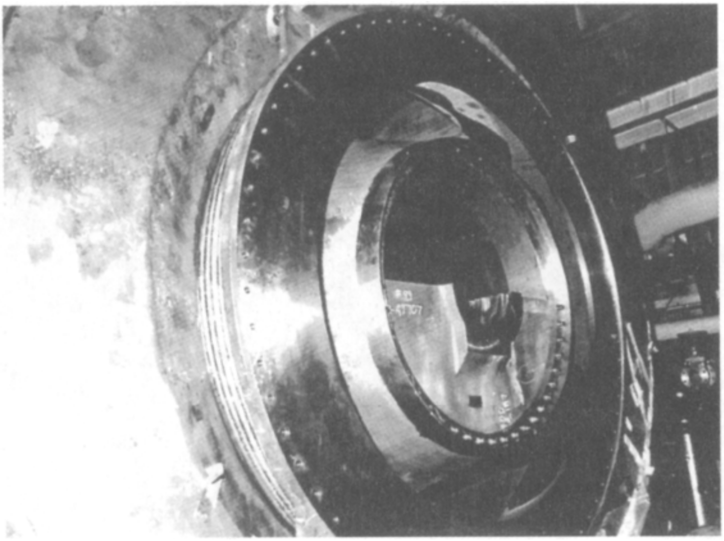

Figure 5-26. The exhaust casing fabrication is stainless steel. In this picture, the bearing housing can be seen in the center of the casing. The inboard (diffuser) end of the inlet casing will be bolted to the exhaust casing bellows.

2.5 Exhaust Casing

2.5.1 The design of the main pressure containing exhaust casing (Figure 5-26) shall be such that the primary stress levels at the metal temperature will not exceed the maximum allowable stress values specified in the ASME BPV Code for the material used. The construction rating for the exhaust casing shall be adequate for the specified condition, but no less than 3 psig at 1,200°F; the rating shall be listed on the data sheets.

2.5.2 The exhaust casing supports (Figure 5-27) shall be designed for true centerline support at the horizontal centerline of the exhaust casing. The support system shall be adequate for the total load, including one times the forces and moments per NEMA SM23 paragraph 8.06, without affecting the rotor blade radial tip clearance.

2.5.3 The exhaust flange shall be of the weldneck type with raised face designed in accordance with ASMEBPV Code Section VIII. The flange shall be vertical up (Figure 5-28)

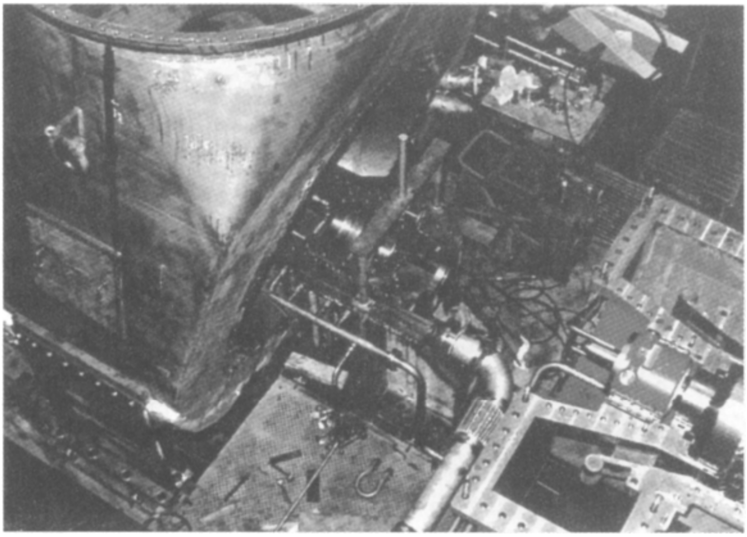

Figure 5-27. The exhaust casing is free-standing on it own wobble foot support. Axial expansion and vertical alignment are allowed by a centering key at the bottom of the casing. The casing is free-floating within the constraints of the wobble feet, bottom key, backup plate, and bellows joint. This view shows the discharge end of an axial compressor in the lower right. The expander rotor support system is pedestal-type with integral bearing housing, independent of the inlet and exhaust casings.

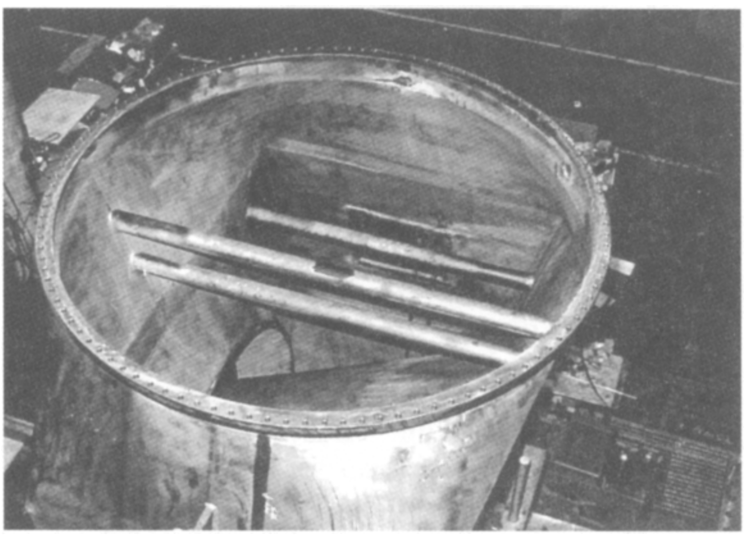

Figure 5-28. Gas exits through the upward-oriented exhaust connection.

with a surface finish of 150–250 micro inches. The gasket shall be of the spiral-wound metal type with a seating stress of 10,000 psi.

2.5.4 The exhaust casing shall be provided with two valved view ports (Figure 5-29) located so their lines of sight intersect at mid-height of the rotor blading. The valves shall be capable of withstanding the conditions specified, but not less than Class 300, with a purge connection between the valve and the sight glass. The valve size shall be the Seller's standard but not less than 4 in.

2.5.5 The exhaust casing shall be provided with at least one manway opening with gasketed cover for internal casing access by personnel.

2.6.6 A drain shall be provided at the low point of the exhaust casing and be at least 1.5 in. in size, Class-300.

2.6 Bearing Housing

2.6.1 A steam buffered shaft seal shall be provided to ensure that hot flue gas cannot escape from the casing at any specified operating condition. The steam supply shall be controlled by

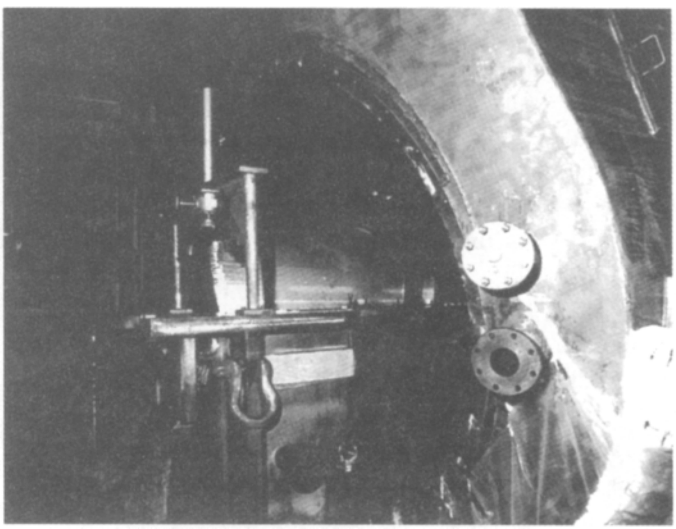

Figure 5-29. This view shows the conical stainless-steel backup plate closing the exhaust casing. The two flanged connections on the right are for the rotor blade viewing ports. The bearing housing is shielded from the backup plate by 3.5 in. (90 mm) of insulation.

differential pressure above the exhaust casing pressure. Seller shall describe in detail the shaft seal arrangement in the proposal.

2.6.2 A buffered oil seal shall be provided at the shaft and bearing case interface to ensure that oil does not escape from the bearing case at any operating condition.

2.6.3 The radial bearings shall be designed to suppress hydrodynamic instabilities and provide sufficient damping over the entire range of allowable bearing clearances to limit rotor vibration to the maximum specified in this document at the specified operating ranges. The radial bearings shall be of the tilting pad or flexure pivot type in horizontally split housings. If the Seller quotes sleeve-type radial bearings as an option, the bearing housing shall be designed for field installation of the tilting pad-type radial bearings without any remachining of the bearing housing.

2.6.4 The hydrodynamic thrust bearings shall be double acting, steel-backed, babbitted, multiple-segment type with continuous pressurized lubrication to each side. Both active and inactive sides of the thrust bearing shall be of the tilting pad type that incorporates a self-leveling feature to ensure equal load to each pad. The thrust bearing shall be selected so that the loading does not exceed 250 psi or 50% of the bearing manufacturer's ultimate load rating, whichever is lower. The thrust bearing shall permit the axial positioning of the rotor relative to the casing and setting of the proper clearance (float).

2.6.5 The thrust collar shall be integral with the shaft. The collar shall be as thick as the thrust bearing manufacturer's usual collar thickness with at least $\frac{1}{8}$ in. of stock for refinishing if the collar is damaged. The faces of the thrust collar shall have a maximum surface finish of 16 micro inches and a maximum runout on the face of 0.0005 in.

2.6.6 Instrumentation

2.6.6.1 Two non-contacting proximity probes positioned at 90° shall be supplied at each radial bearing. The probes shall be supplied complete with proximitors and interconnecting wires.

2.6.6.2 Three non-contacting probes for measuring and monitoring the axial displacement shall be supplied with proximitors and interconnecting wires. The signals shall cause shutdown of the expander train based on a 2-out-of-3 voting system.

2.6.6.3 One key-phasor probe complete with proximitor and interconnecting wires shall be supplied to monitor the expander.

2.6.6.4 All vibration equipment shall conform to API 670. The probes shall be properly locked to prevent movement during operation. Connections from oscillator/demodulators to the Purchaser's wiring shall terminate at suitable terminal blocks located within junction boxes mounted at the edge of the unit or baseplate. The probes shall be externally removable and adjustable without unit shutdown.

2.6.6.5 The radial and thrust bearings shall be equipped with resistance temperature detectors (RTDs). Each radial bearing shall have two embedded RTDs, and each side of the thrust bearing shall have two embedded RTDs. The RTDs shall be 100 Ω at 0°C, platinum with dual element. The RTDs shall be located at positions in the bearings where the highest temperature is anticipated. They shall be terminated in local junction boxes suitable for housing the RTD/mA transmitters working on a 4–20 mA signal.

2.6.6.6 The expander shall be equipped with two speed pickups sensing the rotation of a 30-tooth wheel.

2.6.6.7 The expander shall be equipped with an electronic overspeed trip. The pickups shall sense the rotation of a 30-tooth wheel and be connected to a 2-out-of-3 voting system.

2.6.7 The bearing case shall have provisions for optical alignment flats.

2.7 Expander Construction Materials

Unless agreement is reached to the contrary, construction materials shall be as listed below:

Component	*Material Spec*	*Material*
Inlet casing	AISI 304H	18-8 SS
Inlet flange	AISI 304H	18-8 SS
Nose cone	AISI 304H	18-8 SS
Stator shroud	AISI 304H	18-8 SS
Rotor shroud	AISI 304H	18-8 SS
Stator blades	AMS 5382	Stellite 31
Inlet support	ASTM 516 Gr60	Steel
Exhaust casing	AISI 304H	18-8 SS
Exhaust flange	AISI 304H	18-8 SS
Exhaust diffuser	AISI 304H	18-8 SS

Expansion joint bellows	AISI 321	18-10 SS
Exhaust supports	ASTM 516 Gr60	Steel
Bearing support	ASTM 516 Gr60	Steel
Bearing case cover	ASTM 516 Gr60	Steel
Shaft	AISI 4340 Mod	Ni-Cr-Mo-Va Steel
Disk	AMS 5704 Mod	Waspaloy
Rotor studs	AMS 7471	Waspaloy
Stud nuts	AMS 5704 Mod	Waspaloy
Rotor blades	AMS 5704 Mod	Waspaloy

2.7.1 Manufacturer's standard construction materials will be considered. References and overhaul experience (wear amount, replacement history, etc.) must be submitted with the proposal to be considered for acceptance.

2.8 Testing and Checks

2.8.1 The Seller shall keep the following documents for a minimum of five years after shipment:
2.8.1.1 Material certifications such as mill test reports.
2.8.1.2 The purchase specification for all Bill of Materials items.
2.8.1.3 Final factory assembly clearances.
2.8.1.4 Results of inspections and tests including heat treatment and radiography.
2.8.1.5 Final mechanical test results.
2.8.2 The lateral critical speed of the expander shall be calculated and an unbalance response report shall be issued to the Purchaser for review. The first lateral critical speed should be at least 20% above rated speed.
2.8.3 Hydrostatic/pneumatic tests shall be performed on the main pressure-containing casings (inlet and exhaust) at a pressure of 1.5 times the maximum pressure. Temperature compensation shall be applied where appropriate. Test pressure shall be maintained on the part for at least 30 min. Parts to be tested shall not be painted until testing is complete and satisfactory.
2.8.4 The rotor assembly shall be at-speed balanced. During the at-speed balance, the rotor shall be accelerated to 115% of maximum continuous speed for 3 min to confirm the integrity of the disk and rotor blades. If there is a spare rotor, it shall also be at-speed balanced and oversped. A residual

check shall be performed to confirm the quality of the balance.

2.8.5 A no-load hot running test (Figure 5-30) shall be performed on the expander at the rated speed.

2.8.5.1 The 4 hr hot test shall be at the normal point exhaust temperature or 1,000°F, whichever is higher. The temperature may be attained by recirculating the air heated by windage in a closed loop; the temperature shall be controlled within 25°F of the desired value by adding steam to the loop. During the hot test, the vibration shall be monitored for conformance to the specified limits.

2.8.5.2 During the 4 hr hot no-load test the oil supply temperature shall be varied 10°F above and 10°F below the normal oil supply temperature to demonstrate stability of the rotor-bearing system.

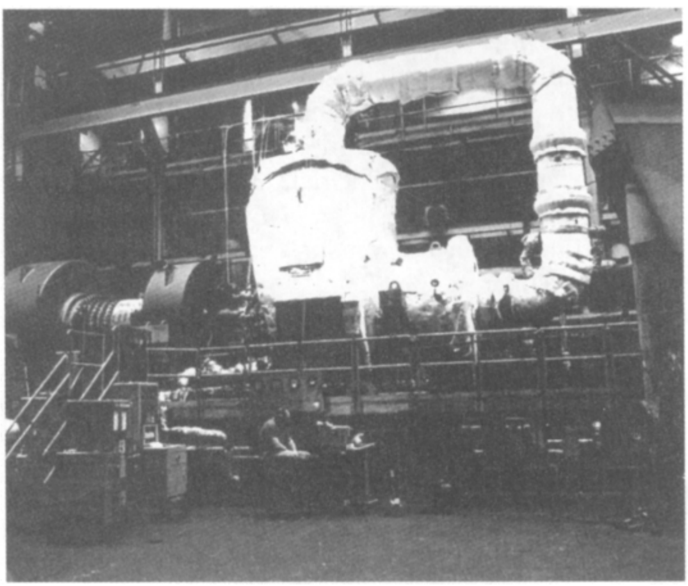

Figure 5-30. Expander during hot mechanical running test in Jeannette, Pennsylvania facility. Four inches (102 mm) of insulation is secured to the casing with refractory-type anchors welded to the casing. Final site treatment includes a layer of 1.1 lb/ft^2 (5 kg/m^2) lead foil for acoustic purposes and two outer coats of open-weave glass cloth and emulsion reinforcement, for an aluminum gray color.

2.8.5.3 After the conclusion of the 4 hr hot test, the expander rotor speed shall be smoothly decreased and increased from rated speed to approximately 500 rpm to obtain a record of the vibration levels.

2.8.6 A factory performance test under load is not required.

2.8.7 Seller shall submit to the Purchaser the hot test procedure for review six weeks prior to the test.

2.8.8 Acceptance of the shop test by the Purchaser is not a waiver of Seller's responsibilities to supply an expander that conforms to these specifications.

2.8.9 Seller shall notify Purchaser at least five working days prior to the start of any test that is to be witnessed by the Purchaser.

2.8.10 Bearings and seals shall be removed, inspected, and reassembled after the mechanical running test is completed. If the bearings or seals require replacement, both parties will mutually decide if a retest is required.

2.9 Lubrication

2.9.1 All bearings and housings shall be compatible with the conventional or synthesized hydrocarbon oil selected.

2.9.2 The oil characteristics shall be specified by the vendor having unit responsibility. Conventional or synthesized hydrocarbon oils, ISO Grade 32, per ISO 3448, are commonly employed.

2.9.3 Oil filtration in the vendor's shop during testing shall be 10 μ or finer.

2.9.4 Each oil drain shall be supplied with a sight flow indicator and 4.5 in. dial thermometer.

2.9.5 Oil piping shall be supplied with removable, turnout-type spools for ease of flushing the oil system.

3.0 Welding

3.1 Welding of all pressure containing parts shall be performed and inspected in accordance with ASME BPV Code Section VIII, Division 1 and Section IX.

3.2 The Seller is responsible for the review of all welding and repairs to ensure that they are properly heat treated, nondestructively examined, and in compliance with the applicable procedures.

3.3 Pressure containing welds shall be full penetration welds.

3.4 Fabricated casings shall be post-weld heat treated. Repairs greater than 10 in.^{2} in size shall be post-weld heat treated. All post-weld heat treatment shall be performed in accordance with ASME BPV Code.

3.5 All circumferential and longitudinal butt welds of pressure containing casings shall be 100% radiographed, if possible. All other welds shall be magnetic-particle or liquid-penetrant examined.

3.6 Permanent weld backing bars are unacceptable.

4.0 Dynamic Simulation

4.1 The expander train supplier shall assist with the selection of the expander inlet and bypass valve configurations and closure rates by performing an open loop dynamic simulation study. For a main air blower train this could be closed loop.

4.2 The dynamic simulation study shall simulate the behavior of the Power Recovery Train (PRT) under various conditions including:

4.2.1 Expander driven equipment coupling break.[1]

4.2.2 String control in the event of motor/generator trip at full load.[1]

4.2.3 Air flow control during normal operation.

4.3 Preliminary simulation results shall be available six weeks after Seller receives all the agreed to information from the Purchaser. The intent is to have results in time for necessary modifications or design changes to be incorporated into the process design without affecting the train startup.

4.4 A simulation report shall be supplied based on the final configuration and controls that will adequately safeguard the system.

5.0 Alarms and Shutdown Provisions

5.1 It is intended to alarm the following items:

a. High radial vibration
b. High axial movement
c. High radial bearing temperature
d. High thrust bearing temperature
e. Low oil pressure

---

[1] *Applies to units in generator drive service*

f. High/low oil temperature
g. High expander inlet temperature
h. High expander inlet pressure
i. High expander exhaust temperature
j. High expander exhaust pressure
k. Low shaft sealing steam pressure differential
l. High expander shaft speed and/or speed differential

5.2 It is intended to trip the following items:

a. High axial movement
b. Low oil pressure
c. High expander shaft speed and/or speed differential

6.0 Miscellaneous Technical Requirements

6.1 The use of asbestos in any component is prohibited.

6.2 The expander shall not be mounted on sole plates.

6.3 The expander shall be mounted on a separate baseplate.

6.4 Anti-friction bearings with non-metallic cages are prohibited on all rotating auxiliaries.

6.5 Insulation for the expander to protect personnel shall be provided (Figure 5-30).

6.6 Oil supply and drain lines shall be type 300 stainless steel.

6.7 Seller shall state in the proposal the recommended and minimum straight run of piping for the expander inlet and exhaust.

6.8 All fixtures and tooling for assembly and disassembly shall be included in the scope of supply.

6.9 Couplings shall be of the non-lubricated, flexible metallic type. Couplings shall be sufficient for the maximum torque application, including full short circuit at the motor/generator terminals. Coupling guards with windage control baffles or similar heat dissipation means shall be provided.

6.10 Openings, connections, pipe, valves, and fittings that are 1.25, 2.5, 3.5, 5, 7, or 9 in. in size are not permitted.

6.11 The speed increasing gear on generator drive applications shall include a turning gear capable of providing the breakaway torque of the train. It shall turn the pinion at a speed compatible with the machinery bearing requirements (approximately 50 rpm).

7.0 Spare Parts

7.1 Seller shall quote both startup and capital spares.

7.2 Startup spares shall be quoted to be shipped with the unit as follows:
a. One set of instrumented radial bearing shoes for both bearings
b. One set of instrumented thrust bearing shoes
c. One set of o-rings, gaskets, and sealants

7.3 Capital spares shall as a minimum include:
a. Spare rotor assembly
b. Spare stator blades
c. One set of all bolting
d. One rotor shroud ring (coated)
e. One stator shroud ring (coated)
f. One shaft steam seal
g. One complete set of all shaft seals

8.0 Drawings and Documents

8.1 An expander performance map of shaft power versus mass flow with lines of constant inlet temperature and pressure shall be provided. There shall be a minimum of four constant pressure lines with increments of approximately 5 psi and a minimum of four constant temperature lines with increments of approximately 100°F. The map shall be valid for rated speed with normal exhaust pressure and gas composition. The normal operating point shall be indicated on the map.

8.2 A Goodman Diagram shall be provided for the highest stressed location of the rotor blade at the normal (guarantee) point.

8.3 A Campbell Diagram shall be provided for the rotor blade including the blade natural frequencies, operating range, and potential exciting frequencies. All natural frequencies shall be at least 10% away from any exciting frequency. The natural frequencies shall be compensated for the operating temperature and centrifugal stiffening.

8.4 Velocity triangles at the mean section of the blading for the normal point shall be provided.

8.5 Blade and disk residual life curves showing the percent of life consumed per unit time versus expander inlet temperature shall be provided.

8.6 Curves of the allowable inlet and exhaust flange forces and moments shall be provided.

8.7 A curve of disk cooling steam flow versus expander inlet temperature shall be provided.

8.8 Completed data sheets shall be provided with the proposal.

8.9 The proposal shall contain preliminary cross-sectional outline and arrangement drawings.

9.0 Prime Vendor Responsibility

9.1 The prime vendor for the PRT shall perform lateral, torsional, and rotor response to unbalance analyses of the complete rotor system and shall issue reports of these analyses to the Purchaser.

9.2 The lateral critical and rotor response to unbalance analyses shall be performed according to APl 612.

9.3 Any torsional natural frequency of the rotor system shall not be closer than 10% to any operating speed (i.e., rated speed).

10.0 Warranty

10.1 The Seller shall warrant all equipment and component parts against defective materials, workmanship, and design in accordance with the terms and conditions of the contract.

10.2 The expander shall be guaranteed to deliver the shaft horsepower at the normal operating conditions (pressures, temperatures, flowrate, speed, and gas analysis) with a tolerance of –0 and +4%.

GUIDELINES FOR FIELD-TESTING HOT GAS TURBOEXPANDERS

Field testing of hot gas expanders is normally intended to establish the unit meets quoted performance or as a set point for future comparisons, which could be used to anticipate or plan maintenance work.

Since there is no standard code which governs the testing of hot gas expanders, related or otherwise applicable code practices should be used whenever possible. Thus, the relevant portions of the ASME PTC-6 and ASME PTC-10-ABCD should be considered. In particular, attention should be given to the paragraphs relating to accuracy of instruments, specifically those in sections 0.01 and 0.02 of PTC-6 on measurement uncertainty, which are quoted as follows:

> "For reasons of expediency and economics, alternative instrumentation and procedures are considered and frequently used. Such alternatives affect the accuracy of the test results. The magnitudes

of the resultant errors and their effects on the final results become subjects to be resolved between the parties to the test."

The environment of a hot gas expander is particularly harsh due to catalyst fines and, therefore, some compromise on instrumentation and test accuracy may be necessary. The following specification is intended to determine the basic requirements that should be considered in any test. Test accuracy can be determined once the actual plant configuration is determined.

1. General

a. Field performance testing procedures should generally be in accordance with ASME PTC-10-ABCD (Compressors and Exhausters).
b. The expander must be clean and in "as new" condition.
c. Casing heat transfer losses are not compensated for because the mass flow is normally high compared to heat loss.
d. Expander shaft horsepower for guarantee purposes will be determined by adding:
    1. Enthalpy change gas horsepower.
    2. Standard values of seal and bearing mechanical losses.
    3. An accurate determination of rotor thrust balance losses could be made by measuring the flow, pressure, and temperature. However, in keeping with the accuracy of item 2, Elliott recommends the use of a calculated design value of the horsepower loss.
    4. Where a torque meter is available to monitor expander shaft horsepower, this option is preferred over the addition of items 1, 2, and 3.
e. To check instrumentation, expander shaft horsepower shall also be determined by subtracting the estimated steam turbine power from the sum of compressor power, generated power, and gear losses.
f. Gas mixture equations (BWR gas properties) are used by Elliott for data reduction for the flue gas mixture.
g. Mass flows will be determined using a process flowmeter located in the upstream expander piping. The meter factor will be adjusted for slight variations from meter design flow conditions. Mass flows are typically calculated per Flow Measurement, PTC L9.5; 4-1959 and Fluid Meters, 6th ed., published by ASME in 1971.

h. The test should be conducted on design gas at design capacity and speed. Under the Power Test Code, the allowable departure from the specified operating conditions requires that the combined effects of inlet pressure, inlet temperature, and specific gravity of gas shall not produce more than 8% departure in the inlet gas density. Agreement should be obtained to accept the ratio of horsepower to volume flow at the guaranteed pressure ratio and temperature as the guarantee criteria. Another option is to create a new performance curve at the inlet temperature and pressure predicted for the time of the field test.

i. Owing to the greater test uncertainties associated with field testing as compared to planned shop testing, the warranty and guarantee should be modified to take into account the non-ideal test set-up.

j. Elliott recommends services of two witnesses be employed during the instrument calibration and test. Expenses associated with the field test would be a per diem rate for the service engineer, travel and living expenses at cost plus 10% administrative charge, and a maximum limit of eight man-day charge for pre- and post-test analysis and report preparation (typical unit).

2. **Performance Test**

a. Test point readings should not be taken until such time as the expander is shown to be at equilibrium. Equilibrium is defined as the discharge temperature varying no more than 2°C over a 5 min period at constant inlet temperature.

b. The scope of the test will be to:
    1. Determine performance at guaranteed point and comparison with quoted performance.
    2. Give a comparison for further tests to estimate power loss.

c. To ensure that the guarantee point is defined by the test data, a minimum of three points should be taken bracketing the guarantee flow.

d. Upon achieving stabilization, each test point should consist of three complete sets of readings, taken over a 20–30 min period and averaged for calculations.

e. Preliminary data reduction will be done during the test to determine whether the test is under control. Final data reduction will be handled within 10 days of returning to the manufacturer's primary office location, using computers.

f. The following mechanical data should be monitored and recorded during the test:
   1. Oil supply temperature/pressure on seals and bearings.
   2. Oil throw-off or mix drain temperatures on seals and bearings.
   3. Vibration readings from all probes.

3. Instrumentation

Due to the dirty environment, the ideal measurements, which should be by fluid manometer, cannot be used.

Since a spool piece in the inlet piping is required for maintenance reasons, it is recommended that this be replaced by a flow measuring section containing the required instrumentation.

a. All pressures should be measured using quality test gauges, having a 6-in. diameter, a 25% sensitivity, and a .5% full-scale accuracy, typically with Class AA labeling. Pressure readings during the test should be at mid-scale or greater. Mounting should be on a vibration-free local panel, connected with pressure lines of at least a .25-in. O.D. tubing; lines should continually slope down toward the expander to limit blocking by catalyst. Block and vent valves should be mounted at the gauges to facilitate calibration of as-mounted gauges. In-place calibration using a certified dead weight tester is preferred.
b. The preferred static pressure connection should have a pressure tap hole no larger than .5 in., deburred and smooth on its inside edge.
c. Gauge locations are suggested as follows:
   1. Four separate pressure gauges read at expander inlet, taps located about one pipe diameter from expander flanges located in spool piece, 90° apart.
   2. Four separate pressure gauges read at expander discharge, taps located about two pipe diameters from expander flange, 90° apart.
   3. Two separate pressure gauges read at the flow measuring section, 180° apart.
   4. Two separate flowmeter differentials should be read. These will probably have to be read with DP transmitter. It is suggested both DP units have one quality calibrated 6-in. gauge on transmitter output to directly read differential in %FS, FR, or psi. DP transmitters should be carefully bench-checked/calibrated, retaining indicated versus actual calibration data.

d. Temperature should be measured using a thermocouple or RTD system having a ±.5°F accuracy. Care should be taken to avoid intermediate TC junctions at terminals and switch boxes with a thermocouple system. Glass stem thermometers are unacceptable.
   1. Four separate temperatures, in spool piece ahead of inlet flange, 90° apart.
   2. Four separate temperatures, close to expander discharge flange.
   3. Temperature locations should be staggered 45° from pressure taps.

e. The temperature sensing portion of the probe should be immersed into the flow from one-third to one-half the pipe diameter.

f. The temperature sensing elements should be in intimate thermal contact if using wells, utilizing a suitable heat transfer filling media, such as graphite paste.

g. Steam conduction errors can be further minimized by wrapping the stem and well with fiberglass or rock-wool insulation.

h. Speed should be determined using two independent systems, one being the steam turbine electronic tachometer with .25% or better accuracy.

i. All instrumentation should be calibrated (pressure gauges, thermocouples, transmitters) before the test to ensure accuracy of instrumentation within specified ranges. Post-test calibration is also recommended to ensure data taken throughout the test were accurate.

Data sheets are generally used to document relevant parameters in easy-to-read, logical fashion. A set of six such sheets is reproduced, for general guidance, on pages 327 through 332. It should be noted that these data sheets serve at least three functions:

- To obtain comprehensive proposals
- To document purchaser's requirements
- To record as-built data

POWER RECOVERY EXPANDER DATA SHEET CUSTOMARY UNITS

Page __1__ of ____

Job No.______________ Item No.______________

Purch. Order No. ______________ Date __________

Requisition No.______________

Inquiry No. ______________

By ______________

Revision ______________ Date __________

Applicable To: O Proposal O Purchase O As Built

For ______________ Unit ______________

Site ______________ Serial No. ______________

Service______________ No. Required ______________

Manufacturere ______________ Model ______________ String Arrangement ______________

Note: O Indicates information to be completed by purchaser ☐ by Manufacturer

O Site and Available Utility Data

Site Data:

O Elevation ________Ft. O Bar. __________ psia

O Temp.: ________F Summer ________ F Winter

O Relative Humidity _____% Design Wet Bulb _____

Unusual Condtions:

O Dust O Fumes ______________

O Other ______________

Location:

O Indoor O Heated O Under Roof

O Outdoor O Unheated O Partial Sides

O Grade O Mezzanine

O Winterization Rq'd O Tropicalization Req'd

O Low Temperature

O Corrosive Agents : ______________

Area Classification: O Non-Hazardous O Hazardous Class____ Group ____ Division _____

Electric:	Drivers	Heating	Instrument & Control	Alarm & Trip
Volts				
Phase				
Cycles				
KW Avail.				

Water:	Min	Max
Psig In		
Psig Out		
F in		
F out		
Velocity, FPS		

Fouling Factor _____ HR*FT2*f/BTU

Water Source ______________ Allowable Temp Rise ________F, Max Delta-P ______________ ps

O Auxiliary Steam Conditions:

		Maximum	Normal	Minimum	
A. Low Press.	Initial Press. (psig) / Initial Temp. (FTT)				
B. Med. Press.	Initial Press. (psig) / Initial Temp. (FTT)				
C. High Press.	Initial Press. (psig) / Initial Temp. (FTT)				

Instrument Air Pressure: Normal _____psig; Maximum ____ psig; Normal Dew Pt. _____ F

☐ Auxiliary Systems - Utility Requirements

Cooling Water ______________ GPM

Aux Steam, Normal ______________ lb/hr

Aux. Steam, Max. ______________ lb/hr

Buffer Air ______________ lbm/hr

Instrument Air ______________ ACFM

POWER RECOVERY EXPANDER DATA SHEET CUSTOMARY UNITS

Page __2__ of ____
Job No.________________ Item No.________________
Purch. Order No. ________________ Date ____________
Requisition No.________________________________
Inquiry No. ________________________________
By ________________________________
Revision ________________________ Date ____________

Operating and Performance Data					
Condition or Operating Point	Normal	Maximum	Minimum		
Inlet:					
○ Mass Flow - lb/hr					
○ Pressure - psia					
○ Temperature - F					
Exhaust:					
○ Pressure - psia					
☐ Temperature - F					
☐ Molecular Weight					
☐ Speed - rpm					
☐ Power - Horsepower					

○ Gas Analysis (Wet) Mol%	
Nitrogen	
Carbon Dioxide	
Water Vapor	
Oxygen	
Carbon Monoxide	
Sulfur Dioxide	
____________	
____________	
____________	

○ Particulate - %wt.	
0 - 1 micron	
1-2 micron	
2-4 micron	
4-6 micron	
6-10 micron	
10-15micron	
15-20 micron	
____________	

Loading: ____________________ lbm/hr.

Catalyst information:

Type	
Grade	
Manufacturer	
Bulk Density	

○ Steam Contaminants ________________________________

Page __3__ of ____

POWER RECOVERY EXPANDER DATA SHEET CUSTOMARY UNITS

Job No.______________ Item No.______________
Purch. Order No. ______________ Date __________
Requisition No.________________________
Inquiry No. ________________________
By ________________________
Revision __________________ Date __________

Turbine Construction - General

Reference Specifications:

○ API 612 Special Purpose Steam Turbines

○ Other ______________________________

Type: ○ ○ ○ Other ______________

Rotation: (Viewed from inlet end)

○ CW ○ CCW

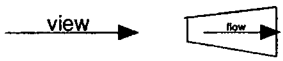

Casings, Nozzles:

☐ Max. Press. Inlet Section ________ psig, Exhaust Section _______ psig, Other _________ psig

☐ Max. Temp. Inlet __________ F, Exhaust __________ F

☐ Hydrostatic Test Press. ☐ Inlet Casing _______ psig ☐ Exhaust Casing ________ psig

☐ ○ Casing Connections:

Connection		☐ Size	☐ Facing	○ Postiion	☐ ○ Flanged or Studded		
Inlet				Axial			
Exhaust				Up			

Allowable Piping forces and Moments:

	Inlet FRC	Inlet Moment	Exhaust FRC	Exhaust Moment
☐ Parallel to Shaft				
☐ Vertical				
☐ Horiz. 90				

Remarks: ____________________

Materials - Casings & Appurtenances:

	Item	Material		Item	Material
☐	Inlet Casing	______	☐	______	______
☐	Exh Casing	______	☐	______	______
☐	Shaft	______	☐	______	______
☐	Disc	______	☐	______	______
☐	Rotor Blades	______	☐	______	______
☐	Stator Blades	______	☐	______	______
☐			☐	______	______
☐	______	______	☐	______	______

Page __4__ of ____

POWER RECOVERY EXPANDER DATA SHEET CUSTOMARY UNITS

Job No.__________ Item No.__________
Purch. Order No. __________ Date __________
Requisition No.__________
Inquiry No. __________
By __________
Revision __________ Date __________

Rotating Elements

Speeds ☐ Normal ________ RPM, Trip ________ RPM, Max. Continuous ________ RPM
☐ Lateral Criticals 1st ________ RPM, 2nd ________ RPM

Shaft Type:
☐ Integral Wheels ☐ Built-Up
☐ Combination
☐ No. of stages _______, Bearing span ________ in
Blades (Buckets):
☐ Max. Tip Speed ________ FPM
☐ Final Stage Blade Length _____ in.

☐ Shaft End: Diameter @ Coupling ________ in.
○ Keyed ○ Taper ________IPF
○ Hydraulic Fit ○ Integral Flange
Remarks: __________

Shaft Seals

End Seals:
☐ Type ○ Labyrinth
○ Other ________

	Disc End	Cplg Eng
☐ Max Seal Press., psig		
☐ Steam Leakage, lb/hr		
☐ Air Leakage, lb/hr		
☐ Shaft Dia. @ Seal, in.		
☐ Stat. laby type		
☐ Rotat. laby type		
☐ Material (stripis)		

Interstage Seals:
☐ Type ○ Labyrinth
○ Other ________
Material: ________

Notes

Bearings and Bearing Housngs

Radial		
☐ Type		
☐ Manufacturer		
☐ Length, in.		
☐ Shaft Dia., in.		
☐ Unit Loading, psi		
☐ Base Material		
☐ No. of Pads		
☐ Load: between/on pad		
☐ Pivot: center/offset, %		

Thrust	active	inactive
☐ Type		
☐ Manufacturer		
☐ Unit Loading, psi		
☐ Unit Loading (ULT.),psi		
☐ Area, sq. in.		
☐ No. of Pads		
☐ Pivot: center/offset, %		
☐ Pad Base Material		

Lubrication: ○ Flooded ○ Directed
Thrust Collar ○ Integral ○ Replaceable Matl________

Gland Sealing

☐ Sealing Stm: Press: ______ psig, flow ______lbs/hr
☐ Sealing Stm Regulator Set Press. ________ psid
furnished by __________
☐ Sealing Stm Temp. ________ F

Vacuum System: Furnished by __________
○ Ship Loose ○ Skid Mounted Other
○ Gland Condenser, see spec. ________
○ Steam Ejector ☐ Steam Press ________ psig
☐ Steam Flow ________lbs/h

Page __5__ of ____

POWER RECOVERY EXPANDER DATA SHEET CUSTOMARY UNITS

Job No.____________ Item No.____________
Purch. Order No. ____________ Date ____________
Requisition No.____________
Inquiry No. ____________
By ____________
Revision ____________ Date ____________

Lubrication and Control Oil Systems

Reference Specs ____________

Furnished by: Expander Mfr. Others

- ○ Separate for Expander only
- ☐ ○ Common with Driven Equip. and including:

____

Expander Mfr. To Supply

- ○ Control Oil Accumulator
- ○ Stainless stl oil supply header piping
- ○ Oil drain header piping
  - ○ Stainless Steel ○ Carbon Steel
- ○ Sight Flow Indicators

Oil Requirements	Lube oil	
☐ Normal Flow, GPM		
☐ Pressure, psig		
☐ Temperature, F		
☐ Total heat rej BTU/hr		
☐ Type Hydrocarbon/Synthetic		
☐ Viscosity,SSU@100F		
☐ Filtration, Microns		
☐ ________		
☐ ________		
☐ ________		

Accessories

Baseplates: furnished by ____________

- ○ Under Expander Only
- ○ Other
- ○ Open ○ Non-Skid Decking
- ○ Drip Rim ○ Leveling Pads
- ○ Column mounting
- ○ Sub-sole plates required
- ○ ____________
- ○ ____________
- ○ ____________

Soleplates: furnished by ____________

Thickness ________.in.

- ○ Subsole plates requied
- ○ Hold-down bolts furnished by ____________
- ○ Primer for expoxy grout required
  Type ____________
- ○ Anchor Bolts Furnished by ____________
- ○ Levleing (Chock) Blocks Required
  furnished by ____________

Gear Unit

Funished By ____________

- ○ Reference API-613, Editiion ________
- ○ Other Specs ____________

Remarks ____________

Page __6__ of ____

POWER RECOVERY EXPANDER DATA SHEET CUSTOMARY UNITS

Job No.________________ Item No.______________
Purch. Order No. ______________ Date __________
Requisition No.______________________________
Inquiry No. _________________________________
By ____
Revision ______________________ Date __________

Inspection and Testing

General: ○ Shop Inspection Extent ____________________
____

Inspection and Material Testing

Component	Mag. Part.	Dye Pene.	Radio graph	Ultra sonic	Obsrd	Record	Wit'n
Inlet Casing					○	○	○
Exh. Casing					○	○	○
Rotor					○	○	○
					○	○	○
					○	○	○
					○	○	○
○ Cleanliness					○	○	○
○ Hardness					○	○	○
○ Hydrostatic Tests					○	○	○
○ Blade Shaker (Static)					○	○	○
Rotor balance							
○ Standard					○	○	○
○ High Speed					○	○	○
○ Final Surface Inspection					○	○	○
○ Crating inspection					○	○	○
○ Spare Rotor Fit					○	○	○

Painting:

○ Manufacturer Standard
○ Other ____________________
○ ____________________

Shipment

○ Domestic ○ Export
○ Exp. Boxing Required
○ Outdoor Storage over 6 months
○ Waterproof boxing required
Spare Rotor Assymbly Packaged for
○ Horz. Storage ○ Vert. Storage

Space Requirements

□ Complete Unit	L ___ in. W ___ in. H ___ in.
□ ____________	L ___ in. W ___ in. H ___ in.
□ ____________	L ___ in. W ___ in. H ___ in.
□ ____________	L ___ in. W ___ in. H ___ in.

Mechanical Running Test

	Obsrd	Wit'n
○ Contract rotor	○	○
○ Spare rotor	○	○
○ Test with job coupling	○	○
○ ____________	○	○
○ ____________	○	○
○ ____________	○	○
○ Complete Unit	○	○
○ Torsional Measurement	○	○
○ Sound Level	○	○
Auxiliary Equipment		
○ Gland Sealing System	○	○
○ Gland vacuum system	○	○
○ Lube Oil System	○	○
○ ____________	○	○
○ Casing integral inspection	○	○
○ Coupling to shaft fit	○	○
○ ____________	○	○
○ ____________	○	○
○ ____________	○	○
Additional Test or Inspection		
○ ____________	○	○
○ ____________	○	○
○ ____________	○	○

Weights

□ Total Shipping Weight____________lb.
□ Expander Only____________lb
□ Max. for Maintenance____________lb
Identify ____________
□ Rotor ____________lb.
□ ____________lb.

Vendor Drawing and Data Requirements

○ Other ____________
○ Progress Reports Required
Frequency ____________
____
____

CHAPTER SIX

Special Features and Controls

This chapter discusses the most popular features and controls that are critical to turboexpander operations. Among those discussed are magnetic bearings, squeeze film dampers, radial fit bolts, valve arrangements for FCC expanders, FCC expander load shedding technology, and surge detection and avoidance.

ACTIVE MAGNETIC BEARINGS[1] AND DRY GAS SEALS[2]

BASIC PRINCIPLES OF ACTIVE MAGNETIC BEARINGS

Active magnetic bearings (Figure 6-1) are an efficient, cost-effective alternative to conventional bearings for rotating machinery. By using electromagnetic forces regulated by an automatic control system, active magnetic bearings eliminate conventional bearing and lube oil systems, significantly reducing maintenance costs and horsepower losses.

The benefits of active magnetic bearings include:

- Reduced maintenance costs, leading to an overall improvement in system integrity and reliability. The mean-times-between-failure for active magnetic bearings are equal to those of an electric motor.
- Elimination of lube oil and auxiliary systems, thereby eliminating certain potential safety problems and maintenance costs.
- Improved rotor dynamic stability. The active magnetic bearing's ability to vary stiffness and damping permits rotation about the rotor's inertial axis, eliminating vibration and noise.
- Simplified system operation.

[1] *Source: Atlas Copco/Rotoflow and S2M Corporation (France).*
[2] *Source: Revolve Technologies, Calgary, Alberta, Canada.*

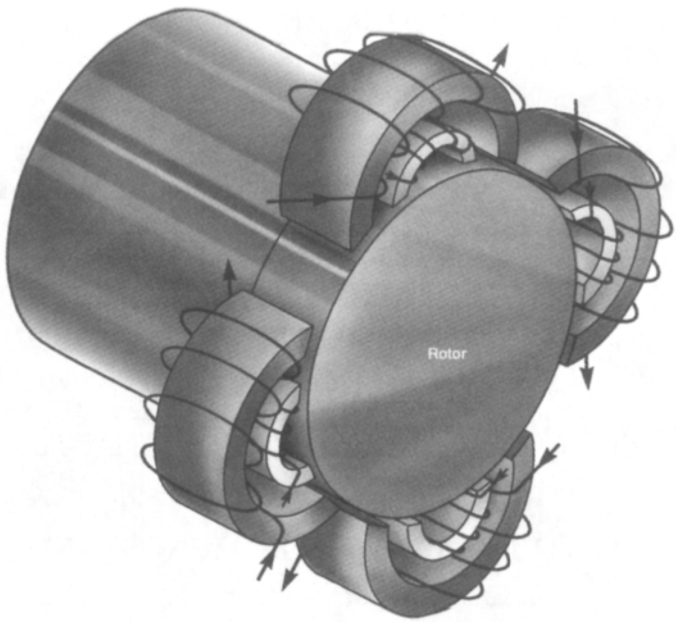

Figure 6-1. Active magnetic bearing principle.

- Elimination of parasitic horsepower losses and oil shear, which may consume up to 2% of the unit's output power.
- Elimination of mechanical wear, which essentially provides unlimited bearing life.
- Continuous monitoring of unit operation providing information on rotor location, balance, speed, and bearing loads, which were previously difficult and costly to obtain.
- System weight and space requirements are reduced by up to 50%.

These benefits directly translate into lower costs and improved operating efficiency for rotating machinery. Lubrication is unnecessary. The bearing is operable in hostile environments and, in many cases, can operate in the process fluid at high pressures and temperatures. Experience shows that total consumption of frictional power is drastically reduced.

Backup features can be incorporated to provide additional operation security. Emergency run-down bearings (Figure 6-2) prevent damage in the case of unforeseen power interruptions or electronic failures.

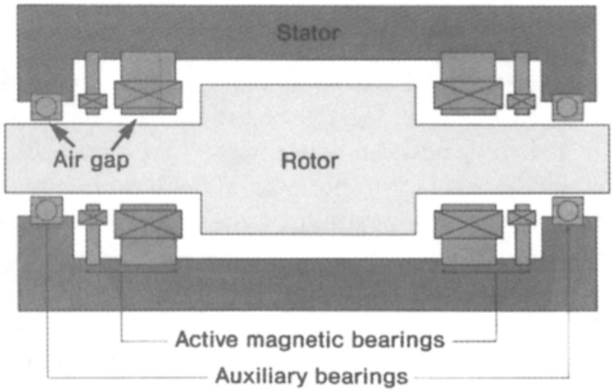

Figure 6-2. Emergency run-down bearings are fitted to the shaft ends.

Operating Principles and Design Features

Radial Bearings

In a radial active magnetic bearing, the rotor is held in position by electromagnets located on the stator (Figure 6-3). The rotor-to-stator position is constantly monitored by sensors that communicate with the electronic control system. If the rotor deviates from its position, the control system adjusts the current flow to the electromagnets to return the rotor back to its proper position.

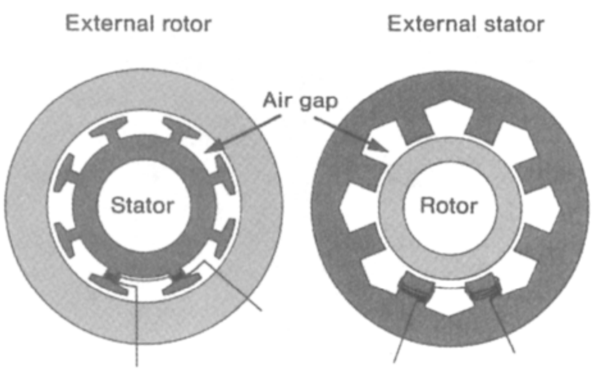

Figure 6-3. Basic radial bearing configurations.

Axial Bearings

An active magnetic axial bearing consists of two stators and a rotor disk (Figure 6-4). A sensor located at the end of the shaft monitors and maintains the rotor position between the two stators. The principle of operation is the same for both axial and radial bearings: any deviation from the normal position of the rotor is communicated to the electronic control system, which adjusts the electric current going to the electromagnets to correct the rotor position.

Turboexpander Applications for Active Magnetic Bearings

Active magnetic bearings are certainly suitable for turboexpanders. These bearings are now being used in the aerospace and machine-tool industries, as well as in a variety of both light and heavy industries.

The active magnetic bearing's versatility allows it to be used in almost any rotating machine. Examples include compressors, blowers, pumps, turbines, centrifuges, x-ray tubes, vacuum pumps, spindles for

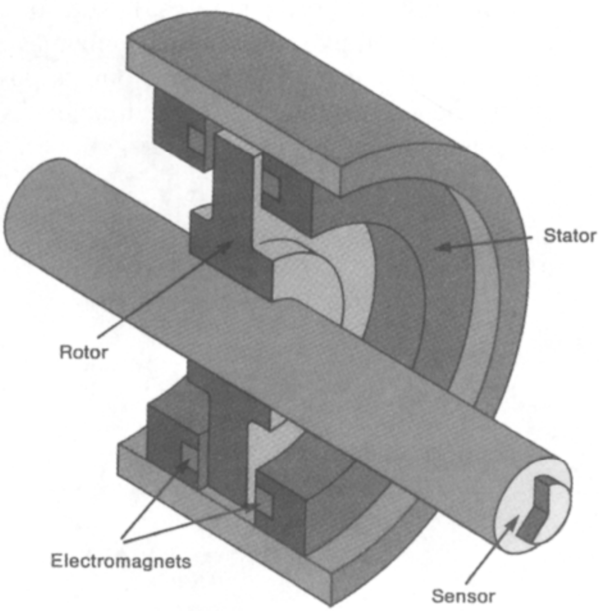

Figure 6-4. Double-acting thrust bearing.

revolving mirrors, gyroscope flywheels and inertia wheels, and machine tool spindles.

In 1985, the first active magnetic bearing in a pipeline compressor for continuous use was installed on the Alberta Gas Transmission System of NOVA Corporation. The bearings have been running smoothly, with a noted improvement in compressor operation and efficiency.

Typical Technical Parameters

Active magnetic bearings attain speeds up to 200 m/s (656 ft/sec) on radial bearings, and 350 m/s (1,148 ft/sec) on axial or thrust bearings. A large variety of process fluids are allowed to flood or surround these bearings. Allowable operating temperatures range from –253°C (–420°F) to as high as +450°C (+840°F). There is no measurable friction and vibration is rarely experienced.

Rotor diameters, or quasi "journals," include dimensions ranging from 14 mm (0.55 in.) to 600 mm (24 in.). Similarly, the load range accommodated by radial magnetic bearings is: 0.3 N (0.007 lb) to 200 kN (45,000 lb). Rotational speeds range from a virtual standstill to as high as 800,000 rpm.

CASE STUDIES ON ACTIVE MAGNETIC BEARINGS (AMB) AND DRY GAS SEALS (DGS)[3]

As previously discussed, cryogenic turboexpanders are used to expand natural gas isentropically. The expansion process is achieved in two locations, the inlet guide vanes and the expander wheel. Isentropic expansion is a more thermally efficient process than conventional Joule-Thomson expansion as shown in Figure 6-5. Expansion through a turboexpander has the additional advantage of making the released energy of expansion available as useable shaft power. Turboexpanders are usually loaded with a compressor, integral to the expander, to recompress the expanded lean gas.

Sealing of turboexpander and compressor process gas from the bearing housing differs for air separation and natural gas applications. The bearing housing is usually sealed in cold expanders and for cases when the process gas contains heavy hydrocarbon components, which may cause condensation in the bearing housing.

[3] *Source: Atlas Copco, Rotoflow Division.*

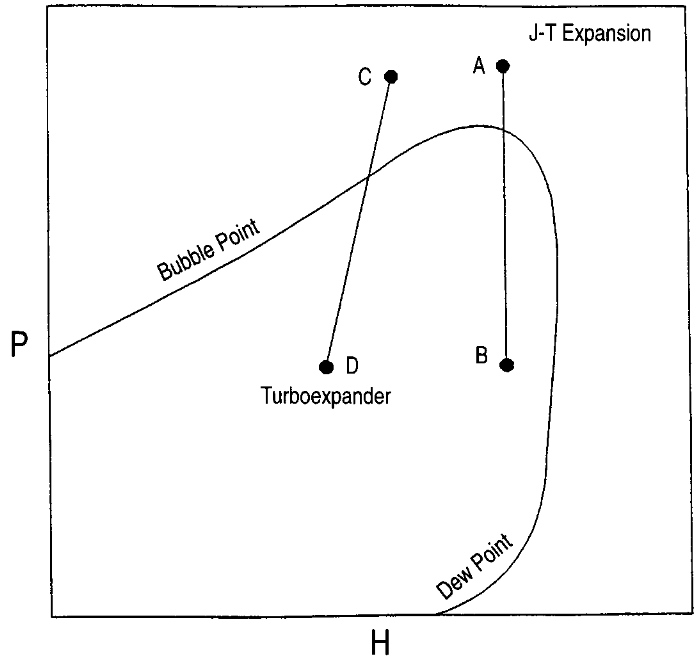

Figure 6-5. Phase diagram for an expansion process.

In turboexpanders with magnetic bearings, some bearing components are not compatible with the corrosive elements of the process gas such as H_2S, CO_2, and C_2H_2. Additionally, hydrocarbon liquids may also be incompatible with certain electrical insulation materials used in magnetic bearing construction. Moreover, since natural gas plant pressure fluctuations can be high, it is conceivable that the thrust capacity of the magnetic bearing is exceeded. Therefore, it is necessary to consider alternative solutions of sealing the magnetic bearing housing against the expander and compressor process gas; it is also appropriate to seek ways of controlling the axial position of the rotor against process fluctuation. The following sections discuss monitoring and controlling schemes used to solve these problems.

Magnetic Bearing Housing Sealing and Cooling Loop Control

Two types of sealing have successfully been used in turboexpander compressors in natural gas processing. The first type of sealing the magnetic bearing housing against cold, corrosive, or saturated natural gas is the conventional labyrinth seal. Here, leakage and/or cross-coupling effects must be considered. Neither of these effects is of much concern in closed system turboexpander compressor applications because the leakage is recovered in the compressor process and the cross-coupling problem does not exist due to large clearances. An important factor, however, is the ease of maintenance and long life. Both of these are achievable by selecting low seal gas velocity and suitable construction materials.

The second option, dry face or gas seals, was developed in the early 1970s. In dry face seals, the hydrodynamic pressure that develops between the rotating and stationary seal faces produces positive sealing with minimal seal gas leakage.

Pressurized Bearing Housing (Offshore Application)

In an offshore application the process gas flowing into a 3,600 kW turboexpander was compatible with the magnetic bearing material and a suitable seal gas source was available. This made it possible to use a pressurized bearing housing.

Figure 6-6 shows a schematic diagram of the sealing system for a pressurized magnetic bearing housing. Since windage loss is increased by higher gas density (Figure 6-7), leakage from the labyrinth seal will

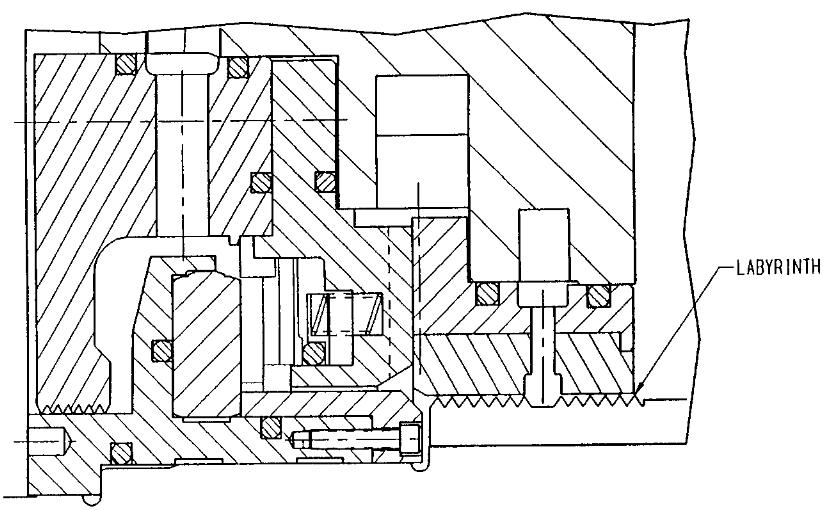

Figure 6-6. Dry face or gas seal.

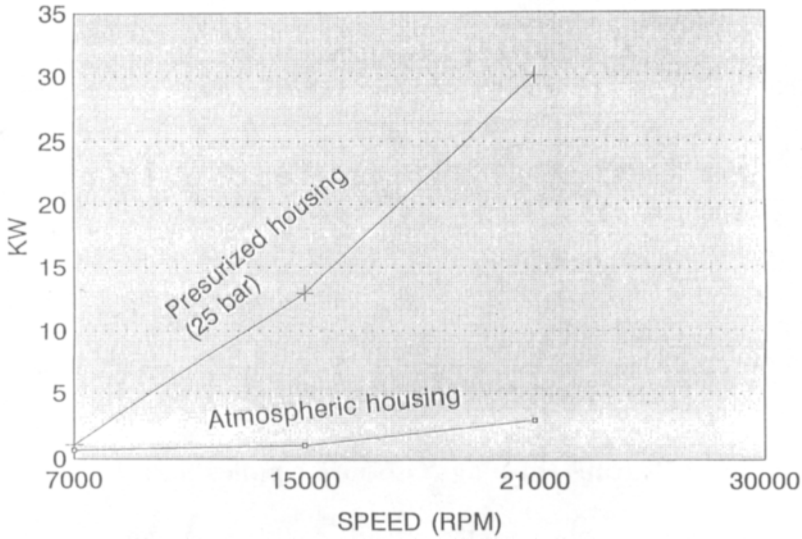

Figure 6-7. Windage loss versus speed for pressurized and unpressurized magnetic bearing environments.

not provide sufficient cooling. Therefore, an internal bypass for the seal is used to dissipate the frictional heat. In this application, the bearing housing is pressurized to 25 bar, which results in a gas density of 19.5 kg/m^3. The total windage loss at this condition is 30 kW and requires 1,200 Nm^3/hr of cooling gas.

Dry Face Seal Application, Atmospheric Bearing Housing (Onshore Application)

Because the process gas in a 6,000 kW turboexpander application was not compatible with the magnetic bearing materials and a purge gas was available, a combination of a dry face seal and a labyrinth seal was used. The seal assembly consisted of a single dry face seal in a cartridge arrangement. Figure 6-7 shows the cross-section of the seal designed for 100 bar static differential pressure. Seal leakage was expected to be 4 Nm^3/hr, which was verified during the shop test. Table 6-1 shows the leakage test results.

The labyrinth portion of the seal was designed to withstand the static and dynamic differential pressure (in the event of a major seal failure) while passing the minimum volume of purge gas.

Table 6-1
Dry face seal leakage test under static and dynamic conditions

Pressure (Barg)	Static gas leakage (Nm^3/hr)	Dynamic gas leakage
49	0.67	2.2
77	1.8	3.5
98	3.3	4.5
118	4.7	—

The gas quality feeding the dry face seal should be clean and dry. Due to the possibility of condensation of the process gas in the seal cavity, it was decided to use a seal gas heater. The heater control was set to provide warm gas at 15°C above the dew point to ensure no condensate entered the seal cavity. Also, a dual filter in series with 5 and 2 μ filtration elements was chosen to provide an ideal sealing environment and maintain the optimum performance of the seal. To reduce the risk of seal damage during reverse rotation of the turbo-expander, programming logic was set to open the compressor bypass valve whenever a shutdown impulse was initiated.

Reverse rotation is not uncommon in magnetic bearing units and could damage unidirectional dry face seals. Note that bidirectional seals have only been available since the 1980s and these would have been insensitive to the rotation direction.

Heat Dissipation

The seal or purge gas flow into the magnetic bearing housing acts as a coolant to carry away frictional heat. There are two sources of heat, magnetic bearing winding and windage loss. While magnetic losses are independent of the type and pressure of the seal and are not affected by the purge gas, windage losses are directly affected by the type of gas.

Magnetic Bearing Winding Loss

Magnetic bearing winding loss is the result of the winding resistance to electrical current. The level of electrical current and, hence, the magnitude of heat generated are functions of rotor position and rotor load.

Magnetic Bearing Windage Loss

Magnetic bearing windage loss is due to friction of the rotor mass rotating in the seal or purge gas medium. A sizeable portion of this loss is caused by thrust disk windage. The following formula estimates windage loss:

For shaft: $W_1 = 2.3 \times 10^{-4} \rho_{gas} N^3 (\Sigma_{i=1}^{\sim} d_i^4 L_i)$ (6-1)

For thrust face: $W_2 = 1.8 \times 10^{-5} \rho_{gas} N^3 (D_1{}^5 - D_2{}^5) C_{f2} P^{0.83}$ (6-2)

where ρ_{gas} = density of the gas at 1 bar and operating temperature
P = operating pressure, bar
N = speed, rpm
D_1 = thrust disk outside diameter, m
D_2 = thrust disk inside diameter, m
L_i = length of the D-section of the shaft, m
d_i = diameter of the ith section of shaft corresponding to the gas velocity at the surface of the shaft and thrust disk, m

C_{f1} and C_{f2} are friction coefficients calculated as follows:

$C_f = 0.073/Re^{0.2}$ (6-3)

where Re is Reynolds number.

These equations convey the fact that windage loss is not only a function of rotating speed, but is also directly proportional to the density of the seal or purge gas filling the bearing housing.

Bearing Housing Temperature Control

Temperature control of the magnetic bearing housing environment is critical to safe operation of turboexpanders. Atlas Copco-Rotoflow has developed several schemes to monitor the bearing housing temperature and maintain it at a safe level.

For an atmospheric bearing housing that is purged with nitrogen, temperature sensors are placed in the vent line. When the exhausting gas temperature approaches 80°C, purge gas pressure is increased to increase purge gas flow and to cool the bearing housing environment. Figure 6-8 shows a typical schematic and control loop.

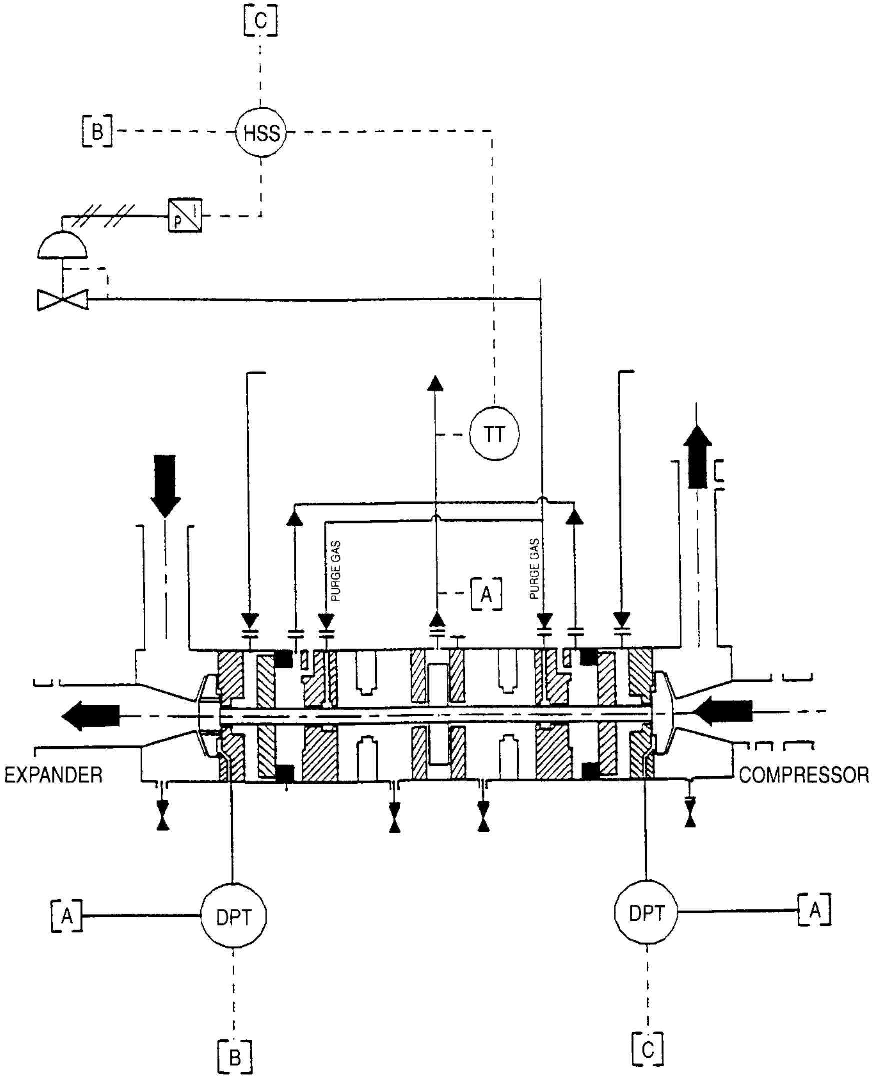

Figure 6-8. Atmospheric bearing housing temperature control.

For the pressurized magnetic bearing housing, temperature sensors are placed in several locations (i.e., compressor side bearing, expander side bearing, and in the vicinity of the thrust disk). In this control scheme, the signal corresponding to the maximum temperature is chosen to adjust seal gas pressure. If the high temperature corresponds to either expander or compressor bearing, the corresponding seal gas control valve is adjusted for higher pressure. If the high temperature is associated with the thrust disk area sensor, then both control valves are reset for higher pressure. Figure 6-9 shows a typical schematic and control loop.

Thrust Balancing Control

The thrust capacity of a magnetic bearing is limited when compared to a conventional oil bearing. Simulation of potential upset conditions

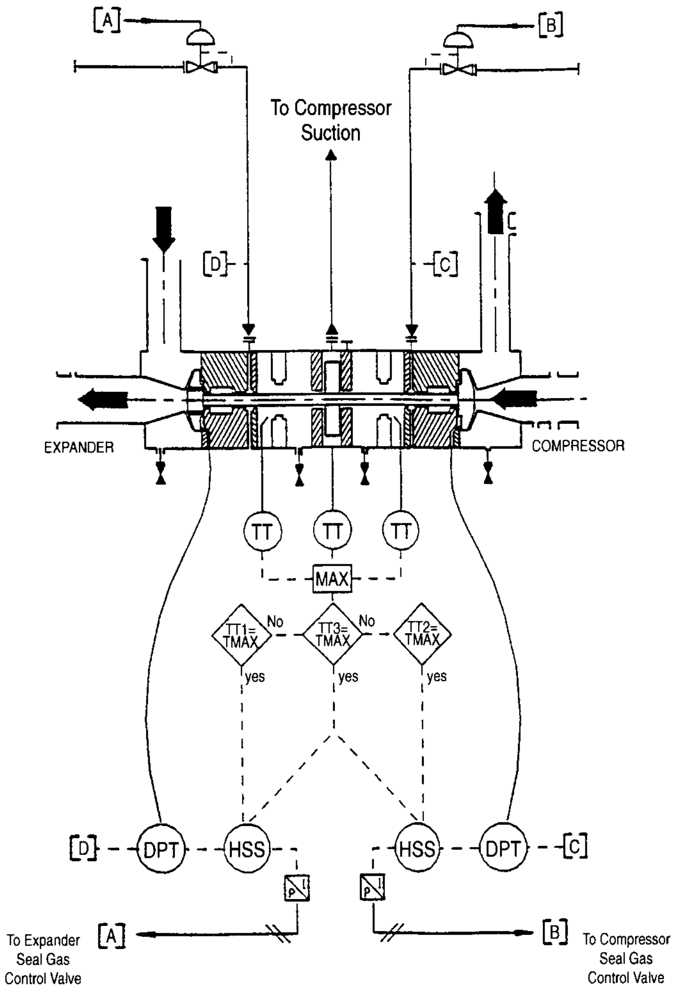

Figure 6-9. Pressurized bearing housing temperature control.

in gas plants indicates that an additional thrust adjusting system, to enhance that of the magnetic bearing, is required. Figure 6-10 shows maximum thrust loads with simulated pressure upsets at the compressor discharge. A typical application is assumed, and a solution is readily available by adapting an existing, patented automated thrust balancing system. This adaptation is called "complementary automatic thrust balancing system," and is shown in Figure 6-11.

In this automatic thrust balancing system, the pressure behind the compressor wheel is controlled to a value between the compressor suction pressure and the wheel peripheral pressure. As the expander inlet pressure increases above the compressor suction pressure level, the resulting thrust force pushes the compressor wheel, and hence the rotor system, towards the compressor suction. In the reverse situation, when the pressure behind the compressor wheel is reduced below the wheel peripheral pressure level, the rotor system moves toward the expander.

When the pressure behind the compressor wheel is adjusted in accordance with the magnitude of the axial force, automatic thrust balancing is achieved. The signal corresponding to the magnitude of

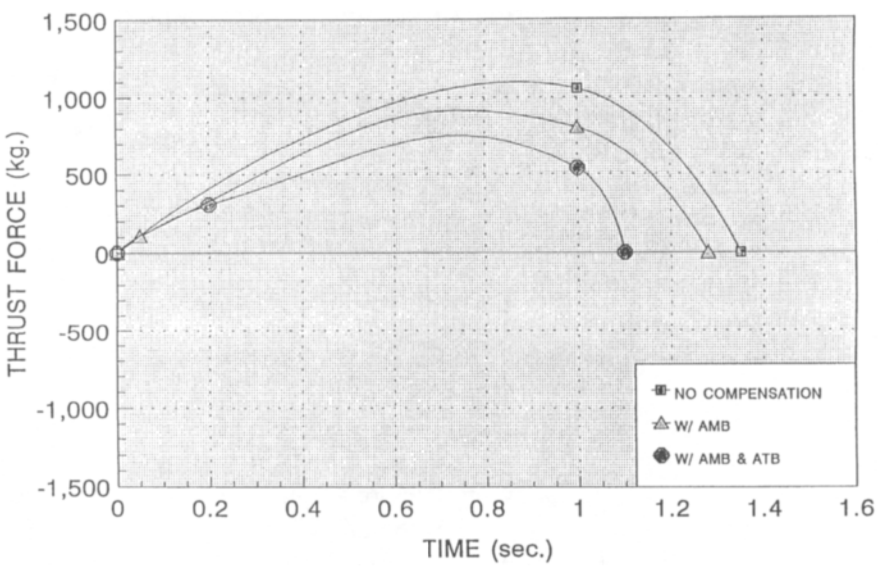

Figure 6-10. Maximum thrust loads with pressure upsets at the compressor discharge.

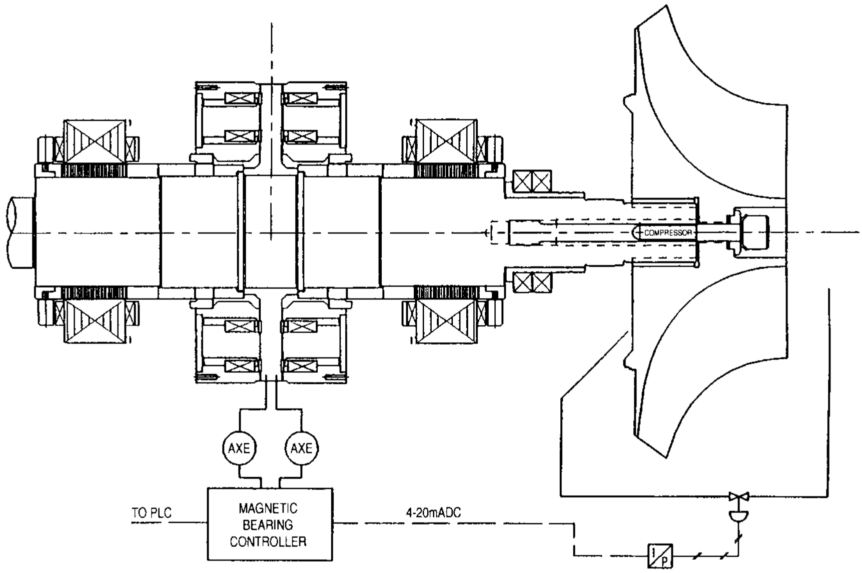

Figure 6-11. Automatic thrust control.

the thrust forces is available from the magnetic bearing thrust sensors. This signal, after being conditioned and biased to prevent oscillation, is used to control the position of a control valve connecting the region behind the wheel to the compressor suction. To prevent the two systems from counteracting each other, the control valve is activated when thrust load exceeds one half of the capability of the magnetic bearings. Also, the response time of the valve is set four times slower than the electronic signal (50 m/sec) to prevent hunting of the valve.

Automatic Clamping System Control

Processing plants are usually designed with a wide range of flow variations. Turboexpanders handle flow variations by variable inlet guide vanes, or IGVs. Variable IGVs maintain the thermal efficiency reasonably constant over a wide range of flows. Process gas pressure variation may cause separation of the nozzle adjusting ring and nozzle segments, resulting in blow-by or excess clamping, which prevents the unit from operating properly. The Automatic Clamping System (ACS) addresses this problem. Implementation of the ACS has improved turboexpander performance. Figure 6-12 shows the control schematic of the automatic clamping system.

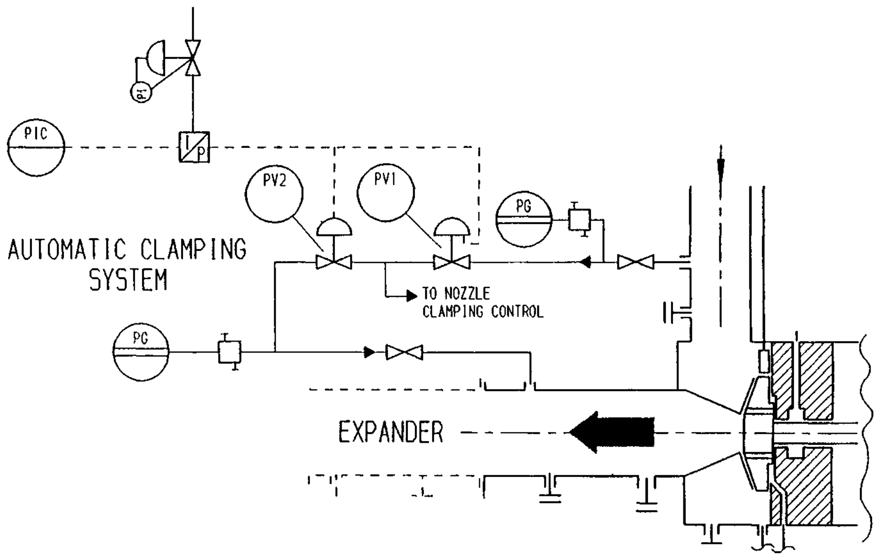

Figure 6-12. Automatic clamping system.

From the foregoing, it can be seen that turboexpanders with magnetic bearings require additional design features to ensure proper cooling and compensation of the axial loads imposed by process fluctuations. Turboexpander/compressor manufacturers are developing several new design features that address AMB requirements. Integration of these new design features with the magnetic bearings makes it possible for large industrial applications of magnetic bearing technology in hydrocarbon processing.

Dry Face Seal Leakage Test Under Static and Dynamic Conditions

Active Magnetic Bearings (AMB) and Dry Gas Seals (DGS) in Hydrocarbon Processing

The following case discusses the use of AMB and DGS in the same application.

A turboexpander was installed in a natural gas processing application for the first time in the early 1960s. This application had two major impacts on the turboexpander industry. On the technical front, the industry had to keep up with the latest developments in natural gas processing equipment. On the marketing front, the gas processing industry would not accept a monopoly of the market by a turboexpander supplier and promoted and financially assisted manufacturers who were willing to enter this market.

The turboexpander industry has met the challenges of improved thermal efficiency, reliability, availability, maintainability, along with compact design, reduced life cycle cost, and process fluid compatibility over the past 30 years. In the late 1980s and early 1990s, it made two major advancements to keep pace with the compressor industry. Turboexpanders with dry face seals were designed in 1989 and turboexpanders with active magnetic bearings were designed in 1991.

In this case, details of turboexpander design with dry gas seals and active magnetic bearings are presented in enough detail that the application to this specific process is clarified.

Turboexpanders with Dry Gas Seals. As mentioned above, the application of dry gas seals in centrifugal compressors dates back to the early 1980s. They are useful in process compressors because seal gas leakage is considerably reduced. Also, the contact of process gas and other constituents that may dilute lubricating oil is minimized.

Figure 6-13 shows the major components of a dry gas seal. In the static condition, the mating ring and primary ring are pushed tightly together by springs. Leakage of high-pressure process or seal gas is a few standard cubic feet per minute in the stand-still condition. The mating ring rotates with the shaft while the primary ring floats on a minutely thin film of gas. The mating ring has logarithmic spiral grooves machined at its surface to a precise depth. As the mating ring rotates, this creates a hydrodynamic effect that draws gas toward the tip of the grooves and forces the two faces apart to form the dynamic seal.

Tandem dry gas seals and other geometric or configurational variations were introduced in the late 1980s. These arrangements not only produced positive sealing between process gas and lubricating oil, but were also a safe design. For instance, with a tandem dry gas seal arrangement, should one seal fail (particularly the one on the process side), the other provides adequate sealing until shutdown.

As stated earlier, turboexpanders are normally used in cryogenic processes to produce isentropic expansion to cool down the process gas. Two common applications are natural gas processing plants and chemical plants. In natural gas processing plants, turboexpanders are installed to liquify heavier hydrocarbon components and produce lean natural gas with specified dew point limits to meet required standards.

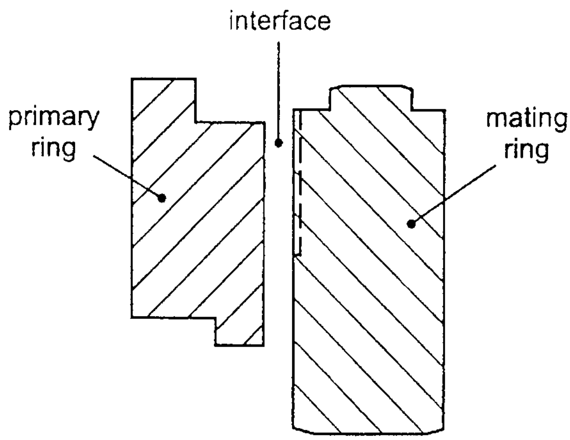

Figure 6-13. Major components of DGS.

In chemical plants, turboexpanders are used to produce refrigeration for cold box installations. In all except energy recovery applications, there are gas-to-gas heat exchangers downstream of the turboexpander. Figure 6-14 recaps a process flow diagram of a natural gas processing gas plant.

The seals in turboexpanders must accomplish two objectives. Their first function is to prevent cryogenic process gas leakage to the bearing housing where lubricating fluid is present. The second function is to prevent lubricating fluid, even in very small quantities, from escaping to the process side. If the latter migration occurs, lubricating fluid will freeze solid in the critical paths in the expander and any oil mist that may escape the turboexpander will freeze solid in the gas-to-gas exchangers. The former mishap may result in problems with turbo-expander operation, and the latter may result in plant shutdown for cleaning. Obviously, neither condition is desirable.

The first documented use of dry gas seals in turboexpanders was in 1989. At that time, an ethylene plant in Scotland worked with a dry gas seal manufacturer to retrofit a turboexpander-integral gear-generator package. The partial success of that project was sufficiently encouraging for both user plant and turboexpander manufacturer to undertake a redesign of all three expander stages. Dry face or gas seals were installed at that time.

This successful experience led to the design, manufacture, and use of turboexpanders with dry gas seals. Table 6-2 lists the installations and major design parameters of dry gas seals.

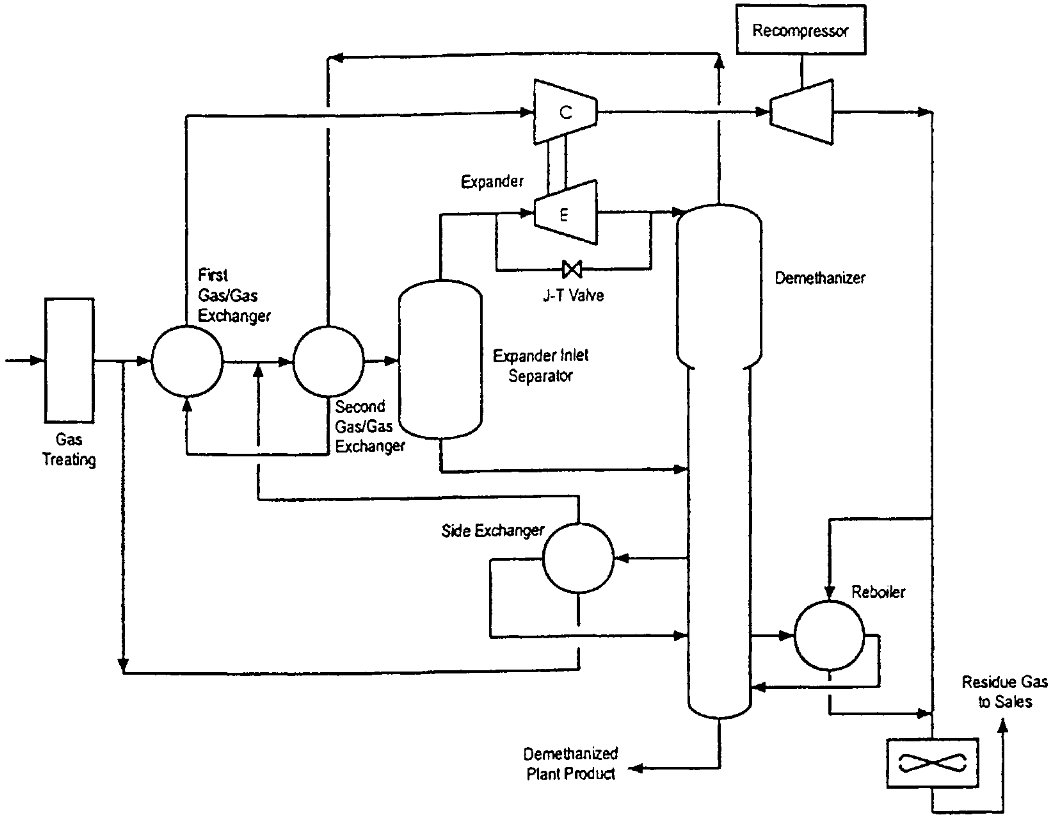

Figure 6-14. Process flow diagram of a typical natural gas processing plant.

Table 6-2
Some turboexpander applications of dry face or gas seals

NO.	Project	Application	Min. Press. Temp. oF	Max. Press. PSIA	Max. RPM	Rated Kw	Year Comm.
1	Job 3090	Exp./Gear/Gen./Ethylene Plant	-190	440	26,400	514	1996
2	ACR-30	Exp./Gear/Gen./Ethylene Plant	-50	1,116	7,600	6,333	1996
3	ACR-68-1	Exp. Oil Brake Ethylene Plant	-227	625	46,200	475	1996
4	ACR-68-2	Exp.-Oil Brake Ethylene Plant	-227	625	46,200	475	1996
5	ACR-68-3	Exp.-Oil Brake Ethylene Plant	-227	625	46,200	475	1996
6	ACR-117	Motor Gear-Comp. Ethylene Plant	-155	34	42,000	37	1995
7	ACR-148	N.G. Exp-Gen	21	1235	24,444	2368	1997
8	ACR-153	Exp./Gear/Gen./Energy Recovery	114	827	15,435	10336	1997
9	ACR-158	Steam, Energy Recovery	333	1123	46,200	2797	1997
10	ACR-166	Exp-Dyno, MTBE Plant	-208	105	40,800	281	1998
11	ACR-201	Exp.-Integ-Gear-Gen. N.G.	-244	449	15,225	1134	1998
12	ACR-209	Exp.-Integ-Gear-Gen., MTBE Plant	-200	163	28,770	391	1998

Purchasers of turboexpanders have occasionally demanded dry face (gas) seals with design configurations and redundancy that duplicate the componentry in their existing centrifugal compressors. Unfortunately, such duplication is not possible. As was demonstrated in our earlier chapters, turboexpanders are machines with high rotational speed and compact design. Figure 6-15 shows a cross-section of a turboexpander oil brake with oil bearings and labyrinth seal. The rotor consists of a short shaft and overhung wheels (i.e., impellers located outside the bearings). The space available on the shaft to install any type of seal is limited. Designs with a tandem seal arrangement, particularly tandem dry gas seals, is either impractical or physically impossible.

Turboexpander manufacturers and dry gas seal vendors recognizing the above limitation, worked together to develop a dry gas seal design that is an excellent compromise given the space limitation and customer requirement. Figure 6-16 shows a cross-section of the dry gas seal developed for turboexpanders.

The turboexpander dry gas seal consists of the conventional dry gas seal mating ring and primary ring, an outboard labyrinth, an inboard labyrinth, and the cavity to be vented, if desired. The outboard labyrinth reduces warm seal gas leakage to the process side; efficiency deterioration is thus minimized. The inboard labyrinth, on one hand, provides an additional seal between the process and lubricating fluids. On the other hand, it allows injection of an inert gas, if desired. In the latter case, inert gas leaks to the bearing side and to the cavity between the

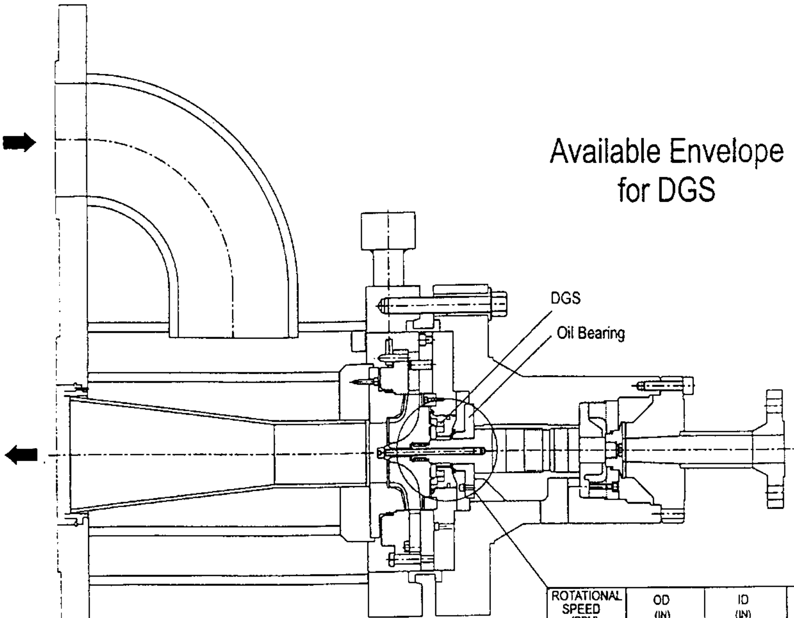

ROTATIONAL SPEED (RPM)	OD (IN)	ID (IN)	LENGTH (IN)
52,000	4.125	1.125	1.00
40,000	6.000	2.875	3.500
30,000	6.625	2.500	2.500
20,000	8.500	4.125	3.250
15,000	6.500	2.500	2.500

Figure 6-15. Cross-section of turboexpander oil brake with oil bearing and DFS.

mating ring and inboard labyrinth, where it can be directed to a vent or flare system.

Turboexpanders with Active Magnetic Bearings Revisited. The rate and extent of AMB applications has been much higher and wider than DGS. Table 6-3 lists some turboexpanders with AMBs in the natural gas processing and chemical industries.

Figures 6-17 through 6-21 show simplified diagrams of AMB systems. Figure 6-18 depicts two pairs of coils suspending the rotor about its inertial axis—as opposed to its geometrical axis as with conventional oil bearing systems. Thus, the rotor is self-balancing and vibration cannot occur. A third pair of coils is used for thrust compensation and to determine the precise shaft position.

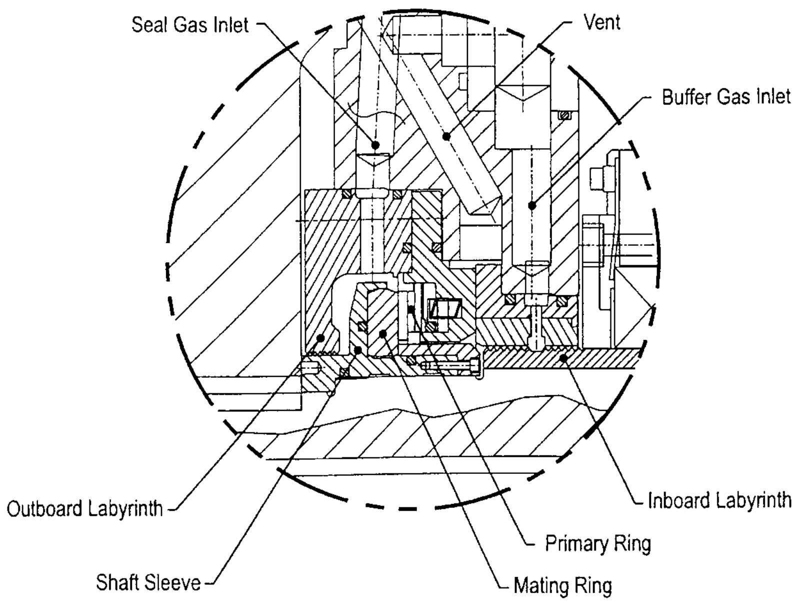

Figure 6-16. Cross-section of DGS for turboexpander compressor.

When the magnetic system is not operating, the shaft is supported by two non-lubricated ball bearings (Figure 6-19) with slightly larger bores than the shaft. During operation, these support bearings do not lend any support to the shaft. They are intended for landing only. During rotation, the levitated rotor will not experience mechanical contact with the bearings. Due to winding and windage losses during rotation, some heat is generated in the bearings. The heat is removed by the flow of seal gas and/or process gas from both the expander and the compressor ends.

AMB control is accomplished through a dedicated programmable logic controller (PLC). Digital controls replaced the early analog controls in the mid-1990s. Digital controls are more user-friendly and adaptable to remote monitoring and diagnostic actions. They greatly simplify and accelerate AMB tuning, which used to require several weeks at the manufacturer's shop and a few weeks at the job site.

Competent ABM manufacturers heat soak the components and test them for compatibility and resistance to corrosion. Extensive chemical soak tests were performed in the early 1990s and the results did not

(text continued on page 356)

Table 6-3
Some turboexpander applications of active magnetic bearings

PROJECT	UNIT	APPLICATION	P1(PSIA)	T2 (°F)	Rated kW	LOCATION	START-UP DATE	AMB SUPPLIER	AMB SYSTEM
ACE-A	ETB	Air Separation Plant	747	-276.8	600	NETHERLANDS	1990	S2M	ANALOG
ACE-B	ETB	Air Separation Plant	138	-264.4	175	JAPAN	1993	S2M	ANALOG
ACR-30-1	EC	Natural Gas Plant	1290	-7.6	6100	NORWAY	1997	S2M	ANALOG
ACR-30-2	EC	Natural Gas Plant	1290	-7.6	6100	NORWAY	1997	S2M	ANALOG
ACR-30-3	EC	Natural Gas Plant	1290	-7.6	6100	NORWAY	1997	S2M	ANALOG
ACR-30-4	EC	Natural Gas Plant	1290	-7.6	6100	NORWAY	1997	S2M	N/A
ACR-44-1	EC	Natural Gas Plant	927	-55	4000	CONGO/OFFSHORE	1996	S2M	ANALOG
ACR-44-2	EC	Natural Gas Plant	927	-55	4000	CONGO/OFFSHORE	1996	S2M	ANALOG
ACR-44-3	EC	Natural Gas Plant	927	-55	4000	CONGO/OFFSHORE	1996	S2M	N/A
ACR-68-1	EC	Ethylene Plant	126	-202.8	500	QATAR	1997	S2M	ANALOG
ACR-68-2	EC	Ethylene Plant	126	-202.8	500	QATAR	1997	S2M	N/A
ACR-161-1	EC	Natural Gas Plant	1100	-50	6000	NORTH SEA/UK	1999	S2M	DIGITAL
ACR-161-2	EC	Natural Gas Plant	1100	-50	6000	NORTH SEA/UK	1999	S2M	DIGITAL
ACR-161-3	EC	Natural Gas Plant	1100	-50	4000	NORTH SEA/UK	1999	S2M	DIGITAL
ACR-180-1	EC	Ethylene Plant	1200	-50	4000	NORTH SEA/UK	1999/2000	S2M	DIGITAL
ACR-180-2	EC	Ethylene Plant	1200	-50	4000	NORTH SEA/UK	2000	S2M	N/A
ACR-207-1	EC	Ethylene Plant	470	-204	500	SWEDEN	1999	S2M	DIGITAL
ACR-207-2	EC	Ethylene Plant	185	-209	600	SWEDEN	1999	S2M	DIGITAL
ACR-207-3	EC	Ethylene Plant	185	-209	600	SWEDEN	1999	S2M	N/A

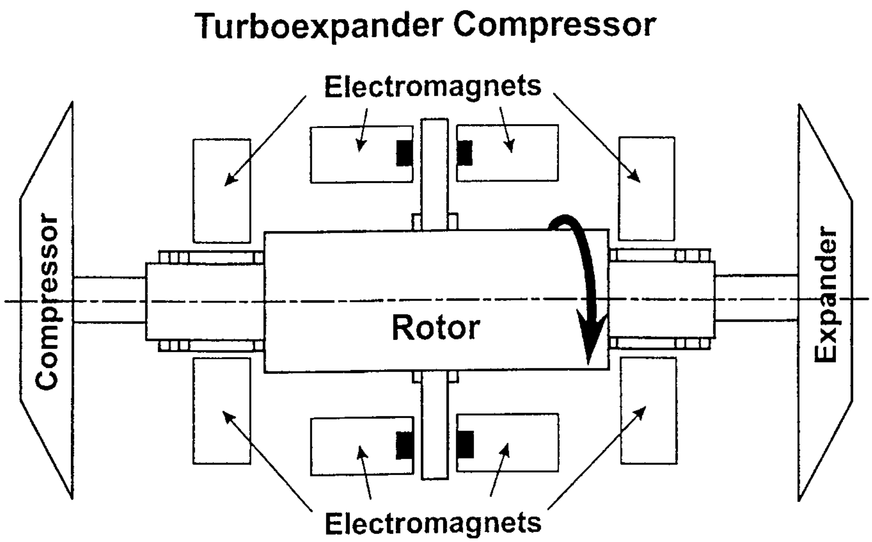

Figure 6-17. Simplified diagram of AMB.

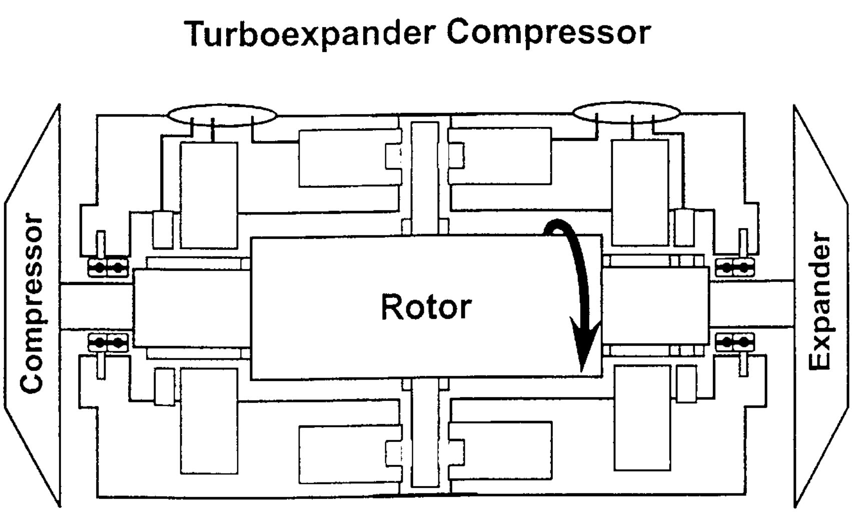

Figure 6-18. Simplified diagram of AMB.

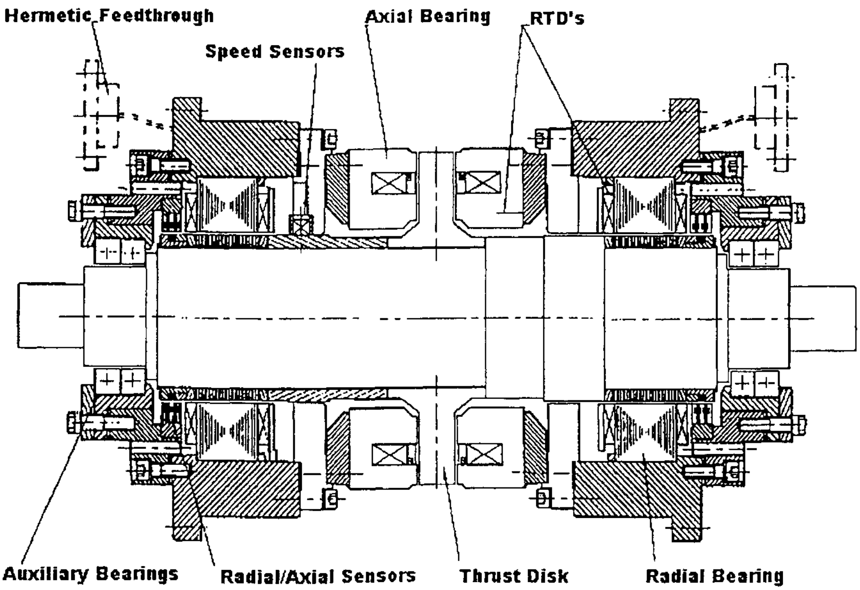

Figure 6-19. Simplified diagram of AMB.

(text continued from page 353)

show any corrosion from such aggressive compositions as hydrogen sulfate, which may be found in natural gas.

AMB design involves considerations and concerns about electrical area classifications and certification by national or international authorities. In the pressurized configuration mentioned earlier in this chapter, the bearing housing is pressurized with process gas and, due to the lack of oxygen, there is no danger of explosion. An international authority such as CENELEC does not consider this design a potential hazard and, therefore, does not require certification. For the atmospheric bearing housing, however, the arrangement is not inherently safe and, hence, CENELEC certification should be issued.

Turboexpanders with AMB and DGS. Due to the advantages of DGS and AMB, a combination of the two is often worthy of consideration. Nevertheless, it should be noted that each serves a completely different purpose and combining the two does not necessarily enhance the total design of the turboexpander. For this reason, a labyrinth may still be the seal component of choice (Figure 6-20). Dry gas systems

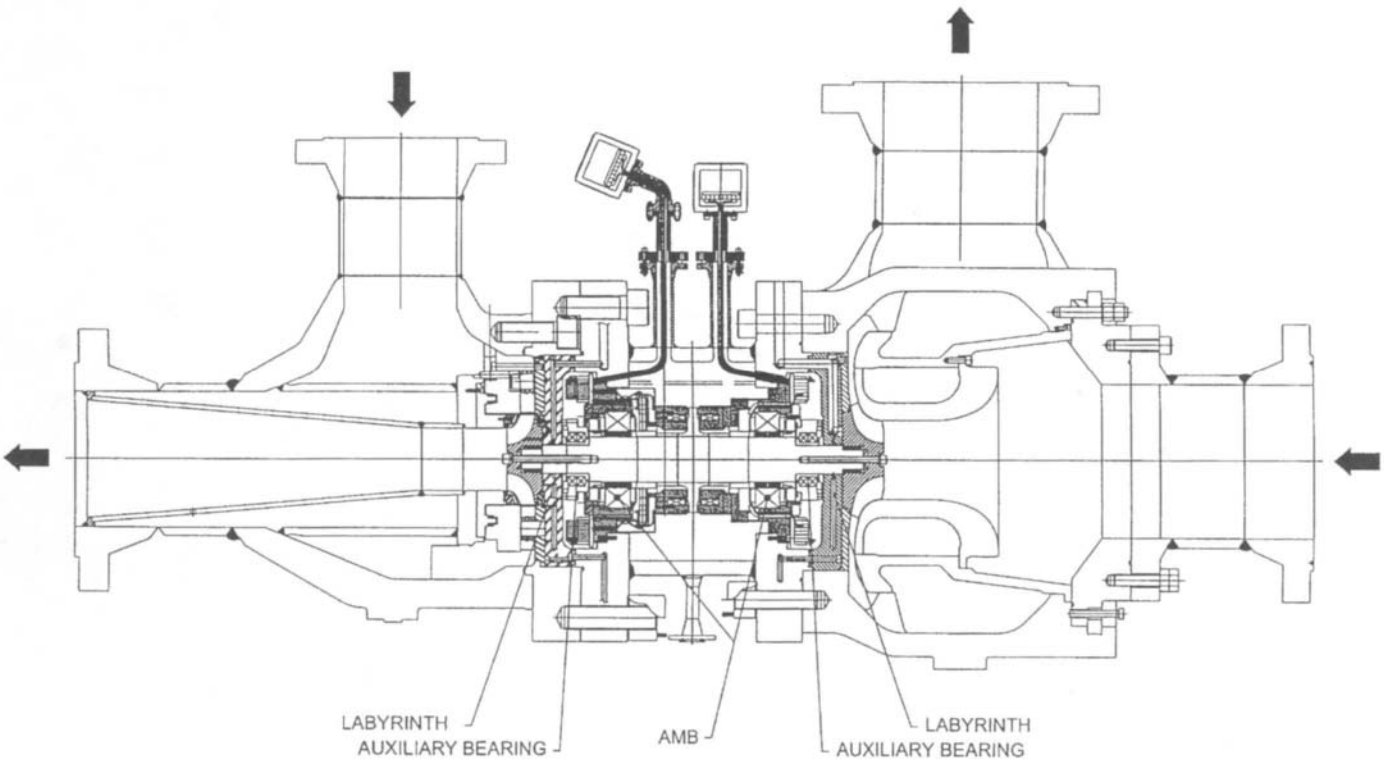

Figure 6-20. Cross-section of turboexpander compressor with AMB and labyrinth seal.

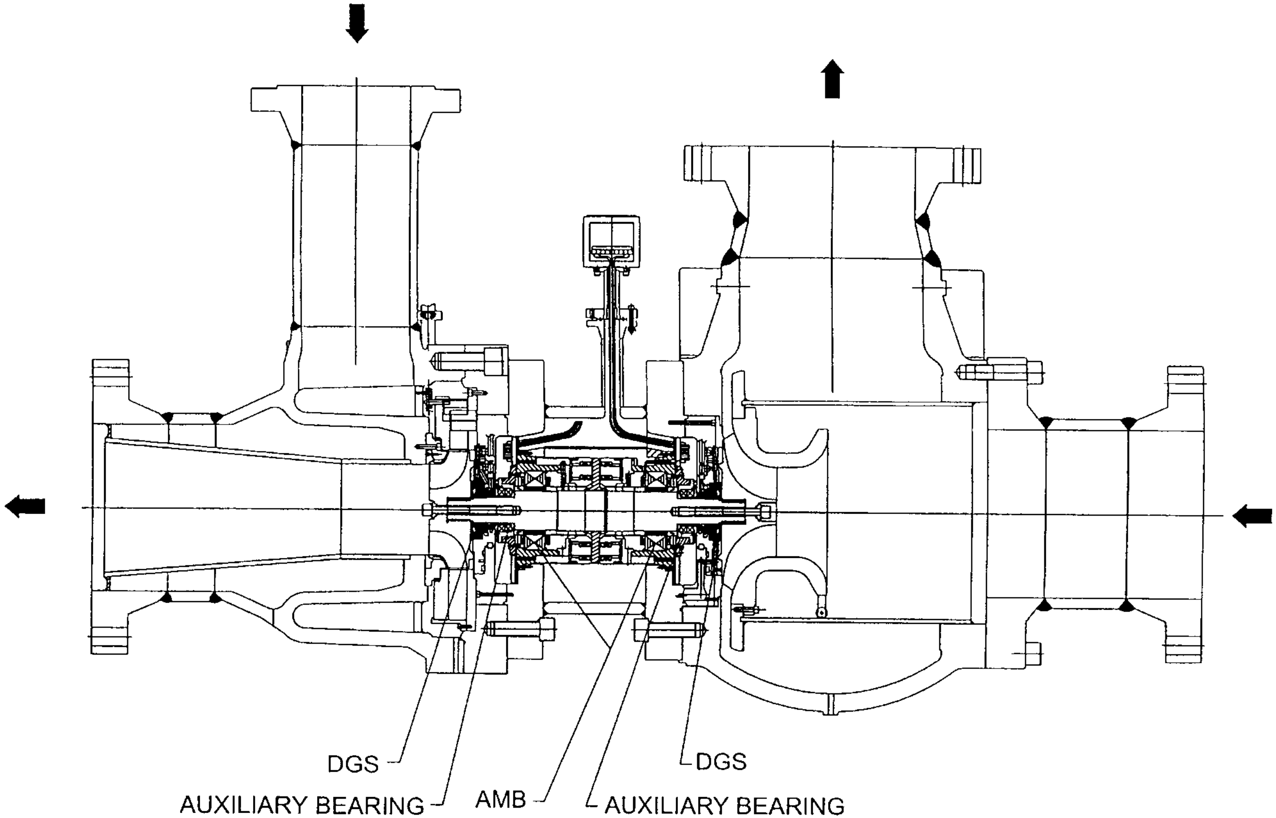

Figure 6-21. Cross-section of turboexpander compressor with AMB and DGS.

protect process gas from oil contamination and reduce seal gas loss. AMB systems, on the other hand, provide an oil-free design. Therefore, a combination of DGS and AMB is of interest when the turboexpander is designed with AMB using an atmospheric bearing housing.

In this design, the inboard labyrinth of the DGS is fed with seal gas that is compatible with the process gas. The outboard labyrinth is injected with an inert gas. With this arrangement, the bearing housing is purged with inert gas, the seal gas leakage is minimized, and the mixture of seal gas and inert gas is vented to a flare or disposal system. Figure 6-21 shows a cross-section of a turboexpander with AMB and DGS.

SQUEEZE FILM DAMPERS[4]

Squeeze film dampers have long been used to combat rotor dynamic and stability problems that conventional bearings cannot solve on turbomachinery rotor systems. The use of squeeze film dampers in problem process machinery has tainted it as a "treat-the-symptom" solution, and many users shy away from using squeeze film dampers for this reason. Also, their limited use is explained by the difficulty in accurately predicting performance, particularly with o-ring supported dampers.

These deficiencies with conventional dampers have been addressed with the novel integral damper centering spring design ("IDCSD"). One of the key attributes of this design is the ability to accurately predict its stiffness and damping characteristics. The IDCSD can also be easily adapted to work with fluid film bearings in a split configuration, as required by certain API specifications. The stability with existing fluid film bearings can, therefore, be extended with this new damper concept. This should allow operation at higher speeds and possibly with longer spans between bearings. The balance limitations and threshold speeds on many existing machines can also be extended.

The ability to center this damper in applications where relatively heavy rotors are used has proven to be very advantageous. The limited axial space present with most machinery does not hinder its applicability. Furthermore, the accuracy in predicting the stiffness and damping is another desirable feature that is missing with conventional damper designs.

---

[4] *Source: F. Y. Zeidan, "Application of Squeeze Film Dampers,"* Turbomachinery International, *September/October 1995.*

Certain facets of squeeze film dampers should be thoroughly understood to properly select the specific design required for a given application. Highlighting the theory of squeeze film dampers is helpful in this regard.

One of the key design features in a squeeze film damper bearing is the introduction of support flexibility and damping in the bearing/support structure. This translates to lower transmitted forces and longer bearing life, particularly for machinery that is designed to operate above rotor critical speeds. Machinery that runs above the first critical speed is classified as supercritical, and constitutes an increasing number of the new high performance machinery manufactured today. Higher efficiency and lower bearing transmitted forces are some of the advantages of running supercritical. Lower damping (not more damping) will also result in lower transmitted forces. However, since some damping is required to allow for safe traversing of the critical speed, an optimum value must be determined to satisfy the two rather conflicting requirements. For this reason, an optimization process is generally required to determine the correct amount of damping.

TYPE OF SQUEEZE FILM DAMPERS

The following describes some of the commonly used squeeze film dampers and introduces one of the more novel damper designs, which clearly has application in turboexpanders. Examples of the optimization process required in the design and selection of squeeze film dampers and their applications to solve stability and critical speed problems are also demonstrated.

Squeeze Film Dampers without a Centering Spring

Figure 6-22 represents the simplest of the squeeze film damper configurations. The outer race, a rolling element bearing or the outer bearing shell in the case of a fluid film bearing, is allowed to float and "whirl" in a clearance space between the bearing outer diameter and the housing inner diameter. As shown in Figure 6-22, the outer race, or bearing shell, forms the damper journal that is allowed to whirl, yet is prevented from spinning by a "loose" antirotation mechanism. This configuration is necessary to allow the damper journal or outer race to orbit (not spin) in a precession motion, squeezing the oil in the small clearance space and generating an oil film pressure and, consequently, a damping force.

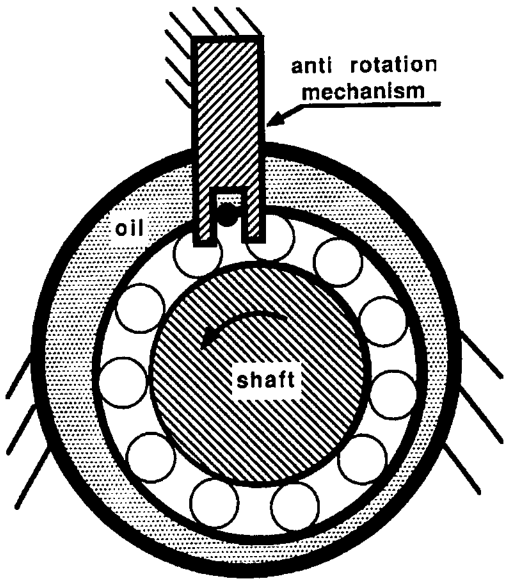

Figure 6-22. Squeeze film damper without a centering spring.

The absence of a mechanical centering spring in this design configuration means that the damper journal is bottomed out at startup. As the speed increases and the shaft starts to whirl, the damper's journal (bearing shell outer surface) lifts off. The oil film in a squeeze film damper does not produce stiffness (i.e., support a static load) like conventional fluid film bearings. However, the damper does develop stiffness-like behavior. This stiffness is due to the cross-coupled damping coefficients, which exhibit stiffness-like (spring) characteristics.

The non-centered damper is one of the most non-linear of the squeeze film damper designs. There are two basic mechanisms that are responsible for this non-linear behavior. The first mechanism is attributed to the non-linear characteristic produced by the cross-coupled damping coefficients. The second source of non-linear behavior present with this type of damper is a direct consequence of the bottoming out of the damper journal. This generally occurs at high side loads or because of excessive unbalance forces. The bottoming out of the damper journal, which is very likely with this design (due to the absence of a centering spring), will result in a bilinear spring behavior. This non-linear behavior can be inferred from the sub-synchronous and super-synchronous vibration characteristics often noted on this type of damper. In some cases, the impact force generated when the damper journal bottoms out excites the lowest natural frequency of the rotor. In the case of flexible casings and support structures, the resonance frequencies of the structure can also be excited.

Non-centered dampers are commonly used on aircraft gas turbines, light-weight process compressor rotors, and automotive turbochargers. In aircraft their use has been limited to the smaller engines, where the use of a conventional style cantering spring (squirrel cage spring) is difficult to implement due to space limitations.

Elastomeric O-Ring Supported Dampers

These dampers constitute the simplest means of providing a centering spring in a squeeze film damper. An illustration of this damper design is shown in Figure 6-23. The advantages of this design are its simplicity, ease of manufacture, and the ability to incorporate the damper into smaller dimensional envelopes. The relatively low radial space required makes it the preferred method to retrofit existing machines in the field. The o-ring doubles as a good end seal, which helps increase the effectiveness of the damper by reducing side leakage.

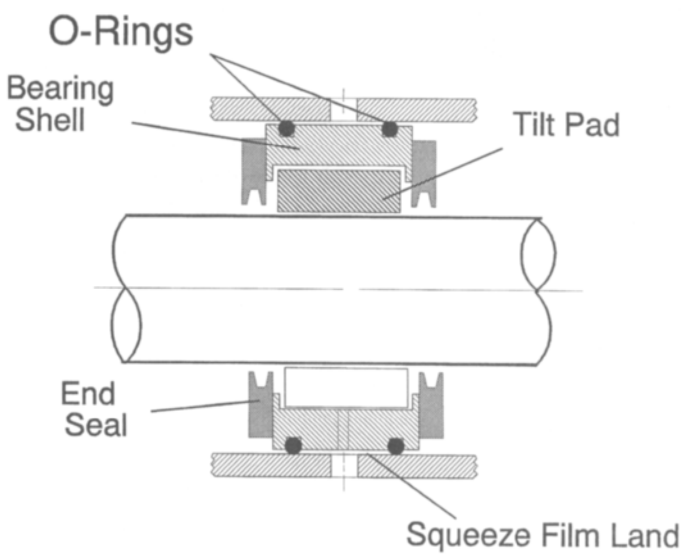

Figure 6-23. Schematic of an o-ring supported squeeze film damper.

Some of the disadvantages with this design are attributed to the limited range of stiffness that can be achieved with elastomers. Predicting the stiffness with a good degree of certainty is difficult in elastomeric materials, due to the material variance and the influence of temperature and time on its properties. Both elastomer stiffness and damping are strongly influenced by temperature. The o-ring design is also susceptible to creep, causing the damper to bottom out, which, as discussed above, may lead to bilinear spring behavior.

O-ring dampers are not capable of taking thrust loads and cannot be easily manipulated for centering the damper journal within the damper clearance space. One means of achieving some centering capability is by making the o-ring groove eccentric. This limitation makes them suitable only for use with light-weight rotors.

High-speed and high-pressure centrifugal compressors prone to stability problems are frequently fitted with these o-ring dampers. The damper is installed in series with tilting pad fluid film bearings to enhance the stability of the compressor. Although most of their use has been primarily aimed at improving stability, they have also been used to reduce the synchronous response due to imbalance, or to shift the peak unbalance response outside the operating speed range.

The o-rings also provide a form of internal friction damping (hysteretic damping), in addition to the squeeze film damping (viscous damping) produced by the oil in the damper. The elastomer material of the o-ring limits the use of such dampers to mostly low-temperature applications. The hysteretic damping from the o-rings has also been used in series with rolling element bearings and gas bearings without any oil in the clearance space (dry o-ring damper). High-speed dentist drills are an example where this configuration is commonly used. These drills are composed of air turbines running on ball or gas bearings, with elastomer o-ring supports for increased damping and improved stability.

Squirrel Cage Supported Dampers

This type of damper is the most commonly used squeeze film damper design, particularly in aircraft engines where its use is widespread. Most large aircraft gas turbine engines employ at least one, and in many instances two or three, of these dampers in one engine. A schematic of this damper is shown in Figure 6-24. A distinctive feature necessary with such a design, is the relatively large axial space

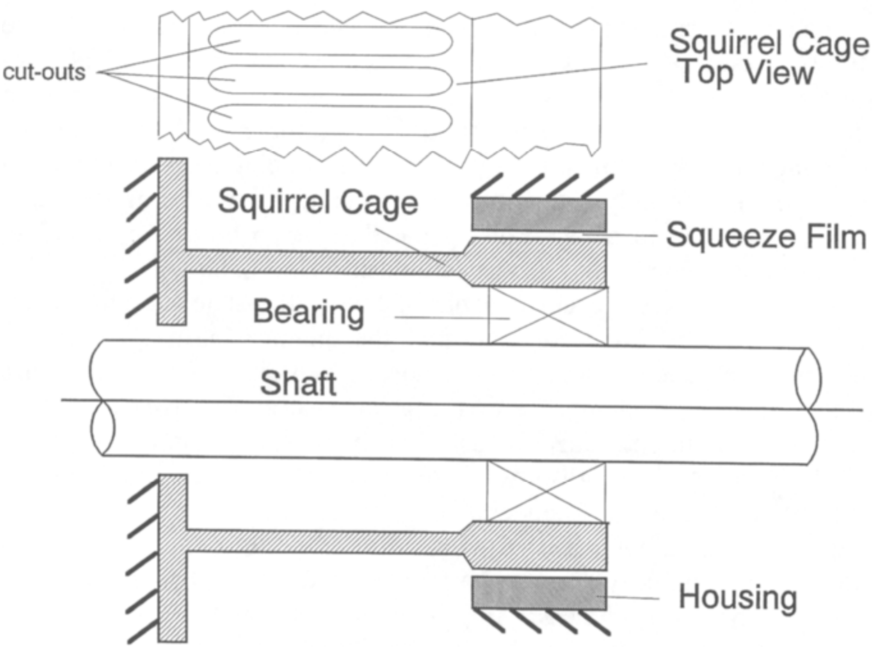

Figure 6-24. Schematic of a squirrel cage supported damper.

required in comparison to the damper length. This is one of the major drawbacks of this damper design. The squirrel cage forming the centering spring for the damper quite often requires three to four times as much axial space as the damper itself.

Assembling the squirrel cage spring and centering the journal within the clearance space requires special tools and skills. The squirrel cage spring also complicates the damper end seal design and assembly. It is also difficult to offset the spring assembly to account for the gravity load due to the shaft weight. Maintaining parallelism between the damper journal and housing is another factor that adds uncertainty and complications to this design.

Integral Damper-Centering Spring

These layouts are configured as shown in Figure 6-25. The cantilevered support ribs, along with the sector they are supporting at both ends, form a centering spring element. The small gap between the sector and the outer ring forms the squeeze film damper clearance

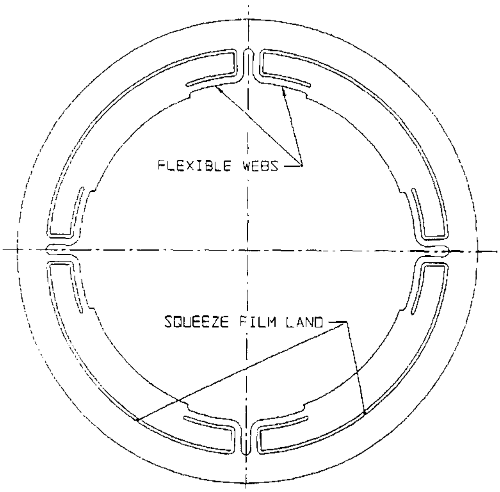

Figure 6-25. Schematic of an integral centering "flexure pivot" spring squeeze film damper.

space. This new, patented centering spring squeeze film damper design does not occupy any additional axial space beyond the existing length occupied by the bearing. This is a major advantage over conventional squirrel cage damper supports. Furthermore, unlike the first two damper configurations (non-centered and o-ring supported dampers), this new design is capable of absorbing axial thrust loads without locking the damper's radial motion.

The integral design makes manufacturing, assembly, and inspection much easier and more reliable than any other configuration. The squeeze film gap can be precisely made using this concept. Wire electric discharge machines (EDM) provide an excellent means of obtaining the desired clearance with high precision and repeatability, maintaining excellent parallelism between the damper journal and housing. Damper retrofits in process type equipment, which are required to meet APl specifications requiring a split bearing configuration, can be easily accommodated with this new concept. This design, unlike conventional style dampers, can be easily provided in a split configuration, as shown in Figure 6-26.

Optimization for Improved Stability

In process equipment, squeeze film dampers are primarily used to improve rotordynamic stability. They are commonly used as a last

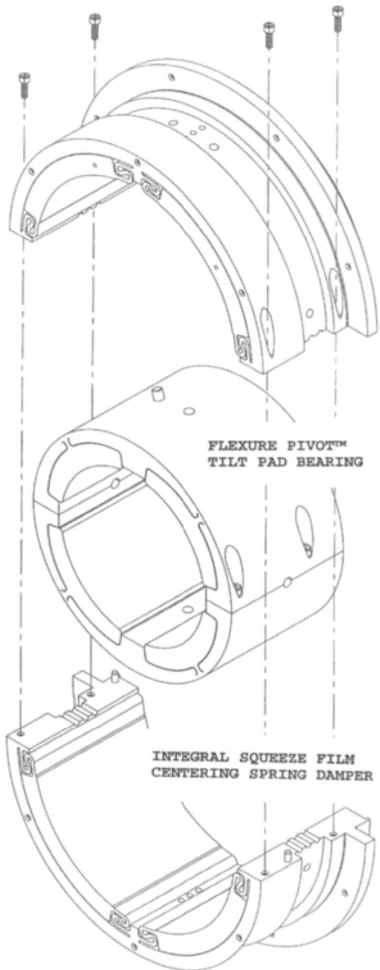

Figure 6-26. Schematic of a split integral squeeze film damper.

resort because of the complexity and drawbacks inherent in conventional dampers. The difficulty associated in accurately predicting damper performance due to cavitation is another reason for their limited use. The new damper design with the integral centering spring overcomes many of these difficulties as shown by the following example.

This example demonstrates the importance of the centered damper in suppressing the subsynchronous vibration exhibited by the relatively heavy rotor shown in Figure 6-27. This rotor was supported by o-ring

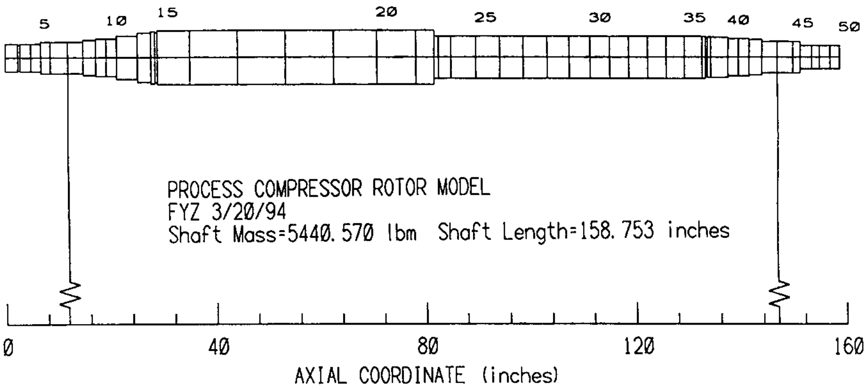

Figure 6-27. Rotor model for a typical heavy process compressor.

dampers, but continued to exhibit subsynchronous vibrations after the damper retrofit. The stability without the squeeze film damper is very low, as indicated by the low logarithmic decrement predicted for the first forward mode shown in Figure 6-28. The rotor is more flexible than the bearings, resulting in small motion at the bearing supports and, consequently, low effective damping. The bearings are virtually at a node, and therefore are ineffective in suppressing the subsynchronous vibrations.

The use of a squeeze film damper in series with the tilting pad bearings introduces flexibility and damping to the bearing support. The

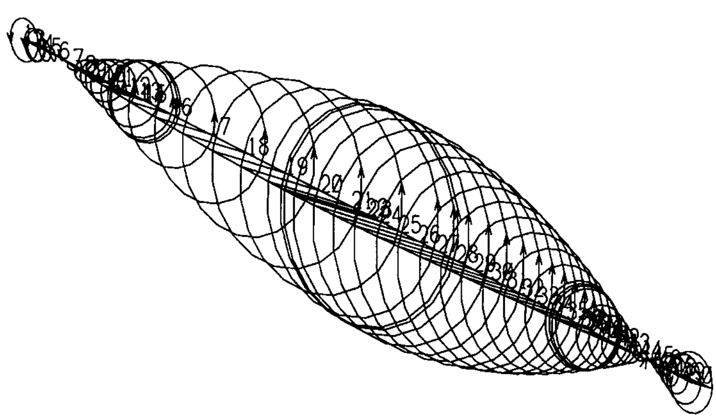

Figure 6-28. First forward mode on fluid film tilt pad bearings.

damping provided by the squeeze film damper, however, must be optimized as shown in Figure 6-29. Low damping values may not be sufficient and high damping may lock the damper and reduce the effective damping, as evidenced by the reduction in the logarithmic decrement at high damping levels.

Using the optimum damping value and varying the squeeze film support stiffness showed that a more flexible spring support allows motion at the bearing, resulting in more effective damping and suppressing of the instability and subsynchronous vibrations. However, if the damper bottoms out, as was the case with the o-ring damper, the stiffness increases and the damper becomes ineffective. The damper is very effective when the damper journal (tilt pad bearing shell OD) can be held close to the centered position within the damper clearance space. This is difficult to accomplish with conventional o-ring dampers, particularly in the case of relatively heavy rotors.

The use of an integral centering spring damper configuration allows precise location of the damper journal and realization of the required stiffness value. To achieve the low stiffness values while still maintaining lower stresses, the damper configuration shown in Figure 6-25 was used.

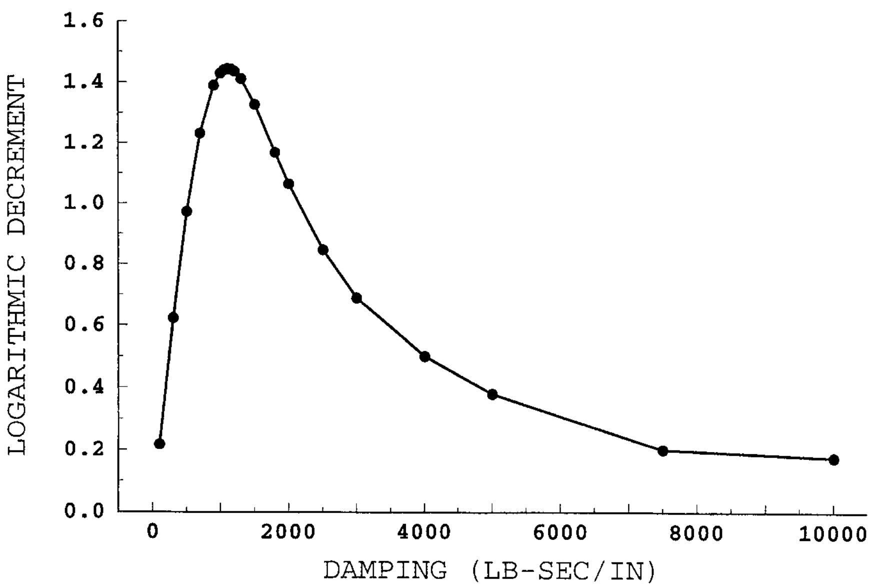

Figure 6-29. Damping optimization for improved stability.

The "S"-shaped flexible elements were required to keep the stiffness and stresses low, due to the relatively heavy rotor weight as evident by the finite element stress analysis shown in Figure 6-30. The wire EDM technology allows the production of such a damper device, which can be easily designed with an offset to compensate for the deflection due to rotor weight.

The stability of the rotor-bearing system was greatly improved with the optimized squeeze film damper. This is evident from the relatively high logarithmic decrement for the first forward mode shown in Figure 6-31. The flexibility introduced with the integral centering spring allows for motion at the bearings, making the damping more effective.

Control of Critical Speeds

The squeeze film damper in series with a fluid film bearing also provides a means for improving the synchronous response, an advantage rarely used with process type equipment. The tight vibration restrictions with the latest API specifications, and the even more restrictive specifications dictated by users, makes the squeeze film damper an attractive and practical alternative to more costly and time

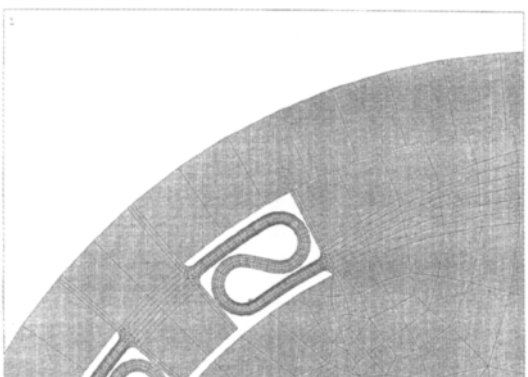

Figure 6-30. Stress and stiffness analysis using ANSYS.

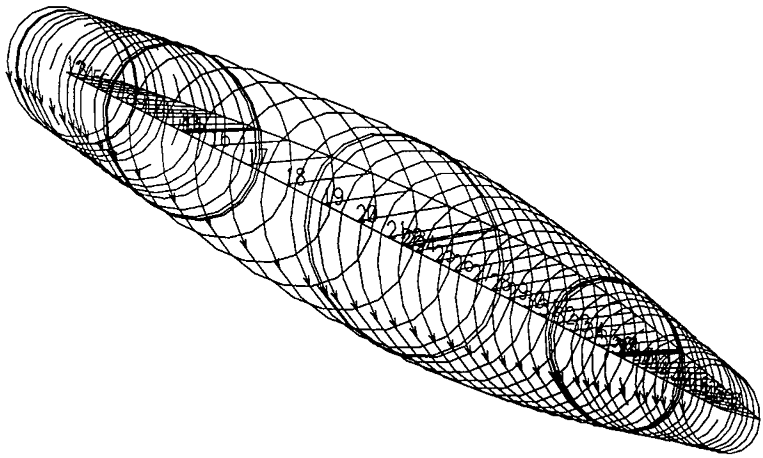

Figure 6-31. First forward mode after including a squeeze film damper in series with the tilt pad bearing.

consuming designs. The squeeze film damper helps reduce the sensitivity to unbalance, which often results in significant delays during shop testing and commissioning of process-type equipment.

RADIAL FIT BOLTS[5]

Radial fit bolts are a special feature used in all types of turbomachinery. They are of increasing importance to users that are both reliability-minded and concerned about life-cycle costs. The radial fit coupling bolt was originally developed for coupling steam turbine shafts by Pilgrim International in Oldham, UK. It is equally useful to coupling other equipment, including, of course, hot gas expander shafts.

Several power stations in England and the U.S. that installed radial fit coupling bolts to turbines five years ago are now finding dramatic savings in outage costs, due to the greater ease of separation and reassembly of turbine shafts and the reusability of the bolts. The bolts, which have been available since the late 1980s, have since then completed several full outage cycles. Bolts removed during a routine service outage at two nuclear power stations were undamaged and could not only be reused, but reinstalled in minutes. This saved

[5] *Source: "Radial-Fit Bolts Save Millions,"* Turbomachinery International, *September/October 1995.*

millions of dollars in alternative power costs through the dramatic shortening of outage times compared with using traditional bolting.

HYDRAULIC BOLT

The hydraulically tensioned, radial-fit bolt (Figure 6-32) replaces the traditional turbine shaft coupling bolt and is reusable. The main body of the bolt is threaded at each end and has a slight taper on the center section, which engages with the similarly internally tapered sleeve and the two nuts. The bolt is taper-bored at each end to accept the puller that is part of the hydraulic tensioning system.

To install the bolt body, it is inserted in the hole through the two flanges with the sleeve in the clearance position. Hydraulic pressure pushes the sleeve into the final (interference) fitted position, and the puller draws the bolt back into the sleeve. The nut is fitted at one end and the bolt is hydraulically tensioned with the other nut. The entire process takes about 15 min per bolt.

The central body of the bolt has circumferential grooves, which allow lubricant to flow between the bolt and sleeve. It can be removed by first removing the nuts and then fitting an oil injector into the

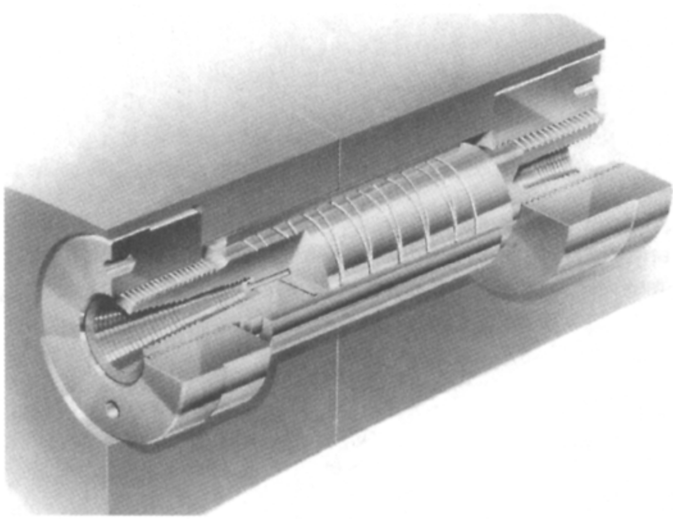

Figure 6-32. The radial-fit bolt fully assembled in the turbine flanges, showing the taper barrel, and the oilways that enable hydraulic pressure to force bolt and sleeve apart.

puller hole. Bolt and sleeve are separated by oil pressure, forcing the tapered surfaces apart. The coupling sleeve is a clearance fit, rather than an interference fit (as with a traditional bolt), and can be easily removed. This is where the time is saved.

When the bolt is removed and the pressure relaxed, the sleeve contracts and can be withdrawn. Normally the bolts and sleeves can be reused. Only if any machining of the holes is required, perhaps to match an old flange with that of a new replacement rotor, would sleeves be replaced, but the same bolts could be used.

ALIGNMENT TOOL

A number of turbomachinery users have specified Pilgrim's CHAT (Coupling Hole Alignment Tool, Figure 6-33), in addition to radial fit bolts. CHAT is a further development of the radial fit bolt, designed to achieve coupling hole alignment in the least amount of time and to a tolerance that permits radial bolt assembly. The CHAT tool is based on the same principle as the bolt and also uses hydraulic power.

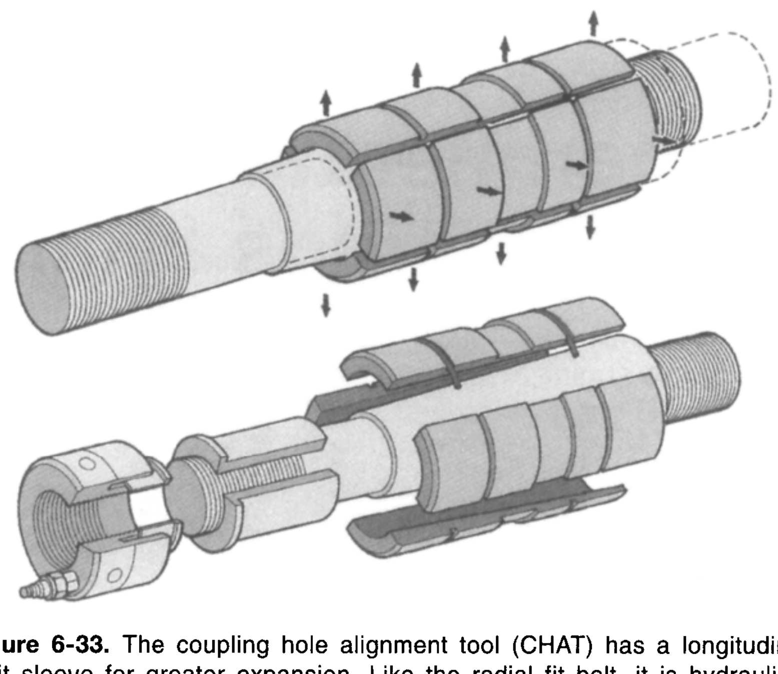

Figure 6-33. The coupling hole alignment tool (CHAT) has a longitudinally split sleeve for greater expansion. Like the radial fit bolt, it is hydraulically tensioned, but there is no hydraulic separation of core and sleeve.

However, the sleeve is segmented, allowing considerable expansion to turn the couplings relative to each other, close the couplings, and maintain alignment while the radial fit bolts are installed.

Depending on the size of the coupling, up to four CHAT tools might be used to effect the alignment. Once enough radial fit bolts are fitted to maintain the alignment, the CHAT tools are removed and the bolting completed.

CONTROLS

Control valve configurations and arrangements are particularly significant in turboexpander applications. Varying configurations are discussed below with specific reference to FCC (fluid catalytic cracking) expander applications.

VALVE ARRANGEMENTS FOR FCC EXPANDERS[6]

One of many decisions that must be made during the planning stage of a FCC expander installation is the valve arrangement that will be used. The train configuration, accuracy of process control, methods of intended operation, and cost must be considered in selecting the valve arrangement. Several possible valve arrangements are of interest and their effects on operation and power recovery train configuration merit consideration.

Full Main Air Blower Train Valve Arrangements

As discussed in Chapter 5, a full main air blower train configuration consists of the power recovery expander, main air blower, steam turbine, motor/generator, and possibly a gear. In large-capacity, 60-cycle installations, the main air blower train may not require a gear. The availability of certain utilities and the operating philosophy influence whether a steam turbine, motor-generator, or both are included in the train. Selection of the valve arrangement can be made concurrent with, or independent of, the train configuration decision. Nevertheless, it is recommended that the train configuration be determined before the valve arrangement is finalized.

Several main air blower train valve arrangements are possible.

[6] *Source: Elliott Company.*

One Valve Arrangement

The simplest arrangement has only one valve, which is located upstream of the expander inlet. This valve maintains the desired pressure control of the regenerator (Figure 6-34). It is the least expensive arrangement, but it does not provide flexibility in operation or upgrading of the reactor throughput. If the expander is out of service, the entire FCC process is inoperable. Due to the lack of flexibility, this arrangement is not desirable.

Two Valve Arrangement

The addition of a second valve that permits the flue gas to bypass the expander and move directly to the waste heat recovery system enhances the flexibility of FCC operation compared to the single valve arrangement. Shown in Figure 6-35, the large single bypass valve can pass all the flow if the expander is out of service. It can protect the regenerator and reactor if an overpressure situation should develop. This valve can also provide regenerator pressure control if the throughput is increased beyond the expander capability.

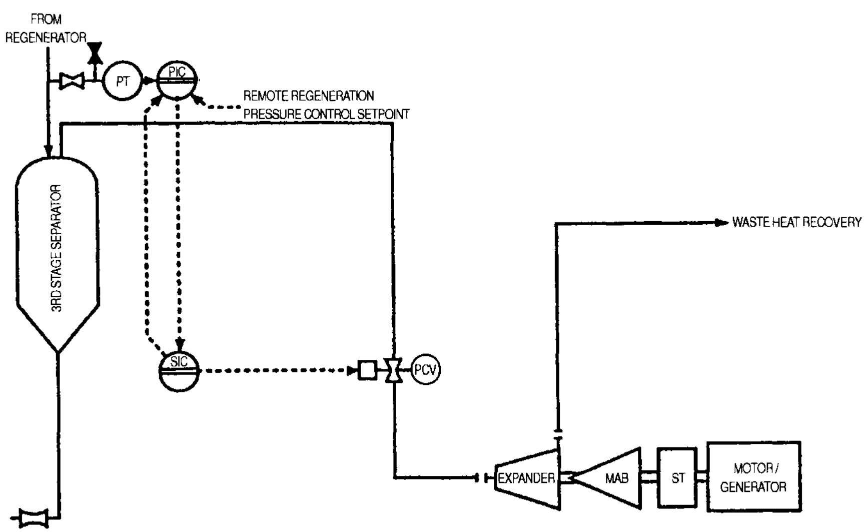

Figure 6-34. One valve arrangement.

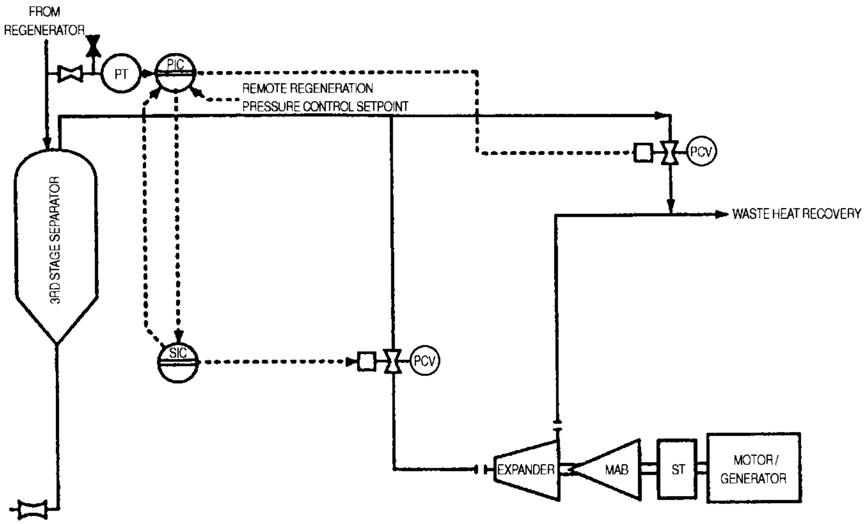

Figure 6-34. Two valve arrangement.

Three Valve Arrangement

Although more expensive, there are advantages to installing a second expander inlet valve in series with the regenerator pressure butterfly control valve (Figure 6-36). The second valve has a faster closure time constant and, therefore, limits the expander terminal speed during an emergency overspeed condition. The expander inlet can be tightly shut off if the expander is out of service. Also, expander blade erosion is eliminated during windmilling because there is no discernible valve leakage. During startup, the second valve in series can take part of the pressure drop, thereby providing a better operating point for the control valve.

Four Valve Arrangement

Installation of a shut-off valve in the expander exhaust line prevents backflow during expander isolation (Figure 6-37). Although the need for this valve may not be immediately obvious, it can be very beneficial if the expander is operated for an extended period in the windmilling mode. Often this type of operation is not anticipated during the initial evaluation of valve requirements, but becomes necessary at some later date. For example, it is useful when it is deemed prudent

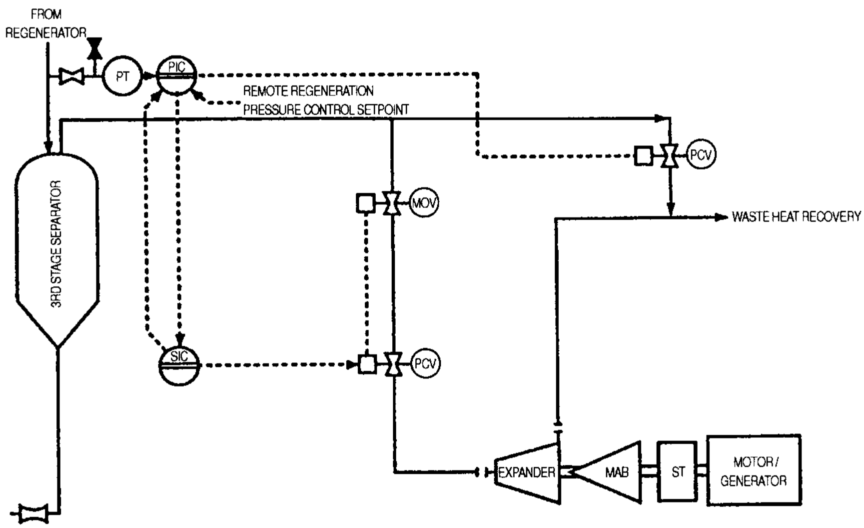

Figure 6-36. Three valve arrangement.

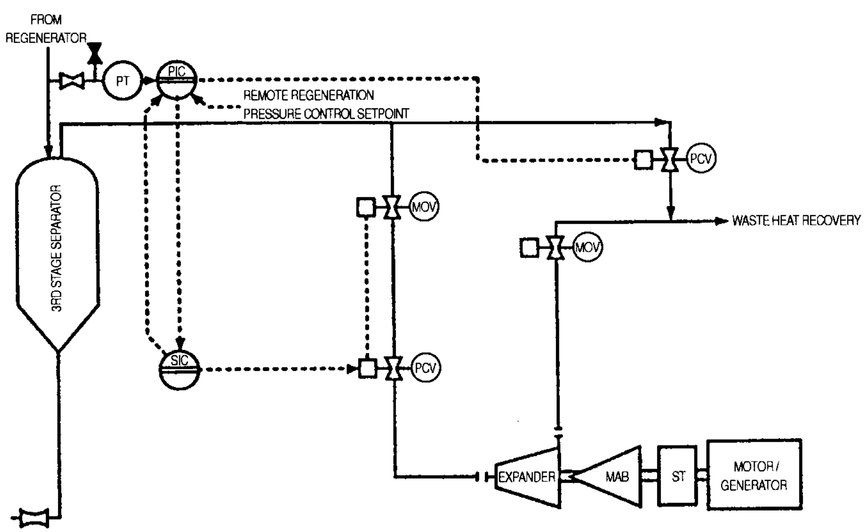

Figure 6-37. Four valve arrangement.

to no longer run the expander due to blade erosion, but the operator does not want to completely shut down the catalytic cracker until the scheduled turnaround.

Five Valve Arrangement

The addition of a second expander main bypass valve (Figure 6-38) in parallel with the initial valve can provide closer process control and flexibility. Both valves may be identical 50% capacity valves; or, one valve may be a 100% capacity main bypass valve and the other a smaller 30% capacity valve. Either approach increases flexibility and provides more precise regenerator pressure control.

Total Power Generation Train

A train that generates only electricity from the hot flue gas is called a Total Power Generation (TPG) train. A TPG train consists of a power recovery expander, gear, generator, and sometimes a steam turbine (Figure 6-39). The valve arrangement for a TPG train requires special attention because the train operation and the process operation are independent.

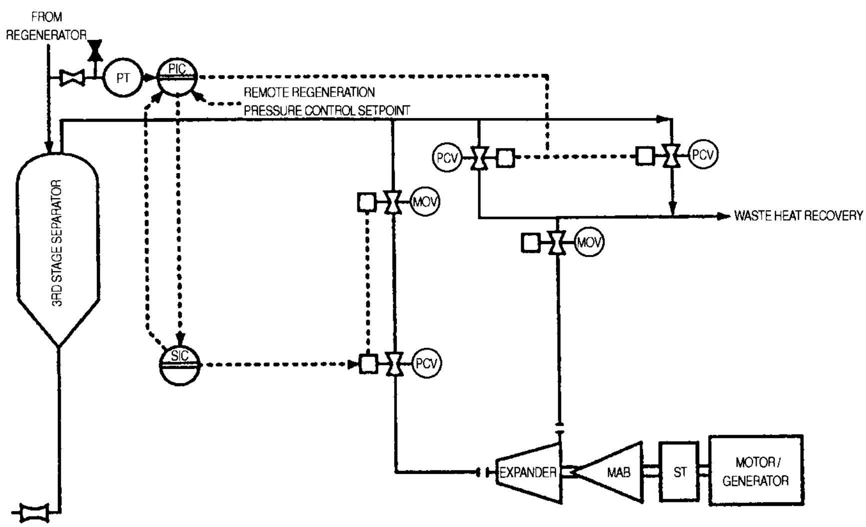

Figure 6-38. Five valve arrangement.

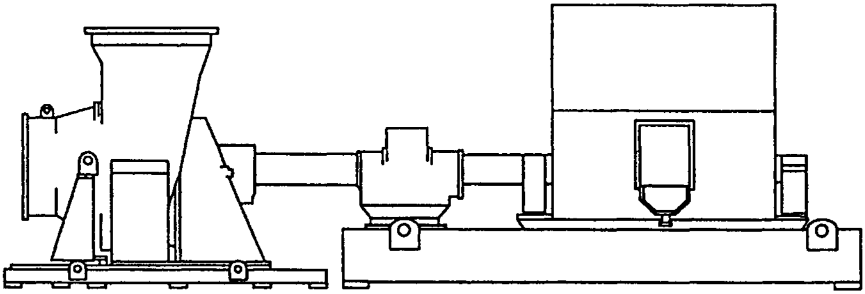

Figure 6-39. Total power generation train.

Six Valve Arrangement

An elaborate system may have as many as six valves (Figure 6-40). A small 30% capacity valve, which enables for flue gas to pass directly from the expander inlet to the expander exhaust, will enhance startup, synchronization, and safety protection for the train. This small inlet bypass valve is modulated to control the ramp-up speed and fine synchronizing of the TPG train. It is also beneficial during emergency situations to divert stored flue gas directly to the expander exhaust, instead of all the flue gas passing through the expander. The six valve arrangement may be used for the main air blower train, as well as the TPG train.

Typical TPG Valve Arrangement

A typical TPG valve arrangement is the five valve system (Figure 6-41). The two expander inlet valves provide regenerator pressure control, overspeed protection, and flue gas shut-off to the expander. The expander exhaust valve enables expander isolation. The full and partial expander bypass valves permit accurate control of the FCC process when the expander is not in operation.

Three Valve TPG Arrangement

The three valve arrangement (Figure 6-42), using one expander inlet valve, one expander exhaust valve, and one expander bypass valve, has been tried with disappointing results. Some users have had to add

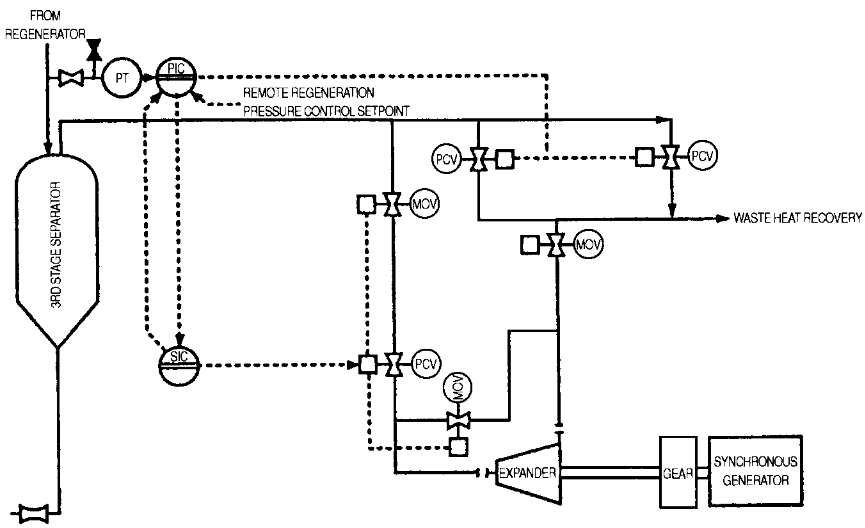

Figure 6-40. Six valve arrangement.

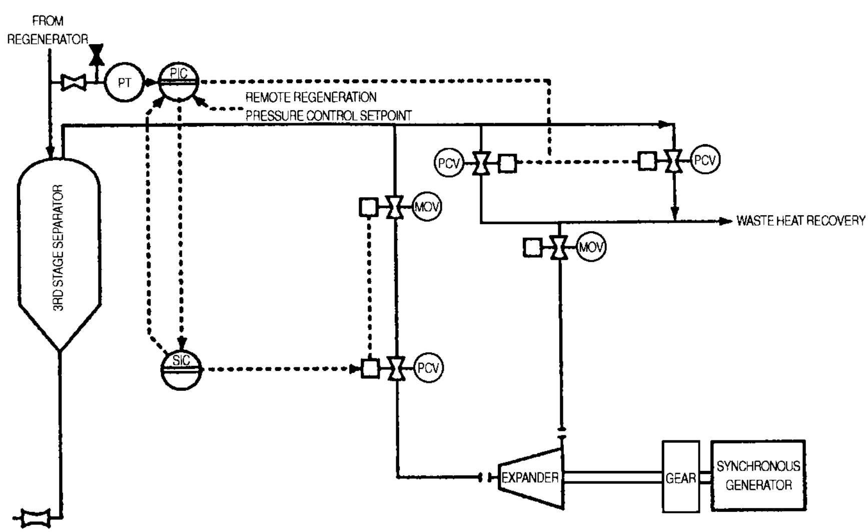

Figure 6-41. Typical TPG valve arrangement.

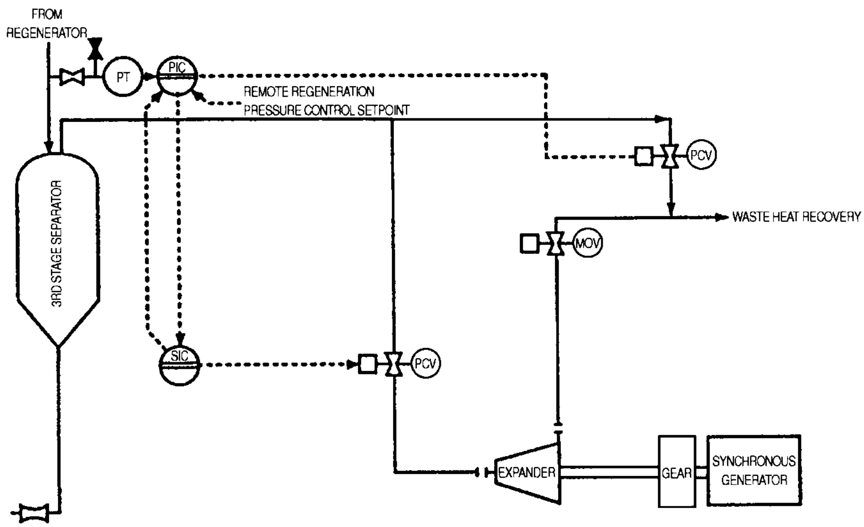

Figure 6-42. Three valve TPG arrangement.

a second expander inlet valve in series on an emergency basis. For this reason, the three valve arrangement is not recommended for TPG trains.

The foregoing comparison of different valve arrangements for both full main air blower trains and TPG trains emphasizes its importance. The range of desired regenerator control, expected modes of operation, and system constraints all influence the choice of valve arrangements. The selected arrangement depends on safety consciousness, cost considerations, and desired process flexibility.

FCC EXPANDER LOAD SHEDDING CONTROL[7]

Load sharing or selective load shedding is of interest to many users of hot gas expanders. A particularly successful European FCC application is illustrated in Figure 6-43. The addition of an expander-generator set to the FCC unit at a major refinery presented a challenge because a trip of the expander could upset the process. The company that is the subject of this application case study, GHH Borsig, solved this problem with the installation of a computerized control system and through computer simulation of trips.

---

[7] *Source: "Expander Load Shedding Control,"* Turbomachinery International, *January/February 1998.*

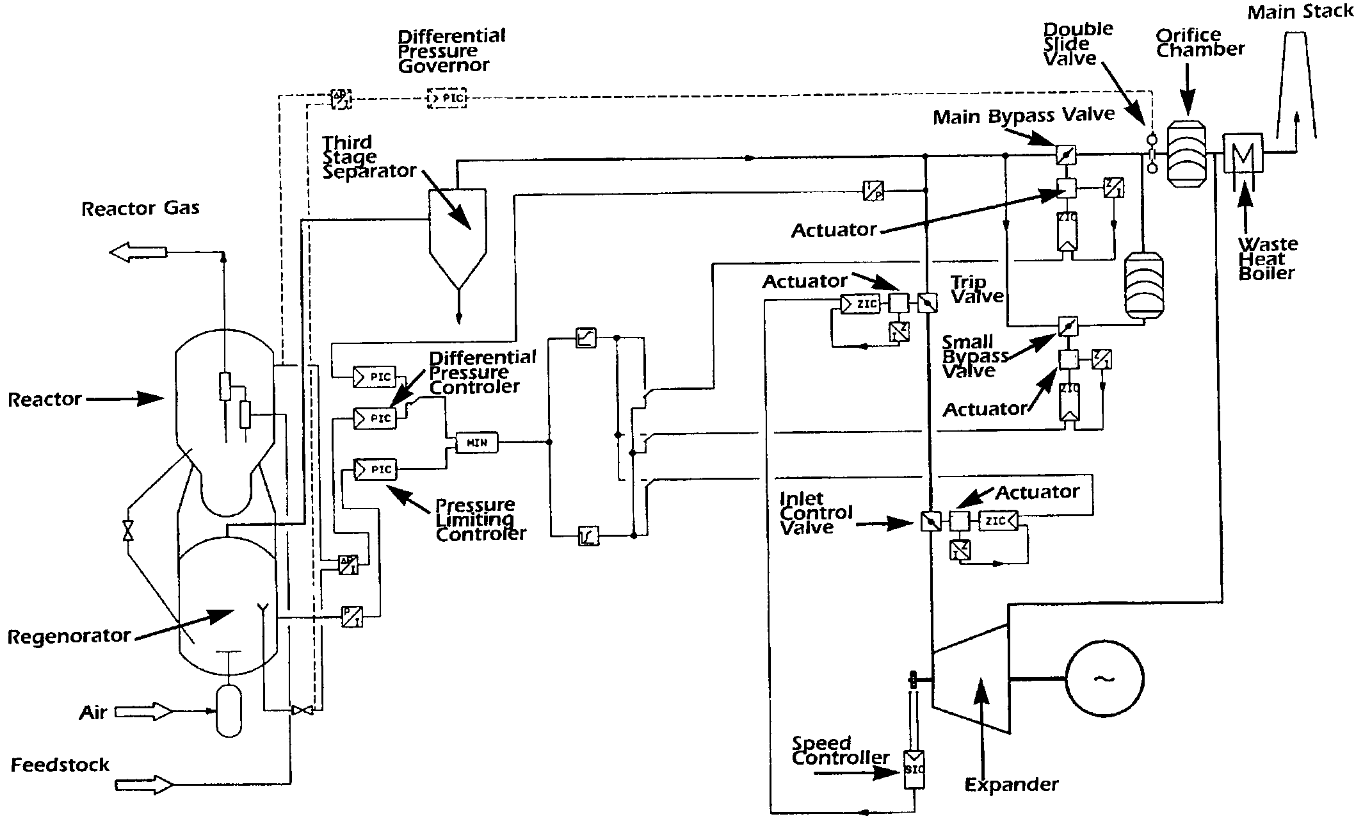

Figure 6-43. Schematic of the FCC system at ERN.

The FCC unit at this refinery was modified through the installation of an expander-generator set. This expander performs the function of expanding the flue gases from a regenerator, converting the residual energy into electric power. The time period allowed for tying the expander into the existing plant was limited to nine days within a 28-day shutdown of the FCC unit. Two days were allowed for optimizing the control system.

To investigate the dynamic behavior of the energy recovery system, particularly when isolating the electric generator from the grid, a dynamic simulation was performed, which incorporated the expander, the associated piping systems, the regenerator, and the control system. The tight time constraints made it necessary to pre-optimize the system during the simulation. Because of this simulation, the time required for "hot" optimization was reduced to five hours.

FCC Plant Layout

Within the FCC plant shown in Figure 6-43, catalyst is continuously circulated between the reactor and the regenerator. In the regenerator, carbon that was deposed on the catalyst is burned off, with combustion air being supplied on a continuous basis. Reactivated catalyst from the regenerator is mixed with FCC feedstock and then returned to the reactor.

In the original system configuration, the hot flue gas leaving the regenerator was expanded in the double slide valve and orifice chamber to atmospheric pressure, and then passed via the waste heat boiler to the main stack. This mode of operation remains possible following the expander retrofit.

After the conversion, the hot flue gas is ducted through the expander and the power extracted from the flue gas is converted into electric power. The exhaust gas from the expander is ducted to the existing waste heat boiler and the downstream electrostatic precipitator, then discharged into the atmosphere through the main stack.

Regenerator Pressure Control

The pressure in the reactor is determined by the controlled pressure at the top of the main column, to which the pressure loss in the reactor header must be added. The pressure loss in the header slowly decreases with time, so that the absolute pressure in the reactor steadily increases with time.

Controlled catalyst circulation is one of the most important prerequisites for trouble-free operation of the FCC unit. Uniform circulation is ensured by controlling the differential pressure between the reactor and regenerator. The differential pressure in the existing plant is controlled by a differential pressure governor adjusting the position of the double slide valve upstream of the orifice chamber.

The expander retrofit required additions to the control system due to the following modifications:

- The main flue gas flow was ducted through the expander instead of through the double slide valve.
- Starting up and shutting down the expander must not adversely affect the differential pressure between the reactor and the regenerator.
- An emergency trip of the expander or generator requires fast closing of the trip valve and inlet control valve. An emergency trip also must not adversely affect the differential pressure between the reactor and regenerator.
- The bypass valves control the differential pressure between the reactor and regenerator by varying the flowrate in the expander bypass.
- A differential pressure controller acts in split range on the inlet control valve and the bypass valves. The differential pressure governor is retained as the standby and backup system.
- A pressure limiting controller, in the event of excessively high absolute pressure in the regenerator, disables the differential pressure controller and limits the pressure to a preset maximum value.
- A speed controller synchronizes the expander/generator with the electricity supply grid, and actuates the inlet trip valve to its fully open position.

All valves are equipped with hydraulic actuators, electronic positioning controllers for precise positioning, and solenoid valves for rapid (trip) opening of bypass valves and emergency closure tripping of trip and inlet control valves.

The actuating time for a quick-closing/quick-opening operation effected by the solenoid valves is 0.6 sec, and the actuating time under normal control is 5 sec for the inlet valves and 0.6 sec for the bypass valves. These actuating times apply to the full valve stroke outside the end position damping range.

At the rated duty point, the differential pressure controller is active. The inlet control valve and trip valve are completely open. The main bypass valve is completely closed and the small bypass valve controls the differential pressure. Approximately 96%–98% of the flue gas flows through the expander, with the rest passing through the small bypass valve, orifice chamber, and double slide valve to the expander outlet to rejoin the main flue gas flow.

Fluctuations in the flue gas flowrate (typically less than 3% of nominal) are detected by the differential pressure controller and compensated for by adjusting the small bypass valve. The main bypass valve is completely closed during normal operations, but can open in the event of sharp increases in the flue gas flowrate. Similarly, in the event the flue gas flowrate decreases, the small bypass valve closes to a mechanically preset minimal opening, and the inlet control valve also partially closes. The minimum opening is necessary to keep the bypass lines to the minimum requisite operating temperature.

The pressure limiting controller prevents the absolute discharge pressure from the regenerator from exceeding an upper threshold. The action signal from this controller overrides the action of the differential pressure controller.

Under normal operations, the existing differential pressure governor is switched to manual and the double slide valve is wide open. This valve must be sufficiently opened so that, even in the event of an emergency expander trip, the entire flue gas flow can pass through the double slide valve without the regenerator discharge pressure increasing to nonpermissible levels.

The maximum permissible variation in the differential pressure between the reactor and regenerator was specified by this refinery as 30 mbar. At the rated duty point, the absolute discharge pressure from the regenerator is 3.75 bar, and the differential pressure between the reactor and the regenerator is 300 mbar.

Dynamic Simulation

In 1993, comparisons between the results of the simulation and the measurement data from the test bed revealed an excellent level of agreement. Such a dynamic simulation model makes it possible to examine the dynamic behavior of the entire system even before the machines and components have been manufactured. It allows the system behavior to be investigated under operating conditions that are difficult to duplicate in practice. For example, it is possible to analyze system behavior under critical failure situations, such as the breakage of a coupling between the expander and generator, with a high degree of detail and without actually physically jeopardizing plant integrity.

In the application described here, a simulation study was performed to develop the ideal control strategy. Additionally, a good model of the system enables the controller parameters to be optimized during the initial engineering phase. This, in turn, means that commissioning time can be substantially reduced.

The GHH Borsig Turbolog DSP control system used for controlling the machine train is designed to enable dynamic system simulation using the control system hardware and software. This offers two major benefits:

- No additional hardware in the form of a separate simulation computer is necessary.
- The control system does not need to be modeled, and can be tested using the original software running on the original hardware.

In the simulation model, the FCC system was subdivided into discrete elements and suitable subsystems. This model provided all the process parameters such as pressures, flowrates, and temperatures. Figure 6-44 shows the corresponding block diagram. (The model for the expander, piping systems, and vessels is based on a gas turbine model described by GHH Borsig in a paper by W. Blotenberg.)

The Turbolog DSP System

The strict requirements placed on the quality of the regenerator pressure control system necessitate complex control strategies that can only be achieved using modern freely programmable control systems, while the short actuating times of the control valves require controllers with ultrafast response.

Each digital controller operates sequentially within a total program execution time (TPET). The current process variables are entered, and from these the CPU calculates the relevant control outputs, which are then transmitted via converters to the actuators and control valves. At the start of the next cycle, new, updated process variables are entered and the program run begins again. Between one and two program cycles (TPET) may pass between a change in the process variable (input) and the necessary correction to the control output signals.

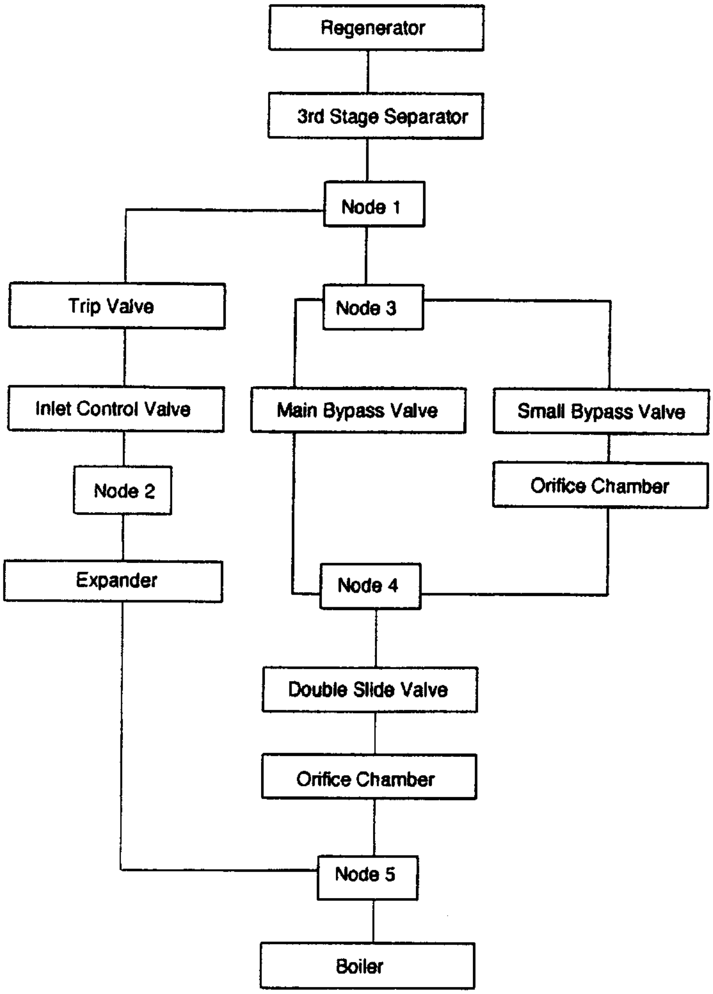

Figure 6-44. Block diagram for the simulation model.

The control valves have a full-stroke actuating time of 600 msec; thus, in 6 msec the valves are actuated through 1% of their full stroke. Only controllers with a TPET of less than 3 msec are able to meet the strict requirements of this application.

The Turbolog DSP digital control system was installed to meet these requirements. This system is based on off-the-shelf hardware that is adapted to this application, running GHH-Borsig's custom-designed software. The signal process system employed makes this machine control system suitable for performing complex control tasks with TPET values of less than 1 msec.

The software in the Turbolog DSP controller includes a control algorithm called "SHEDCON," which controls the regenerator differential pressure under all operating conditions. This software was designed in 1984 specifically for FCC applications and was improved for the refinery project described here.

System Behavior During Load Shedding

In the event that certain faults occur in the electrical equipment of the generator, the load circuit breaker must be opened immediately. The result is that the machine train is accelerated with the full power of the expander. Only if the inlet valves are closed within 0.6 sec can excessive overspeed be avoided. For this reason, both inlet valves must be able to close within this time window in the event of an emergency trip.

Such an emergency trip has a catastrophic effect on the regenerator pressure. Because the gas flow path is completely closed off within 0.6 sec, this pressure increases rapidly. This cannot be allowed for operational reasons (i.e., production of the FCC unit must not be adversely affected by a shutdown of the power recover system). The maximum permissible fluctuations in the differential pressure between the reactor and regenerator were specified by the purchaser as 30 mbar. As the pressure in the reactor is only able to follow changes in regenerator pressure with a major time lag, the requirement for a maximum of 30 mbar variation means that in the event of generator load shedding, the absolute regenerator outlet pressure must not vary by more than 30 mbar. This is less than 1% of the operating pressure value. Such a requirement can only be met with highly specialized control algorithms.

Controller Structure

The FCC unit operating requirements make it necessary for the bypass control valves to open as soon as the expander inlet valves start to close. Optimum control response is achieved if the bypass valves open so that the pressure at the outlet of the regenerator remains completely unaffected by the expander shutdown.

The inlet valves and the bypass valves are operated in a split range mode (i.e., in a staggered sequence). Rising regenerator pressure causes the inlet valves to open first, followed by the small bypass valve, and then the main bypass valve. Without additional control interventions, regenerator pressure (and thus differential pressure) automatically rises if the expander is shut down. The pressure controller reacts to this pressure increase and opens the bypass valves. The regenerator pressure increases by 122 mbar. Although this pressure rise may be undesirable for many FCC units, it nevertheless represents a generally acceptable value.

The manufacturer of this system has developed a control strategy by which the bypass valves are controlled in the event of an expander trip. This enables the valves to precisely assume the position in which, in conjunction with the downstream orifice chambers, they precisely emulate the flow loss caused by the expander prior to the trip event. A properly adjusted and calibrated control output jump function is applied so that the pressure fluctuations that occur at a given duty point are kept to a minimum.

If, however, the FCC unit should be operated at a different duty point, whether this is due to a different flue gas flowrate or a different regenerator pressure, the bypass valves would either open too wide or not wide enough. The result is fluctuation in the regenerator outlet pressure.

Switching Between Control Characteristics

Generally, butterfly valves are used for the inlet control and bypass valves. They are inexpensive to manufacture, and their actuators are able to operate in accordance with the requisite response times. Butterfly valves do, however, have the disadvantage of a tightly curved characteristic.

Additional non-linearities arise from the fact that valves of different nominal sizes are operated in sequence. An initial improvement in the control response was achieved in that the steady-state duty point characteristics for operation with and without the expander were stored in function generators in the controller. Depending on the operational state, the output of the process controller (regenerator pressure, or differential pressure, between the regenerator and the reactor) is applied to one or the other of these characteristics. In the event of an expander trip, the system immediately switches from one characteristic to the other. This results in linearization of the characteristic profile, so that the process controller is able to operate independent of the duty point concerned and independent of the operating mode (i.e., with or without the expander). This switching between characteristics in the event of an emergency trip also ensures that the bypass valves are always driven at maximum actuating speed to their new steady-state position in accordance with the prevailing operating conditions. All this is performed independent of the prevailing duty point (i.e., whether the system is operating at partial load or at overload).

In the event of an expander trip, the regenerator pressure decreases by 46 mbar, and then increases to overshoot the steady-state value by 16 mbar. This constitutes a substantial improvement over the previously described process, but still did not meet the specifications of the end-user.

Advanced Control Algorithms

In the dynamic simulation run, the pressures and flowrates at the input and output of each module are known. It is, therefore, possible to perform non-linear correction of the control mode, such that the changes in regenerator pressure in the event of load shedding are minimized. In a test performed with a correspondingly corrected controller structure, the pressure drop after load shedding was reduced from 46 mbar to 19 mbar. The subsequent pressure rise of 27 mbar is just below the specified threshold.

A further substantial improvement in control response was achieved by including the expander inlet pressure into the control algorithm. With this change, the regenerator pressure falls by only 5 mbar, thereafter rising by 9 mbar, representing a fluctuation that is substantially below the contractual agreement.

A further improvement in control response can be achieved by a variable gain of the controller. With this change, the simulated pressure fluctuation totals no more than 6 mbar.

Commissioning of the Power Recovery Train

The machine control system was set in accordance with the parameters determined during simulation prior to delivery to the site. Following re-routing and hook-up of the piping, the compressors were run to a maximum flow at 2.71 bar (absolute) and 480°C. The generator was disconnected from the grid and the expander tripped accordingly.

The regenerator pressure fell by 28 mbar. This value was within the contractually agreed limits. Nevertheless, two further tests were performed with modified parameters. Five hours after beginning the optimization process, a test was performed in which the regenerator pressure dropped by just 8 mbar. This value is within the normal operating spread of the regenerator output pressure.

The refinery restarted their FCC plant approximately 30 hours earlier than originally scheduled.

SURGE CONTROL[8]

Aside from being one of the largest concerns in rotating machinery operation, surge control is an integral part of a machine's capacity sharing and control. Although primarily applicable to the driven equipment, a discussion of surge control strategies is deemed appropriate.

Surge protection is necessary for all turbocompressors. Antisurge control systems have evolved over the years from simple pneumatic minimum-flow controllers, to analog electronic controllers with special algorithms and numerous computing elements, to microprocessor-based controllers with special surge control algorithms and the flexibility to handle a wide variety of applications.

Understanding Surge

Surge is defined as self-oscillations of discharge pressure and flow reversal. A basic understanding of the surge phenomenon can be attained by observing the movement of the compressor operating point on its characteristic curve during surge.

Figure 6-45 shows a simple compressor system with surge protection. The characteristic curve of this compressor at a constant rotation speed and constant inlet conditions is illustrated in Figure 6-46. The two measured variables in Figure 6-47 are the coordinates for the compressor curve in Figure 6-45 and are defined as:

ΔP_c = differential pressure across the compressor
ΔP_o = differential pressure across the flow measuring element in the compressor suction line

---

[8] *Source: John Hampel, "Basic Turbocompressor Control and Protection,"* Turbomachinery International, *July/August 1995, Compressor Controls Corporation, Des Moines, Iowa.*

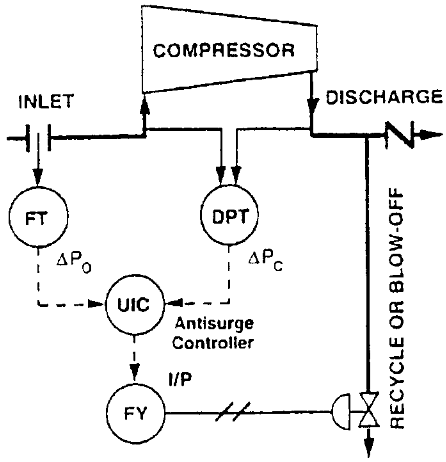

Figure 6-45. Simple compressor system.

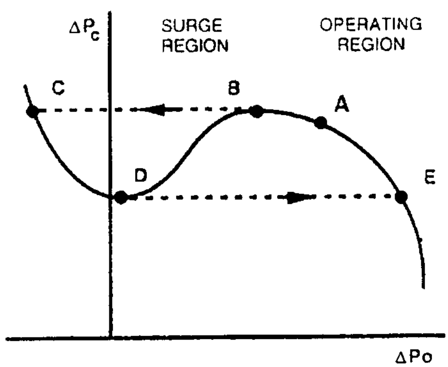

Figure 6-46. Compressor characteristic curve.

The shape of the curve to the right of point B in Figure 6-46 is familiar. This is the normal operating region of the compressor. The shape of the curve to the left of point B shows the theoretical characteristic of the surge region.

Consider this compressor operating in steady state at point A, with the recycle valve closed. If the resistance in the compressor discharge system were to rise to point B, the compressor would encounter the surge region—essentially a region of flow instability. Catastrophic surge incidents can result in complete destruction of the rotor.

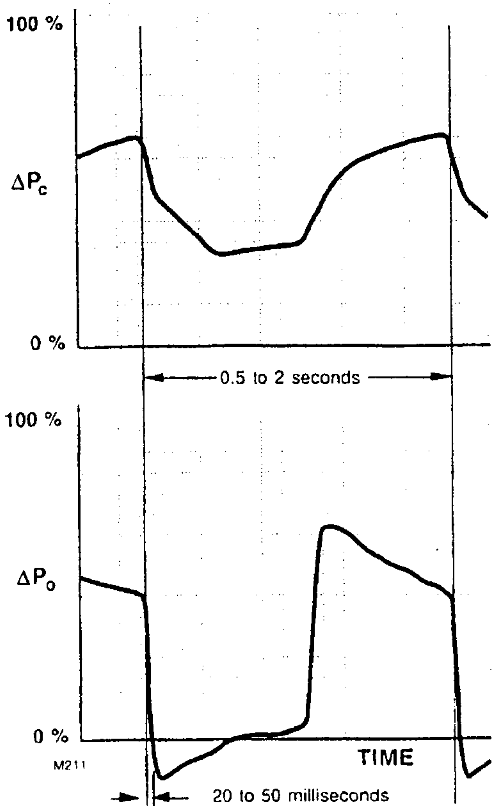

Figure 6-47. Surge characteristic of a centrifugal compressor.

Closed-Loop Surge Protection

Surge protection is almost always based on manipulating a recycle valve, as shown earlier in Figure 6-45. This recycle valve is called a blow-off valve on air compressors. Opening the valve decreases the discharge resistance to flow, reduces the pressure rise across the compressor (ΔP_c), and increases the flowrate through the compressor (ΔP_o). This moves the compressor operating point away from surge.

The essence of surge protection is determining when and how much to open or close the recycle valve. In the simple application of Figure 6-45, the antisurge controller (UIC) will position the recycle valve using a control algorithm based on ΔP_o, ΔP_c, and data on the location of the surge limit.

The set point of the antisurge controller is represented on the compressor map by a line parallel to the surge limit line. The controller calculates the deviation of the operating point from this surge control line by the equation:

$$\text{Deviation} = \Delta P_o - K\Delta P_c + b_1$$

where K = slope of the surge limit line
ΔP_c = differential pressure across the compressor
ΔP_o = differential pressure across the flow measuring element in suction
b_1 = control margin between the surge limit line and the surge control line

Limit Line and Surge Control Line. Figure 6-48 shows this approach on the compressor map. A proportional-plus-integral (PI) control alogarithm calculates the position of the recycle valve according to deviation and its proportional and integral gains. Integral limiting (anti-rest windup) is required because the operating point often will be to the right of the control line, where the recycle valve will be closed despite a non-zero deviation.

Under steady-state conditions, the PI algorithm provides enough recycle to maintain operation on, or to the right of, the surge control line. Preventing surge is not a steady-state problem. Surge almost always occurs due to either a process disturbance or a machine disturbance.

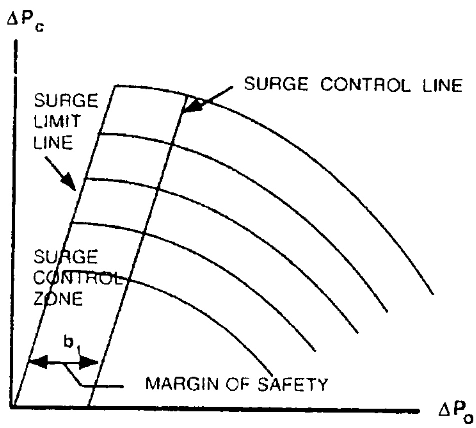

Figure 6-48. Proportional-plus-integral control.

The first objective of the antisurge control system is to protect the compressor. This can be accomplished for some disturbances by using the PI algorithm with a large value of b_1. However, it is also necessary to maximize the region in which the compressor can operate with the recycle valve closed. This increases the efficiency of the compressor at lower throughputs. Steady-state operation with recycle is extremely inefficient. Therefore, from this perspective, small values of b_1 are highly desirable.

Operating close to the surge limit in steady-state with small values of b_1 requires a fast control loop. This allows the valve to open rapidly to prevent surge when necessary.

The speed of the controller is adjusted by the proportional band and reset rate (proportional and integral gains). These parameters also influence the stability of the control loop. All control loops are limited to a gain of less than one at their critical frequency. Higher closed-loop gain will make the loop unstable.

In most cases, closed-loop control can be improved by moving the surge control line to a more conservative position in response to disturbances. When the flow measurement is sufficiently stable (good signal-to-noise ratio), the controller can calculate the time derivative of the compressor map.

It has been shown that the higher the value of this derivative, the stronger the disturbance. This signal can be used to temporarily increase the surge control margin (b_1). This makes the closed-loop PI control more effective, allowing the steady-state surge control margin to be reduced. Because the approach to surge is so fast, even an optimally tuned closed-loop controller would be unable to prevent surge during large or fast disturbances. Moreover, such a controller would be unable to stop surge should it occur. The controller would simply cycle the recycle valve open and closed in response to successive surge cycles.

Open-Loop Control

To prevent surges, a well-trained operator would put the controller in manual mode and freeze the valve in an open position. This stops the control loop oscillations and decreases the compressor discharge resistance, thus breaking the surge cycle. Unfortunately, the operator has no way of knowing how much to open the valve and, subsequently, how much to close it.

The PI controller, even when optimally tuned, is also unable to prevent surge. Furthermore, it is unable to stop surge once it occurs. In the above situation, the operator would correctly identify the problem as instability of the closed-loop PI controller. The only viable action would be to open the closed control loop by placing the controller in manual, thereby freezing the valve open. In this scenario, open-loop control will stop surge.

A similar type of open-loop control response is combined with closed-loop control in a patented method of surge protection. In this control method an open-loop control response is added before surge occurs.

Figure 6-49 shows the addition of a recycle trip line between the surge control and the surge limit lines. In essence, recycle trip is an overshoot limit. Small or slow disturbances are managed by the closed-loop algorithm, which keeps the compressor operating point to the right of the recycle trip line. For large or fast disturbances, the compressor operating point will reach the recycle trip line. At that point, the open-loop control algorithm is initiated.

Figure 6-50 shows how such an antisurge controller responded to a strong disturbance. When the operating point crossed the surge control line, the PI control algorithm began to open the valve. The PI control algorithm responded for 1 sec, reaching a requested valve position of 10% open. This appears to have influenced the compressor operating point somewhat, slowing the rate of flow decrease, but surge was still rapidly approaching. Then, when the operating point hit the

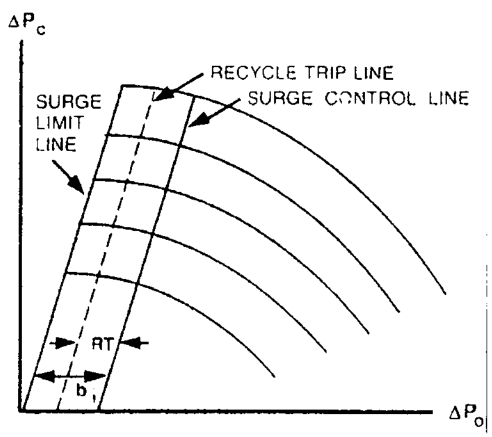

Figure 6-49. PI plus open-loop recycle trip strategy.

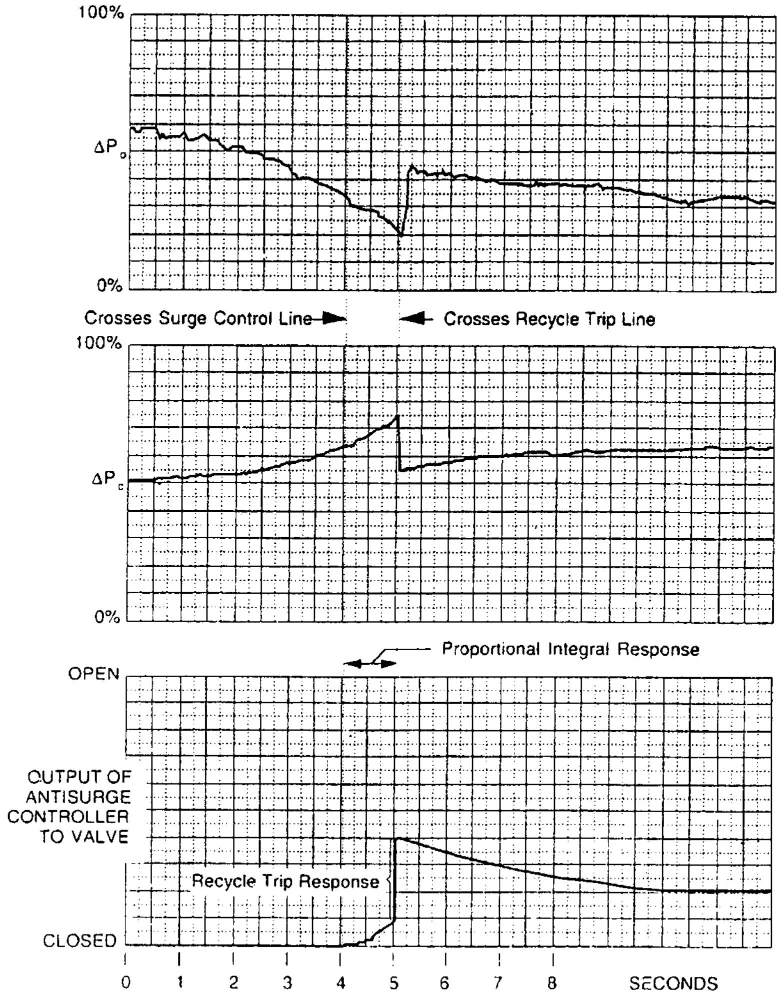

Figure 6-50. PI plus recycle trip responding to a large disturbance.

recycle trip line, the open-loop control algorithm added a step change to the controller output. The magnitude of the step change (C) is a function of the derivative of the compressor operating point at the moment it touches the recycle trip line. The faster the operating point is moving toward surge, the larger the derivative value and the larger the step change will be to open the antisurge valve. The recycle trip function added a 30% step to the controller output. This produced a nearly instantaneous reversal of the operating point movement direction. Surge was avoided and the system moved toward steady state as the constant Tl decayed, ending on the surge control line with the valve 20% open.

The step change and the exponential decay are open-loop because these responses are not affected by feedback. Because the operating point reached the recycle trip line, it is assumed that the disturbance was strong. The fast opening of the valve was able to prevent surge. Because the step size was related to the size of the disturbance, the valve was opened just enough to prevent surge. A larger step would add to the process disturbance. The exponential decay brought the compressor and the process back to steady state smoothly while the initial disturbance decayed. With this method, the closed-loop algorithm is never turned off and, therefore, can open the valve farther if necessary. The exponential decay of the recycle trip signal becomes the low limit for the valve signal.

It has been observed that the value of the combined closed-loop PI control and the open-loop recycle trip control justifies its use on all turbocompressors.

Minimizing Process Upsets

Most processes are sensitive to rapid movement of the antisurge valve. Figure 6-51 shows how this conflict of protecting the compressor and protecting the process can be resolved. A value of the maximum step change (C) is selected that does not cause an excessive process upset. To protect the compressor from larger disturbances, a parameter C2 is established. C2 is a timer that is set to match the response time of the recycle loop. When recycle trip is activated, the controller output is incremented by C, as calculated based on the derivative of the operating point. The C2 timer is started at this time. After C2 times out, the controller can evaluate the results of the initial increment of C. If the operating point is to the right of the recycle trip line, the initial increment of C is enough. If the operating point is on or to the left of the recycle trip line, an additional increment of C is provided, again based on the derivative of the operating point. The C2 timer is started again. This continues until the operating point moves to the right of the recycle trip line. This method provides a balance of strong action to protect the compressor, and a constraint on the maximum opening of the recycle valve in one step to avoid excessive process upset. An appropriate balance accomplishes these

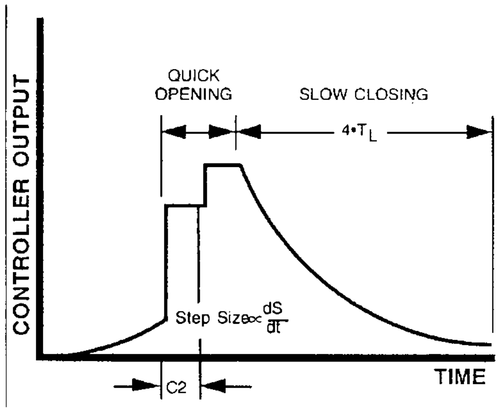

Figure 6-51. Recycle trip configured to minimize process disturbances.

conflicting goals while preventing the even greater process disturbance of surge.

Adaptive Surge Detection

Surge can still occur if, among other reasons, the controller is not optimally tuned, or if the surge limit shifts due to a change in the molecular weight of the gas. Therefore, the antisurge controller must be able to detect the surge flow reversal. The PI plus recycle trip algorithms will stop surge, typically after only one cycle. The controller then adds an additional bias, b_2, to the surge control line. Additional surges are prevented by this larger surge control margin. The surge detection produces an alarm, which should initiate a review of the incident to determine why surge occurred. The additional margin b_2 should be reset only after the cause is determined and corrected.

Complex Antisurge Protection

The surge protection described above is for a simple, single section, constant geometry compressor with constant inlet conditions and constant speed of rotation. Many compressor installations involve more complex configurations and applications.

Compressors driven by steam turbines, gas turbines, hot gas expanders, or variable speed electric motors usually employ variable rotation speed for capacity control. Generally, the surge limit slope varies with rotation speed. Multisection compressors usually require multiple antisurge controllers and recycle valves. Because these control loops interact, steps must be taken to automatically decouple the interactions.

Compressors with adjustable inlet or diffuser guide vanes introduce another complexity. Vane position affects the location of the surge limit and must be considered in the antisurge control algorithm. Compressors with sidestreams, widely varying inlet conditions, and varying molecular weight gas are other examples of more complex applications. More sophisticated algorithms are used in these cases to calculate the operating point distance from surge.

Antisurge Valve Requirements

Proper selection of the antisurge valve is of utmost importance in the design of a surge prevention system. The valve capacity must be large enough to prevent surge under all possible operating conditions, including startup and shutdown, without being oversized. An excessively large valve will provide poor control precision and will drive the compressor into stonewall (choke flow) when fully opened. Because of the different requirements of the many different compressor configurations, and the widely varying shapes of different compressor characteristic curves, no single method of valve sizing is appropriate for all applications.

The preferred characteristic is linear. Rotary valves with nonlinear characteristics may be appropriate in some applications.

Positioners should be used to achieve accuracy and repeatability of the control-loop response. This is particularly important with the open-loop control method discussed above.

Fast stroking speed is important. The entire control valve assembly should be designed with fast stroking speed as a major design goal. An adequate air supply is required to power the valve. Tubing runs should be minimized to reduce lag time. One or more volume boosters are required to ensure fast response, and equal opening and closing times.

In most applications, the valve should be designed so that in the event of an air supply loss, it defaults to the open position. This failure default mode will protect the compressor by allowing full recycle.

Attention to noise may be required because antisurge valves usually have large pressure drops. Appropriate valve style, noise attenuation trim, and in-line devices, as well as attention to line velocities and pipe schedules, can eliminate or minimize the noise.

Capacity Control

While protecting the compressor from surge is the most compelling control problem, it is not the only requirement. The compressor throughput must be adjusted to match its load. Capacity control interacts with surge protection, which reduces the effectiveness of the antisurge control system if they are not decoupled.

Capacity control is more complex in compressor networks where two or more compressors operate in series or parallel. Automatic distribution of the load between compressors is required. The antisurge and load sharing control loops must be coordinated to ensure surge protection while the load distribution and energy consumption are optimized.

When designing a control system for a turbocompressor, it must be realized that surge protection and capacity control are parts of the same problem. Therefore, an integrated control solution is needed.

BIBLIOGRAPHY AND ADDITIONAL READING

1. Agahi, R., Ershaghi, B., Bosen, W., and Leonhard, M., "Turbo-expanders with Magnetic Bearings in Air Separation and in Hazardous Areas," MAG'92, Alexandria, VA, 1992.
2. "Application of Active Magnetic Bearings to Industrial Rotating Machinery," printed material of Bearing Manufacturer S2M, Vernon, France.
3. Swearingen, J. S., U.S. Patent Number 3,895,689.
4. Clair, M., "Application of Magnetic Bearings and Dry Gas Seals to an Overhung Compressor," Revolve Proceedings, April 1992.

CHAPTER SEVEN

Turboexpander Protection and Upgrading

The troubleshooting process—how easy it is to troubleshoot a machine, how often it needs to be done, and so forth—depends largely on the type of maintenance philosophy applied during the machine's operational life. This basic philosophy affects how often the machine must be monitored.

Not surprisingly, the same strategies and philosophy that govern turboexpander selection play a key role in defining maintenance requirements. Unfortunately, a number of operators never link maintenance philosophy and troubleshooting to an appropriate extent. They either leave themselves wide open for disastrous repair bills or spend more than they need to on maintenance.

This is poor risk management. Applied to a turboexpander in critical service it translates into bad business practice. This segment will describe three basic strategies appropriate for turboexpanders (and indeed all rotating machinery). The choice of strategy should not be left to the manufacturer. It needs to fit the operator's specific application and comfort level. The manufacturer's resources and technical expertise should be used to support the decision process by providing relevant information.

MAINTENANCE STRATEGIES

Typically, an operator proceeds to itemize basic goals. The highest priority is to maximize production. Optimizing production per unit of energy is part of that aim. Maximum availability and reliability (i.e., no unplanned downtime) are also critical. Operators struggle with financial budgets and the pressure of reducing costs in the attempt to minimize maintenance, service, and repair activity.

Too little maintenance results in unexpected failures and consequential major losses of production and/or customers (Figure 7-1). This impractical approach is termed "reactive strategy" and should be avoided on all important machinery. Optimum maintenance strategy balances reasonable costs with maxmium possible availability and reliability. The two main maintenance strategies employed by companies today are labelled predictive strategy and preventive strategy. These are part of a "balanced" approach as shown in Figure 7-2.

PREDICTIVE STRATEGY

Predictive maintenance strategies operate without a regular plan for service work or exchange of parts. A maintenance plan is only set up if there is proof of deterioration. Consequently, a company with a predictive strategy favors minimizing cost over maximizing use. The annual cost of this strategy may typically only average 1%–2% of the prime equipment price.

With a predictive maintenance strategy, long-term plans typically involve as few as only two regular procedures:

- Monitoring of operating data as follows:
  –gas path (mass flow, head, efficiency)
  –water coolant (differential temperature)
  –oil analysis (water content, deterioration of anti-oxidation additives)

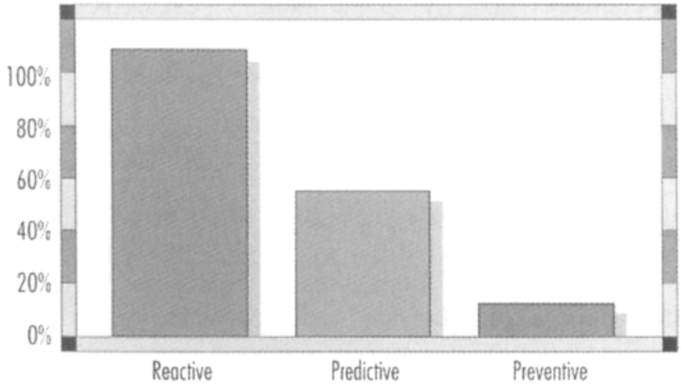

Figure 7-1. Probability of unexpected breakdowns.

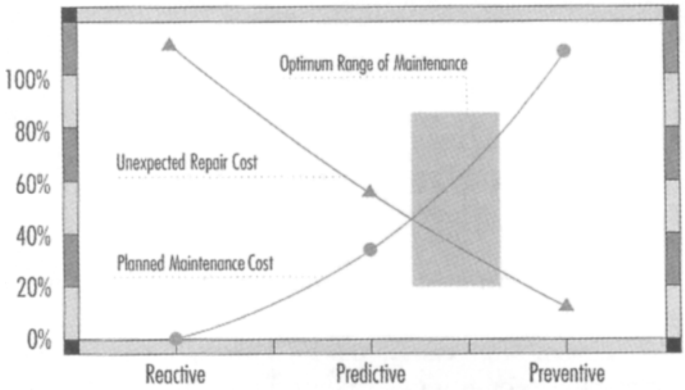

Figure 7-2. Balancing your maintenance budget.

- Vibration analysis measurements as follows:
  –Spectrum analysis (shaft, pinions), using eddy current probes at normal load and turndown
  –Velocity readings (all bearing housings), at normal load

PREVENTIVE STRATEGY

In contrast with the predictive strategy, a preventive strategy aims toward maximum safety against unexpected failures. The basic concept is to predict the average lifespan of a part and then replace it before the end of that lifespan. Annual cost is therefore higher (8%–10% of the prime equipment price) because it is necessary to purchase and warehouse more spare parts.

Aside from the effects of a given maintenance strategy on troubleshooting time and effort required, the application service of the unit also has an effect. With increasingly tough environmental legislation that in turn demands maximum energy usage and/or recovery, power recovery processes are increasing in number. The deregulation of the power industry that results in the increase of small power producers (such as process plants) also serves to increase this number.

PRT LOAD SHEDDING CONCERNS

In a power recovery train, a breaker trip is one of the more complex problems that is experienced. An algorithm that models the train's recovery after such a trip is therefore of considerable benefit to turboexpander users. The development and use of such an algorithm is detailed below.

ALGORITHM FOR FCCU POWER RECOVERY TRAIN BREAKER TRIP RECOVERY[1]

As previously mentioned in Chapter 5, one of the most severe disturbances for the power recovery train (PRT) is a generator breaker opening. This event often causes the PRT to trip on overspeed or other process or machine conditions. A control solution has been developed to keep the PRT and the process under control during breaker opening.

What Is Needed

A PRT in an FCCU significantly increases total plant efficiency. In practice, many PRTs are not operated at their design capacity. Generally, two categories of problems prohibit users from getting the maximum out of their PRT:

- Mechanical and erosion problems on the expander
- Control problems on the PRT

To get good control of the entire PRT, not only should the expander be controlled, but a completely integrated control system for this application should be designed. Most conventional control systems consist of individual control loops that only consider their specific tasks. The PRT—from a control perspective—is a multivariable system that requires integration between the different control loops. Further, some of the disturbances on the PRT are so fast that closed-loop control is too slow to keep the train under control.

As a result of these poorly designed control systems, users experience significant operational problems, including machine and process shutdowns. As with any process plant, the first objective is to achieve reliable production from the FCCU. Only with reliable production will operators start optimizing the unit. Users, therefore, are not using the

---

[1]*Source: Compressor Controls Corporation.*

expander on the PRT (full bypass operation), or are only partly using the power recovery capability of the PRT by having the bypass valve open continuously.

One of the biggest PRT disturbances is motor/generator breaker opening. When the breaker is opened during electrical power generation, there is an instantaneous drop in power consumption on the PRT shaft. As a result, the machine starts to accelerate. The more electricity generated before the breaker trip, the more power is available to accelerate the PRT after the breaker trip. With conventional control systems, it is common for the PRT to trip on overspeed within seconds after breaker opening.

This segment focuses on the breaker trip event and how both the train speed and the differential pressure between the regenerator and reactor stripper can be controlled during this event. Based on the breaker status, action is immediately initiated on the expander. Due to the improved reliability in train operation with these patented control techniques, the PRT can be better utilized without sacrificing plant reliability. This leads to more efficient FCCU operation and the pay-back period for the improved control system can be extremely short.

Expander Operation and Control

The PRT is started by the motor/generator and/or steam turbine. As the air blower starts to provide air to the regenerator, coke burning on the catalyst starts and the energy in the flue gases increases. The flue gas flows through the expander, and the expander starts to take load away from the steam turbine and the motor/generator. When the process comes online, the motor becomes a generator and electricity is exported into the refinery grid.

Since the generator is connected to the electrical grid, PRT speed is fixed. For induction-type motor/generators, some speed variation is possible due to motor/generator slip, but this is only a small percentage of rated speed. In any event, the speed cannot be used to control other process parameters (e.g., air mass flow to the regenerator).

The differential pressure between the regenerator and reactor stripper must be maintained at all times to prevent hydrocarbon vapors or liquids from entering the regenerator and causing an explosion. At the same time, maintaining differential pressure avoids air ingress into the reactor, which could lead to major equipment damage. This is achieved by a controller that controls this differential pressure by manipulating, in split range, the expander inlet and bypass valves under normal running conditions.

Further, the absolute regenerator pressure needs to be limited to a maximum value. This is achieved by a controller PIC that manipulates the expander bypass valve using a high signal selector (HSS).

Equation of Motion

Power applied to a rotating equipment train shaft must be balanced by the power absorbed on that shaft to maintain a constant speed. However, these parameters are not truly dimensionless. Because the geometry of the expander is fixed, dimensions of length can be eliminated by a constant characteristic length. Constants can be dropped and ignored for control purposes. The equation describing this is:

$$\frac{I dN^2}{2dt} = J^+ - J^- \tag{7-1}$$

where J^+ implies the power added by the driver(s) on the shaft and J is the power absorbed by the load(s) on the shaft. From Equation 7-1, it is easy to see that the speed will not change with time if the power applied to the shaft is exactly absorbed by the load(s). However, this equation also describes the rotational dynamics when these powers are not balanced.

Expander Characteristics

A hot gas expander is typically described by a map of shaft power versus mass flowrate (Figure 7-3). Notice that there are four parameters changing in this particular map: w, J, P_1, and T_1. Figure 7-3 is most useful when the family of curves (which are for a constant rotational speed) reduces to a single curve in a two-dimensional space. Usually, expander characteristics are a very weak function of angular speed. However, in cases where the variations due to rotational speed are important, a third dimension is required. This dimension should be equivalent speed, N_e.

If using dimensionless parameters obtained through dimensional analysis, or similitude, the data will collapse into a single curve. In this case, the useful parameters are reduced flow, q_r, reduced power,

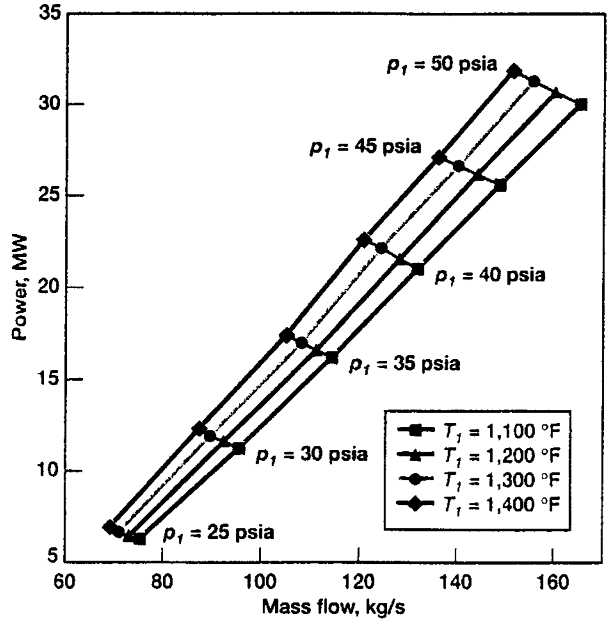

Figure 7-3. Speed will not change with time if power is absorbed by the load.

j_r, and pressure ratio, R_c (see "Definitions" at the end of this chapter). The resulting maps are shown in Figures 7-4 and 7-5.

Breaker Trip Triggers Open-loop Control

When the breaker opens, the load (or a portion of it) on the expander is suddenly shed. This event is detected by the breaker status before the speed increase is detected by the control system. Therefore, a feedforward approach is employed to anticipate the need for control action before feedback indicates this need.

The power applied by the expander to the shaft must be reduced in this situation. Open-loop control can be applied, but an intelligent application of the open-loop response should be made. How much to reduce this power is described in the following paragraphs. The characteristics described in the section "Expander characteristics" are needed to determine expander power output under any conditions.

The objective is to balance the power applied to the shaft with that absorbed—making the right side of Equation 7-1 close to zero, thus

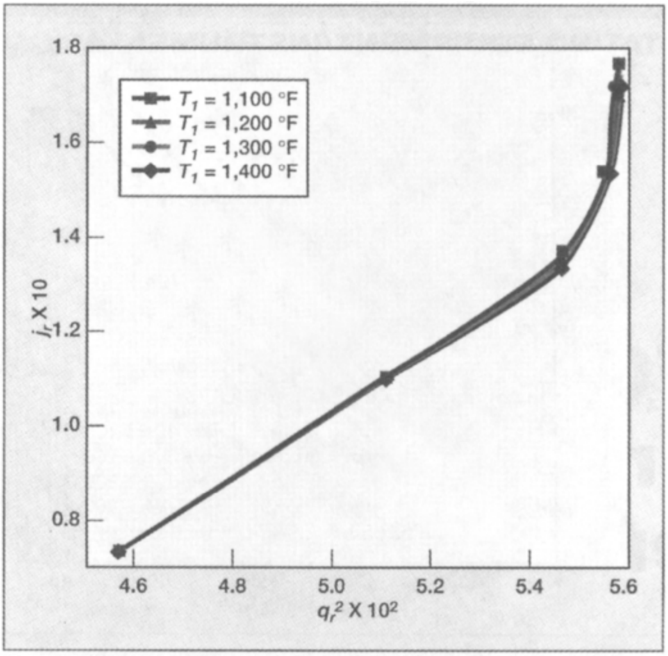

Figure 7-4. Reduced power versus reduced flow.

keeping the speed under tight control. This reduction in expander power is achieved by closing the expander inlet valve.

Breaker opening causes the expander inlet valve to close. This, however, would disturb the differential pressure between the regenerator and the reactor stripper. To keep this pressure constant, the bypass valve needs to be opened to keep pressure, P_0, upstream of the inlet and bypass valves constant. Again, this needs to be done carefully. Opening the bypass valve too much can cause the pressure to drop to such a level that catalyst enters the expander. This must be prevented under all circumstances.

To follow through with the open-loop approach, there must first be a signal that warns the speed control function of load loss (or breaker opening) and impending speed increase. This is provided by a digital contact that indicates motor/generator breaker status. Next, a load loss estimate is needed. This is provided by a kilowatt transducer on the motor/generator.

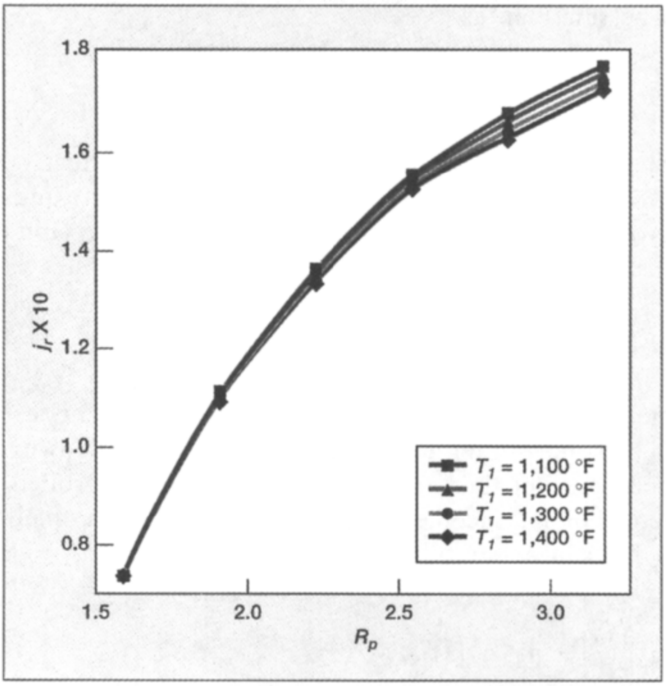

Figure 7-5. Reduced power versus pressure ratio.

Closing the Inlet Valve and Opening the Bypass Valve

The following steps outline the correct manner in which to close the inlet valve and open the bypass valve (Figure 7-6):

Step 1: Calculate actual expander power before breaker opening. To determine the required power from the expander after the breaker opening, it is necessary to know the actual power developed by the expander before breaker opening based on readily available and reliable measurements on the expander. Typically these are P_1, T_1, P_2, T_2, and N. The PRT speed can be ignored because it is nearly constant before and after the breaker trip and the expander performance curve is typically a weak function of rotational speed.

The reduced power of the expander has been defined as:

$$j_r = \frac{J}{P_1\sqrt{ZRT_1}} \tag{7-2}$$

This can be rewritten as:

$$j_{bef} = j_{r,bef} P_{1,bef} \sqrt{ZRT_{1,bef}} \tag{7-3}$$

As previously mentioned, R_c versus j_r is an invariant coordinate system. This means that the reduced power, j_r, can be expressed as a function of pressure ratio, R_c, across the expander (Figure 7-5). Knowing this, Equation 7-5 can be rewritten as:

$$j_{bef} = f_1(R_{c,bef}) P_{1,bef} \sqrt{ZRT_{1,bef}} \tag{7-4}$$

Assume Z and R to be constant for the expander. This assumption can lead to some minor errors in the calculation. However, if P_2 is assumed constant then the variation for Z can be rolled into the new function of R_c and the total error becomes even smaller. Now, Equation 7-4 can be simplified to:

$$j_{bef} = f_2\left(\frac{P_{1,bef}}{P_{2,bef}}\right) P_{1,bef} \sqrt{T_{1,bef}} \tag{7-5}$$

It is now possible to calculate j_{bef} based on P_1, P_2, and T_1, which are all readily available transmitters.

Step 2: Calculate required expander power after breaker opening. The power required from the expander after the breaker opening can be calculated as the expander power produced before the breaker opening minus the electrical power produced by the generator immediately prior to the breaker opening. This can be expressed as:

$$J_{aft} = J_{bef} - J_{gen} \tag{7-6}$$

Calculating power developed by the expander before breaker opening, J_{bef}, is described in Step 1. The generator power, J_{gen}, can be measured by using a kilowatt transducer. The kilowatt transducer (or current transducer) is typically available in the motor/generator control panel. If not, it can be added to the machine at a low cost. Knowing both J_{bef} and J_{gen}, J_{aft} can be calculated.

Step 3: Calculate new inlet pressure, $P_{1,aft}$, *for the expander.* As the breaker opens, the PRT will start to accelerate if immediate action is not taken. Therefore, the inlet valve is going to be closed by a step.

Closing the inlet valve will potentially change the expander inlet and outlet parameters. The parameters that influence the expander power calculation are P_1, P_2, and T_1. Therefore, it is important to consider what happens to these three parameters during breaker opening.

- *Inlet pressure,* P_1. As the expander inlet valve is closed, the differential pressure across it will increase. The amount of change depends on the flowrate and valve characteristics. Closing the valve can also potentially change the pressure upstream of the inlet valve. This pressure, P_o, is one side of the differential pressure control loop and, as such, it is desirable to keep it constant for a given process condition. Therefore, closing the inlet valve can have a negative effect on the pressure in the process. However, in this control system, the inlet valve is closed and the bypass valve is opened simultaneously. This is done in such a way that the total flow through the inlet and bypass valves before and after the step changes remains the same:

$$W_{total} = W_{inlet} + W_{bypass} \tag{7-7}$$

$$W_{total,bef} = W_{total,aft} \tag{7-8}$$

  Keeping the flow through the valves constant will cause P_o to stay constant. As a result, P_1 will vary with the step change on the inlet valve, but P_o will stay constant.
- *Outlet pressure,* P_2. Since total flow through the bypass and inlet valves will remain constant, it is assumed that P_2 will remain constant.
- *Inlet temperature,* T_1. Assuming that the gas is ideal and the kinetic energy is negligible, the pressure drop across the inlet valve maintains a constant temperature line. The flue gas mainly consists of air and is at high temperature and relatively low pressure. These types of gases behave closely to ideal gases. Thus, it is assumed that T_1 is equal to T_o at different valve opening positions.

Based on this, it is assumed that only P_1 changes as the inlet valve is closed. This is a good approximation, given that all calculations are based on given process conditions that only need to remain stable for a short time (seconds rather than minutes).

Calculating $P_{1,\,aft}$: It is necessary to determine $P_{1,aft}$ to be able to determine the inlet and bypass valve steps. As seen in the invariant coordinate systems, the reduced power, j_r is a function of the pressure ratio, R_c:

$$j_r = f_1(R_c) \tag{7-9}$$

Equation 7-3 can be rewritten for conditions after the breaker opening:

$$j_{aft} = j_{r,aft} P_{1,aft} \sqrt{ZRT_{1,aft}} \tag{7-10}$$

It is known that T_1 and P_2 will stay constant before and after the inlet valve closing. Using the same invariant coordinate systems as before, Equation 7-10 can be rewritten as:

$$j_{aft} = f_2\left(\frac{P_{1,aft}}{P_2}\right) P_{1,aft} \sqrt{T_1} \tag{7-11}$$

Rewriting Equation 7-11 demonstrates how $P_{1,aft}$ is calculated:

$$P_{1,aft} = \frac{j_{aft}}{f_2\left(\frac{P_{1,aft}}{P_2}\right)\sqrt{T_1}} \tag{7-12}$$

Knowing that T_1 and P_2 are constant and that J_{aft} is calculated, the only unknown in Equation 7-12 is the expander inlet pressure, $P_{1,aft}$. Pressure $P_{1,aft}$ is present on both sides of the equation, but can still be calculated by iteration. As a result, the required expander inlet pressure after closing the inlet valve is known. This calculated $P_{1,aft}$ corresponds to the inlet pressure that causes the expander to develop j_{aft} for the given outlet pressure, P_2, and inlet temperature, T_1.

Step 4: Calculate $q_{r,exp,aft}$ *for the expander.* To shed generator load, the inlet valve is closed until the bypass valve is opened. This causes the flowrate through both valves to change. To calculate the required flowrate changes (to calculate the step changes on the valves) it is necessary to determine the flowrate through the expander. Knowing the expander flow and correlating this to the inlet and bypass valves makes it possible to calculate the new valve positions.

The invariant coordinate, q_r, is used to determine the flow calculation independent of inlet conditions. To determine the reduced flow

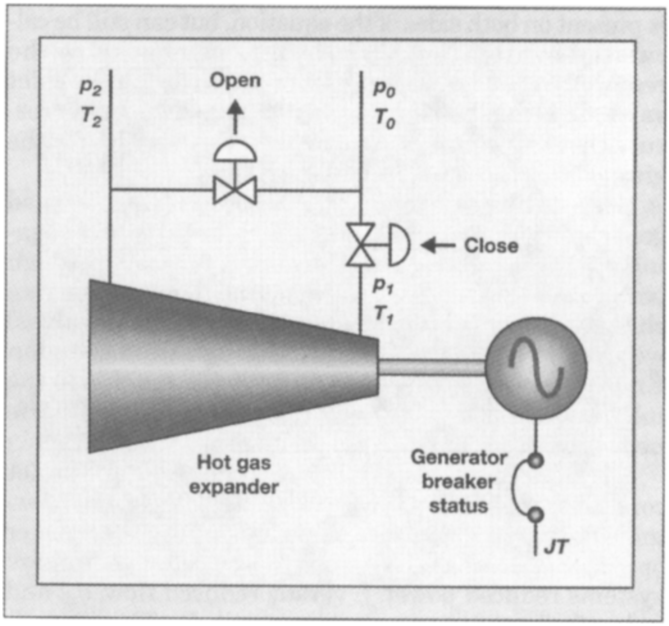

Figure 7-6. Breaker opening causes the expander inlet valve to close.

for the expander after the breaker opening, $q_{r,aft}$, use the invariant coordinate systems reduced power j_r versus reduced flow q_r, and reduced power j_r versus pressure ratio R_c. These invariant coordinate systems can also be described as functions. Thus, reduced power, j_r, is a function of pressure ratio, R_c (Equation 7-9) and reduced flow, q_r, is a function of reduced power, j_r, or:

$$q_{r,exp} = f_3(j_r) \tag{7-13}$$

As can be seen from Equation 7-9 and Equation 7-13, it is now possible to calculate the reduced expander flow, if the expander pressure ratio is known. To calculate pressure ratio, P_1 and P_2 are needed. In this situation, this calculation is for conditions after the breaker opening. Since $P_{1,aft}$ and $P_{2,aft}$ are known, it is possible to calculate $q_{r,exp,aft}$. This is clearly illustrated in Figure 7-7.

Step 5: Calculate $c_{v,inlet}$ *for* $q_{r,exp,aft}$. To make the step on the inlet and bypass valves, it is necessary to know what c_v is needed through the valve. This corresponds to the flow through the valve for certain

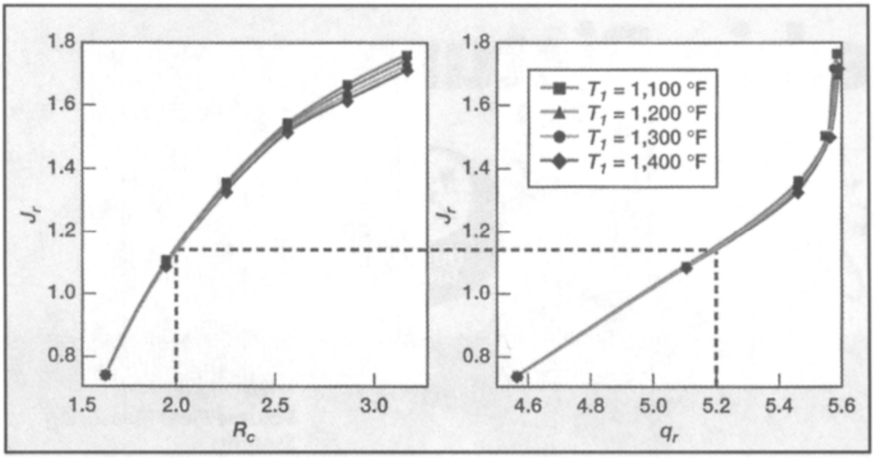

Figure 7-7. Determine q_r from R_c.

pressure conditions on the valve. The flow through the valve is related to the flow through the expander. Step 5 calculates the valve c_v for the reduced valve flow after the breaker opening, $q_{r,inlet,aft}$. This $q_{r,inlet,aft}$ is related to $q_{r,exp,aft}$.

To begin, start with the flow equation for valves from ISA standards:

$$w = N_8 F_p c_v P_o Y \sqrt{\frac{xMW}{T_o Z}} \tag{7-14}$$

Multiply both sides of the equation by the term $\sqrt{T_o Z / MW}$. Now, Equation 7-14 can be rewritten as:

$$w\sqrt{\frac{T_o Z}{MW}} = N_8 F_p c_v P_o Y \sqrt{x} \tag{7-15}$$

Dividing both sides by P_o results in a term that is proportional to the reduced valve flow on the left side of Equation 7-15. Simultaneously, $x = \Delta P/P_o$ is applied. This results in:

$$\frac{w\sqrt{\frac{T_o Z}{MW}}}{P_o} = N_8 F_p c_v Y \sqrt{\frac{\Delta P}{P_o}} \tag{7-16}$$

The expansion factor, Y, can be seen as a function of pressure ratio, R_v, across the inlet valve:

$$Y = 1 - \frac{x}{3F_k x_T} = f_4(R_v) \tag{7-17}$$

Also, the factor $\sqrt{x}$ is a function of pressure ratio R_v across the inlet valve:

$$\sqrt{x} = \sqrt{\frac{\Delta P}{P_o}} = \sqrt{\frac{P_o - P_1}{P_o}} = \sqrt{1 - \frac{P_1}{P_o}} = f_5(R_v) \tag{7-18}$$

It is now possible to rewrite Equation 7-16 and fill in the results of Equations 7-17 and 7-18. This yields:

$$w\frac{\sqrt{T_o Z / MW}}{P_o} = N_8 F_p c_v f_4(R_v) f_5(R_v) \tag{7-19}$$

Factors N_8 and F_p are constants and as such can be rolled into a function. It is also possible to combine the two functions f_4 and f_5 of R_v into a new function of R_v. Combining these two steps yields:

$$w\frac{\sqrt{T_o Z / MW}}{P_o} = f_6(R_v) c_v \tag{7-20}$$

The left side of Equation 7-20 is proportional to the reduced valve flow (defined under "Definitions"). Equation 7-20 can now be rewritten as:

$$q_{r,inlet} = f_7\left(\frac{P_o}{P_1}\right) c_v \tag{7-21}$$

The reduced inlet valve flow, $q_{r,inlet}$, can also be calculated by compensating the reduced expander flow, $q_{r,exp}$, from expander inlet conditions to valve inlet conditions; in other words, from conditions at point 1 to the conditions at point 0. It is already assumed that $T_o = T_1$ and $Z_o = Z_1$ and, therefore, it is only necessary to compensate for pressure from P_1 to P_o. This can be formulated as:

$$q_{r,inlet} = q_{r,exp}\left(\frac{P_1}{P_o}\right) \tag{7-22}$$

Combining Equations 7-21 and 7-22 and defining the formula for the conditions after the breaker opening yields:

$$c_{v,inlet,aft} = \frac{q_{r,exp,aft}}{f_7(P_o / P_{1,aft})}\left(\frac{P_{1,aft}}{P_o}\right) \tag{7-23}$$

All parameters of Equation 7-23 are known except $c_{v,inlet,aft}$. Step 3 calculated for $P_{1,aft}$ and $q_{r,exp,aft}$ was calculated in Step 4. Therefore, it is possible to determine $c_{v,inlet,aft}$.

Step 6: Calculate step on the inlet valve. Now that the new inlet valve c_v after the breaker opening has been determined, this can be translated into a valve position. This is a simple process using the valve characteristic of the manufacturer. Figure 7-8 shows a typical butterfly valve characteristic. This curve shows the calculated $c_{v,inlet,aft}$. Using the valve curve, the new valve position is determined.

The actual valve position is measured by the control system. The step on the valve is determined as the difference between the current valve position and the new valve position.

Step 7: Calculate the differential in $\Delta c_{v,bypass}$. One PRT control objective is to maintain the differential pressure between the regenerator and the reactor stripper. At the time of the breaker opening, it is assumed that the reactor stripper pressure will not vary. Therefore, to keep the differential pressure constant, the regenerator pressure needs to also remain constant. For the expander, this means that P_o must remain constant. To keep P_o constant, the mass flow before and after the breaker opening must remain constant (Equations 7-7 and 7-8). This implies that whatever mass flow is reduced on the inlet valve must be rerouted over the bypass valve.

The criterion of equal mass flows before and after the breaker opening is the same as keeping the total reduced flow through the inlet and bypass valves equal. This is only true when valve inlet conditions are the same, which they are in this case.

To calculate the $\Delta c_{v,bypass}$ it is necessary to know the reduced flow on the inlet valve. The change in reduced flow, $\Delta q_{r,inlet}$, can be determined by calculating the inlet valve reduced flow before and after the breaker opening. This reduced flow can be calculated by compensating the reduced expander flow for pressure conditions. In formula form:

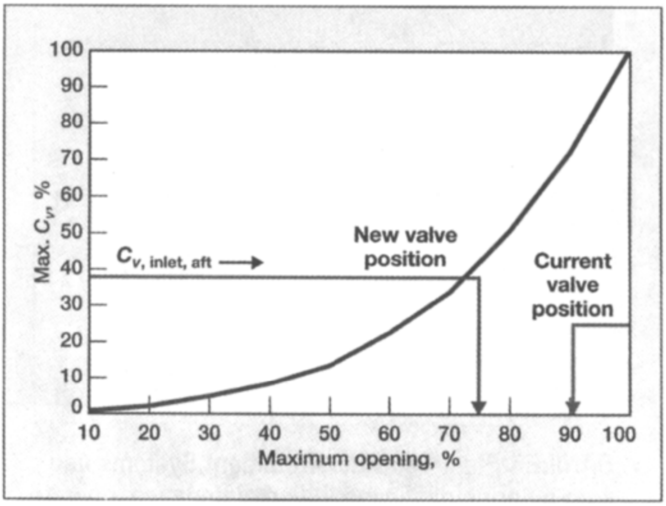

Figure 7-8. The new inlet valve position can be determined from the valve curve.

$$\Delta c_{v,bypass} = \frac{q_{r,exp,aft}(P_{1,bef} / P_o) - q_{r,exp,aft}(P_{1,aft} / P_o)}{f_8(P_o / P_2)} \qquad (7\text{-}24)$$

All parameters are known in the control system and the required $\Delta c_{v,bypass}$ can be calculated.

Step 8: Calculate step on the bypass valve. Now that the $\Delta c_{v,bypass}$ of the bypass valve is known, this must be translated into a new valve position. A similar process as described in Step 6 is used. However, in this case there is not an absolute value of c_v, but instead a Δc_v. Therefore, first determine the actual $c_{v,bypass,bef}$. This is accomplished by taking the actual bypass valve position and using the manufacturer's curve (Figure 7-9). From this point, the method to determine the new valve position is the same as described in Step 6.

Step 9: Apply steps to inlet and bypass valves. Now that the new inlet and bypass valve positions are determined, the outputs to the valves can be changed. Before doing this, however, due to flexibility in the control system, it is still possible to manipulate the step on the valve. For this purpose, the control system provides scaling factors between the actual step and the calculated step. These scaling factors can help compensate for calculation errors and/or process dynamics. This is formulated as:

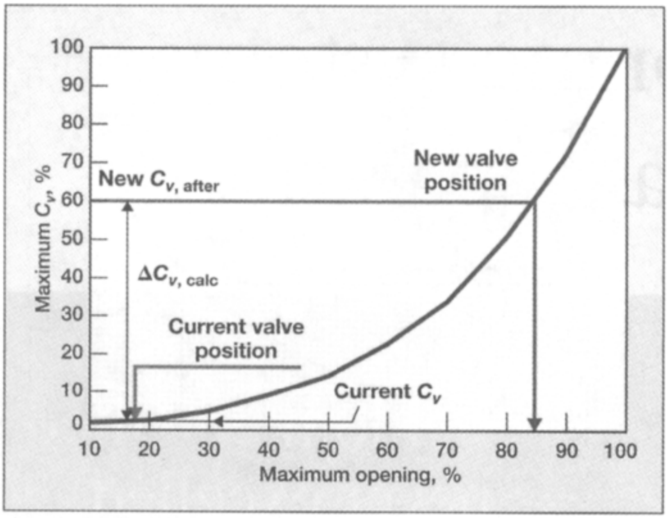

Figure 7-9. The bypass valve position can also be determined from the valve's curve.

$$\Delta \text{Output}_{\text{inlet,act}} = \Delta \text{Output}_{\text{inlet,calc}} C_1 \tag{7-25}$$

$$\Delta \text{Output}_{\text{bypass,act}} = \Delta \text{Output}_{\text{bypass,calc}} C_2 \tag{7-26}$$

These trimming factors can, for instance, be used to reduce the bypass valve step in comparison to that calculated. Opening the bypass valve too much can cause the regenerator pressure to drop, causing catalyst to enter the expander and exit the stack. This should be avoided, which can be achieved by the trimming factors.

Method Simplification

Clearly, the calculations are quite extensive and machine data must be available to perform the calculations to make the system work. If those data are not available, a simpler method can be used. As seen in the figures, the relationships between the different parameters are nonlinear and, therefore, simplification will lead to errors in the algorithm. Nevertheless, it is better to do something than to do nothing with this specific disturbance.

One of the simplifications is to assume that power is a function of valve position. This basically assumes that valve and expander inlet conditions are constant, which is not always the case. However, knowing the process conditions around the expander are fairly constant during a significant percentage of the FCCU operating time, this method can still yield good results.

The next simplification is to assume that there is a linear relationship between a change in power and a change in valve position. This is even less accurate than the previous method, but can still yield reasonable results if the expander typically runs in the same operating conditions and, for example, the bypass valve is usually closed. However, due to the nonlinear characterisitics, this method can cause significant over or under reaction depending on actual FCCU operating conditions.

ROTOR DYNAMICS AND VIBRATION ANALYSIS

Because the study of rotor dynamics and vibration analysis is contained in numerous texts only some basic troubleshooting tables and guidelines are presented. They describe the most common peaks in a typical vibration analysis spectrum and how these symptoms might be mitigated.

VIBRATION FREQUENCIES AND VELOCITIES

Of all vibration frequencies, the most dangerous are the synchronous vibrations, where an externally forced vibration excites one of the natural (resonant) frequencies in the machine. Campbell diagrams constructed by the manufacturers will help the operator avoid these frequencies during run-up or commissioning of the machine in question.

Tables 7-1 through 7-7 give commonly accepted "guideline" limits for vibration readings. These limits apply to turboexpanders and all associated machinery in the process train.

Guide Basis

The limits expressed in Table 7-3 (x-axis = operating speed in rpm, y-axis = overall vibration level in mils [peak to peak]) are based on experience in refineries. The guide reflects the typical proximity probe installation close to and supported by the bearing housing and assumes the main vibration component to be of [1× rpm] frequency. The

Table 7-1
"Normal" vibration levels on bearing housings in ips (in. per second, peak) highest noted on smooth machine

MACHINE TYPE:	1	2	3	4	VP1	VP2	GMF1	GMF2	BP1	BP2
BLOWERS (6000 RPM MAX)	.05	.02	.01	.01	.04	.01				
HORIZONTAL CENTRIFUGAL COMPRESSORS	.05	.02	.01	.01	.04	.01				
BARREL COMPRESSORS	.03	.01	.005	.005	.05	.005				
GEARS: PARALLEL SHAFT	.1	.05	.02	.02			.05	.02		
EPICYCLIC	.05	.02	.02	.02			.05	.01		
STEAM TURBINES	.1	.02	.02	.02					.05	.01
GAS TURBINES/ AXIAL COMPRESSORS	.2	.02	.01	.01					.05	.01
PUMPS	.1	.05	.01	.01						
MOTORS	.1	.1	.05	.05						
			LP1	LP2	LP3	LP4	LP5			
SCREW COMPRESSORS	. 1	. 01	. 1	. 1	. 1	. 05	. 05			

VP = VANE PASS
BP = BLADE PASS
GMF = GEAR MESH FREQUENCY
LP = LOBE PASS

seemingly high allowable vibration levels above 20,000 rpm reflect the experience of high-speed air compressors (up to 50,000 rpm) and jet engine type gas turbines with their light rotors and light bearing loads.

Readings must be taken on machined surfaces with runout below .5 mil up to 20,000 rpm, and below .25 mil above 12,000 rpm.

Table 7-2
Maximum allowable vibration limits on bearing housings in ips (peak) for operation up to earliest possible corrective shutdown

	SPEED HARMONICS									
MACHINE TYPE	1	2	3	4	VP1	VP2	GMF1	GMF2	BP1	BP2
BLOWERS (6000 RPM MAX)	.5	.4	.25	.25	.1	.05				
HORIZONTAL CENTRIFUGAL COMPRESSORS	.25	.2	.15	.15	.1	.05				
BARREL COMPRESSORS	.15	.1	.1	.1	.05	.025				
GEARS: PARALLEL SHAFT	.25	.2	.15	.15			.1	.05		
EPICYCLIC	.15	.1	.1	.1			.1	.05		
STEAM TURBINES	.25	.2	.15	.15					.1	.05
GAS TURBINES/ AXIAL COMPRESSORS	.5	.4	.25	.25					.1	.05
PUMPS	.25	.2	.15	.15	.1	.05				
MOTORS	.25	.2	.15	.15						
			LP1	LP2.	LP3	LP4	LP5			
SCREW COMPRESSORS	.25	.2	.2	.2	.2	.2	.2			

VP =VANE PASS BP = BLADE PASS
GMF=- GEAR MESH FREQUENCY LP =- LOBE PASS

Warning: Judgement must be used especially when experiencing frequencies in multiples of operating rpm on machines with standard bearing loads. Such machines cannot operate at the indicated limits for frequencies higher than [1× rpm]. In such cases, enter the graph with the predominant frequency of vibration instead of the operating speed.

(text continued on page 428)

Table 7-3
Turbomachinery shaft vibration guide

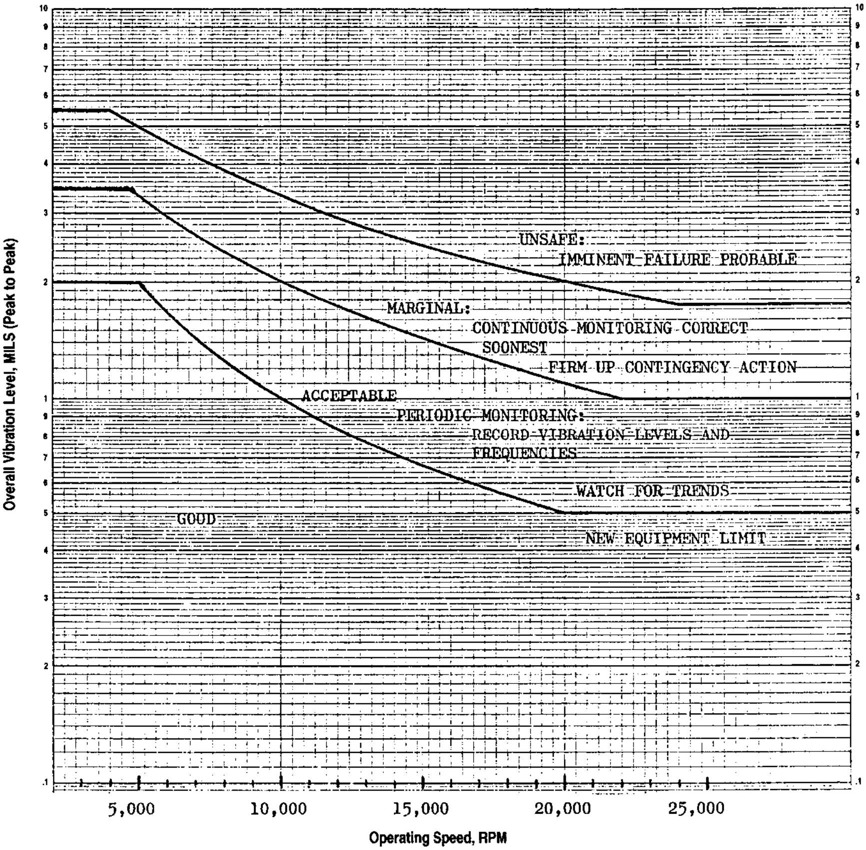

Table 7-4
Machinery lateral vibrations, less than [0.5× rpm]

Symptom	Probable cause	Examples
Appears suddenly at a frequency of 40–50% of rpm. Often disappears when speed is reduced. Lube oil temperature increase will often eliminate or reduce vibration severity.	Bearing oil whirl	• Bearing clearance too large • Bearing lightly loaded • Oil viscosity too high • Improper bearing design
Same symptoms as bearing oil whirl except a decrease in lube oil temperature will often eliminate or reduce vibration severity.	Seal ring oil whirl	• Oil ring seal acting as lightly loaded bearing
Same symptoms as bearing oil whirl, however, vibration frequency is constant even though speed is changed.	Resonant whirl	• Same as oil whirl except triggered by resonant component such as rotor, casing, piping, etc.
Appears suddenly at or above rotor critical speed when critical is below one-half operating speed. Increasing speed increases vibration amplitude, but whirl frequency remains constant. When speed is decreased, vibration disappears below where it first appeared.	Friction-induced rotor whirl	• Encountered in built-up rotors or rotors with shrink fits or rotor disassembly to inspect fits, increase shrink fits • Coupling friction has been known to induce whirl
Vibration appears/disappears suddenly with increasing/decreasing speed, respectively.	Loose component	• Rotor sleeves/impellers become loose as speed is increased • Bearing liners, housings, or self-aligning spherical casts have loose fits • Loose casing or supports
Vibration peaks at specific speeds/high axial vibration is often present.	Sub-harmonic	Usually occurs as a result of loose components or as a result of aerodynamic or hydrodynamic excitations; areas to be investigated for correction are seals, thrust clearance, couplings, and rotor/stator clearance

Table 7-5
Machinery lateral vibrations [1× operating frequency]

Symptom	Probable cause	Examples
Increasing vibration amplitude with speed; behavior repeats for successive runs.	Unbalance	• Loose rotor component • Foreign object lodged in rotor • Fouling • Poor balance (initial startup of rotor or components added to rotor (coupling, etc.) • Off-center journal
Vibration peaks at specific speeds; peaks can usually be shifted with change in oil temperature	Rotor critical speeds	
Vibration peaks at specific speeds; oil temperature changes will generally not change the speed at which the peak occurs.	Structural resonance	• Any machine part or supporting structure could have its natural frequency in the operating speed range
Increasing vibration with speed.	Casing distortion	• Uneven casing warmup • External forces
Increasing vibration with speed; may or may not repeat for successive runs (prime 1×, also up to 5× present).	Bowed or bent rotor	• Temporary heat bow • Permanent (no change with time)

Vibration amplitude varies with time in a definite rhythm (beat).	Beat frequency	• Occurs when two or more machines mounted on common foundations operate at nearly the same speed • Occasionally, a beat can develop in one machine if its operating speed is close to a structural component resonance
Increasing vibration with speed; other frequencies and axial vibration usually present.	Thrust bearing damage	• Usually a result of off-design operation (surge, liquid slugging) or balance piston problem (design, plugged, or worn labyrinths)
Increasing vibration with speed. Shaft bearing housing amplitude about equal.	Sleeve bearing damage	• Increased clearance • Wiped bearing
Increasing vibration with speed (prime frequency is 1× rpm plus many other frequencies).	Seal rub	• Rub usually relieves itself and, therefore, appears as erratic vibration.
High axial vibration, vibration erratic (prime frequency is 1×, also 2× present).	V or other drive belts Component eccentricity	• Mismatched V-belts • Drive and driven pulley not aligned • Gear pitchline has excessive runout • Thrust collar may be cocked
Electric motors. Vibration behaves like unbalance but disappears when power is off.	Electric motor armature	• High eccentricity
Appears on gears like rotor critical speed. Vibration peaks at specific speeds.	Torsional resonance	• Usually occurs only during startup or drastic load-speed change

Table 7-6
Machinery lateral vibrations [2× operating frequency]

Symptom	Probable cause	Examples
Increasing vibration with speed (prime 2×, also 1× and/or 5× present. Often accompanied by high axial vibration).	Misalignment of coupling or bearing	• Thermal casing growth • Piping forces • Bearing housing alignment
Increasing vibration with speed.	Loose rotor components	• Loose coupling hub • Loose impellers or sleeves
Increasing vibration with speed. Appears on adjacent rotors.	Coupling machining inaccuracies	• Replace coupling
Increasing vibration with speed. Vibration appears/disappears suddenly. Appears on adjacent rotors.	Coupling damage	• Pitting of coupling teeth • Loose coupling spacer • Dirt in coupling teeth
Increasing vibration with speed.	Unbalanced reciprocating part(s)	• Crankshaft or piston type machinery • Loose piston or rod
Vibration peaks at specific speed.	Harmonic resonance	• Same as critical or resonance

Table 7-7
Machinery lateral vibrations [frequencies > 2× rpm]

Symptom	Probable cause	Examples
Erratic high-frequency vibration amplitude and possibly an audible sound.	Rotor rub	• Labyrinth rubs generally self-correct • Disc rubs due to thrust bearing failure often self-correct temporarily through wear; steel on steel shrill noise during wear • Rotor deflection is critical speed
Rpm × number of vanes/blades Rpm × number of guide vanes/nozzles.	Vane/blade aerodynamic or hydraulic forces.	• No concern for normal operations • Record signal for machine as new condition to permit identification of possible future problem; also record harmonics
Rpm × number of gear teeth (always present)	Gear mesh frequency	• Record signal for reference • Distress noisy and shows increase in GMF and harmonics • One-half GMF—even number of teeth with machining error
Rpm × number of lobes (always present)	Lobe pass frequency	• Record for future reference
Rpm × number of pads (always present)	Journal tilt pad bearing	• Increased vibration with increasing clearance
High-frequency, destructive vibrations. Unaffected by operating speed.	Steam turbine valve vibration	• Rare occurrence; change valve plug, seat shape, and/or increase valve gear rigidity
Multiples of running frequency	Harmonic resonance	• Multiples of component natural frequencies (rotor casing, foundation, bearing housing, diaphragms, etc.)

(text continued from page 421)

OPTIMIZED/REENGINEERED DESIGN AND ECONOMICS[2]

Turboexpanders are usually custom designed to what the customer defines as "normal" operating conditions. Normal operating conditions, however, rarely remain unchanged for a long period of time. In fact, there have been cases where the normal operating conditions changed during manufacture of the turboexpander or shortly thereafter.

In natural gas applications, changes in normal design conditions are common over time, but even relatively stable applications such as air separation are not totally immune from change. However, since the frequency of changes in normal design conditions for air separation plants is much less than for natural gas processing plants, the following addresses turboexpanders in natural gas plant applications.

The design of a turboexpander and its sensitivity to changes in design conditions are well known facts. Extensive performance data collected from actual operating sites support this premise. Likewise, retrofitting and upgrading gas processing plant equipment to accommodate changes in normal design conditions of the feed gas have been studied as has the restaging of centrifugal gas compressors. However, the economic impact of operating a turboexpander at an off-design condition has not been the subject of rigorous study.

The following examines the sensitivity of a turboexpander and brake to changes in normal design conditions, as well as the degradation of a turboexpander's thermal efficiency (TTE) as a result of changes in individual normal design condition parameters. The economic impact of drops in TTE are presented along with the cost impact of redesigning a turboexpander. Recommendations about the timing of a turboexpander redesign are also provided.

TURBOEXPANDER DESIGN AND PERFORMANCE

Earlier chapters explained that air separation expanders are "turbines" that expand gases in two steps, using primary and secondary gas expansion devices. Inlet guide vanes (or inlet nozzles) are the primary expansion device. Their function is to convert almost half of

[2]*Source: Atlas Copco, Rotoflow Division.*

the total pressure head across the turboexpander into velocity head. The secondary expansion device is the turboexpander impeller. This is where velocity head and the other half of total pressure head are converted into useful torque. Figure 7-10 illustrates primary and secondary expansion with velocity triangles at the inlet and outlet of the turboexpander.

Turboexpander thermal efficiency (TTE isentropic) is defined as the ratio of actual work produced by the fluid, divided by the work produced from the isentropic expansion process. Depending on gas composition, expansion ratio, and liquid formation, TTE varies between 80%–90%. These high efficiencies are the result of improvements to the thermodynamic and mechanical design of turboexpanders since the early 1960s and their use in gas processing plant applications.

Consider the normal design conditions as shown in Table 7-8, with process gas compositions shown in Table 7-9. The turboexpander is

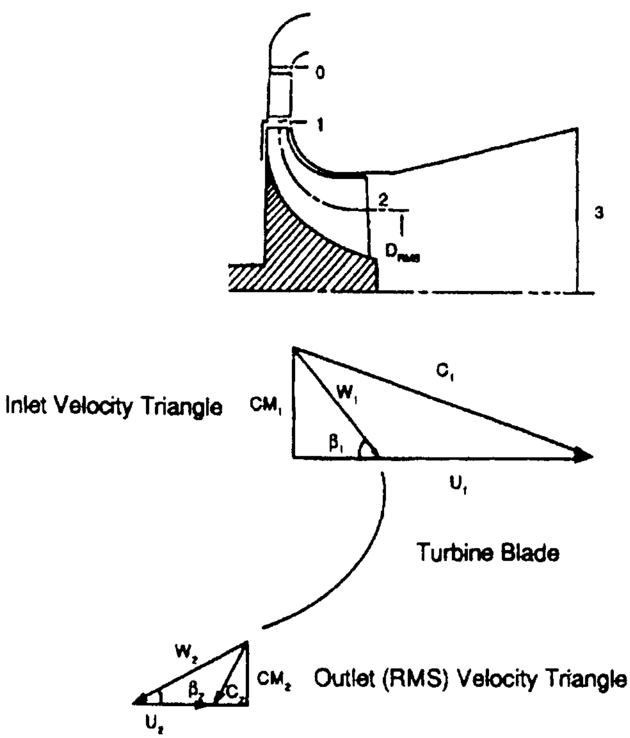

Figure 7-10. One-dimensional turbine model and turbine velocity triangles.

Table 7-8

Normal design parameter	Expander	Compressor
Inlet flowrate, lb/hr	221,000	208,000
Inlet molecular weight, lb/mol	17.46	16.5
Inlet gas rate, MMscfd	115.6	115.2
Inlet pressure psia	1,080	470
Inlet temperature, °F	–50	60
Discharge pressure, psia	480	576
Discharge temperature, °F	–113.6	93.5
Liquid formation, wt%	19.3	—
Speed, rpm	22,000	22,000
Power, BHP	1,380	1,350
Efficiency, %	83	74

Table 7-9

	Mol %	
Process gas composition	**Turboexpander**	**Compressor**
C_1H_4	93.00	97.33
C_2H_6	4.41	1.85
C_3H_8	1.13	0.13
i-C_4H_{10}	0.28	0.01
n-C_4H_{10}	0.25	—
i-C_5H_{12}	0.25	—
n-C_5H_{12}	—	—
C_6-H_{14}	—	—
N_2	0.55	0.56
CO_2	0.13	0.12
Totals:	100.00	100.00

designed to optimize TTE at normal design conditions. The turboexpander thermal efficiency curve is shown in Figure 7-11. TTE is a function of μ/C_0, or "spouting velocity."

Turboexpanders may be used in variable speed (compressor, blower, or oil brake) or constant speed (generator brake) and pre-boost or post-boost applications. In variable speed applications, the performance characteristics of turboexpanders, particularly those driving compressors, are more sensitive to changes in normal design conditions. This examination of turboexpander-compressors is limited to post-boost applications only.

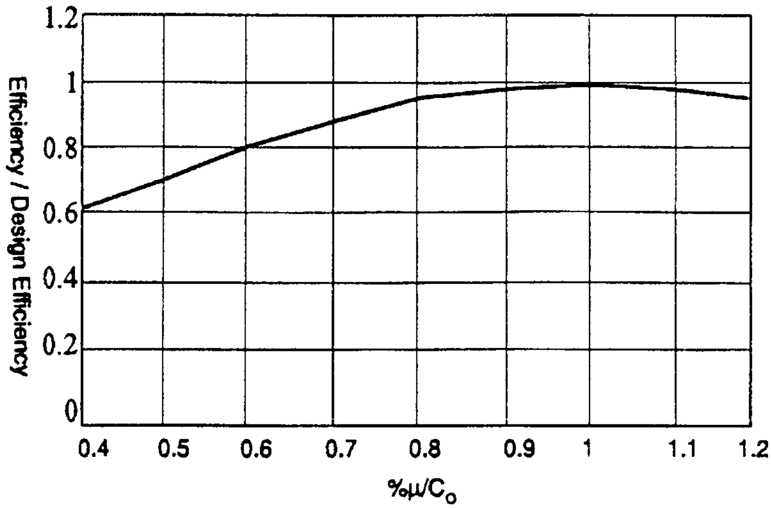

Figure 7-11. Expander thermal efficiency versus μ/C_0.

In pre-boost applications, an integral booster compressor feeds an expander and the complexity of interactions is different than in post-boost applications where the integral booster compressor is downstream from the turboexpander.

In the following discussion on TTE degradation, it is assumed that for constant speed cases the turboexpander drives an induction generator and for variable speed cases it drives a compressor with normal design conditions as given in Table 7-8.

TTE DEGRADATION

Consider the sensitivity of TTE to four process gas normal design condition parameters: inlet gas pressure (P_t), inlet gas temperature (T_1), gas mass flow (M), and gas molecular weight (MW).

Constant Speed Turboexpander

Turboexpander sensitivity to process gas inlet pressure. Figure 7-12a shows that TTE is more sensitive to a reduction than to an increase in the inlet gas pressure. For example, a 20% reduction of inlet gas pressure results in a 4% reduction of design TTE, while a 20% increase in inlet gas pressure produces only a 0.25% reduction in thermal efficiency.

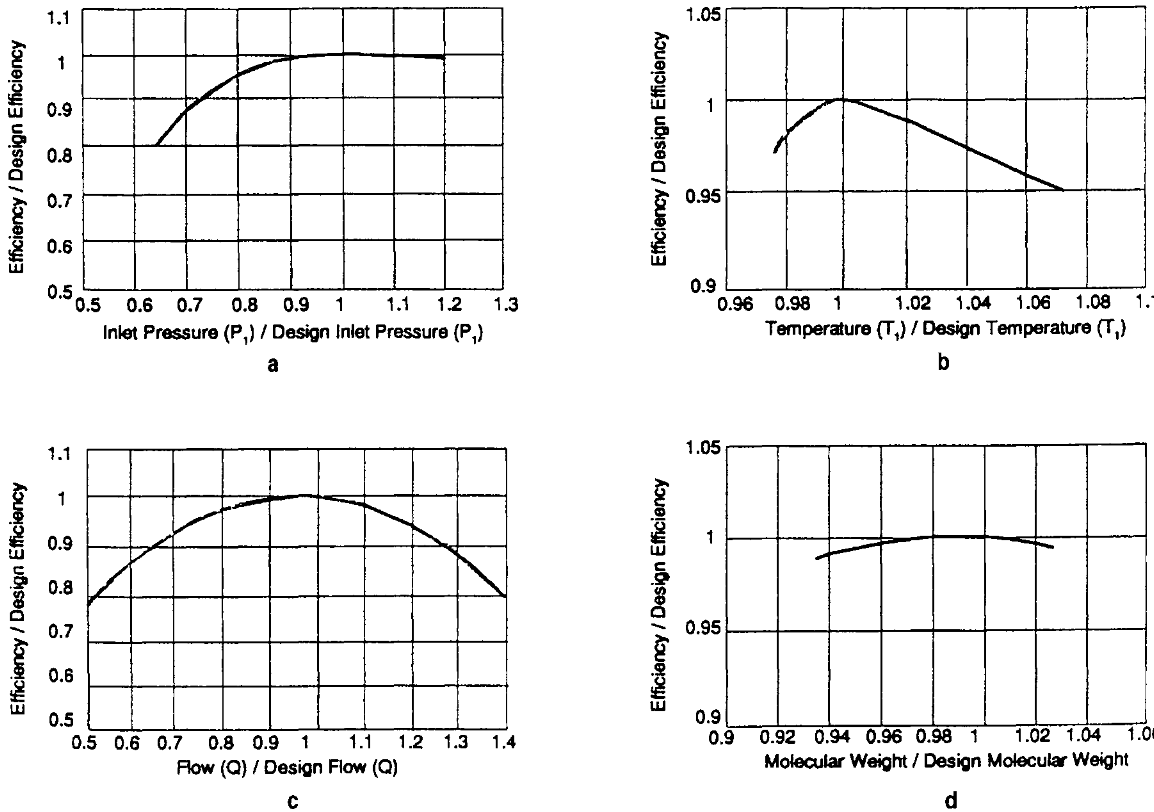

Figure 7-12. Turboexpander parameters at constant speed.

Turboexpander sensitivity to process gas inlet temperature. Figure 7-12b shows that TTE reduces near-symmetrically with decreases or increases in the process gas inlet temperature. For example, a 3% increase or decrease in inlet temperature reduces TTE by 2%.

Sensitivity to process gas inlet flow. Figure 7-12c shows that TTE is more sensitive to increases in mass flow than to decreases. For instance, a 20% increase in mass flow reduces TTE to 94% of the design efficiency, while a 20% decrease reduces TTE to 97% of design value.

Sensitivity to process gas molecular weight. Figure 7-12d shows that TTE is not sensitive to process gas molecular weight.

Variable Speed Turboexpander

Turboexpander sensitivity to process gas inlet pressure. As previously mentioned, variable speed turboexpanders are more sensitive to changes in normal operating conditions. The pattern of TTE degradation, however, is the same as for constant speed turboexpanders (Figure 7-13a). In other words, TTE is more sensitive to pressure drop than to pressure rise. For instance, a 20% drop in gas inlet pressure will reduce TTE to 90% of the design value, whereas a 20% increase in gas inlet pressure reduces TTE to 99% of the design value.

Sensitivity to process gas inlet temperature. Figure 7-13b shows TTE variation with changes in process gas inlet temperature. The sensitivity of variable speed machines to temperature variation is less than constant speed machines. The pattern and symmetry around the design point, however, are the same for constant speed machines. For example, note that a 3% decrease in the inlet temperature causes TTE to drop to 98% and that the same percentage drop in TTE occurs when gas inlet temperature rises by 3%.

Sensitivity to process gas mass flow. Figure 7-13c depicts the sensitivity of TTE to changes in process gas mass flow. For example, a 20% drop or rise in gas mass flow reduces TTE to 96% of design efficiency.

Sensitivity to process gas molecular weight. Figure 7-13d shows that TTE is not sensitive to changes in the molecular weight of the process gas. Constant speed machines show the same results.

Hydrocarbon Extraction

Only TTE is considered because it directly impacts the turboexpander's hydrocarbon extraction (liquid production), thereby directly

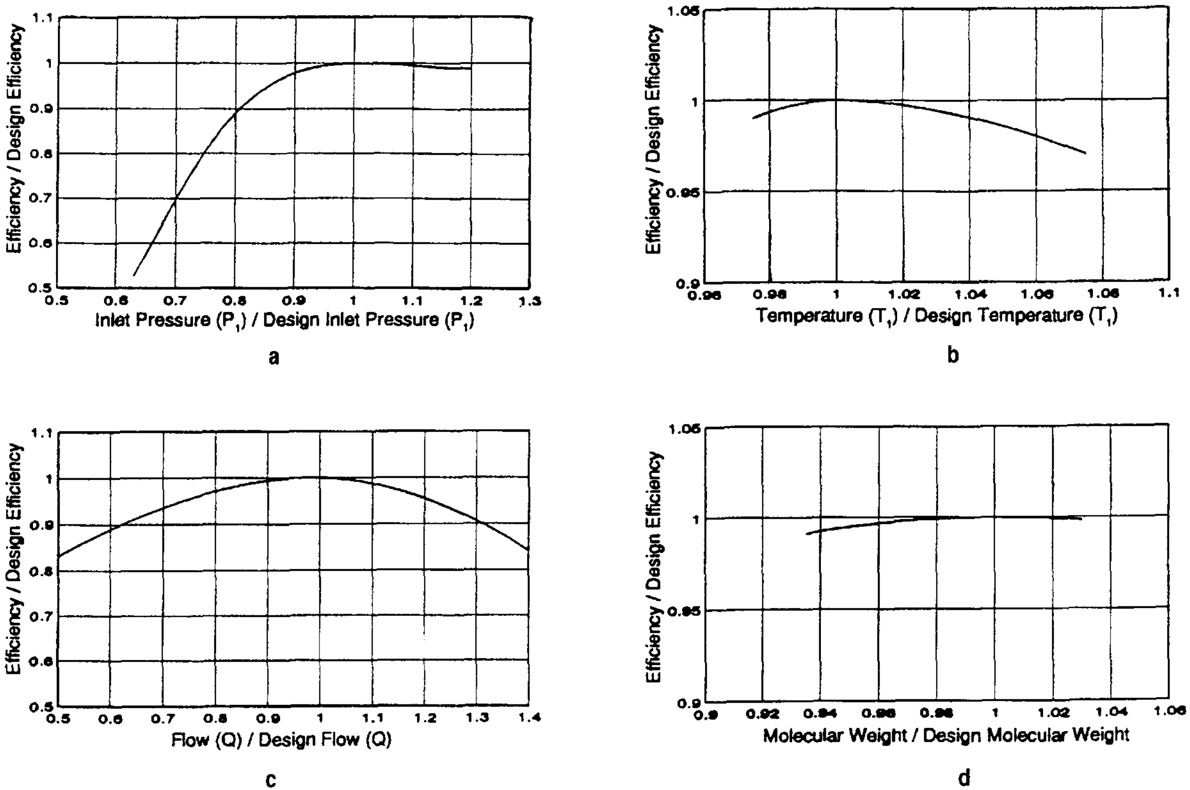

Figure 7-13. Turboexpander parameters at variable speed.

impacting the plant operation as a whole. Given the composition in Table 7-9 and normal design conditions in Table 7-8, Figure 7-14 shows hydrocarbon extraction as a function of TTE variation.

Clearly, the turboexpander is one of several key components in a process plant and liquid production is related to the performance of all components of the plant, not the turboexpander alone. It has previously been assumed that changes in the normal design conditions of turboexpanders have not adversely affected other equipment in the plant because adverse impact on other equipment, if any, would further reduce liquid production. This simplifies the assumptions, but does not affect the general validity of the findings.

Liquid production is usually the main objective of any gas plant. Reductions in liquid production result in reductions in plant revenue. Revenue reduction is a major concern and is often what initiates a redesign project.

Turboexpander Redesign Concepts

The modular design of a turboexpander allows some flexibility in modifying parts to accommodate changes in normal design conditions. The extent to which modification is possible depends on how much the original design conditions have changed. Sometimes existing parts can be modified at low cost. In other cases, when changes are

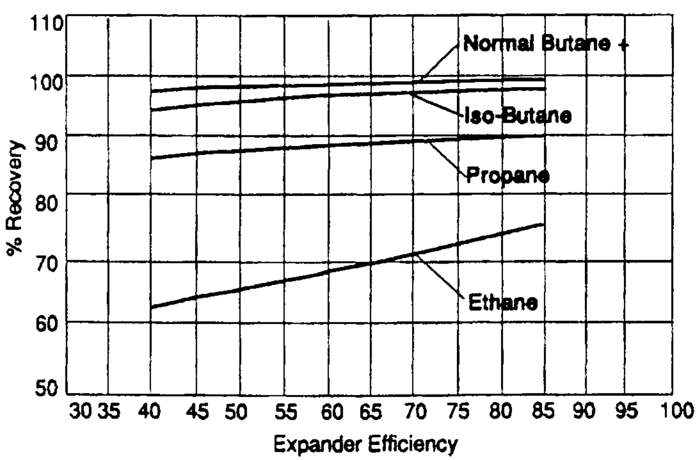

Figure 7-14. Typical gas plant liquid recovery.

extensive, engineering redesign and new manufacturing requirements can render the modification quite costly.

For the purpose of conceptual presentation, cost may be considered in terms of TTE improvement. Figure 7-15 shows such an approximation and makes it clear that modification cost as a function of modification rate follows an exponential trend.

Break-even Analysis

Any degradation of TTE, reduction in liquid production, and decrease in revenue associated with deviation from the normal design conditions is important, but may not justify redesign. Redesign is justified only if the economic value of the performance improvement outweighs the economic disadvantage of deviation from the normal design conditions. Figure 7-16 evaluates the disadvantages of change and the advantages of redesign. This figure depicts the break-even point. In this application, break-even is the point at which the gas plant has net zero gain. If TTE degradation goes above the break-even point, the gas plant is losing net profit if it does not proceed with the redesign. If TTE degradation is below the break-even point, it is better to delay redesign.

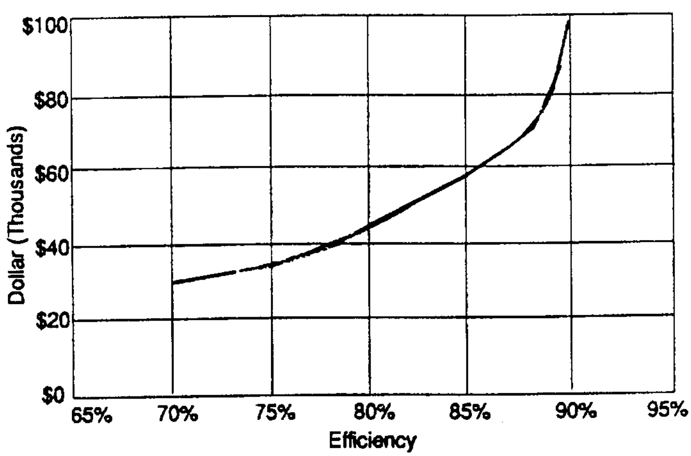

Figure 7-15. Typical cost of expander redesign.

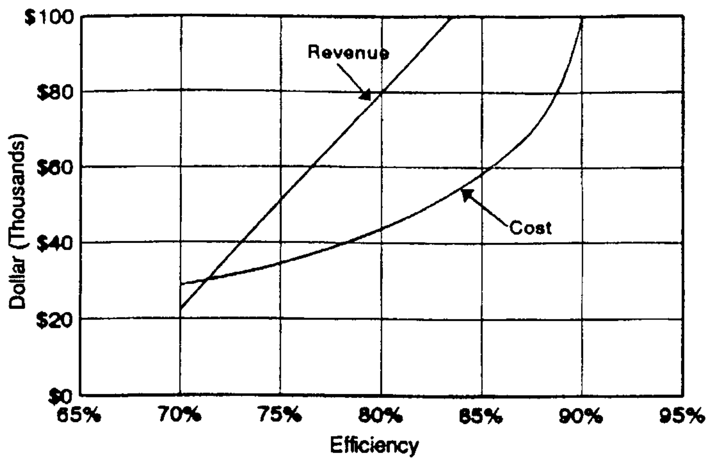

Figure 7-16. Typical revenue increase compared to expander upgrade costs (6 months).

NOMENCLATURE

c_v	conductance through a valve
C	constant
F_k	ratio of specific heats, dimensionless
F_p	piping geometry factor, dimensionless
I	moment of inertia
J, j	power
j_r	reduced power
k	isentropic exponent
K	orifice coefficient
MW	molecular weight
N	rotational speed
N_8	numerical constant for units of measurement used
N_e	equivalent speed
P	absolute pressure
ΔP_o	differential pressure across flow measurement device
q_r	reduced flowrate
R	gas constant (R_u/MW)
R_c	pressure ratio across expander
R_u	universal gas constant
R_v	pressure ratio across valve

T	temperature
w	mass flowrate
x	ratio of pressure drop to absolute inlet pressure ($\Delta p/p_o$) for valves, dimensionless
x_r	pressure drop ratio factor, dimensionless
Y	expansion factor, ratio of flow coefficient for a gas to that for a liquid at the same Reynolds number, dimensionless
Z	compressibility factor

Subscripts:

0	upstream of bypass and expander inlet valve
1	expander inlet
2	expander and bypass valve outlet
act	actual
aft	after breaker opening
bef	before breaker opening
bypass	expander bypass valve
calc	calculated
exp	expander
inlet	expander inlet valve
gen	generator
r	reduced

Definitions:

Reduced flow for the expander:

$$q_{r,exp} = \frac{w\sqrt{ZRT}}{P_1} = K\sqrt{\frac{P_{o,1}}{P_1}} \qquad (7\text{-}27)$$

Pressure ratio expander:

$$R_{c,exp} = \frac{P_1}{P_2} \qquad (7\text{-}28)$$

Pressure ratio inlet valve:

$$R_{v,inlet} = \frac{P_o}{P_1} \qquad (7\text{-}29)$$

Pressure ratio bypass valve:

$$R_{v,\text{bypass}} = \frac{P_o}{P_2} \tag{7-30}$$

Reduced power expander:

$$\dot{j}_{r,\exp} = \frac{J}{P_1\sqrt{ZRT}} \tag{7-31}$$

Equivalent speed:

$$N_e = \frac{N}{\sqrt{ZRT_1}} \tag{7-32}$$

BIBLIOGRAPHY AND ADDITIONAL READING

1. Gulsby, I. and Coo, G. D., "Retrofitting for Increased Capacity," 67th Annual GPA Convention. March 14–16, 1955, Dallas, Texas.
2. Wardall, R. M., "Restaging Centrifugal Gas Compressors," Turbomachinery International, September 1983.
3. Wilkinson, I. D. and Hudson, H. M., "Upgrading Turboexpander Plants for Higher Ethane Recoveries," Texas Regional GPA Meeting, February 20, 1986.

CHAPTER EIGHT

Specific Applications and Case Histories

The following specific case applications indicate the present, potential, and growing diversity of turboexpander use. The case histories do not occur in any particular sequence, but the key words or phrases that synopsize the application are included in the index. The demographics, statistical data, and geographic details about the plant locations involved have generally been retained in these case studies. They present the reader with a perspective on how far turboexpander technology has spread throughout the world, and the difficult process conditions this technology has overcome. It is shown that cost and maintenance complexity are not prohibitive even in countries or locations where sophisticated local overhaul facilities are scarce.

CASE 1: CRYOGENIC TECHNOLOGY HELPS OPTIMIZE PRODUCTIVITY[1]

New Mexico's San Juan Gas Plant is one of the United States' newest and largest natural gas liquids recovery plant. Commissioned in November 1986, its levels of productivity are high by industry standards. Located near Bloomfield, New Mexico, just south of the Colorado border, the plant is jointly owned by Conoco Inc. (then a subsidiary of the DuPont Company) and Tenneco Inc., both of Houston. It is operated by Conoco and is named after its location in the San Juan basin, an area of oil, gas, and coal production.

The San Juan plant can process up to 500 MMcfd of gas, and extract 40,000 bbl of EPBC liquids. EPBC liquids include ethane (E), propane (P), butanes (B), and condensate (natural gasoline) products

[1] *Source for case histories is Atlas Copco Corporation, unless otherwise stated.*

that the oil and chemical industries use as feedstocks in the manufacture of chemical and petroleum-related products.

Ethane is used by petrochemical plants to make ethylene, a primary building block for many plastic products. Butane and condensate are used by refineries producing automotive fuel. For production of NGL's (natural gas liquids), the plant's recovery rate of 98% of ethane and 100% of all other liquid products contained in natural gas, is among the best in the world.

To extract the EPBC liquids, the plant employs a cryogenic temperature process in combination with a refluxed demethanizer process in two trains. The two turboexpander trains are the heart of the process and both have operated at efficiencies higher than originally expected at the design stage.

Computerized controls allow remote monitoring and control of temperatures, pressures, liquid levels, and fluid flows at three separate locations in the plant. Computer keyboards allow an operator to electronically perform precise processing adjustments from any of the three strategic plant locations.

The raw material at this plant is natural gas supplied by the El Paso Natural Gas Company from a nearby pumping station. In each process train, gas is compressed to 850 psig, dehydrated by an adsorption method to remove 100% of the water, then passed through a refrigeration unit to lower the temperature to –60°F. A separator removes liquids upstream of the turboexpander.

The turboexpander lowers the temperature of the product to –100°F, causing it to liquify. Now at 350 psig pressure, the liquid from this process enters the demethanizer tower where it mingles with the previously introduced stream of liquid. The turboexpanders provide a 92% recovery rate while the former system, a backup Joule-Thomson valve, was able to provide only a 60% recovery rate. The volume of gas entering the turboexpanders can vary up to 10%; yet, the different flowrates do not significantly affect the efficiency of these units, which are rated at 2,400 hp at 16,000 rpm.

The liquid collected at the bottom of the demethanizer tower is a mixture of ethane, propane, butane, and condensate (EPBC), which is taken off in a stream and pumped—as a liquid, at 1,000 psig—to a customer facility. Another part of the EPBC is introduced into a deethanizer tower. The stream of EPBC liquid entering the deethanizer tower is further separated into PBC liquid and pumped to the El Paso Natural Gas facility in Gallup, New Mexico. EP (ethane and propane) from this process can be routed to residue, as well as being returned to liquid and co-mingled with EPBC liquid prior to sale.

A methane gas stream taken off the demethanizer process, and still at 350 psig, is compressed via byproduct energy from the turboexpanders and raised to 410 psig. The gas is then introduced into a 15,000 hp compressor and raised to 850 psig for delivery back to the El Paso Natural Gas Company. The 60 psig boost by each turboexpander represents a 15% reduction in required horsepower. This amounts to considerable energy saved and is yet another reason why the turboexpander is useful in a cryogenic process of this type.

CASE 2: TURBOEXPANDERS INSTALLED AT AN OLDER METHANOL PRODUCING PLANT PROVIDE MAJOR ENERGY SAVINGS

In the energy markets of a few decades ago, oil and gas fuels were inexpensive. Thus, very little thought was given to energy conservation in the planning and construction of industrial and processing plants. However, starting in the early 1970s, this thinking began to change and plants built prior to that time have had to be upgraded or expanded to reduce energy costs.

An older processing plant that is now a model of energy conservation (achieved through upgrading) is the Bishop, Texas, Engineering Plastics Division of the Hoechst Celanese Corporation. The plant is a major producer of methanol, formaldehyde, and formaldehyde derivatives. Situated on a site of over 1,000 acres, the Bishop plant was originally built and owned by the U.S. Government during World War II to produce synthetic rubber. It was purchased in 1946 by the Celanese Corporation, and operated under Celanese ownership until 1987 when it became a member of the Hoechst Group of companies worldwide. Hoechst Celanese is a multinational corporation involved in the development, production, and marketing of a broad spectrum of chemicals, pharmaceuticals, advanced materials, and other high-technology products.

One of the major energy saving innovations that has been introduced into the Bishop, Texas, plant is an energy recovery process that takes advantage of excess hydrogen production. Hydrogen is a byproduct in the manufacture of methanol. Although the byproduct has always been used as a fuel supplement in the Bishop, Texas, plant, it was not until an energy shortage and sharply rising energy costs prompted the plant to install turboexpanders. These machines can tap the energy potential of a pressure reduction process.

The raw product in the production of methanol is natural gas (CH_4). It is delivered to the plant at 800 psi pressure. In a process that combines the CH_4 with steam, the gas is converted to a synthesis gas consisting of carbon monoxide (CO) + carbon dioxide (CO_2) + hydrogen (H_2) + water (H_2O). This gas is subsequently converted to methanol (Figure 8-1).

However, not all the hydrogen that is produced is used in the production of methanol. To prevent an excessive buildup of hydrogen in the recirculating methanol synthesis loop, a slipstream is drawn off consisting of hydrogen and some CO and CO_2. It is fed to the boiler as supplemental fuel to the main natural gas fuel supply. The slipstream is at approximately 800 psi pressure and must be reduced to 75 psi before it can be fed to the boilers.

When the plant was first constructed, the pressure reduction was accomplished using a series of pressure reducing valves, which did not take advantage of the energy recovery potential. This was the conventional operating mode in the mid-to-late 1940s technology. In the mid-1970s it was determined that substituting turboexpanders for pressure reducing valves would result in capturing energy that could serve to turn generators for producing electricity.

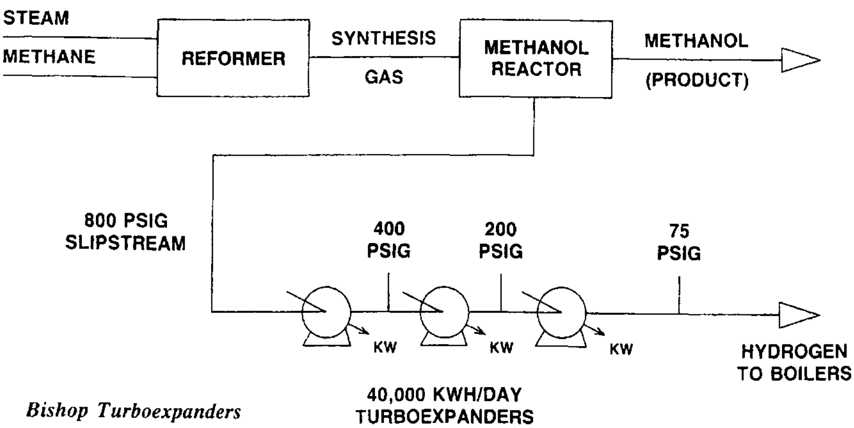

Bishop Turboexpanders

Figure 8-1. Energy recovery process taking advantage of excess hydrogen production.

Three turboexpanders were installed at the plant to reduce the slipstream pressure from 800 psi to 100 psi and to thus capture the kinetic energy made available. The energy captured by the turboexpanders provides 40,000 kWh of electric energy per day. One 23,000 rpm turboexpander with a 2:1 pressure reduction ratio takes the gas stream from 800 psi to 400 psi. A second 19,000 rpm turboexpander with the same 2:1 ratio takes the 400 psi gas down to 200 psi, and a third 19,000 rpm turboexpander with a 2:1 ratio takes the 200 psi gas down to 100 psi.

The units have been disassembled for maintenance by plant engineering personnel on a scheduled 3-year basis. Although a "preventive" maintenance philosophy was used where others might have opted to employ the "predictive" maintenance approach, the machines have operated well with an on-stream factor in excess of 99%.

CASE 3: MANUFACTURE OF COPPER AND MOLYBDENUM

BACKGROUND DATA

The arid open pit copper mine of Chuquicamata is located at an altitude of 9,000 ft (2,800 m) in the Atacama desert of Chile (Figure 8-2). It is a gigantic oval-shaped cavity, 4 km in length by 2.5 km in width, and constitutes one of the few man-made features that can be seen from space.

Chuquicamata—Chuqui for short—is one of five copper mines owned by the state and operated by the government of Chile, under the name of Codelco Copper Corporation. The Codelco mines have typically contributed annually 4% to the country's gross national product, of which more than 59% has been contributed by Chuquicamata. Situated in the northern part of Chile, 1,700 km from the capital of Santiago and close to the border of Bolivia, the Chuqui mine was scheduled to produce approximately 640,000 t of refined copper and 12,000 t of molybdenum as concentrate and technical oxide grade during 1997. About 3.12 t of rocky material are needed to obtain 1 t of ore, which at the end of the process results in 10 kg of refined copper. The known reserve of deposits amounts to 2.7 bt.

Codelco has invested $650 million (U.S.) in decontamination equipment and technology, allowing the Chuqui mine to catch more than

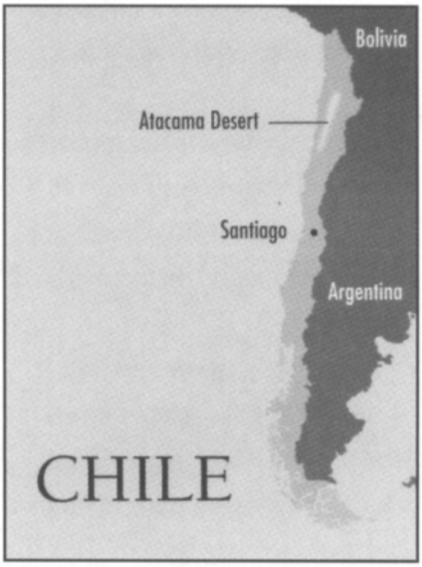

Figure 8-2. The Chuquicamata copper mine is located in the Atacama desert in Chile.

80% of sulphur trioxide and approximately 85% of arsenic emissions produced by mining operations.

HOW THE PROCESS WORKS

The production process starts with the extraction of the ore from blasting of banks or graded levels (Figure 8-3). The ore is transferred to a series of milling and storing silos for later delivery for further processing. The first grinding in the mill reduces the ore to pieces 6 in. in diameter, after which it is transferred by truck to a primary grinder. At the end of the process it enters the concentrate plant where it is reduced in size in a grinder comprised of bar mills and ball mills.

The pulp from this grinding process is introduced into a floating process to which water and chemical reactants are added. This process results in a collective concentrate, Cu-Mo, containing approximately 30% copper and 1% molybdenum. In a follow-up process, the copper and sulfur-molybdenum concentrate are separated.

The copper concentrate is filtered and dried in rotary kilns and later sent to the concentrate smelter, where it is melted at high temperatures

Figure 8-3. Copper and molybdenum-containing ore being mined by Codelco in Chile.

in an oxygen-enriched atmosphere in either flash furnace-type melting units or in holding-type converters. Both units employ state-of-the-art technology that was developed and patented by Codelco who sell it to other mining companies. The concentrate smelter produces 99.7% pure copper anodes, which are transferred to refineries where they are subjected to an electrolytic refining process, the final result of which are copper cathodes with a purity of 99.9%.

The sulfur molybdenum concentrate is subjected to a molybdenum recovery stage. This consists of a selective floating process in conventional and colonnade cells wherein the concentrate interacts with a form of diluted pulp. It is this pulp that contains specific chemicals together with nitrogen delivered at the rate of 10,000 Nm^3/h at 7 psig. Nitrogen production is a key step in the process as it inhibits the oxidation of the chemical agents, allowing them to maintain their properties.

The nitrogen is obtained as a byproduct of an oxygen production process (1,200 tpd of oxygen) in a dedicated oxygen plant. In this plant, parallel expansion turbines are used that were designed especially for the process. The first expansion turbine train (two turbines) went into service in 1986, and was followed by two turbines commissioned in 1993.

Some 45,000 Nm^3/h of filtered, compressed, and purified air pass through the expansion turbines, contributing a cooling factor to the process and allowing the separation of oxygen and nitrogen into cryogenic rectification columns. Next, the nitrogen flows toward a single-stage compressor where the pressure is increased, allowing it to be sent to the molybdenum plant located approximately 1.5 km away.

Although operating in a dry, hot, and dusty desert environment, compressor and expansion turbines must perform reliably if the Chuqui mine is to remain competitive in copper and molybdenum production.

The maintenance staff at the plant changed the high-speed pinion bearings in the train's gear box, but only as part of preventive maintenance and as a precautionary measure. Otherwise, machinery availability has been high.

CASE 4: NICKEL SMELTER AND OXYGEN PRODUCTION

BACKGROUND DATA

The Kalgoorlie nickel mine is about 6 m south of Kalgoorlie, Australia. It is operated by Western Mining Corporation and fed by a modern oxygen plant. Nickel was first discovered at nearby Kambalda in 1966. By 1970, concentrated nickel sulfide ore was being mined and delivered to the Kwinana refinery near Perth. Then, in 1972, a smelter was built near Kalgoorlie so that production at the Kambalda mine could be increased.

Dry nickel concentrate is brought from the mine by rail and stored in eight 1,000-t silos before being combined with flux and recycled furnace dust. Eventually, it is fed into Kalgoorlie's flash furnace where temperatures reach 1,350°C (2,500°F).

In Western Mining's flash smelting process, reaction air is preheated to 480°C (920°F) and enriched until the oxygen content is 24%. The reaction charge and combustion air are mixed, and heat for smelting comes from the combustion of fuel oil (some of it present in the flux) and sulfur in the concentrate. The process yields matte, a refined ore with 44% nickel content.

Batches of matte are then tapped from the sides of the furnace into ladles and transferred to converters. More flux is added, and air is blown through to oxidize the iron and sulfur. This results in a high-grade matte containing 72% nickel, 19% sulfur, and 5%–6% copper. Slag formed on the surface of the molten ore is poured off before the matte is dried. It is then either packaged for export or shipped by rail to the Kwinana nickel refinery.

In a business where oxygen plants play a key role in the cost of the end product, Western Mining needs high process efficiencies. This prompted the company to select a custom-built centrifugal compressor and turboexpander.

The 100-t compressor is 7 m tall and 15 m long (23 ft by 49 ft). Replacing two 40-year-old air units, it delivers 87,700 m^3/h (51,600 acfm) for oxygen production and process air. The 6,800-kW (9,900-hp) compressor produces higher pressures and more oxygen per kilowatt than its predecessors. As a result, daily oxygen production at the smelter has increased from 180 to 525 mt. About half that capacity goes into the flash furnace; the rest feeds converters and other smelting operations.

Two expanders are coupled to the compressor, recovering energy from high-pressure gas streams leaving the flash furnace. The expanders specification called for an efficiency of 80% and the actual efficiency exceeds this value. Gases heated to 1,350°C (2,500°F) pass through a waste heat boiler producing about 100 t of steam per hour; this steam, drives two generators and provides most of the electricity needed by the smelter.

Today, the capacity of Western Mining's smelter exceeds half-million tons annually and may reach up to 750,000 tpy with the addition of a fourth booster stage and ancillary equipment. Engineers at the smelter find the turbomachinery availability and reliability are satisfactory. Efficiency values of up to 91% are observed with the turboexpander models in use at this location. This particular model range offers five computer-generated geometries to meet the most specific application requirements, in either open or closed designs. Impellers are cast or milled to withstand erosion.

CASE 5: LNG PARALLEL EXPANDERS

In MESA Inc.'s facility in Satanta, Kansas, expander/compressor packages (Figure 8-4) give the operators a cost savings in horsepower on both ends of the configuration, and a much lower initial installation outlay. Without the expanders they would have had the additional

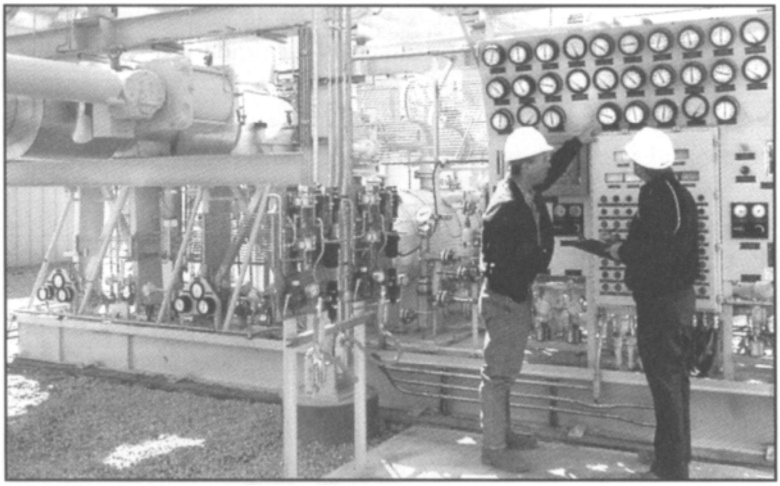

Figure 8-4. At Mesa, Inc., process units convert gas into LNG with two compressor-loaded expanders instead of conventional refrigeration and condenser equipment.

major capital expense of building a chiller, condenser, and associated piping. Additionally, MESA would have had the ongoing expense of propane supply for refrigeration.

The Satanta plant went online in September 1993, processing natural gas from some 1,000 wells drilled in the Hugoton fields of southern Kansas. A day's production yields 13,000 bbl of liquified natural gas (LNG), 5.1 million Nm^3 (190 MMscf) of residue natural gas, and 21,600 Nm^3 (800,000 scf) of helium.

LNG—consisting of ethane, propane, butane, and "natural gasoline" (condensate)—arrives at the plant for upgrading before it is sent to petrochemical plants and refineries as feedstock. Residue gas is sold to the interstate and intrastate pipeline network. MESA, one of the world's major crude helium producers, also delivers helium to a pipeline operated by the U.S. Bureau of Mines.

Natural gas from MESA's wells flows into a gathering system where pressure is increased to 7 bar (100 psig). Multiple booster stations raise it to 34 bar (500 psig) before gas enters the plant for separation. When gas enters the LNG recovery unit, its pressure must be raised again to 66 bar (950 psig). It is then subjected to a molecular sieve process for moisture removal. A series of heat exchangers lowers the temperature to –34°C (–30°F).

Instead of using conventional refrigeration and condensers to convert incoming gas into LNG, the system was designed to feed 2,340 Nm^3/day (86,800 scfd) into each of two expanders. Both are connected in parallel, with compressors attached at the back end. The compressors are connected in series to boost a single stream of returning gas.

Gas emerges from each expander cooled to –61°C (–77°F). Additional heat exchangers lower the temperature to –84°C (–120°F), at which point all the LNG is removed for delivery. Residue gas, now under reduced pressure, is passed along to the nitrogen rejection unit (NRU) where inert nitrogen is separated and vented into the atmosphere. Helium is also recovered in the NRU. The remaining residue gas is 90% methane.

Next, the upgraded residue gas is raised back to 34 bar (500 psig) for delivery to customers. The gas stream is introduced into the compressor end, where it is boosted from 8 to 10 bar (120 to 145 psig). The stream continues to the second compressor, where pressure is raised to 12 bar (170 psig).

Attached to the expanders, the compressors provide an additional 60 psig without energy cost outlay. Further compression ultimately raises gas pressure to 34 bar. MESA estimates that the arrangement at its Satanta plant saves 45 kW (60 hp) while reliably handling the daily production of natural gas.

CASE 6: NEW GAS RESERVOIR PRODUCTION WITH OFFSHORE OIL SITE

At a cost of more than 1 billion guilders (about US $570 million), BP-Amoco Netherlands Petroleum Company has built a natural gas project that brings together four offshore licensing areas, eight North Sea gas reservoirs, and 10 separate companies. BP-Amoco has also bridge-linked an existing oil platform with a new gas processing platform, saving the cost of an onshore gas treatment facility.

Since going online in 1993, the joint venture has reaped large dividends from the P15/P18 blocks of Holland's Rijn field, some 40 km (25 miles) from Rotterdam. BP-Amoco processes 13 MMm^3 (500 $MMft^3$) of natural gas from the field each day; also, nearly 2,000 m^3 (12,300 bbl) of condensate are produced daily. The project marks the first time Dutch gas has been produced to sales specification at an offshore location. Seven reservoirs, developed separately, are tied back to a central processing platform; an eighth reservoir has been accessed by directional drilling from one of four satellite platforms.

Gas is treated on the processing platform, then transferred to the oil production platform. From there it goes to an onshore metering station in Maasvlakte, traveling through a new 660-mm (26-in.) diameter pipeline buried 1 m (3 ft) beneath the sea bed. Condensate is sent through the existing Rijn crude oil pipeline to Europoort, near Rotterdam. BP-Amoco's approach has several advantages. It not only eliminates the cost of an onshore gas treatment plant, but also extends the life of the Rijn oil platform and makes offshore support much easier.

To meet sales specifications, gas produced at the wellheads must be free of water and hydrocarbon liquids. Twin turboexpanders are a key component in this process, providing dewpoint control with optimal efficiency. Initial processing takes place at the wellhead platforms, where methanol is injected to inhibit hydrate formation. A corrosion inhibitor is also added to prevent gas from damaging downstream equipment.

At the central platform, water and hydrocarbon liquids are first removed in knockout drums. Then saturated natural gas, free of any liquid droplets, enters the twin expanders. The gas is cooled below its dewpoint, allowing heavy hydrocarbon components and water vapor to condense in the discharge stream. Turboexpanders were chosen for two main reasons: They are more compact than competing methods of controlling the dewpoint and their operating costs are typically lower than those of many alternatives.

The expanders also remove energy from the gas, using that energy to drive a centrifugal compressor for pipeline recompression. As gas expands through the expander's inlet nozzle, pressure drops from 90 bar (1,300 psig) to 55 bar (800 psig). Temperature drops as well, below the dewpoint, and the liquids formed can be separated from the main gas stream.

Energy removed by the isentropic expansion process powers the expander shaft, which also drives a centrifugal compressor connected at the opposite end. Dry, lean gas is then recompressed for delivery to the pipeline. With space at a premium on the platform, the expanders' small size represents an important advantage over desiccant plants or refrigeration systems. Expander output can be adjusted down to 30% of capacity by either lowering throughput in each machine or by shutting down one and running the other at half flow or less. Flows below those that can be accommodated by an expander are being handled by Joule-Thomson valves.

Since the platform was commissioned in 1993, it has reached flows of 14.5 MMcmd (550 MMcfd), well above design capacity values. BP-Amoco expects the field to produce gas at full capacity for the next five to seven years before production tapers off. As levels decline, off-shore compression will be applied to the wells to maintain gas deliveries.

Control and data collection are managed by a computer monitoring system. More than 24 gas and liquid meters feed data into a metering control system. Further downstream, the platform's Data Management and Gas Allocation System does a number of jobs, including distributing gas to BP-Amoco's partners. A distributive control system linked to the main allocation apparatus monitors all facilities and operations, ensuring that each reservoir meets its production quota. Potential hazards are also computer-controlled through a safety management system.

After production is completed, natural gas from the P15 platform is sent through a new pipeline, much of it laid alongside the existing oil line. Condensate liquids extracted by the expanders follow a different route, undergoing stabilization and then moving through the Rijn crude oil pipeline before they reach Europoort. Once it reaches Hoek van Holland, the gas pipeline veers south across the estuary of the River Maas. It terminates at the Maasvlakte metering station, where gas is piped to the national distribution system.

CASE 7: NATURAL GAS "STRADDLE" PIPELINE APPLICATION

Probably the largest natural gas processing "straddle plant" in North America is BP-Amoco's Empress, Alberta facility. Here, EPBC (ethane, propane, butanes, and condensate) are extracted as liquids from natural gas before the gas is delivered to the TransCanada and Foothills (Saskatchewan) pipelines (Figure 8-5). The term "straddle plant" refers to the fact that the plant straddles the natural gas pipeline and extracts liquid components before passing the natural gas further along the pipeline.

Located at the eastern terminus of the NOVA and Foothills (Alberta) pipeline systems and about one mile west of the Alberta/Saskatchewan border, the BP-Amoco Empress NGL processing plant extracts liquids equivalent to approximately 2% of the (maximum value of) 5.2 Bcf of natural gas that passes through the facility every day. Most of the

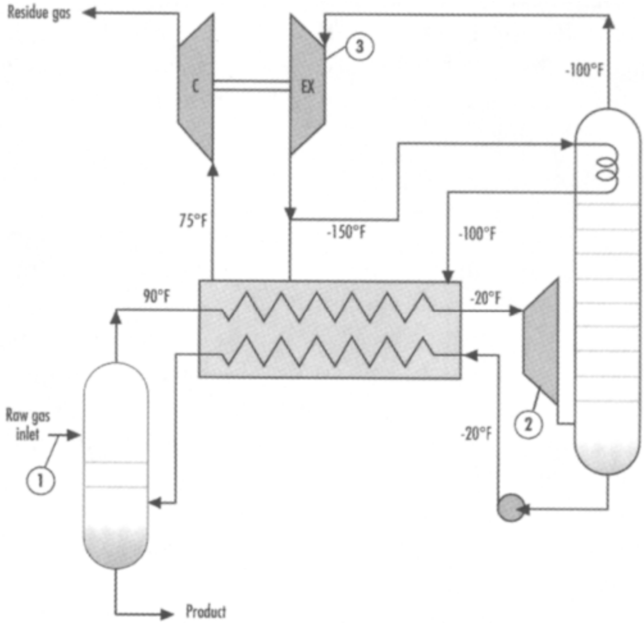

Figure 8-5. Typical turboexpander process for recovering ethane and LPG from natural gas.

extracted liquid ethane is delivered from the plant by pipeline to an ethylene plant 125 miles away, and the liquid propanes, butanes, and condensates that are extracted are stored underground in salt caverns until the required shipment to BP-Amoco fractionating plants in Wisconsin and Ontario.

The BP-Amoco Empress plant complex consists of three interconnected facilities located on a one mile square site. It operates 24 hours a day, 365 days a year, employing 70 personnel who work two shifts. If the plant were to shut down for a period of time, suppliers would have to sell their product on the spot market and forego profits. Also, from the customer's perspective, even a plant with reserves would soon run out of products.

The original plant (Phase 1) was constructed by Fluor in 1971, and can remove 45% of the ethane, 90% of the propane, and 100% of the butanes and condensates from the gas stream. Phase 1 has a capacity of 1.7 Bcfd. The second plant (Phase 2) can remove up to 70% of the ethane, 95% of the propane, and 100% of the butanes and condensates. Phase 2 was designed with a capacity of 2 Bcfd. Phase 1 was expanded in 1994. Together, Phase 1 and Phase 2 have a processing capability of 3.7 Bcfd, making the complex the highest capacity gas processing plant in North America.

REDUCING THE PRESSURE WITH EXPANSION TURBINES

The extraction process at BP-Amoco Empress begins with natural gas arriving at the plant at about 15°C and 600 psi pressure. The gas is dehydrated to a –90°C dewpoint by means of molecular sieves. Still at 600 psi, the gas is introduced into heat exchangers and cooled to –70°C, at which point it begins to liquify in a separator.

Expansion turbines—three in Phase 1 and two in Phase 2—cool the gas to –90°C, at which point more liquid drops out in another separator. In this system, the cold methane gas emerges from the expansion turbines at a reduced pressure of 325 psi and is recirculated to the original heat exchanger to reduce the temperature of the natural gas entering the plant.

The methane warms to 10°C. It then passes through the booster compressors on the expansion turbine shaft, increasing in pressure from 325 psi to 375 psi before being introduced into other gas compressors that boost the pressure back up to 600 psi. This is the pressure needed for reintroduction of the natural gas back into the TransCanada pipeline. This 50 psi boost, which makes use of available energy from the expansion turbines, provides a significant savings in electrical power.

Following initial installation in 1971, the Phase 1 expansion turbines have proven extremely reliable. The redesign effort of Phase 2 in 1992 incorporated improved aerodynamics and changed inlet guide vane profiles in the expansion turbines. This redesign yielded an additional .40 to .50 Bcf of gas per year without any increase in recompression horsepower. This translates to an increase in propane and butane production of an additional 3,600 to 4,500 bbl of liquid without an increase in electrical power consumption.

The efficiencies of the modified machines are 2%–4% higher than those achieved with comparable traditional machines. Higher efficiencies enhance the rate of condensate extraction. In a plant the size of Empress, this could result in \$100,000 to \$200,000 worth of additional production per year.

CASE 8: A NEW H_2O_2 PLANT DESIGN

Solvay Interox of Longview, Washington, a major chemical company that produces hydrogen peroxide, contracted to jointly build and test a new product with a turboexpander manufacturer (Atlas Copco) in 1994. One of the challenges of this product was that it incorporated an entirely new design: a three-stage integrally geared compressor that also includes one expander stage.

The compressor consists of three centrifugal compressor stages mounted on two high-speed pinions. Both pinions are driven by a 3,600 rpm/2,500 hp induction motor through a bullgear. The first and second stages, mounted on opposite ends of one pinion, operate at 16,076 rpm. The third compressor stage and the expander wheel, on opposite ends of the other pinion, operate at 19,403 rpm. Each pinion is supported by two tilting pad bearings. The gearbox and motor are mounted on a fabricated base that also forms the oil sump and interstage cooler shells.

The Solvay Interox plant in Longview produces hydrogen peroxide by the Auto Oxidation (AO) process. The AO process consists of three phases—hydrogenation, oxidation, and extraction. During hydrogenation, pure hydrogen is absorbed into an organic solution in the presence of a non-consumable catalyst. In the oxidation phase, air is introduced into the bottom of a liquid-filled tower full of the hydrogenated organic solution. Oxygen is absorbed into the solution, where it bonds with hydrogen to form H_2O_2. Extraction occurs when the peroxide is stripped out of the organic solution, which is then recirculated through the system in an endless loop. Oxygen-depleted air exits the top of the oxidizer tower. At this point there is no further process use for the pressurized "off gas," which has a depleted oxygen content and is saturated with solvents, water vapor, and traces of H_2O_2. The off gas must be stripped of organic vapor and vented back into the atmosphere. It is always advantageous to reduce the temperature to remove as many condensibles as possible before stripping the gas through a low-pressure carbon bed.

As is the case in most chemical and petrochemical plants, energy consumption accounts for a major portion of plant operating costs. In the AO process, air compression is the greatest energy user. However, this is not the case with this new compressor/expander design. By using a turboexpander stage coupled directly to two equally-sized air compressors operating in parallel, Solvay's compressor horsepower consumption was reduced by 30%.

Several constraints were faced in the design phase of the project. For example, special attention was given to the fact that 400 Series stainless steel, carbon, and some grades of aluminum were not compatible with the process. Additionally, the expander discharge temperature was required to stay between 35–70°F. The operating rpm of the expander wheel was determined by the rpm required by the third stage of the air compressor.

The required suction pressure to the expander is not available until the oxidizer tower reaches design pressure. With two compressors in operation this takes approximately 15 min. Since the expander wheel is mounted on the compressor pinion, enough flow must be available at startup to prevent overheating. The calculated windage loss of the expander wheel (40 hp) requires about 16,000 lb/hr of flow to prevent overheating.

Startup flow to the expander is designed to be supplied from the discharge of the compressor through a throttle valve and cooler. A careful study of the characteristics of the compressor blow-off valve and the expander startup valve was performed by Solvay process engineers. Based on these calculations, the startup cooler and valve were sized to supply the minimum required flow to the expander wheel.

CASE 9: USE OF MAGNETIC BEARINGS BY NORSKE SHELL IN AN ONSHORE APPLICATION

The development and commercialization of magnetic bearings has been swift and intense. When an Aker-Kellogg joint venture requested bids on behalf of Norske Shell's Troll onshore process plant for three identical turboexpander units, they stipulated that these turboexpander-compressor units be offered with active magnetic bearings (Figure 8-6) and dry-face (gas) seals. Norske Shell had concluded that magnetic bearings promoted long-term reliability.

In many cases, the most frequent cause of equipment outage is the lubrication system. Because magnetic bearings do not "wear out," and do eliminate oil, pumps, filters, coolers, and regulating and mixing valves, the potential for improved reliability is obvious. Reliability is also enhanced by the control system, which offers continuous real-time protection. The system automatically shuts down before machinery damage can occur.

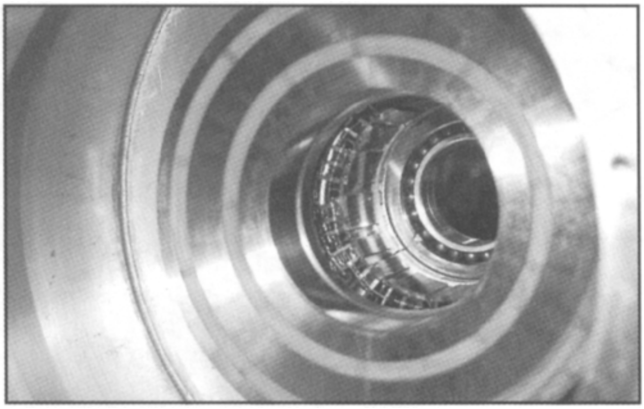

Figure 8-6. View of radial magnets. The construction is very similar to an electric motor.

Magnetic bearings (Figure 8-7) were discussed in Chapter 6. The operating principle can be restated by noting that the rotor assembly is suspended, or levitated, in a magnetic field generated by radial bearings at each end. Axial position is maintained by a thrust bearing located either in the center or at one end of the rotor. When the magnetic bearings are deenergized, auxiliary bearings at each end of the shaft provide support. These auxiliary bearings are dry, or non-lubricated, and remain unloaded during normal operation. Once the magnetic bearings are energized, an electronic control system centers the shaft within the field and uses signals from sensors to control the current, and hence magnetic flux.

However, each application has its challenges. What made Norske Shell's application so different from other turboexpander units using magnetic bearings was the combination of power level and speed: 6,000 kW (8,046 hp) on each shaft at 7,000 rpm, with typical pressures of 90 bar (1,305 psi).

Because Norske Shell was using these turboexpanders in a dewpoint control process, it was necessary to factor in other specific conditions. For instance, these turboexpanders could be exposed to possibly violent process transient conditions. For this reason, the magnetic bearings required a flux control system to increase the response capability, which was developed by the original equipment manufacturer in concert with the magnetic bearing manufacturer. The load factor of

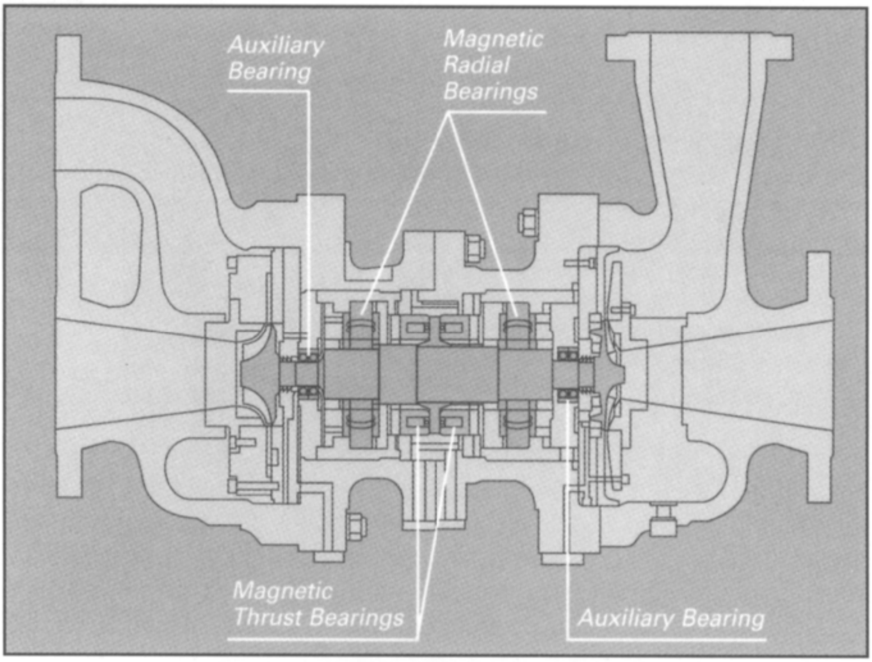

Figure 8-7. Turboexpander equipped with magnetic bearings.

this magnetic bearing was increased to 40 g compared to only 5 g with the conventional design. This system improved the dynamic characteristic of the magnetic bearings to 300,000 n/s, allowing the total maximum axial load to be available in 100 ms. With this feature, the turboexpander's magnetic bearings could withstand the unexpected shock loading occasionally experienced during emergency shutdowns.

Each aspect of the turboexpander's bearing systems was carefully tailored. For instance, the radial bearings for Norske Shell were built larger—200-mm (7.88-in.) in diameter—than required to provide additional overload capacity. Axial thrust was contained by a double-acting magnetic thrust bearing using the "thrust disk" concept that has seen decades of satisfactory use in traditional high-capacity turbomachinery bearings.

The thrust disk consists of solid steel material with a linear speed of 160 m/sec (528 fps) at the outside diameter. This compares with a maximum allowable peripheral speed of 400 m/sec (1,320 fps) and eliminates the necessity for the thrust disk to be laminated. Because the bearing is not subject to significant magnetization change during rotation, eddy current losses are minimized.

As previously mentioned, auxiliary bearings are used to protect electromechanical parts in case of bearing overload or electronic failure. These auxiliary bearings are used for both radial and axial motion and are mounted on damping bands. The maximum air gap between the shaft and the auxiliary bearings is 0.25 mm (.010 in.) radial and 0.30 mm (.012 in.) axial, including band deflection of 0.07 mm (.003 in.).

The auxiliary bearings should be designed to withstand a number of de-levitations during trip at nominal speed and load conditions. To avoid any damage to the rotor itself, sleeves hardened by nitriding are typically fitted to the rotor portion that would contact the auxiliary bearings. These bearings remain stationary during normal operation. In the event of main power failure, batteries must supply power to the magnetic bearings to avoid de-levitation.

The bearing environment may have to be purged with nitrogen. However, to ensure that every magnetic bearing component can withstand the aggressiveness of the process gas in case of a nitrogen purge loss, special soak tests are typically performed.

When the compressor back wheel pressure is adjusted in accordance with the magnitude of the axial force, automatic thrust balancing is achieved. The signal corresponding to the magnitude of the thrust forces is available from the magnetic bearing thrust sensors. This signal, after being conditioned and biased to prevent oscillation, is used to adjust the position of a control valve connecting the back wheel void to the compressor suction. To prevent the two systems from counteracting each other, the control valve is activated when thrust load exceeds one-fifth of the capability of the magnetic bearings. Also, the response time of the valve is selected to be four times slower than the electronic signal to prevent hunting of the valve.

This Norske Shell case proves that there is a growing interest among large gas plant operators to use state-of-the-art technology, such as active magnetic bearings and dry-face seals, when it has the potential for long-term benefits. Engineering design and manufacture of magnetic bearings for large industrial applications have shown that magnetic bearing technology is well suited for use in hydrocarbon, high power, and sour-natural gas applications. Dry gas seals are capable of providing a positive and dependable barrier between the process gas and the magnetic bearing.

CASE 10: GAS SEPARATION PLANT IN THAILAND

Thailand's sole producer of methane, propane, and LNG/NGL is operating at least four gas separation plants. From these state-owned sites, the company supplies more than 90% of its production to the domestic market. A small percentage of NGL is exported.

The various plants each have a daily input capacity of natural gas of 220–350 MMcfd. All operate 24 hours a day, providing an estimated total daily production capacity of 1,000 MMcf of methane, 1,450 t of ethane, 1,414 t of propane, 2,670 t of LPG and 5,700 bbl of NGL.

A vital part of the process system for each of the plants includes a turboexpander-compressor set. This turbomachinery string has two main functions. The first function reduces the pressure and temperature of the incoming gas to facilitate separation of the methane. The second function raises the pressure of the methane after it leaves the fractionation tower and is transferred directly to the customers through an underground pipeline.

The oldest of the various systems was commissioned when the plant first opened in 1985; it has been operating continuously 24 hours a day. The turboexpander-compressor set has proved its durability, requiring only lube oil skid maintenance prior to its first overhaul after many years of operation.

Operating at a flowrate of 203,714 kg/hr (449,190 lb/hr) the compressor raises the methane pressure 14.3 bar (207 psia) to 17.9 bar (259 psia), with a power consumption of 2,373 kWh. The compressor is driven by the turboexpander, which in turn is powered by the gas pressure from natural gas in the offshore inlet pipeline. This gas enters the expander at 42.1 bar and exits at 16 bar with a flowrate of 169,480 kg/hr (373,700 lb/hr). This provides a power recovery of 2,412 kWh. The natural gas then flows into the fractionation tower where the methane, propane, LPG, and NGL are separated. A relay logic control system performs the startup, running, alarm, and shutdown sequences. A wide range of flow is controlled by adjusting the inlet guide vanes of the turboexpander.

Refer to Figure 8-8 for a typical NGL plant schematic.

CASE 11: ETHYLENE PLANT IN KUWAIT

Equate, a joint venture between Petroleum Industrial Corporation in Kuwait and Union Carbide Corporation, built a grass-roots petrochemical

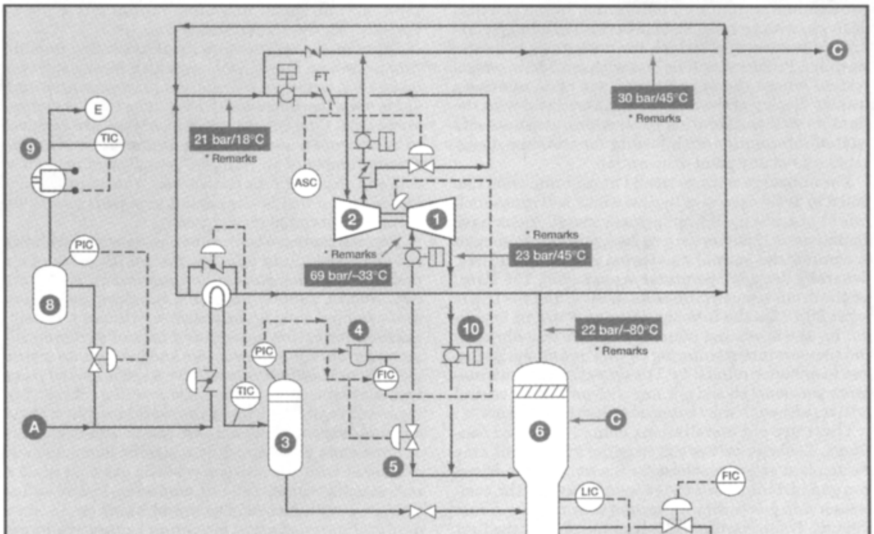

ID	Description	ID	Description
A	Natural gas inlet after dehydration	3	Chill down flash drum
B	Gas supply	4	Expander feed gas drum
C	Reflux inlet	5	Bypass valve (JT valve)
D	Raw NGL outlet	6	Demethanizer column
E	Seal gas supply outlet (startup)	7	Raw NGL pump
1	Turboexpander	8	Vessel for seal gas
2	Compressor	9	Seal gas heater
		10	Motor operated valve

* Remarks

The figures given in the bracket refer to normal operation when the turboexpander is working. When out of service, the demethanizer column pressure will go up and line pressure 'B' will be less than before.

Figure 8-8. Typical NGL plant schematic showing a turboexpander.

complex in Kuwait featuring a world-class ethylene plant. At the heart of this ethylene plant are two expander-compressors in series, which are used for ethylene recovery (Figure 8-9). The expander recovers the ethylene by running the gas through the expander, which results in a temperature drop. This temperature drop then causes the ethylene to liquify.

Most ethylene plants operate continuously with the expander functioning at or near design point. However, by using inlet guide vanes, the expander can still provide optimum performance at off-design conditions. Also, the expansion process generates power, which is used by the compressor. The ethylene enters the expanders at approximately 26 bar (377 psia) and exits at approximately 6 bar (87 psia). The expanders generate over 2,000 hp for gas compression.

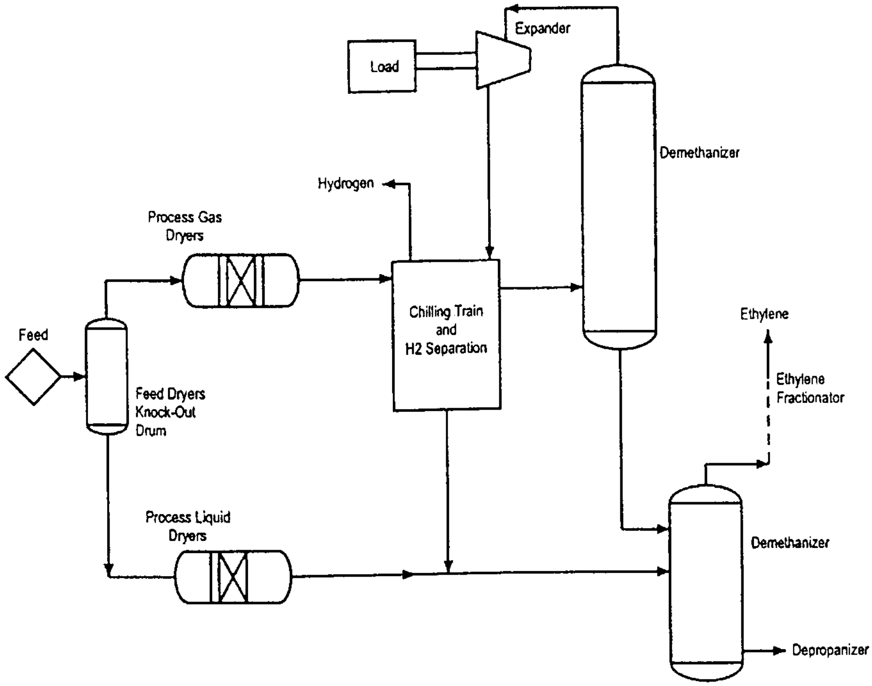

Figure 8-9. Process flow diagram of a typical ethylene plant.

CASE 12: MTBE PLANT IN TEXAS

In 1993, the Valero Refining Company of Corpus Christi, Texas, commissioned a highly efficient MTBE gasoline additive production unit. The Corpus Christi plant went online in 1983, and the MTBE facility was added in 1993. The plant produces up to 125,000 bpd of reformulated gasoline (RFG) containing 12% MTBE for purifying oxygenation. Seventy-five percent of Valero's production is regular gasoline, and 25% is premium gasoline.

Some 14,700 gal of MTBE are produced each day. The MTBE production facility relies on an "Olefiex" design system that converts isobutane to isobutylene, the basic ingredient in MTBE. The Olefiex unit manages to recycle isobutane so that ultimately 100% is converted to isobutylene, and byproduct hydrogen used in the process is recycled and processed to 99.9% purity.

The hydrogen recycling process uses two turboexpanders that cool the gas stream to –120°F (–84°C), separating out 87% of the hydrogen.

Energy released by the turboexpanders powers a two-stage compressor for recirculating the gas. The hydrogen is later purified to 99.9% through the removal of chlorides and H_2S.

At the Corpus Christi plant, liquid supplies of C_4, C_5, and C_6 are delivered by truck and pipelines from nearby refineries. These liquids are processed through light end fractionating units that remove the propane (C_5 and C_6), and drop out isobutane and normal butane (which is reintroduced into the stream for reprocessing.)

The liquid C_4 is fed into the Olefiex unit where it is introduced into a cold box for drying. It is then introduced into a series of three heat exchangers, combined with hydrogen and a catalyst, and heated to 1,192°F (644°C). The process converts the isobutane to 48% isobutylene solution.

The remaining gas stream is cooled to 120°F (49°C) through heat exchangers, then compressed to 145 psia (11 bar) before being introduced into the first of two turboexpanders.

The gas emerging at –100°F (–73°C) and less than 70 psia (4.8 bar) is 85% pure hydrogen. The hydrogen gas stream entering a second turboexpander emerges at –120°F (–84°C) and under 36 psia (2.5 bar) with a purity of 87%.

CASE 13: MORE ENERGY FOR A PHENOL PLANT

Phenol compounds are vital ingredients of processes that ultimately lead to the production of nylon, aspirin, and polycarbonate. EniChem SpA is one of the world's leading producers of phenol. When the company was looking to boost phenol production at its plant in Mantova, Italy, they decided to recover the energy being used in their process.

EniChem has been producing this caustic chemical compound at Mantova since the plant opened in the 1960s. Initially, the total annual output was approximately 10,000 tons. This output figure increased rapidly and, in 1987, a combined centrifugal compressor and expander were installed to boost production from about 230,000 to 270,000 tpy. Operating at a flowrate of 23,000 kg/hr (50,715 lb/hr), the three-stage compressor raises air pressure from 1 bar (14.5 psia) to 9.5 bar (137.8 psia) and is used to feed the reactor in the phenol production plant.

The plant recognized the energy potential of the off gas from the reactor—a combination of nitrogen and oxygen at a temperature of 125°C, a pressure of 6.4 bar (92.8 psia), and a flowrate of 19,000 kg/

hr (41,895 lb/hr). Hence, the decision to incorporate a turboexpander. Mounted on the same shaft as the first stage of the compressor, the turboexpander provides 680 kW of the 2,023 kW total power requirement to drive the compressor.

The main power source is a 2,200 kW rated motor, which drives two high-speed pinions through integral gears. The first stage of the compressor operates at 17,900 rpm, while the second and third stages operate at 21,800 rpm. The unit is controlled by a local control system, but operators can also monitor the operating parameters from the plant control room.

CASE 14: IMPROVING FCC EXPANDER RELIABILITY UNDER OFF-DESIGN CONDITIONS[2]

Rotating machinery usually performs efficiently if it works under "design point" conditions. However, "off-design" conditions require a predictive model of the machine's performance. In a FCC power train system, mass flow deviation is quite common for adjusting production capacity to meet the requirements of petrochemical product markets.

There are many reasons for significant investment in FCC power trains and, thus, power train maintenance. These power recovery machines handle catalyst-laden gas at high temperature. Because the recovery system is connected to the processing plant, the steam pipe network and the electrical power grid, a power train upset is likely to rapidly extend from the FCC unit to the entire plant.

Evaluating off-design performance is strongly recommended for the purpose of improving the operating reliability of both power recovery sets and processing plants. To do this evaluation, a simulation analysis should be based on velocity diagrams, the law of similarity, and expander performance maps.

It would be an understatement to say that the gas expander turbine forms a major part of the power train. Evaluating off-design performance for the expander installed in the Sinopec Jinan Oil Refinery is presented as an example of an appropriate evaluation method. It should be noted that calculations are based on actual field measurements and plant experience.

[2] *Source: Zhang and Wang, Sinopec Jinan Oil Refinery, Jinan, Shandong, P.R. China.*

The power train (Figure 8-10) was commissioned in May 1989. Table 8-1 provides data on the machine in question. Tables 8-2 and 8-3 show flue gas analysis from the regenerator to the gas expander turbine inlet and the relevant metallurgy, respectively. There are many possible failure modes in gas expanders, which include erosion, catalyst deposition, and excessive mechanical vibration. Obviously, these factors may also cause power loss, and some power trains do indeed fall short of producing the expected power. Nevertheless, in some cases operation at off-design expander system conditions could be the primary cause of performance deficiencies.

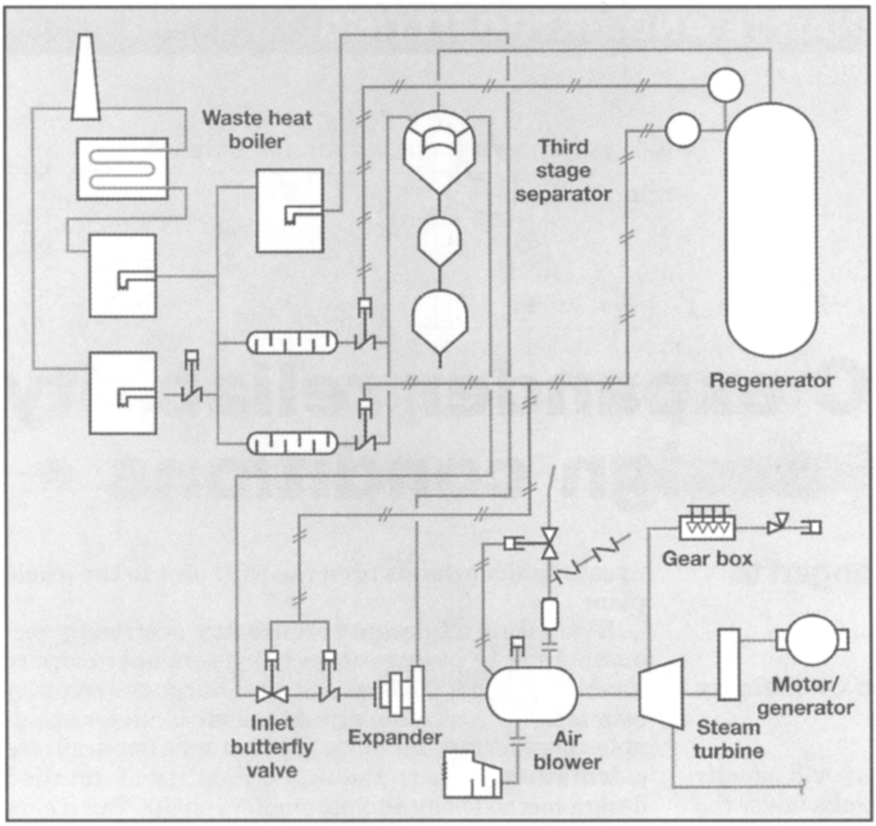

Figure 8-10. At Jinan Oil, the FCC power recovery system is integral to the plant.

Table 8-1
Specification of power train in Sinopec Jinan oil refinery

Items	Expander	Air blower	Steam turbine	Motor/ generator
Inlet pressure, MPa	0.3138	0.0961	3.43	
Inlet temperature, °C	700	27.6	400	
Discharge pressure, MPa	0.10787	0.393	1.28	
Discharge temperature, °C	537	198.5	283	
Flow, Nm^3/min	1,800–2,000	2,000	65,000 (kg/hr)	
Power, kW	8,700–9,700	7,240	3,920	7,200
Speed, rpm	5,714	5,714	5,714	1,506
Voltage, V				6,300
Current, A				733

Table 8-2
Flue gas analysis and expander data

Composition					
Gas Component	Rated Vol%	Actual Vol%	Actual Wt%	Mol. wt., gm/mol	29.02
N_2	71.84	74.05	70.06	Average Cp value, kcal/kg-K	0.3293
O_2	1.75	5.4	5.88	Adiabatic enthalpy drop, kcal/kg	63.7658
CO_2	13.76	12.2	18.27	C_p/C_v	1.2623
CO	—	0.5	0.47	Density of gas at std. condition, kg/Nm^3	1.296
H_2O	12.65	7.85	4.81		

Table 8-3
Metallurgy of expander components

Components	Material
1. Rotor disks	GH864
2. Rotor blades	GH864
3. Stator blades	K13
4. Flame coating for blades	C–1
5. Studs (Bolting)	GH169

As previously mentioned, FCC units produce hot flue gas as a byproduct. Hot gas is expanded in the expander turbine and then supplies mechanical energy for processing. The excess power is converted into electrical energy by the motor-generator. Therefore, the power recovery system is likely to raise the energy efficiency and profitability of the plant by substantial margins.

For analytical purposes, consider that the mass carrier in the expander with higher temperature and lower pressure could be thought of as an ideal gas. Because exhaust gas pressure and temperature are nearly unchangeable once selected (unless the efficiency degrades), its residual enthalpy may be assumed constant. The expander operating condition mainly depends on the inlet parameters, and the power developed by an expander may be calculated from the equation:

$$W_a = m \bullet \eta \bullet C_p \bullet T_1[1-(p_2/p_1)^{k-1/k}] \qquad (8\text{-}1)$$

where m = gas mass flow
η = overall efficiency
C_p = specific heat at constant pressure
T_1 = gas inlet temperature
p_2 = gas exhaust pressure
p_1 = gas inlet pressure
k = gas specific heat ratio (= C_p/C_υ)

It follows from the equation that the power output of an expander is a function of gas mass flow, inlet temperature, and pressure.

However, when an expander has to operate at mismatched conditions, the actual mismatch usually occurs in the inlet butterfly valve, which attempts to maintain regenerator pressure. Fortunately, processing parameters can also be modulated under different production capacities. In such circumstances, it is important to keep the volume flow in the normal range to maintain system efficiency. For an ideal gas, the conditional equation is:

$$p_1\upsilon_1 = RT_1 \qquad (8\text{-}2)$$

where p_1 = gas inlet pressure
υ_1 = gas inlet volume flow
R = gas constant
T_1 = gas inlet temperature

The effects of gas temperature and pressure are significant. The higher the gas temperature and/or the lower the gas pressure, the larger the gas volume that flows through the expander. Higher inlet temperatures and lower inlet pressures would result from reduced gas mass flow.

When actual mass flow through the expanders is lowered, efficiency varies according to power loss, deflective angle of gas in the leading edge of the rotating blades, and pressure drop across the inlet butterfly valve. The pressure drop increases as the valve closes.

As long as the volume flow is kept near design point, both the deflection angle and pressure drop can be corrected. Temperature differential increase is limited by metallurgy, so it is neglected in analytical calculations. This evaluation is based on inlet pressure changes. The "new" volume at a different pressure is calculated by the ideal gas equation:

$$p_1'\upsilon_1' = p_1\upsilon_1 \tag{8-3}$$

In cases where gas flow is about 20% less than rated, the inlet pressure should also decline by 20%. In the Jinan expander, this pressure decrease is about 0.25 MPa.

The pressure in the regenerator depends on several factors. As the actual inlet pressure is adjusted to 0.22–0.24 MPa, the expander matches the system, but power loss is considerable. The power consumption on the air blower may be reduced at the same time as the pressure in the regenerator is lowered. However, the overall efficiency of the power recovery system is not significantly affected.

Other suggestions that address gas flow deviation include a retrofit of the stator-nozzle assembly or replacing rotors with shorter blades. However, it is easier to increase volume flow by lowering inlet pressure. Increased capacity of the third-stage separator and the auxiliary equipment avoids the possibility that excess catalyst will pass through the equipment.

In a hot gas expander, the major problems associated with catalyst fines are centered on erosion of components and particulate plugging. Either problem can cause machine vibration and sometimes power train emergency shutdown. Because many failures have resulted from these factors, machinery manufacturers recommend that the maximum permissible solids concentration upstream of an expander not exceed 200 ppm. It is further stipulated that 97% of the particles be smaller than 10 μ. Allowing concentrations of 160 ppm with 95% of the particle less than 10 μ is considered reasonable.

However, excessive catalyst flow may be experienced during occasional process upsets. Off-design condition analysis can anticipate and prepare for these negative circumstances.

The following discusses two main cases. Consider, however, that the actual problem could be a combination of excessive concentration of larger particles (10 μ or larger) and excessive concentration of fine dust (smaller than 10 μ).

Erosion occurs due to the impact of catalyst particles larger than 10 μ. Larger dust particles possess more kinetic energy, which is represented by mv^2 (mass times velocity squared). Note that dust particles in the blade path would deflect away from the flow line due to inertia. The larger the particles, the greater the deflection.

Inspection during shutdown showed evidence of blade erosion and pits located on the leading edge and the concave side of the trailing edge. For expanders operating at a constant speed, the velocity diagram depends on the absolute speed of the mass carrier. The absolute speed, C_1, may be calculated from the nozzle formula:

$$C_1 = \sqrt{2\Delta h + C_o^{\,2}} \tag{8-4}$$

where C_1 = absolute gas speed at the first stage of rotor blades
C_o = primary gas velocity due to the gas volume flow
Δh = enthalpy drop across the first stator row

Using the example of Jinan's expander, if primary velocity is 89 m/s (rated flow 30 Nm^3/s), the absolute speed, C_1, is about 376 m/s. Figure 8-11a shows the velocity diagram at the inlet of the first-stage rotor blades.

When C_1 is reduced by 50%, the velocity diagram is now represented by Figure 8-11b and, as the relative flow angle, B, changes, the point of impact would change and blade life may be extended. It stands to reason that a reduction in gas mass flow and/or gas inlet temperature is beneficial whenever an excessive concentration of larger particles is noticed.

When mass flow is on the increase, an excessive concentration of fine dust (smaller than 10 μ), could occur and catalyst deposits may be detected. Because of the highly sophisticate dust-plugging mechanism, there has been no unanimous explanation for this malfunction. However, field experience indicates that catalyst fines settle in lower velocity areas such as stator paths, the trailing edges of rotor blades, and between the rotor disks after dust ingestion events.

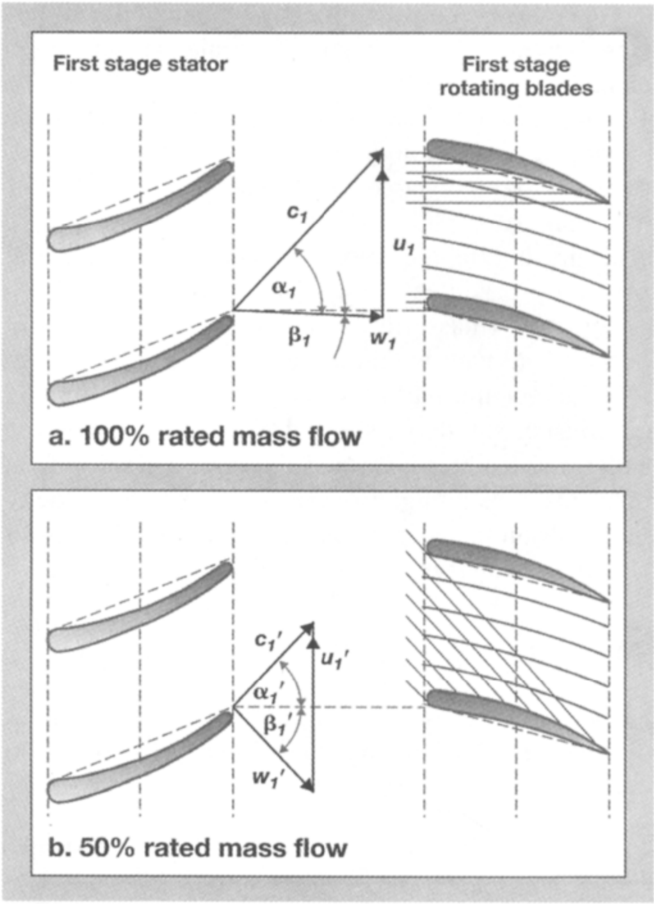

Figure 8-11. When the absolute speed is reduced, the velocity diagram changes.

It has been proposed that rapidly cooling the expander with steam combined with flue gas would leave the expander free of deposits. This suggestion is unlikely to work with multi-stage expanders because catalyst residue is likely to remain in the space between the disks. Moreover, there is a concern that this type of cooling could cause localized cooling in the expander and partial deformation of components.

Prevention rather than "cure" is always preferable for keeping machines free from dust plugging. A steady blast of superheated steam prevents catalyst carryover from entering the space between the disks.

Other recommended remedial measures include raising the gas inlet temperature and/or lowering the gas inlet pressure. These measures would increase the volume flow of gas and then reduce the possibility of catalyst buildup in the expanders.

CASE 15: GENERATING ELECTRICITY FROM EXCESS ENERGY WITH A LETDOWN GAS COMPRESSOR

San Diego Gas & Electric has been operating a turboexpander-driven generator on their natural gas transmission system (Figure 8-12) since April 1983. This system is capable of recovering the energy that is normally lost in the process of reducing gas pressure as it flows from a high-pressure system into a low-pressure system. San Diego Gas & Electric's system is installed at a city gate station. Energy available in the pressure drop is converted into shaft horsepower, which can then be used to drive a generator.

The process of reducing gas pressure with an expander is an isentropic process, which is able to recover both the energy from the gas pressure and also the gas temperature. A conventional gas regulator station is an isenthalpic process, which only reduces pressure. As a result, an expander system produces much lower gas temperatures downstream compared to a pressure regulator operating under the same pressure conditions.

San Diego Gas & Electric's expander is installed in parallel to a major city gate station. This type of system could be installed on a pressure reducing station supplying natural gas to an electric power plant. Large regulator stations serving industrial customers are another possible application.

San Diego Gas & Electric's system was originally installed as a research project. The intent of the research project was to test the hardware in this application, test the feasibility of operating such a system remotely with no local operators, and to prove the economics. Similar systems had been installed within process plants where operators were present to start and stop the system and monitor its operation. However, this was the first system installed on a natural gas transmission system with completely remote operation.

The economics of such a system are very complex, and there are many variables that must be considered. Some of the major considerations are total installed cost, the load factor or capacity factor, the

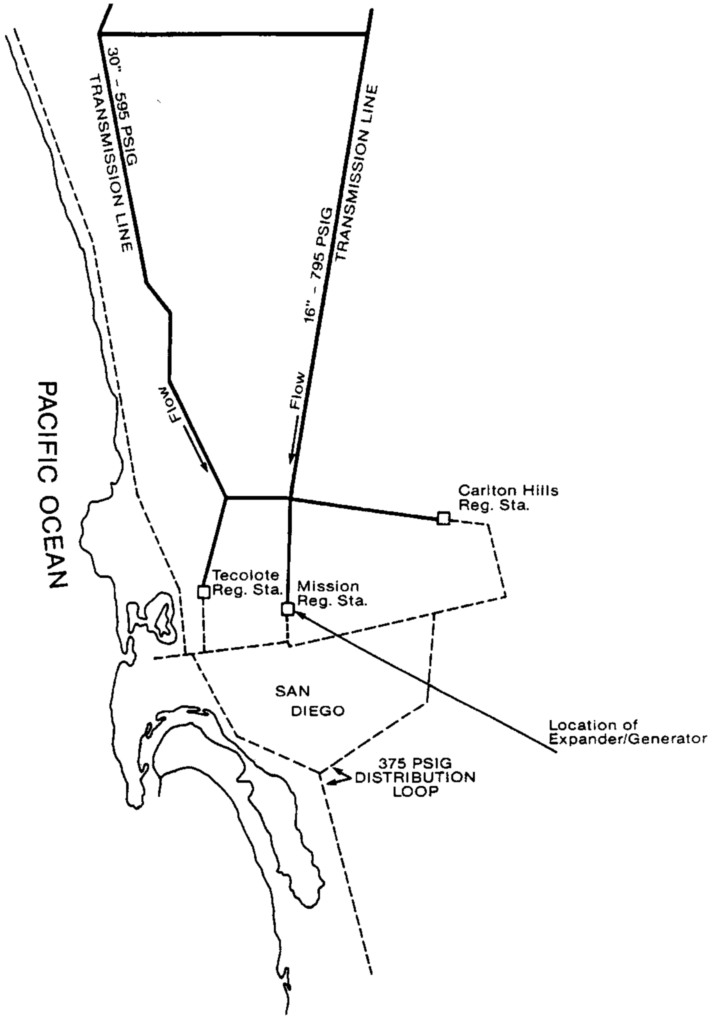

Figure 8-12. San Diego Gas & Electric Company's gas transmission system.

value of the electricity, and, where preheat is required, the cost differential between the electricity produced and the fuel used. Any design must make assumptions about these variables and then the final design must be a series of compromises, which will yield the optimum combination.

The original proposal stimulated considerable interest. However, because this was a new application for this type of facility, it also raised several questions. Again, previous applications for expander-driven generators had all been in process plant environments where operators would monitor it during operation. Process plant applications also had relatively constant flowrates and pressure available for the expander. This would be the first facility installed on a natural gas transmission system. The ability to remotely operate and monitor the system was a key factor in the economic justification of the system. In addition to these concerns, there were questions regarding possible hydrate formation, noise levels, control stability, and coordination with an existing regulator station.

The first major step of the project was to select the location for the installation. The existing configuration of San Diego Gas & Electric's gas transmission system consisted of two major high-pressure gas transmission lines, which transport gas into San Diego from the north. There are two compressor stations on the north end of the system that pump gas down the lines. One of the lines operated at a maximum pressure of 595 psig, and the other operated at a maximum of 795 psig. These transmission lines then terminated at three city gate stations, which reduced the pressure to 375 psig and supplied a distribution loop system that encompassed the major populated area of San Diego.

The gas system did not include any storage other than pipeline pack and one relatively small high-pressure pipe-type holder. Therefore, pressures and flows in all areas of the system varied widely on a daily and seasonal basis. Several years of operating data were reviewed and analyzed to select a location that met the flow and pressure drop requirements for installation of an expander. Site selection also gave consideration to the requirements for connection to the gas system, connection to the electric system, and sound attenuation measures necessary to eliminate any impact on the surrounding area.

The location that was finally selected was the Mission Regulator Station. This was one of the three city gate stations supplying the distribution loop from the transmission system. Mission is on the southern end of the 16-in. transmission line, which was rated at 795 psig maximum.

The expander was installed in parallel with the existing pressure regulating station (Figure 8-13). The existing station consisted of three parallel runs. Each run included a working regulator and a monitor regulator. The monitor regulator would control pressure if the working regulator malfunctioned. The setpoints of the runs were offset so they would come on and off line in response to downstream demand and provide sufficient turndown for adequate control at all flowrates. The station had a history of stable, reliable operation.

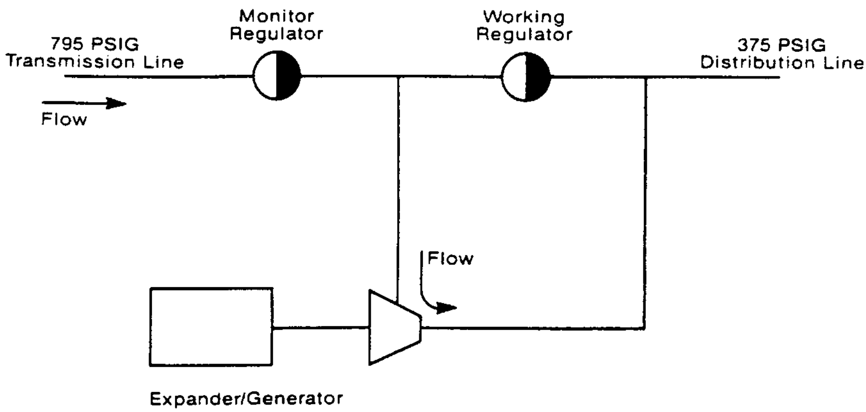

Figure 8-13. Regulator station schematic.

The pipeline to the expander inlet was taken from a point downstream of the monitor regulators and upstream of the working regulators. The monitor regulators were, therefore, still able to provide back-up pressure control in the event of a malfunction. The expander control system included the capability to throttle flow to maintain downstream pressure. The setpoint of the expander control system was set slightly above the regulator setpoints. Therefore, gas flowed through the expander first, then the regulator runs would open as the flow exceeded the expander's capability. The chosen location was very close to a major electric substation, so connection to the electric system was relatively simple. It was also fairly remote, so the noise impact was minimized.

The final design for the station resulted in a 365 hp, single-stage, radial reaction turbine. Rotating at 18,000 rpm, the turbine was integrally connected to a 5:1 reduction gear box, which was directly coupled to a 260 kW, 3,600 rpm, 480-V, 3-phase/60-cycle induction generator. The generator was actually a 350 hp induction motor. The expander/gearbox/generator train was mounted on a single skid with its support systems. The support systems included a lubrication system with an air-to-oil fin fan heat exchanger, a seal gas system, and an electrical control panel with instrumentation. Natural gas was used as both the seal gas for the lube system and as the control fluid for the control system.

The control system was a relatively simple pneumatic control system consisting of two main control modes (Figure 8-14). The first mode controlled pressure in the piping system downstream of the

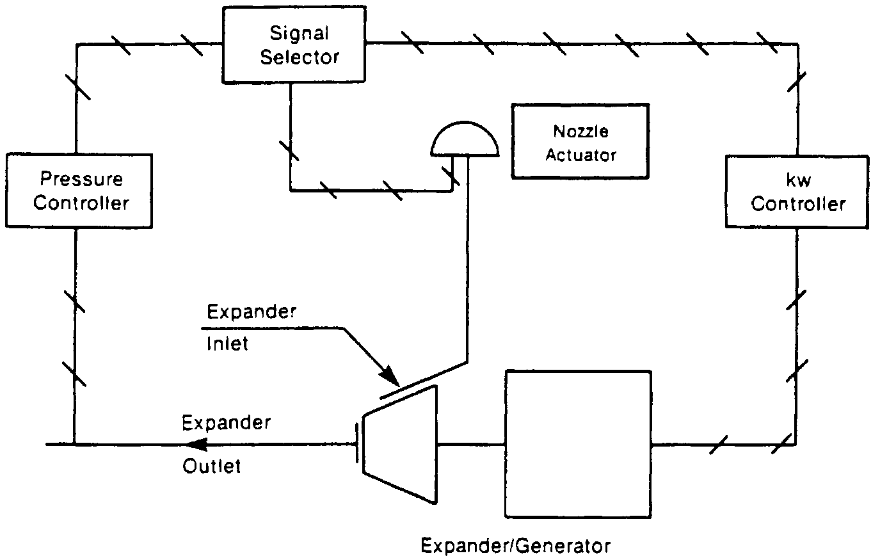

Figure 8-14. Control system schematic.

expander. This system would be in control when downstream pressure was high and the limiting factor. In this case, generator output was generally less than maximum. The second mode controlled generator output and limited the output to the generator design maximum. This system would be in control when high flows and high pressure differentials were available and generator output was the limiting factor. A signal selector provided automatic and smooth transfers between these two modes during normal operation. Additional control loops provided automatic startup and manual control capabilities.

The remote control and indicator panel in the Gas Operations Control Center were designed to be as simple as possible. The controls consisted of momentary start and stop buttons for the lube oil system and the expander/generator. There was an instantaneous generator kilowatt output indicator, although there were no remote controls for output. There were also indicators for lube oil pump status and expander/generator status. Alarm indications consisted of a single light for an alarm condition and another light for a shutdown. To determine the exact cause of an alarm, it was necessary to dispatch personnel to the facility.

The electrical system consisted of a walk-in motor control center that contained the generator breaker and all the necessary generator protection relays (Figure 8-15). The motor starters for lube oil pumps, the fan, and lube oil pump heater were also in the motor control center. A step-up transformer increased the generator voltage from 480 V to the 12,000 V required by the electric distribution system.

OPERATING AND MAINTENANCE HISTORY

Operation of the unit has proven to be successful. The generator is started and stopped by the dispatcher in the control center. It is also designed to automatically shut down if the electrical output drops below a predetermined level. Due to the widely varying conditions in the pipeline, there are times when the generator is started and stopped once or twice a day. At other times, it runs continuously for two or more weeks. There has been no impact on the operation of the existing regulator station resulting from the operation of the expander. The transfer of flow as the expander starts and stops has not caused any pressure excursions downstream of the station.

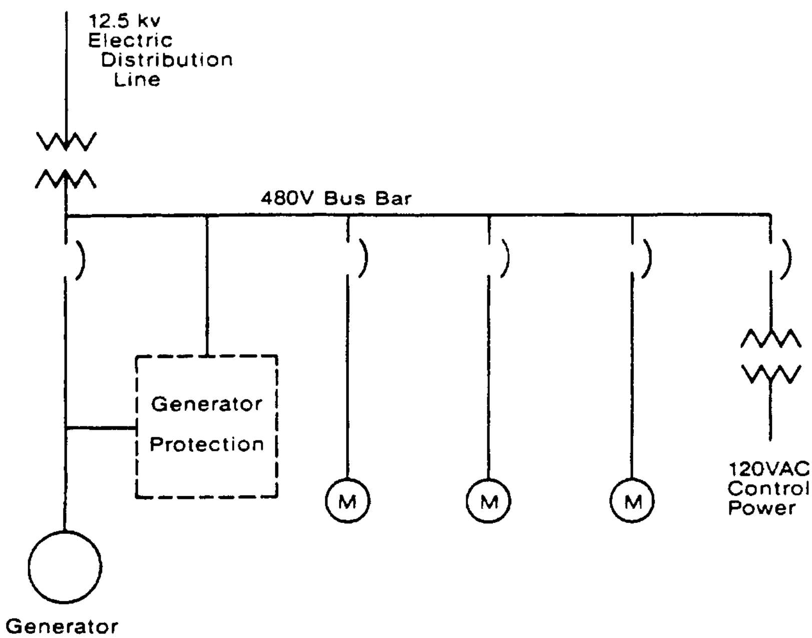

Figure 8-15. Electrical one-line diagram.

The equipment has also proven to be failsafe in all modes of normal operation, as well as all abnormal modes that have been discovered. This was a concern because there were no personnel near the site to detect blowing gas, lube oil spills, or any number of other undesirable conditions. The system has been thoroughly tested and has always operated safely.

The majority of the maintenance of the station has been routine preventive maintenance. The only major problem was due to a failure of an inboard roller bearing in the generator. The expander shaft and gearbox had a vibration protection system; however, the generator had no vibration sensors. The bearing failure was not detected until the bearing disintegrated, causing the generator to trip electrically. This resulted in extensive damage to the motor shaft, rotor, stator windings, the end bells, and the bearing retainers.

The generator was repaired, and design started immediately on a new vibration protection package for the unit. The new package upgraded all the expander protection, as well as including protection for the generator. Further follow-up generator repairs were necessary to improve the rotor balance and correct a rotor misalignment. However, this work was relatively minor; similarly, the remaining maintenance has been routine. The expander controls require calibration one or two times per year. Generator alignment and balance are critical, prompting routine vibration readings and adjustments where necessary.

The formation of hydrates downstream of the expander does not appear to be a problem in this facility. The original design studies indicated that hydrates should not form with this pipeline gas above temperatures of 20°F. The downstream temperature was not expected to drop this low. In operation, the downstream temperature has been above 25°F most of the time and has not dropped below 20°F. This is with inlet temperatures normally above 65°F. There have been no indications of hydrate formation downstream of the expander. Indeed, electric power production has acutually exceeded the quantity estimated for all years of operation.

When the unit was initially placed in service, sound level measurement data were collected. Within 3 ft of the expander case, sound levels were measured at 92–99 dBA. At the property line 25 ft away from the case, the levels were 68–85 dBA. At the time of installation, there were no structures near enough to the facility to be impacted by any noise. However, as the surrounding area continues to develop, it may be necessary to install sound attenuation equipment.

The operation of the facility has been so successful that after one year the facility was converted from research status to commercial operation. It has proven to be very reliable and trouble-free.

ECONOMIC ANALYSIS

The economics regarding the installation of expander-driven generator facilities can be rather complex. There are several variables that must be considered, most of which change with time and are difficult to accurately predict. In all cases, the installed cost of the system, the expected capacity or load factor, and the value of electric energy are all very important factors. In those cases where either pre- or post-heating is required, the cost of energy for heating is also very important. Some installations are able to take advantage of government regulations.

The installed cost is primarily determined by the size of the unit. However, other factors may have a significant impact on this cost. The connection to the gas system could be expensive if special hot tap fittings are required. If sound attenuation is necessary for the chosen location, this can also have an impact on the overall cost. The connection to the electrical system can add significant cost if distances are far or high-voltage switchgear is necessary. Equipment manufacturers are able to provide cost estimates for major equipment. The installation costs are site specific and require individual studies and estimates.

The capacity factor or load factor is the ratio of the electric energy actually produced or expected to be produced, and the maximum amount of electric energy that could be produced if the generator operated at full load all the time. The net capacity factor is similar, except the auxiliary electric load is subtracted from the energy actually produced. The capacity or load factor is a trade-off between the maximum possible size of the unit and the profile of the available energy versus time. Some installations could have a constant gas flow and pressure drop. However, most will probably have flowrates and pressure differentials that vary with time of day, day of the week, and even seasons of the year. In these situations, it is necessary to decide whether it is better to install the largest capacity unit for the highest flows and pressure drops, or if a smaller size, which may end up online at a higher load factor, is more desirable.

A larger unit may have a lower capacity factor and may be required to go offline at a higher minimum output. This could result in less energy production than a smaller unit that may operate at 100% load much of the time. The operating characteristics of an expander in this type of application are typically represented by a family of curves. At a given available pressure drop, the expander power will vary with flowrate. At elevated pressure differentials, the expander may well produce the same power levels at lower flowrates. An estimate must be made of the differential pressure drop profile for the proposed site. An expander can then be sized to best take advantage of the available energy.

Another important economic consideration is the value of the electrical energy being produced and where it will be used. Some installations will make use of the electrical energy onsite. In these instances, the value of the energy will be the cost to the customer of the electric energy that is being displaced.

The other situation would be those that could not use any or all of the electric energy produced onsite and would require the utility to purchase the excess power. In some areas, local utilities may not permit such a facility to be connected to their electric system; in other areas utilities are very receptive to such equipment. This is an area where government regulations may provide incentives to some operators. If certain conditions are met an expander/generator facility could qualify as a small power producer under U.S. government regulations. If the conditions are met, the application regulations would, in fact, require the utility to allow the generator to be connected to their system and purchase the power at the utility's "avoided cost." To qualify, certain requirements must be met. First, for a small producer, the facility capacity cannot exceed 80 MW. Second, the primary source of energy must be waste energy or a renewable resource. Excess pressure in pipelines is considered a "waste energy." To qualify as the primary source of energy, it must be 75% of the energy consumed. Finally, the operator of the facility cannot be a utility.

The need for auxiliary heating is another factor that must be carefully evaluated. Due to the nature of the thermodynamic process, the gas discharging from an expander is at a much lower temperature than gas discharging from a regulator station operating within the same pressure bounds. If temperatures downstream of the expander are allowed to drop too low, potential problems may arise, such as hydrate formation and material compatibility.

There are several methods available to avoid problems with low discharge temperature. One solution is auxiliary heating. The gas can be heated upstream of the expander; this is called pre-heating. The gas can also be heated downstream of the expander, known as post-heating.

Once again, whether or not to use auxiliary heating is an economic decision. The heating allows more energy to be extracted from the gas stream, but the cost of the heat source or fuel must be subtracted from the value of the energy recovered. If the facility is to qualify under U.S. governmental regulations, auxiliary heating must be included when calculating the primary energy source.

Another alternative is to place a limit on the minimum downstream temperature and design the expander system to only recover energy available above that limit. This decreases the available energy for recovery, but eliminates the heating cost and is the base case against which cases with heating are compared. A similar approach involves a bypass regulator station that bypasses the expander and mixes a slightly warmer gas stream downstream of the expander. Again, this reduces the amount of energy being recovered because part of it is bypassed. Many other alternatives probably also exist, including the use of waste energy if a source is available. Again, each case will be different and the various alternatives must be carefully evaluated.

Due to the complexity of the economics, it is necessary to look at each installation individually. It is very difficult to state generalities, but the SDG&E story provides important feedback.

In any event, the economics for San Diego Gas & Electric's expander facility were fairly straightforward. There was no need for auxiliary heating, so the most difficult and critical decision concerned the capacity of the generator being installed. This capacity was finally determined based on historical flow data and a desire to maximize the amount of time the unit was operating. Because this was a research project, the need to gather operating experience was weighted heavily when selecting the size unit to install.

After four years of operation, the net electric energy produced each year had exceeded the estimate of 890,000 kW per year. However, this was, initially, offset by a steady decline in the value of the electricity. Since then, the payback period has decreased nicely. Follow-up studies have also indicated that a larger capacity unit may have resulted in better economics. Still, the operation of San Diego Gas & Electric's expander/generator has been very successful. The equipment has been thoroughly tested during four years of operation. It has demonstrated that an expander-driven generator can operate in conjunction with a gas pressure regulator station. The remote operation of such a facility has also been successfully demonstrated over that four-year time span.

CASE 16: THE USE OF MAGNETIC BEARINGS FOR OFFSHORE APPLICATIONS

As previously noted in Chapter 6, there are two primary parameters that encourage the use of magnetic bearings in turbomachinery: oil-free process and space requirements. For cryogenic processes such as hydrogen purification and ethylene plants, oil-free process is the primary objective. In the case of offshore platforms for oil and gas production, the occupied space and weight are of prime concern. In offshore operations, the process gas density is usually higher than in normal process plants because the gas is untreated and at high pressure. High-density process gas generates more windage loss and may also cause excessive radial load to journal bearings. Additionally, the bearing assembly design should be suitable for sour gas environments. Furthermore, the thrust bearing system should withstand process fluctuations, which are more severe due to high pressure.

In one successful offshore installation, the turboexpander receives rich natural gas at 80 bar and produces an 80/20 gas-to-liquid mass ratio at the discharge. The integral compressor recompresses expander discharge gases from 25–37 bar after the liquid is removed. The magnetic bearings operate in environments where natural gas is at 25 bar.

The 110-kg rotor is supported by 150-mm magnetic journal and thrust bearings. The maximum load capacity is 3,000 N per axis. These bearings were designed larger than necessary to withstand any unexpected side loads from uneven pressure distribution around the expander and compressor wheels. The thrust bearing diameter is 280 mm, with maximum load capacity of 20,000 N. Axial forces in the turboexpander are supported by double-acting thrust bearings. The rotor consists of a solid-steel material with a linear speed of 308 m/s (maximum allowable is 400 m/s.). The thrust disk is not laminated because the bearing is not subject to significant magnetization change during rotation and, therefore, eddy current losses are nominal. The maximum axial force slope is 200,000 N/s. To protect the electromechanical parts in the event of bearing overload or electronic failure, a set of auxiliary bearings is used for both radial and axial motions. The auxiliary bearings are dry ("paste-lubricated") ball bearings mounted on damping bands.

Active magnetic bearing load capabilities, both radially and axially, are much lower than those of conventional oil-lubricated bearings. The radial load limitation is mostly due to the limited magnetic flux density of the materials used. The axial load restriction is, for the most part, governed by the mechanical limitations of the thrust disk. Currently, the limit for radial unit loading is 0.5 N/mm^2 compared to 3.5 N/mm^2 for hydrodynamic oil bearings. The limit for axial loading is 0.3 N/mm^2 and 2.0 N/mm for the AMB and the conventional oil bearing, respectively. Therefore, the size of an AMB must be much larger than the conventional oil bearing for a given radial load. However, mechanical constraints do not allow the AMB's physical size to be sufficiently enlarged to carry the radial and/or axial load equivalent of the conventional oil bearing.

Turbomachinery bearing systems are normally designed for radial loads corresponding to the weight of the rotor. Non-uniform pressure distribution around the wheel(s) of a turbomachine may also contribute to the magnitude of gas dynamic radial load, occasionally called "side load." The sources of gas dynamic radial loads on the compressor wheel are different from those at the expander wheel.

In a compressor with a vaned diffuser followed by a typical casing, the non-uniform, circumferential flow resistance across the diffuser walls induces an asymmetric gas pressure around the wheel. Non-uniform peripheral gas pressure results in unbalanced loading on the wheel and, hence, a radial bearing load.

On the expander side, the expander wheel is surrounded by the nozzle vanes. The nozzle vanes, in turn, receive gas from a toroidal space that is connected to the expander inlet piping. Any non-uniformity in the torus space and/or in the nozzle vane design may result in a non-uniform pressure distribution around the expander wheel. Non-uniform gas pressure around the expander wheel will result in a non-uniform load and, hence, produce a gas dynamic radial load on the bearing. In the expander case, however, the nozzle throat flow resistance is much larger than the casing peripheral pressure non-uniformity. The latter acts as a buffer making the expander wheel circumferential pressure variations smaller than those of the compressor side. This smaller pressure variation produces much less radial load when compared to that of the compressor side.

Proper cooling of the bearings is one of the design challenges in magnetic bearing turbomachinery. This challenge is more serious when magnetic bearings are used in a high-pressure, closed environment. In once such application, the bearing housing is vented to the compressor suction at 25 bar. As discussed in Chapter 6, the high-density gas causes high rotor windage losses of approximately 22 kW.

Temperature sensors were placed in three locations in the magnetic bearing housing, the compressor side bearing, the expander side bearing, and in the vicinity of the thrust disk. In this control scheme, the signal corresponding to the maximum temperature was chosen to adjust seal/cooling gas flow and pressure. If the high temperature corresponds to either the expander or compressor bearings, the corresponding seal/cooling gas control valve is adjusted for higher pressure. If the high temperature is associated with the thrust disk area sensor, then both control valves are reset for higher flow and pressure.

Each turboexpander/compressor is supported by an independent programmable logic controller (PLC). The expander/compressor process and the seal gas treatment package are monitored by other PLCs. The control functions related to design features, such as automatic clamping systems, automatic thrust controls, compressor surge controls, inlet guide vane (IGV) ramping functions, and startup and shutdown logic, are all incorporated in the PLC program.

Offshore applications inherently have a wide range of flow and pressure variations. This is mostly due to production levels and decay of the oil/gas reservoir over time. Turboexpanders handle flow variations by IGVs. IGVs maintain thermal efficiency reasonably constant over a wide range of flow. Process gas pressure variation may cause separation of the nozzle adjusting ring and nozzle segments resulting in a blow-by or excess clamping, which will disable the unit. The automatic clamping system (ACS) addresses this problem. With ACS as part of the design, IGV operation and, therefore, turboexpander performance significantly improves (see Chapter 6).

Turboexpanders with magnetic bearings are an attractive solution for offshore applications. Several design features are implemented to ensure proper cooling and compensation of the axial loads imposed by process fluctuations. In high-density natural gas applications, magnetic bearings are subject to gas dynamic and process induced radial loads. Proper bearings selection and design features can prevent field problems.

BIBLIOGRAPHY AND ADDITIONAL READING

1. Agahi, R. R. and Ershaghi, B., 1993. "Engineering of Turbo-expander-Compressor Units for Off-Shore Installation," Fifth International Congress on Fluid Machinery, The Hague, Netherlands.

2. Agahi, R. R., Ershaghi, B., Leonhard, M., and Bosen, W., 1992. "Turboexpander with Magnetic Bearings in Air Separation and Hazardous Area," MAG'92, Alexandria, VA.
3. Agahi, R. R., Ershaghi, B., Leonhard, M., Bosch, W., and Brunet M., 1994. "The First High-Power Natural Gas Turboexpander-Compressor with Magnetic Bearings and Dry Face Seal," ASME, Revolve, National Petroleum Show, Calgary, Canada.
4. Agahi, R. R. and Ershaghi, B., 1994. "Integrated Monitoring and Controlling of Turboexpander Compressor with Active Magnetic Bearings Turbomachinery Asia," World Trade Center, Singapore.
5. Agahi, R. R., Ershaghi, B., and Leonhard, M., 1994. "Side Load Effect on Turbomachines with AMB," ICMB (International Center for Magnetic Bearings), Zurich, Switzerland.

APPENDIX A

Conversion Tables

Energy Conversions

	Joule	Calorie	Btu	Chu	kW.h	Hp.h	ft.lbf	ft.pdl	erg.
1 J	1	0.239	9.48 − 04	5.27 − 04	2.78 − 07	3.72 − 07	0.738	23.7	1 + 07
1 Cal	4.18	1	3.97 − 03	2.20 − 03	1.162 − 06	1.559 − 06	3.09	99.3	4.18 + 07
1 Btu	1.055 + 03	252	1	0.556	2.93 − 04	3.93 − 04	778	2.50 + 04	1.055 + 10
1 Chu	1.889 + 03	454	1.8	1	5.28 − 04	7.07 − 04	1.401 + 03	4.51 + 04	1.899 + 10
1 kW.h	3.60 + 06	8.60 + 05	3.41 + 03	1.896 + 03	1	1.341	2.66 + 06	8.54 + 07	3.60 + 13
1 Hp.h	2.68 + 06	6.42 + 05	2.54 + 03	1.41 + 03	0.746	1	1.980 + 06	6.37 + 07	2.68 + 13
1 ft.lbf	1.356	0.324	1.285 − 03	7.14 − 04	3.77 − 07	5.05 − 07	1	32.2	1.356 + 07
1 ft.pdl	4.21 − 02	1.007 − 02	3.99 − 05	2.22 − 05	1.171 − 08	1.570 − 08	3.11 − 02	1	4.21 + 05
1 erg	1 − 07	2.39 − 08	9.48 − 11	5.27 − 11	2.78 − 14	3.72 − 14	7.38 − 08	2.37 − 06	1

1 J = 1 W.s = 1 N.m
1 ft. lbf = 1 slug.ft^2/s^2
1 ft. poundal = 1 lbm.ft^2/s^2
1 erg = 1 dyne.cm

Power Conversions

	Watt	ft.pdl/s	cal/s	kcal/h	Btu/s	Btu/h	ft.lbf/s	Chu/s	Hp
1 W	1	23.7	0.239	0.860	9.48 − 04	3.41	0.738	5.27 − 04	1.341 − 03
1 ft.pdl/s	4.21 − 02	1	1.007 − 02	3.63 − 02	3.99 − 05	0.1438	3.11 − 02	2.22 − 05	5.64 − 05
1 cal/s	4.18	99.3	1	3.6	3.97 − 03	14.28	3.09	2.20 − 03	5.61 − 03
1 kcal/h	1.162	27.6	0.278	1	1.102 − 03	3.97	0.857	6.12 − 04	1.559 − 03
1 Btu/s	1.055 + 03	2.50 + 04	252	908	1	3.60 + 03	778	0.556	1.415
1 Btu/h	0.293	6.96	7.00 − 02	0.252	2.78 − 04	1	0.216	1.543 − 04	3.93 − 04
1 ft.lbf/s	1.356	32.2	0.324	1.167	1.285 − 03	4.63	1	7.14 − 04	1.818 − 03
1 Chu/s	1.899 + 03	4.51 + 04	454	1.634 + 03	1.8	6.48 + 03	1.401 + 03	1	2.55
1 Hp	74	1.774 + 04	178.2	642	0.707	2.54 + 03	550	0.393	1

1 W = 1 J/s
1 ft.pdl/s = 1 lbm.ft^2/s^3
1 ft.lbf/s = 1 slug.ft^2/s^3

Pressure Conversions

	Pa	bar	atm	Torr	In H_2O	In Hg	psi	pdl/ft^2	lbf/ft^2
1 Pa	1	1 + 05	9.87 − 06	7.50 − 03	4.20 − 03	2.95 − 04	1.450 − 04	0.672	2.09 − 02
1 bar	1 + 05	1	0.987	750	402	29.5	14.5	6.72 + 04	2.09 + 03
1 atm	1.013 + 05	1.013	1	760	407	29.9	14.70	6.81 + 04	2.12 + 03
1 Torr	133.3	1.33 − 03	1.316 − 03	1	0.535	3.94 − 02	1.934 − 02	89.6	2.78
1 In H_2O	249	2.49 − 03	2.46 − 03	1.868	1	7.36 − 02	3.61 − 02	167.4	5.20
1 In Hg	3.39 + 03	3.39 − 02	3.34 − 02	25.4	13.60	1	0.491	2.28 + 03	70.7
1 psi	6.90 + 03	6.90 − 02	6.80 − 02	51.7	27.7	2.04	1	4.63 + 03	144
1 pdl/ft^2	1.488	1.488 − 05	1.469 − 05	1.116 − 02	5.97 − 03	4.40 − 04	2.16 − 04	1	3.11 − 02
1 lbf/ft^2	47.9	4.79 − 04	4.72 − 04	0.359	0.1922	1.414 − 02	6.94 − 03	32.2	1

1 Pa = 1 N/m^2
1 poundal/ft^2 = 1 lbm./($ft.s^2$)
1 lbf/f^2 = 1 slug/($ft.s^2$)
1 Torr = 1 mm Hg

NOTE: 1 + 04 corresponds to 1 x 10^4
1 − 04 corresponds to 1 x 10^{-4}

Source: TMI Handbook.

APPENDIX B

Turboexpander Specifications

Atlas Copco Energas GmbH (1) — Cologne, Germany
Rotoflow Corporation Inc (2) — Gardena, California, USA

MODEL	INLET PRESSURE (BAR A)	INLET TEMPERATURE (°C)	INLET FLOW (kg/hr)	NUMBER OF STAGES	RPM	TYPE OF CASING SPLIT	TYPE OF SEALS	TYPE OF GAS EXPANDER CAN HANDLE	TYPE OF DESIGN
(1)									
ETF	2 to 64	-210 to	500 to	1	to 105,000	V	L/O	Air, N_2,	R
		+20	5,000					H_2, CO,	
ETB	2 to 80	-260 to	3,000 to	1	to 81,000	V	L/O/D	Tail Gas,	R
		+40	150,000					Hydrocarbons,	
ETG	2 to 150	-150 to	5,500 to	1 to 4	to 44,000	V	L/O/D	gas	R
		+510	150,000					mixtures,	
								Natural	
								gas, etc.	
(2)									
10	2 to	-250 to	235 to	1	86,000	V	L/O/D	Air, N_2,	R
15	207	+510	500,000	1	70,000	V	L/O/D	H_2, NH_3,	R
20				1	55,000	V	L/O/D	Steam,	R
30				1	35,000	V	L/O/D	Hydrocarbons	R
40				1	26,000	V	L/O/D	Refrigerants	R
50				1	20,000	V	L/O/D	and other	R
60				1	15,000	V	L/O/D	technical	R
								gases.	

Note: Symbol "D" at "Type of Seal" = Dynamic Dry Gas Seal.

Dresser Rand, Turbo Products Division — Olean, New York, USA

MODEL	INLET PRESSURE (BAR A)	INLET TEMPERATURE (°C)	INLET FLOW (kg/hr)	NUMBER OF STAGES	RPM	TYPE OF CASING SPLIT	TYPE OF SEALS	TYPE OF GAS EXPANDER CAN HANDLE	TYPE OF DESIGN
E-516	15.0	700	45,000	5	10,930	H	L	Nitric	A
E-520	15.0	700	75,000	5	8,780	H	L	Acid,	A
E-522	15 0	700	135,000	5	8,400	H	L	Ethylene	A
E-526	15.0	700	165,000	5	7,100	H	L	Oxide,	A
E-232	4.8	760	200,000	2	7,500	V	L	FCC,	A
E-132	3.2	760	165,000	1	8,400	V	L	Coal Gas,	A
E-238	4.8	760	345,000	2	6,000	V	L	Blast	A
E-138	3.2	760	285,000	1	6,000	V	L	Furnace	A
E-248	4.8	760	555,000	2	4,000	V	L		A
E-148	3 2	760	425,000	1	4,000	V	L		A
E-156	3.2	760	640,000	1	3,600	V	L		A

Elliott Company — Jeannette, Pennsylvania, USA

MODEL	INLET PRESSURE (BAR A)	INLET TEMPERATURE (°C)	INLET FLOW (kg/hr)	NUMBER OF STAGES	RPM	TYPE OF CASING SPLIT	TYPE OF SEALS	TYPE OF GAS EXPANDER CAN HANDLE	TYPE OF DESIGN
TH-85	3.4	760	220,000	1 or 2	6,700	V	L	FCC	A
TH-100	3.4	760	315,000	1 or 2	5,600	V	L	Blast Furnace,	A
								Coal Gas	
TH-120	3 4	760	370,000	1 or 2	4,700	V	L	Blast Furnace,	A
								Coal Gas	
TH-140	3.4	760	635,000	1 or 2	3,600	V	L	Blast Furnace,	A
								Coal Gas	

GHH BORSIG Turbomaschinen GmbH — Oberhausen, Germany

MODEL	INLET PRESSURE (BAR A)	INLET TEMPERATURE (°C)	INLET FLOW (m³/hr)	NUMBER OF STAGES	RPM	TYPE OF CASING SPLIT	TYPE OF SEALS	TYPE OF GAS EXPANDER CAN HANDLE	TYPE OF DESIGN
EN	max. 130	max. 520	150,000	multi	max. 20,000	H	L,O,G	all	A
EH	80	760	200,000	1 + 2	24,000	H/V	L,O	industrial	A
ER	100	520	60,000	1/2 or multi	48,000	V	L,O,G	gases	R

Note: Inlet flow specifications are in m³/hr.

Mafi-Trench Corporation — Santa Maria, California, USA

MODEL	INLET PRESSURE (BAR A)	INLET TEMPERATURE (°C)	INLET FLOW (kg/hr)	NUMBER OF STAGES	RPM	TYPE OF CASING SPLIT	TYPE OF SEALS	TYPE OF GAS EXPANDER CAN HANDLE	TYPE OF DESIGN
Frame 1	to 125	-200 to +200	from 500 to 750,000	1	to 100,00	V	L	all industrial	R
Frame 2	to 125	-200 to +200		1	to 60,00	V	L	gases and hydro-	R
Frame 2.5	to 125	-200 to +200		1	to 45,000	V	L/O	carbon gas mixtures	R
Frame 3	to 125	-200 to +200		1	to 35,000	V	L/O/D	including condensing	R
Frame 3.5	to 125	-200 to +200		1	to 28,000	V	L/O/D	streams	R
Frame 4	to 125	-200 to +200		1	to 24,000	V	L/O/D		R
Frame 5	to 125	-200 to +200		1	to 20,000	V	L/O/D		R
Frame 6	to 125	-200 to +200		1	to 15,000	V	L/O/D		R
Frame 10	to 50	-29 to +300		1	to 8,000	V	L/O/D		R

Notes: 1. Load devices include: integrally mounted turbocompressor, dynometer or gearbox/generator.
2. "Oil free" design using magnetic bearings also available.

Mannesmann Demag Verdichter — Duisburg, Germany

MODEL	INLET PRESSURE (BAR A)	INLET TEMPERATURE (°C)	INLET FLOW (kg/hr)	NUMBER OF STAGES	RPM	TYPE OF CASING SPLIT	TYPE OF SEALS	TYPE OF GAS EXPANDER CAN HANDLE	TYPE OF DESIGN
PRT	25	+550	240,000	1 - 4	50,000	V	L,G	all gases	C

Mitsui Engineering & Shipbuilding Co, Ltd — Japan

MODEL	INLET PRESSURE (BAR A)	INLET TEMPERATURE (°C)	INLET FLOW (kg/hr)	NUMBER OF STAGES	RPM	TYPE OF CASING SPLIT	TYPE OF SEALS	TYPE OF GAS EXPANDER CAN HANDLE	TYPE OF DESIGN
GE-Series	20	670	100,000	9	12,000	H	L	NG,TPA,EO Phenol	A
MAT-W Series	4.5	60	1,000,000	4	3,600	H	L	BFG (Wet)	A
MAT-D Series	4.5	200	1,000,000	4	3,600	H	L	BFG (Dry)	A

Nuovo Pignone — Florence, Italy

MODEL	INLET PRESSURE (BAR A)	INLET TEMPERATURE (°C)	INLET FLOW (kg/hr)	NUMBER OF STAGES	RPM	TYPE OF CASING SPLIT	TYPE OF SEALS	TYPE OF GAS EXPANDER CAN HANDLE	TYPE OF DESIGN
PGE Series	80	800	550,000	1 - 6	4-12,000	V	L	Nitric Acid FCC Coal Gasif.	A

Stewart & Stevenson International Inc Gas Turbine Products Division — Houston, Texas, USA

MODEL	INLET PRESSURE (BAR A)	INLET TEMPERATURE (°C)	INLET FLOW (kg/hr)	NUMBER OF STAGES	RPM	TYPE OF CASING SPLIT	TYPE OF SEALS	TYPE OF GAS EXPANDER CAN HANDLE	TYPE OF DESIGN
EXP-Gen 250	68	260	10,400 SCFM	1	3,600	—	Carbon	NG, air	—

Sulzer Turbo GmbH — Ravensburg, Germany

MODEL	INLET PRESSURE (BAR A)	INLET TEMPERATURE (°C)	INLET FLOW (kg/hr)	NUMBER OF STAGES	RPM	TYPE OF CASING SPLIT	TYPE OF SEALS	TYPE OF GAS EXPANDER CAN HANDLE	TYPE OF DESIGN
GT, integral geared with compressor	up to 10	up to 400	up to 100,000	2	to suit driven compressor	V	L	Nitric Acid Tailgas	—

Sulzer Turbo Ltd. — Zurich, Switzerland

MODEL	INLET PRESSURE (BAR A)	INLET TEMPERATURE (°C)	INLET FLOW (kg/hr)	NUMBER OF STAGES	RPM	TYPE OF CASING SPLIT	TYPE OF SEALS	TYPE OF GAS EXPANDER CAN HANDLE	TYPE OF DESIGN
E (8 frame sizes)	up to 17	up to 510	up to 360,000	4	to suit driven equipment	H	L	air, N_2, Tailgas	A
EH (2 frame sizes)	up to 17	up to 710	up to 300,000	6	to suit driven equipment	H	L	air, N_2, Tailgas	A

APPENDIX C

Turboexpander Contacts and Addresses

Listed below are companies that have provided hardware, services, information, or data used by the authors in conjunction with work involving turboexpanders. Their past and present contributions are gratefully acknowledged.

Three important points should be noted:

- This list is not complete. There are undoubtedly other suppliers that can satisfy user needs.
- The product slate of the companies listed is often much greater than indicated here. For most large manufacturers, turboexpanders are only one of several product types or categories. These manufacturers often also produce compressors, steam turbines, gas turbines, and other machinery.
- Many equipment manufacturers have entire divisions engaging in field service and repair activities.

Keeping in mind the above extension of probable scopes of supply, the entries are limited to those of primary interest to turboexpander users. An alphabetical listing follows:

Atlas Copco Incorporated 46 School Road Voorheesville, NY 12186, USA Tel: 518-765-3344 Fax: 518-765-3357	Turboexpanders
Atlas Copco Rotoflow, Inc. 540 Rosecrans Avenue Gardena, CA 90248, USA Tel: 310-329-8447 Fax: 310-329-8502	Turboexpanders

Bearings Plus Corporation 8525 W. Monroe Street Houston, TX 77061, USA Tel: 713-944-1005 Fax: 713-944-3950	Flexure Pivot Bearings; Dampers
Bently Nevada Corporation 1617 Water Street Minden, NV 89423, USA Tel: 702-782-3611 Fax: 702-782-9337	Vibration Monitoring Equipment and Diagnostic Services
BHS-Sonthofen Hans-Boeckler-Strasse 7 87527 Sonthofen, Allgaeu Germany Tel: 49-8321-8020 Fax: 49-08321-802-689	High-Speed Gears, Clutches, Couplings
Borsig (*see* GHH-Borsig)	Turboexpanders
Clarion Technical Conferences 3401 Louisiana Street Houston, TX 77002, USA Tel: 713-521-5929 Fax: 713-521-9255	Conferences and Exhibitions
Compressor Controls Corporation 11359 Aurora Avenue Des Moines, IA 50322, USA Tel: 515-270-0857 Fax: 515-270-1331	Surge Control Devices, Governing Systems
Compressor Tech/Two 20855 Watertown Road Waukesha, Wl 53186-1873, USA Tel: 262-832-5000 Fax: 262-832-5075	Publications
Demag DeLaval Turbomachinery Wolfgang-Reuter-Platz 47053 Duisburg, Germany Tel: 49-203-6051 Fax: 49-203-61061	Turboexpanders

Demag DeLaval Turbomachinery 840 Nottingham Way Trenton, NJ 08650-0788, USA Tel: 609-890-5000 Fax: 609-890-9180	Turboexpanders
Dresser-Rand Control Systems 1202 W. Sam Houston Pkwy N. Houston, TX 77043, USA Tel: 713-365-2601 Fax: 713-365-2660	Control Systems
Dresser-Rand Turbo Products Division P.O. Box 560 Olean, NY 14760, USA Tel: 716-375-3000 Fax: 716-375-3178	Turboexpanders
Elliott Company 901 North Fourth Street Jeannette, PA 15644-1473, USA Tel: 724-527-2811 Fax: 724-527-8442	Turboexpanders
Elliott Support Services 2001 W. Sam Houston Pkwy N. Houston, TX 77043-2121, USA Tel: 713-984-3837 Fax: 713-984-3905	Turboexpander Field Support and Repairs
Flender-Graffenstaden 1, Rue du Vieux Moulin Illkirch-Graffenstaden 67400 France Tel: 33-8867-6000 Fax: 33-8867-0617	Gears, Clutches, and Couplings
Gas-Path Technology, Inc. 8301 W. Monroe Street Houston, TX 77061, USA Tel: 713-947-1396 Fax: 713-947-1084	Gas Path Repairs

GHH Borsig Turbomaschinen GmbH Bahnhofstrasse 66 46145 Oberhausen, Germany Tel: 49-208-69207 Fax: 49-208-6922019	Turboexpanders
Gulf Publishing Company Hydrocarbon Processing Magazine P.O. Box 2608 Houston, TX 77252-2608, USA Tel: 713-529-4301 Fax: 713-520-4433	Publications
Hickham Industries, Inc. 11518 Old LaPorte Road LaPorte, TX 77571, USA Tel: 713-471-6540 Fax: 713-471-4821	Turboexpander Field Support and Repairs
Howmet Corporation 475 Steamboat Road Greenwich, CT 06830, USA Tel: 203-661-4600 Fax: 203-625-8796	Investment Castings, Coatings, and Blade Repairs
Kingsbury, Inc. 10385 Drummond Road Philadelphia, PA 19154, USA Tel: 215-824-4000 Fax: 215-824-4999	Fluid Film Bearings, LEG Technology
KMC Incorporated 20 Technology Way West Greenwich, RI 02817, USA Tel: 401-392-1900 Fax: 401-397-6702	Flexure Pivot Bearings; Dampers
Liburdi Engineering Ltd. 400 Highway 6 North Hamilton, Ontario L9J 1E7, Canada Tel: 905-689-0734 Fax: 905-689-0739	Coating Services, Blade Repairs

Lucas Aerospace Power Transmission 211 Seward Avenue Utica, NY 13503-0457, USA Tel: 315-793-1419 Fax: 315-793-1415	Clutches and Couplings
Ludeca, Inc. 1527 NW 89th Court Miami, FL 33172, USA Tel: 305-591-8935 Fax: 305-591-1537	Alignment Technology (Laser Optics)
Lufkin Industries, Inc. 407 Kiln Street Lufkin, TX 75902, USA Tel: 936-637-5612 Fax: 936-637-5883	Gears
MAAG Gear Company, Ltd. Hardstrasse 219 Zurich 8023, Switzerland Tel: 41-1-278-7878 Fax: 41-1-278-7880	Gears, Clutches, and Couplings
Mafi-Trench Corporation 3037 Industrial Parkway Santa Maria, CA 93455, USA Tel: 805-928-5757 Fax: 805-925-3861	Turboexpanders
Magnetic Bearings Inc. 5241 Valleypark Drive Roanoke, VA 24019, USA Tel: 703-563-4936 Fax: 703-563-4937	Bearings, magnetic
Mitsui Engineering Ltd. Energy Plant Division 6-4, Tsukiji 5-Chome, Chuo-ku Tokyo, 104, Japan Tel: 81-3-3544-3639 Fax: 81-3-3544-3045	Turboexpanders

Nuovo Pignone Via Felice Matteucci, 2 50127 Florence, Italy Tel: 39-55-423-2272 Fax: 39-55-423-2901	Turboexpanders
Mannesmann Demag (*see* Demag DeLaval)	Turboexpanders
Odessa Babbitt Bearing Company 6112 W. County Road Odessa, TX 79764, USA Tel: 915-366-2836 Fax: 915-366-4887	Fluid Film Bearings
Olympus America Inc. Industrial Products Group Two Corporate Center Drive Melville, NY 11747, USA Tel: 800-446-5260 Fax: 516-844-5620	Borescopes
Orion Corporation 1111 Cedar Creek Road Grafton, WI 53024, USA Tel: 414-377-2210 Fax: 414-377-0729	Fluid Film Bearings
Philadelphia Gear Corporation 181 South Gulph Road King of Prussia, PA 19406, USA Tel: 610-265-3000 Fax: 610-337-5637	Gears, including Epicyclic Type
Pioneer Motor Bearing 116 Beacon Street South San Francisco, CA 94080, USA Tel: 415-871 -8144 Fax: 415-873-5717	Fluid Film Bearings
Praxair Surface Technologies, Inc. 1500 Polco Street Indianapolis, IN 46224, USA Tel: 317-240-2400 Fax: 317-240-2380	Coatings

Prueftechnik AG Oskar-Messter-Strasse 19-21 85737 Ismaning, Germany Tel: 49-89-996-160 Fax: 49-89-99616-200	Alignment Technology Vibration Monitoring and Analysis Equipment
Renk Aktiengesellschaft Gogginger Strasse 73 86159 Augsburg, Germany Tel: 49-821-5700-534 Fax: 49-821-5700-460	Gears, Fluid Film Bearings, Couplings, and Clutches
Revolve Magnetic Bearings, Inc. 300, 707-10th Avenue SW Calgary, Alberta T2R OB3, Canada Tel: 403-232-9292 Fax: 403-232-9255	Bearings, magnetic; Gas Sealing Technology
SRS Rotordynamics Seal Research 3628 Madison Avenue, Suite 20 North Highlands, CA 95660, USA Tel: 916-344-9500 Fax: 916-344-8400	Damper Technology
Schenk Trebel 535 Acorn Street Deer Park, NY 11729, USA Tel: 516-242-4010 Fax: 516-242-4147	Balancing Equipment
Sermatech International 155 South Limerick Road Limerick, PA 19468 Tel: 610-948-5100 Fax: 610-948-2771	Coating Services; Blade Repair
SKF USA Industrial Division 1510 Gehman Road Kulpsville, PA 19443 Tel: 215-513-4512 Fax: 215-513-4401	Rolling Element Bearings

Société de Méchanique Magnetique S2M America 5241 Valleypark Drive Roanoke, VA 24019, USA Tel: 540-563-5191 Fax: 540-563-4937	Bearings, magnetic
Sohre Turbomachinery Inc. 132 Gilbertville Road Ware, MA 01082-0889, USA Tel: 413-967-0968 Fax: 413-967-5846	Shaft Riding (Grounding) Brushes
Sulzer Turbo Ltd. Hardstrasse 319 8023 Zurich, Switzerland Tel: 41-1-278-2211 Fax: 41-1-278-2989	Turboexpanders
Sulzer Turbosystems International 2901 Wilcrest Drive, Suite 450 Houston, TX 77042, USA Tel: 713-780-4200 Fax: 713-780-2848	Turboexpanders
Triconex Corporation Tri-Sen Turbomachinery Controls 4916 FM 1765 LaMarque, TX 77568, USA Tel: 409-935-3555 Fax: 409-935-3881	Controls and Governors
Turbine Metal Technology, Inc. 7327 Elmo Street Tujinga, CA 91042, USA Tel: 818-352-8721 Fax: 818-352-8726	Coatings; Blade Repairs
TurboCare Div. of Demag DeLaval 2140 Westover Road Chicopee, MA 01022, USA Tel: 413-593-0500 Fax: 413-593-3424	Field Service; Repairs

Turbomachinery International Publications P.O. Box 5550 Norwalk, CT 06856, USA Tel: 203-853-6015 Fax: 203-856-8175	Books and Magazines
Turbomachinery Maintenance Congress (*see above*)	Conference and Exhibition
Voith Turbo GmbH Power Transmission Voithstrasse 1 74564 Crailsheim, Germany Tel: 49-7951-320 Fax: 49-7951-32500	Clutches and Couplings; Torque Converters
Waukesha Bearings Corporation P.O. Box 1616 Waukesha, WI 53187, USA Tel: 414-547-3381 Fax: 414-547-5508	Fluid Film Bearings
Westech Gear Corporation 2600 East Imperial Highway Lynwood, CA 90262, USA Tel: 310-605-2600 Fax: 310-635-6080	Gears
Woodward Governor Company 3800 N. Wilson Avenue Loveland, CO 80539-2072, USA Tel: 970-663-3900 Fax: 970-962-7050	Controls and Governors

Index

This Page Intentionally Left Blank